INTERSPECIES INTERACTIONS: EFFECTS ON VIRULENCE AND ANTIMICROBIAL SUSCEPTIBILITY OF BACTERIAL AND FUNGAL PATHOGENS

EDITED BY: Giuseppantonio Maisetta and Giovanna Batoni
PUBLISHED IN: Frontiers in Microbiology

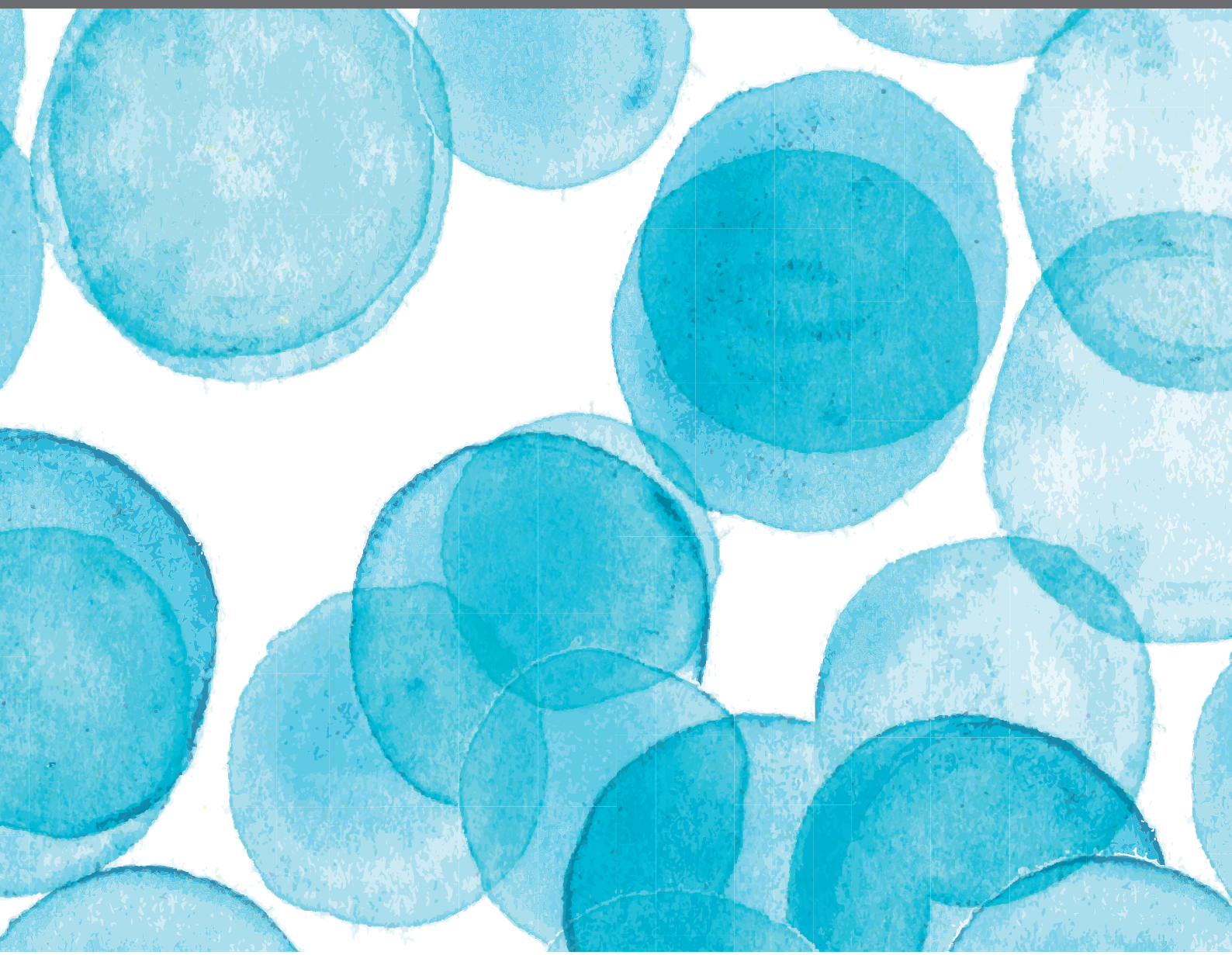

frontiers Research Topics

frontiers

ISSN 1664-8714
ISBN 978-2-88966-097-1
DOI 10.3389/978-2-88966-097-1

About Frontiers

Frontiers is more than just an open-access publisher of scholarly articles: it is a pioneering approach to the world of academia, radically improving the way scholarly research is managed. The grand vision of Frontiers is a world where all people have an equal opportunity to seek, share and generate knowledge. Frontiers provides immediate and permanent online open access to all its publications, but this alone is not enough to realize our grand goals.

Frontiers Journal Series

The Frontiers Journal Series is a multi-tier and interdisciplinary set of open-access, online journals, promising a paradigm shift from the current review, selection and dissemination processes in academic publishing. All Frontiers journals are driven by researchers for researchers; therefore, they constitute a service to the scholarly community. At the same time, the Frontiers Journal Series operates on a revolutionary invention, the tiered publishing system, initially addressing specific communities of scholars, and gradually climbing up to broader public understanding, thus serving the interests of the lay society, too.

Dedication to Quality

Each Frontiers article is a landmark of the highest quality, thanks to genuinely collaborative interactions between authors and review editors, who include some of the world's best academicians. Research must be certified by peers before entering a stream of knowledge that may eventually reach the public - and shape society; therefore, Frontiers only applies the most rigorous and unbiased reviews.
Frontiers revolutionizes research publishing by freely delivering the most outstanding research, evaluated with no bias from both the academic and social point of view. By applying the most advanced information technologies, Frontiers is catapulting scholarly publishing into a new generation.

What are Frontiers Research Topics?

Frontiers Research Topics are very popular trademarks of the Frontiers Journals Series: they are collections of at least ten articles, all centered on a particular subject. With their unique mix of varied contributions from Original Research to Review Articles, Frontiers Research Topics unify the most influential researchers, the latest key findings and historical advances in a hot research area! Find out more on how to host your own Frontiers Research Topic or contribute to one as an author by contacting the Frontiers Editorial Office: researchtopics@frontiersin.org

INTERSPECIES INTERACTIONS: EFFECTS ON VIRULENCE AND ANTIMICROBIAL SUSCEPTIBILITY OF BACTERIAL AND FUNGAL PATHOGENS

Topic Editors:
Giuseppantonio Maisetta, University of Pisa, Italy
Giovanna Batoni, University of Pisa, Italy

Citation: Maisetta, G., Batoni, G., eds. (2020). Interspecies Interactions: Effects On Virulence and Antimicrobial Susceptibility of Bacterial and Fungal Pathogens. Lausanne: Frontiers Media SA. doi: 10.3389/978-2-88966-097-1

Table of Contents

frontiers in Microbiology

EDITORIAL
published: 26 August 2020
doi: 10.3389/fmicb.2020.01922

Editorial: Interspecies Interactions: Effects on Virulence and Antimicrobial Susceptibility of Bacterial and Fungal Pathogens

Giuseppantonio Maisetta and Giovanna Batoni**

Department of Translational Research and New Technologies in Medicine and Surgery, University of Pisa, Pisa, Italy

Keywords: interspecies interactions, polymicrobial infections, virulence, biofilm, susceptibility

Editorial on the Research Topic

Interspecies Interactions: Effects on Virulence and Antimicrobial Susceptibility of Bacterial and Fungal Pathogens

One of the most exciting achievements that microbiologists have pursued over the last decades is the recognition that microorganisms rarely live as single fluctuating entities but strictly interact with each other in complex communities known as biofilms. Studies on dental biofilms, intestinal communities, chronic wounds, or respiratory infections in patients with cystic fibrosis clearly demonstrate that community interactions greatly influence microbial survival and disease progression (Dalton et al., 2011; Caverly et al., 2015; Reynolds et al., 2015; Marsh and Zaura, 2017). These interactions range from synergism to competition and involve, among others, physical interactions, chemical signaling, and exchange of genetic information. There is no doubt that consideration of the social behavior of microorganisms can reveal emergent traits and mechanisms of pathogenicity that would be overlooked by studying bacteria in isolation. For instance, community establishment provides members with additional properties such as enhanced tolerance to antimicrobials, ability to evade host immune responses or to survive in harmful environments (Batoni et al., 2016).

This Research Topic gathers 11 articles from 71 authors exploring different aspects of species-to-species interactions. We believe that a deep understanding of the mechanisms at the basis of the ecological interactions among microbial species will provide the knowledge needed to translate novel interventions for the diagnosis, treatment, and prevention of poly-microbial infections into the clinic, and hope that this Research Topic may contribute to this purpose.

Certainly, the study of interspecies interactions strongly relies on the availability of suitable experimental models that enable the stable and long-term cultivation of poly-microbial communities (Røder et al., 2020). In this respect, the Topic includes three studies aimed at reproducing the features of specific body sites and at exploring the multiple interactions among commensals and pathogenic organisms, as well as antimicrobials. O'Brien and Welch described a new continuous-flow model for *in vitro* cultivation of mixed bacteria associated with cystic fibrosis airway infections, while Jordana-Lluch et al. developed and validated a simple 2D skin infection model for investigating commensals, pathogens and keratinocytes interactions. Finally, by employing an *in vitro* nasopharyngeal colonization model that mimics the conditions of the human

OPEN ACCESS

Edited by:
Natalia V. Kirienko,
Rice University, United States

Reviewed by:
Alexandra R. Lucas,
Arizona State University, United States
Milya Davlieva,
Quantapore, United States

****Correspondence:***
Giuseppantonio Maisetta
giuseppantonio.maisetta@dps.unipi.it
Giovanna Batoni
giovanna.batoni@med.unipi.it

Specialty section:
This article was submitted to Antimicrobials, Resistance and Chemotherapy, a section of the journal Frontiers in Microbiology

Received: *27 May 2020*
Accepted: *21 July 2020*
Published: *26 August 2020*

Citation:
Maisetta G and Batoni G (2020) Editorial: Interspecies Interactions: Effects on Virulence and Antimicrobial Susceptibility of Bacterial and Fungal Pathogens. Front. Microbiol. 11:1922. doi: 10.3389/fmicb.2020.01922

nasopharynx including temperature, nutrient availability, aeration, and epithelial attachment, Bair and Campagnani studied the co-colonization dynamics of three main othopatogens: *Moraxella catarrhalis*, non-typable *Haemophilus influenzae* (NTHi), and *Streptococcus pneumoniae* and found that the presence of *M. catarrhalis* is essential for NTHi to survive the bactericidal effects of *S. pneumoniae*.

One of the most obvious translational aspect of interspecies interactions is the use of "friend" microorganisms, the so-called probiotics, to prevent or cure diseases caused by microorganisms endowed high pathogenic potential. Although traditionally used to restore intestinal flora after prolonged antibiotic therapy, probiotics have been considered as means to prevent/treat a variety of diseases during the last decade (Sales-Campos et al., 2019). In this Research Topic, two papers concerning the employment of candidate probiotics against oral pathogens are included. Moman et al. demonstrated that bacterial strains such as *Lactobacillus reuteri* and *Streptococcus salivarius* decrease the toxic effects of the periodontal pathogens *Porphyromonas gingivalis* and *Aggregatibacter actinomycetemcomitans* toward oral keratinocytes and in an *in vivo* model of *G. mellonella* larvae. Zhang et al. reported that *Lactobacillus plantarum* K41 is able to inhibit biofilm formation of the highly cariogenic species *Streptococcus mutans* and observed a significant reduction in the incidence and severity of dental caries in rats pretreated with this probiotic strain.

Kang et al. showed that competitive interactions among microorganisms can be exploited to protect plants by phytopathogens. They studied how the gene expression of the pathogenic fungus *Gaeumannomyces graminis* var. *tritici* was affected by *Bacillus velezensis*, an endophytic biocontrol bacterium exhibiting a broad antifungal spectrum against many phytopathogens.

The close relationship between interspecies interactions and susceptibility to antimicrobials is a rapidly expanding research area that is likely to provide new clues to face the worrisome and world- spreading problem of antimicrobial resistance (AMR) (Radlinski and Conlon, 2018). In this direction, Banerji et al. present a comprehensive and interesting review addressing the relation between microbial interactions and AMR from an ecological point of view. Highlighting that human, animal, and environmental systems are strictly interconnected, the Authors show that species interactions may play significant and sometimes multifaceted roles in determining the prevalence and distribution of AMR and antimicrobial resistance-associated genes (ARGs).

The effects of interspecies interactions on antibiotic susceptibility are not limited to closely related microorganisms but can actually cross kingdom borders (Harriott and Noverr, 2009). Nabb et al. disclose an interesting mechanism by which *C. albicans* may promote multi-drug tolerance in *S. aureus*. They report that *S. aureus* grown in dual cultures with *C. albicans* displays decreased intracellular ATP concentrations as well as lower membrane potential when compared to cultures lacking *C. albicans*. Collectively, the data reported demonstrate that decreased metabolic activity through nutrient deprivation may induce the formation of persister cells and represent a mechanism for increased antibiotic tolerance within polymicrobial cultures.

Interestingly, three articles from the Research Topic highlight how interactions between species can not only negatively affect the susceptibility of microbial populations to antimicrobials, but also be exploited for the identification of new drugs or drug targets. In the first of these articles, Hardy et al. screened a number of clinical bacterial isolates obtained from a variety of body sites for the ability to inhibit multiple *S. aureus* strains. They found that the majority of the isolates inhibited at least one *S. aureus* strain including MRSA. Furthermore, many of the clinical isolates belonging to the *Staphylococcus* and *Corynebacterium* genera mediated contact-independent inhibitory or bactericidal activity against *S. aureus* warranting the characterization of the active entities at the molecular level to reveal novel *S. aureus* therapeutics. In the second article, Herbrik et al. studied a strain of *Streptomyces* (TR1341) isolated from the sputum of a tuberculosis patient. They demonstrated that TR1341 produces at least two bioactive compounds with fungicidal or antibacterial/anti-virulence activity. Finally, in the third article (Veerapandian and Vediyappan), an *in vitro* study was carried out demonstrating the inhibition of mono-species or dual-species biofilms of *S. gordonii* and *C. albicans*, by gymnemic acid (GAs), a non-toxic small molecule inhibitor of fungal hyphae. The study shows that *S. gordonii* stimulates the expression of adhesive materials in *C. albicans* by direct interaction and/or signaling, and that the adhesive material expression can be inhibited by GAs.

Overall, we believe that the articles collected in this Research Topic represent a step forward for a better understanding of microbe-microbe interactions and their effects on infection outcome and antibiotic susceptibility. We hope that this article collection may encourage further studies in this research field aimed to develop new preventive and/or therapeutic approaches against poly-microbial infections.

AUTHOR CONTRIBUTIONS

GM and GB equally contributed to the writing of the manuscript. All authors contributed to the article and approved the submitted version.

FUNDING

This work was supported by institutional funds from the University of Pisa.

ACKNOWLEDGMENTS

We thank Dr. Semih Esin for critical reading of the manuscript.

REFERENCES

Batoni, G., Maisetta,. G., and Esin, S. (2016). Antimicrobial peptides and their interaction with biofilms of medically relevant bacteria. *Biochim. Biophys. Acta.* 1858, 1044–1060. doi: 10.1016/j.bbamem.2015.10.013

Caverly, L. J., Zhao, J., and LiPuma, J. J. (2015). Cystic fibrosis lung microbiome: opportunities to reconsider management of airway infection. *Pediatr. Pulmonol.* 50(Suppl. 40):S31–S38. doi: 10.1002/ppul.23243

Dalton, T., Dowd, S. E., Wolcott, R. D., Sun, Y., Watters, C., Griswold, J. A., et al. (2011). An *in vivo* polymicrobial biofilm wound infection model to study interspecies interactions. *PLoS ONE* 6:e27317. doi: 10.1371/journal.pone.0027317

Harriott, M. M., and Noverr, M. C. (2009). *Candida albicans* and *Staphylococcus aureus* form polymicrobial biofilms: effects on antimicrobial resistance. *Antimicrob. Agents Chemother.* 53, 3914–3922. doi: 10.1128/AAC.00657-09.

Marsh, P. D., and Zaura, E. (2017). Dental biofilm: ecological interactions in health and disease. *J. Clin. Periodontol.* 44(Suppl. 18):S12–S22. doi: 10.1111/jcpe.12679

Radlinski, L., and Conlon, B. P. (2018). Antibiotic efficacy in the complex infection environment. *Curr. Opin. Microbiol.* 42, 19–24. doi: 10.1016/j.mib.2017.09.007

Reynolds, L. A., Finlay, B. B., and Maizels, R. M. (2015). Cohabitation in the intestine: interactions among helminth parasites, bacterial microbiota, and host immunity. *J. Immunol.* 195, 4059–4066. doi: 10.4049/jimmunol.1501432

Røder, H. L., Olsen, N. M. C., Whiteley, M., and Burmølle, M. (2020). Unravelling interspecies interactions across heterogeneities in complex biofilm communities. *Environ. Microbiol.* 22, 5–16. doi: 10.1111/1462-2920.14834

Sales-Campos, H., Soares, S. C., and Oliveira, C. J. F. (2019). An introduction of the role of probiotics in human infections and autoimmune diseases. *Crit. Rev. Microbiol.* 45, 413–432. doi: 10.1080/1040841X.2019.1621261

Conflict of Interest: The authors declare that the research was conducted in the absence of any commercial or financial relationships that could be construed as a potential conflict of interest.

frontiers in Microbiology

ORIGINAL RESEARCH
published: 09 July 2019
doi: 10.3389/fmicb.2019.01474

Comparative Transcriptome Profiling of *Gaeumannomyces graminis* var. *tritici* in Wheat Roots in the Absence and Presence of Biocontrol *Bacillus velezensis* CC09

Xingxing Kang[1], Yu Guo[1], Shuang Leng[1], Lei Xiao[2], Lanhua Wang[1], Yarong Xue[1] and Changhong Liu[1]**

[1] State Key Laboratory of Pharmaceutical Biotechnology, School of Life Sciences, Nanjing University, Nanjing, China,
[2] School of Chemical Engineering and Technology, China University of Mining and Technology, Xuzhou, China

OPEN ACCESS

Edited by:
Giovanna Batoni, University of Pisa, Italy

Reviewed by:
Patricia Ann Okubara, Agricultural Research Service (USDA), United States
Melissa Kay LeTourneau, Agricultural Research Service (USDA), United States

***Correspondence:**
Yarong Xue
xueyr@nju.edu.cn
Changhong Liu
chliu@nju.edu.cn

Specialty section:
This article was submitted to Microbial Physiology and Metabolism, a section of the journal Frontiers in Microbiology

Received: *15 February 2019*
Accepted: *13 June 2019*
Published: *09 July 2019*

Citation:
Kang X, Guo Y, Leng S, Xiao L, Wang L, Xue Y and Liu C (2019) Comparative Transcriptome Profiling of Gaeumannomyces graminis var. tritici in Wheat Roots in the Absence and Presence of Biocontrol Bacillus velezensis CC09. Front. Microbiol. 10:1474. doi: 10.3389/fmicb.2019.01474

This study aimed to explore potential biocontrol mechanisms involved in the interference of antagonistic bacteria with fungal pathogenicity *in planta*. To do this, we conducted a comparative transcriptomic analysis of the "take-all" pathogenic fungus *Gaeumannomyces graminis* var. *tritici* (*Ggt*) by examining *Ggt*-infected wheat roots in the presence or absence of the biocontrol agent *Bacillus velezensis* CC09 (*Bv*) compared with *Ggt* grown on potato dextrose agar (PDA) plates. A total of 4,134 differentially expressed genes (DEGs) were identified in *Ggt*-infected wheat roots, while 2,011 DEGs were detected in *Bv*+*Ggt*-infected roots, relative to the *Ggt* grown on PDA plates. Moreover, 31 DEGs were identified between wheat roots, respectively infected with *Ggt* and *Bv*+*Ggt*, consisting of 29 downregulated genes coding for potential *Ggt* pathogenicity factors – e.g., para-nitrobenzyl esterase, cutinase 1 and catalase-3, and two upregulated genes coding for tyrosinase and a hypothetical protein in the *Bv*+*Ggt*-infected roots when compared with the *Ggt*-infected roots. In particular, the expression of one gene, encoding the ABA3 involved in the production of *Ggt*'s hormone abscisic acid, was 4.11-fold lower in *Ggt*-infected roots with *Bv* than without *Bv*. This is the first experimental study to analyze the activity of *Ggt* transcriptomes in wheat roots exposed or not to a biocontrol bacterium. Our results therefore suggest the presence of *Bv* directly and/or indirectly impairs the pathogenicity of *Ggt* in wheat roots through complex regulatory mechanisms, such as hyphopodia formation, cell wall hydrolase, and expression of a papain inhibitor, among others, all which merit further investigation.

Keywords: endophytic bacteria, pathogenic fungi, phytopathology, RNA sequencing, wheat disease

INTRODUCTION

"Take-all" is one of the most severe soil-borne diseases of wheat plants worldwide, caused by the necrotrophic fungus *Gaeumannomyces graminis* var. *tritici* (Bithell et al., 2016). This pathogen infects healthy wheat roots via infectious hyphae that penetrate the cortical cells of the root and progress upward into the stem base. Because this process invariably disrupts water flow,

it eventually results in the premature death of infected plants. However, since the well-known virulence mechanism of *Ggt* might contribute to improved control of this fungal pathogen, considerable research effort has sought to better understand the mechanisms underlying *Ggt* pathogenicity (Dori et al., 1995; Yu et al., 2010; Yang et al., 2012). Consequently, many genes that contribute to *Ggt* pathogenicity have been identified, such as cellulase, endo-β-1,4-xylanase, pectinase, xylanase, β-1,3-exoglucanase, glucosidase, aspartic protease, and β-1,3-glucanase of cell wall degrading enzymes (CWDEs) (Yang et al., 2015). Based on their comparative transcriptome analysis of *Ggt* in axenic culture and *Ggt*-infected wheat, Yang et al. (2015) recently pointed out that many genes related to signaling, penetration, fungal nutrition, and host colonization are highly expressed during *Ggt* pathogenesis in wheat roots. Nevertheless, because of the complexity of the interaction between *Ggt* and its host plants, the pathogenesis of *Ggt* in wheat roots remains unclear. Additionally, control of the disease is hindered by a lack of resistant varieties and environmentally friendly fungicides.

Several studies have shown that beneficial bacteria, such as *Bacillus subtilis* (Liu et al., 2009, 2011; Durán et al., 2014; Yang et al., 2018), *Bacillus velezensis* (Wu et al., 2012; Luo et al., 2013; Kang et al., 2018), and *Pseudomonas fluorescens* (Daval et al., 2011; Kwak and Weller, 2013; Lagzian et al., 2013; Yang et al., 2014, 2017), could be used as effective and eco-friendly biocontrol agents to protect wheat from take-all disease. Among them, *B. velezensis* is a newly reported species that may be used to control take-all and other fungal diseases, such as spot blotch and powdery mildew (Cai et al., 2017; Kang et al., 2018). More specifically, *B. velezensis* CC09 (*Bv*) is an endophytic biocontrol bacterium, originally isolated from healthy *Cinnamomum camphora* leaves, that has broad antifungal spectra against many phytopathogens (Cai et al., 2016). It possesses several key biocontrol traits, namely, the production of strong antifungal metabolites (e.g., iturins and fengycins), promotion of plant growth, and induction of plant resistance (Cai et al., 2017; Kang et al., 2018). Recently, we found that this strain can cause the swelling, deformation, and cell content release of *Ggt* mycelia *in vitro*, inhibiting *Ggt* mycelia density and spread in wheat (Kang et al., 2018). Moreover, we also found that *Bv* could colonize and migrate in plants, leading to a 66.67% disease-control efficacy of take-all and 21.64% of spot blotch, with a single treatment inoculated on roots (Kang et al., 2018). These attributes make *Bv* a promising biocontrol agent for the long-term and effective protection of wheat from soil-borne and leaf diseases.

Yet, despite these established biocontrol features of *Bv*, limited information is available concerning its direct and indirect effects upon *Ggt*'s fungal pathogenicity *in planta*. For example, how *Ggt* responds to the presence of *Bv* in *Ggt*-infected plants remains unknown. In this study, we performed an RNA sequencing (RNA-Seq) analysis of *Ggt* in wheat roots with and without *Bv*. Since the *Ggt* transcriptome in axenic culture and *Ggt*-infected wheat roots differed markedly and varied during the infection process (Yang et al., 2015), the transcriptome of *Ggt* grown on potato dextrose agar (PDA) plates was also determined to serve as the control (*CK*). Through a comparative analysis of *Ggt* transcriptomes under three different conditions (e.g., grown on PDA, within wheat roots in the presence or absence of *Bv*), we sought to reveal the possible pathogenicity gene(s) of *Ggt* and its regulation by *Bv in planta* during the early infection of wheat roots.

MATERIALS AND METHODS

The Wheat, Bacterium, and Fungus

The winter wheat (*Triticum aestivum* "Sumai 188") used in this study was purchased from the Jiangsu Academy of Agricultural Sciences, Nanjing, China. The endophytic bacterium *Bv* was isolated from *C. camphora* leaf tissue (Cai et al., 2016) and deposited in the China Center of Industrial Culture Collection (No. CICC24093). The genome sequence of *Bv* was deposited in the GenBank database under accession number CP015443. *Bv* was cultured in LB medium at 37°C and 200 rpm for 12 h (exponential growth phase), and then harvested by centrifugation at 8,000 rpm for 10 min at 4°C, and finally resuspended in distilled water to a final concentration of 1.0×10^8 CFU/mL (Kang et al., 2018). The take-all causative pathogen, *Gaeumannomyces graminis* var. *tritici* strain Ggt-C2 (*Ggt*), was deposited in Agricultural Culture Collection of China (No. ACCC 30310); it was a gift from Prof. Jian Heng (Department of Plant Pathology, Chinese Agricultural University, Beijing, China). The pathogenicity of *Ggt* was evaluated on *T. aestivum* Sumai 188 in our prior study (Kang et al., 2018). The periphery of 10-day-old colonies of *Ggt* on PDA plates at 25°C was used for inoculations.

Root Inoculation and Sampling

Seeds of winter wheat were surface disinfected and germinated, as described by Kang et al. (2018). Germinated wheat seeds were cultured on a sterilized 72-cell seedling tray containing 120 mL of 1/2 MS (Duchefa Biochemie, Haarlem, Netherlands, catalog number M022250) and incubated at 25°C under a 14-h light/10-h dark cycle for 7 days. The roots of 15 7-day-old seedlings were inoculated with 30 mL of *Bv* inoculum (1.0×10^8 CFU/mL). An equal amount of sterile distilled water was used to treat the roots, as a negative control. Five days after inoculation with *Bv*, the seedlings were gently removed from the tray, their roots were rinsed with sterile water, and then they were placed on water agar plates. Half of the seedling roots, whether inoculated with *Bv* or not, were fully covered by the fresh periphery of the 10-day-old colonies of *Ggt* and maintained for 3 days in a plant growth chamber at 25°C, under 50% relative humidity and a 14-h light/10-h dark cycle (light intensity of 200 μmol m^{-2} s^{-1}). At this time, the mycelium had invaded the root cortex of wheat roots, but these lacked obvious symptoms (Kang et al., 2018). Approximately 15 seedling roots were pooled for each biological replicate of the *Ggt* or *Bv*+*Ggt* treatment; they were immediately flash frozen, and stored in liquid nitrogen until later usage, while 0.1 g of the periphery of the 10-day-old *Ggt* colony was remove from PDA plates and maintained in liquid nitrogen as well. Assays were repeated for three independent experiments. Thus, the total number of seedlings used was 45 (three replicates) per treatment or control group.

RNA-Seq and Data Analysis

Total RNA was extracted from *Ggt*- and *Bv*+*Ggt*-infected roots of wheat seedlings using an RNAiso Plus kit (TaKaRa, Otsu, Japan). The same method was used to extract total RNA from *Ggt* (periphery of 10-day-old colony) grown on PDA plates. The purity and integrity of the total RNA were determined using an Agilent 2100 Bioanalyzer RNA chip (Agilent Technologies, Santa Clara, CA, United States). The mRNA was purified from 3 μg of total RNA per sample using oligo(dT) magnetic beads and then cleaved into short fragments using divalent cations under elevated temperature. The short fragments were used for first-strand cDNA synthesis by using random primers and reverse transcriptase (Invitrogen, Carlsbad, CA, United States), followed by a second-strand cDNA synthesis, performed using DNA polymerase I and RNaseH. After the end repair process and ligation of adaptors, these second-strand cDNA products were purified and amplified via polymerase chain reaction (PCR) to create the final cDNA library.

The cDNA libraries were sequenced on an Illumina HiSeq^{TM} 4000 platform by following the default Illumina Stranded RNA protocol (Personalbio, Shanghai, China). Clean reads were obtained by removing adapter sequences, any reads with more than 10% N, along with low-quality sequences (e.g., more than 50% of each read that had a Phred score Q ≤ 5). The Q20, Q30, and GC contents of the cleaned data were calculated (Yang et al., 2015). Each sample resulted in approximately 17 million 150-bp clean reads (sequencing data >2 gigabases per sample) for *Ggt* on PDA plates and 180 million 150-bp clean reads (sequencing data >25 gigabases per sample) for *Ggt*- or *Bv*+*Ggt*-infected root sample. Filtered clean reads were aligned to the reference *Ggt* genome in the genome website[1] using SOAPaligner/SOAP2 (Li et al., 2009). All RNA-Seq data generated for this study were deposited in the National Center for Biotechnology Information Sequence Read Archive under BioProject IDs PRJNA485739 and PRJNA496308. Reads per kilobase per million (RPKM) were used to normalize the levels of gene expression for each replicate. To evaluate the reproducibility of RNA-Seq, a hierarchical cluster analysis (HCA) was done using the command "heatmap3::heatmap3" in the R (v3.5.3) package "gplots" (Warnes et al., 2015) with the hclust command (R Core Team, 2009). The "DESeq" package (1.10.1) of R was used to analyze differentially expressed genes (DEGs) in *Ggt* among the three conditions under the criteria of *P* values < 0.05 and an absolute log2 ratio ≥1 (Anders and Huber, 2012).

Functional Analysis of RNA-Seq Data

Two enrichment analyses of DEGs between samples were performed, topGO, and KEGG (Kyoto Encyclopedia of Genes and Genomes), by respectively, using the AgriGO analytical tools[2] and the KEGG website[3] (Alexa and Rahnenfuhrer, 2010; Yang et al., 2015). GO terms and KEGG pathways were considered significantly enriched by DEGs if the *P* values were < 0.05. All Venn diagrams were produced using Venny Tools[4]. Pathogenesis-related genes were identified through a BLAST search of the pathogen–host interaction (PHI) database (identity >25, *E*-value: 1e-10) (Jing et al., 2017).

The STEM (short time-series expression miner) software[5] (Ernst et al., 2005) was used to identify the significantly enriched expression profiles (*P* values < 0.05) in *Ggt* on PDA plates and in *Ggt*- and *Bv*+*Ggt*-infected wheat roots. The log2-transformed RPKM values of *Ggt* on plates and in *Ggt*-infected roots in the absence or presence of *Bv* were used as the input data set. The software parameters for this STEM analysis were as follows: maximum number of model profiles = 8; maximum unit change in model profiles between treatments = 2; and calculated method of significance level = permutation test corrected by Bonferroni correction.

Validation of RNA-Seq Results via Quantitative Reverse Transcription PCR

The expression levels of six pathogenicity DEGs were determined by using quantitative reverse transcription PCR (qRT-PCR) to confirm the prior results of the RNA-Seq analysis. Total RNA from *Ggt*- and *Bv*+*Ggt*-infected wheat roots was each reverse transcribed into cDNA with the PrimeScript^{TM} 1st Strand cDNA Synthesis kit (Takara, Dalian, China, Code No. 6110A) according to the manufacturer's protocol. The qRT-PCR was carried out by an Applied Biosystems 7500 Real-Time PCR System (Applied Biosystems, Foster City, CA, United States) using a SYBR®Advantage®qPCR premix (Toyobo, Osaka, Japan). Each qRT-PCR was performed with a 20-μL volume containing 2 μL of cDNA, 0.4 μL of each primer (10 μM), 10 μL of 2 × SYBR Green PCR Master Mix, and 7.2 μL of nuclease-free water. The amplification went as follows: 95°C for 30 s, 40 cycles at 95°C for 5 s, and 60°C for 5 s. The qRT-PCR primers used for the DEGs' validation are listed in **Supplementary Table S1**. Three housekeeping genes – encoding actin, tubulin beta, and elongation factor2-1 – served as internal reference for qRT-PCR. Each reaction was performed in triplicate independent experiments for the reference and selected genes. Gene expression was evaluated by applying the $2^{-\Delta\Delta Ct}$ method (Livak and Schmittgen, 2001).

Statistical Analyses

The qRT-PCR amplification data are expressed here as mean ± standard deviation (SD) of at least three independent biological experiments. PRISM software v7.0 (Graph-Pad Software, San Diego, CA, United States) was used to perform one-way analysis of variance (ANOVA) that compared the three conditions. Tukey's multiple pairwise comparison test was applied to the mean relative expression levels of selected pathogenicity genes (first normalized by the three internal reference genes). A *P*-value of less than 0.05 was deemed statistically significant.

[1] http://fungi.ensembl.org/info/website/ftp/index.html

[2] http://systemsbiology.cau.edu.cn/agriGOv2/

[3] https://www.kegg.jp/

[4] http://bioinfogp.cnb.csic.es/tools/venny/index.html

[5] http://www.cs.cmu.edu/~jernst/stem/

RESULTS

General Analyses of RNA-Seq Data

After removing the low-quality reads and adaptors, a total of 67,293,916, 553,791,342, and 553,453,160 clean reads were generated from the mRNA of *Ggt* on PDA and *Ggt* in wheat roots with and without *Bv*, which accounted for 91.6%, 83.2%, and 84.9% of raw reads, respectively (**Supplementary Table S2**). The quality of each library was similar, ranging from 97.02% to 98.63% of the raw reads with quality values of $Q \geq 20$, and likewise from 92.16% to 96.03% of the raw reads with quality values of $Q \geq 30$. Their average GC contents were 59.52%, 56.67%, and 57.77% for *Ggt* on PDA and *Ggt* in wheat roots with and without *Bv*, respectively. Together, these results confirmed the high quality of our sequencing data and their robust suitability for further analysis.

Identification of DEGs

A total of 9,588, 9,389, and 8,826 expressed genes were, respectively detected in *Ggt* on PDA and in wheat roots in the absence and presence of *Bv*, which corresponded to 64.19%, 62.86%, and 59.09% of all genes (14,936) in the *Ggt* genome. We found 8,395 genes expressed in *Ggt* (RPKM > 1) under all three conditions. Based on the respective RPKM values of these 8,395 genes, HCA showed that the three biological replicates from each treatment clustered into an independent branch (**Supplementary Figure S1**), thus indicating RNA-Seq data were reliable, being highly repeatable between biological replicates. When compared with *Ggt* grown on PDA, 4,134 DEGs (2,142 upregulated, 1,992 downregulated) and 2,011 DEGs (957 upregulated, 1,054 downregulated) were identified in *Ggt* in wheat roots in the absence and presence of *Bv*, respectively (**Supplementary Figure S2A**). The total numbers of upregulated and downregulated genes in the *Ggt*-treated samples were, respectively, 2.24- and 1.89-fold higher than those observed in the *Bv*+*Ggt*-treated group. As the Venn diagram shows, 1,251 and 66 upregulated DEGs, as well as 1,000 and 62 downregulated DEGs, were uniquely found in *Ggt* in wheat roots without and with *Bv*, respectively (**Supplementary Figure S2B**). However, overall rates of gene expression were similar between these two treatments (**Supplementary Figure S2C**).

In addition, a total of 31 DEGs were detected between the *Ggt*- and *Bv*+*Ggt*-infected wheat root libraries, with two upregulated genes (GGTG_06400 and GGTG_05929) and 29 downregulated genes in *Bv*+*Ggt*-infected roots relative to *Ggt*-infected roots (**Table 1**). Among the downregulated DEGs in *Bv*+*Ggt*-infected wheat roots, 13 genes (41.94%) were associated with secreted proteins, three genes (9.68%) encoded pathogenicity proteins (para-nitrobenzyl esterase, cutinase 1, and catalase-3), two genes were linked to cell wall lysis enzymes (esterase and cutinase), and one gene encoded peroxidases (catalase-3). In particular, the expression of ABA3 protein-encoding gene involved in the biosynthesis of abscisic acid was downregulated 4.11 times in *Bv*+*Ggt*-infected wheat roots compared with *Ggt*-infected wheat roots; this suggested that *Bv* might inhibit mycelial infection by regulating *Ggt*-derived abscisic acid. All these results indicated that the presence of *Bv* in wheat root directly or indirectly reduced the expression of pathogenicity genes.

HCA of DEGs

The HCA was conducted using those 4,260 DEGs that underwent significant changes in their expression in at least one replicate sample. This analysis revealed clear clustering of *Ggt*-infected wheat roots whether precolonized with *Bv* (*Bv*+*Ggt*) or not (*Ggt*), with the *Ggt* sample on PDA clustered into another branch entirely (**Figure 1**). Based on the expression levels of the DEGs, gene expression patterns were divided into five groups for the three experimental conditions. Clusters A and D contained the bulk of the DEGs. Cluster A and B were enriched in transcripts showing lower expression levels in *Ggt*-infected wheat roots, regardless of precolonization with *Bv*, versus the *Ggt* on PDA. Cluster C and D contained transcripts that were highly upregulated in the *Ggt*-infected wheat roots but whose upregulation was significantly suppressed in the presence of *Bv* or in *Ggt* on PDA. Cluster E contained those DEGs with very lower expression levels for *Ggt* on PDA while representing a higher expression level in the infected wheat roots with or without *Bv*.

Functional Enrichment of DEGs

A total of 4,260 transcripts that showed significant differential expression in at least one sample were used for the STEM analysis, resulting in three significantly enriched expression profiles (**Figure 2**) out of the eight enriched expression profiles (P values <0.05). Profile 1 contained 1,016 transcripts, which were significantly enriched in 10 pathways based on the KEGG database. These pathways were mainly involved in carbohydrate metabolism, such as for starch and sucrose, pentose and glucuronate interconversions, galactose, glycolysis/gluconeogenesis, and inositol phosphate. Compared with *Ggt* on PDA, all of the included DEGs were downregulated in *Ggt* in wheat roots with or without *Bv*. Yet, the expression levels of genes in *Ggt* in the *Bv*+*Ggt*-infected wheat roots were lower than those observed in *Ggt*-infected wheat roots. Profile 2 had 881 genes, enriched in 10 pathways, of which three were related to amino acid metabolism (e.g., taurine and hypotaurine; tryptophan, glycine, serine; and threonine and phenylalanine), while two pathways were involved in DNA replication and pyrimidine metabolism. These genes were downregulated in both the *Ggt*- and the *Bv*+*Ggt*-infected wheat roots relative to *Ggt* on PDA. Profile 6 contained the highest numbers of transcripts (1,706), which were enriched into 12 pathways, including lipid metabolism (e.g., sphingolipid, fatty acid, glycerophospholipid, and fatty acid degradation), tricarboxylic acid cycle, and peroxisome metabolism assigned to primary metabolism. Expression of these genes in *Ggt*-infected wheat roots was much higher than that on PDA plates or in *Bv*+*Ggt*-infected roots; hence, *Bv* might inhibit *Ggt* infection by regulating its primary metabolism.

DEGs for Secreted Proteins

During the process of host infection, fungi generally secrete a suite of proteins and enzymes to evade or counteract plant defense systems and alter the microenvironment of their

TABLE 1 | The expression profile of *Ggt* DEGs that were only affected by *Bv in planta* based on the analysis comparing *Bv+Ggt* and *Ggt* transcriptomic data.

Gene ID	*Ggt*	*Bv+Ggt*	*Bv+Ggt_vs_Ggt*	Protein name	Secreted protein	PHI
GGTG_03282	5.29	2.90	−2.33	Para-nitrobenzyl esterase	Yes	PHI:2032
GGTG_10566	11.38		−4.80	Cutinase 1	Yes	PHI:2383
GGTG_10011			−2.38	Catalase-3	Yes	PHI:1034
GGTG_08754	4.39	1.79	−2.54	Endothiapepsin	Yes	
GGTG_06400		2.97	1.96	Tyrosinase	Yes	
GGTG_12447	3.94		−2.56	Arylsulfatase-like protein	Yes	
GGTG_06631	9.83		−3.93	Cell wall protein	Yes	
GGTG_05929	−2.09		1.42	Hypothetical protein	Yes	
GGTG_13651	10.54	8.25	−2.23	Hypothetical protein	Yes	
GGTG_07328	8.98	6.96	−1.96	Hypothetical protein	Yes	
GGTG_00233	12.22	9.88	−2.28	Diaminopimelate decarboxylase	Yes	
GGTG_08345	10.69	8.20	−2.44	Hypothetical protein	Yes	
GGTG_08028	10.15		−4.05	Cell wall protein	Yes	
GGTG_07717	5.68	3.97	−1.65	Copper-transporting ATPase 1		
GGTG_08722	4.03		−2.50	Sodium/phosphate symporter		
GGTG_07931	3.18	1.65	−1.47	Putative nucleosome assembly protein		
GGTG_12291	2.03		−1.53	2-hydroxyacid dehydrogenase		
GGTG_05152	3.04		−2.48	Arsenical-resistance protein		
GGTG_08620	3.95	2.36	−1.52	L-ornithine 5-monooxygenase		
GGTG_05151	3.94		−2.20	NADPH-dependent FMN reductase ArsH		
GGTG_02030	3.32		−2.13	Aldehyde reductase ii		
GGTG_02188		−1.62	−1.94	Glycosyl Hydrolase-glycosidase superfamily		
GGTG_03806	4.28		−2.32	NAD(P)-binding protein		
GGTG_09078	4.86		−4.59	ubiE/COQ5 methyltransferase		
GGTG_10994	4.11		−2.25	Glycosyl transferase, family 25		
GGTG_11842	10.71	7.84	−2.82	Putative cytochrome P450 monooxygenase		
GGTG_03493	1.95		−2.85	Integral membrane protein		
GGTG_11826	9.68	5.97	−3.66	Cyclohexanone –monooxygenase		
GGTG_11845	7.77		−4.11	Putative ABA3 protein		
GGTG_03814	5.90		−2.92	AhpD-like protein		
GGTG_11844	5.97		−3.62	Putative cytochrome p450 monooxygenase protein/pisatin demethylase protein		

Ggt, the comparison of total Ggt transcriptome on wheat roots compared to Ggt on PDA plate; Bv+Ggt, the comparison of total Ggt transcriptome on wheat roots pretreated by Bv compared to Ggt on PDA plates; Bv+Ggt_vs_Ggt, the comparison of total Ggt transcriptome on wheat roots pretreated by Bv compared to Ggt on wheat roots. "−" represents negative values (downregulation).

host. *Ggt* reportedly harbors 1,001 secreted proteins with structures consisting of signal peptides and cleavage sites, subcellular targeting, transmembrane (TM) spanning regions, and glycosylphosphatidylinositol (GPI) anchor proteins (Xu et al., 2016). When compared to the gene ID of secreted proteins recently predicted by Xu et al. (2016), we identified a total of 458 (372 upregulated, 86 downregulated) and 198 (161 upregulated, 37 downregulated) secreted protein-coding DEGs (**Supplementary Figure S3**) among the 4,260 DEGs (**Supplementary Figure S2A**) in *Ggt*- and *Bv+Ggt*-infected roots, respectively. This clearly suggested that precolonization by *Bv* significantly regulated the expression of genes associated with secreted proteins in *Ggt* in wheat roots.

The STEM analysis revealed that all 469 DEGs encoding secreted proteins clustered significantly into profiles 5 and 6 (P values < 0.05) (**Figure 3**) but not so (P values > 0.05) in the other six profiles (not shown). Profile 5 included 266 genes whose expression was activated in *Ggt*-infected wheat roots but were mostly unaltered in the *Bv+Ggt*-infected roots or in *Ggt* on PDA (**Figure 3**). Profile 6 included 100 genes upregulated in the *Ggt*- and *Bv+Ggt*-infected wheat roots compared with *Ggt* grown on PDA (**Figure 3**). Moreover, the genes of both profiles were largely enriched in categories of catalytic activity, carbohydrate binding, and pattern binding. In profiles 5 and 6, a total of 137 genes (37.43%) participated in catalytic activities primarily related to hydrolases and oxidoreductases (**Supplementary Tables S3**, **S4**). Among these hypothesized hydrolase genes, most of them encode pectase, cellulase, xylanase, keratase, and peptidase, all of which play key roles in cell wall degradation. All the genes encoding oxidoreductase are capable of peroxidase activity with the function of pathogen self-defense against plant immune response. Additionally, the expression of *Ggt* genes encoding papain inhibitors involved in suppressing host protease activity was distinctly suppressed in *Bv+Ggt*-infected wheat roots. Collectively, these results suggested the presence of *Bv* directly and/or indirectly impaired the pathogenicity (e.g.,

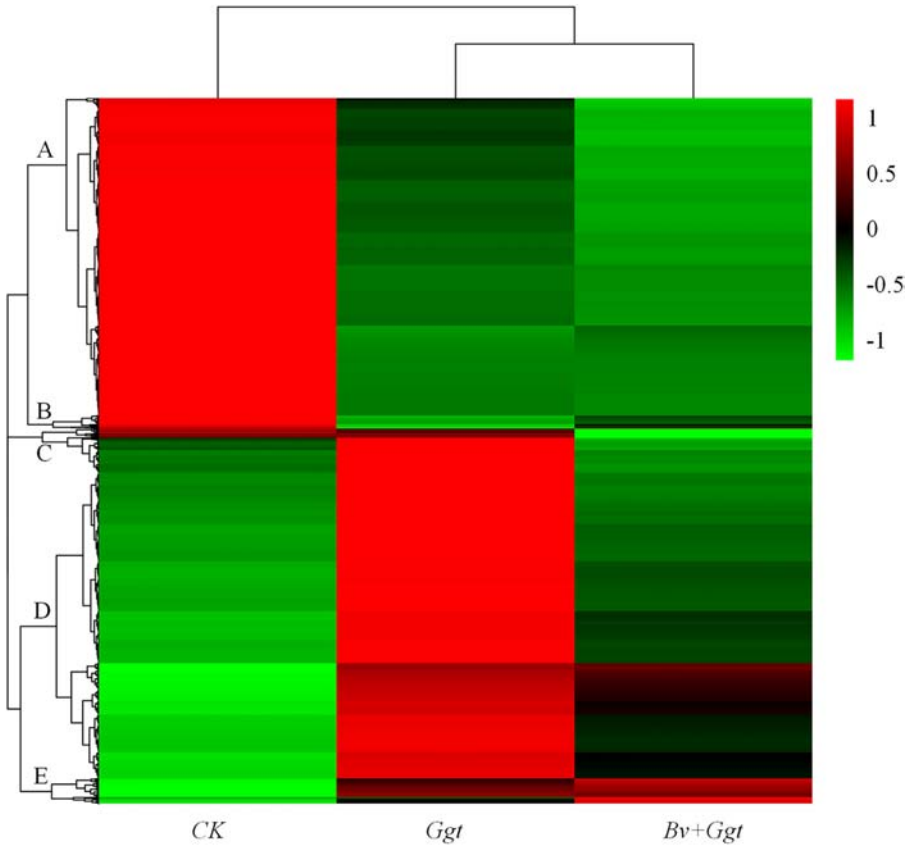

FIGURE 1 | Hierarchical clustering analyses of all DEGs. The analysis was based on three treatments' RPKM value from the transcriptomic data of *CK*, *Ggt*, and *Bv+Ggt* treatments; red indicates high expression of genes, while green indicates low expression of genes. *CK*, the *Ggt* sample on the PDA plates; *Ggt*, the wheat roots infected with pathogen *Ggt*; *Bv+Ggt*, the *Ggt*-infected wheat roots in the presence of *Bv*.

cell wall degradation enzymes, oxidoreductases, and papain inhibitors, among others) of *Ggt* in wheat roots through complex regulatory mechanisms.

DEGs for Fungal Pathogenicity

Based on the BLAST analyses of the PHI database, a total of 151 pathogenicity-related genes were identified in the *Ggt* genome (**Supplementary Table S5**). Of those, 83 genes are recognized as established determinants of pathogenicity in various pathogenic fungi (**Supplementary Table S5**), for which 44 (34 upregulated, 10 downregulated) were significantly expressed in *Ggt*-infected wheat roots in the absence of *Bv*, whereas 17 (11 upregulated, 6 downregulated) were significantly expressed in *Bv+Ggt*-infected wheat roots. The distribution of up- and downregulated *Ggt* pathogenicity DEGs is depicted in the Venn diagram (**Figure 4**). Evidently, 28 pathogenicity genes were uniquely regulated in *Ggt*-infected wheat roots, of which 4 genes – CTB5, Sc Srb10, ACP, and DEP4 – were downregulated during *Ggt* infection (**Supplementary Table S6**). Only one gene coding for appressorial penetration-associated GAS2 was found upregulated (2.69 fold change) in *Bv+Ggt*-infected wheat roots but not in *Ggt*-infected wheat roots. These results suggested that the presence of the biocontrol bacterium *Bv* reduces the pathogenesis of *Ggt* during its infection of wheat roots.

qRT-PCR Validation

The expression of the target genes, normalized by three internal reference genes, was downregulated between *Ggt*- and *Bv+Ggt*-infected wheat roots. Comparing the ratio of qRT-PCR expression and RPKM values for the *Bv+Ggt*-infected to the *Ggt*-infected wheat roots revealed they were mostly consistent, indicating the RNA-Seq data were robust (**Supplementary Table S7**).

DISCUSSION

This study compared the transcriptomes of *Ggt* and *Ggt*-infected wheat root in the absence and presence of the biocontrol bacterium *Bv* using the RNA-Seq platform. A total of 4,134 and 2,011 twofold DEGs were, respectively identified from the *Ggt* in the *Ggt*-infected roots without and with *Bv* relative to *Ggt* grown on PDA plates. Numbers of the upregulated and downregulated DEGs in the *Ggt*-infected roots were, respectively reduced by 55.3% and 47.1% when *Bv* had precolonized wheat

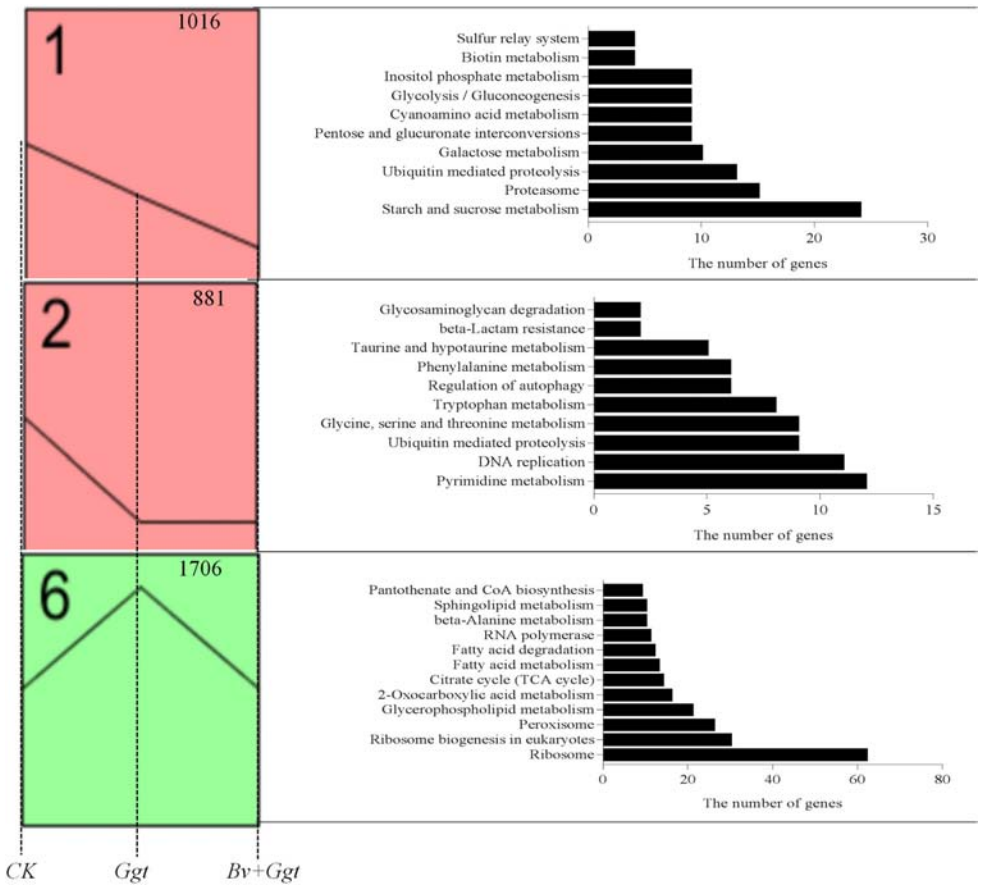

FIGURE 2 | The significant (*P* values < 0.05) expression profiles generated by the analysis of the RPKM value based on the *Ggt* transcriptomic data of *CK*, *Ggt*, and *Bv+Ggt* treatments. The figure at the upper right corner represents the gene number. All significant annotated KEGG pathways for each profile are listed on the right shown by histograms. *CK*, the *Ggt* sample on the PDA plates; *Ggt*, the wheat roots infected with pathogen *Ggt*; *Bv+Ggt*, the *Ggt*-infected wheat roots in the presence of *Bv*.

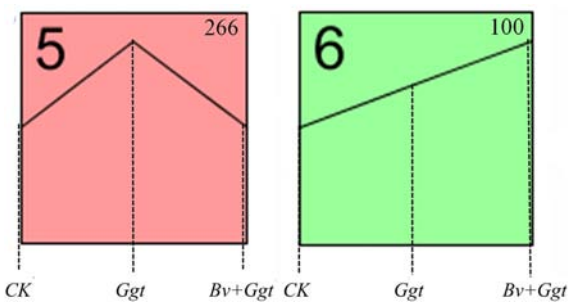

FIGURE 3 | The significant (*P* values < 0.05) expression profiles for identified secreted protein-coding genes. The analysis was based on the RPKM value of the *Ggt* transcriptomic data from *CK*, *Ggt*, and *Bv+Ggt* treatments. *CK*, the *Ggt* sample on the PDA plates; *Ggt*, the wheat roots infected with pathogen *Ggt*; *Bv+Ggt*, the *Ggt*-infected wheat roots in the presence of *Bv*.

roots. Some of these DEGs, whether related to *Ggt* pathogenicity or not, are consistent with those reported by Yang et al. (2015), but many of them were newly identified and, thus, warrant future investigation. However, only 31 DEGs (2 upregulated, 29 downregulated) were detected by directly comparing the *Ggt*- and *Bv+Ggt*-infected wheat root libraries (**Table 1**). These limited numbers of DEGs may truly reflect the direct or indirect (e.g., induced plant resistance) regulation of *Ggt*'s gene expression by endophytic *Bv* in wheat roots. Previous studies have shown that *Bv* can mutually coexist with plants and produce antifungal metabolites such as iturins *in vitro* and *in vivo*, which might have contributed to the changed *Ggt* transcriptome in the infected wheat roots (Gong et al., 2015; Cai et al., 2017; Kang et al., 2018). Moreover, beneficial bacteria impose small impacts upon plant root transcriptomes (Pieterse et al., 2014), and they may impose similarly small impacts upon fungal transcriptomes. This may explain the small number of DEGs observed between *Ggt*- and *Bv+Ggt*-infected wheat roots in this study.

Many secretory proteins have crucial functions in the fungal infection process. For example, CWDEs are the major pathogenicity factors involved in plant cell wall breakdown and are secreted by many pathogens during infection, such as *Fusarium graminearum* (Zhang et al., 2012), *Colletotrichum orbiculare* (Gan et al., 2013), *Colletotrichum gloeosporioides*

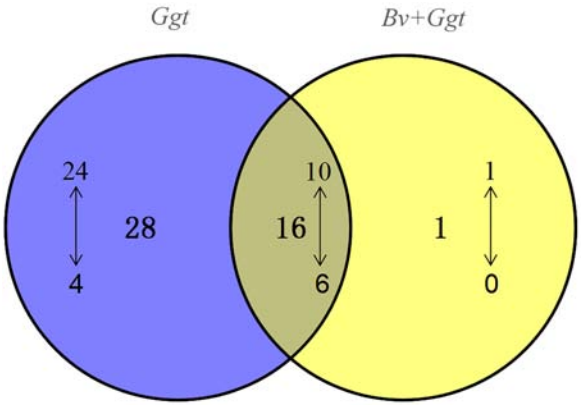

FIGURE 4 | The numbers of DEGs encoding *Ggt* pathogenicity proteins. The Venn diagram illustrates the shared and specific pathogenicity genes generated by the comparative *Ggt* transcriptomic data analysis of *Ggt*-infected wheat roots with or without *Bv* compared to *Ggt* on PDA plates. The upward (or downward)-pointing arrow represents up (or down)-regulated gene expression. *Ggt*, the comparison of total *Ggt* transcriptome on wheat roots compared to *Ggt* on PDA plate; *Bv+Ggt*, the comparison of total *Ggt* transcriptome on wheat roots pretreated by *Bv* compared to *Ggt* on PDA plates.

(Alkan et al., 2015), *Zymoseptoria tritici* (McDonald et al., 2015), *Colletotrichum graminicola* (Torres et al., 2016), *Dothistroma septosporum* (Bradshaw et al., 2016), and *Leptosphaeria maculans* (Gervais et al., 2017). For example, the expression of genes encoding CWDEs (e.g., endo-1,4-b-xylanase, glycoside hydrolase family 61) were highly upregulated in *Magnaporthe oryzae*, a rice fungus closely related to the pathogen *Ggt* (Kawahara et al., 2012). Thus, inhibition of CWDE gene expression is one of the mechanisms by which bacteria exert biocontrol *in vitro* (Mela et al., 2011; Gkarmiri et al., 2015). Our *in vivo* test also demonstrated the biocontrol efficacy of *Bv* against *Ggt* might contribute to the inhibition of gene expression encoding CWDEs, since these genes were significantly upregulated in *Ggt*-infected roots but downregulated in *Bv+Ggt*-infected wheat roots compared to *Ggt* grown on PDA plates (**Figure 3**, **Table 1**, and **Supplementary Tables S3**, **S4**). For instance, the expression of cutinase 1 and xylanase in *Bv+Ggt*-infected roots was at least twofold lower than that in *Ggt*-infected roots.

Papain-like cysteine proteases (PLCPs) are a large class of proteolytic enzymes found in most plant species (Misas-Villamil et al., 2016). According to recent studies, a plant can protect itself from pest or pathogen attacks by producing PLCPs (Misas-Villamil et al., 2016; Liu et al., 2018); however, in the long-term battle waged between pathogens and plants, pathogens will evolve a PLCP inhibitor (e.g., EPIC2B and avirulence protein 2) to counteract host-derived PLCPs (Kruger et al., 2002; Tian et al., 2004, 2005, 2007). In line with this, we found that the expression of PLCP inhibitor-encoding genes was upregulated in *Ggt*-infected wheat roots compared with *Ggt* grown on PDA (**Figure 3** and **Supplementary Table S4**), indicating that one or more PLCP inhibitors may play an important role in the process of *Ggt* infection. In stark contrast, the expression of PLCP inhibitor-encoding genes in *Ggt*-infected wheat roots precolonized by *Bv* was reduced substantially (**Figure 3** and **Supplementary Table S4**). This result strongly suggests that low-level expression of PLCP inhibitor-encoding genes may be one of the biocontrol mechanisms exerted by *Bv* toward the fungal pathogen *Ggt*.

As a member of the peroxidases, catalase could mediate the decomposition of hydrogen peroxide into water and molecular oxygen, so as to protect the pathogens from reactive oxygen species (ROS) produced by both fungi themselves and host plants (Gardiner et al., 2015; Mir et al., 2015). Work by Singh et al. (2012) revealed that in the response of the fungal pathogen *Verticillium longisporum* to *Brassica napus* xylem sap, catalase peroxidase (VlCPEA) was the most upregulated protein, whereas knockdowns of VlCPEA-encoding genes resulted in sensitivity against ROS. In our study, many genes with predicted peroxidase activity (e.g., catalase) were found upregulated (**Figure 3**, **Table 1**, and **Supplementary Table S4**) during the pathogen *Ggt*'s infection of wheat roots, a result that agrees with previous reports (Govrin and Levine, 2000; Singh et al., 2012; Bao et al., 2014). This result suggests that, similar to the mechanism underlying other pathogenic infections, catalase peroxidase might also participate in protecting the fungus *Ggt* from the oxidative stress generated by wheat plants (Singh et al., 2012). Yet, because the expression of genes encoding peroxidase (e.g., catalase) was decreased in *Bv+Ggt*-infected wheat roots (**Figure 3**, **Table 1**, and **Supplementary Table S4**), the presence of biocontrol bacteria *in planta* could have diminished such detoxification activity by reducing peroxidase secretion.

ABA is a crucial molecule for regulating the growth and development of plants, and their stress responses and pathogenicity, and it has been widely studied (Spence et al., 2015). By examining the role of ABA produced by *M. oryzae* in rice leaves, Spence et al. (2015) suggested that it enhances disease severity in two ways, by increasing plant susceptibility and accelerating the pathogenicity of the pathogen itself. For instance, *Pseudomonas syringae* indirectly utilizes ABA as an effector molecule to modulate endogenous host biosynthesis of ABA, thus perturbing the ABA-mediated host defense responses (Lievens et al., 2017). In this current study, we identified a homologous gene (ABA3) encoding an enzyme involved in ABA biosynthesis (Siewers et al., 2006; Fan et al., 2009). The expression of this gene was 7.77-fold higher in *Ggt*-infected wheat roots but was lowered by almost 50% to being 4.11-fold higher in *Bv+Ggt*-infected wheat roots relative to PDA (**Table 1**). This result suggests that ABA, at least, is likely a critical component in plant–pathogen interactions between wheat and *Ggt*, whereas *Bv* might also use this ABA functioning to impair pathogen infection by disturbing *Ggt*-derived ABA synthesis and thus limiting fungal pathogenesis. Targeting these candidate pathogenicity genes/factor through further experimental analysis, such as gene knockouts in *Ggt*, will enable a better understanding of the biocontrol mechanisms of *Bv* that act on the pathogen *Ggt*.

Many plant pathogenic fungi have evolved the capacity to breach intact cuticles of their plant hosts by using an infection

structure called the appressorium (Ryder and Talbot, 2015). Previous studies reported that during infection with a pathogen, the accumulation of glycerol in appressoria/hyphopodia results in highly localized turgor pressure upon the cell wall, and this further assists fungal pathogens to overcome cellular barriers for successful hyphal infection and extension (DeJong et al., 1997). For example, Martin-Urdiroz et al. (2016) have shown that glycerol accumulation of the appressorium in rice blast fungus *Magnaporthe oryzae* drives turgor-mediated penetration of the rice leaf. However, work by Sha et al. (2016) indicated that, *in vitro*, the biocontrol strain *Bacillus subtilis* suppressed the appressorial formation of *Magnaporthe oryzae*. The metabolism of glycerophospholipids, carbohydrate, and peroxisome may have direct or indirect effects on the biosynthesis of glycerol or its precursors' replenishment (**Supplementary Figure S4**). As shown in profile 6, the activation or enhancement of the metabolism of glycerol (**Figure 2**) could be beneficial for *Ggt* to infect wheat roots. Conversely, the metabolism of glycerol was suppressed in *Bv*+*Ggt*-infected wheat roots. Thus, limiting the expression of glycerol synthesis-related genes in *Ggt* may be among the biocontrol strategies that *Bv* employs *in planta*.

Inexplicably, when compared with *Ggt* on PDA, 10 pathogenicity-related genes were downregulated in *Ggt*-infected wheat roots, and likewise six genes in *Bv*+*Ggt*-infected wheat root (**Figure 4**). These genes mainly encode MoAAT (4-aminobuty-rate aminotransferase), Chi2 (endochitinase), avenacinase, Ss-ggt1 (gamma-glutamyl transpeptidase), and SS-odc2 (oxalate decarboxylase). Although we do not know why these pathogenicity-related genes are downregulated in infected wheat roots, plausible reasons include the following: (1) these genes are host dependent and their activation is not essential in the *Ggt*–wheat ecological system; (2) the internal environment of wheat roots is not suitable for the expression of these genes; and (3) these genes are highly expressed in PDA, resulting in relatively low expression in wheat. As to which explanation is most probable and operative, this ought to be tested in the future.

CONCLUSION

This study has provided novel insights into a potential pathogenicity mechanism of *Ggt* in wheat roots, whether strain CC09 is present or absent (relative to the *Ggt* grown on PDA plates) through comparative analysis of their transcriptomes using the Illumina platform. Many novel candidate genes related to *Ggt* pathogenesis were identified, and some potential targets of biocontrol bacteria were discussed. The gene expression data presented in this study suggest that the following mechanisms likely play a role in the biocontrol efficacy of *Bv* against *Ggt* in wheat: (a) decreased amount of fungus-derived CWDEs; (b) repressed genes encoding papain inhibitors, catalase-3, and ABA3; and (c) limited hyphopodia formation that impedes pathogen infection. In addition, our results enhance our knowledge of not only the pathogenicity of *Ggt* at the early infection stage in wheat roots but also the potential mechanism of an endophytic biocontrol bacterium *in planta*. Nonetheless, to what extent *Bv*-induced plant defense fosters the biological control effect of *Bv* upon *Ggt* infection remains to be elucidated.

DATA AVAILABILITY

The datasets generated for this study are available in the National Center for Biotechnology Information, PRJNA 485739 and PRJNA496308.

AUTHOR CONTRIBUTIONS

CL, YX, and XK designed the research study. XK, YG, and SL performed the experiments. XK and CL wrote the manuscript and analyzed the data. CL, XK, SL, YG, LX, and LW assisted in structuring and editing the work. All authors contributed substantially to revisions and approved the final manuscript.

FUNDING

This work was supported by the Natural Science Foundation of China (Grant Nos. 31471810, 41773083, and 31272081), the National Key R&D Project from the Minister of Science and Technology, China (Grant No. 2017YFD0800705), and the Program B for Outstanding Ph.D. Candidate of Nanjing University.

ACKNOWLEDGMENTS

We are grateful to Prof. Jian Heng (Department of Plant Pathology, Chinese Agricultural University, Beijing, China) for providing the fungal pathogen *Gaeumannomyces graminis* var. *tritici*. We thank the two reviewers and Charlesworth Author Services for reviewing the manuscript and improving the quality of the writing, respectively.

SUPPLEMENTARY MATERIAL

The Supplementary Material for this article can be found online at: https://www.frontiersin.org/articles/10.3389/fmicb.2019.01474/full#supplementary-material

FIGURE S1 | Hierarchical clustering of transcripts for each replicate from *Ggt* and *Bv*+*Ggt* treatments. Hierarchical clustering analysis of the transcriptional profiles was performed using the hclust command in R and the default complete linkage method. Each gene's expression was Z-score normalized separately within each of the three data sets. Rows (genes) were clustered hierarchically. Columns (RNA samples) were sorted by sample metadata. The genes with higher (red) or lower (blue) expression are represented. *CK*, the *Ggt* sample on the PDA plates; *Ggt*, the wheat roots infected with pathogen *Ggt*; *Bv*+*Ggt*, the *Ggt*-infected wheat roots in the presence of *Bv*.

FIGURE S2 | The DEG expression profile obtained from the comparison of total *Ggt* transcriptome on wheat roots pretreated by *Bv* or not compared to *Ggt* on the PDA plate. **(A)** The number of *Ggt* DEGs in response to *Ggt*- and

Bv+*Ggt*-infected wheat roots, respectively. **(B)** Venn diagram illustrating the number of *Ggt* DEGs upregulated or downregulated in *Ggt*- and *Bv*+*Ggt*-infected wheat roots. **(C)** The level of *Ggt* gene expression in response to *Ggt*- and *Bv*+*Ggt*-infected wheat roots, respectively. The expression level is shown along the horizontal axis, while values on the vertical axis indicate the gene number. *CK*, the *Ggt* sample on the PDA plates; *Ggt*, the wheat roots infected with pathogen *Ggt*; *Bv*+*Ggt*: the *Ggt*-infected wheat roots in the presence of *Bv*.

FIGURE S3 | The number of DEGs encoding secreted proteins obtained from the comparison of total *Ggt* transcriptome on wheat roots pretreated by *Bv* or not compared to *Ggt* on the PDA plate.

FIGURE S4 | Overview of the glycerol biosynthesis in fungus. The solid lines, dashed lines, circle marks, and frames represent the direct link, indirect links/unknown reaction, chemical compound, and metabolism/enzymes, respectively.

TABLE S1 | The selected DEGs and the sequences of primer pairs used for the qRT-PCR experiment.

TABLE S2 | Summary of the sequence analysis after Illumina sequencing.

TABLE S3 | List of molecular functions for the identified secreted protein-coding genes, based on the data of profile 6 in **Figure 3**.

TABLE S4 | List of molecular functions for identified secreted protein-coding genes, based on the data of profile 5 in **Figure 3**.

TABLE S5 | The pathogenicity-related genes identified in the *Ggt* genome.

TABLE S6 | The expression profile of DEGs assigned to pathogenicity proteins.

TABLE S7 | Relative expression levels of selected pathogenicity-related DEGs in *Ggt*- and *Bv*+*Ggt*-infected wheat roots.

REFERENCES

Alexa, A., and Rahnenfuhrer, J. (2010). *topGO: Enrichment Analysis for Gene Ontology. R Package Version 2.36.0*.

Alkan, N., Friedlander, G., Ment, D., Prusky, D., and Fluhr, R. (2015). Simultaneous transcriptome analysis of *Colletotrichum gloeosporioides* and tomato fruit pathosystem reveals novel fungal pathogenicity and fruit defense strategies. *New Phytol.* 205, 801–815. doi: 10.1111/nph.13087

Anders, S., and Huber, W. (2012). *Differential Expression of RNA-Seq Data at the Gene Level—the DESeq Package*. Heidelberg: EMBL.

Bao, G. H., Bi, Y., Li, Y. C., Kong, Z. H., Hu, L. G., Ge, Y. H., et al. (2014). Overproduction of reactive oxygen species involved in the pathogenicity of *Fusarium* in potato tubers. *Physiol. Mol. Plant Pathol.* 86, 35–42. doi: 10.1016/j.pmpp.2014.014

Bithell, S. L., McKay, A. C., Butler, R. C., and Cromey, M. G. (2016). Consecutive wheat sequences: effects of contrasting growing seasons on concentrations of *Gaeumannomyces graminis* var. tritici DNA in soil and take-all disease across different cropping sequences. *J. Agric. Sci.* 154, 472–486. doi: 10.1017/S002185961500043X

Bradshaw, R. E., Guo, Y., Sim, A. D., Kabir, M. S., Chettri, P., Ozturk, I. K., et al. (2016). Genome-wide gene expression dynamics of the fungal pathogen *Dothistroma septosporum* throughout its infection cycle of the gymnosperm host *Pinus radiata*. *Mol. Plant Pathol.* 17, 210–224. doi: 10.1111/mpp.12273

Cai, X. C., Kang, X. X., Xi, H., Liu, C. H., and Xue, Y. R. (2016). Complete genome sequence of the endophytic biocontrol strain *Bacillus velezensis* CC09. *Genom. Announc.* 4:e01048-16. doi: 10.1128/genomeA.01048-16

Cai, X. C., Liu, C. H., Wang, B. T., and Xue, Y. R. (2017). Genomic and metabolic traits endow *Bacillus velezensis* CC09 with a potential biocontrol agent in control of wheat powdery mildew disease. *Microbiol. Res.* 196, 89–94. doi: 10.1016/j.micres.2016.12007

Daval, S., Lebreton, L., Gazengel, K., Boutin, M., Guillerm-Erckelboudt, A., and Sarniguet, A. (2011). The biocontrol bacterium *Pseudomonas fluorescens* Pf29Arp strain affects the pathogenesis-related gene expression of the take-all fungus *Gaeumannomyces graminis* var. *tritici* on wheat roots. *Mol. Plant Pathol.* 12, 839–854. doi: 10.1111/J.1364-3703.2011715.X

DeJong, J. C., MCCormack, B. J., Smirnoff, N., and Talbot, N. J. (1997). Glycerol generates turgor in rice blast. *Nature* 389, 244–245. doi: 10.1038/38418

Dori, S., Solel, Z., and Barash, I. (1995). Cell wall-degrading enzymes produced by *Gaeumannomyces graminis* var. *tritici in vitro* and *in vivo*. *Physiol. Mol. Plant Pathol.* 46, 189–198. doi: 10.1006/pmpp.1995.1015

Durán, P., Acuña, J. J., Jorquera, M. A., Azcón, R., Paredes, C., Rengel, Z., et al. (2014). Endophytic bacteria from selenium-supplemented wheat plants could be useful for plant-growth promotion, biofortification and *Gaeumannomyces graminis* biocontrol in wheat production. *Biol. Fertil. Soils* 50, 983–990. doi: 10.1007/s00374-014-0920-0

Ernst, J., Nau, G. J., and Bar-Joseph, Z. (2005). Clustering short time series gene expression data. *Bioinformatics* 21, i159–i168. doi: 10.1093/bioinformatics/bti1022

Fan, J., Hill, L., Crooks, C., Doerner, P., and Lamb, C. (2009). Abscisic acid has a key role in modulating diverse plant–pathogen interactions. *Plant Physiol.* 150, 1750–1761. doi: 10.1104/pp.109.137943

Gan, P., Ikeda, K., Irieda, H., Narusaka, M., O'Connell, R. J., Narusaka, Y., et al. (2013). Comparative genomic and transcriptomic analyses reveal the hemibiotrophic stage shift of *Colletotrichum* fungi. *New Phytol.* 197, 1236–1249. doi: 10.1111/nph.12085

Gardiner, M., Thomas, T., and Egan, S. (2015). A glutathione peroxidase (GpoA) plays a role in the pathogenicity of *Nautella italica* strain R11 towards the red alga *Delisea pulchra*. *FEMS Microbiol. Ecol.* 91, 1–5. doi: 10.1093/femsec/fiv021

Gervais, J., Plissonneau, C., Linglin, J., Meyer, M., Labadie, K., Cruaud, C., et al. (2017). Different waves of effector genes with contrasted genomic location are expressed by *Leptosphaeria maculans* during cotyledon and stem colonization of oilseed rape. *Mol. Plant Pathol.* 18, 1113–1126. doi: 10.1111/mpp.12464

Gkarmiri, K., Finlay, R. D., Alstrom, S., Thomas, E., Cubeta, M. A., and Hogberg, N. (2015). Transcriptomic changes in the plant pathogenic fungus *Rhizoctonia solani* AG-3 in response to the antagonistic bacteria *Serratia proteamaculans* and *Serratia plymuthica*. *BMC Genom.* 16:630. doi: 10.1186/s12864-015-1758-z

Gong, A., Li, H., Yuan, Q., Song, X., Yao, W., He, W., et al. (2015). Antagonistic mechanism of iturin A and plipastatin A from *Bacillus amyloliquefaciens* S76-3 from wheat spikes against *Fusarium graminearum*. *PLoS One* 10:e0116871. doi: 10.1371/journal.pone.0116871

Govrin, E. M., and Levine, A. (2000). The hypersensitive response facilitates plant infection by the necrotrophic pathogen *Botrytis cinerea*. *Curr. Biol.* 10, 751–757. doi: 10.1016/S0960-9822(00)00560-1

Jing, L., Guo, D. D., Hu, W. J., and Niu, X. F. (2017). The prediction of a pathogenesis-related secretome of *Puccinia helianthi* through high-throughput transcriptome analysis. *BMC Bioinform.* 18:166. doi: 10.1186/s12859-017-1577-0

Kang, X. X., Zhang, W. L., Cai, X. C., Zhu, T., Xue, Y. R., and Liu, C. H. (2018). *Bacillus velezensis* CC09: a potential 'vaccine' for controlling wheat diseases. *Mol. Plant Microbe Interact.* 31, 623–632. doi: 10.1094/MPMI-09-17-0227-R

Kawahara, Y., Oono, Y., Kanamori, H., Matsumoto, T., and Itoh, T. (2012). Simultaneous RNA-seq analysis of a mixed transcriptome of rice and blast fungus interaction. *PLoS One* 7:e49423. doi: 10.1371/journal.pone.0049423

Kruger, J., Thomas, C. M., Golstein, C., Dixon, M. S., Smoker, M., Tang, S. K., et al. (2002). A tomato cysteine protease required for Cf-2-dependent disease resistance and suppression of autonecrosis. *Science* 296, 744–747. doi: 10.1126/science.1069288

Kwak, Y. S., and Weller, D. M. (2013). Take-all of wheat and natural disease suppression: a review. *Plant Pathol. J.* 29, 125–135. doi: 10.5423/PPJ.SI.07.2012.0112

Lagzian, A., Riseh, R. S., Khodaygan, P., Sedaghati, E., and Dashti, H. (2013). Introduced *Pseudomonas fluorescens* VUPf5 as an important biocontrol agent for controlling *Gaeumannomyces graminis* var. *tritici* the causal agent of take-all disease in wheat. *Arch. Phytopathol. Plant Protoc.* 46, 2104–2116. doi: 10.1080/03235408.2013.785123

Li, R. Q., Yu, C., Li, Y. R., Lam, T. W., Yiu, S. M., Kristiansen, K., et al. (2009). SOAP2: an improved ultrafast tool for short read alignment. *Bioinformatics* 25, 1966–1967. doi: 10.1093/bioinformatics/btp336

Lievens, L., Pollier, J., Goossens, A., Beyaert, R., and Staal, J. (2017). Abscisic acid as pathogen effector and immune regulator. *Front. Plant Sci.* 8:587. doi: 10.3389/fpls.2017587

Liu, B., Huang, L. L., Kang, Z. S., and Buchenauer, H. (2011). Evaluation of endophytic bacterial strains as antagonists of take-all in wheat caused by *Gaeumannomyces graminis* var. *tritici* in greenhouse and field. *J. Pest Sci.* 84, 257–264. doi: 10.1007/s10340-011-0355-4

Liu, B., Qiao, H. P., Huang, L. L., Buchenauer, H., Han, Q. M., Kang, Z. H., et al. (2009). Biological control of take-all in wheat by endophytic *Bacillus subtilis* E1R-j and potential mode of action. *Biol. Control* 49, 277–285. doi: 10.1016/j.biocontrol.2009.027

Liu, H. J., Hu, M. H., Wang, Q., Cheng, L., and Zhang, Z. B. (2018). Role of papain-like cysteine proteases in plant development. *Front. Plant Sci.* 9:1717. doi: 10.3389/fpls.2018.01717

Livak, K. J., and Schmittgen, T. D. (2001). Analysis of relative gene expression data using real-time quantitative PCR and the 2[-delta delta C(T)] method. *Methods* 25, 402–408. doi: 10.1006/meth.2001.1262

Luo, J., Zhang, X., Huang, H., Zhai, F., An, T. C., and An, D. R. (2013). Control effect and mechanism of *Bacillus amyloliquefaciens* Ba-168 on wheat take-all. *Acta Phyto-phylac. Sin.* 40, 475–476. doi: 10.13802/j.cnki.zwbhxb.2013.05.014

Martin-Urdiroz, M., Oses-Ruiz, M., Ryder, L. S., and Talbot, N. J. (2016). Investigating the biology of plant infection by the rice blast fungus *Magnaporthe oryzae*. *Fungal Genet. Biol.* 90, 61–68. doi: 10.1016/j.fgb.2015.12.009

McDonald, M. C., McDonald, B. A., and Solomon, P. S. (2015). Recent advances in the *Zymoseptoria tritici*–wheat interaction: insights from pathogenomics. *Front. Plant Sci.* 6:102. doi: 10.3389/fpls.2015.00102

Mela, F., Fritsche, K., de Boer, W., van Veen, J. A., de Graaff, L. H., van den Berg, M., et al. (2011). Dual transcriptional profiling of a bacterial/fungal confrontation: *Collimonas fungivorans* versus *Aspergillus niger*. *ISME J.* 5, 1494–1504. doi: 10.1038/ismej.2011.29

Mir, A. A., Park, S., Abu Sadat, M., Kim, S., Choi, J., Jeon, J., et al. (2015). Systematic characterization of the peroxidase gene family provides new insights into fungal pathogenicity in *Magnaporthe oryzae*. *Sci. Rep.* 5:11831. doi: 10.1038/srep11831

Misas-Villamil, J. C., van der Hoorn, R. A. L., and Doehlemann, G. (2016). Papain-like cysteine proteases as hubs in plant immunity. *New Phytol.* 212, 902–907. doi: 10.1111/nph.14117

Pieterse, C. M., Zamioudis, C., Berendsen, R. L., Weller, D. M., Van Wees, S. C., and Bakker, P. A. (2014). Induced systemic resistance by beneficial microbes. *Annu. Rev. Phytopathol.* 52, 347–375. doi: 10.1146/annurev-phyto-082712-102340

R Core Team (2009). *R: A Language and Environment for Statistical Computing*. Vienna: R Foundation for Statistical Computing.

Ryder, L. S., and Talbot, N. J. (2015). Regulation of appressorium development in pathogenic fungi. *Curr. Opin. Plant Biol.* 26, 8–13. doi: 10.1016/j.pbi.2015.05.013

Sha, Y. X., Wang, Q., and Li, Y. (2016). Suppression of *Magnaporthe oryzae* and interaction between *Bacillus subtilis* and rice plants in the control of rice blast. *Springerplus* 5:1238. doi: 10.1186/s40064-016-2858-1

Siewers, V., Kokkelink, L., Smedsgaard, J., and Tudzynski, P. (2006). Identification of an abscisic acid gene cluster in the grey mold *Botrytis cinerea*. *Appl. Environ. Microbiol.* 72, 4619–4626. doi: 10.1128/AEM.02919-05

Singh, S., Braus-Stromeyer, S. A., Timpner, C., Valerius, O., Von, T. A., Karlovsky, P., et al. (2012). The plant host *Brassica napus* induces in the pathogen *Verticillium longisporum* the expression of functional catalase peroxidase which is required for the late phase of disease. *Mol. Plant Microbe Interact.* 25, 569–581. doi: 10.1094/MPMI-08-11-0217

Spence, C. A., Lakshmanan, V., Donofrio, N., and Bais, H. P. (2015). Crucial roles of abscisic acid biogenesis in virulence of rice blast fungus *Magnaporthe oryzae*. *Front. Plant Sci.* 6:1082. doi: 10.3389/fpls.2015.01082

Tian, M., Win, J., Song, J., van der Hoorn, R., van der Knaap, E., and Kamoun, S. (2007). A *Phytophthora infestans* cystatin-like protein targets a novel tomato papain-like apoplastic protease. *Plant Physiol.* 143, 364–377. doi: 10.1104/pp.106.090050

Tian, M. Y., Benedetti, B., and Kamoun, S. (2005). A second Kazal-like protease inhibitor from *Phytophthora infestans* inhibits and interacts with the apoplastic pathogenesis-related protease P69B of tomato. *Plant Physiol.* 138, 1785–1793. doi: 10.1104/pp.105.061226

Tian, M. Y., Huitema, E., Da Cunha, L., Torto-Alalibo, T., and Kamoun, S. (2004). A Kazal-like extracellular serine protease inhibitor from *Phytophthora infestans* targets the tomato pathogenesis-related protease P69B. *J. Biol. Chem.* 279, 26370–26377. doi: 10.1074/jbc.M400941200

Torres, M. F., Ghaffari, N., Buiate, E. A. S., Moore, N., Schwartz, S., Johnson, C. D., et al. (2016). A *Colletotrichum graminicola* mutant deficient in the establishment of biotrophy reveals early transcriptional events in the maize anthracnose disease interaction. *BMC Genom.* 17:202. doi: 10.1186/s12864-016-2546-0

Warnes, G. R., Bolker, B., Bonebakker, L., Gentleman, R., Huber, W., Liaw, A., et al. (2015). *Gplots: Various R Programming Tools for Plotting Data. R Package Version* 3.0.1. Available at: https://cran.r-project.org/web/packages/gplots/index.html (accessed January 27, 2019).

Wu, X. B., Sun, R. K., Wu, Y. X., Wang, Z. Y., Wu, X. X., Mao, Z. C., et al. (2012). Screening and identification of biocontrol *Bacillus* strains against take-all of wheat. *Acta Agric. Jiangxi* 24, 53–55. doi: 10.3969/j.issn.1001-8581.2012.11.017

Xu, X. H., He, Q., Chen, C., and Zhang, C. L. (2016). Differential communications between fungi and host plants revealed by secretome analysis of phylogenetically related endophytic and pathogenic fungi. *PLoS One* 11:e0163368. doi: 10.1371/journal.pone.0163368

Yang, L., Han, X., Zhang, F., Goodwin, P. H., Yang, Y., Li, J., et al. (2018). Screening Bacillus species as biological control agents of *Gaeumannomyces graminis* var. *tritici* on wheat. *Biol. Control* 118, 1–9. doi: 10.1016/j.biocontrol.2017.11.004

Yang, L. R., Huang, Y., Liang, S., Xue, B. G., and Quan, X. (2012). "Screening wheat take-all disease mutant by *Agrobacterium*-mediated genetic transformation," in *Proceedings of the Annual Meeting of Chinese Society for Plant Pathology*, ed. Z. J. Guo (Beijing: China Agriculture Press), 555.

Yang, L. R., Xie, L. H., Xue, B. G., Goodwin, P. H., Quan, X., Zheng, C. L., et al. (2015). Comparative transcriptome profiling of the early infection of wheat roots by *Gaeumannomyces graminis* var. *tritici*. *PLoS One* 10:e0120691. doi: 10.1371/journal.pone.0120691

Yang, M., Wen, S., Mavrodi, D. V., Mavrodi, O. V., von Wettstein, D., Thomashow, L. S., et al. (2014). Biological control of wheat root diseases by the CLP-producing strain *Pseudomonas fluorescens* HC1-07. *Phytopathology* 104, 248–256. doi: 10.1094/PHYTO-05-13-0142-R

Yang, M. M., Mavrodi, D. V., Mavrodi, O. V., Thomashow, L. S., and Weller, D. M. (2017). Construction of a recombinant strain of *Pseudomonas fluorescens* producing both phenazine-1-carboxylic acid and cyclic lipopeptide for the biocontrol of take-all disease of wheat. *Eur. J. Plant Pathol.* 149, 683–694. doi: 10.1007/s10658-017-1217-6

Yu, Y. T., Kang, Z. S., Han, Q. M., Buchenauer, H., and Huang, L. L. (2010). Immunolocalization of 1, 3-β-glucanases secreted by *Gaeumannomyces graminis* var. *tritici* in infected wheat roots. *J. Phytopathol.* 158, 344–350. doi: 10.1111/j.1439-0434.2009.01614.x

Zhang, X. W., Jia, L. J., Zhang, Y., Jiang, G., Li, X., Zhang, D., et al. (2012). In planta stage-specific fungal gene profiling elucidates the molecular strategies of *Fusarium graminearum* growing inside wheat coleoptiles. *Plant Cell* 24, 5159–5176. doi: 10.1105/tpc.112.105957

Conflict of Interest Statement: The authors declare that the research was conducted in the absence of any commercial or financial relationships that could be construed as a potential conflict of interest.

frontiers in Microbiology

ORIGINAL RESEARCH
published: 11 October 2019
doi: 10.3389/fmicb.2019.02328

Gymnemic Acids Inhibit Adhesive Nanofibrillar Mediated *Streptococcus gordonii–Candida albicans* Mono-Species and Dual-Species Biofilms

*Raja Veerapandian and Govindsamy Vediyappan**

Division of Biology, Kansas State University, Manhattan, KS, United States

OPEN ACCESS

Edited by:
Giovanna Batoni,
University of Pisa, Italy

Reviewed by:
Marlise Inez Klein,
Universidade Estadual Paulista (UNESP), Brazil
Jintae Lee,
Yeungnam University, South Korea
Shunmugiah Karutha Pandian,
Alagappa University, India

***Correspondence:**
Govindsamy Vediyappan
gvediyap@ksu.edu

Specialty section:
This article was submitted to Infectious Diseases, a section of the journal Frontiers in Microbiology

Received: *13 June 2019*
Accepted: *24 September 2019*
Published: *11 October 2019*

Citation:
Veerapandian R and Vediyappan G (2019) Gymnemic Acids Inhibit Adhesive Nanofibrillar Mediated Streptococcus gordonii–Candida albicans Mono-Species and Dual-Species Biofilms. Front. Microbiol. 10:2328. doi: 10.3389/fmicb.2019.02328

Dental caries and periodontitis are the most common oral disease of all age groups, affecting billions of people worldwide. These oral diseases are mostly associated with microbial biofilms in the oral cavity. *Streptococcus gordonii*, an early tooth colonizing bacterium and *Candida albicans*, an opportunistic pathogenic fungus, are the two abundant oral microbes that form mixed biofilms with augmented virulence, affecting oral health negatively. Understanding the molecular mechanisms of the pathogen interactions and identifying non-toxic compounds that block the growth of biofilms are important steps in the development of effective therapeutic approaches. In this *in vitro* study we report the inhibition of mono-species or dual-species biofilms of *S. gordonii* and *C. albicans*, and decreased levels of biofilm extracellular DNA (eDNA), when biofilms were grown in the presence of gymnemic acids (GAs), a non-toxic small molecule inhibitor of fungal hyphae. Scanning electron microscopic images of biofilms on saliva-coated hydroxyapatite (sHA) surfaces revealed attachment of *S. gordonii* cells to *C. albicans* hyphae and to sHA surfaces via nanofibrils only in the untreated control, but not in the GAs-treated biofilms. Interestingly, *C. albicans* produced fibrillar adhesive structures from hyphae when grown with *S. gordonii* as a mixed biofilm; addition of GAs abrogated the nanofibrils and reduced the growth of both hyphae and the biofilm. To our knowledge, this is the first report that *C. albicans* produces adhesive fibrils from hyphae in response to *S. gordonii* mixed biofilm growth. Semi-quantitative PCR of selected genes related to biofilms from both microbes showed differential expression in control vs. treated biofilms. Further, GAs inhibited the activity of recombinant *S. gordonii* glyceraldehyde-3-phosphate dehydrogenase (GAPDH). Taken together, our results suggest that *S. gordonii* stimulates the expression of adhesive materials in *C. albicans* by direct interaction and/or signaling, and the adhesive material expression can be inhibited by GAs.

Keywords: bacteria–fungi interactions, *Candida albicans*, *Streptococcus gordonii*, nanofibrils, gymnemic acid, biofilm inhibition, GAPDH, mixed oral biofilms

INTRODUCTION

Dental caries is a polymicrobial biofilm-induced disease affecting 3.5 billion people globally (Kassebaum et al., 2017). The worldwide annual total costs due to dental diseases are estimated to be around $545 billion in 2015 (Righolt et al., 2018). New therapeutic approaches are required to manage these biofilm-associated oral diseases. We need an efficient antimicrobial agent which inhibits biofilm formation, while not exerting selective pressure on the oral microbiome. *Candida albicans* is a fungus that is the etiologic agent of oral thrush and denture stomatitis, two mucosal oral biofilm infections that particularly affect immunocompromised patients and elderly people, respectively (Odds, 1987). *C. albicans* and *Streptococcus* bacterial species are abundant in the oral cavity and readily form mixed biofilms which are resistant to antimicrobials and serve as a source for systemic infections (Dongari-Bagtzoglou et al., 2009; Silverman et al., 2010; Diaz et al., 2012; Ricker et al., 2014; O'Donnell et al., 2015). Some of the streptococci (e.g., *Streptococcus mutans*) are the causative agents of dental caries and gum disease. Recent studies have shown that a complex interaction and aggregation occurs between streptococci and *C. albicans*, and the molecular mechanisms are poorly understood (Dutton et al., 2014; Hwang et al., 2017).

Candida albicans is a commensal and an opportunistic human fungal pathogen found in cutaneous, oral, intestinal, and genital regions, and can initiate various forms of Candidiasis. Various groups of oral bacteria are shown to interact with *C. albicans* and influence the disease severity (Dongari-Bagtzoglou et al., 2009; Harriott and Noverr, 2011). Oral streptococcal species, including *Streptococcus gordonii, Streptococcus oralis*, and *S. mutans,* interact with *C. albicans* and augment both fungal and bacterial virulence (Silverman et al., 2010; Ricker et al., 2014; O'Donnell et al., 2015; Hwang et al., 2017). Other bacteria, including *Staphylococcus aureus* (Harriott and Noverr, 2009) and *Acinetobacter baumannii* (Uppuluri et al., 2018), use *C. albicans* hyphae as a substratum for attachment, and form robust biofilms.

Candida albicans exists in yeast, pseudohyphae, and hyphal growth forms. The transition from yeast or pseudohyphae to hyphae is required for its tissue invasion and biofilm formation. Mutants that are defective in hyphal growth are avirulent and unable to form biofilms (Lo et al., 1997; Nobile and Mitchell, 2006). Hence, *C. albicans* hyphae play a pivotal role in biofilm growth and virulence. Some of the oral bacteria, including *S. gordonii* are shown to promote the hyphal growths of *C. albicans* and bind preferably to these hyphal surfaces (Bamford et al., 2009). This hyphal binding increases biofilm mass, and chemical inhibition of candida hyphae reduces biofilm mass (Bamford et al., 2009). Several bacterial pathogens exploit *C. albicans* hyphae for their attachments (Silverman et al., 2010; Diaz et al., 2012; Dutton et al., 2014; Xu et al., 2014b; O'Donnell et al., 2015). A recent study has shown that yeast cells of *Candida glabrata* bind to *C. albicans* hyphae and form fungal-fungal biofilms in the oral milieu (Tati et al., 2016). Microbial biofilms are highly resistant to antimicrobial agents, sequestering them and causing tissue inflammation (Nett et al., 2010; Vediyappan et al., 2010; Xu et al., 2014b). It is plausible that inhibiting *C. albicans* hyphal growth with non-toxic small molecules could abrogate the hyphae-related virulence, including *C. albicans* interaction with bacteria and the growth of polymicrobial biofilms.

Gymnemic acids (GAs), a family of triterpenoid molecules from the medicinal plant *Gymnema sylvestre*, were shown to block *C. albicans* yeast-to-hypha transition and hyphal growth *in vitro* and in a worm (*Caenorhabditis elegans*) model of invasive candidiasis (Vediyappan et al., 2013). GAs contain various pharmacological properties, including antagonistic activity against the β-isoform of Liver-X-Receptor (LXR) which could result in decreased lipid accumulation in liver cells (Renga et al., 2015), suppressing sweet taste sensation by binding to taste receptors, T1R2, and T1R3 (Sanematsu et al., 2014), and blocking the uptake of glucose in the intestinal cells (Wang et al., 2014). The GA-rich gymnema extract has been used in humans to treat diabetes and obesity (Baskaran et al., 1990; Porchezhian and Dobriyal, 2003; Leach, 2007). A recent clinical study confirmed the traditional use of *G. sylvestre* for diabetes (Zuniga et al., 2017). Since *S. gordonii* and other oral bacteria use *C. albicans* hyphae for their attachment (Bamford et al., 2009) and GAs block the hyphal growth of *C. albicans*, we wanted to test the hypothesis that prevention of *C. albicans* hyphal growth using GAs could abolish bacteria – *C. albicans* interactions and the formation of mixed biofilms. In the current study, we show a synergistic interaction between *S. gordonii* and *C. albicans in vitro,* and the addition of gymnemic acids (GAs) prevented the growth of mono-species or dual-species biofilms. Our results show, for the first time to our knowledge, formation of "nanofibrillar" structures from *C. albicans* hyphae in response to *S. gordonii* co-culture, which correlates with their enhanced interaction and biofilms growth. Treating mono-species or dual-species biofilms with GAs abolished these structures and reduced biofilm growth.

MATERIALS AND METHODS

Strains, Culture Conditions, and Compounds

Streptococcus gordonii ATCC 10558 (generously provided by Dr. Indranil Biswas, Kansas University Medical Center, Kansas City, KS) and *C. albicans* SC5314 (genome sequenced) were used to generate mono-species or dual-species biofilms in 24-well microtiter plates (TPP, Cell culture treated) under static condition. *Escherichia coli* 10-Beta (NEB) and BL21(DE3) (Novagen, Madison, WI, United States) were used for cloning and expression of recombinant protein, and were routinely grown in Luria-Bertani (LB) broth or on LB agar. GAs were purified from *G. sylvestre* plant leaf extract, obtained from Suan Forma Inc., NJ, United States, according to the published protocols (Vediyappan et al., 2013; Sanematsu et al., 2014) and a mixture of GAs was used in this study. The GA mixture contains at least five species (GA-III, GA-IV, GA-XIII, GA-XIV, and GA-I) and therefore, the term GAs was used throughout in the text. All five GA species that we used have similar bioactivities of yeast-to-hypha inhibition (Vediyappan et al., 2013; Sanematsu et al., 2014).

We have isolated GA-I recently and it was included in the GA mixture. There are 18 different species of GA that have been reported (Liu et al., 1992; Porchezhian and Dobriyal, 2003; Di Fabio et al., 2013). The GA mixture (50 mg/ml) was solubilized as a stock solution in TYES growth medium, filter sterilized (0.4 μm syringe filter), and diluted in the growth medium as required.

Determination of Minimum Biofilm Inhibition Concentrations (MBICs) and Growth Kinetics

Streptococcus gordonii and *C. albicans* co-exist in the oral cavity as abundant microbes, and the former is known to attach to the hyphal surfaces of the latter, forming a mixed-species biofilm with enhanced virulence. Preventing the growth of these biofilms by non-toxic small molecules would limit oral diseases and their systemic dissemination. Since GAs are known to inhibit *C. albicans* hyphal growth, we wanted to know if GAs can inhibit *S. gordonii* and *C. albicans* biofilms. First, we wanted to determine the MBIC of GAs against these microbial biofilms. The MBIC is the lowest concentration of GAs that inhibit maximum amount of biofilm growth. MBIC was determined in 24-well plates as previously described (Saputo et al., 2018), with slight modifications using TYES broth medium (1% tryptone and 0.5% yeast extract at pH 7.0 with 1% (wt/vol) sucrose). Briefly, suspensions of *S. gordonii* ($\sim 2 \times 10^6$ CFU/ml) or *C. albicans* yeast cells (2×10^4 CFU/ml), according to Kim et al. (2017), were added into 24-well plates containing serially diluted GAs at concentrations ranging from 0 to 600 μg/mL. The plates were incubated at 37°C with 5% CO_2 for 18 h statically. Medium alone and medium with GAs were also included in parallel as blanks to rule out that the observed readings were not due to precipitation of GAs or non-specific absorbance. After washing off unbound cells and medium with PBS, the adhered biofilms were stained with crystal violet (0.1%, CV solubilized in water) solution (Merritt et al., 2005). After removing the unbound CV, the wells were washed (at least two times) with PBS and dried to remove residual buffer. Biofilm attached CV stains were solubilized in 95% ethanol, and the absorbance was measured at 595 nm with a Victor 3 multimode reader (Perkin Elmer, United States). Experiments were repeated at least three times, each with triplicates, and representative results are shown.

To determine the effect of GAs on the growth rates of *S. gordonii* and *C. albicans*, we used a Bioscreen-C real time growth monitoring system (Oy Growth Curves Ab Ltd., Finland). In this method, 200 μl of growth medium containing exponentially growing *S. gordonii* or *C. albicans* yeast cells (each at A_{600} = 0.1) were added into the honeycomb wells (triplicate) with GAs (400, 500, and 600 μg/mL in 200 μl total volume) or without GAs (control), and their growth rates were measured for 24 h. The plates were incubated at 37°C without shaking except for 10-s of shaking before reading absorbance at 600 nm at 30-min intervals. The overall objective of the kinetic growth readings of *S. gordonii* and *C. albicans* in the presence or absence of GAs was to determine if GAs exert any toxic effect on the microbes.

Unstimulated Whole Saliva Preparation

Human saliva collection and processing were done as described previously (Jack et al., 2015). Briefly, unstimulated whole human saliva was collected from six healthy volunteers with Institutional Review Board (IRB) protocol approval (#9130.1) from Kansas State University. All the subjects gave written informed consent approved by the IRB committee. Saliva was pooled and mixed with 2.5 mM dithiothreitol and kept in ice for 10 min before clarification by centrifugation (10,000 × *g* for 10 min). The supernatant was diluted to 10% in distilled water and filter sterilized through a 0.22-μm nitrocellulose filter and stored at −80°C in aliquots. Diluted saliva was used to coat the microtiter wells and hydroxyapatite (HA) disks (Clarkson Chromatography Products, PA, United States) overnight.

Mono-Species and Dual-Species Biofilm Assay

To test the effect of GAs on biofilm formation in saliva-coated wells and on hydroxyapatite (sHA) disks, *S. gordonii* and *C. albicans* were grown alone or in combination in TYES medium with or without GAs (500 μg/ml) statically for 18 h at 37°C and in 5% CO_2, as reported with some minor modifications (Dutton et al., 2014; Ricker et al., 2014). Two types of biofilm models were used. (i) Biofilms grown on saliva-coated hydroxyapatite (sHA) disks that were used for Scanning Electron Microscopic (SEM) analysis, and (ii) biofilms grown on the bottom of the saliva coated polystyrene microplates (24-wells, TPP cell culture treated). The biofilms developed on the microplate surfaces were used for CV staining, RNA, and for eDNA isolations. Briefly, sHA disks were placed in a 24-well plate and inoculated with approximately 2×10^6 (CFU/ml) of *S. gordonii* or/and 2×10^4 (CFU/ml) of *C. albicans* according to Kim et al. (2017) in the TYES medium with or without GAs. The effect of GAs against biofilm formation in the microtiter wells was determined using CV staining (Merritt et al., 2005), as described above (MBIC section). Experiments were repeated at least three times each with triplicates, and representative results are shown.

Measurement of Biofilm Extracellular DNA (eDNA)

Extracellular DNA was measured as described by Jack et al. (2015). Briefly, biofilms were scraped from saliva-coated wells into 0.5 mL TE buffer (10 mM Tris–HCl, pH 7.5, 1 mM EDTA), sonicated for 15 s at low speed (20 pulse, Branson Ultrasonic 250), and the cell-free DNA was collected by centrifugation at 10,000 × *g* for 5 min. The DNA concentration was then analyzed from the supernatant using a NanoDrop 2000 spectrophotometer (Thermo Scientific, United States).

Scanning Electron Microscopy (SEM)

Scanning Electron Microscopy was done as per the standard protocol described previously (Erlandsen et al., 2004). Briefly, sHA disks with biofilms on their surfaces were fixed with 2% paraformaldehyde and 2% glutaraldehyde in 0.15 M sodium cacodylate buffer, pH 7.4, containing 0.15% Alcian blue. Biofilms grown on sHA disks were washed with 0.15 M cacodylate buffer

and dehydrated in a graded series of ethanol concentrations. Specimens were mounted on adhesive carbon films and then coated with 1 nm of platinum using an Ion Tech argon ion beam coater. Prepared samples were observed in a SEM (Field Emission Scanning Electron Microscope, Versa 3D Dual Beam, Nikon).

RNA Isolation, cDNA Synthesis, and Semi-Quantitative RT–PCR

Biofilms grown in 24-well microtiter plates were treated with RNAprotect bacteria reagent (Qiagen, Valencia, CA, United States) for 5 min to stabilize RNA, and stored at −80°C. Total RNA was isolated from the biofilms using the TRIzol reagent (Invitrogen, Carlsbad, CA, United States) as per manufacturer instructions. The concentration of RNA was determined by measuring the A_{260} in a NanoDrop 2000 spectrophotometer (Thermo Scientific, United States). Total RNA (1 μg) was reverse transcribed into cDNA using the SuperScript III indirect cDNA labeling kit (Invitrogen), as per the manufacturer's instructions with slight modifications. The semi-quantitative RT-PCR using 2X PCR Master Mix (Promega Corporation, Madison, WI, United States) and primers was carried out in a 20 μL reaction volume (1 μL cDNA, 10 μL Master Mix, 0.5 μM of each primer). Primers were designed using PrimerQuest® (Integrated DNA Technologies), and the details are given in **Tables 1**, **2**. The internal control was *16S rRNA* for *S. gordonii* and *TDH3* for *C. albicans*. The cycling conditions consisted of initial denaturation at 94°C for 3 min followed by denaturation at 94°C for 30 s, annealing at 50 or 58°C for 30 s, and extension at 72°C for 45 s, then final extension at 72°C for 7 min. Twenty microliters of each PCR product was electrophoresed on an agarose gel (1.2% w/v) containing ethidium bromide (0.5 μg/ml). Images of the amplified products were acquired with an Alpha Imager; the intensity was quantified using the Image J software (NIH, United States). The band intensity was expressed as mRNA fold expression [specific gene expression/internal control gene (*16S rRNA* or *TDH3*)]. The intensity of each DNA band in the control cells was determined, taken as 1, and compared with the respective treated group (Sivaprakasam et al., 2016).

Cloning, Expression, and Purification of rGAPDH

Glyceraldehyde-3-phosphate dehydrogenase is reported to be present in various streptococcal cell surfaces which mediates cell adhesion and plays an important role in bacterial infection and invasion (Brassard et al., 2004; Jin et al., 2011; Wang et al., 2012). For example, *S. gordonii* cell surface GAPDH binds to the FimA protein of Porphyromonas *gingivalis* and forms a mixed biofilm (Maeda et al., 2004a,b). GAPDH has multiple functions in various organisms (Sirover, 2017). Further, our semi-quantitative RT-PCR results showed reduced transcripts of *gapdh* in both mono-species and mixed-species biofilms, and hence we pursued to analyze the role of this protein. GAPDH gene from *S. gordonii* was PCR amplified using primers GAPDH-F (5′-ATTCCATATGGTAGTTAAAGTTGGTATTAACGGT-3′) and GAPDH-R (5′-GCGCTCGAGTTTAGCGATTTTCGCGAAGTATTCAAG-3′), where the underlined sequences in the forward and in reverse primers indicate *Nde*I and *Xho*I restriction sites, respectively. Following PCR amplification of chromosomal DNA from *S. gordonii* strain ATCC 10558, amplicons of 1008 bp were digested with *Nde*I and *Xho*I and inserted into the predigested pET28b plasmid (Novagen, Madison, WI, United States). Successful cloning of the gene was confirmed by restriction endonuclease and DNA sequence analyses (**Supplementary Figures S1**, **S2**). Recombinant plasmid was transformed into *E. coli* BL21 (DE3) for overexpression. Expression of GAPDH-6His protein was induced with 1 mM isopropyl-β-d-thiogalactopyranoside (IPTG) when cultures reached an optical density at 600 nm (OD600) of 0.6, and cells were harvested after 4 h. The cell pellet from 2 L of culture was resuspended in 40 ml of a buffer containing 50 mM NaH_2PO_4 pH 8.0, 300 mM NaCl, 20 mM imidazole with 1× protease inhibitor cocktail (Roche) and 1 mM phenylmethylsulfonyl fluoride (PMSF), and cells were lysed by French press (∼19,000 psi). The lysate was centrifuged at 10,000 × *g* for 20 min at 4°C.

TABLE 1 | List of *S. gordonii* specific primers used for semi-quantitative RT-PCR.

Gene name	Description	Direction	Sequence (5′-3′)	Product Size (bp)
*csh*A	Cell surface hydrophobicity	Forward	GACAAGCAGTTCGTTGGTAAAC	264
		Reverse	GGTTCCTTGACCTGGAATAGAC	
ldh	Lactate dehydrogenase	Forward	CGTTCAGTTCACGCCTACAT	328
		Reverse	CAGCTGGTTGACCGATAAAGA	
gapdh	Glyceraldehyde-3-phosphate dehydrogenase	Forward	CTCGCATCAACGACCTTACA	557
		Reverse	AGCAGCACCAGTTGAGTTAG	
gftG1	Glucosyltransferase G	Forward	CCATCCCTTGAGTACGAGTTTC	564
		Reverse	GTGGAGTAGAGCCAACGATTAC	
scaA	Metal ABC transporter substrate-binding lipoprotein	Forward	GGGAATATC TTGGCGGTACAA	288
		Reverse	GGTCTTGAGACTCTTGGCATAG	
scaR	Iron-dependent transcriptional regulator	Forward	TAGTCCACCATCTGGGCTATAC	281
		Reverse	GCCAACTTGAAGGCCATTTC	
16S rRNA	16S ribosomal RNA	Forward	CCATAGACTGTGAGTTGCGAAC	427
		Reverse	CCGTCCCTTTCTGGTAAGATAC	

TABLE 2 | List of *C. albicans* primers used for semi-quantitative RT-PCR.

Genename	Description	Direction	Sequence (5′-3′)	Product Size (bp)
CSH1	Cell surface hydrophobicity	Forward	GCTGTCGGTACTATGAGATTGG	245
		Reverse	CTGTCTTCTGCGTCGTCTTT	
ZRT1	Zinc-regulated transporter	Forward	ATGCCCGTGATACTGGAAAG	312
		Reverse	GGGTGATCAATGCAAACATGAG	
NRG1	Transcription factor/co-repressor	Forward	ACTACAACAACCTCAGCCATAC	254
		Reverse	CAAGGGAGTTGGCCAGTAAA	
PRA1	pH-regulated antigen	Forward	CGCTGACACTTATGAGGAAGTC	258
		Reverse	CTAGGGTTGCTATCGGTATGTTG	
TDH3	Glyceraldehyde-3-phosphate dehydrogenase	Forward	GTCGCCGTCAACGATCC	455
		Reverse	GTGATGGAGTGGACAGTGGTC	

Recombinant His-tagged GAPDH was purified using Ni-NTA Agarose (Qiagen, Valencia, United States) in native conditions according to the manufacturer's recommendations. GAPDH was eluted using gradients of increasing imidazole concentration (100–300 mM). Fractions containing rGAPDH were pooled and dialyzed against distilled water and used for subsequent analysis.

SDS-PAGE and Immunoblotting

The purity of the proteins was checked using SDS-PAGE electrophoresis in a vertical electrophoretic mini-cell unit (Bio-Rad, Hercules, CA), in Tris-glycine running buffer (25 mM Tris, 192 mM glycine, 0.1% SDS [pH 8.3]), for 1 h at 120 V. Proteins were transferred to an Immobilon-P PVDF membrane (pore size, 0.45 μm; Millipore Sigma, United States) and blocked with 5% non-fat dry milk in Tris-buffered saline (20 mM Tris, 150 mM NaCl, 0.2% Tween 20 [pH 7.5]). Membranes were incubated with anti-*Sg*GAPDH immune sera raised in rabbits, followed by incubation with secondary antibody (anti-rabbit IgG; Cell Signaling Technology, United States). Reacted protein bands were visualized by using Pierce^{TM} ECL 2 Western Blotting Substrate (Thermo Scientific, United States) and imaging.

Determination of GAPDH Activity

Glyceraldehyde-3-phosphate dehydrogenase activity was measured in the presence and absence of GAs using Glyceraldehyde 3 Phosphate Dehydrogenase Activity Colorimetric Assay Kit (ab204732, Abcam, Cambridge, MA, United States) as per the manufacturer's instructions. Briefly, purified rGAPDH protein (0.1 μM) was mixed with and without GAs (100 and 200 μM), followed by the addition of reaction mix supplied from the kit components. The conversion of NAD to NADH was monitored every 10 s spectrometrically using a Victor 3 multimode reader (Perkin Elmer, United States) at 450 nm.

Statistical Analysis

Data from multiple experiments ($\geq$3) were quantified and expressed as mean ± SD, and differences between groups were analyzed using one-way ANOVA. Tukey multiple comparison test was used to analyze significance among the groups. $p \leq 0.05$ was considered significant in all analyses. The data were computed with GraphPad Prism version 7.0 software.

RESULTS

Determination of Minimum Biofilm Inhibition Concentration

To determine the minimum amount of GAs needed to inhibit maximum biofilm growth of *S. gordonii* and *C. albicans*, an MBIC assay was performed with increasing concentrations of GAs (0–600 μg/mL). Biofilms were quantified by CV staining, and the results showed a concentration-dependent antibiofilm activity of GAs against *S. gordonii* and *C. albicans* (**Figures 1A,C**, respectively). A significant inhibition of biofilm formation was found from concentrations >400 μg/mL for *S. gordonii* and from concentrations >200 μg/mL for *C. albicans*. While maximum biofilm growth inhibition (80–90%) was found between 500 and 600 μg/mL for *S. gordonii*, about 50% biofilm growth was inhibited for *C. albicans* at that GAs concentration (**Figure 1C**).

Impact of GAs on the Growth Kinetics of *S. gordonii* and *C. albicans*

To determine if GAs are toxic to *S. gordonii* and *C. albicans*, we measured their growth kinetics as planktonic cells in the presence or absence of GAs using Bioscreen-C growth monitor at 37°C in TYES medium, as described in the section "Materials and Methods." Since GAs inhibited *S. gordonii* biofilm growth from a concentration of 400 μg/ml upward, we used three different concentrations of GAs (400, 500, and 600 μg/mL) to assess its effects. As shown in **Figure 1B**, the growth of *S. gordonii* is slightly reduced in the presence of GAs. When *S. gordonii* was exposed to 400 and 500 μg/mL, GAs showed only slight growth inhibition, while GAs at 600 μg/mL affected *S. gordonii* growth to a greater extent. In contrast, GAs did not affect *C. albicans* growth rate until 12 h. At that point, GAs (400, 500, and 600 μg/mL) promoted the growth of *C. albicans* (**Figure 1D**), and each concentration had a similar effect. The mechanism for the growth induction is not known. One possibility may be that GAs may interfere with the carbohydrate metabolism of *C. albicans,* and as an adaptive response, the fungus turns on a different metabolic pathway for its cellular energy needs, resulting in an increased growth rate compared to the control. This conjecture is based on the fact that GAs are used for treating

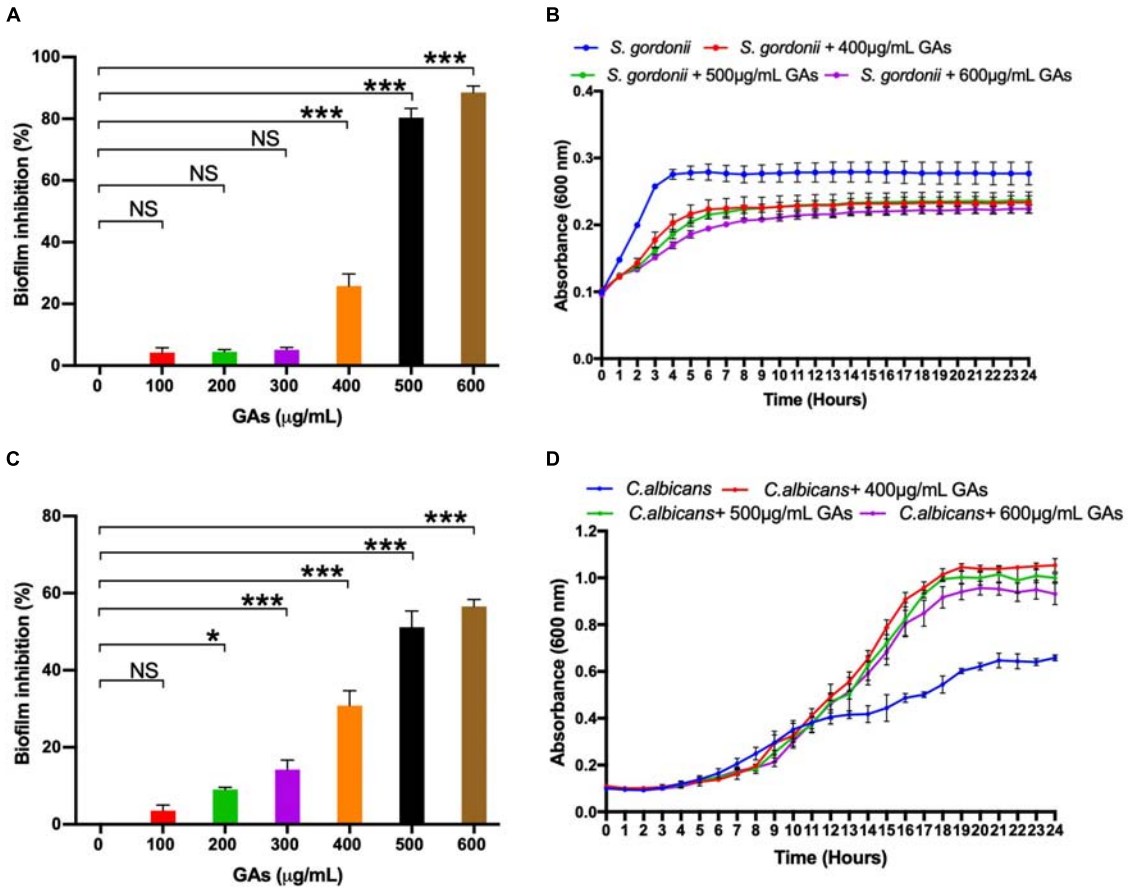

FIGURE 1 | Determination of minimum biofilm inhibition concentration (MBIC) of GAs against *S. gordonii* **(A)** and *C. albicans* **(C)**. Varying concentrations of GAs (0–600 μg/ml) were used in TYES medium containing *S. gordonii* or *C. albicans* in 24-wells with triplicates and incubated at 37°C with 5% CO_2 statically for 18 h. Biofilms grown without GAs served as controls. Inhibition of biofilm growth was analyzed by CV staining and % inhibition of biofilm was calculated. The results represent means ± standard deviations for three independent experiments. Statistical significance was determined by ANOVA and a Dunnett's multiple comparison test. *$p < 0.05$, ***$p < 0.0001$, NS, not significant. Analysis of planktonic growths of *S. gordonii* **(B)** and *C. albicans* **(D)** with and without GAs. Honeycomb wells containing *S. gordonii* or *C. albicans* in 200 μl TYES medium with or without GAs were used to monitor their growth rates in a Bioscreen-C system for 24 h. Three different concentrations of GAs (400, 500, 600 μg/ml) were used. Absorbance was recorded every 30-min intervals at 600 nm as described in the section "Materials and Methods." The results represent means ± standard deviations for three independent experiments.

metabolic diseases in humans (e.g., lowering plasma glucose in diabetes) (Baskaran et al., 1990; Leach, 2007). Further studies on biofilm gene expression in the presence of GAs and biochemical validation are warranted. Taken together, GAs inhibited the growth of *S. gordonii* slightly at 400–600 μg/mL but did not inhibit *C. albicans*' growth under the conditions used. Since 500 μg/ml GAs maximally inhibited biofilms of both microbes with minimal impacts on their growth rates, we employed this concentration (500 μg/mL) throughout the study to determine its effect on mono-species or dual-species biofilms.

Inhibition of *S. gordonii* and *C. albicans* Mono-Species and Dual-Species Biofilms Grown in 24-Well Microtiter Plates by GAs

The anti-biofilm efficacy of GAs was assessed under *in vitro* condition by measuring the binding of CV to *S. gordonii* biofilms cells grown in 24-well plates. The antibiofilm activity of GAs was effective at 500 μg/ml against *S. gordonii* and *C. albicans* mono-species and dual-species biofilms (**Figure 2A**). GAs treatment significantly reduced the amount of *S. gordonii* biofilms (**Figure 2A**). Similarly, the mixed biofilms were also reduced with GAs treatment, and are significant as analyzed by one-way ANOVA ($p = 0.001$). When Tukey multiple comparison test was used, the *S. gordonii* biofilm was significantly inhibited by GAs compared to *C. albicans* or dual-species biofilms (**Figure 2A**).

Effective Reduction of eDNA in Mono-Species and Dual-Species Biofilm by GAs Treatment

Extracellular DNA is a part of the polymeric materials in the extracellular matrix of biofilms (Xu and Kreth, 2013). To examine the effects of GAs on biofilm eDNA, mono-species and dual-species biofilms were grown in TYES medium.

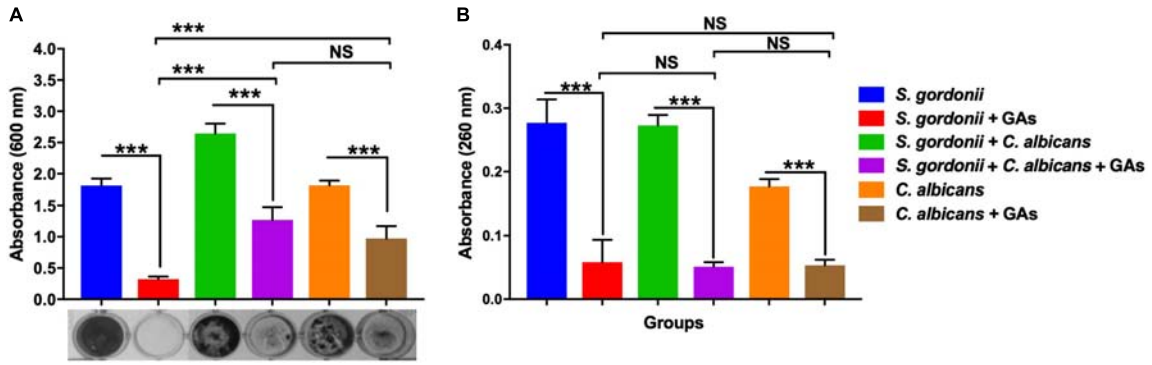

FIGURE 2 | Effect of GAs on *S. gordonii* and *C. albicans* mono-species or dual-species biofilms. **(A)** Crystal violet staining of *S. gordonii* and *C. albicans*, either as mono-species or as dual-species biofilms with and without GAs in saliva coated 24-well plates. **(B)** Measurement of eDNA from mono-species and dual-species biofilms with and without GAs. eDNA from pooled biofilms was released by gentle sonication as mentioned in the methods. The results represent means ± standard deviations for three independent experiments. Data were analyzed by one-way ANOVA followed by Tukey's multiple comparison test. NS, not significant; ***$p < 0.001$.

High levels of eDNA were found in both mono-species and dual-species biofilms. Interestingly, a significant reduction in eDNA concentrations were observed in the biofilms treated with GAs (p = 0.001, **Figure 2B**). There was no significant difference in the amount of eDNA reduction among the three groups as determined by Tukey multiple comparison test (**Figure 2B**), suggesting GAs treatment affects eDNA in all these biofilms similarly.

Inhibition of *S. gordonii* and *C. albicans* Mono-Species and Dual-Species Biofilms on sHA Disks

Scanning Electron Microscopy analysis was carried out to examine the structures of mono-species and dual-species biofilms formed on sHA disks that were treated with GAs. Biofilms formed on sHA disks were fixed, stained with Alcian blue, and processed as described (Erlandsen et al., 2004). These authors used different cationic stains to visualize bacterial surface structures by SEM. Since the microbial surface structures are negatively charged, the positively charged Alcian blue stain binds to the cell surface nanofibrils and improves their detection by SEM. SEM micrographs of *S. gordonii* revealed the formation of biofilms with thick aggregates of cells and patches of exopolysaccharide (EPS) on the surface of sHA (**Figure 3A**). Interestingly, very little biofilm of *S. gordonii* was found on the GAs treated-sHA disk, and large empty areas were seen mostly (**Figure 3G**). The SEM results are consistent with the results of the *in vitro* biofilm growth assay (**Figure 2A**). As expected, *C. albicans* control biofilms (B) contained multilayers of hyphae and in the GAs exposed biofilms, very little yeast and pseudohyphal cells were present on the sHA disks (H-I). It is worth mentioning that although GAs promote the growth rate of *C. albicans* (**Figure 1D**), the cells that grow are mostly planktonic yeast cells, and they poorly attach or fail to form biofilms. *S. gordonii* and *C. albicans* dual biofilms contained both dense bacterial and fungal hyphal cells (**Figure 3C**), and their abundance was decreased by GAs treatment (**Figure 3I**). The inhibitory effect of GAs was clearly demonstrated in the SEM micrographs of biofilms. Interestingly, mono-species and dual-species biofilms grown on sHA disks treated with GAs has no or few cell surface nanofibrils and instead exhibited smooth hyphal surfaces (**Figures 3J–L**).

S. gordonii and *C. albicans* Co-culture Promotes Formation of Extracellular Fibrils

Viewing the biofilms at higher magnification (50,000× or 1 μm) revealed that, without GAs exposure, there were short fibrils between *S. gordonii* cells, and some of these fibrils were attached to sHA (**Figure 4C**, arrows). As expected, *C. albicans* biofilms without GAs treatment produced mostly hyphae. Interestingly, *C. albicans* biofilms co-cultured with *S. gordonii* (dual-species biofilm) without GAs showed several closely attached bacterial-fungal cells with extracellular materials (**Figure 4A**). Strikingly, we found several thin fibrils from hypha that are in close contact with the sHA disk (**Figure 4A**, arrows) or to the neighboring hypha (**Figure 4D**, arrows). *S. gordonii* was in close contact with the *C. albicans* hyphae as the bacterium coiled around the hypha, and also appeared to be directly attached with the help of fibrils (**Figures 4C,D**, arrows).

Modulation of Gene Expression in Mono-Species and Dual-Species Biofilms With and Without GAs

Few studies have described differential expressions of genes during *S. gordonii* (Gilmore et al., 2003) or *Streptococci* + *C. albicans* dual-species biofilm growth (Dutton et al., 2016). To determine if some of these genes are affected by GAs treatment, a semi-quantitative RT-PCR analysis was used to examine variation in the expression of genes related to biofilm formation, i.e., *cshA, ldh, gapdh, gftG1, scaA,* and *scaR* for *S. gordonii* and *CSH1*, *ZRT1, NRG1,* and *PRA1,* for *C. albicans*. Treatment with GAs significantly reduced the expression of genes, including *scaA, gapdh,* and *gtfG1* in

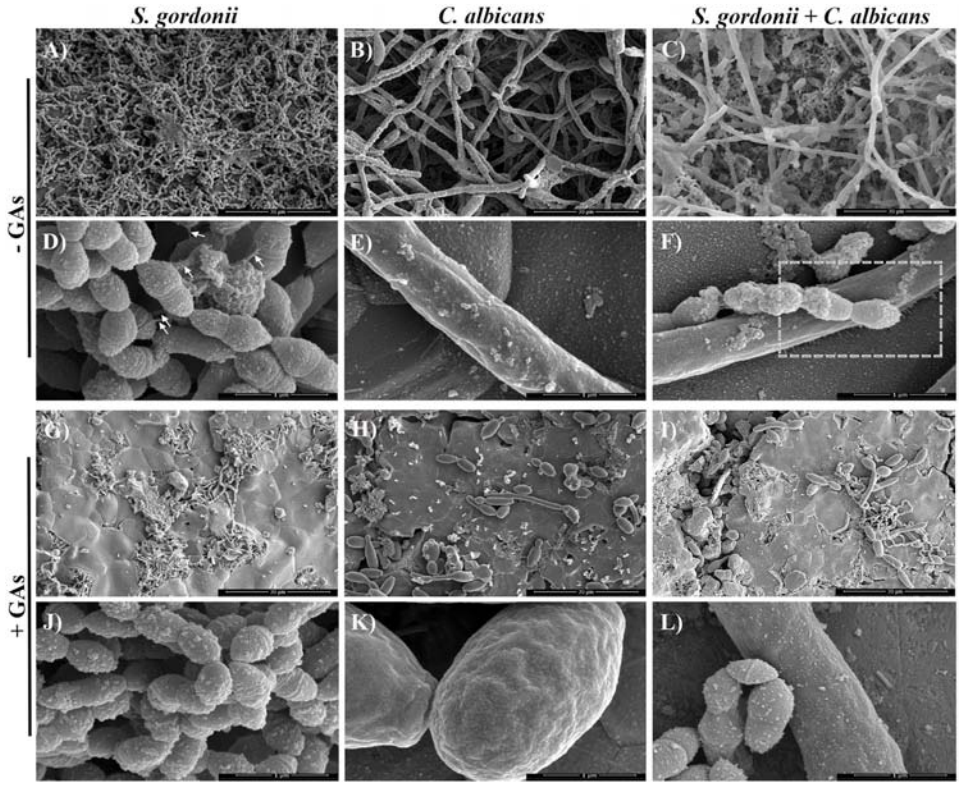

FIGURE 3 | Scanning electron microscopy (SEM) observations of mono-species and dual-species biofilms grown on sHA in the presence or absence of GAs. Images of mono-species and dual-species biofilms grown for 18 h in the absence (control, **A–F**) and in the presence of GAs **(G–L)** at 500 μg/ml concentration. Magnifications: **(A–C,G–I)** scale bar 20 μm, and **(D–F,J–L)** scale bar 1 μm. Biofilms grown with GAs show few cells on the sHA surfaces compared to dense layers of cells with exopolysaccharides (EPS) in the control groups. Short fibrils in the control *S. gordonii* biofilms that are attached to neighboring cells are shown (**D**, arrows). Changes in the biofilm surface textures and absence of fibrils were observed in the GAs treated biofilm groups **(G–L)**. GAs treated *C. albicans* show mostly yeast or pseudohyphal cells with few hyphae **(H,K)**. Dashed box in **F** was further magnified in **Figure 4** to show nanofibrillar structures. In GAs treated dual-species biofilms, weak or no fibrillar structures from *S. gordonii* and none from *C. albicans* were found **(J–L)**.

S. gordonii mono-species biofilms, whereas, in dual-species biofilms, *scaA*, *ldh,* and *cshA* were reduced in their expression when compared with their respective controls (**Figure 5A**). Interestingly, the expression of *ldh* was enhanced ninefold in GAs treated *S. gordonii* mono-species biofilms but not in dual-species biofilms (**Figure 5A**). In mono-species biofilms of *C. albicans*, the expression of *NRG1* was increased twofold in GAs treated samples compared to the untreated control (**Figure 5B**). No change was observed for *NRG1* and *CSH1* in GAs treated dual biofilms (**Figure 5B** and **Supplementary Figure S3**). The expression of *PRA1* was increased twofold in GAs exposed *C. abicans* mono-species biofilms, whereas, in dual-species biofilms, the expression of *PRA1* was decreased in GAs treated biofilms. In contrast, *ZRT1*, the regulator of *PRA1*, was overexpressed about fivefold in dual-species biofilms in the presence of GAs, but not in the GAs-exposed *C. albicans* mono-species biofilms.

Inhibition of GAPDH Activity by GAs

Glyceraldehyde-3-phosphate dehydrogenase from streptococcal species is involved in pathogenesis and biofilm formation. Also, GAs treatment of *S. gordonii* mono-species or dual-species biofilms showed a reduction in its, gene expression. To assess the potential inhibitory activity of GAs against the GAPDH from *S. gordonii*, we cloned the gene, overexpressed and purified the rGAPDH protein using the *E. coli* expression system (**Figure 6A**). The purified rGAPDH migrated at an apparent molecular weight of ∼40 kDa and reacted to polyclonal anti-*Sg*GAPDH antibody (**Figure 6B**). We next tested the effect of GAs (100 and 200 μM) against the purified rGAPDH protein (0.1 μM). The assay depends on the conversion of glyceraldehyde-3-phosphate to 1,3-diphosphoglycerate by GAPDH enzyme in the presence of NAD. Interestingly, GAs appears to bind to GAPDH and block its enzyme activity in a dose-dependent manner. At 200 μM concentration, GAs block the activity of GAPDH completely when compared to the reaction without GAs where it shows strong enzyme activity (**Figure 6C**).

DISCUSSION

Microbial infection in the oral cavity of humans is biofilm-associated, where a significant proportion of infection was mixed biofilms. *S. gordonii*, an early colonizer of the oral cavity, forms

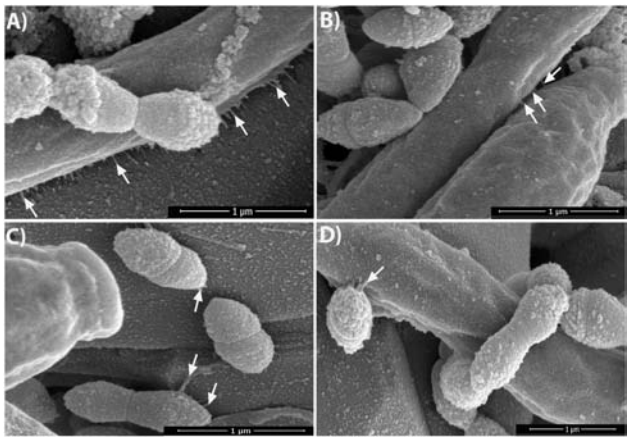

FIGURE 4 | Dual-species biofilms in the absence of GAs promote nanofibrillar-mediated interactions. SEM images of dual-species biofilms showing nanofibrillar structures from *C. albicans* hypha that are attached to the sHA (**A**, arrows) as well as between two hyphae (**B**, arrows). *S. gordonii* exhibits high affinity to hypha by its fibrillar attachment and by tight coiling around the hypha **(D)**, and also to sHA **(C)** which mimics teeth. The images were zoomed to show the nanofibrils. Scale bar, 1 μm.

an adhering biofilm on oral surfaces via cell surface adhesins (Bamford et al., 2009), leads to stable colonization in the oral cavity, and also attaches to *C. albicans* hyphae via protein-protein interactions (Holmes et al., 1996). In addition, *S. gordonii* colonization on the tooth surface allows other microbes to adhere and develop mixed biofilms such as dental caries, which is the most prevalent human oral disease, especially among the children. We have investigated the *S. gordonii* mono-species and *S. gordonii* – *C. albicans* dual-species biofilms and their inhibition by gymnemic acids (GAs) *in vitro*. GAs, a medicinal plant-derived small molecule, was shown to prevent *C. albicans* yeast-to-hypha transition and hyphal growth without affecting its viability or yeast growth rate (Vediyappan et al., 2013). However, GAs' effect on bacterial and or bacterial-fungal mixed biofilms are unknown. GAs are a family of triterpenoid saponin compounds which are the major active principles of *G. sylvestre* plant leaves. The extract of this plant is widely used for its various medicinal properties, including lowering blood glucose activity in diabetic patients and reducing obesity (Porchezhian and Dobriyal, 2003; Leach, 2007; Zuniga et al., 2017).

Antibiofilm efficacy of GAs was investigated in terms of CV staining and eDNA reduction in the saliva-coated microtiter wells, where the results were found to be significant compared to untreated controls. This is the first report to provide evidence that the GAs shows antibiofilm efficacy against both mono-species and dual-species biofilms of *S. gordonii* and *C. albicans*. The microbial biofilms are protected by self-produced exopolysaccharides (EPS). EPS are generally made up of different types of polysaccharides, proteins, glycoproteins, glycolipids, and eDNA. The importance of eDNA release during early stages of biofilm is to preserve the structural firmness, enhancing the mixed biofilm and protection against antimicrobial agents (Mulcahy et al., 2008; Jack et al., 2015; Jung et al., 2017). Therefore, reduction of eDNA accumulation and other components could substantively diminish the development of biofilm formation. As such, we found that GAs was able to reduce a significant amount of eDNA in both mono-species and dual-species biofilms (**Figures 1**, **2**).

It was reported earlier that *S. gordonii* cells form surface fibrils, which have multiple properties like cell surface hydrophobicity, co-aggregate with other oral bacteria, saliva-coated hydroxyapatite (sHA) and bind to host fibronectin (McNab et al., 1996; Back et al., 2017). These results emphasize that fibril-mediated attachment is the critical factor for the initial oral colonization for Streptococci. In the present study, we observed an extracellular nanofibrillar-mediated attachment of *S. gordonii* cells to sHA by SEM. Interestingly, these nanofibrils were not peritrichous as previously reported (McNab et al., 1999) and instead, the scattered fibrils were attached to neighboring streptococci cells, sHA substratum and to *C. albicans* hyphae (**Figures 3**, **4A–D**) confirming its role in adherence. To our surprise, synthesis of these fibrils was abolished in the GAs treated *S. gordonii* biofilms. These fibrils could be related to EPS and we believe GAs might be affecting their synthesis and/or their incorporation into the biofilms. One of the unexpected findings of *S. gordonii*–*C. albicans* mixed biofilms was the formation of short fibrils from the *C. albicans* hyphae (**Figures 4A,B**). These fibrils show attachment to neighboring hypha and to the sHA substratum. This shows that there is an enhanced mutual synergism between these two microbes. However, in GAs treated mixed biofilms, these fibrils were absent (**Figure 3L**) and significant inhibition of biofilms was found. Djaczenko and Cassone (1972) have reported the presence of fimbriae in *C. albicans* yeast cells and known to contain mannosylated glycoprotein (Yu et al., 1994). We believe the fibrils that we observe in hyphae could be different from the fimbriae described above. For example, the fimbriae reported by Djaczenko and Cassone (1972) were found on the surface of "yeast cells" grown on agar plates for several days. These fimbriae are short and continuous throughout the cell surface of mother yeast cells but very little on the daughter cells.

In contrast, our results show the fibrils are discontinuous and found only from hyphae of *S. gordonii*–*C. albicans* co-cultured biofilms where they have close contacts with abiotic or biotic surfaces (**Figure 4**). These fibrils were not observed in biofilms grown in the presence of GAs, suggesting that GAs can prevent adhesive fibrils, in part, by inhibiting its synthesis and or hyphae associated adhesive proteins.

To understand the mechanisms of biofilm inhibition by GAs, we determined the expression of selected genes that have predicted roles in the growth of *S. gordonii* and *C. albicans* biofilms (Gilmore et al., 2003; Dutton et al., 2016). EPSs are the core parts for the assembly and maintenance of biofilm architectural integrity in the oral cavity. The oral streptococci produce glucosyltransferase enzymes, Gtfs, that split and use glucose from extracellular sucrose to synthesize glucans, which helps the streptococci adhere to the tooth surface and to the surfaces of other oral microbes. *S. gordonii*, the primary colonizer of the oral cavity, produces *gtfG1* (Vickerman et al., 1997). The RT-PCR analysis of *S. gordonii* biofilm cells shows basal

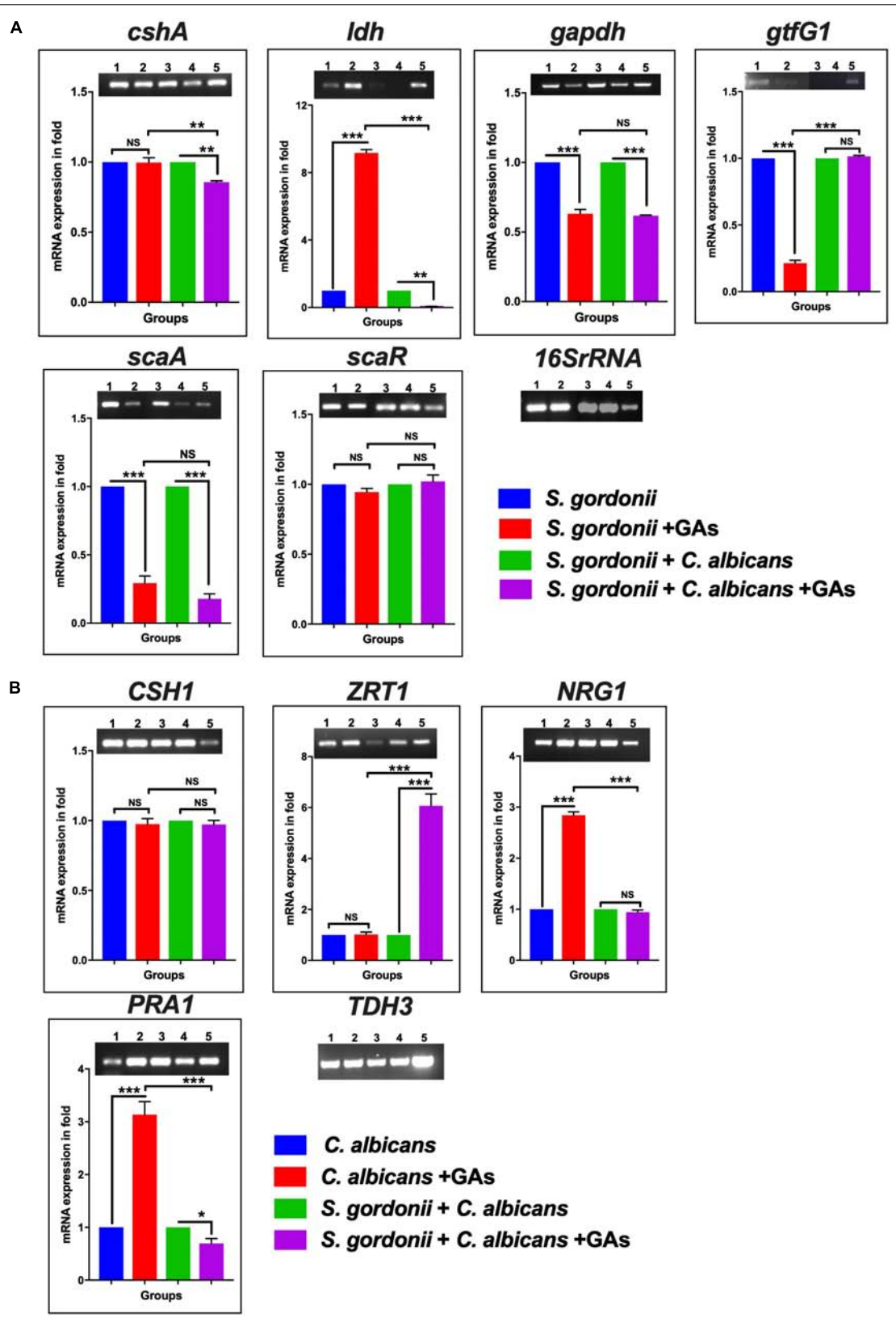

FIGURE 5 | The mRNA expression level of biofilm genes as determined by RT-PCR. **(A)** Representative semi-quantitative mRNA expression profile for streptococcal primers showing the amplicons of mono-species and dual-species biofilms. (1) *S. gordonii*, (2) *S. gordonii* + GAs, (3) *S. gordonii* + *C. albicans*, (4) *S. gordonii* +

(Continued)

FIGURE 5 | Continued
C. albicans + GAs, (5) Positive PCR control (gDNA used as template). Bar graphs represent the densitometry analysis of respective genes and a constant level of expression of 16S rRNA. **(B)** Representative semiquantitative mRNA expression profile for candida primers showing the amplicons of mono-species and dual-species biofilms. (1) *C. albicans*, (2) *C. albicans* + GAs, (3) *S. gordonii* + *C. albicans*, (4) *S. gordonii* + *C. albicans* + GAs, (5) Positive PCR control (gDNA as template). Bar graph represents the densitometry analysis of respective genes and a constant level of expression of *TDH3*. The results represent means ± standard deviations for three independent experiments. NS, not significant, $*p < 0.05$, $**p < 0.01$, $***p < 0.001$. *P* values were obtained by one-way ANOVA followed by Tukey's multiple comparison test.

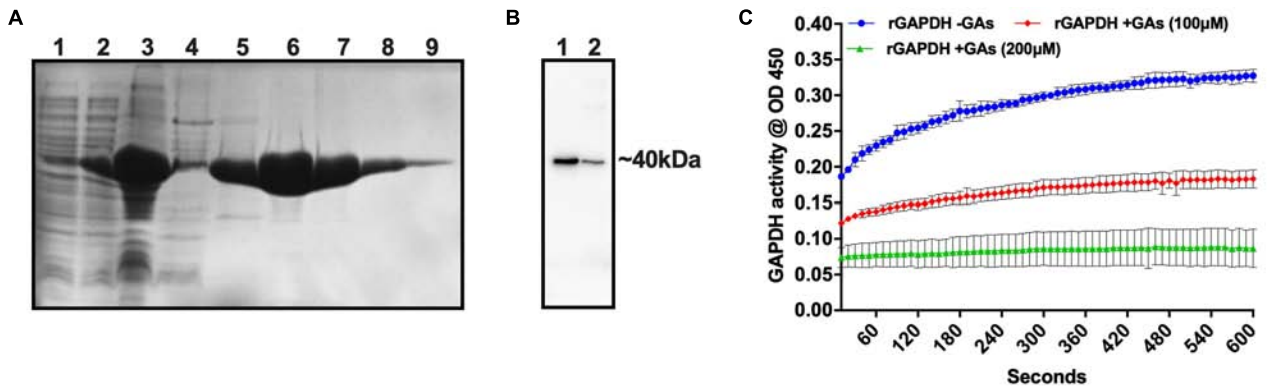

FIGURE 6 | Purification of *S. gordonii* rGAPDH and determination of its enzyme activity. **(A)** SDS-PAGE gel showing purified fractions of rGAPDH protein from *E. coli* cell lysates. (1) Uninduced whole cell lysate, (2) Induced whole cell lysate, (3) French pressed cell lysate, (4) Unbound fraction, 5 to 9–100, 150, 200, 250, 300, and 350 mM imidazole eluted fractions, respectively. **(B)** Western blot of rGAPDH protein against anti-GAPDH antibody (anti rabbit *S. gordonii* GAPDH). Lanes, 1 and 2 – Purified rGAPDH protein at two different concentrations (3 and 1 μg). **(C)** Measurement of GAPDH activity in the presence and absence of GAs (treated, 200 μm equal to ∼160 μg/mL and 100 μm equal to ∼80 μg/mL).

level expression of *gtfG1*. However, GAs treatment reduced its expression, signifying the inhibitory potential of biofilm glucan by GAs (**Figure 5A**). This result agrees with SEM data where the *S. gordonii* biofilms treated with GAs show absence of adhesive fibrils when compared to the control biofilm where the fibrils can be seen between the biofilms cells and on the sHA (**Figures 3D,J**). The other roles of Gtfs include glycosylation of adhesive proteins such as GspB of *S. gordonii* and Fap1 of *Streptococcus parasanguinis* (Zhu et al., 2015). GAs are known to bind several proteins, including glucose transporter (Wang et al., 2014), taste receptors T1R2/T1R3 (Sanematsu et al., 2014), and Liver X-receptor (LXR) that regulates lipid metabolism in the liver (Renga et al., 2015). It has been reported that administration of GAs containing fraction, GS4, decreased the glycosylated hemoglobin (HbA1c) and glycosylated plasma protein in diabetic patients (Baskaran et al., 1990), and a similar mechanism may occur in microbial biofilms. Bacterial Gtfs play a critical role in enhancing the accumulation of *C. albicans* cells during mixed biofilm growths (Ellepola et al., 2017). GAs may affect the polysaccharide synthesis pathway in *S. gordonii* biofilms, through a reduced *gtfG1* expression and or its enzyme activity. Further, Gtfs use metal co-factor Mn^{2+} for enzyme catalytic activity (Zhu et al., 2015) and the downregulation of *scaA*, the gene that encodes Mn^{2+} binding lipoprotein, in GAs treated *S. gordonii* mono-species as well as dual-species biofilms (**Figure 5**) may also contribute to the reduction of adhesive fibrils/polysaccharides. For growth and survival in the human host, *S. gordonii* will have to acquire Mn^{2+} with the help of ScaA, a prominent surface antigen. It has been shown that inactivation of *scaA* gene resulted in both impaired growth of cells and >70% inhibition of Mn^{2+} uptake (Kolenbrander et al., 1998).

Oral bacteria, including *S. gordonii,* can sense the redox status of the biofilm niche and respond accordingly. Among the genes examined for differential expression in biofilms, we found lactate dehydrogenase (*ldh*) is one of the highly upregulated genes in GAs treated biofilms of *S. gordonii* (**Figure 5**). The ldh enzyme interconverts pyruvate into lactate and back, as it converts NADH to NAD and back. In GAs treated *S. gordonii*, ldh may be converting lactate into pyruvate as the *gapdh* mRNA is downregulated in GAs treated mono-species or mixed biofilms of *S. gordonii* but not in *C. albicans*. GAPDH uses NAD during glycolytic activity and the reduced amount of GAPDH may lead to the accumulation of NAD, which in turn activates the overexpression of *ldh* through a redox-sensing system (Bitoun and Wen, 2016). To determine if GAs has any effect on GAPDH enzyme activity, we cloned the *gapdh* gene from *S. gordonii,* overexpressed in *E. coli*, and tested the purified rGAPDH with or without GAs. We found the inhibition of rGAPDH enzyme activity in a dose-dependent manner (**Figure 6**). GA was shown to inhibit rabbit GAPDH enzyme activity (Izutani et al., 2005). Maeda et al. (2004a,b) have showed that oral streptococcal (e.g., *S. oralis, S. gordonii*) cell surface-associated GAPDH binds to the long fimbriae (FimA) of *P. gingivalis* and play a role in the development of oral polymicrobial biofilms (Kuboniwa et al., 2017). In addition to glycolytic function, GAPDH is also a moonlighting protein and known to carry out multiple functions (Sirover, 2017). It is worth mentioning that natural products (anacardic acid and curcumin) have been shown to bind and

inhibit *Streptococcus pyogenes* GAPDH activity. GAPDH is a major virulence factor (Gomez et al., 2019), and the GAPDH serves as a drug target for other pathogens (Freitas et al., 2009) as well. GAs appear to impact *S. gordonii* GAPDH both at the transcriptional and translational level and could account, at least partially, for the observed inhibition of *S. gordonii* growth and or biofilm. Comparison of amino acid sequences of both *S. gordonii* and *C. albicans* GAPDH revealed about 50% similarity, leaving open the possibility that GAs impact on them could be different. In fact, the expression of GAPDH gene in *C. albicans* (*TDH3*) biofilms grown in the presence or absence of GAs is not affected (**Figure 5B**, *TDH3* RT-PCR bands). However, GAs impact on *C. albicans* GAPDH (Tdh3) enzyme activity and its role in biofilms can't be ruled out and remains to be determined. Global gene expression and biochemical analyzes are necessary steps to reveal the mechanism(s) of GAs-mediated inhibition of *S. gordonii* mono-species and dual-species biofilms.

Among the genes examined in *C. albicans* mono-species or dual-species biofilms, *NRG1, PRA1,* and *ZRT1* are the most differentially expressed. It is well known from the literature that Nrg1 of *C. albicans* is a DNA binding protein that represses its filamentous growth (Braun et al., 2001). GAs treatment shows a significant increase of *NRG1* mRNA expression in *C. albicans* biofilms compared to control biofilms (**Figure 5B**), which may correspond to the observed yeast or pseudohyphal growth forms of *C. albicans* mono-species biofilm (**Figure 3**). However, no change of *NRG1* expression level was observed in dual-species biofilms, yet their biofilm growth was inhibited, underscoring the unknown regulatory mechanism in the GAs treated dual-species biofilms. *C. albicans* sequesters environmental zinc through a secreted protein, the pH-regulated antigen 1 (Pra1) and transports it through the membrane transporter (Zrt1) for its invasive growth in the host (Citiulo et al., 2012). *C. albicans* has biphasic mechanisms for its environmental and cellular zinc homeostasis and Pra1 expresses when cells are at pH 7 and above or at zinc limitation (Crawford et al., 2018; Wilson, 2019). Kurakado et al. (2018) have also reported that the hypha-related Pra1 and Zrt1 play a major regulatory role *C. albicans* biofilm formation through zinc homeostasis. GAs treatment to *C. albicans* mono-species biofilm appears to cause zinc limitation and or change in cellular pH, which could be altered when grown with *S. gordonii* as mixed-species biofilms (**Figure 5B**).

Our understanding about mixed species biofilms in caries pathogenesis is still in its infancy (Metwalli et al., 2013). It was well known that from various host defense factors, microbes in mixed biofilms act synergistically for their survival (Morales and Hogan, 2010; Xu et al., 2014a). Great attention is needed on mitis group streptococci (*S. gordonii*, *S. oralis*, *Streptococcus mitis*, *S. parasanguinis,* and *Streptococcus sanguinis*), which form multispecies biofilms when aggregating with other bacterial and fungal species (Xu et al., 2014b). These oral microbial infections pose a significant threat to public health, as many pathogenic bacteria readily develop resistance to multiple antibiotics and form biofilms with additional protection from antibiotic treatment (Lebeaux et al., 2014). Currently available antimicrobial agents were most effective at drastically reducing the cell viability, rather than reducing the virulence via inhibiting the biofilm growth. For instance, fluoride is a proven agent for caries prophylaxis; however, excess use of fluoride causes fluorosis and hardening of cartilage. Also, these synthetic antimicrobial agents lead to negative effects in the gastrointestinal system and several other side effects. We are in need of efficient antimicrobial agent which inhibit biofilm formation, while at the same time the agent should not exert selective pressure over oral microbiome.

Recently, many studies have targeted medicinal plants in finding effective anticaries agents (Islam et al., 2008; Yang et al., 2017; Gartika et al., 2018; Henley-Smith et al., 2018). Medicinal plants have been used to prevent and treat microbial diseases since ancient times, which can target several antigens or pathways of the pathogens for inhibition without adverse effects. Earlier studies on medicinal plant extracts described biofilm inhibition by hindering hydrophobic properties of *S. mutans* (Nostro et al., 2004; Khan et al., 2012). Any antimicrobial agent that reduces or hinders interactions/attachment represents a novel strategy to overcome oral infection. Interestingly, our GAs treatment shows a significant reduction in both mono-species and dual-species biofilms and appear to act via more than one mechanism. GAs affect the transcription of *S. gordonii gapdh* and its enzyme activity in addition to *gtfG1*, which is involved in glucan polysaccharide synthesis. Further, GAs are able to curtail the development of nanofibrils that mediate cell-cell and substrate adhesion both in *S. gordonii* and *C. albicans*. In summary, our findings offer an anti-virulence approach for preventing mixed oral biofilms and by further optimization, and natural products have high potential as a useful source for developing mixed biofilm inhibitors.

DATA AVAILABILITY STATEMENT

All datasets generated for this study are included in the manuscript/**Supplementary Files**.

ETHICS STATEMENT

The studies involving human participants were reviewed and approved by Institutional Review Board, Kansas State University. The patients/participants provided their written informed consent to participate in this study.

AUTHOR CONTRIBUTIONS

GV designed the study. RV and GV conducted the experiments, analyzed the data, and wrote the manuscript.

FUNDING

This work was supported by American Heart Association SDG Grant #14SDG18910036 to GV, and by an Institutional Development Award (IDeA) from the National Institute of

General Medical Sciences of the National Institutes of Health under grant number P20 GM103418. The content is solely the responsibility of the authors and does not necessarily represent the official views of the National Institute of General Medical Sciences or the National Institutes of Health. Publication of this article was funded in part by the Kansas State University Open Access Publishing Fund to GV.

ACKNOWLEDGMENTS

We acknowledge the generous gift of streptococcal strains by Indranil Biswas, KUMC, Kansas City. We thank Kansas Idea Network of Biomedical Research Excellence (K-INBRE) for CORE Facility support and Johnson Cancer Research Center, KSU for IRA funding supports to GV and K-INBRE postdoctoral support to RV. We also thank Erick Saenz-Gardea's assistance under the Developing Scholar Program during the initial phase of this project. We also acknowledge SEM technical support by Ravindra Thakkar, NICKS, KSU and Prem Thapa Chetri, MAI, KU.

SUPPLEMENTARY MATERIAL

The Supplementary Material for this article can be found online at: https://www.frontiersin.org/articles/10.3389/fmicb.2019.02328/full#supplementary-material

REFERENCES

Back, C. R., Sztukowska, M. N., Till, M., Lamont, R. J., Jenkinson, H. F., Nobbs, A. H., et al. (2017). The *Streptococcus gordonii* adhesin CshA protein binds host fibronectin via a catch-clamp mechanism. *J. Biol. Chem.* 292, 1538–1549. doi: 10.1074/jbc.M116.760975

Bamford, C. V., D'mello, A., Nobbs, A. H., Dutton, L. C., Vickerman, M. M., and Jenkinson, H. F. (2009). *Streptococcus gordonii* modulates *Candida albicans* biofilm formation through intergeneric communication. *Infect. Immun.* 77, 3696–3704. doi: 10.1128/IAI.00438-09

Baskaran, K., Kizar Ahamath, B., Radha Shanmugasundaram, K., and Shanmugasundaram, E. R. (1990). Antidiabetic effect of a leaf extract from *Gymnema sylvestre* in non-insulin-dependent diabetes mellitus patients. *J. Ethnopharmacol.* 30, 295–300.

Bitoun, J. P., and Wen, Z. T. (2016). Transcription factor Rex in regulation of pathophysiology in oral pathogens. *Mol. Oral Microbiol.* 31, 115–124. doi: 10.1111/omi.12114

Brassard, J., Gottschalk, M., and Quessy, S. (2004). Cloning and purification of the *Streptococcus suis* serotype 2 glyceraldehyde-3-phosphate dehydrogenase and its involvement as an adhesin. *Vet. Microbiol.* 102, 87–94. doi: 10.1016/j.vetmic.2004.05.008

Braun, B. R., Kadosh, D., and Johnson, A. D. (2001). NRG1, a repressor of filamentous growth in *Candida albicans*, is down-regulated during filament induction. *EMBO J.* 20, 4753–4761. doi: 10.1093/emboj/20.17.4753

Citiulo, F., Jacobsen, I. D., Miramon, P., Schild, L., Brunke, S., Zipfel, P., et al. (2012). *Candida albicans* scavenges host zinc via Pra1 during endothelial invasion. *PLoS Pathog.* 8:e1002777. doi: 10.1371/journal.ppat.1002777

Crawford, A. C., Lehtovirta-Morley, L. E., Alamir, O., Niemiec, M. J., Alawfi, B., Alsarraf, M., et al. (2018). Biphasic zinc compartmentalisation in a human fungal pathogen. *PLoS Pathog.* 14:e1007013. doi: 10.1371/journal.ppat.1007013

Di Fabio, G., Romanucci, V., Zarrelli, M., Giordano, M., and Zarrelli, A. (2013). C-4 gem-dimethylated oleanes of *Gymnema sylvestre* and their pharmacological activities. *Molecules* 18, 14892–14919. doi: 10.3390/molecules181214892

Diaz, P. I., Xie, Z., Sobue, T., Thompson, A., Biyikoglu, B., Ricker, A., et al. (2012). Synergistic interaction between *Candida albicans* and commensal oral streptococci in a novel in vitro mucosal model. *Infect. Immun.* 80, 620–632. doi: 10.1128/IAI.05896-11

Djaczenko, W., and Cassone, A. (1972). Visulization of new ultrastructural components in the cell wall of *Candida albicans* with fixatives containing TAPO. *J. Cell Biol.* 52, 186–190. doi: 10.1083/jcb.52.1.186

Dongari-Bagtzoglou, A., Kashleva, H., Dwivedi, P., Diaz, P., and Vasilakos, J. (2009). Characterization of mucosal *Candida albicans* biofilms. *PLoS One* 4:e7967. doi: 10.1371/journal.pone.0007967

Dutton, L. C., Nobbs, A. H., Jepson, K., Jepson, M. A., Vickerman, M. M., Aqeel Alawfi, S., et al. (2014). O-mannosylation in *Candida albicans* enables development of interkingdom biofilm communities. *mBio* 5:e911-14. doi: 10.1128/mBio.00911-14

Dutton, L. C., Paszkiewicz, K. H., Silverman, R. J., Splatt, P. R., Shaw, S., Nobbs, A. H., et al. (2016). Transcriptional landscape of trans-kingdom communication between *Candida albicans* and *Streptococcus gordonii*. *Mol. Oral Microbiol.* 31, 136–161. doi: 10.1111/omi.12111

Ellepola, K., Liu, Y., Cao, T., Koo, H., and Seneviratne, C. J. (2017). Bacterial GtfB augments *Candida albicans* accumulation in cross-kingdom biofilms. *J. Dent. Res.* 96, 1129–1135. doi: 10.1177/0022034517714414

Erlandsen, S. L., Kristich, C. J., Dunny, G. M., and Wells, C. L. (2004). High-resolution visualization of the microbial glycocalyx with low-voltage scanning electron microscopy: dependence on cationic dyes. *J. Histochem. Cytochem.* 52, 1427–1435. doi: 10.1369/jhc.4a6428.2004

Freitas, R. F., Prokopczyk, I. M., Zottis, A., Oliva, G., Andricopulo, A. D., Trevisan, M. T., et al. (2009). Discovery of novel *Trypanosoma cruzi* glyceraldehyde-3-phosphate dehydrogenase inhibitors. *Bioorg. Med. Chem.* 17, 2476–2482. doi: 10.1016/j.bmc.2009.01.079

Gartika, M., Pramesti, H. T., Kurnia, D., and Satari, M. H. (2018). A terpenoid isolated from *Sarang semut* (Myrmecodia pendans) bulb and its potential for the inhibition and eradication of *Streptococcus mutans* biofilm. *BMC Complement. Altern. Med.* 18:151. doi: 10.1186/s12906-018-2213-x

Gilmore, K. S., Srinivas, P., Akins, D. R., Hatter, K. L., and Gilmore, M. S. (2003). Growth, development, and gene expression in a persistent *Streptococcus gordonii* biofilm. *Infect. Immun.* 71, 4759–4766. doi: 10.1128/iai.71.8.4759-4766.2003

Gomez, S., Querol-Garcia, J., Sanchez-Barron, G., Subias, M., Gonzalez-Alsina, A., Franco-Hidalgo, V., et al. (2019). The antimicrobials anacardic acid and curcumin are not-competitive inhibitors of gram-positive bacterial pathogenic Glyceraldehyde-3-phosphate dehydrogenase by a mechanism unrelated to human C5a anaphylatoxin binding. *Front. Microbiol.* 10:326. doi: 10.3389/fmicb.2019.00326

Harriott, M. M., and Noverr, M. C. (2009). *Candida albicans* and *Staphylococcus aureus* form polymicrobial biofilms: effects on antimicrobial resistance. *Antimicrob. Agents Chemother.* 53, 3914–3922. doi: 10.1128/AAC.00657-09

Harriott, M. M., and Noverr, M. C. (2011). Importance of *Candida*-bacterial polymicrobial biofilms in disease. *Trends Microbiol.* 19, 557–563. doi: 10.1016/j.tim.2011.07.004

Henley-Smith, C. J., Botha, F. S., Hussein, A. A., Nkomo, M., Meyer, D., and Lall, N. (2018). Biological activities of heteropyxis natalensis against micro-organisms involved in oral infections. *Front. Pharmacol.* 9:291. doi: 10.3389/fphar.2018.00291

Holmes, A. R., Mcnab, R., and Jenkinson, H. F. (1996). *Candida albicans* binding to the oral bacterium *Streptococcus gordonii* involves multiple adhesin-receptor interactions. *Infect. Immun.* 64, 4680–4685.

Hwang, G., Liu, Y., Kim, D., Li, Y., Krysan, D. J., and Koo, H. (2017). *Candida albicans* mannans mediate *Streptococcus mutans* exoenzyme GtfB binding to modulate cross-kingdom biofilm development in vivo. *PLoS Pathog.* 13:e1006407. doi: 10.1371/journal.ppat.1006407

Islam, B., Khan, S. N., Haque, I., Alam, M., Mushfiq, M., and Khan, A. U. (2008). Novel anti-adherence activity of mulberry leaves: inhibition of *Streptococcus*

mutans biofilm by 1-deoxynojirimycin isolated from *Morus alba*. *J. Antimicrob. Chemother.* 62, 751–757. doi: 10.1093/jac/dkn253

Izutani, Y., Murai, T., Imoto, T., Ohnishi, M., Oda, M., and Ishijima, S. (2005). Gymnemic acids inhibit rabbit glyceraldehyde-3-phosphate dehydrogenase and induce a smearing of its electrophoretic band and dephosphorylation. *FEBS Lett.* 579, 4333–4336. doi: 10.1016/j.febslet.2005.06.070

Jack, A. A., Daniels, D. E., Jepson, M. A., Vickerman, M. M., Lamont, R. J., Jenkinson, H. F., et al. (2015). *Streptococcus gordonii* comCDE (competence) operon modulates biofilm formation with *Candida albicans*. *Microbiology* 161, 411–421. doi: 10.1099/mic.0.000010

Jin, H., Agarwal, S., Agarwal, S., and Pancholi, V. (2011). Surface export of GAPDH/SDH, a glycolytic enzyme, is essential for *Streptococcus pyogenes* virulence. *mBio* 2:e68-11. doi: 10.1128/mBio.00068-11

Jung, C. J., Hsu, R. B., Shun, C. T., Hsu, C. C., and Chia, J. S. (2017). AtlA mediates extracellular DNA release, which contributes to *Streptococcus mutans* biofilm formation in an experimental rat model of infective Endocarditis. *Infect. Immun.* 85:e252-17. doi: 10.1128/IAI.00252-17

Kassebaum, N. J., Smith, A. G. C., Bernabe, E., Fleming, T. D., Reynolds, A. E., Vos, T., et al. (2017). Global, regional, and national prevalence, incidence, and disability-adjusted life years for oral conditions for 195 countries, 1990-2015: a systematic analysis for the global burden of diseases, injuries, and risk factors. *J. Dent. Res.* 96, 380–387. doi: 10.1177/0022034517693566

Khan, R., Adil, M., Danishuddin, M., Verma, P. K., and Khan, A. U. (2012). *In vitro* and *in vivo* inhibition of *Streptococcus mutans* biofilm by *Trachyspermum ammi* seeds: an approach of alternative medicine. *Phytomedicine* 19, 747–755. doi: 10.1016/j.phymed.2012.04.004

Kim, D., Sengupta, A., Niepa, T. H., Lee, B. H., Weljie, A., Freitas-Blanco, V. S., et al. (2017). *Candida albicans* stimulates *Streptococcus mutans* microcolony development via cross-kingdom biofilm-derived metabolites. *Sci. Rep.* 7:41332. doi: 10.1038/srep41332

Kolenbrander, P. E., Andersen, R. N., Baker, R. A., and Jenkinson, H. F. (1998). The adhesion-associated sca operon in *Streptococcus gordonii* encodes an inducible high-affinity ABC transporter for Mn2+ uptake. *J. Bacteriol.* 180, 290–295.

Kuboniwa, M., Houser, J. R., Hendrickson, E. L., Wang, Q., Alghamdi, S. A., Sakanaka, A., et al. (2017). Metabolic crosstalk regulates *Porphyromonas gingivalis* colonization and virulence during oral polymicrobial infection. *Nat. Microbiol.* 2, 1493–1499. doi: 10.1038/s41564-017-0021-6

Kurakado, S., Arai, R., and Sugita, T. (2018). Association of the hypha-related protein Pra1 and zinc transporter Zrt1 with biofilm formation by the pathogenic yeast *Candida albicans*. *Microbiol. Immunol.* 62, 405–410. doi: 10.1111/1348-0421.12596

Leach, M. J. (2007). *Gymnema sylvestre* for diabetes mellitus: a systematic review. *J. Altern. Complement. Med.* 13, 977–983. doi: 10.1089/acm.2006.6387

Lebeaux, D., Ghigo, J. M., and Beloin, C. (2014). Biofilm-related infections: bridging the gap between clinical management and fundamental aspects of recalcitrance toward antibiotics. *Microbiol. Mol. Biol. Rev.* 78, 510–543. doi: 10.1128/MMBR.00013-14

Liu, H. M., Kiuchi, F., and Tsuda, Y. (1992). Isolation and structure elucidation of gymnemic acids, antisweet principles of *Gymnema sylvestre*. *Chem. Pharm. Bull.* 40, 1366–1375. doi: 10.1248/cpb.40.1366

Lo, H. J., Kohler, J. R., Didomenico, B., Loebenberg, D., Cacciapuoti, A., and Fink, G. R. (1997). Nonfilamentous *Candida albicans* mutants are avirulent. *Cell* 90, 939–949. doi: 10.1016/s0092-8674(00)80358-x

Maeda, K., Nagata, H., Nonaka, A., Kataoka, K., Tanaka, M., and Shizukuishi, S. (2004a). Oral streptococcal glyceraldehyde-3-phosphate dehydrogenase mediates interaction with *Porphyromonas gingivalis* fimbriae. *Microbes Infect.* 6, 1163–1170. doi: 10.1016/j.micinf.2004.06.005

Maeda, K., Nagata, H., Yamamoto, Y., Tanaka, M., Tanaka, J., Minamino, N., et al. (2004b). Glyceraldehyde-3-phosphate dehydrogenase of *Streptococcus oralis* functions as a coadhesin for *Porphyromonas gingivalis* major fimbriae. *Infect. Immun.* 72, 1341–1348. doi: 10.1128/iai.72.3.1341-1348.2004

McNab, R., Forbes, H., Handley, P. S., Loach, D. M., Tannock, G. W., and Jenkinson, H. F. (1999). Cell wall-anchored CshA polypeptide (259 kilodaltons) in *Streptococcus gordonii* forms surface fibrils that confer hydrophobic and adhesive properties. *J. Bacteriol.* 181, 3087–3095.

McNab, R., Holmes, A. R., Clarke, J. M., Tannock, G. W., and Jenkinson, H. F. (1996). Cell surface polypeptide CshA mediates binding of *Streptococcus gordonii* to other oral bacteria and to immobilized fibronectin. *Infect. Immun.* 64, 4204–4210.

Merritt, J. H., Kadouri, D. E., and O'toole, G. A. (2005). Growing and analyzing static biofilms. *Curr. Protoc. Microbiol.* 0 1:Unit–1B.1. doi: 10.1002/9780471729259.mc01b01s00

Metwalli, K. H., Khan, S. A., Krom, B. P., and Jabra-Rizk, M. A. (2013). *Streptococcus mutans*, *Candida albicans*, and the human mouth: a sticky situation. *PLoS Pathog.* 9:e1003616. doi: 10.1371/journal.ppat.1003616

Morales, D. K., and Hogan, D. A. (2010). *Candida albicans* interactions with bacteria in the context of human health and disease. *PLoS Pathog.* 6:e1000886. doi: 10.1371/journal.ppat.1000886

Mulcahy, H., Charron-Mazenod, L., and Lewenza, S. (2008). Extracellular DNA chelates cations and induces antibiotic resistance in *Pseudomonas aeruginosa* biofilms. *PLoS Pathog.* 4:e1000213. doi: 10.1371/journal.ppat.1000213

Nett, J. E., Sanchez, H., Cain, M. T., and Andes, D. R. (2010). Genetic basis of *Candida* biofilm resistance due to drug-sequestering matrix glucan. *J. Infect. Dis.* 202, 171–175. doi: 10.1086/651200

Nobile, C. J., and Mitchell, A. P. (2006). Genetics and genomics of *Candida albicans* biofilm formation. *Cell Microbiol.* 8, 1382–1391. doi: 10.1111/j.1462-5822.2006.00761.x

Nostro, A., Cannatelli, M. A., Crisafi, G., Musolino, A. D., Procopio, F., and Alonzo, V. (2004). Modifications of hydrophobicity, *in vitro* adherence and cellular aggregation of *Streptococcus* mutans by Helichrysum italicum extract. *Lett. Appl. Microbiol.* 38, 423–427. doi: 10.1111/j.1472-765x.2004.01509.x

Odds, F. C. (1987). *Candida* infections: an overview. *Crit. Rev. Microbiol* 15, 1–5.

O'Donnell, L. E., Millhouse, E., Sherry, L., Kean, R., Malcolm, J., Nile, C. J., et al. (2015). Polymicrobial *Candida* biofilms: friends and foe in the oral cavity. *FEMS Yeast Res.* 15:fov077. doi: 10.1093/femsyr/fov077

Porchezhian, E., and Dobriyal, R. M. (2003). An overview on the advances of *Gymnema sylvestre*: chemistry, pharmacology and patents. *Pharmazie* 58, 5–12.

Renga, B., Festa, C., De Marino, S., Di Micco, S., D'auria, M. V., Bifulco, G., et al. (2015). Molecular decodification of gymnemic acids from *Gymnema sylvestre*. Discovery of a new class of liver X receptor antagonists. *Steroids* 96, 121–131. doi: 10.1016/j.steroids.2015.01.024

Ricker, A., Vickerman, M., and Dongari-Bagtzoglou, A. (2014). *Streptococcus gordonii* glucosyltransferase promotes biofilm interactions with *Candida albicans*. *J. Oral. Microbiol.* 6. doi: 10.3402/jom.v6.23419

Righolt, A. J., Jevdjevic, M., Marcenes, W., and Listl, S. (2018). Global-, Regional-, and Country-level economic impacts of dental diseases in 2015. *J. Dent. Res.* 97, 501–507. doi: 10.1177/0022034517750572

Sanematsu, K., Kusakabe, Y., Shigemura, N., Hirokawa, T., Nakamura, S., Imoto, T., et al. (2014). Molecular mechanisms for sweet-suppressing effect of gymnemic acids. *J. Biol. Chem.* 289, 25711–25720. doi: 10.1074/jbc.M114.560409

Saputo, S., Faustoferri, R. C., and Quivey, R. G. Jr. (2018). A drug repositioning approach reveals that *Streptococcus mutans* is susceptible to a diverse range of established antimicrobials and nonantibiotics. *Antimicrob. Agents Chemother.* 62:e1674-17. doi: 10.1128/AAC.01674-17

Silverman, R. J., Nobbs, A. H., Vickerman, M. M., Barbour, M. E., and Jenkinson, H. F. (2010). Interaction of *Candida albicans* cell wall Als3 protein with *Streptococcus gordonii* SspB adhesin promotes development of mixed-species communities. *Infect. Immun.* 78, 4644–4652. doi: 10.1128/IAI.00685-10

Sirover, M. A. (2017). *Glyceraldehyde-3-Phosphate Dehydrogenase (GAPDH). The Quintessential Moonlighting Protein in Normal Cell Function and in Human Disease*. Cambridge, MA: Academic Press, 324.

Sivaprakasam, C., Vijayakumar, R., Arul, M., and Nachiappan, V. (2016). Alteration of mitochondrial phospholipid due to the PLA2 activation in rat brains under cadmium toxicity. *Toxicol. Res.* 5, 1680–1687. doi: 10.1039/c6tx00201c

Tati, S., Davidow, P., Mccall, A., Hwang-Wong, E., Rojas, I. G., Cormack, B., et al. (2016). *Candida glabrata* binding to *Candida albicans* hyphae enables its development in oropharyngeal candidiasis. *PLoS Pathog.* 12:e1005522. doi: 10.1371/journal.ppat.1005522

Uppuluri, P., Lin, L., Alqarihi, A., Luo, G., Youssef, E. G., Alkhazraji, S., et al. (2018). The Hyr1 protein from the fungus *Candida albicans* is a cross kingdom immunotherapeutic target for Acinetobacter bacterial infection. *PLoS Pathog.* 14:e1007056. doi: 10.1371/journal.ppat.1007056

Vediyappan, G., Dumontet, V., Pelissier, F., and D'enfert, C. (2013). Gymnemic acids inhibit hyphal growth and virulence in *Candida albicans*. *PLoS One* 8:e74189. doi: 10.1371/journal.pone.0074189

Vediyappan, G., Rossignol, T., and D'enfert, C. (2010). Interaction of *Candida albicans* biofilms with antifungals: transcriptional response and binding of antifungals to beta-glucans. *Antimicrob. Agents Chemother.* 54, 2096–2111. doi: 10.1128/AAC.01638-09

Vickerman, M. M., Sulavik, M. C., Nowak, J. D., Gardner, N. M., Jones, G. W., and Clewell, D. B. (1997). Nucleotide sequence analysis of the *Streptococcus gordonii* glucosyltransferase gene, gtfG. *DNA Seq.* 7, 83–95. doi: 10.3109/10425179709020155

Wang, Y., Dawid, C., Kottra, G., Daniel, H., and Hofmann, T. (2014). Gymnemic acids inhibit sodium-dependent glucose transporter 1. *J. Agric. Food Chem.* 62, 5925–5931. doi: 10.1021/jf501766u

Wang, Y., Yi, L., Wu, Z., Shao, J., Liu, G., Fan, H., et al. (2012). Comparative proteomic analysis of *Streptococcus suis* biofilms and planktonic cells that identified biofilm infection-related immunogenic proteins. *PLoS One* 7:e33371. doi: 10.1371/journal.pone.0033371

Wilson, D. (2019). *Candida albicans*. *Trends Microbiol.* 27, 188–189. doi: 10.1016/j.tim.2018.10.010

Xu, H., Jenkinson, H. F., and Dongari-Bagtzoglou, A. (2014a). Innocent until proven guilty: mechanisms and roles of *Streptococcus-Candida* interactions in oral health and disease. *Mol. Oral Microbiol.* 29, 99–116. doi: 10.1111/omi.12049

Xu, H., Sobue, T., Thompson, A., Xie, Z., Poon, K., Ricker, A., et al. (2014b). Streptococcal co-infection augments *Candida* pathogenicity by amplifying the mucosal inflammatory response. *Cell Microbiol.* 16, 214–231. doi: 10.1111/cmi.12216

Xu, Y., and Kreth, J. (2013). Role of LytF and AtlS in eDNA release by *Streptococcus gordonii*. *PLoS One* 8:e62339. doi: 10.1371/journal.pone.0062339

Yang, H., Li, K., Yan, H., Liu, S., Wang, Y., and Huang, C. (2017). High-performance therapeutic quercetin-doped adhesive for adhesive-dentin interfaces. *Sci. Rep.* 7:8189. doi: 10.1038/s41598-017-08633-3

Yu, L., Lee, K. K., Ens, K., Doig, P. C., Carpenter, M. R., Staddon, W., et al. (1994). Partial characterization of a *Candida albicans* fimbrial adhesin. *Infect. Immun.* 62, 2834–2842.

Zhu, F., Zhang, H., and Wu, H. (2015). Glycosyltransferase-mediated sweet modification in oral *Streptococci*. *J. Dent. Res.* 94, 659–665. doi: 10.1177/0022034515574865

Zuniga, L. Y., Gonzalez-Ortiz, M., and Martinez-Abundis, E. (2017). Effect of *Gymnema sylvestre* administration on metabolic syndrome, insulin sensitivity, and insulin secretion. *J. Med. Food* 20, 750–754. doi: 10.1089/jmf.2017.0001

Conflict of Interest: The authors declare that the research was conducted in the absence of any commercial or financial relationships that could be construed as a potential conflict of interest.

frontiers in Microbiology

REVIEW
published: 15 November 2019
doi: 10.3389/fmicb.2019.02626

Bringing Community Ecology to Bear on the Issue of Antimicrobial Resistance

Aabir Banerji, Michael Jahne, Michael Herrmann, Nichole Brinkman and Scott Keely*

Office of Research and Development, Center for Environmental Measurement and Modeling, US Environmental Protection Agency, Cincinnati, OH, United States

Antimicrobial resistance (AMR) is a global concern, pertaining not only to human health but also to the health of industry and the environment. AMR research has traditionally focused on genetic exchange mechanisms and abiotic environmental constraints, leaving important aspects of microbial ecology unresolved. The genetic and ecological aspects of AMR, however, not only contribute separately to the problem but also are interrelated. For example, mutualistic associations among microbes such as biofilms can both serve as a barrier to antibiotic penetration and a breeding ground for horizontal exchange of antimicrobial resistance genes (ARGs). In this review, we elucidate how species interactions promote and impede the establishment, maintenance, and spread of ARGs and indicate how management initiatives might benefit from leveraging the principles and tools of community ecology to better understand and manipulate the processes underlying AMR.

Keywords: antibiotic, biofilm, competition, consortia, mutualism, predation, indirect effects

OPEN ACCESS

Edited by:
Giuseppantonio Maisetta, University of Pisa, Italy

Reviewed by:
Jinxin Liu, University of California, Davis, United States
Henry P. Godfrey, New York Medical College, United States

****Correspondence:***
Aabir Banerji
lycanthropuslor@comcast.net

Specialty section:
This article was submitted to Antimicrobials, Resistance and Chemotherapy, a section of the journal Frontiers in Microbiology

Received: *30 August 2019*
Accepted: *29 October 2019*
Published: *15 November 2019*

Citation:
Banerji A, Jahne M, Herrmann M, Brinkman N and Keely S (2019) Bringing Community Ecology to Bear on the Issue of Antimicrobial Resistance. Front. Microbiol. 10:2626. doi: 10.3389/fmicb.2019.02626

INTRODUCTION

As pathogens and other microbes become increasingly and more frequently resistant to antibiotics, concern is growing world-wide that the use of antibiotics for treating and preventing diseases in humans, animals, and plants is rapidly becoming less effective and unsustainable (Nerlich and James, 2009; Defoirdt et al., 2011; Stockwell and Duffy, 2012; Wellington et al., 2013; Aćimović et al., 2015). Antimicrobial resistance (AMR) may, in addition, threaten the health of ecosystems (Grenni et al., 2018) and the performance of businesses that rely on large-scale maintenance of microbial monocultures or AMR-related reporter genes for culinary and industrial fermentation processes (Teuber et al., 1999; Bourdichon et al., 2012; Shaw et al., 2016), food and nutritional supplement cultivation (Richmond and Preiss, 1980; Hallmann and Rappel, 1999; Mišurcová et al., 2012; Wells et al., 2017), bioremediation (Jebelli et al., 2018), energy harvesting and biofuel production (Arora et al., 2015; Wang et al., 2015; Oliver et al., 2016), and the derivation of bioprospects (Strobel and Daisy, 2003; Ferrer et al., 2016) such as dyes (Tuli et al., 2015; Sen et al., 2019) and self-healing concrete (Seifan et al., 2016). Although many strategies to mitigate the threat and current impacts of AMR are presently being explored and enacted, such as altering how antibiotics are administered and regulated to sustain or improve their effectiveness (Fridkin and Gaynes, 1999; Drusano, 2003; Pruden et al., 2013; Chakradhar, 2016), discovering or developing new classes of natural and synthetic antibiotics to supplement or replace the old (Livermore, 2011; Moloney, 2016; Wiese and Imhoff, 2019),

and employing bacteriocins and other scalable alternatives to the use of antibiotics (Joerger, 2003; Reardon, 2015; Czaplewski et al., 2016; Willing et al., 2018), the problem remains. At the root of this problem is the One Health nature of AMR; i.e., the interconnectedness among human, animal, and environmental systems (**Figure 1A**; Collignon and McEwen, 2019).

To begin to address this interconnectedness, we must acknowledge that resistance to antibiotics may not be the primary or original (evolutionary) purpose of antimicrobial resistance genes (ARGs). ARGs occur naturally in the environment, where they have been shown or posited to confer protection against toxins such as heavy metals and host-produced biocides and to perform important roles in cellular processes such as quorum sensing (the detection of conspecific or cooperative cells in the environment, associated with cell-to-cell communication/signaling and group activity) and biosynthesis (the enzymatic conversion of simple compounds into more complex products by living things; **Figure 1B**; Allen et al., 2010; Martinez, 2018). Indeed, ARGs are detected even in habitats that have historically been sheltered from antibiotic pollution and other forms of anthropogenic disturbance (McArthur et al., 2016; Van Goethem et al., 2018). Many antibiotic-producing microbes possess ARGs, ensuring that they are resistant or immune to their own antibiotics (Benveniste and Davies, 1973). Antibiotic-producing microbes may thus be a

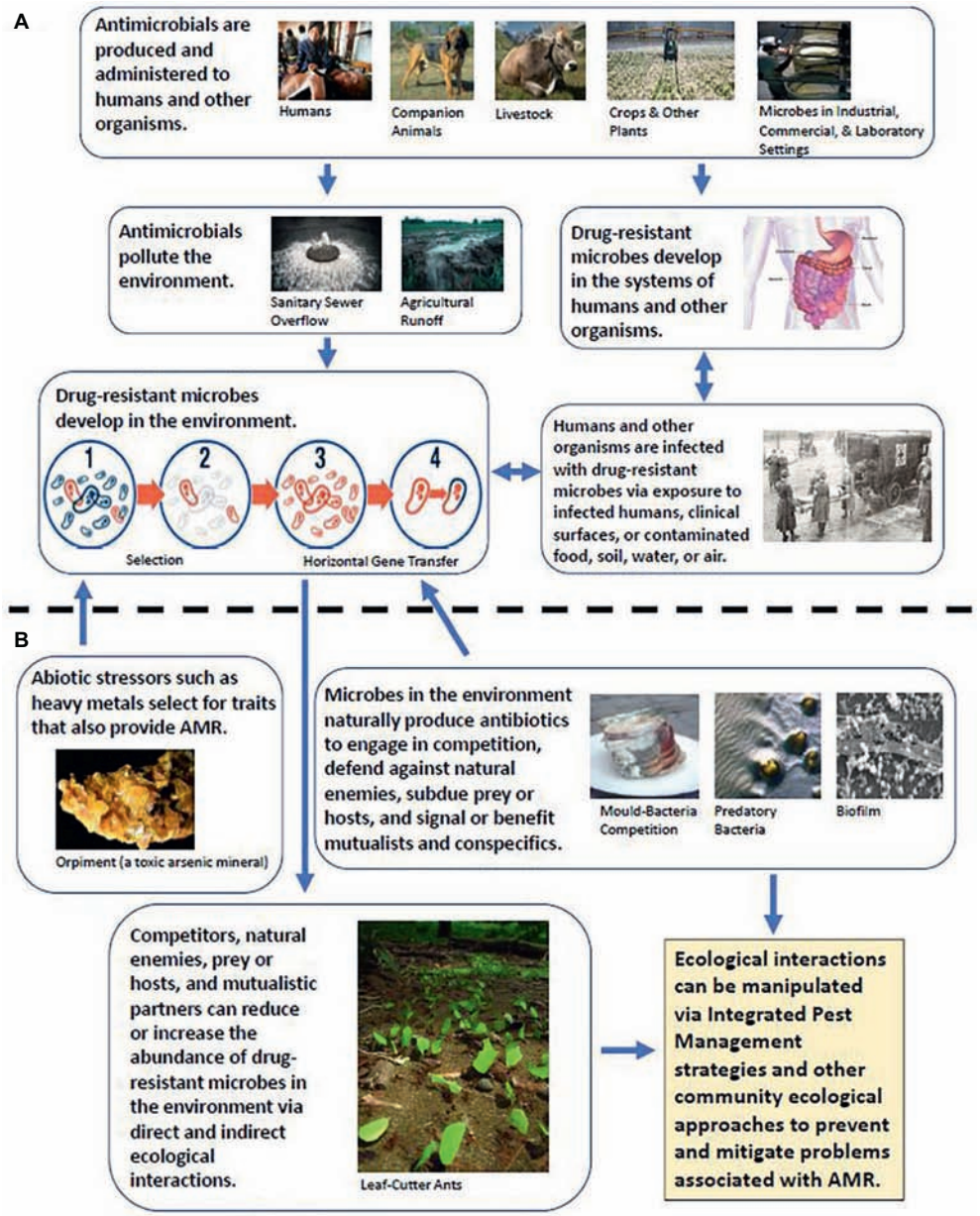

FIGURE 1 | (A) Traditional view of AMR, wherein the environment and wildlife mostly represent opportunities for exposure and/or reservoirs of drug-resistant microorganisms. **(B)** Expansion of the traditional view of AMR to include the effects and potential management implications of species interactions.

source of ARGs in sympatric species *via* horizontal gene transfer (Jiang et al., 2017; Ringel et al., 2017) or select for AMR in the targets of their antibiotics (Wellington et al., 2013), resulting in an "arms race" of cyclical coevolutionary dynamics known as "Red Queen" dynamics (Baron et al., 2018; Decaestecker and King, 2019). From the standpoint of managing AMR, this poses two separate challenges. First, for any new class of antibiotic discovered in nature, there may already be a corresponding suite of ARGs among or transferrable to pathogens (Bengtsson-Palme and Larsson, 2015). Second, efforts to monitor changes in ARG prevalence and identify areas of concern based on comparison to a "least disturbed" reference site may need to account for natural environmental variations in the reference site that favor the natural producers or production of antibiotics. Reference sites may themselves become areas of concern under certain conditions and should, in any case, be critically reviewed to ensure their appropriateness as a baseline of comparison (White and Walker, 1997; Whittier et al., 2007; Berendonk et al., 2015; Rothrock et al., 2016; Vikesland et al., 2017).

High-throughput "-omics" techniques, including genomics, transcriptomics, metabolomics, and proteomics, have greatly enhanced our ability to detect and quantify presence of antibiotic-resistant strains, identify modes of transmission of ARGs, and illuminate complex expression pathways and epigenetic mechanisms (Cockerill, 1999; Cohen et al., 2015; Huijbers et al., 2015; Motta et al., 2015; dos Santos et al., 2016; Anjum et al., 2017). These techniques can be useful for establishing best management practices to reduce antimicrobial resistance (Durante-Mangoni and Zarrilli, 2011; Cohen et al., 2015), estimating and monitoring risk of exposure to antibiotic-resistant pathogens (Brul et al., 2012; Tyson et al., 2015; Haddad et al., 2018; Brockhurst et al., 2019), and assessing environmental impacts of antibiotic pollution (Cairns et al., 2018b; Danner et al., 2019). They have helped to uncover critical roles that the environment plays in determining the establishment, maintenance, and spread of ARGs *via* mechanisms such as co-selection, co-resistance, cross-resistance, hypermutation, and exchanges of plasmids, transposons, and integrons (Seiler and Berendonk, 2012; Singer et al., 2016; Pal et al., 2017). However, while the value of these insights and of the as-yet untapped potential of -omics techniques in general cannot be overstated, elucidation of the molecular biology of AMR should complement, not overshadow, our understanding of underlying ecological processes, such as the relationships that microbes have with other species in the environment (US Centers for Disease Control and Prevention and UK Science and Innovation Network, 2018; Brockhurst et al., 2019). Here, we review some of these ecological relationships, discuss their implications for AMR management, and highlight existing frameworks in community ecology that could be used to address the problem of AMR holistically and robustly.

SPECIES INTERACTIONS INVOLVING ANTIMICROBIAL RESISTANCE

Competition

Although the intracellular and ecological functions of antibiotics in nature are varied and, in many cases, uncertain, at least some of the organisms that produce antibiotics appear to use them for allelopathy, "chemical warfare" with competing species (Sturz et al., 1998; Baquero et al., 2009; Raaijmakers and Mazzola, 2012; Chevrette and Currie, 2019). *Penicillium notatum*, for example, the mold famously discovered by Alexander Fleming to produce penicillin, was found, in that instance, to compete for resources and space with the bacterium *Staphylococcus aureus* (Demain and Elander, 1999; Bennett and Chung, 2001). This situation could increase the prevalence of ARGs in the environment, as ARG-possessing antibiotic producers outcompete their targets or as targets evolve ARGs in response to their competitors' antibiotics. Even if microbes do not engage in allelopathy, possessing ARGs may increase their biological fitness due to co-benefits of the resistance mechanisms (e.g., ARGs coding for or regulating efflux pumps simultaneously provide resistance to heavy metals and other toxic compounds; Allen et al., 2010). On the other hand, if resource limitation is the predominant driver of microbial population dynamics and phenotypic plasticity in the expression of ARGs is insufficient to reduce costs (Auld et al., 2009), then microbes that do not house ARGs may have a competitive advantage over microbes that do, due to the energetic expenses or other physiological tradeoffs associated with ARGs (Kang and Park, 2010; Basra et al., 2018).

Moreover, under certain conditions, ARG-possessing microbes might facilitate rather than competitively exclude other microbes (Klümper et al., 2019). This has been shown to occur in one of two ways: through mutualism, which we describe in the next section, or through exploitation of "leaky" or "public" resistance mechanisms. For example, susceptible microbes can benefit from neighboring ARG-possessing competitors' production and release of signaling compounds such as indole, a compound which activates drug efflux pumps and oxidative-stress protective mechanisms (Lee et al., 2010). As previously mentioned, antibiotics themselves may serve as signaling compounds, though they are more likely to be utilized by conspecifics and mutualistic symbionts than by competitors (Allen et al., 2010). Relative costliness of ARGs may create a selection pressure favoring exploiters over resistance builders, so that only the microbes that require ARGs for essential life processes retain their ARGs over time. Such "race to the bottom" coevolutionary dynamics are known as "Black Queen" dynamics (Morris et al., 2012; Cairns et al., 2018a). Microbes exhibiting Black Queen dynamics would represent a best-case scenario for human priorities regarding the evolution of AMR in pathogens, since it would entail selection against ARGs even under conditions favoring AMR.

Mutualism

The term "mutualism" refers to a relationship of mutually beneficial exchanges between different species (Hoeksema and Bruna, 2000). Certain mutualisms can enable microbes to acquire AMR without necessarily possessing their own independent ARGs. Two such mutualisms that have garnered attention in clinical settings and nutritional science are microbial biofilms and syntrophic consortia. Biofilms are structured associations of microbes that form on surfaces, including within

food processing and water treatment facilities, various medical devices, and the human body (Donlan, 2002; Chmielewski and Frank, 2006; Ling et al., 2015; Kovach et al., 2017; Hu et al., 2018). They provide microbes with defenses against adverse conditions, increased efficiency in sequestering and assimilating nutrients, and other cooperative benefits (Jefferson, 2004; Nadell et al., 2016; Zhang et al., 2018). Syntrophic consortia are symbiotic associations of two or more microbial groups that allow for synthesis or degredation of substances that few or none of the constituent microbes would be able to synthesize or degrade on their own (Madigan et al., 2009; Morris et al., 2013; Bradáčová et al., 2019). Note that these characterizations are not mutually exclusive of one another: a biofilm can be a consortium and vice versa, depending on its location, form, and benefits.

The formation of biofilms can not only enhance the horizontal exchange of ARGs among constituent microbes (Molin and Tolker-Nielsen, 2003) but also confer AMR based on the physical and chemical structure of exopolysaccharides and other features of biofilm architecture shielding the constituent microbes' cell envelopes (Mah and O'Tool, 2001; Jałowiecki et al., 2018). In addition, biofilms can provide resistance based on less intuitive mechanisms, such as slowed growth and inhibition of targeted metabolic processes (Olsen, 2015), achieved through the release of toxins by core constituent microbes (Lewis, 2005). Similarly, syntrophic consortia can allow microbes to gain AMR by creating enzymes in assembly-line fashion that degrade or inhibit antibiotics (e.g., β-lactamases; Olsen, 2015). This can be based on a small number of constituent microbes synthesizing the enzymes and the rest either supplying essential resources (Fan and He, 2011; Liu et al., 2017) or ameliorating factors such oxidative stress (Shatalin et al., 2011), or it can be based on multiple constituent microbes each synthesizing complementary parts of the enzymes (Burmølle et al., 2006; Islas-Espinoza et al., 2012). Mutualisms giving rise to exogenous or emergent AMR may call for the development of new methods of assessing antibiotic susceptibility that go beyond screening for conventional ARGs, at least in the case of the microbes known to engage in such mutualisms.

Predation and Parasitism

Microbes are often the prey or hosts of other species, including other microbes. Use of these natural enemies as biological control agents to combat clinical pathogens is a hot-topic area of research (which we delve deeper into in a later section) and has been shown to be effective under certain circumstances (Kutateladze and Adamia, 2010), including where pathogens already exhibit AMR (Willis et al., 2016). In natural environmental contexts, the influence of predation and parasitism on ARGs and AMR is complicated by the fact that certain predators and parasites produce antibiotics to subdue their prey or hosts and certain prey and hosts produce antibiotics to defend themselves from predators and parasites. For instance, predatory myxobacteria utilize antibiotics (myxovirescin and corallopyronin) to subdue prey such as *Escherichia coli* (Xiao et al., 2011), as does the non-obligate predator *Aristabacter necator* Strain 679-2 (pyrrolnitrin, maculosin, and banegasine; Cain et al., 2003). Antarctic sponges of the genus *Crella* produce antibiotic steroids (norselic acids A–E) that deter predators such as the amphipod *Gondogeneia antarctica*, as well as protozoan parasites of the genus *Leishmania* (Ma et al., 2009). Antibiotic-producing consumers and resources, like other antibiotic-producing organisms, may be sources of ARGs in sympatric species and select for AMR in the targets of their antibiotics.

Complex Associations and Indirect Effects

Although the broad categories of competition, mutualism, and predation/parasitism accommodate the entire spectrum of fundamental pairwise relationships within ecology (from mutually detrimental to mutually beneficial), these pairwise relationships do not exist in a vacuum. In the context of real-world ecological communities, mutualisms can enable predators and parasites to subdue their prey or hosts (Hwang et al., 1989; Mlot, 1997; Jones and Nishiguchi, 2004; Shiga, 2005), enable prey or hosts to fend off their predators and parasites (Soler et al., 2010; Pauli et al., 2014; Flórez et al., 2015; Van Arnam et al., 2018; Chevrette and Currie, 2019), and enable competitors to exclude their rivals (Preer et al., 1953; Brown et al., 2008; Mangla et al., 2008). Some of these complex associations and indirect interactions are mediated by antibiotics and ARGs. For example, the medicinal plant *Leptospermum scoparium* relies on endophytic bacteria to produce antibiotics such as phenazine and 2,4-diacetylphloroglucinol, which inhibit infection of the plant by pathogens such as *Pseudomonas syringae* pv. actinidiae (Wicaksono et al., 2018). Wicaksono et al. (2018) found that these bacteria were transmissible to other plants and could therefore be used for biological control of the plant diseases. Similarly, the pest beetle *Lagria villosa* relies on *Burkholderia gladioli* to produce icosalide, a lipocyclopeptide antibiotic that protects the beetle's offspring from entomopathogenic bacteria (Dose et al., 2018), bacteria which predatory nematodes often rely on to envenomate prey (Mlot, 1997). Fungus-growing attine ants weed out microfungal parasites (competitors for the ants' food) of the genus *Escovopsis* from their fungal gardens using antibiotics produced by a streptomycete bacterium that resides within their cuticles (Currie et al., 2003; Little and Currie, 2007). There is evidence to suggest that the ants might deliberately (arguably "artificially") select their antibiotic-producing bacteria (Barke et al., 2011) and that the nature of the relationship has permitted the antibiotics to remain effective in controlling the parasitic fungi despite millions of years of coevolution (Pathak et al., 2019). In a study that had implications for agriculture, Li and Alexander (1988) found that use of antibiotic-producing soil inoculants can enhance crop yield and resilience by increasing colonization and nodulation by rhizobia.

Antibiotics and ARGs associated with symbionts of macroscopic hosts seem, at first glance, unlikely to be an important source of antibiotics and ARGs in clinical, industrial, or water treatment settings. If they have shared a long co-evolutionary history with their macroscopic hosts, the symbionts will likely have lost certain functional traits that are important to the fitness of their free-living counterparts (Bennett and Moran, 2015) and have as restricted a geographical distribution as their hosts (Martiny et al., 2006; Joseph et al., 2016). Three caveats to consider, however, are that: (1) even

if the symbionts die when their hosts die, the symbionts' antibiotics and genes are released into the environment; (2) animal migration, human globalization, and other modes of dispersal all permit spread to management-relevant environments (Brown and Barker, 1999; Molmeret et al., 2005; Allen et al., 2010; Forsberg et al., 2012; Zurek and Ghosh, 2014); and (3) many hosts of microbial symbionts are known vectors of disease. Investigating what Galimand et al. (2006) have referred to as a "clinically ominous event," Hinnebusch et al. (2002) demonstrated that horizontal gene transfer among the microbes inside the Oriental rat flea *Xenopsylla cheopis* may have been the cause of AMR in *Yersinia pestis* strains isolated from bubonic plague patients in Madagascar.

COMMUNITY ECOLOGICAL APPROACHES TO ADDRESSING ANTIMICROBIAL RESISTANCE

While using methods such as -omics to comprehensively profile microbial communities both in and out of clinical settings is still a major priority, the biological data produced through these methods must ultimately be interpreted and synthesized for there to be progress in addressing the problem. The frameworks for this synthesis currently exist within community ecology. Two that are well-established and appropriate for the task are "integrated pest management" and "ecological succession."

Integrated Pest Management

Integrated pest management (IPM) is a strategy designed to safeguard human health and the environment while avoiding, attenuating, or delaying pest outbreaks or associated damages (Kogan, 1998; Liang et al., 2015). Historically, the major focus of IPM has been minimization of pesticide use and enhancement of its efficacy in targeting herbivorous insects, weeds, and vectors of disease. Part of the motivation for this focus is that pesticides, globally, have promoted pesticide resistance among target species, adversely impacted non-target and beneficial organisms, and, in some cases, proven to be persistent in the environment (Barzman et al., 2015). The issue is analogous to that of antibiotics promoting AMR and other adverse outcomes. Although Magarey et al. (2019) and others (Fidler, 1998; Orzech and Nichter, 2008) have noted that complex cultural, legal, and socioeconomic factors underlie both issues and must be addressed for management practices to be successful, we focus here on providing basic understanding of relevant IPM approaches and elucidating how they might be applied in the context of AMR. Specifically, we consider the approaches of biological control and habitat manipulation.

Biological control is the use of living organisms to control pests. As previously stated, microbes, including those possessing ARGs, have natural enemies such as predators and parasites. A few studies highlight the potential of using these natural enemies to control pathogens responsible for post-harvest diseases of fruits and vegetables (Wilson et al., 1993), tree and woody plant diseases (Cazorla and Mercado-Blanco, 2016), and even diseases within humans and domesticated animals (Negus et al., 2017). Among the presently favored candidate biological control agents are protozoan bacterivores and plasmid-dependent bacteriophages. By decreasing microbial population abundance (the prerequisite for heritable variation and population viability) and exacting opposing selection pressures (compared to those exacted by antibiotics, other natural enemies, or competing microbes), these consumers can theoretically replace antibiotics or enhance the effectiveness of antibiotics and reduce the likelihood of AMR (Hiltunen et al., 2017; Cairns et al., 2018a,b).

Unfortunately, evidence is conflicting as to whether there are tradeoffs between AMR and defense against natural enemies. For example, whereas Chen et al. (2017b) found that AMR coincides with increased susceptibility to bacteriophages, Allen et al. (2017) found that AMR is associated with increased resistance to bacteriophages. If indeed AMR provides the co-benefit of defense against natural enemies, introduction of natural enemies may amplify the effectiveness and prevalence of AMR rather than decrease it. Moreover, in the environment of a gut or epiphytic microbiome, bacteriophages or other natural enemies of microbes may affect microbes that are necessary or beneficial for overall health more than they affect ARG-possessing pathogens. Equivalently, the natural enemies may prevent competitively inferior ARG-possessing microbes from being excluded by other microbes (Bohannan et al., 2002), in a manner akin to "keystone predation" (where apex predators preferentially feed on superior resource competitors, promoting biodiversity among the prey; Amarasekare, 2008).

Due to these concerns, biological control of pathogens, especially within humans and domesticated animals, requires forethought and the means to ensure that "ecological release" of the biological control agents and other potential adverse outcomes do not occur within or on the patients (Miller and Aplet, 1993; Louda et al., 2003; Shanmuganathan et al., 2009). Barratt et al. (2010) noted that numerous recent advances in risk assessment methodologies have helped to minimize the possibility of adverse outcomes of biological control. These include multi-factorial assessments of control agent viability, quarantine laboratory host range testing, pre- and post-release studies incorporating mechanistic population dynamics models, and meta-analysis of cumulative data from past introductions. Each of these advances (with the possible exception of meta-analysis of past introductions) can be tailored to evaluate the efficacy of biological control of pathogens and AMR. For example, comprehensive profiles of microbial communities both in and out of clinical settings can be assembled *via* sampling and manipulative experiments and be used to establish the host/prey specificity of putative biological control agents or select the most appropriate stage of infection or population growth at which to introduce biological control agents.

Habitat manipulation entails altering the physical, chemical, or biological structure of the landscape to inhibit pests or to benefit or manipulate the natural enemies and competitors of the pests. This includes creating or manipulating breeding grounds and refuges against adverse abiotic conditions, such as overwintering sites in terrestrial systems (Griffiths et al., 2008) or zones of oxygenated hypolimnion in aquatic systems

(Klumb et al., 2004). It also includes providing incentives for pests to leave or reduce their impacts (e.g., trap crops; Badenes-Perez et al., 2004), targeting the pests' symbionts and vectors (Beard et al., 2002; Pocquet et al., 2014), and introducing alternative prey or hosts to amplify the effects of natural enemies *via* apparent competition (Holt and Bonsall, 2017). In the context of managing AMR, the "landscape" may be outdoor environments and open public spaces serving as source pools of ARGs or hubs of transmission; indoor facilities and equipment; or individual vector, host, or patient microbiomes. At the larger scale, habitat manipulation might thus entail familiar tactics such as regulating and remediating pollutants, employing safe and sustainable hygiene practices, and removing conditions that favor human, plant, or animal exposure to vectors of disease. In the case of microbiomes, analogues of altering abiotic conditions, targeting of pests' symbionts, and introducing alternative prey or hosts to amplify natural enemies' effects might include manipulating dietary nutrients, utilizing prophylactics and probiotics (see, however, Gueimonde et al., 2013 for a cautionary perspective on this approach), and targeting non-pathogenic (or less pathogenic) mutualistic partners of pathogens rather than the pathogens themselves. Recent preliminary studies have even suggested that microbes not ordinarily present in the hosts' organs could be employed for this purpose; e.g., photosynthetic cyanobacteria could be injected into the heart to convert blood carbon dioxide to oxygen and thereby inhibit the causes and symptoms of heart disease and necrosis (Cohen et al., 2017). Treatment strategies that counteract the benefit of exogenous or emergent AMR, such as the use of agents that disrupt quorum sensing or target specific components of the biofilm matrix and the use of biofilm-penetrating antibiotics, would also be a worthwhile extension of the principle of habitat manipulation (Donlan, 2000; Sully et al., 2014).

Ecological Succession

Ecological succession is the phenomenon of biological communities forming or re-assembling and changing over time following natural or anthropogenic disturbances. These disturbances can include influx or loss of resources or habitat structure (e.g., due to urban development), invasion of the ecological community by exotic species, and changes in abiotic conditions due to seasonality or pollution. They can also often be autochthonous, as in the case of pioneer lichen creating soil from bare rock (Shure and Ragsdale, 1977). Patterns of succession affect functional traits within species and interaction strengths among species and depend on factors such as disturbance severity and species' dispersal limitations (Chang and Turner, 2019). Ecological succession theory has been developed within classical microbiology, even including versions of the concepts of *r*- and *K*-strategists (Dorodnikov et al., 2009). However, two popular microbiological paradigms have created some divergence between microbial ecological succession theory and classical ecological succession theory: that of "everything is everywhere, and the environment selects" (O'Malley, 2007) and of microbial utilization of resources being determined thermodynamically by reduction-oxidation reaction-related processes (a.k.a. the "Redox Tower"; Delattre et al., 2019). Through the lens of these paradigms, antibiotics constitute two separate forms of disturbance: a selection pressure against non-resistant microbes (which would release some of their metabolic resources and space, making them available to other microbes) and a metabolic resource for AMR-exhibiting microbes. Combining this concept with an understanding of the previously mentioned syntrophic consortia, it may be possible to predict the rate at which and extent to which antibiotics would be enzymatically degraded in the presence of particular microbial assemblages and the likelihood of ARG spread within those assemblages. This information could be used to assess or predict environmental impacts and legacy effects of antibiotics or to develop novel mitigation strategies. To some extent, it has already been used to develop or enhance certain bioremediation techniques (US Environmental Protection Agency, 2013).

However, real-world microbial succession is typically more complicated (Chen et al., 2017a). Within microbiomes of macroscopic hosts, various potential metabolic resources can become available simultaneously (e.g., *via* mixed diets), and host immune responses, natural enemies, and competitors of various kinds may also be present. Furthermore, as stated previously, microbes can obtain exogenous or emergent AMR *via* exploitation of ARG-possessing microbes, potentially promoting Black Queen coevolutionary dynamics (see *Competition* subsection of Species Interactions Involving AMR). Depending on the level of impact it has on the ARG-possessing microbes, this could allow for coexistence or be analogous to successional replacement of "pioneer" and "nurse" plants (Whittaker, 1993; Tewksbury and Lloyd, 2001). Conceptual models within classical ecological succession theory that could be used to predict such outcomes include that of "alternative stable states" (Fukami and Nakajima, 2011) and that of the "Stress-Gradient Hypothesis" (Bertness and Callaway, 1994). The latter, originally developed for terrestrial plant communities (and later refined by Malkinson and Tielbörger, 2010), posits that, among potential competitors, intense grazing pressure or abiotic stress can increase the prevalence and importance of facilitative interactions such as "associational defense" and "neighborhood habitat amelioration," provided that the competitors possess adequate complementarity in their physiological traits. Studies of AMR across gradients of antibiotic pollution, other abiotic stress, and bacterivore biodiversity (e.g., Baquero and Negri, 1997; Dunivin and Shade, 2018; Harmand et al., 2018) could be used to parameterize numerical simulations based on the hypothesis and test whether facilitative interactions in the form of AMR-conferring multi-species syntrophic consortia and biofilms occur as predicted along these gradients.

DISCUSSION

AMR is a global human health concern, exacerbated by human population growth and socioeconomic inequity (Allcock et al., 2017; Jensen et al., 2019), climate change (MacFadden et al., 2018), and biological warfare/terrorism (Inglesby et al., 2000). It is also a pressing concern within the realms of industry, food production, and environmental health (**Figure 1**). The approach of "kill everything susceptible for as long as it is susceptible" has proven to be short-sighted and costly, with

far-reaching implications. The relationships that microbes have with other species are an integral component of AMR ecology and should therefore be accounted for in both management initiatives and basic research. As we have described above, these relationships can have significant and sometimes multifaceted roles in determining the prevalence and distribution of AMR and ARGs. They and their effects call for subtle changes in our thinking regarding the boundaries of the problem that allow for innovations in the management of AMR, innovations that could easily and appropriately draw from existing frameworks within the field of community ecology. Priorities that would enable this progress include further characterizing AMR ecology in complex microbial communities and formally articulating and evaluating the links between this ecology and the risks to human and environmental health *via* mechanistic models and experimental tests of ecological theory.

Among the many questions still needing to be addressed regarding AMR ecology is what impact ARGs have on the longevity and infectivity of pathogens in the environment, outside of their hosts. Although many studies have traced ARGs introduced through human activities such as the generation of wastewaters, few have examined how the microbes associated with these ARGs persist and interact with other species in their new surroundings (Rodriguez-Mozaz et al., 2015; Bengtsson-Palme et al., 2017; Smalla et al., 2018). Knowing how frequently horizontal gene transfer of ARGs occurs among mutualistic symbionts, across trophic levels of microbial food webs, and in general (and, more importantly, knowing why) would enable researchers to better estimate the probability of non-pathogenic organisms with ARGs spreading resistance to the pathogens of humans, plants, and domesticated animals (Cairns et al., 2018a,b). Ideally, future research and mitigation efforts will leverage the fundamentals of modern microbial ecology, bringing together the principles and tools of molecular genetics, classical microbiology, and community ecology to allow us to better understand and manage the processes driving this complex challenge.

AUTHOR CONTRIBUTIONS

AB provided the premise and framework of the manuscript and contributed the bulk of the writing and literature review pertaining to ecological theory and applications. MJ, MH, NB, and SK each contributed to the background regarding molecular/genetic aspects of AMR and AMR-related exposure risks, assisted in proof-reading, and helped to finalize the overall scope of the manuscript.

FUNDING

The U.S. Environmental Protection Agency, through its Office of Research and Development, partially funded and participated in the research described herein. Any opinions expressed in this paper are those of the authors and do not necessarily reflect the views of the agency; therefore, no official endorsement should be inferred. Any mention of trade names or commercial products does not constitute endorsement or recommendation for use.

ACKNOWLEDGMENTS

We gratefully acknowledge Jay Garland, Eric Villegas, Mark Bagley, Jorge Santo Domingo, and our reviewers for their insights. All photographic images were obtained from the public domain (Wikimedia Commons, the free media repository).

REFERENCES

Aćimović, S. G., Zeng, Q., McGhee, G. C., Sundin, G. W., and Wise, J. C. (2015). Control of fire blight (*Erwinia amylovora*) on apple trees with trunk-injected plant resistance inducers and antibiotics and assessment of induction of pathogenesis-related protein genes. *Front. Plant Sci.* 6:16. doi: 10.3389/fpls.2015.00016

Allcock, S., Young, E. H., Holmes, M., Gurdasani, D., Dougan, G., Sandhu, M. S., et al. (2017). Antimicrobial resistance in human populations: challenges and opportunities. *Glob. Health Epidemiol. Genom.* 2:e4. doi: 10.1017/gheg.2017.12

Allen, H. K., Donato, J., Wang, H. H., Cloud-Hansen, K. A., Davies, J., and Handelsman, J. (2010). Call of the wild: antibiotic resistance genes in natural environments. *Nat. Rev. Microbiol.* 8, 251–259. doi: 10.1038/nrmicro2312

Allen, R. C., Pfrunder-Cardozo, K. R., Meinel, D., Egli, A., and Hall, A. R. (2017). Associations among antibiotic and phage resistance phenotypes in natural and clinical *Escherichia coli* isolates. *MBio* 8, e01341–e01317. doi: 10.1128/mBio.01341-17

Amarasekare, P. (2008). Spatial dynamics of keystone predation. *J. Anim. Ecol.* 77, 1306–1315. doi: 10.1111/j.1365-2656.2008.01439.x

Anjum, M. F., Zankari, E., and Hasman, H. (2017). Molecular methods for detection of antimicrobial resistance. *Microbiol. Spectr.* 5. doi: 10.1128/microbiolspec.ARBA-0011-2017

Arora, R., Behera, S., and Kumar, S. (2015). Bioprospecting thermophilic/thermotolerant microbes for production of lignocellulosic ethanol: a future perspective. *Renew. Sust. Energ. Rev.* 51, 699–717. doi: 10.1016/j.rser.2015.06.050

Auld, J. R., Agrawal, A. A., and Relyea, R. A. (2009). Re-evaluating the costs and limits of adaptive phenotypic plasticity. *Proc. R. Soc. B* 277, 503–511. doi: 10.1098/rspb.2009.1355

Badenes-Perez, F. R., Shelton, A. M., and Nault, B. A. (2004). Evaluating trap crops for diamondback moth, *Plutella xylostella* (Lepidoptera: Plutellidae). *J. Econ. Entomol.* 97, 1365–1372. doi: 10.1093/jee/97.4.1365

Baquero, F., Alvarez-Ortega, C., and Martinez, J. L. (2009). Ecology and evolution of antibiotic resistance. *Environ. Microbiol. Rep.* 1, 469–476. doi: 10.1111/j.1758-2229.2009.00053.x

Baquero, F., and Negri, M. C. (1997). Selective compartments for resistant microorganisms in antibiotic gradients. *BioEssays* 19, 731–736. doi: 10.1002/bies.950190814

Barke, J., Seipke, R. F., Yu, D. W., and Hutchings, M. I. (2011). A mutualistic microbiome: how do fungus-growing ants select their antibiotic-producing bacteria? *Commun. Integr. Biol.* 4, 41–43. doi: 10.4161/cib.4.1.13552

Baron, S. A., Diene, S. M., and Rolain, J.-M. (2018). Human microbiomes and antibiotic resistance. *Hum. Microbiome J.* 10, 43–52. doi: 10.1016/j.humic.2018.08.005

Barratt, B. I. P., Howarth, F. G., Withers, T. M., Kean, J. M., and Ridley, G. S. (2010). Progress in risk assessment for classical biological control. *Biol. Control* 52, 245–254. doi: 10.1016/j.biocontrol.2009.02.012

Barzman, M., Bàrberi, P., Birch, A. N. E., Boonekamp, P., Dachbrodt-Saaydeh, S., Graf, B., et al. (2015). Eight principles of integrated pest management. *Agron. Sustain. Dev.* 35, 1199–1215. doi: 10.1007/s13593-015-0327-9

Basra, P., Alsaadi, A., Bernal-Astrain, G., O'Sullivan, M. L., Hazlett, B., Clarke, L. M., et al. (2018). Fitness tradeoffs of antibiotic resistance in extraintestinal

pathogenic *Escherichia coli*. *Genome Biol. Evol.* 10, 667–679. doi: 10.1093/gbe/evy030

Beard, C. B., Cordon-Rosales, C., and Durvasula, R. V. (2002). Bacterial symbionts of the triatominae and their potential use in control of Chagas disease transmission. *Annu. Rev. Entomol.* 47, 123–141. doi: 10.1146/annurev.ento.47.091201.145144

Bengtsson-Palme, J., Kristiansson, E., and Larsson, D. G. J. (2017). Environmental factors influencing the development and spread of antibiotic resistance. *FEMS Microbiol. Rev.* 42:p.fux053. doi: 10.1093/femsre/fux053

Bengtsson-Palme, J., and Larsson, D. G. J. (2015). Antibiotic resistance genes in the environment: prioritizing risks. *Nat. Rev. Microbiol.* 13:396. doi: 10.1038/nrmicro3399-c1

Bennett, J. W., and Chung, K.-T. (2001). Alexander Fleming and the discovery of penicillin. *Adv. Appl. Microbiol.* 49, 163–184. doi: 10.1016/S0065-2164(01)49013-7

Bennett, G. M., and Moran, N. A. (2015). Heritable symbiosis: the advantages and perils of an evolutionary rabbit hole. *Proc. Natl. Acad. Sci. USA* 112, 10169–10176. doi: 10.1073/pnas.1421388112

Benveniste, R., and Davies, J. (1973). Aminoglycoside antibiotic-inactivating enzymes in actinomycetes similar to those present in clinical isolates of antibiotic-resistant bacteria. *Proc. Natl. Acad. Sci. USA* 70, 2276–2280.

Berendonk, T. U., Manaia, C. M., Merlin, C., Fatta-Kassinos, D., Cytryn, E., Walsh, F., et al. (2015). Tackling antibiotic resistance: the environmental framework. *Nat. Rev. Microbiol.* 13, 310–317. doi: 10.1038/nrmicro3439

Bertness, M. D., and Callaway, R. (1994). Positive interactions in communities. *Trends Ecol. Evol.* 9, 191–193.

Bohannan, B. J. M., Kerr, B., Jessup, C. M., Hughes, J. B., and Sandvik, G. (2002). Trade-offs and coexistence in microbial microcosms. *Antonie Van Leeuwenhoek* 81, 107–115. doi: 10.1023/A:1020585711378

Bourdichon, F., Casaregola, S., Farrokh, C., Frisvad, J. C., Gerds, M. L., Hammes, W. P., et al. (2012). Food fermentations: microorganisms with technological beneficial use. *Int. J. Food Microbiol.* 154, 87–97. doi: 10.1016/j.ijfoodmicro.2011.12.030

Bradáčová, K., Florea, A. S., Bar-Tal, A., Minz, D., Yermiyahu, U., Shawahna, R., et al. (2019). Microbial consortia versus single-strain inoculants: an advantage in PGPM-assisted tomato production? *Agronomy* 9:105. doi: 10.3390/agronomy9020105

Brockhurst, M. A., Harrison, F., Veening, J.-W., Harrison, E., Blackwell, G., Iqbal, Z., et al. (2019). Assessing evolutionary risks of resistance for new antimicrobial therapies. *Nat. Ecol. Evol.* 3, 515–517. doi: 10.1038/s41559-019-0854-x

Brown, M. R. W., and Barker, J. (1999). Unexplored reservoirs of pathogenic bacteria: protozoa and biofilms. *Trends Microbiol.* 7, 46–50.

Brown, S. P., Le Chat, L., and Taddei, F. (2008). Evolution of virulence: triggering host inflammation allows invading pathogens to exclude competitors. *Ecol. Lett.* 11, 44–51. doi: 10.1111/j.1461-0248.2007.01125.x

Brul, S., Bassett, J., Cook, P., Kathariou, S., McClure, P., Jasti, P. R., et al. (2012). 'Omics' technologies in quantitative microbial risk assessment. *Trends Food Sci. Technol.* 27, 12–24. doi: 10.1016/j.tifs.2012.04.004

Burmølle, M., Webb, J. S., Rao, D., Hansen, L. H., Sørensen, S. J., and Kjelleberg, S. (2006). Enhanced biofilm formation and increased resistance to antimicrobial agents and bacterial invasion are caused by synergistic interactions in multispecies biofilms. *Appl. Environ. Microbiol.* 72, 3916–3923. doi: 10.1128/AEM.03022-05

Cain, C. C., Lee, D., Waldo, R. H. III, Henry, A. T., Casida, E. J. Jr., Wani, M. C., et al. (2003). Synergistic antimicrobial activity of metabolites produced by a nonobligate bacterial predator. *Antimicrob. Agents Chemother.* 47, 2113–2117. doi: 10.1128/AAC.47.7.2113-2117.2003

Cairns, J., Koskinen, K., Penttinen, R., Patinen, T., Hartikainen, A., Jokela, R., et al. (2018a). Black queen evolution and trophic interactions determine plasmid survival after the disruption of the conjugation network. *mSystems* 3, e00104–e00118. doi: 10.1128/mSystems.00104-18

Cairns, J., Ruokolainen, L., Hultman, J., Tamminen, M., Virta, M., and Hiltunen, T. (2018b). Ecology determines how low antibiotic concentration impacts community composition and horizontal transfer of resistance genes. *Commun. Biol.* 1:35. doi: 10.1038/s42003-018-0041-7

Cazorla, F. M., and Mercado-Blanco, J. (2016). Biological control of tree and woody plant diseases: an impossible task? *BioControl* 61, 233–242. doi: 10.1007/s10526-016-9737-0

Chakradhar, S. (2016). What's old is new: reconfiguring known antibiotics to fight drug resistance. *Nat. Med.* 22, 1197–1199. doi: 10.1038/nm1116-1197

Chang, C. C., and Turner, B. L. (2019). Ecological succession in a changing world. *J. Ecol.* 107, 503–509. doi: 10.1111/1365-2745.13132

Chen, J., Hanke, A., Tegetmeyer, H. E., Kattelmann, I., Sharma, R., Hamann, E., et al. (2017a). Impacts of chemical gradients on microbial community structure. *ISME J.* 11, 920–931. doi: 10.1038/ismej.2016.175

Chen, L.-K., Kuo, S.-C., Chang, K.-C., Cheng, C.-C., Yu, P.-Y., Chang, C.-H., et al. (2017b). Clinical antibiotic-resistant *Acinetobacter baumannii* strains with higher susceptibility to environmental phages than antibiotic-sensitive strains. *Sci. Rep.* 7:6319. doi: 10.1038/s41598-017-06688-w

Chevrette, M. G., and Currie, C. R. (2019). Emerging evolutionary paradigms in antibiotic discovery. *J. Ind. Microbiol. Biotechnol.* 46, 257–271. doi: 10.1007/s10295-018-2085-6

Chmielewski, R. A. N., and Frank, J. F. (2006). Biofilm formation and control in food processing facilities. *Compr. Rev. Food Sci. Food Saf.* 2, 22–32. doi: 10.1111/j.1541-4337.2003.tb00012.x

Cockerill, F. R. III. (1999). Genetic methods for assessing antimicrobial resistance. *Antimicrob. Agents Chemother.* 43, 199–212.

Cohen, A., Bont, L., Engelhard, D., Moore, E., Fernández, D., Kreisberg-Greenblatt, R., et al. (2015). A multifaceted 'omics' approach for addressing the challenge of antimicrobial resistance. *Future Microbiol.* 10, 365–376. doi: 10.2217/fmb.14.127

Cohen, J. E., Goldstone, A. B., Paulsen, M. J., Shudo, Y., Steele, A. N., Edwards, B. B., et al. (2017). An innovative biologic system for photon-powered myocardium in the ischemic heart. *Sci. Adv.* 3:e1603078. doi: 10.1126/sciadv.1603078

Collignon, P. J., and McEwen, S. A. (2019). One health—its importance in helping to better control antimicrobial resistance. *Trop. Med. Infect. Dis.* 4:22. doi: 10.3390/tropicalmed4010022

Currie, C. R., Wong, B., Stuart, A. E., Schultz, T. R., Rehner, S. A., Mueller, U. G., et al. (2003). Ancient tripartite coevolution in the attine ant-microbe symbiosis. *Science* 299, 386–388. doi: 10.1126/science.1078155

Czaplewski, L., Bax, R., Clokie, M., Dawson, M., Fairhead, H., Fischetti, V. A., et al. (2016). Alternatives to antibiotics—a pipeline portfolio review. *Lancet Infect. Dis.* 16, 239–251. doi: 10.1016/S1473-3099(15)00466-1

Danner, M. C., Robertson, A., Behrends, V., and Reiss, J. (2019). Antibiotic pollution in surface fresh waters: occurrence and effects. *Sci. Total Environ.* 664, 793–804. doi: 10.1016/j.scitotenv.2019.01.406

Decaestecker, E., and King, K. (2019). "Red queen dynamics" in *Reference module in earth systems and environmental sciences, volume 3 – encyclopedia of ecology.* 2nd Edn. ed. B. Fath (Amsterdam, The Netherlands: Elsevier), 185–192.

Defoirdt, T., Sorgeloos, P., and Bossier, P. (2011). Alternatives to antibiotics for the control of bacterial disease in aquaculture. *Curr. Opin. Microbiol.* 14, 251–258. doi: 10.1016/j.mib.2011.03.004

Delattre, H., Quéméner, E. D.-L., Duquennoi, C., Filali, A., and Bouchez, T. (2019). Consistent microbial dynamics and functional community patterns derived from first principles. *ISME J.* 13, 263–276. doi: 10.1038/s41396-018-0272-0

Demain, A. L., and Elander, R. P. (1999). The β-lactam antibiotics: past, present, and future. *Antonie Van Leeuwenhoek* 75, 5–19. doi: 10.1023/A:1001738823146

Donlan, R. M. (2000). Role of biofilms in antimicrobial resistance. *ASAIO J.* 46, S47–S52. doi: 10.1097/00002480-200011000-00037

Donlan, R. M. (2002). Biofilms: microbial life on surfaces. *Emerg. Infect. Dis.* 8, 881–890. doi: 10.3201/eid0809.020063

Dorodnikov, M., Blagodatskaya, E., Blagodatsky, S., Fangmeier, A., and Kuzyakov, Y. (2009). Stimulation of *r*- vs. *K*-selected microorganisms by elevated atmospheric CO_2 depends on soil aggregate size. *FEMS Microbiol. Ecol.* 69, 43–52. doi: 10.1111/j.1574-6941.2009.00697.x

dos Santos, B. S., da Silva, L. C. N., da Silva, T. D., Rodrigues, J. F. S., Grisotto, M. A. G., dos Santos Correia, M. T., et al. (2016). Application of omics technologies for evaluation of antibacterial mechanisms of action of plant-derived products. *Front. Microbiol.* 7:1466. doi: 10.3389/fmicb.2016.01466

Dose, B., Niehs, S. P., Scherlach, K., Flórez, L. V., Kaltenpoth, M., and Hertweck, C. (2018). Unexpected bacterial origin of the antibiotic icosalide: two-tailed depsipeptide assembly in multifarious burkholderia symbionts. *ACS Chem. Biol.* 13, 2414–2420. doi: 10.1021/acschembio.8b00600

Drusano, G. L. (2003). Prevention of resistance: a goal for dose selection for antimicrobial agents. *Clin. Infect. Dis.* 36, S42–S50. doi: 10.1086/344653

Dunivin, T. K., and Shade, A. (2018). Community structure explains antibiotic resistance gene dynamics over a temperature gradient in soil. *FEMS Microbiol. Ecol.* 94:fiy016. doi: 10.1093/femsec/fiy016

Durante-Mangoni, E., and Zarrilli, R. (2011). Molecular epidemiology and management of antimicrobial resistance. *Future Microbiol.* 6. doi: 10.2217/fmb.11.23

Fan, C., and He, J. (2011). Proliferation of antibiotic resistance genes in microbial consortia of sequencing batch reactors (SBRs) upon exposure to trace erythromycin or erythromycin-H_2O. *Water Res.* 45, 3098–3106. doi: 10.1016/j.watres.2011.03.025

Ferrer, M., Martínez-Martínez, M., Bargiela, R., Streit, W. R., Golyshina, O. V., and Golyshin, P. N. (2016). Estimating the success of enzyme bioprospecting through metagenomics: current status and future trends. *Microb. Biotechnol.* 9, 22–34. doi: 10.1111/1751-7915.12309

Fidler, D. P. (1998). Legal issues associated with antimicrobial drug resistance. *Emerg. Infect. Dis.* 4, 169–177. doi: 10.3201/eid0402.980204

Flórez, L. V., Biedermann, P. H., Engl, T., and Kaltenpoth, M. (2015). Defensive symbioses of animals with prokaryotic and eukaryotic microorganisms. *Nat. Prod. Rep.* 32, 904–936. doi: 10.1039/C5NP00010F

Forsberg, K. J., Reyes, A., Wang, B., Selleck, E. M., Sommer, M. O. A., and Dantas, G. (2012). The shared antibiotic resistome of soil bacteria and human pathogens. *Science* 337, 1107–1111. doi: 10.1126/science.1220761

Fridkin, S. K., and Gaynes, R. P. (1999). Antimicrobial resistance in intensive care units. *Clin. Chest Med.* 20, 303–316. doi: 10.1016/S0272-5231(05)70143-X

Fukami, T., and Nakajima, M. (2011). Community assembly: alternative stable states or alternative transient states? *Ecol. Lett.* 14, 973–984. doi: 10.1111/j.1461-0248.2011.01663.x

Galimand, M., Carniel, E., and Courvalin, P. (2006). Resistance of *Yersinia pestis* to antimicrobial agents. *Antimicrob. Agents Chemother.* 50, 3233–3236. doi: 10.1128/AAC.00306-06

Grenni, P., Ancona, V., and Caracciolo, A. B. (2018). Ecological effects of antibiotics on natural ecosystems: a review. *Microchem. J.* 136, 25–39. doi: 10.1016/j.microc.2017.02.006

Griffiths, G. J. K., Holland, J. M., Bailey, A., and Thomas, M. B. (2008). Efficacy and economics of shelter habitats for conservation biological control. *Biol. Control* 45, 200–209. doi: 10.1016/j.biocontrol.2007.09.002

Gueimonde, M., Sánchez, B., de los Reyes-Gavilán, C. G., and Margolles, A. (2013). Antibiotic resistance in probiotic bacteria. *Front. Microbiol.* 4:202. doi: 10.3389/fmicb.2013.00202

Haddad, N., Johnson, N., Kathariou, S., Métris, A., Phister, T., Pielaat, A., et al. (2018). Next generation microbiological risk assessment—potential of omics data for hazard characterization. *Int. J. Food Microbiol.* 287, 28–39. doi: 10.1016/j.ijfoodmicro.2018.04.015

Hallmann, A., and Rappel, A. (1999). Genetic engineering of the multicellular green alga *Volvox*: a modified and multiplied bacterial antibiotic resistance gene as a dominant selectable marker. *Plant J.* 17, 99–109.

Harmand, N., Gallet, R., Martin, G., and Lenormand, T. (2018). Evolution of bacteria specialization along an antibiotic dose gradient. *Evol. Lett.* 2, 221–232. doi: 10.1002/evl3.52

Hiltunen, T., Virta, M., and Laine, A.-L. (2017). Antibiotic resistance in the wild: an eco-evolutionary perspective. *Philos. Trans. R. Soc. Lond. Ser. B Biol. Sci.* 372:20160039. doi: 10.1098/rstb.2016.0039

Hinnebusch, B. J., Rosso, M.-L., Schawn, T. G., and Carniel, E. (2002). High-frequency conjugative transfer of antibiotic resistance genes to *Yersinia pestis* in the flea midgut. *Mol. Microbiol.* 46, 349–354. doi: 10.1046/j.1365-2958.2002.03159.x

Hoeksema, J. D., and Bruna, E. M. (2000). Pursuing the big questions about interspecific mutualism: a review of theoretical approaches. *Oecologia* 125, 321–330. doi: 10.1007/s004420000496

Holt, R. D., and Bonsall, M. B. (2017). Apparent competition. *Annu. Rev. Ecol. Evol. Syst.* 48, 447–471. doi: 10.1146/annurev-ecolsys-110316-022628

Hu, X., Huang, Y.-Y., Wang, Y., Wang, X., and Hamblin, M. R. (2018). Antimicrobial photodynamic therapy to control clinically relevant biofilm infections. *Front. Microbiol.* 9:1299. doi: 10.3389/fmicb.2018.01299

Huijbers, P. M. C., Blaak, H., de Jong, M. C. M., Graat, E. A. M., Vandenbroucke-Grauls, C. M. J. E., and de Roda Husman, A. M. (2015). Role of the environment in the transmission of antimicrobial resistance to humans: a review. *Environ. Sci. Technol.* 49, 11993–12004. doi: 10.1021/acs.est.5b02566

Hwang, D. F., Arakawa, O., Saito, T., Noguchi, T., Simidu, U., Tsukamoto, K., et al. (1989). Tetrodotoxin-producing bacteria from the blue-ringed octopus *Octopus maculosus*. *Mar. Biol.* 100, 327–332. doi: 10.1007/BF00391147

Inglesby, T. V., Dennis, D. T., Henderson, D. A., Bartlett, J. G., Ascher, M. S., Eitzen, E., et al. (2000). Plague as a biological weapon: medical and public health management. *JAMA* 283, 2281–2290. doi: 10.1001/jama.283.17.2281

Islas-Espinoza, M., Reid, B. J., Wexler, M., and Bond, P. L. (2012). Soil bacterial consortia and previous exposure enhance the biodegradation of sulfonamides from pig manure. *Microb. Ecol.* 64, 140–151. doi: 10.1007/s00248-012-0010-5

Jałowiecki, L., Żur, J., Chojniak, J., Ejhed, H., and Płaza, G. (2018). Properties of antibiotic-resistant bacteria isolated from onsite wastewater treatment plant in relation to biofilm formation. *Curr. Microbiol.* 75, 639–649. doi: 10.1007/s00284-017-1428-2

Jebelli, M. A., Maleki, A., Amoozegar, M. A., Kalantar, E., Gharibi, F., Darvish, N., et al. (2018). Isolation and identification of the native population bacteria for bioremediation of high levels of arsenic from water resources. *J. Environ. Manag.* 212, 39–45. doi: 10.1016/j.jenvman.2018.01.075

Jefferson, K. K. (2004). What drives bacteria to produce a biofilm? *FEMS Microbiol. Lett.* 236, 163–173. doi: 10.1111/j.1574-6968.2004.tb09643.x

Jensen, C. S., Nielsen, S. B., and Fynbo, L. (2019). "Risking antimicrobial resistance: a one health study of antibiotic use and its societal aspects" in *Risking antimicrobial resistance*. eds. C. Jensen, S. Nielsen, and L. Fynbo (Cham: Palgrave Macmillan), 1–24.

Jiang, X., Ellabaan, M. M. H., Charusanti, P., Munck, C., Blin, K., Tong, Y., et al. (2017). Dissemination of antibiotic resistance genes from antibiotic producers to pathogens. *Nat. Commun.* 8:15784. doi: 10.1038/ncomms15784

Joerger, R. D. (2003). Alternatives to antibiotics: bacteriocins, antimicrobial peptides and bacteriophages. *Poult. Sci.* 82, 640–647. doi: 10.1093/ps/82.4.640

Jones, B. W., and Nishiguchi, M. K. (2004). Counterillumination in the Hawaiian bobtail squid, *Euprymna scolopes* Berry (Mollusca: Cephalopoda). *Mar. Biol.* 144, 1151–1155. doi: 10.1007/s00227-003-1285-3

Joseph, M. B., Stutz, W. E., and Johnson, P. T. J. (2016). Multilevel models for the distribution of hosts and symbionts. *PLoS One* 11:e0165768. doi: 10.1371/journal.pone.0165768

Kang, Y.-S., and Park, W. (2010). Trade-off between antibiotic resistance and biological fitness in *Acinetobacter* sp. strain DR1. *Environ. Microbiol.* 12, 1304–1318. doi: 10.1111/j.1462-2920.2010.02175.x

Klumb, R. A., Bunch, K. L., Mills, E. L., Rudstam, L. G., Brown, G., Knauf, C., et al. (2004). Establishment of a metalimnetic oxygen refuge for zooplankton in a productive Lake Ontario embayment. *Ecol. Appl.* 14, 113–131. doi: 10.1890/02-5054

Klümper, U., Recker, M., Zhang, L., Yin, X., Zhang, T., Buckling, A., et al. (2019). Selection for antimicrobial resistance is reduced when embedded in a natural microbial community. *ISME J.* doi: 10.1038/s41396-019-0483-z

Kogan, M. (1998). Integrated pest management: historical perspectives and contemporary developments. *Annu. Rev. Entomol.* 43, 243–270. doi: 10.1146/annurev.ento.43.1.243

Kovach, K., Davis-Fields, M., Irie, Y., Jain, K., Doorwar, S., Vuong, K., et al. (2017). Evolutionary adaptations of biofilms infecting cystic fibrosis lungs promote mechanical toughness by adjusting polysaccharide production. *npj Biofilms Microbiomes* 3:1. doi: 10.1038/s41522-016-0007-9

Kutateladze, M., and Adamia, R. (2010). Bacteriophages as potential new therapeutics to replace or supplement antibiotics. *Trends Biotechnol.* 28, 591–595. doi: 10.1016/j.tibtech.2010.08.001

Lee, H. H., Molla, M. N., Cantor, C. R., and Collins, J. J. (2010). Bacterial charity work leads to population-wide resistance. *Nature* 467, 82–85. doi: 10.1038/nature09354

Lewis, K. (2005). Persister cells and the riddle of biofilm survival. *Biochemistry* 70, 267–274. doi: 10.1007/s10541-005-0111-6

Li, D.-M., and Alexander, M. (1988). Co-inoculation with antibiotic-producing bacteria to increase colonization and nodulation by rhizobia. *Plant Soil* 108, 211–219. doi: 10.1007/BF02375651

Liang, J., Tang, S., Cheke, R. A., and Wu, J. (2015). Models for determining how many natural enemies to release inoculatively in combinations of biological and chemical control with pesticide resistance. *J. Math. Anal. Appl.* 422, 1479–1503. doi: 10.1016/j.jmaa.2014.09.048

Ling, F., Hwang, C., LeChevallier, M. W., Andersen, G. L., and Liu, W.-T. (2015). Core-satellite populations and seasonality of water meter biofilms in a metropolitan drinking water distribution system. *ISME J.* 10, 582–595. doi: 10.1038/ismej.2015.136

Little, A. E. F., and Currie, C. R. (2007). Symbiotic complexity: discovery of a fifth symbiont in the attine ant-microbe symbiosis. *Biol. Lett.* 3, 501–504. doi: 10.1098/rsbl.2007.0253

Liu, Y., Chang, H., Li, Z., Feng, Y., Cheng, D., and Xue, J. (2017). Biodegradation of gentamicin by bacterial consortia AMQD4 in synthetic medium and raw gentamicin sewage. *Sci. Rep.* 7:11004. doi: 10.1038/s41598-017-18286-x

Livermore, D. M. (2011). Discovery research: the scientific challenge of finding new antibiotics. *J. Antimicrob. Chemother.* 66, 1941–1944. doi: 10.1093/jac/dkr262

Louda, S. M., Pemberton, R. W., Johnson, M. T., and Follett, P. A. (2003). Nontarget effects — the Achilles' heel of biological control? Retrospective analyses to reduce risk associated with biocontrol introductions. *Annu. Rev. Entomol.* 48, 365–396. doi: 10.1146/annurev.ento.48.060402.102800

Ma, W. S., Mutka, T., Vesley, B., Amsler, M. O., McClintock, J. B., Amsler, C. D., et al. (2009). Norselic acids A-E, highly oxidized anti-infective steroids that deter mesograzer predation, from the Antarctic sponge Crella sp. *J. Nat. Prod.* 72, 1842–1846. doi: 10.1021/np900382x

MacFadden, D. R., McGough, S. F., Fisman, D., Santillana, M., and Brownstein, J. S. (2018). Antibiotic resistance increases with local temperature. *Nat. Clim. Chang.* 8, 510–514. doi: 10.1038/s41558-018-0161-6

Madigan, M. T., Bender, K. S., Buckley, D. H., Sattley, W. M., and Stahl, D. A. (2009). *Brock biology of microorganisms*. San Francisco: Pearson.

Magarey, R. D., Chappell, T. M., Trexler, C. M., Pallipparambil, G. R., and Hain, E. F. (2019). Social ecological system tools for improving crop pest management. *J. Integr. Pest Manag.* 10, 1–6. doi: 10.1093/jipm/pmz004

Mah, T.-F., and O'Tool, G. A. (2001). Mechanisms of biofilm resistance to antimicrobial agents. *Trends Microbiol.* 9, 34–39. doi: 10.1016/S0966-842X(00)01913-2

Malkinson, D., and Tielbörger, K. (2010). What does the stress-gradient hypothesis predict? Resolving the discrepancies. *Oikos* 119, 1546–1552. doi: 10.1111/j.1600-0706.2010.18375.x

Mangla, S., Inderjit, and Callaway, R. M. (2008). Exotic invasive plant accumulates native soil pathogens which inhibit native plants. *J. Ecol.* 96, 58–67. doi: 10.1111/j.1365-2745.2007.01312.x

Martinez, J. L. (2018). Ecology and evolution of chromosomal gene transfer between environmental microorganisms and pathogens. *Microbiol. Spectr.* 6. doi: 10.1128/microbiolspec.MTBP-0006-2016

Martiny, J. B. H., Bohannan, B. J. M., Brown, J. H., Colwell, R. K., Fuhrman, J. A., Green, J. L., et al. (2006). Microbial biogeography: putting microorganisms on the map. *Nat. Rev. Microbiol.* 4, 102–112. doi: 10.1038/nrmicro1341

McArthur, J. V., Fletcher, D. E., Tuckfield, R. C., and Baker-Austin, C. (2016). Patterns of multi-antibiotic-resistant *Escherichia coli* from streams with no history of antimicrobial inputs. *Microb. Ecol.* 72, 840–850. doi: 10.1007/s00248-015-0678-4

Miller, M., and Aplet, G. (1993). Biological control: a little knowledge is a dangerous thing. *Rutgers Law Rev.* 45, 285–334.

Mišurcová, L., Škrovánková, S., Samek, D., Ambrožová, J., and Machů, L. (2012). Chapter 3 – health benefits of algal polysaccharides in human nutrition. *Adv. Food Nutr. Res.* 66, 75–145. doi: 10.1016/B978-0-12-394597-6.00003-3

Mlot, C. (1997). A soil story. *Sci. News* 152, 58–59. doi: 10.2307/3981065

Molin, S., and Tolker-Nielsen, T. (2003). Gene transfer occurs with enhanced efficiency in biofilms and induces enhanced stabilisation of the biofilm structure. *Curr. Opin. Biotechnol.* 14, 255–261. doi: 10.1016/S0958-1669(03)00036-3

Molmeret, M., Horn, M., Wagner, M., Santic, M., and Kwaik, Y. A. (2005). Amoebae as training grounds for intracellular bacterial pathogens. *Appl. Environ. Microbiol.* 71, 20–28. doi: 10.1128/AEM.71.1.20-28.2005

Moloney, M. G. (2016). Natural products as a source for novel antibiotics. *Trends Pharmacol. Sci.* 37, 689–701. doi: 10.1016/j.tips.2016.05.001

Morris, B. E. L., Henneberger, R., Huber, H., and Moissl-Eichinger, C. (2013). Microbial syntrophy: interaction for the common good. *FEMS Microbiol. Rev.* 37, 384–406. doi: 10.1111/1574-6976.12019

Morris, J. J., Lenski, R. E., and Zinser, E. R. (2012). The Black Queen Hypothesis: evolution of dependencies through adaptive gene loss. *MBio* 3, e00036–e00012. doi: 10.1128/mBio.00036-12

Motta, S. S., Cluzel, P., and Aldana, M. (2015). Adaptive resistance in bacteria requires epigenetic inheritance, genetic noise, and cost of efflux pumps. *PLoS One* 10:e0118464. doi: 10.1371/journal.pone.0118464

Nadell, C. D., Drescher, K., and Foster, K. R. (2016). Spatial structure, cooperation and competition in biofilms. *Nat. Rev. Microbiol.* 14, 589–600. doi: 10.1038/nrmicro.2016.84

Negus, D., Moore, C., Baker, M., Raghunathan, D., Tyson, J., and Sockett, R. E. (2017). Predator versus pathogen: how does predatory *Bdellovibrio bacteriovorus* interface with the challenges of killing Gram-negative pathogens in a host setting? *Annu. Rev. Microbiol.* 71, 441–457. doi: 10.1146/annurev-micro-090816-093618

Nerlich, B., and James, R. (2009). "The post-antibiotic apocalypse" and the "war on superbugs": catastrophe discourse in microbiology, its rhetorical form and political function. *Public Underst. Sci.* 18, 574–590. doi: 10.1177/0963662507087974

O'Malley, M. A. (2007). The nineteenth century roots of 'everything is everywhere'. *Nat. Rev. Microbiol.* 5, 647–651. doi: 10.1038/nrmicro1711

Oliver, N. J., Rabinovitch-Deere, C. A., Carroll, A. L., Nozzi, N. E., Case, A. E., and Atsumi, S. (2016). Cyanobacterial metabolic engineering for biofuel and chemical production. *Curr. Opin. Chem. Biol.* 35, 43–50. doi: 10.1016/j.cbpa.2016.08.023

Olsen, I. (2015). Biofilm-specific antibiotic tolerance and resistance. *Eur. J. Clin. Microbiol. Infect. Dis.* 34, 877–886. doi: 10.1007/s10096-015-2323-z

Orzech, K. M., and Nichter, M. (2008). From resilience to resistance: political ecological lessons from antibiotic and pesticide resistance. *Annu. Rev. Anthropol.* 37, 267–282. doi: 10.1146/annurev.anthro.37.081407.085205

Pal, C., Asiani, K., Arya, S., Rensing, C., Stekel, D. J., Larsson, D. G. J., et al. (2017). Metal resistance and its association with antibiotic resistance. *Adv. Microb. Physiol.* 70, 261–313. doi: 10.1016/bs.ampbs.2017.02.001

Pathak, A., Kett, S., and Marvasi, M. (2019). Resisting antimicrobial resistance: lessons from fungus farming ants. *Trends Ecol. Evol.* S0169-5347, 30256–30253. doi: 10.1016/j.tree.2019.08.007

Pauli, J. N., Mendoza, J. E., Steffan, S. A., Carey, C. C., Weimer, P. J., and Peery, M. Z. (2014). A syndrome of mutualism reinforces the lifestyle of a sloth. *Proc. R. Soc. B Biol. Sci.* 281:20133006. doi: 10.1098/rspb.2013.3006

Pocquet, N., Darriet, F., Zumbo, B., Milesi, P., Thiria, J., Bernard, V., et al. (2014). Insecticide resistance in disease vectors from Mayotte: an opportunity for integrated vector management. *Parasit. Vectors* 7:299. doi: 10.1186/1756-3305-7-299

Preer, J. R., Siegel, R. W., and Stark, P. S. (1953). The relationship between kappa and paramecin in *Paramecium aurelia*. *Proc. Natl. Acad. Sci. USA* 39, 1228–1233. doi: 10.1073/pnas.39.12.1228

Pruden, A., Larsson, D. G. J., Amézquita, A., Collignon, P., Brandt, K. K., Graham, D. W., et al. (2013). Management options for reducing the release of antibiotics and antibiotic resistance genes to the environment. *Environ. Health Perspect.* 121, 878–885. doi: 10.1289/ehp.1206446

Raaijmakers, J. M., and Mazzola, M. (2012). Diversity and natural functions of antibiotics produced by beneficial and plant pathogenic bacteria. *Annu. Rev. Phytopathol.* 50, 403–424. doi: 10.1146/annurev-phyto-081211-172908

Reardon, S. (2015). Antibiotic alternatives rev up bacterial arms race. *Nature* 521, 402–403. doi: 10.1038/521402a

Richmond, A., and Preiss, K. (1980). The biotechnology of algaculture. *Interdiscip. Sci. Rev.* 5, 60–70.

Ringel, P. D., Hu, D., and Basler, M. (2017). The role of type VI secretion system effectors in target cell lysis and subsequent horizontal gene transfer. *Cell Rep.* 21, 3927–3940. doi: 10.1016/j.celrep.2017.12.020

Rodriguez-Mozaz, S., Chamorro, S., Marti, E., Huerta, B., Gros, M., Sànchez-Melsió, A., et al. (2015). Occurrence of antibiotics and antibiotic resistance genes in hospital and urban wastewaters and their impact on the receiving river. *Water Res.* 69, 234–242. doi: 10.1016/j.watres.2014.11.021

Rothrock, M. J. Jr., Hiett, K. L., Guard, J. Y., and Jackson, C. R. (2016). Antibiotic resistance patterns of major zoonotic pathogens from all-natural, antibiotic-free, pasture-raised broiler flocks in the southeastern United States. *J. Environ. Qual.* 45, 593–603. doi: 10.2134/jeq2015.07.0366

Seifan, M., Samani, A. K., and Berenjian, A. (2016). Bioconcrete: next generation of self-healing concrete. *Appl. Microbiol. Biotechnol.* 100, 2591–2602. doi: 10.1007/s00253-016-7316-z

Seiler, C., and Berendonk, T. U. (2012). Heavy metal driven co-selection of antibiotic resistance in soil and water bodies impacted by agriculture and aquaculture. *Front. Microbiol.* 3:399. doi: 10.3389/fmicb.2012.00399

Sen, T., Barrow, C. J., and Deshmukh, S. K. (2019). Microbial pigments in the food industry—challenges and the way forward. *Front. Nutr.* 6, 7–21. doi: 10.3389/fnut.2019.00007

Shanmuganathan, T., Pallister, J., Doody, S., McCallum, H., Robinson, T., Sheppard, A., et al. (2009). Biological control of the cane toad in Australia: a review. *Anim. Conserv.* 13, 16–23. doi: 10.1111/j.1469-1795.2009.00319.x

Shatalin, K., Shatalina, E., Mironov, A., and Nudler, E. (2011). H_2S: a universal defense against antibiotics in bacteria. *Science* 334, 986–990. doi: 10.1126/science.1209855

Shaw, A. J., Lam, F. H., Hamilton, M., Consiglio, A., MacEwen, K., Brevnova, E. E., et al. (2016). Metabolic engineering of microbial competitive advantage for industrial fermentation processes. *Science* 353, 583–586. doi: 10.1126/science.aaf6159

Shiga, D. (2005). Poisonous partnership: parasitoid wasps use viruses as a weapon. *Sci. News* 167, 136–137. doi: 10.2307/4015898

Shure, D. J., and Ragsdale, H. L. (1977). Patterns of primary succession on granite outcrop surfaces. *Ecology* 58, 993–1006. doi: 10.2307/1936920

Singer, A. C., Shaw, H., Rhodes, V., and Hart, A. (2016). Review of antimicrobial resistance in the environment and its relevance to environmental regulators. *Front. Microbiol.* 7:1728. doi: 10.3389/fmicb.2016.01728

Smalla, K., Cook, K., Djordjevic, S. P., Klümper, U., and Gillings, M. (2018). Environmental dimensions of antibiotic resistance: assessment of basic science gaps. *FEMS Microbiol. Ecol.* 94:p.fiy195. doi: 10.1093/femsec/fiy195

Soler, J. J., Martín-Vivaldi, M., Peralta-Sánchez, J. M., and Ruiz-Rodríguez, M. (2010). Antibiotic-producing bacteria as a possible defence of birds against pathogenic microorganisms. *Open Ornithol. J.* 3, 93–100. doi: 10.2174/1874453201003010093

Stockwell, V. O., and Duffy, B. (2012). Use of antibiotics in plant agriculture. *Rev. Sci. Tech.* 31, 199–210. doi: 10.20506/rst.31.1.2104

Strobel, G., and Daisy, B. (2003). Bioprospecting for microbial endophytes and their natural products. *Microbiol. Mol. Biol. Rev.* 67, 491–502. doi: 10.1128/mmbr.67.4.491-502.2003

Sturz, A. V., Christie, B. R., and Matheson, B. G. (1998). Associations of bacterial endophyte populations from red clover and potato crops with potential for beneficial allelopathy. *Can. J. Microbiol.* 44, 162–167. doi: 10.1139/w97-146

Sully, E. K., Malachowa, N., Elmore, B. O., Alexander, S. M., Femling, J. K., Gray, B. M., et al. (2014). Selective chemical inhibition of agr quorum sensing in *Staphylococcus aureus* promotes host defense with minimal impact on resistance. *PLoS Pathog.* 10:e1004174. doi: 10.1371/journal.ppat.1004174

Teuber, M., Meile, L., and Schwarz, F. (1999). "Acquired antibiotic resistance in lactic acid bacteria from food" in *Lactic acid bacteria: Genetics, metabolism and applications*. eds. W. N. Konings, O. P. Kuipers, and J. H. J. H. In't Veld (Dordrecht: Springer).

Tewksbury, J. J., and Lloyd, J. D. (2001). Positive interactions under nurse-plants: spatial scale, stress gradients and benefactor size. *Oecologia* 127, 425–434. doi: 10.1007/s004420000614

Tuli, H. S., Chaudhary, P., Beniwal, V., and Sharma, A. K. (2015). Microbial pigments as natural color sources: current trends and future perspectives. *J. Food Sci. Technol.* 52, 4669–4678. doi: 10.1007/s13197-014-1601-6

Tyson, G. H., McDermott, P. F., Li, C., Chen, Y., Tadesse, D. A., Mukherjee, S., et al. (2015). WGS accurately predicts antimicrobial resistance in *Escherichia coli*. *J. Antimicrob. Chemother.* 70, 2763–2769. doi: 10.1093/jac/dkv186

US Centers for Disease Control and Prevention and UK Science and Innovation Network (2018). Initiatives for addressing antimicrobial resistance in the environment: Current situation and challenges. Available at: https://wellcome.ac.uk/sites/default/files/antimicrobial-resistance-environment-report.pdf (Accessed July 31, 2019).

US Environmental Protection Agency (2013). Introduction to in situ bioremediation of groundwater. Available at: https://www.epa.gov/sites/production/files/2015-04/documents/introductiontoinsitubioremediationofgroundwater_dec2013.pdf (Accessed July 31, 2019).

Van Arnam, E. B., Currie, C. R., and Clardy, J. (2018). Defense contracts: molecular protection in insect-microbe symbioses. *Chem. Soc. Rev.* 47, 1638–1651. doi: 10.1039/C7CS00340D

Van Goethem, M. W., Pierneef, R., Bezuidt, O. K. I., Van De Peer, Y., Cowan, D. A., and Makhalanyane, T. P. (2018). A reservoir of 'historical' antibiotic resistance genes in remote pristine Antarctic soils. *Microbiome* 6:40. doi: 10.1186/s40168-018-0424-5

Vikesland, P. J., Pruden, A., Alvarez, P. J. J., Aga, D., Bürgmann, H., Li, X.-D., et al. (2017). Toward a comprehensive strategy to mitigate dissemination of environmental sources of antibiotic resistance. *Environ. Sci. Technol.* 51, 13061–13069. doi: 10.1021/acs.est.7b03623

Wang, H., Park, J.-D., and Ren, Z. J. (2015). Practical energy harvesting for microbial fuel cells: a review. *Environ. Sci. Technol.* 49, 3267–3277. doi: 10.1021/es5047765

Wellington, E. M. H., Boxall, A. B. A., Cross, P., Feil, E. J., Gaze, W. H., Hawkey, P. M., et al. (2013). The role of the natural environment in the emergence of antibiotic resistance in Gram-negative bacteria. *Lancet Infect. Dis.* 13, 155–165. doi: 10.1016/S1473-3099(12)70317-1

Wells, M. L., Potin, P., Craigie, J. S., Raven, J. A., Merchant, S. S., Helliwell, K. E., et al. (2017). Algae as nutritional and functional food sources: revisiting our understanding. *J. Appl. Phycol.* 29, 949–982. doi: 10.1007/s10811-016-0974-5

White, P. S., and Walker, J. L. (1997). Approximating nature's variation: selecting and using reference information in restoration ecology. *Restor. Ecol.* 5, 338–349. doi: 10.1046/j.1526-100X.1997.00547.x

Whittaker, R. J. (1993). Plant population patterns in a glacier foreland succession: pioneer herbs and later-colonizing shrubs. *Ecography* 16, 117–136. doi: 10.1111/j.1600-0587.1993.tb00064.x

Whittier, T. R., Stoddard, J. L., Larsen, D. P., and Herlihy, A. T. (2007). Selecting reference sites for stream biological assessments: best professional judgment or objective criteria. *J. N. Am. Benthol. Soc.* 26, 349–360. doi: 10.1899/0887-3593(2007)26[349:SRSFSB]2.0.CO;2

Wicaksono, W. A., Jones, E. E., Casonato, S., Monk, J., and Ridgway, H. J. (2018). Biological control of *Pseudomonas syringae* pv. actinidiae (Psa), the causal agent of bacterial canker of kiwifruit, using endophytic bacteria recovered from a medicinal plant. *Biol. Control* 116, 103–112. doi: 10.1016/j.biocontrol.2017.03.003

Wiese, J., and Imhoff, J. F. (2019). Marine bacteria and fungi as promising source for new antibiotics. *Drug Dev. Res.* 80, 24–27. doi: 10.1002/ddr.21482

Willing, B. P., Pepin, D. M., Marcolla, C. S., Forgie, A. J., Diether, N. E., and Bourrie, B. C. T. (2018). Bacterial resistance to antibiotic alternatives: a wolf in sheep's clothing? *Anim. Front.* 8, 39–47. doi: 10.1093/af/vfy003

Willis, A. R., Moore, C., Mazon-Moya, M., Krokowski, S., Lambert, C., Till, R., et al. (2016). Injections of predatory bacteria work alongside host immune cells to treat *Shigella* infection in zebrafish larvae. *Curr. Biol.* 26, 3343–3351. doi: 10.1016/j.cub.2016.09.067

Wilson, C. L., Wisniewski, M. E., Droby, S., and Chalutz, E. (1993). A selection strategy for microbial antagonists to control postharvest diseases of fruits and vegetables. *Sci. Hortic.* 53, 183–189. doi: 10.1016/0304-4238(93)90066-Y

Xiao, Y., Wei, X., Ebright, R., and Wall, D. (2011). Antibiotic production by myxobacteria plays a role in predation. *J. Bacteriol.* 193, 4626–4633. doi: 10.1128/JB.05052-11

Zhang, S., Merino, N., Okamoto, A., and Gedalanga, P. (2018). Interkingdom microbial consortia mechanisms to guide biotechnological applications. *Microb. Biotechnol.* 11, 833–847. doi: 10.1111/1751-7915.13300

Zurek, L., and Ghosh, A. (2014). Insects represent a link between food animal farms and the urban environment for antibiotic resistance traits. *Appl. Environ. Microbiol.* 80, 3562–3567. doi: 10.1128/AEM.00600-14

Conflict of Interest: The authors declare that the research was conducted in the absence of any commercial or financial relationships that could be construed as a potential conflict of interest.

frontiers in Microbiology

ORIGINAL RESEARCH
published: 22 November 2019
doi: 10.3389/fmicb.2019.02713

A Continuous-Flow Model for *in vitro* Cultivation of Mixed Microbial Populations Associated With Cystic Fibrosis Airway Infections

*Thomas James O'Brien and Martin Welch**

Department of Biochemistry, University of Cambridge, Cambridge, United Kingdom

The airways of people with cystic fibrosis (CF) provide a nutrient-rich environment which favours colonisation by a variety of bacteria and fungi. Although the dominant pathogen associated with CF airway infections is *Pseudomonas aeruginosa*, it is becoming increasingly clear that inter-species interactions between *P. aeruginosa* and other colonists in the airways may have a large impact on microbial physiology and virulence. However, there are currently no suitable experimental models that permit long-term co-culture of *P. aeruginosa* with other CF-associated pathogens. Here, we redress this problem by describing a "3R's-compliant" continuous-flow *in vitro* culture model which enables long-term co-culture of three representative CF-associated microbes: *P. aeruginosa*, *Staphylococcus aureus* and *Candida albicans*. Although these species rapidly out-compete one another when grown together or in pairs in batch culture, we show that in a continuously-fed setup, they can be maintained in a very stable, steady-state community. We use our system to show that even numerically (0.1%) minor species can have a major impact on intercellular signalling by *P. aeruginosa*. Importantly, we also show that co-culturing does not appear to influence species mutation rates, further reinforcing the notion that the system favours stability rather than divergence. The model is experimentally tractable and offers an inexpensive yet robust means of investigating inter-species interactions between CF pathogens.

Keywords: cystic fibrosis, continuous-flow, co-culture, *in vitro*, *Pseudomonas aeruginosa*, *Staphylococcus aureus*, *Candida albicans*

OPEN ACCESS

Edited by:
Giovanna Batoni, University of Pisa, Italy

Reviewed by:
Giordano Rampioni, Roma Tre University, Italy
Emanuela Frangipani, University of Urbino Carlo Bo, Italy

***Correspondence:**
Martin Welch
mw240@cam.ac.uk

Specialty section:
This article was submitted to Microbial Physiology and Metabolism, a section of the journal Frontiers in Microbiology

Received: *17 September 2019*
Accepted: *08 November 2019*
Published: *22 November 2019*

Citation:
O'Brien TJ and Welch M (2019) A Continuous-Flow Model for in vitro Cultivation of Mixed Microbial Populations Associated With Cystic Fibrosis Airway Infections. Front. Microbiol. 10:2713. doi: 10.3389/fmicb.2019.02713

INTRODUCTION

Cystic fibrosis (CF) is the most common life-limiting genetic disorder within the Caucasian population (Cystic Fibrosis Foundation, 2019), with 1 in 40 people estimated to carry the common ΔF508 mutation in the CF transmembrane conductance regulator (CFTR) gene (Bobadilla et al., 2002; Cystic Fibrosis Mutation Database, 2019). The most striking consequence of dysfunctional CFTR activity is the overproduction of nutrient-rich, mucilaginous sputum. This blocks the airways and generates a heterogenous environment with steep oxygen gradients and a lowered pH (Boucher, 2002; Tate et al., 2002; Worlitzsch et al., 2002). This environmental niche is rich in nutrients such as mucin, amino acids, iron, and nitrate making the CF airway prone to colonisation by a variety of microbial species (Grasemann et al., 1998; Jones et al., 2000; Palmer et al., 2007; Ghio et al., 2013).

The resulting infections often persist for decades, leading to respiratory failure and eventually, premature death (Lyczak et al., 2002; Rajan and Saiman, 2002; Carmody et al., 2013, 2015; Elborn, 2016). Traditionally, these CF-associated infections have been linked with a relatively small number of easily-culturable pathogens, such as *Pseudomonas aeruginosa* or *Staphylococcus aureus*. However, the introduction of culture-independent molecular profiling approaches revealed that expectorated CF sputum samples often contain a much wider range of bacterial and fungal species (Sibley et al., 2006, 2008; Rogers et al., 2010a; Zhao et al., 2012; Carmody et al., 2013, 2015; Short et al., 2014; Boutin et al., 2015). This suggests that the CF airways may harbour a highly-diverse microbial community, although this notion has been challenged recently through the direct sampling of lavage fluid from the lungs of CF children. These new data suggest that to a large extent, the diversity of the previously reported CF-associated microbiome arises from contamination of the sample during passage through the oral cavity, and following sample processing (Jorth et al., 2019). Nevertheless, these newer studies still suggest that the CF airways harbour a core population of "non-conventional" pathogens, including *Prevotella*, *Veillonella* and *Staphylococcus* species, as well as "traditional CF pathogens" such as *P. aeruginosa* (PA).

The polymicrobial character of many CF-associated airway infections makes it crucial to consider what impact inter-species interactions have on the physiology and composition of the microbial consortium. Previous reports demonstrate that co-culturing bacterial species *in vitro* and *in vivo* causes significant alterations in gene essentiality (Ibberson et al., 2017). This can lead to changes in microbial lifestyle, impacting upon the expression of virulence factors (Rogers et al., 2009, 2010a,b; Hibbing et al., 2010; Leekha et al., 2011; Elias and Banin, 2012; Quinn et al., 2014; Limoli et al., 2016). For example, PA senses peptidoglycan shed from Gram-positive bacteria, and this stimulates the production of extracellular lytic virulence factors (Korgaonkar et al., 2013). Polymicrobial communities also display altered responses to therapeutic intervention. This may explain why many of the currently used clinical interventions designed to target PA show varying degrees of efficacy between patients (Lopes et al., 2012; Peters et al., 2012). As a consequence of these conceptual realisations, research focus is gradually moving away from studying individual species in isolation toward co-cultivating the major CF associated pathogens (Spasenovski et al., 2010; Bragonzi et al., 2012; Filkins et al., 2015; Magalhães et al., 2016; Lopes et al., 2017; Makovcova et al., 2017). However, these efforts are hampered by the paucity of adequate polymicrobial infection models. The development of a model which enables the stable and long-term recapitulation of CF polymicrobial communities is therefore highly-desirable.

Here we describe the development of a simple *in vitro* continuous-flow co-culture model which utilises artificial sputum medium (ASM). ASM is known to physiologically recapitulate the nutritional composition of CF airway secretions (Palmer et al., 2007; Kirchner et al., 2012; Turner et al., 2015). To the best of our knowledge, our co-culture model (**Figure 1**) is the first to permit the long-term, steady-state co-culture of three distinct microbial species: PA, *Staphylococcus aureus* (SA), and *Candida albicans* (CA). Through viable cell counting and optical density measurements, we demonstrate that the abundance of each member of this microbial population remains unchanged over the course of 4 days and that a total carrying capacity can be reached and maintained within the culture vessel. By contrast, and in line with previous reports, when these species are co-cultured under batch conditions, PA rapidly outcompetes the other species (Machan et al., 1992; Duan et al., 2003; Hogan et al., 2004; Mashburn et al., 2005; McAlester et al., 2008; Cugini et al., 2010; Holcombe et al., 2010; Morales et al., 2010; Park et al., 2012; Korgaonkar et al., 2013; Baldan et al., 2014; Fugère et al., 2014; Rüger et al., 2014; Barnabie and Whiteley, 2015; Filkins et al., 2015; Nguyen et al., 2015; Zago et al., 2015; Nguyen and Oglesby-Sherrouse, 2016). Our *in vitro* model provides a defined and experimentally tractable system which can be used to dissect interspecies interactions and determine the long-term impact of co-cultivation on the physiology and gene expression profiles of CF-associated pathogens. Our *in vitro* model also provides a robust and cheaper alternative to existing *in vivo* infection models, making it compliant with the current trend toward the refinement, replacement and reduction (3Rs) of animal models in research.

The species chosen for inoculation into our co-culture model represent three distinct classes of microorganisms; a Gram-negative species and dominant CF-associated pathogen (PA), a Gram-positive species, often associated with CF airway infections (SA) and a dimorphic fungus (CA), also commonly found in CF airway secretions (Conrad et al., 2013). As such, our continuous-flow model lays a solid groundwork for the development and optimisation of an *in vitro* co-culture model which can be directly inoculated with expectorated CF sputum. This will hopefully enable, in the longer-term, full recapitulation of the CF-associated polymicrobial community in defined laboratory conditions.

MATERIALS AND METHODS

Microbial Strains and Culture Conditions

The bacterial/fungal strains used in this study are shown in **Table 1**. All bacterial strains were routinely cultured in lysogeny broth (LB) (Formedium) with vigorous aeration at 37°C overnight. Where necessary, cultures were supplemented with 50 μg mL^{-1} carbenicillin (to maintain pSB1057 in the *N*-(3-Oxododecanoyl)-L-homoserine lactone OdDHL biosensor strain) or 10 μg mL^{-1} tetracycline (to maintain pSB536 in the *N*-butanoyl-L-homoserine lactone BHL biosensor strain).

Artificial sputum medium was used for every mono-, dual-, and triple-species cultivation. ASM was made using a modified version of the recipe published by Turner et al. (2015). Briefly, bovine maxillary mucin was replaced with 1.25 g L^{-1} porcine stomach mucin type-II (Sigma-Aldrich) and salmon sperm DNA was replaced with 1 g L^{-1} fish sperm DNA (Sigma-Aldrich) as described by Kirchner et al. (2012). A detailed protocol for preparing ASM can be found in the **Supplementary Information** (SI.1).

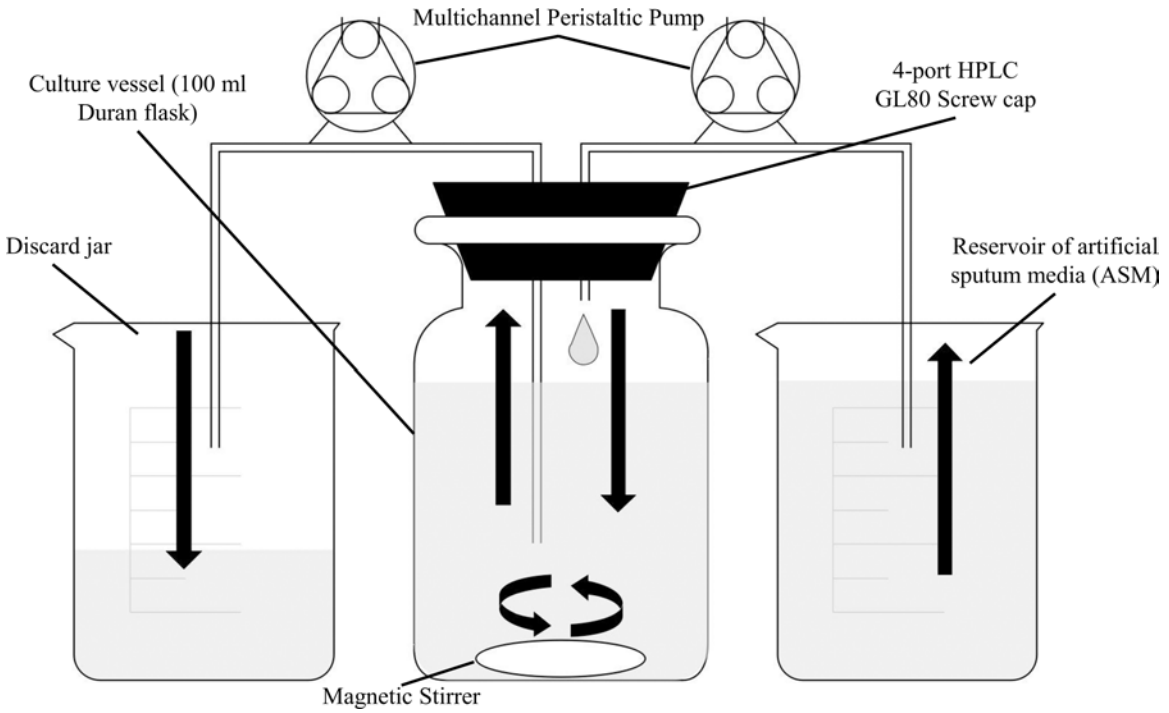

FIGURE 1 | Schematic diagram of the *in vitro* continuous-flow culture system used in this study. The main culture vessel (centre) is a 100 mL Duran bottle fitted with a 4-port HPLC GL80 screwcap lid, containing 4 sealable inlet/outlet ports. A multichannel peristaltic pump delivers fresh media (ASM) into the culture vessel from a reservoir, and also removes waste culture at the same rate of flow (Q). Arrows show the direction of flow. The culture vessel is incubated at 37°C and the contents are kept homogenous through gentle stirring. If required, an in-line spectrophotometer fitted with a continuous-flow cuvette can be included in the setup prior to the discard jar. The value for Q depends on the microbial species being cultured within the vessel.

Continuous-Flow Culture Vessel and Culture Conditions

A schematic of the continuous-flow culture system is shown in **Figure 1**. The culture vessel consists of a 100 mL flask (Duran), fitted with an assembled 4-port HPLC GL80 screw cap (Duran). A 24-channel IPC ISM934C standard-speed digital peristaltic pump (Ismatec) was used to deliver sterile ASM at a defined flow rate (Q) through 1.5 mm bore sterilin silicon tubing (Fisher Scientific) to the culture vessel. A different channel on the same pump was used to remove waste culture into a discard jar at the same flow-rate. The culture vessel was maintained at 37°C and its contents were kept homogenous by stirring (100 rpm) using a magnetic stir bar. When necessary, the culture optical density was monitored at 600 nm ($OD_{600\ nm}$) by passing the removed waste culture through an in-line 6715 UV series spectrophotometer (Jenway) fitted with a continuous-flow cuvette.

Overnight cultures were washed three times in sterile 1 × phosphate buffered saline (PBS, Oxoid) prior to inoculating the culture vessel. Pre-warmed ASM (100 mL) in the culture vessels was inoculated with the required combination of microbial species. Each species was introduced into the culture vessel to achieve a starting $OD_{600\ nm}$ of 0.05. The vessel was incubated for 3 h prior to staring the flow of medium. For mono-species and co-culture experiments not containing CA, the flow rate (Q) was set at 170 μL min^{-1}. For co-culture experiments including CA, Q was decreased to 145 μL min^{-1}. For all continuous-flow experiments, samples (1 mL volume) for cell enumeration were withdrawn using a syringe fitted with a sterile needle inserted through the rubber septa in the HPLC ports.

Aerobic and Stirred Batch Culture Conditions

For aerobic batch cultures, 250 mL Erlenmeyer flasks containing pre-warmed ASM (inoculated with the indicated strains to a starting $OD_{600\ nm}$ of 0.05) were incubated at 37°C with vigorous shaking (180 rpm). Stirred batch cultures were set up as described for the continuous-flow experiments (see section "Continuous-Flow Culture Vessel and Culture Conditions"), except with Q = 0 μL min^{-1}. For both types of batch culture, samples (1 mL volume) were taken from the culture vessel for $OD_{600\ nm}$ analysis and viable cell counting.

Microbial CFU mL^{-1} Enumeration

Colony forming units (CFU) per mL of culture were determined using the single plate-serial dilution spotting (SP-SDS), as described previously (Thomas et al., 2015). Serial dilutions were made in sterile PBS and 20 μL of each dilution was spotted onto the appropriate selective agar. PA was isolated using pseudomonas agar base (Oxoid) supplemented with cetrimide (200 μg mL^{-1}) and sodium nalidixate (15 μg mL^{-1}). SA was isolated on mannitol salt agar (Oxoid). CA was isolated on BiGGY agar (Oxoid). During co-culture experiments involving CA, the agar plates used to isolate PA and SA were further

TABLE 1 | Microbial strains used in this study.

Strain	Description	References
PAO1	*Pseudomonas aeruginosa*, spontaneous chloramphenicol-resistant derivative. Used worldwide as a laboratory reference strain (isolated Melbourne, 1954).	Holloway, 1955
ATCC 25923	*Staphylococcus aureus* Rosenbach (ATCC® 25923D-5™), methicillin sensitive clinical isolate. Laboratory reference strain lacking recombinases and *mecA* (isolated Seattle, 1945).	Treangen et al., 2014
SC5314	*Candida albicans,* clinical isolate commonly used as a wild-type laboratory reference strain (isolated New York, 1980s).	Gillum et al., 1984
PAO1 Δ*pqsA* CTX-*lux*::*pqsA*	PQS biosensor strain. Δ*pqsA* mutant of PAO1 containing a *pqsA* promoter:: *luxCDABE* fusion integrated at a neutral site in the chromosome.	Fletcher et al., 2007
JM109 (pSB1057)	OdDHL biosensor strain. *Escherichia coli* JM109 containing pSB1057.	Winson et al., 1998
JM109 (pSB536)	BHL biosensor strain. *Escherichia coli* JM109 containing pSB536.	Winson et al., 1998

supplemented with 5 μg mL^{-1} itraconazole to inhibit the growth of CA. All plates were incubated at 37°C. Pseudomonas agar base and mannitol salt plates were incubated overnight (16 h). BiGGY agar plates were incubated for 24 h. CFU mL^{-1} counts are averages taken from three technical repeats. There was no significant difference between total CFU mL^{-1} counts of pure microbial cultures plated onto either non-selective (LB-agar) or any of the selective agar (*data not shown*).

Quantification of Quorum Sensing Molecules

Aliquots (1.5 mL) of culture were collected after 24 and 96 h (as indicated) of incubation. The cells were pelleted by centrifugation (15,000 × *g*, 5 min, 20°C) and the supernatant was filtered (0.22 μm pore size). Aliquots of the supernatant were snap frozen in liquid N_2 and stored at −20°C until use. OdDHL was detected using JM109 (pSB1057). BHL was detected using JM109 (pSB536). PQS was detected using PAO1 Δ*pqsA* CTX-*lux*::*pqsA*. Overnight starter cultures of the reporter strains were sub-cultured in LB supplemented with the appropriate antibiotics and grown to OD_{600nm} = 1.0. Following this, aliquots (60 μL volume) of the normalised cell culture were transferred to a sterile clear-bottomed black opaque 96-well plate (Greiner Bio-One) containing an equal volume of thawed culture supernatant. The plates were incubated at 30°C with shaking (100 rpm) for 3 h. Bioluminescence was recorded using a FLOUstar Omega plate reader (BMG). Standard curves to calibrate the biosensor outputs were constructed using known concentrations of synthetic quorum sensing molecules dissolved in ASM.

Quantification of Pyocyanin

Pyocyanin quantification was performed following chloroform extraction of the pigment (Knight et al., 1979). Aliquots (10 mL volume) of culture were collected after 96 h growth and the cells were pelleted (4000 × *g*, 30 min, 4°C). The culture supernatants were filter sterilised (0.22 μm pore size). Chloroform (4.5 mL) was added to 7.5 mL of the cell-free culture supernatant and the suspension was vigorously vortexed for 30 s. The immiscible layers were separated by centrifugation (4000 × *g*, 10 min, 4°C). An aliquot (3 mL volume) of the blue-green chloroform phase was removed and mixed with 1.5 mL 0.2M HCl. The immiscible layers were then separated by centrifugation and 1 mL of the rose-pink phase was transferred to a cuvette. The pyocyanin absorbance was measured at 520 nm using a BioSpectrometer Kinetic spectrophotometer (Eppendorf) and converted to concentration (μg mL^{-1}) by multiplying the $A_{520\ nm}$ value by 26.6.

Estimation of Mutation Rates

Mutation rates in the chemostat were measured as described by Foster (2006). Initially, the rate constant (λ) associated with exponential growth of PA and SA co-cultured in ASM, was determined by enumeration of CFU mL^{-1} on selective agar plates. Next, the total cell count (*N*) within the culture vessel at steady-state growth was determined. The number of spontaneous rifampicin resistant PA or SA mutants, *r*, was measured after t_1 = 0 h, t_2 = 24 h and t_3 = 96 h of incubation. Total cell numbers in the chemostat did not change appreciably between 24 and 96 h. The value of *r* was determined by plating aliquots (100 μL volume) of culture onto either pseudomonas isolation agar supplemented with 60 μg mL^{-1} rifampicin (for PA), or mannitol salt agar supplemented with 0.05 μg mL^{-1} rifampicin (for SA). The mutation rate per cell per generation (m) was calculated according to Eq. 2 in Foster (2006);

$$\mu = \frac{1}{N\lambda}\frac{(r_2 - r_1)}{(t_2 - t_1)}$$

Statistical Analysis

Unless otherwise stated, all data represent the mean ± SD of three independent biological experiments. Results were analysed by one-way or two-way ANOVA (as indicated), or Student's unpaired *t*-test using GraphPad Prism version 8.2.0, with $P < 0.05$ being considered statistically significant.

RESULTS

Mono-Species Continuous-Flow Culture (PAO1)

As a first step, we confirmed that PA, SA and CA could all grow in ASM. This was done by inoculating each species into flat-bottomed microtitre plates containing ASM. The plates were incubated at 37°C with vigorous shaking (180 rpm) in a FluoStar Omega plate reader, and the culture optical density (OD_{600})

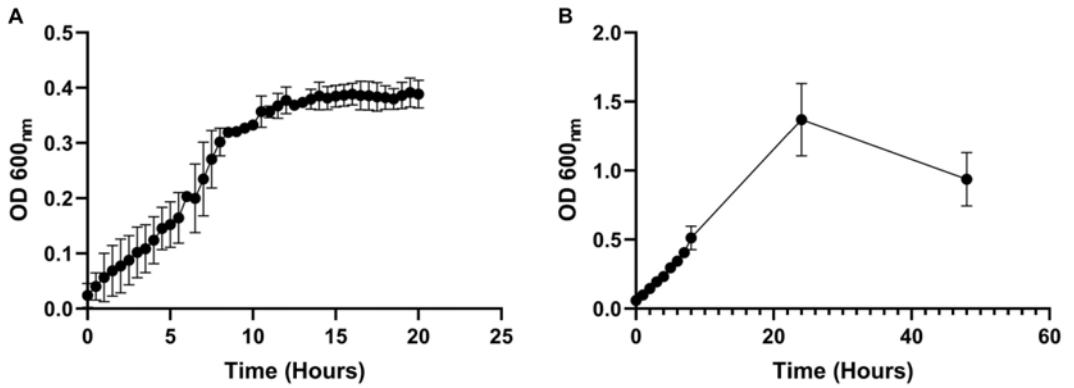

FIGURE 2 | Growth of *P. aeruginosa* in ASM in batch and continuous flow culture conditions. Growth (monitored as OD_{600}) of PA in ASM during **(A)** continuous-flow culture (Q = 170 μL min^{-1}); **(B)** batch culture (Q = 0 μL min^{-1}). Data represent the mean ± standard deviation from three independent experiments.

was monitored every 15 min. PA, SA and CA grew rapidly in ASM, achieving a final OD_{600} of > 1 after 24 h in all cases (**Supplementary Figure S1**).

Next, we measured whether a mono-species culture of PA could be maintained with stable steady-state titres in our continuous-flow setup. The laboratory reference strain, PAO1, was inoculated into the continuous-flow system using a flow-rate Q = 170 μL min^{-1} and the OD_{600} was measured every 30 min as described in Section "Continuous-Flow Culture Vessel and Culture Conditions." The OD_{600} increased almost linearly for the first 8 h and then reached a plateau ($OD_{600} \approx 0.4$) after 10 h of incubation (**Figure 2A**). By comparison, during growth in the same medium and experimental setup with Q = 0 μL min^{-1} (i.e., in stirred batch mode), the PA culture reached a final OD_{600} of > 1 (**Figure 2B**). We conclude that during continuous-flow operation, the setup allows the culture to achieve a steady-state carrying capacity with an OD_{600} well-below the final OD_{600} associated with entry into the stationary phase of growth in the same medium.

Dual-Species Co-culture (PA-SA)

Staphylococcus aureus is also associated with CF airway infection and is particularly prevalent in adolescent patients (Goss and Muhlebach, 2011; Conrad et al., 2013; Jorth et al., 2019). Despite PA and SA being frequently co-isolated from CF patients, numerous antagonistic interactions have been identified between these species, and PA readily outcompetes SA *in vitro* in mixed cultures (Machan et al., 1992; Duan et al., 2003; Mashburn et al., 2005; Park et al., 2012; Korgaonkar et al., 2013; Baldan et al., 2014; Fugère et al., 2014; Rüger et al., 2014; Filkins et al., 2015; Nguyen et al., 2015). We therefore wanted to determine if the two species could be stably maintained in our continuous-flow culture system. We found that a mixed species co-culture of PA and SA could be readily maintained to yield an apparently stable steady-state composition using Q = 170 μL min^{-1}. The CFU counts for each species are shown in **Figure 3A**, and the co-culture OD_{600} measurements are shown in **Supplementary Figure S2**. A steady state composition of around 10^7 SA CFU mL^{-1} and 10^8 PA CFU mL^{-1} was established by 24 h of growth, and there were no significant differences in the viable cell counts following this ($P > 0.05$) up to 96 h of growth. By contrast, during aerobic batch culture in flasks, PA rapidly outcompeted SA and no viable SA could be recovered at the 96 h sampling point (**Figure 3B**). PA also outcompeted SA during stirred batch co-culture conditions (Q = 0 μL min^{-1}) in the continuous-flow vessel (**Figure 3C**), albeit at a slower rate. Taken together, these data indicate that a continual supply of fresh media and removal of waste products is crucial for permitting a successful PA-SA co-culture *in vitro*.

Dual-Species Co-culture (PA-CA)

Fungi, such as *Candida* sp. and *Aspergillus* sp. are also associated with CF airway infections (Williams et al., 2016; Bouchara et al., 2018). We therefore examined whether *Candida albicans* (CA) could be maintained alongside PA in the continuous-flow setup. This is important because inter-kingdom interactions between PA and CA have been previously shown to affect virulence factor production by both species (Hogan et al., 2004; McAlester et al., 2008; Cugini et al., 2010; Holcombe et al., 2010). We found that a co-culture of PA and CA could be readily maintained in the continuous-flow setup (**Figure 4A**), although to prevent a wash-out of CA from the culture vessel over time we had to decrease the flow rate (Q = 145 μl min^{-1}). The culture carrying capacity for CA (ca. 10^5 CFU mL^{-1}) was lower than it was for PA (ca. 10^8 CFU mL^{-1}), but once a steady-state had been achieved (after 24 h incubation) no statistically significant differences in PA or CA viable cell counts were observed ($P > 0.05$). In contrast, CA titres rapidly declined during aerobic batch co-culture (**Figure 4B**). A similar, albeit slower decline in CA titres was observed during stirred batch growth (**Figure 4C**).

Dual-Species Co-culture (SA-CA)

We next wanted to confirm that a stable co-culture of SA and CA could be maintained independent of PA. Using Q = 145 μL min^{-1}, this was indeed the case (**Figure 5A**), and after 24 h growth, the ratio of SA:CA remained essentially unchanged. As in the PA-CA co-culture, at steady-state, the carrying capacity (ca. 10^5 CFU mL^{-1}) for CA was lower than

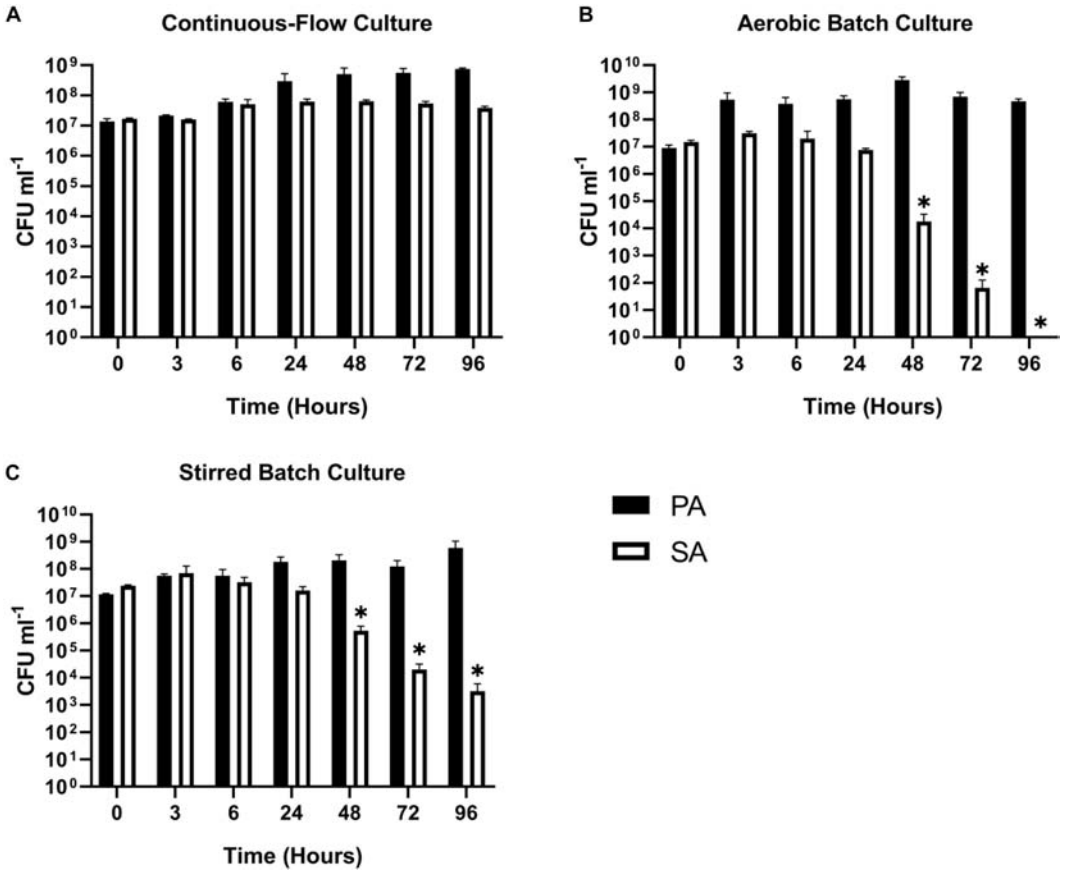

FIGURE 3 | Continuous-flow culture allows *P. aeruginosa* and *S. aureus* to be maintained in a stable steady-state. Viable cell counts [colony forming units (CFUs)] of *P. aeruginosa* PAO1 (PA, black bars) and *S. aureus* 25923 (SA, white bars) during co-culture in ASM using: **(A)** a continuous-flow setup; **(B)** aerobic batch culture; and **(C)** stirred batch culture. Data represent as mean ± standard deviation from three independent experiments. Asterisks represent significant (*$P < 0.05$) differences in CFU mL^{-1} counts in comparison with the data from the 24 h time point.

it was for SA (ca. 10^8 CFU mL^{-1}). Unexpectedly, we noted that following aerobic and stirred batch culture, the CA outcompeted the SA (**Figures 5B,C**). This confirms that in mixed cultures, a species comprising just 0.1% of the microbiota can potentially have a major impact on titres of the [initially] numerically-dominant organism.

Triple-Species Co-culture

With the continuous-flow culture system clearly capable of maintaining dual-species co-cultures of PA-SA, PA-CA and CA-SA, we next wanted to determine if all three species could be co-cultured to achieve a stable steady-state composition. We found that setting Q = 145 μL min^{-1}, a mixed population of all three microbial species could be maintained at a steady state for 96 h of incubation (**Figure 6A**; the corresponding in-line OD_{600} data are shown in **Supplementary Figure S3**). Once the steady-state had been achieved (i.e., after 24 h of growth) there were no significant differences in the CFU mL^{-1} counts for each species for the remaining duration of the co-culture ($P > 0.1$). The PA and SA titres remained at around 10^8–10^9 CFU mL^{-1}, and the CA titres remained at around 10^5 CFU mL^{-1}. By contrast, when co-cultured in aerobic batch culture, both SA and CA were outcompeted by PA (**Figure 6B**). Indeed, there was a progressive decrease in the number of SA CFUs in each of the samples harvested after the 24 h time-point ($P < 0.0005$), and by 72 h, no viable CA CFU could be recovered. However, and unlike the PA-SA aerobic dual cultures (**Figure 3B**), SA could still be recovered at the 96 h sampling point, suggesting that the presence of CA affords a degree of protection, perhaps by decreasing the direct competition between PA and SA for shared resources. The stirred batch co-cultures yielded a somewhat different pattern (**Figure 6C**). Here, following the 24 h sampling point, PA titres remained high (ca. 10^9–10^{10} CFU mL^{-1}) and constant, but there was a significant and progressive decrease in SA titres ($P < 0.05$). Unlike the aerobic batch culture, this was accompanied by a much slower decline in CA titres.

Quantification of *P. aeruginosa* Quorum Sensing Molecules

Quorum sensing (QS) mediated signalling pathways are linked to the regulation of secondary metabolite and extracellular virulence factor production by PA. Some of these QS-regulated

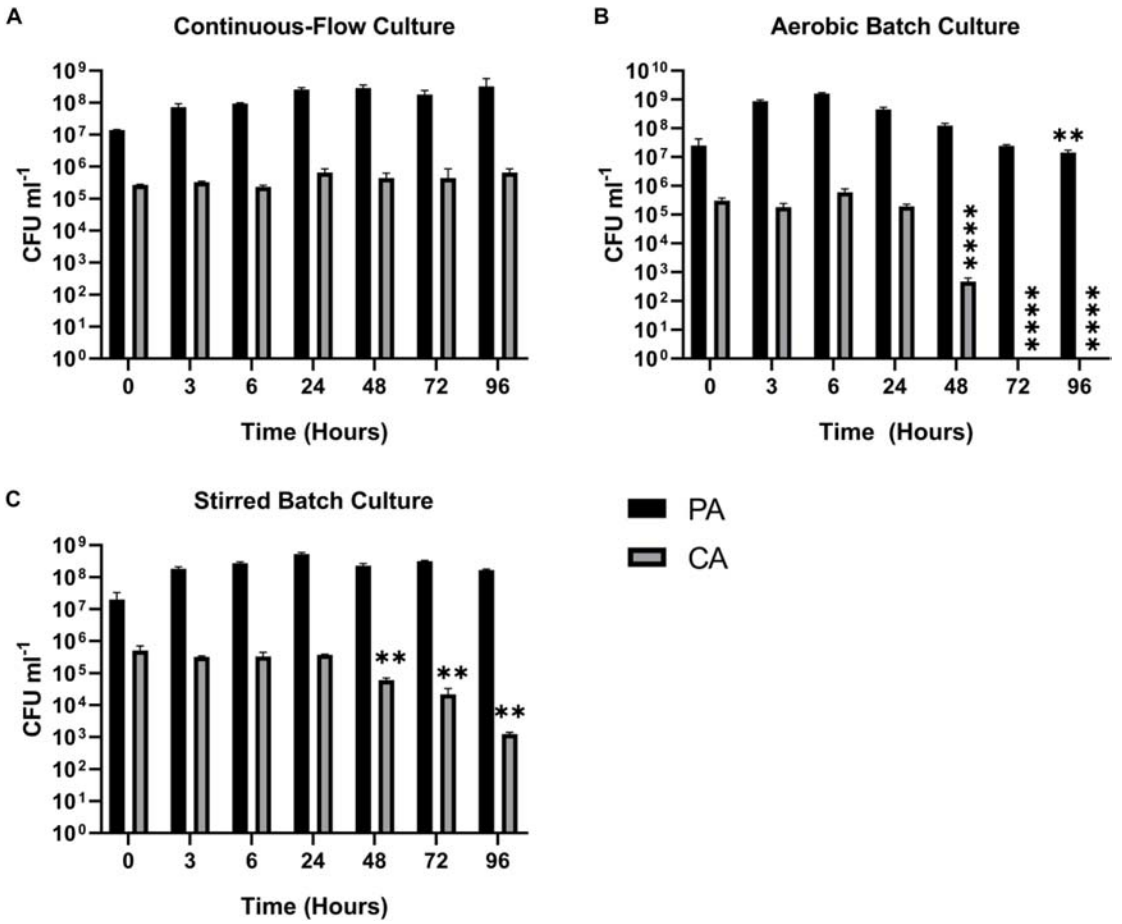

FIGURE 4 | Continuous-flow culture allows *P. aeruginosa* and *C. albicans* to be maintained in a stable steady-state. Viable cell counts (CFU) of *P. aeruginosa* PAO1 (PA, black bars) and *C. albicans* SC5314 (CA, grey bars) during co-culture in ASM using: **(A)** a continuous-flow setup; **(B)** aerobic batch culture; and **(C)** stirred batch culture. Data represent as mean ± standard deviation from three independent experiments. Asterisks represent significant differences in CFU mL^{-1} counts in comparison with the data from the 24 h time point (**$P < 0.005$, ****$P < 0.0001$).

factors have been implicated in mediating interactions with other microbial species (Gambello et al., 1993; Smith and Iglewski, 2003; Lau et al., 2004; Schuster and Greenberg, 2006; Dekimpe and Déziel, 2009; Antunes et al., 2010). To examine how other microbial species might impinge on QS in PA, we therefore determined the concentration of the Pseudomonas quinolone signal (PQS), *N*-(3-Oxododecanoyl)-L-homoserine lactone (OdDHL) and *N*-butanoyl-L-homoserine lactone (BHL) in the culture supernatant of single and mixed species co-cultures (**Figures 7A–C**, respectively).

The concentration of all three QS molecules was significantly ($P < 0.0001$) lower in the continuous-flow setup compared with the aerobic- and stirred-batch cultures. In the continuous-flow setup, there was no significant difference in the concentration of PQS between the 24 and 96 h sampling points, or of OdDHL between these sampling points ($P > 0.1$), although we did note an increase in BHL concentration in the PA-CA co-culture over this period ($P > 0.05$). In contrast, QS molecules accrued to much higher concentrations in the aerobic- and stirred-batch cultures. Moreover, the presence of co-cultivated species had a large, but differential impact on QS molecule production by PA. For example, in batch culture, SA appeared to stimulate OdDHL production, whereas CA appeared to depress OdDHL levels and stimulate PQS (and to a lesser extent, also BHL) production. Taken together, our data indicate that QS molecules accumulate to a much lower concentration in the continuous-flow setup compared with batch cultures.

Quantification of Pyocyanin

Pyocyanin is a redox-active PA secondary metabolite, and is linked with virulence and competition between microbial species in the CF lung (Castric, 1975; Hoffman et al., 2006; Voggu et al., 2006; Biswas et al., 2009; Filkins et al., 2015; Noto et al., 2017). We measured pyocyanin levels in the different culture setups at the endpoint of each experiment (**Figure 8**). Pyocyanin concentrations were significantly lower for all microbial species combinations in the continuous-flow setup compared with the aerobic- or stirred-batch cultures ($P < 0.0001$). No significant differences were observed in pyocyanin accumulation between the different microbial co-culture combinations following growth

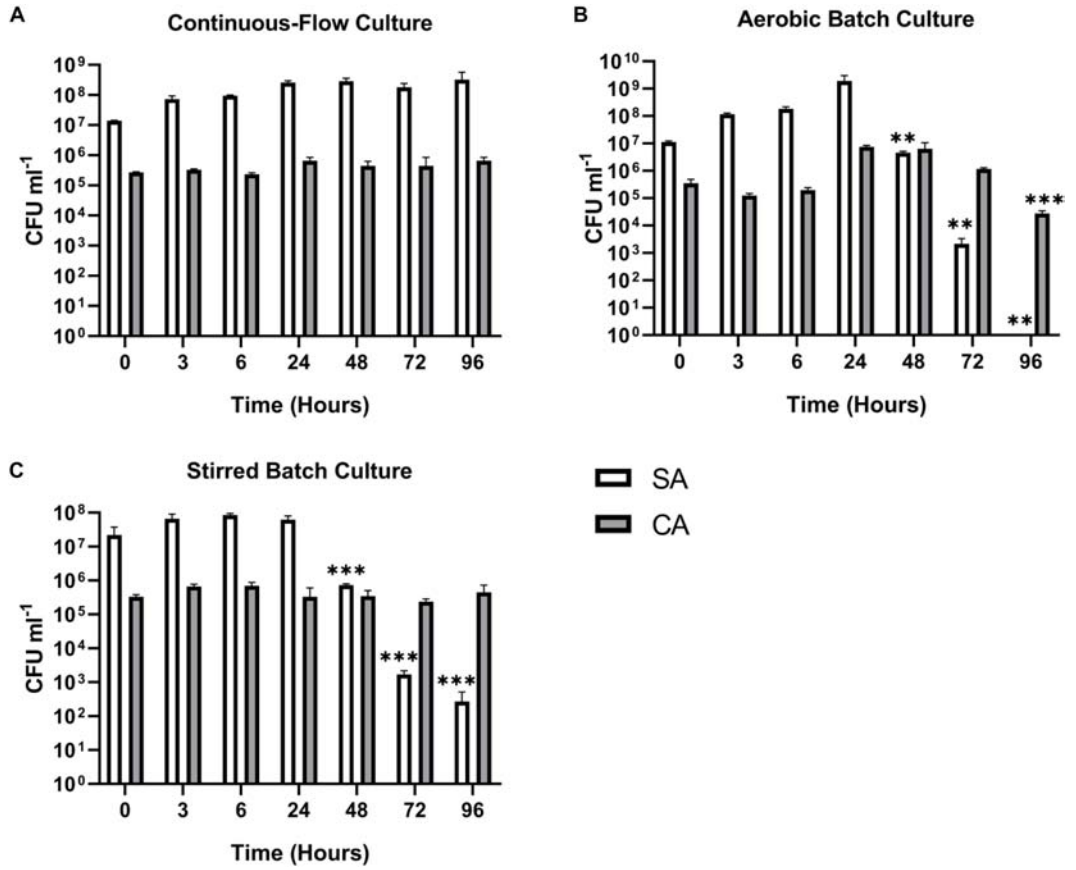

FIGURE 5 | Continuous-flow culture allows *S. aureus* and *C. albicans* to be maintained in a stable steady-state. Viable cell counts of *S. aureus* 25923 (SA, white bars) and *C. albicans* SC5314 (CA, grey bars) co-cultures in ASM in: **(A)** a continuous-flow setup; **(B)** aerobic batch culture; and **(C)** stirred batch culture. Data represented as mean ± standard deviation of three independent experiments. CFU mL^{-1} values are plotted on a $\log_{10}$ scale and asterisks represent significant differences in CFU mL^{-1} counts in comparison with the data from the 24 h time point (**$P < 0.005$, ***$P < 0.001$, ****$P < 0.0001$).

in the continuous-flow setup ($P > 0.3$). However, we did note that in the batch cultures, the presence of CA depressed pyocyanin accumulation.

Estimation of Mutation Rates in Co-cultures of *P. aeruginosa* and *S. aureus*

One possible use of the continuous-flow system described here would be to investigate how the presence of co-habiting species affects evolutionary trajectory(s). To gauge this, we measured the mutation rate of each species during co-culture. Mutation rates were measured as described by Foster (2006) and were assessed shortly after the steady-state had been attained (i.e., at the 24 h time-point) and at the end of the experiment (96 h time-point). The mean number of Rif^R-conferring mutations per cell division was comparable with previously-reported values [$\approx 10^{-8}$–10^{-9} mutations/cell/division (Schaaff et al., 2002; Dettman et al., 2016)] and was consistently low for both PA and SA, with no statistically significant differences between the 24 and 96 h sampling points ($P > 0.1$) (**Figure 9**). We conclude that PA and SA do not exhibit abnormal mutability in the continuous-flow setup and that co-culture of these species has no apparent impact on their respective mutation rate.

Continuous-Flow Cultures Maintain a Constant pH

We also examined the endpoint pH of mixed-species cultures to see whether this differed from the starting pH of ASM (pH 6.7). We found that irrespective of the microbes and combinations of microbes being tested, the continuous flow cultures maintained a remarkably constant pH that was close to the starting pH. Stirred batch cultures maintained a pH of ca. 7, whereas aerobic batch cultures exhibited an endpoint pH > 8 (**Supplementary Figure S4**).

DISCUSSION

In this work, we have shown that a simple *in vitro* continuous-flow co-culture system enables long-term co-culture of three distinct microbial species (PA, SA and CA) associated with CF airway infections. When co-cultured in batch, these organisms ordinarily outcompete one another, leading to domination by

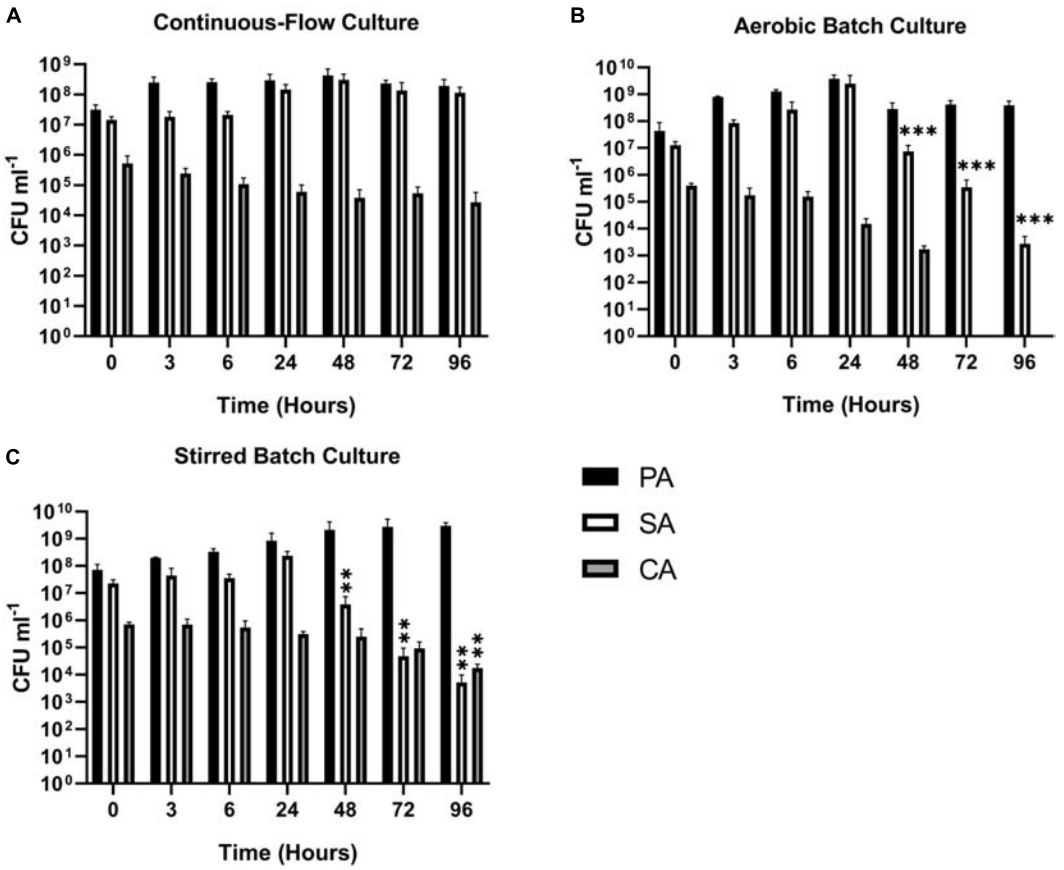

FIGURE 6 | Continuous-flow culture allows *P. aeruginosa*, *C. albicans,* and *S. aureus* to be maintained in a stable steady-state. Viable cell counts of *P. aeruginosa* PAO1 (PA, black bars) *S. aureus* 25923 (SA, white bars) and *C. albicans* SC5314 (CA, grey bars) co-cultures in ASM in: **(A)** a continuous-flow setup; **(B)** aerobic batch culture; and **(C)** stirred batch culture. Data represented as mean ± standard deviation of three independent experiments. CFU mL^{-1} values are plotted on a log_{10} scale and asterisks represent significant differences in CFU mL^{-1} counts in comparison with the data from the 24 h time point (**$P < 0.05$, ***$P < 0.001$).

a single species. However, in the setup described here, once a steady-state has been achieved (after around 24 h incubation) each inoculated species can be maintained at a constant titre, presumably reflecting the carrying capacity for each organism in the culture. Significantly, we show that even low-abundance species (represented by CA in our model) can be stably maintained, and that the presence of such species can have a major impact on the population trajectory of numerically more-abundant organisms such as SA, as well as inter-cellular signalling by PA.

The airways of people with CF have been shown to harbour a diverse polymicrobial community, comprising both bacteria and fungi (Sibley et al., 2006, 2008; Rogers et al., 2010a; Zhao et al., 2012; Carmody et al., 2013, 2015; Short et al., 2014; Boutin et al., 2015), and through the efforts of several teams, we now have a well-defined ASM for *in vitro* analyses. Indeed, PA grown in ASM has an almost identical gene expression profile compared with PA grown directly in sputum derived from CF patients (Turner et al., 2015). In spite of this, to date, there have been no reports describing the successful, long-term co-culture of CF-associated microbes in ASM. As we demonstrate in the current work, simply adding mixed-species inocula into ASM is not a recipe for the long-term maintenance of a stable population. Perhaps the best measure of the lack of progress on this front is seen when considering PA and SA. These two species are common in CF infections, and decades of work have revealed a wealth of knowledge about their physiology and nutritional requirements in axenic culture. However, until now, there have been no studies describing the successful long-term co-cultivation of these two species *in vitro*. One possible reason for this is that in iron limited conditions, PA lyses SA and uses the resulting lysate as a source of iron (Mashburn et al., 2005). By providing a continual supply of fresh media (which presumably mimics the unrelenting and exuberant production of airway secretions in the CF lung) we speculate that this nutritional limitation may be overcome.

The *in vitro* system described here offers a number of advantages. First, it is inexpensive to set up, making it accessible as a model to most researchers. Second, it is compliant with the "3Rs" (the replacement, refinement and reduction of animal research). Third, it is robust, as attested by the remarkably constant titres of each species following attainment of the steady-state condition. Fourth, early indications are that it can faithfully

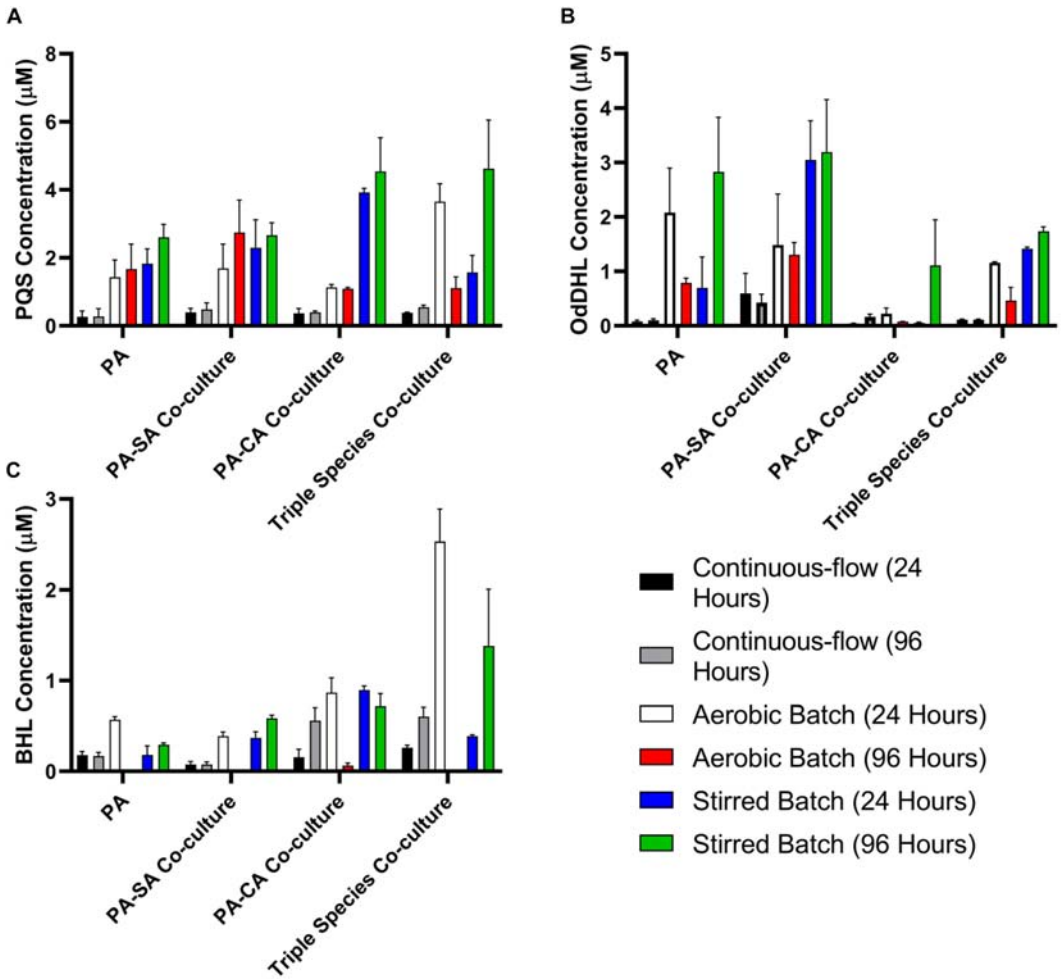

FIGURE 7 | Quorum sensing molecule accumulation in the different culture setups. Concentration of the indicated *P. aeruginosa* quorum sensing molecules in the supernatant of single-species or multi-species co-cultures after 24 and 96 h incubation (as indicated). **(A)** Pseudomonas quinolone signal (PQS); **(B)** *N*-(3-oxododecanoyl)-L-homoserine lactone (OdDHL); **(C)** *N*-butanoyl-L-homoserine lactone (BHL). Data represented as mean ± standard deviation of three independent experiments.

maintain species diversity when patient-derived CF sputum is being used to inoculate the system, and our progress on that aspect of the model will be published presently. Fifth, the system is far more defined and controlled than an animal model, allowing facile experimental perturbation. This experimental tractability means that we can address biological questions in a way that is just not possible with, e.g., animal models. For example, new species or defined mutants can be readily introduced to examine their impact on succession dynamics, and the action of antibiotics on the entire community can be accessed. We have also been exploring ways of modifying the setup to promote biofilm growth in the culture vessel, and again, these findings will be published in the near future.

Our *in vitro* setup is also subject to a number of perceived disadvantages. Unlike an animal model, it does not incorporate any immune response. This may be significant since the immune response would be expected to play a major role in clearance of microbes from the airways, and therefore exerts a selective pressure on the microbial community. Also, our model does not incorporate other types of host cell. This may be significant because in some circumstances (e.g., in patients carrying the DF508 CFTR mutation) the altered cell surface on the epithelia lining the airways has been implicated in promoting microbial colonisation (Campodónico et al., 2008). Mitigating these features, we note that few animal models accurately recapitulate the human CF airway environment, and aside from the difficulties associated with controlling and sampling such models, as far as we are aware, none of these models have yet been developed for maintaining a polymicrobial community of CF pathogens (O'Brien and Welch, 2019). One other potential disadvantage of our model is the requirement for continual flow. On the one hand, this is a feature that does allow maintenance of a stable steady-state community of microbes. On the other hand, even at low Q values, "washout" may prevent slow-growing species/variants from thriving, or key molecules from accumulating. For example, we noted that QS

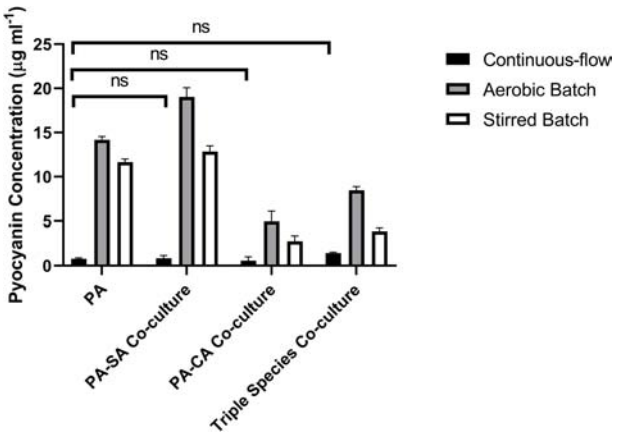

FIGURE 8 | Pyocyanin accumulation in the different culture setups. The concentration (μg mL^{-1}) of pyocyanin in the supernatants of single-species and co-cultures after 96 h of incubation under: continuous-flow (black bars); aerobic batch (grey bars) and; stirred batch (white bars) culture conditions. Data represented as mean ± standard deviation of three independent experiments, $P > 0.05$ is considered no significant difference (ns).

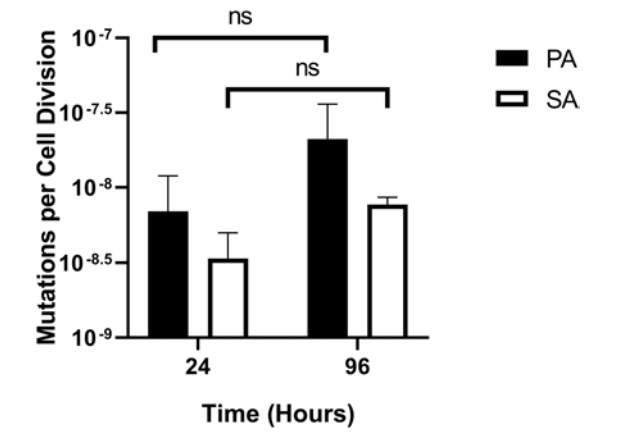

FIGURE 9 | Mutation rates of *P. aeruginosa* and *S. aureus* during co-culture in the continuous-flow setup. Assumed mutation rates of *P. aeruginosa* PAO1 (black bars) and *S. aureus* 25923 (white bars) in the continuous-flow culture vessel after 24 and 96 h of incubation. Mutation rates were calculated as the number of Rif^R-conferring mutations per cell per cell division, calculated as described by Foster (2006). The bars represent the mean ± standard deviation from three independent experiments. $P > 0.05$ is considered not significantly different (ns).

molecules (and pyocyanin) fail to accumulate in the continuous-flow system, whereas these compounds reached high levels in batch culture. The most likely explanation for this is simple washout (through continual dilution) of the QS signals. However, it should be noted that with Q = 170 μL min^{-1}, it would take > 6 h to dilute the vessel contents by 50%, and all the while, the contained culture continues to grow and elaborate more QS molecules. To put this into context, previous work has shown that QS molecules more than double their concentration in batch cultures in a 2 h period (Davenport et al., 2015), so assuming similar kinetics in ASM, these molecules should accumulate faster than they are diluted. If so, this suggests that QS plays a less important role in continuous-flow cultures than it does in batch cultures. The low steady-state concentrations of QS molecules documented here may also be advantageous (for the experimenter). First of all, the metabolic physiology of the community is defined and stable over the experiment's time course and we would not expect to see the bursts of metabolic activity which would normally accompany the accumulation of QS molecules in the post-quorate period (Davenport et al., 2015). Second, and if the effect(s) of QS molecules on community interactions does need to be examined, this can be easily be done through the addition of defined concentrations of exogenous QS molecules.

We conclude that the setup described here enables facile maintenance of PA, SA and CA (a Gram-negative bacterial species, a Gram-positive bacterial species and dimorphic fungus, respectively). Our approach provides a framework for potentially recapitulating the entire polymicrobial community associated with CF airway infections. The setup will provide leverage to access to key biological problems regarding inter-species interactions, the impact of antibiotics, and the impact that newly-introduced species may have on the community trajectory.

DATA AVAILABILITY STATEMENT

The raw data supporting the conclusions of this manuscript will be made available by the authors, without undue reservation, to any qualified researcher.

AUTHOR CONTRIBUTIONS

TO'B and MW conceived and designed the work and revised the manuscript. TO'B executed the experiments, analysed the data, and drafted the manuscript.

FUNDING

This work was supported by a studentship (NC/P001564/1) from the NC3Rs to support TO'B, and consumables support from the UK Cystic Fibrosis Trust and British Lung Foundation.

ACKNOWLEDGMENTS

Andres Floto is acknowledged for helpful discussions and for providing the *C. albicans*.

SUPPLEMENTARY MATERIAL

The Supplementary Material for this article can be found online at: https://www.frontiersin.org/articles/10.3389/fmicb.2019.02713/full#supplementary-material

REFERENCES

Antunes, L. C., Ferreira, R. B., Buckner, M. M., and Finlay, B. B. (2010). Quorum sensing in bacterial virulence. *Microbiology* 156(Pt 8), 2271–2282. doi: 10.1099/mic.0.038794-0

Baldan, R., Cigana, C., Testa, F., Bianconi, I., De Simone, M., and Pellin, D. (2014). Adaptation of *Pseudomonas aeruginosa* in cystic fibrosis airways influences virulence of *Staphylococcus aureus in vitro* and murine models of co-infection. *PLoS One* 9:e89614. doi: 10.1371/journal.pone.0089614

Barnabie, P. M., and Whiteley, M. (2015). Iron-mediated control of *Pseudomonas aeruginosa-Staphylococcus aureus* interactions in the cystic fibrosis lung. *J. Bacteriol.* 197, 2250–2251. doi: 10.1128/JB.00303-15

Biswas, L., Biswas, R., Schlag, M., Bertram, R., and Götz, F. (2009). Small-colony variant selection as a survival strategy for *Staphylococcus aureus* in the presence of *Pseudomonas aeruginosa*. *Appl. Environ. Microbiol.* 75, 6910–6912. doi: 10.1128/AEM.01211-09

Bobadilla, J. L., Macek, M., Fine, J. P., and Farrell, P. M. (2002). Cystic fibrosis: a worldwide analysis of CFTR mutations–correlation with incidence data and application to screening. *Hum. Mutat.* 19, 575–606. doi: 10.1002/humu.10041

Bouchara, J. P., Symoens, F., Schwarz, C., and Chaturvedi, V. (2018). Fungal respiratory infections in cystic fibrosis (cf): recent progress and future research agenda. *Mycopathologia* 183, 1–5. doi: 10.1007/s11046-017-0241-6

Boucher, R. C. (2002). An overview of the pathogenesis of cystic fibrosis lung disease. *Adv. Drug Delivery Rev.* 54, 1359–1371. doi: 10.1016/S0169-409X(02)00144-8

Boutin, S., Graeber, S. Y., Weitnauer, M., Panitz, J., Stahl, M., and Clausznitzer, D. (2015). Comparison of microbiomes from different niches of upper and lower airways in children and adolescents with cystic fibrosis. *PLoS One* 10:e0116029. doi: 10.1371/journal.pone.0116029

Bragonzi, A., Farulla, I., Paroni, M., Twomey, K. B., Pirone, L., and Lorè, N. I. (2012). Modelling co-infection of the cystic fibrosis lung by *Pseudomonas aeruginosa* and *Burkholderia cenocepacia* reveals influences on biofilm formation and host response. *PLoS One* 7:e52330. doi: 10.1371/journal.pone.0052330

Campodónico, V. L., Gadjeva, M., Paradis-Bleau, C., Uluer, A., and Pier, G. B. (2008). Airway epithelial control of *Pseudomonas aeruginosa* infection in cystic fibrosis. *Trends Mol. Med.* 14, 120–133. doi: 10.1016/j.molmed.2008.01.002

Carmody, L. A., Zhao, J., Kalikin, L. M., LeBar, W., Simon, R. H., and Venkataraman, A. (2015). The daily dynamics of cystic fibrosis airway microbiota during clinical stability and at exacerbation. *Microbiome* 3:12. doi: 10.1186/s40168-015-0074-9

Carmody, L. A., Zhao, J., Schloss, P. D., Petrosino, J. F., Murray, S., and Young, V. B. (2013). Changes in cystic fibrosis airway microbiota at pulmonary exacerbation. *Ann. Am. Thorac Soc.* 10, 179–187. doi: 10.1513/AnnalsATS.201211-107OC

Castric, P. A. (1975). Hydrogen cyanide, a secondary metabolite of *Pseudomonas aeruginosa*. *Can. J. Microbiol.* 21, 613–618. doi: 10.1139/m75-088

Conrad, D., Haynes, M., Salamon, P., Rainey, P. B., Youle, M., and Rohwer, F. (2013). Cystic fibrosis therapy: a community ecology perspective. *Am. J. Respir. Cell Mol. Biol.* 48, 150–156. doi: 10.1165/rcmb.2012-0059PS

Cugini, C., Morales, D. K., and Hogan, D. A. (2010). Candida albicans-produced farnesol stimulates *Pseudomonas* quinolone signal production in LasR-defective *Pseudomonas aeruginosa* strains. *Microbiology* 156(Pt 10), 3096–3107. doi: 10.1099/mic.0.037911-0

Cystic Fibrosis Foundation (2019). *Cystic Fibrosis Foundation (http://www.cff.org)*. Bethesda: Cystic Fibrosis Foundation

Cystic Fibrosis Mutation Database (2019). *Cystic Fibrosis Mutation Database*. Cystic Fibrosis Mutation Database: Bethesda.

Davenport, P. W., Griffin, J. L., and Welch, M. (2015). Quorum sensing is accompanied by global metabolic changes in the opportunistic human pathogen *Pseudomonas aeruginosa*. *J. Bacteriol.* 197, 2072–2082. doi: 10.1128/JB.02557-14

Dekimpe, V., and Déziel, E. (2009). Revisiting the quorum-sensing hierarchy in *Pseudomonas aeruginosa*: the transcriptional regulator RhlR regulates LasR-specific factors. *Microbiology* 155(Pt 3), 712–723. doi: 10.1099/mic.0.022764-0

Dettman, J. R., Sztepanacz, J. L., and Kassen, R. (2016). The properties of spontaneous mutations in the opportunistic pathogen *Pseudomonas aeruginosa*. *BMC Genomics* 17:27. doi: 10.1186/s12864-015-2244-3

Duan, K., Dammel, C., Stein, J., Rabin, H., and Surette, M. G. (2003). Modulation of *Pseudomonas aeruginosa* gene expression by host microflora through interspecies communication. *Mol. Microbiol.* 50, 1477–1491. doi: 10.1046/j.1365-2958.2003.03803.x

Elborn, J. S. (2016). Cystic fibrosis. *Lancet* 388, 2519–2531. doi: 10.1016/S0140-6736(16)00576-6

Elias, S., and Banin, E. (2012). Multi-species biofilms: living with friendly neighbors. *FEMS Microbiol. Rev.* 36, 990–1004. doi: 10.1111/j.1574-6976.2012.00325.x

Filkins, L. M., Graber, J. A., Olson, D. G., Dolben, E. L., Lynd, L. R., and Bhuju, S. (2015). Coculture of *Staphylococcus aureus* with *Pseudomonas aeruginosa* Drives S. aureus towards fermentative metabolism and reduced viability in a cystic fibrosis model. *J. Bacteriol.* 197, 2252–2264. doi: 10.1128/JB.00059-15

Fletcher, M. P., Diggle, S. P., Cámara, M., and Williams, P. (2007). Biosensor-based assays for PQS, HHQ and related 2-alkyl-4-quinolone quorum sensing signal molecules. *Nat. Protoc.* 2, 1254–1262. doi: 10.1038/nprot.2007.158

Foster, P. L. (2006). Methods for determining spontaneous mutation rates. *Methods Enzymol.* 409, 195–213. doi: 10.1016/S0076-6879(05)09012-9

Fugère, A., Lalonde Séguin, D., Mitchell, G., Déziel, E., Dekimpe, V., and Cantin, A. M. (2014). Interspecific small molecule interactions between clinical isolates of *Pseudomonas aeruginosa* and *Staphylococcus aureus* from adult cystic fibrosis patients. *PLoS One* 9:e86705. doi: 10.1371/journal.pone.0086705

Gambello, M. J., Kaye, S., and Iglewski, B. H. (1993). LasR of *Pseudomonas aeruginosa* is a transcriptional activator of the alkaline protease gene (apr) and an enhancer of exotoxin A expression. *Infect Immun.* 61, 1180–1184.

Ghio, A. J., Roggli, V. L., Soukup, J. M., Richards, J. H., Randell, S. H., and Muhlebach, M. S. (2013). Iron accumulates in the lavage and explanted lungs of cystic fibrosis patients. *J. Cyst. Fibros* 12, 390–398. doi: 10.1016/j.jcf.2012.10.010

Gillum, A. M., Tsay, E. Y., and Kirsch, D. R. (1984). Isolation of the Candida albicans gene for orotidine-5′-phosphate decarboxylase by complementation of S. *cerevisiae ura*3 and E. coli pyrF mutations. *Mol. Gen. Genet.* 198, 179–182. doi: 10.1007/bf00328721

Goss, C. H., and Muhlebach, M. S. (2011). Review: *Staphylococcus aureus* and MRSA in cystic fibrosis. *J. Cyst. Fibros* 10, 298–306. doi: 10.1016/j.jcf.2011.06.002

Grasemann, H., Ioannidis, I., Tomkiewicz, R. P., de Groot, H., Rubin, B. K., and Ratjen, F. (1998). Nitric oxide metabolites in cystic fibrosis lung disease. *Arch. Dis. Child* 78, 49–53. doi: 10.1136/adc.78.1.49

Hibbing, M. E., Fuqua, C., Parsek, M. R., and Peterson, S. B. (2010). Bacterial competition: surviving and thriving in the microbial jungle. *Nat. Rev. Microbiol.* 8, 15–25. doi: 10.1038/nrmicro2259

Hoffman, L. R., Déziel, E., D'Argenio, D. A., Lépine, F., Emerson, J., and McNamara, S. (2006). Selection for Staphylococcus aureus small-colony variants due to growth in the presence of *Pseudomonas aeruginosa*. *Proc. Natl. Acad. Sci. U.S.A.* 103, 19890–19895. doi: 10.1073/pnas.0606756104

Hogan, D. A., Vik, A., and Kolter, R. (2004). A *Pseudomonas aeruginosa* quorum-sensing molecule influences Candida albicans morphology. *Mol. Microbiol.* 54, 1212–1223. doi: 10.1111/j.1365-2958.2004.04349.x

Holcombe, L. J., McAlester, G., Munro, C. A., Enjalbert, B., Brown, A., and Gow, J. P. (2010). *Pseudomonas aeruginosa* secreted factors impair biofilm development in Candida albicans. *Microbiology* 156(Pt 5), 1476–1486. doi: 10.1099/mic.0.037549-0

Holloway, B. W. (1955). Genetic recombination in *Pseudomonas aeruginosa*. *J. Gen. Microbiol.* 13, 572–581. doi: 10.1099/00221287-13-3-572

Ibberson, C. B., Stacy, A., Fleming, D., Dees, J. L., Rumbaugh, K., and Gilmore, M. S. (2017). Co-infecting microorganisms dramatically alter pathogen gene essentiality during polymicrobial infection. *Nat. Microbiol.* 2:17079. doi: 10.1038/nmicrobiol.2017.79

Jones, K. L., Hegab, A. H., Hillman, B. C., Simpson, K. L., Jinkins, P. A., and Grisham, M. B. (2000). Robbins: elevation of nitrotyrosine and nitrate concentrations in cystic fibrosis sputum. *Pediatr. Pulmonol.* 30, 79–85. doi: 10.1002/1099-0496(200008)30:2<79::aid-ppul1>3.0.co;2-1

Jorth, P., Ehsan, Z., Rezayat, A., Caldwell, E., Pope, C., and Brewington, J. J. (2019). Direct lung sampling indicates that established pathogens dominate

early infections in children with cystic fibrosis. *Cell Rep.* 27:1190-1204.e3. doi: 10.1016/j.celrep.2019.03.086

Kirchner, S., Fothergill, J. L., Wright, E. A., James, C. E., Mowat, E., and Winstanley, C. (2012). Use of artificial sputum medium to test antibiotic efficacy against *Pseudomonas aeruginosa* in conditions more relevant to the cystic fibrosis lung. *J. Vis. Exp.* 5:e3857. doi: 10.3791/3857

Knight, M., Hartman, P. E., Hartman, Z., and Young, V. M. (1979). A new method of preparation of pyocyanin and demonstration of an unusual bacterial sensitivity. *Anal. Biochem.* 95, 19–23. doi: 10.1016/0003-2697(79)90179-9

Korgaonkar, A., Trivedi, U., Rumbaugh, K. P., and Whiteley, M. (2013). Community surveillance enhances *Pseudomonas aeruginosa* virulence during polymicrobial infection. *Proc. Natl. Acad. Sci. U.S.A.* 110, 1059–1064. doi: 10.1073/pnas.1214550110

Lau, G. W., Hassett, D. J., Ran, H., and Kong, F. (2004). The role of pyocyanin in *Pseudomonas aeruginosa* infection. *Trends Mol. Med.* 10, 599–606. doi: 10.1016/j.molmed.2004.10.002

Leekha, S., Terrell, C. L., and Edson, R. S. (2011). General principles of antimicrobial therapy. *Mayo Clin. Proc.* 86, 156–167. doi: 10.4065/mcp.2010.0639

Limoli, D. H., Yang, J., Khansaheb, M. K., Helfman, B., Peng, L., and Stecenko, A. A. (2016). Staphylococcus aureus and *Pseudomonas aeruginosa* co-infection is associated with cystic fibrosis-related diabetes and poor clinical outcomes. *Eur. J. Clin. Microbiol. Infect Dis.* 35, 947–953. doi: 10.1007/s10096-016-2621-0

Lopes, S. P., Azevedo, N. F., and Pereira, M. O. (2017). Developing a model for cystic fibrosis sociomicrobiology based on antibiotic and environmental stress. *Int. J. Med. Microbiol.* 307, 460–470. doi: 10.1016/j.ijmm.2017.09.018

Lopes, S. P., Ceri, H., Azevedo, N. F., and Pereira, M. O. (2012). Antibiotic resistance of mixed biofilms in cystic fibrosis: impact of emerging microorganisms on treatment of infection. *Int. J. Antimicrob. Agents* 40, 260–263. doi: 10.1016/j.ijantimicag.2012.04.020

Lyczak, J. B., Cannon, C. L., and Pier, G. B. (2002). Lung infections associated with cystic fibrosis. *Clin. Microbiol. Rev.* 15, 194–222. doi: 10.1128/cmr.15.2.194-222.2002

Machan, Z. A., Taylor, G. W., Pitt, T. L., Cole, P. J., and Wilson, R. (1992). 2-Heptyl-4-hydroxyquinoline N-oxide, an antistaphylococcal agent produced by *Pseudomonas aeruginosa*. *J. Antimicrob. Chemother.* 30, 615–623. doi: 10.1093/jac/30.5.615

Magalhães, A. P., Lopes, S. P., and Pereira, M. O. (2016). Insights into cystic fibrosis polymicrobial consortia: the role of species interactions in biofilm development, phenotype, and response to in-use antibiotics. *Front. Microbiol.* 7:2146. doi: 10.3389/fmicb.2016.02146

Makovcova, J., Babak, V., Kulich, P., Masek, J., Slany, M., and Cincarova, L. (2017). Dynamics of mono- and dual-species biofilm formation and interactions between *Staphylococcus aureus* and Gram-negative bacteria. *Microb. Biotechnol.* 10, 819–832. doi: 10.1111/1751-7915.12705

Mashburn, L. M., Jett, A. M., Akins, D. R., and Whiteley, M. (2005). Staphylococcus aureus serves as an iron source for *Pseudomonas aeruginosa* during *in vivo* coculture. *J. Bacteriol.* 187, 554–566. doi: 10.1128/JB.187.2.554-566.2005

McAlester, G., O'Gara, F., and Morrissey, J. P. (2008). Signal-mediated interactions between *Pseudomonas aeruginosa* and Candida albicans. *J. Med. Microbiol.* 57(Pt 5), 563–569. doi: 10.1099/jmm.0.47705-0

Morales, D. K., Jacobs, N. J., Rajamani, S., Krishnamurthy, M., Cubillos-Ruiz, J. R., and Hogan, D. A. (2010). Antifungal mechanisms by which a novel *Pseudomonas aeruginosa* phenazine toxin kills Candida albicans in biofilms. *Mol. Microbiol.* 78, 1379–1392. doi: 10.1111/j.1365-2958.2010.07414.x

Nguyen, A. T., Jones, J. W., Ruge, M. A., Kane, M. A., and Oglesby-Sherrouse, A. G. (2015). Iron depletion enhances production of antimicrobials by *Pseudomonas aeruginosa*. *J. Bacteriol.* 197, 2265–2275. doi: 10.1128/JB.00072-15

Nguyen, A. T., and Oglesby-Sherrouse, A. G. (2016). Interactions between *Pseudomonas aeruginosa* and *Staphylococcus aureus* during co-cultivations and polymicrobial infections. *Appl. Microbiol. Biotechnol.* 100, 6141–6148. doi: 10.1007/s00253-016-7596-3

Noto, M. J., Burns, W. J., Beavers, W. N., and Skaar, E. P. (2017). Mechanisms of pyocyanin toxicity and genetic determinants of resistance in *Staphylococcus aureus*. *J. Bacteriol.* 199:e221-17. doi: 10.1128/JB.00221-17

O'Brien, , T. J., and Welch, M. (2019). Recapitulation of polymicrobial communities associated with cystic fibrosis airway infections: a perspective. *Future Microbiol.* (in press). doi: 10.2217/fmb-2019-0200

Palmer, K. L., Aye, L. M., and Whiteley, M. (2007). Nutritional cues control *Pseudomonas aeruginosa* multicellular behavior in cystic fibrosis sputum. *J. Bacteriol.* 189, 8079–8087. doi: 10.1128/JB.01138-07

Park, J. H., Lee, J. H., Cho, M. H., Herzberg, M., and Lee, J. (2012). Acceleration of protease effect on Staphylococcus aureus biofilm dispersal. *FEMS Microbiol. Lett.* 335, 31–38. doi: 10.1111/j.1574-6968.2012.02635.x

Peters, B. M., Jabra-Rizk, M. A. O., May, G. A., Costerton, J. W., and Shirtliff, M. E. (2012). Polymicrobial interactions: impact on pathogenesis and human disease. *Clin. Microbiol. Rev.* 25, 193–213. doi: 10.1128/CMR.00013-11

Quinn, R. A., Lim, Y. W., Maughan, H., Conrad, D., Rohwer, F., and Whiteson, K. L. (2014). Biogeochemical forces shape the composition and physiology of polymicrobial communities in the cystic fibrosis lung. *MBio* 5:e956-13. doi: 10.1128/mBio.00956-13

Rajan, S., and Saiman, L. (2002). Pulmonary infections in patients with cystic fibrosis. *Semin Respir Infect* 17, 47–56. doi: 10.1053/srin.2002.31690

Rogers, G. B., Carroll, M. P., and Bruce, K. D. (2009). Studying bacterial infections through culture-independent approaches. *J. Med. Microbiol.* 58(Pt 11), 1401–1418. doi: 10.1099/jmm.0.013334-0

Rogers, G. B., Hoffman, L. R., Whiteley, M., Daniels, T. W., Carroll, M. P., and Bruce, K. D. (2010a). Revealing the dynamics of polymicrobial infections: implications for antibiotic therapy. *Trends Microbiol.* 18, 357–364. doi: 10.1016/j.tim.2010.04.005

Rogers, G. B., Stressmann, F. A., Walker, A. W., Carroll, M. P., and Bruce, K. D. (2010b). Lung infections in cystic fibrosis: deriving clinical insight from microbial complexity. *Expert Rev. Mol. Diagn* 10, 187–196. doi: 10.1586/erm.09.81

Rüger, M., Ackermann, M., and Reichl, U. (2014). Species-specific viability analysis of *Pseudomonas aeruginosa*, Burkholderia cepacia and *Staphylococcus aureus* in mixed culture by flow cytometry. *BMC Microbiol.* 14:56. doi: 10.1186/1471-2180-14-56

Schaaff, F., Reipert, A., and Bierbaum, G. (2002). An elevated mutation frequency favors development of vancomycin resistance in *Staphylococcus aureus*. *Antimicrob. Agents Chemother.* 46, 3540–3548. doi: 10.1128/aac.46.11.3540-3548.2002

Schuster, M., and Greenberg, E. P. (2006). A network of networks: quorum-sensing gene regulation in *Pseudomonas aeruginosa*. *Int. J. Med. Microbiol.* 296, 73–81. doi: 10.1016/j.ijmm.2006.01.036

Short, F. L., Murdoch, S. L., and Ryan, R. P. (2014). Polybacterial human disease: the ills of social networking. *Trends Microbiol.* 22, 508–516. doi: 10.1016/j.tim.2014.05.007

Sibley, C. D., Parkins, M. D., Rabin, H. R., Duan, K., Norgaard, J. C., and Surette, M. G. (2008). A polymicrobial perspective of pulmonary infections exposes an enigmatic pathogen in cystic fibrosis patients. *Proc. Natl. Acad. Sci. U.S.A.* 105, 15070–15075. doi: 10.1073/pnas.0804326105

Sibley, C. D., Rabin, H., and Surette, M. G. (2006). Cystic fibrosis: a polymicrobial infectious disease. *Future Microbiol.* 1, 53–61. doi: 10.2217/17460913.1.1.53

Smith, R. S., and Iglewski, B. H. (2003). P. aeruginosa quorum-sensing systems and virulence. *Curr. Opin. Microbiol.* 6, 56–60. doi: 10.1016/s1369-5274(03)00008-0

Spasenovski, T., Carroll, M. P., Lilley, A. K., Payne, M. S., and Bruce, K. D. (2010). Modelling the bacterial communities associated with cystic fibrosis lung infections. *Eur. J. Clin. Microbiol. Infect Dis.* 29, 319–328. doi: 10.1007/s10096-009-0861-y

Tate, S., MacGregor, G., Davis, M., Innes, J. A., and Greening, A. P. (2002). Airways in cystic fibrosis are acidified: detection by exhaled breath condensate. *Thorax* 57, 926–929. doi: 10.1136/thorax.57.11.926

Thomas, P., Sekhar, A. C., Upreti, R., Mujawar, M. M., and Pasha, S. S. (2015). Optimization of single plate-serial dilution spotting (SP-SDS) with sample anchoring as an assured method for bacterial and yeast cfu enumeration and single colony isolation from diverse samples. *Biotechnol. Rep.* 8, 45–55. doi: 10.1016/j.btre.2015.08.003

Treangen, T. J., Maybank, R. A., Enke, S., Friss, M. B., Diviak, L. F., and Karaolis, D. K. (2014). Complete genome sequence of the quality control strain *Staphylococcus aureus* subsp. *aureus* ATCC 25923. *Genome Announc.* 2:e1110-14. doi: 10.1128/genomeA.01110-14

Turner, K. H., Wessel, A. K., Palmer, G. C., Murray, J. L., and Whiteley, M. (2015). Essential genome of *Pseudomonas aeruginosa* in cystic fibrosis sputum. *Proc. Natl. Acad. Sci. U.S.A.* 112, 4110–4115. doi: 10.1073/pnas.1419677112

Voggu, L., Schlag, S., Biswas, R., Rosenstein, R., Rausch, C., and Götz, F. (2006). Microevolution of cytochrome bd oxidase in *Staphylococci* and its implication in resistance to respiratory toxins released by *Pseudomonas*. *J. Bacteriol.* 188, 8079–8086. doi: 10.1128/JB.00858-06

Williams, C., Ranjendran, R., and Ramage, G. (2016). Pathogenesis of fungal infections in cystic fibrosis. *Curr. Fungal Infect Rep.* 10, 163–169. doi: 10.1007/s12281-016-0268-z

Winson, M. K., Swift, S., Fish, L., Throup, J. P., Jørgensen, F., and Chhabra, S. R. (1998). Construction and analysis of luxCDABE-based plasmid sensors for investigating N-acyl homoserine lactone-mediated quorum sensing. *FEMS Microbiol. Lett.* 163, 185–192. doi: 10.1111/j.1574-6968.1998.tb13044.x

Worlitzsch, D., Tarran, R., Ulrich, M., Schwab, U., Cekici, A., and Meyer, K. C. (2002). Effects of reduced mucus oxygen concentration in airway *Pseudomonas* infections of cystic fibrosis patients. *J. Clin. Invest* 109, 317–325. doi: 10.1172/JCI13870

Zago, C. E., Silva, S., Sanitá, P. V., Barbugli, P. A., Dias, C. M., and Lordello, V. B. (2015). Dynamics of biofilm formation and the interaction between Candida albicans and methicillin-susceptible (MSSA) and -resistant Staphylococcus aureus (MRSA). *PLoS One* 10:e0123206. doi: 10.1371/journal.pone.0123206

Zhao, J., Schloss, P. D., Kalikin, L. M., Carmody, L. A., Foster, B. K., and Petrosino, J. F. (2012). Decade-long bacterial community dynamics in cystic fibrosis airways. *Proc. Natl. Acad. Sci. U.S.A.* 109, 5809–5814. doi: 10.1073/pnas.1120577109

Conflict of Interest: The authors declare that the research was conducted in the absence of any commercial or financial relationships that could be construed as a potential conflict of interest.

frontiers in Microbiology

ORIGINAL RESEARCH
published: 05 December 2019
doi: 10.3389/fmicb.2019.02803

Polymicrobial Interactions Induce Multidrug Tolerance in *Staphylococcus aureus* Through Energy Depletion

*Dan L. Nabb, Seoyoung Song, Kennedy E. Kluthe, Trevor A. Daubert, Brandon E. Luedtke and Austin S. Nuxoll**

Department of Biology, University of Nebraska at Kearney, Kearney, NE, United States

Staphylococcus aureus is responsible for a high number of relapsing infections, which are often mediated by the protective nature of biofilms. Polymicrobial biofilms appear to be more tolerant to antibiotic treatment, however, the underlying mechanisms for this remain unclear. Polymicrobial biofilm and planktonic cultures formed by *S. aureus* and *Candida albicans* are 10- to 100-fold more tolerant to oxacillin, vancomycin, ciprofloxacin, delafloxacin, and rifampicin compared to monocultures of *S. aureus*. The possibility of *C. albicans* matrix components physically blocking antibiotic molecules from reaching *S. aureus* was ruled out as oxacillin, ciprofloxacin, delafloxacin, and rifampicin were able to diffuse through polymicrobial biofilms. Based on previous findings that *S. aureus* forms drug tolerant persister cells through ATP depletion, we examined nutrient deprivation by determining glucose availability, which indirectly correlates to ATP production via the tricarboxylic acid (TCA) cycle. Using an extracellular glucose assay, we confirmed that *S. aureus* and *C. albicans* polymicrobial cultures depleted available glucose faster than the respective monocultures. Supporting this finding, *S. aureus* exhibited decreased TCA cycle activity, specifically fumarase expression, when grown in the presence of *C. albicans*. In addition, *S. aureus* grown in polymicrobial cultures displayed 2.2-fold more cells with low membrane potential and a 13% reduction in intracellular ATP concentrations than in monocultures. Collectively, these data demonstrate that decreased metabolic activity through nutrient deprivation is a mechanism for increased antibiotic tolerance within polymicrobial cultures.

Keywords: *Staphylocccus aureus*, persister, *Candida albicans*, energy depletion, polymicrobial

OPEN ACCESS

Edited by:
Giuseppantonio Maisetta, University of Pisa, Italy

Reviewed by:
Jianfeng Wang, Jilin University, China
Rohitashw Kumar, University at Buffalo, United States

****Correspondence:***
Austin S. Nuxoll
nuxollas@unk.edu

Specialty section:
This article was submitted to Microbial Physiology and Metabolism, a section of the journal Frontiers in Microbiology

Received: *28 August 2019*
Accepted: *19 November 2019*
Published: *05 December 2019*

Citation:
Nabb DL, Song S, Kluthe KE, Daubert TA, Luedtke BE and Nuxoll AS (2019) Polymicrobial Interactions Induce Multidrug Tolerance in Staphylococcus aureus Through Energy Depletion. Front. Microbiol. 10:2803. doi: 10.3389/fmicb.2019.02803

INTRODUCTION

Globally, 1 in 20 patients are currently suffering from a nosocomial infection (Zarb et al., 2012; Koch et al., 2015a,b), with *Staphylococcus aureus* being a prevalent organism associated with these infections (Hassoun et al., 2017). *S. aureus* is a leading cause of infective endocarditis, osteomyelitis, skin and soft tissue infections, and prosthetic device-related infections (Tong et al., 2015).

A number of *S. aureus* mediated infections can be attributed to the contamination of the device surface with a biofilm (Wolcott et al., 2010). Interestingly, biofilm mediated *S. aureus* infections are difficult to eradicate, yet are caused primarily by drug-susceptible strains (Conlon, 2014; Ericson et al., 2015). Moreover, in polymicrobial biofilms, *S. aureus* is interacting with other pathogens, including the fungus *Candida albicans*. Polymicrobial infections are of concern as they result in a higher mortality rate than monomicrobial infections (Goetghebeur et al., 2007; Perlroth et al., 2007). However, underlying mechanisms for these observations remain inconclusive (McKenzie, 2006; Lin et al., 2010; Fengcai et al., 2015; Royo-Cebrecos et al., 2017). Polymicrobial biofilms have been reported to increase pathogen virulence, antibiotic resistance, and biofilm robustness (Harriott and Noverr, 2009, 2010, 2011; Kong et al., 2016). More specifically, tolerance to vancomycin in polymicrobial biofilms with *C. albicans* through an increase in biofilm robustness due to the extracellular matrix products secreted by the *C. albicans*, which restricted vancomycin penetration into the biofilm (Singh et al., 2010; Kong et al., 2016). However, similar results were found in *S. aureus* monomicrobial biofilms treated with vancomycin (Singh et al., 2010); therefore, it is difficult to make any direct inferences about the underlying causes of tolerance to antibiotics.

Until recently, literature on the mechanisms of persister cell formation was limited to two themes, toxin-antitoxin (TA) modules and stringent response (Lewis, 2010; Maisonneuve et al., 2013). However, it was recently demonstrated that TA modules did not have a role in *S. aureus* persister cell formation (Conlon et al., 2016), and the stringent response, when disrupted in *S. aureus* had no effect on persister formation. Instead, it was observed that *S. aureus* cells exhibiting lower intracellular ATP had increased persister formation and tolerance to antibiotics (Conlon et al., 2016). Additional work confirmed an association between decreased metabolic activity in the TCA cycle and membrane potential with *S. aureus* persister formation (Wang et al., 2018). The metabolic status of *S. aureus* and nutrient acquisition has become of interest for explaining bacterial survival during chronic infection and more recently has been associated with antibiotic tolerance in *S. aureus*. Nutrients such as amino acids, iron, nitrogen, and carbon metabolism have been a focal point of recent *in vivo* investigations (Haley and Skaar, 2012; Halsey et al., 2016; Spahich et al., 2016). While glucose is required for initial infection, in mature abscesses, non-preferred carbon sources are often a limiting factor (Kelly and O'Neill, 2015; Spahich et al., 2016; Thurlow et al., 2018). Similarly, bacteria appear to form more robust biofilms when grown in the presence of abundant glucose. As the biofilm matures, glucose is exhausted leading to the formation of persisters (Amato and Brynildsen, 2014). These environments provide examples where glucose is required for initial establishment of infection, but as the infection progresses glucose availability becomes less important. Furthermore, nutrient sparse environments are frequently associated with relapsing chronic infection following antibiotic therapy. This points to a need for further exploration of the role of nutrient depletion in relapsing infections.

In this study, glucose exhaustion and the subsequent decrease in energy availability was explored as a mechanism for multidrug tolerance within *S. aureus* and *C. albicans* polymicrobial cultures. It was found that polymicrobial cultures depleted glucose more rapidly compared to monomicrobial cultures. Additionally, *S. aureus* grown in polymicrobial cultures demonstrated decreased intracellular ATP concentrations as well as lower membrane potential when compared to cultures lacking *C. albicans*. Evidence for increased antibiotic tolerance within polymicrobial cultures due to matrix composition or biomolecules secreted by *C. albicans* was not found. Overall, these studies highlight the importance of metabolism in bacterial persistence, and demonstrate a potential mechanism for relapse in polymicrobial infection following antibiotic treatment.

MATERIALS AND METHODS

Strains and Growth Conditions

The methicillin susceptible *S. aureus* strain HG003 was used in all assays (Herbert et al., 2010). The community acquired *C. albicans* strain SC5314 was used for all experiments (Gillum et al., 1984; Odds et al., 2004). For experiments demonstrating this phenotype occurs across staphylococcal species, *Staphylococcus epidermidis* 1457, *S. aureus* UAMS-1, and *S. aureus* JE2 were used. *S. epidermidis* was grown to late log ($\sim 1 \times 10^9$ CFU/mL) as this species is more sensitive to antibiotics an eradication occurs at early log phase. *S. aureus* JE2 is highly tolerant to antibiotics in later phases of growth and therefore assays were performed in early log (3×10^7 CFU/mL). *S. aureus* UAMS-1 and HG003 are similar in persister formation and assays were performed in mid-log ($2–5 \times 10^8$ CFU/mL). SC5314 was grown to $\sim 3 \times 10^6$ CFU/mL for each biofilm and time-dependent kill assay where polymicrobial cultures were utilized. The P*spa:gfp* plasmid was provided by Kim Lewis (Conlon et al., 2016). For construction of the P*fumC:gfp* reporter, the promoter of *fumC* was amplified (5′-gggccc*gaattc*ttgatgatgttaatgcgcaaa-3′ and 5′-gggccc*ctctaga*tcaatttctcccccttatcac-3′) and cloned upstream of *gfp* into the *Eco*RI and *Xba*I sites in pALC1434 (Cheung et al., 1998). Once cloned, P*fumC:gfp* was electroporated into *S. aureus* RN4220 and subsequently transduced into HG003 using Φ11 phage. Unless otherwise stated, all growth steps and time-dependent kill assays were grown in 3 mL Tryptic Soy Broth (TSB) at 37°C at 225 rpm in 14 mL snap cap tubes.

96-Well Static Biofilm Tolerance Assays

Overnight cultures of *S. aureus* were diluted 1:1000 and *C. albicans* overnight cultures were diluted 1:100 in 100 μL of TSB within a 96-well polystyrene flat-bottom plate. Plates were incubated statically for 8 h. Non-adherent cells were washed with 1% NaCl, fresh TSB was added, and biofilms were subsequently challenged with antibiotics (10–100× MIC) for 24 h. MICs were previously determined for HG003: ciprofloxacin (0.5 μg/mL),

gentamicin (1 μg/mL), oxacillin (0.5 μg/mL), vancomycin (1 μg/mL), rifampicin (0.008 μg/mL). Finally, biofilms were solubilized and plated on TSA containing amphotericin B (25 μg/mL) using a standard serial dilution technique. Error bars represent the standard deviation and statistical significance was determined using a *t*-test, $P \leq 0.05$.

Planktonic Time-Dependent Kill Assays

Planktonic cultures were grown to mid-exponential phase in 3 mL TSB and challenged with antibiotics (10–100× MIC) as described previously (Conlon et al., 2016; Zalis et al., 2019). Cultures were placed in a shaking incubator at 225 rpm at 37°C. 100 μL aliquots were removed from samples, washed to remove antibiotic, and surviving bacteria were enumerated at 18, 24, 48, and 72 h by serial dilution and plating on TSA containing amphotericin B (25 μg/mL).

Antibiotic Diffusion Through Mono- and Polymicrobial Biofilms

Polycarbonate filters (13 mm) were sterilized by UV light for 30 min per side and placed on a TSA plate. Overnight *S. aureus* cultures were diluted 1:1000, *C. albicans* overnight cultures were diluted 1:100 in TSB. 100 μL of this solution was placed onto the filter and grown statically for 24 h. Biofilms were placed on fresh TSA plates seeded with 1×10^6 CFU *S. aureus*. A 13 mm polycarbonate disk was placed on the biofilm, followed by a diffusion disk. Each respective antibiotic (1 mg/mL ciprofloxacin, 10 mg/mL oxacillin, 1 mg/mL rifampicin, 10 mg/mL vancomycin) was added (10 μL) to the disk and plates were incubated for 24 h. The diameter of the zone of inhibition was then measured in millimeters. The average and standard deviation was obtained from biological triplicates. Significance was determined using a *t*-test, $P \leq 0.05$.

Visualization of Antibiotic Diffusion Throughout a Biofilm Using Confocal Scanning Laser Microscopy

To visualize antibiotic diffusion through single and polymicrobial biofilms, fluorescently labeled vancomycin and delafloxacin were used as described previously with modification (Pereira et al., 2007). Biofilms were grown on 8-chambered glass coverslips (cat. 154941, MatTek Co.) for 24 h at 37°C statically in TSB containing 1% glucose. Following incubation, non-adherent cells were washed gently with 1% NaCl, and stained for 1 h. In order to visualize vancomycin, the fluorescent vancomycin BODIPY FL conjugate (ex488/em511) was added (5 μg/mL). Delafloxacin was visualized using the intrinsic fluorescence of the molecule (ex405/em450) at a concentration of (10 μg/mL). Concanavalin A (ex488/em545) was added (50 μg/mL) to visualize the biofilm matrix. The coverslip was mounted on the slides using Prolong Diamond Antifade (ThermoFisher) according to the manufactures recommendation. Biofilms were observed using a 60× oil immersion objective and an Olympus FV3000 laser scanning confocal microscope (Olympus, Tokyo, Japan). Images were acquired at a resolution of 512 by 512 pixels. To analyze the biofilms, a series of images at ≤ 1 μm intervals in the z axis were acquired through the depth of the biofilm. For each condition, at least three fields of view were imaged and processed equally using cellSens Dimension Desktop V1.18 (Olympus). Representative images are displayed.

Analysis of Matrix Coating and Antibiotic Accessibility Using Flow Cytometry

To determine whether coating of *S. aureus* by *C. albicans* matrix components blocked antibiotic access to the cell we utilized vancomycin BODIPY FL and the intrinsic fluorescence of delafloxacin. Cultures were grown to mid-exponential phase, fluorescent compounds were added 10^6 CFU/mL in 1% NaCl at the same concentration that was used in the confocal experiments for 1 h at room temperature. Samples were analyzed using a Sony SH800 cell sorter.

Concentrated Supernatant Time-Dependent Kill Assay

Cultures (25 mL) of each strain (HG003 and SC5314) were grown in a shaking incubator overnight. These cultures were then pelleted and the supernatant removed. Supernatants were passed through a 0.45 micron filter then spun through a 3000 MW filter and concentrated to approximately 1500 μL. Concentrated supernatant (300 μL) was then added to planktonic HG003 cultures and incubated for 4 h. These cultures were challenged with rifampicin (0.8 μg/mL). The bacteriostatic antibiotic, chloramphenicol (4 μg/mL), was added to prevent rifampicin resistant cells from regrowing. Aliquots (100 μL) were removed from samples, and surviving bacteria were enumerated at 18, 24, 48, and 72 h by serial dilution and plating on TSA.

Farnesol Time-Dependent Kill Assay

Overnight *S. aureus* cultures were diluted 1:1000 in TSB containing 40 μM farnesol and grown to mid-exponential phase. Rifampicin (0.8 μg/mL) and chloramphenicol (4 μg/mL) were added and bacteria were enumerated over 72 h.

Spent Media Time-Dependent Kill Assay

Overnight cultures were diluted 1:1000 and were grown to mid-exponential phase in 3 mL of either HG003 or SC5314 spent media collected from overnight cultures via centrifugation and challenged with rifampicin (0.8 μg/mL) and chloramphenicol (4 μg/mL). Bacteria were cultured and enumerated as described above.

Determination of Intracellular ATP Concentration

Intracellular ATP concentration was measured using the Promega BacTiter-Glo Microbial Cell Viability Assay according to manufacturer's instructions. Late exponential phase cultures were filtered through a 5 μM filter to remove *C. albicans*. The remaining *S. aureus* cells were pelleted and washed with 1% NaCl prior to measuring luminescence. A sample was also taken for serial dilution and enumeration of bacteria. Luminescence was divided by surviving cells to account for any growth

differences. Six replicates were used for obtaining averages and standard deviation. Significance was determined using a student's *t*-test, $P \leq 0.05$.

Measurement of Membrane Potential in Individual Cells

Membrane potential was measured using BacLight Bacterial Membrane Potential Kit according to manufacturer's instructions. Briefly, samples were taken from mid-exponential phase ($t = 5$ h) in *S. aureus* either grown alone or in the presence of *C. albicans*. Samples were diluted to 1×10^6 cells in PBS and were stained with $DiOC_2(3)$ for 30 min and analyzed by flow cytometry. Carbonyl cyanide m-chlorophenylhydrazone (CCCP) was used to dissipate membrane potential and was used to gate low membrane potential cells. Bacterial cells were separated from fungal cells and debris using back scatter (BSC) and forward scatter (FSC) parameters with 50,000 events collected for each sample. $DiOC_2(3)$ was excited at 488 nm and emissions of the green and red fluorescence were detected with bandpass filters of 525/50- and 600/60-nm, respectively. Samples were analyzed using FlowJo software. The average and standard deviation was obtained from six biological replicates. Significance was determined using a student's *t*-test, $P \leq 0.05$.

Quantifying Extracellular Glucose Availability

Overnight cultures of *S. aureus* (1:1000) and *C. albicans* (1:100) were diluted in TSB and placed in a shaking incubator. Every hour, 500 uL media was removed and pelleted. Supernatant was then used to measure glucose concentration using an Invitrogen glucose detection colorimetric assay kit according to manufacturer's instructions. Averages and standard deviation were calculated using six biological replicates.

Measuring Fumarase C Expression

Overnight cultures of *S. aureus* (1:100) containing P*fumC:gfp* or P*spa:gfp* plasmids and *C. albicans* (1:50) were diluted in Mueller Hinton Broth (MHB) in a microtiter plate. Growth and fluorescence were (485ex/528em) were monitored over 22 h in a Biotek microplate reader at 37°C with continuous shaking. Averages and standard deviation were calculated from biological triplicates.

RESULTS

Polymicrobial Cultures Demonstrate Increased Tolerance to Antibiotics in Both Biofilm and Planktonic Environments

Polymicrobial infections are more tolerant to antibiotic therapy than single organism infections, though the underlying mechanisms remain unclear. Recent work has demonstrated that the presence of *C. albicans* increases *S. aureus* tolerance to vancomycin within a biofilm (Kong et al., 2016). We sought to determine if interactions between *C. albicans* and *S. aureus* lead to multidrug tolerance. Since mature biofilms often do not respond to antibiotics, it is often impossible to observe decreased antibiotic effectiveness between various cultures. In order to overcome this, immature biofilms were used. It is important to note that two distinct phenotypes of the wild type HG003 strain were observed. Following antibiotic treatment, cultures showed up to 3 logs of killing, or little to no effect. Polymicrobial biofilms led to significantly more survival in six of eight antibiotic treatments (ciprofloxacin $p = 0.006$, oxacillin $p = 0.019$, rifampicin $p = 0.006$, rifampicin/ciprofloxacin $p = 0.001$, rifampicin/gentamicin $p = 0.003$, and vancomycin/ciprofloxacin $p = 0.008$) compared to *S. aureus* monomicrobial biofilms (**Figure 1**). Interestingly, no increase in tolerance was observed when biofilms were challenged with vancomycin.

To determine if the increase in tolerance was specific to biofilms, planktonic cultures were challenged with antibiotics during the mid-exponential growth phase. Following antibiotic challenge with rifampicin, ciprofloxacin, oxacillin, delafloxacin, and vancomycin, *S. aureus* exhibited 10 to 100-fold more persisters when grown in the presence of *C. albicans* (**Figure 2**). To further determine these effects were not strain or species specific, another MSSA strain, a MRSA strain, and a *S. epidermidis* strain were tested for antibiotic tolerance in the presence and absence of *C. albicans* (**Supplementary Figures S1A–C**). With all three strains, there was increased antibiotic tolerance when the staphylococcal species was grown in the presence of *C. albicans*. These experiments demonstrate the presence of *C. albicans* increases *S. aureus* persister cells

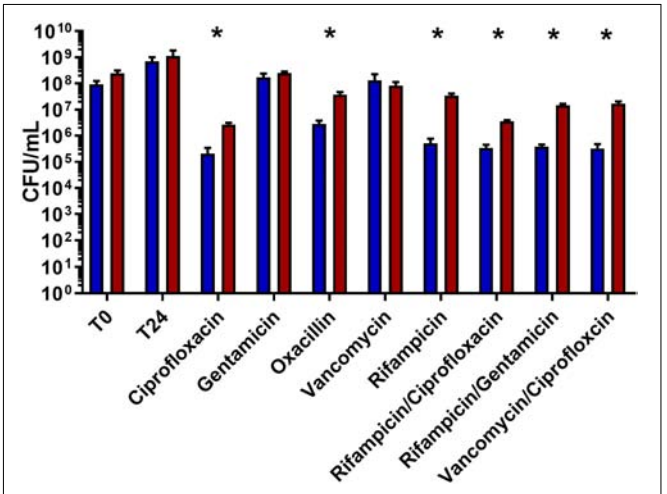

FIGURE 1 | Polymicrobial biofilms show increased tolerance to a variety of antibiotic. Overnight cultures of *S. aureus* were diluted 1:1000 and *C. albicans* overnight cultures were diluted 1:100 in TSB using a microtiter plate. Plates were incubated for 8 h at 37°C statically. Non-adherent cells washed, fresh media was added, and biofilms were subsequently challenged with antibiotics (10–100× MIC) for 24 h. *S. aureus* growing in polymicrobial biofilms (red) had significantly higher survival compared to biofilms only containing *S. aureus* (blue). Experiment was performed in biological triplicate and error bars represent standard deviation. Significance (as indicated by *) was determined using a *t*-test ($p < 0.05$).

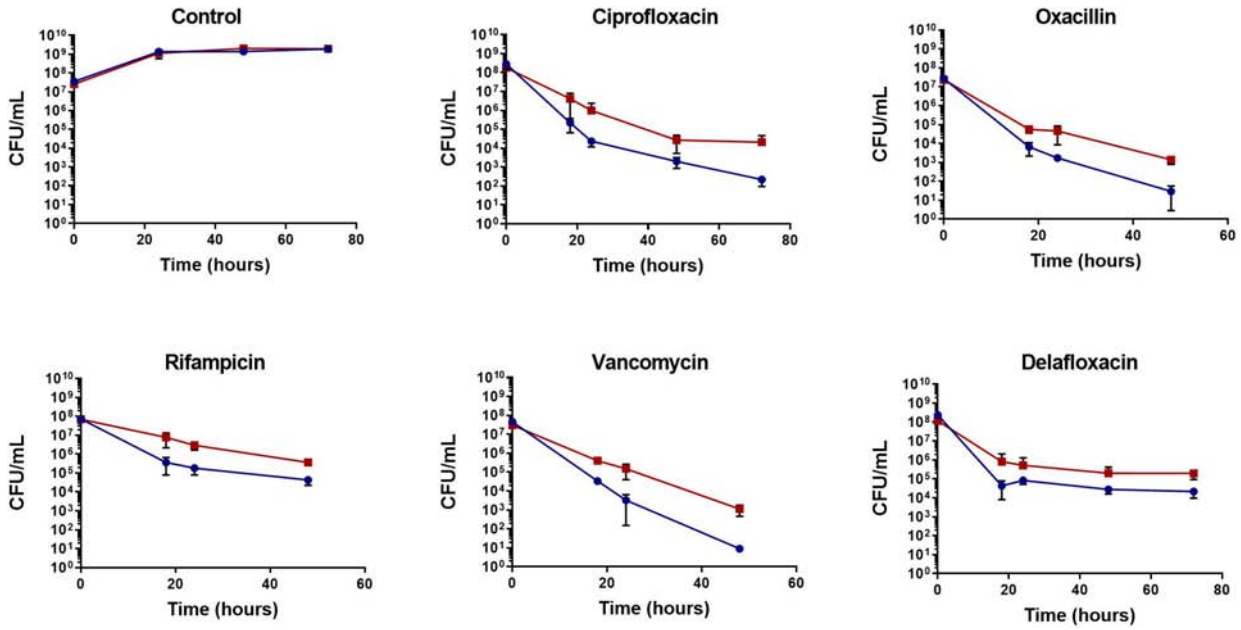

FIGURE 2 | Polymicrobial planktonic cultures have increased antibiotic tolerance. Planktonic cultures were grown to mid-exponential phase in TSB and challenged with antibiotic (10–100× MIC), the surviving bacteria were enumerated over 48 or 72 h by plating on TSA containing amphotericin B (25 μg/mL). The presence of *C. albicans* increases *S. aureus* (red) antibiotic tolerance compared to *S. aureus* monocultures (blue). Experiment was performed in biological triplicate and error bars represent standard deviation.

when challenged with most antibiotics, regardless of whether growing in planktonic or biofilm environments.

With the Exception of Vancomycin, Antibiotics Diffuse Freely Through Polymicrobial Biofilms

One mechanism that could explain the increased tolerance in polymicrobial biofilms is that antibiotics are not able to completely penetrate the polymicrobial biofilm matrix. To determine whether this was the case for other classes of antibiotics, antibiotic penetration assays were performed. The respective zone of inhibition for oxacillin, rifampicin, delafloxacin, and ciprofloxacin indicated that these antibiotics are not impeded by the biofilm matrix created by *S. aureus*, *C. albicans*, or the combination of both organisms (**Table 1**). As previously demonstrated, vancomycin diffusion was inhibited by the polymicrobial biofilm (p = 0.041). A decrease in vancomycin diffusion was also seen with *S. aureus* monoculture biofilms, although this was found to not be significantly different (p = 0.052) from diffusion in the absence of biofilm.

To confirm these findings, vancomycin and delafloxacin penetration throughout the biofilm were examined using confocal scanning laser microscopy (**Figure 3**). *S. aureus*, *C. albicans*, or polymicrobial biofilms were grown. Formed biofilms were visualized by staining the polysaccharide matrix with concanavalin A (ConA, red). To visualize vancomycin, a fluorescent BODIPY conjugate was used (green). For delafloxacin, its intrinsic fluorescence was used (ex405/em450, blue). Contrary to the biofilm penetration assay and previously published work, vancomycin diffusion did not appear to be inhibited by the polymicrobial biofilm. The only exception to this

TABLE 1 | Zone of inhibition (mm) following antibiotic diffusion through biofilms.

	Zone of Inhibition (MM)			
Antibiotic	**No biofilm**	***S. aureus* biofilm**	***C. albicans* biofilm**	**Polymicrobial biofilm**
Ciprofloxacin	76.67 ± 5.77	78.33 ± 7.63	75 ± 8.66	76.67 ± 5.77
Delafloxacin	160 ± 5	150 ± 5	150 ± 0	151.67 ± 2.89
Oxacillin	120 ± 17.32	123.33 ± 15.27	115 ± 18.03	121.67 ± 16.07
Rifampicin	100 ± 5	95 ± 5	96.67 ± 2.89	96.67 ± 5.77
Vancomycin	40 ± 5	13.33 ± 12.58	35 ± 0	13.33 ± 11.55*
No antibiotic	0 ± 0			

**Denotes significance using t-test ($p \leq 0.05$).*

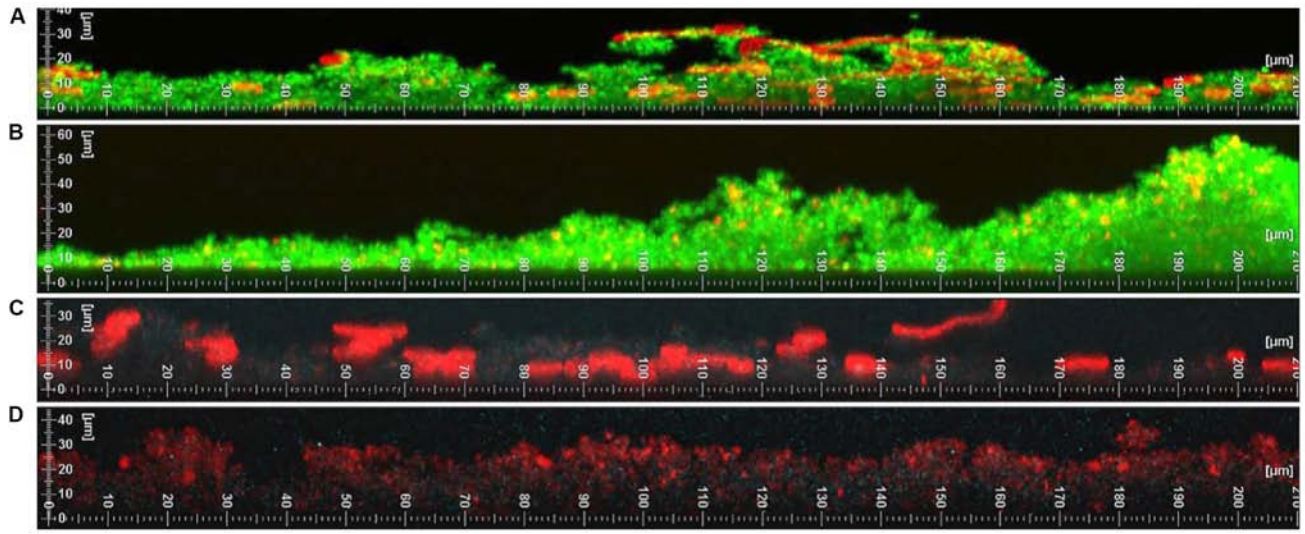

FIGURE 3 | Vancomycin has limited diffusion while Delafloxacin does not have restricted diffusion through polymicrobial biofilms. **(A)** Vancomycin BODIPY FL conjugate (green) and concanavalin A (red) was added to a polymicrobial biofilm. The diffusion of vancomycin is modestly reduced in areas with a complex and thick biofilm. **(B)** Vancomycin BODIPY FL conjugate (green) and concanavalin A (red) was added to a monomicrobial *S. aureus* biofilm. The *S. aureus* biofilm has unrestricted diffusion of vancomycin. **(C)** Delafloxacin (blue) and concanavalin A (red) was added to a polymicrobial biofilm. The diffusion of delafloxacin is not restricted throughout the biofilm. **(D)** Delafloxacin (blue) and concanavalin A (red) was added to a monomicrobial *S. aureus* biofilm. The *S. aureus* biofilm has unrestricted diffusion of delafloxacin. Images are respective images from three random fields of view.

observation is a slight decrease in vancomycin fluorescence in basal layers of the biofilm that reached 30 μM in height. However, a similar decrease in fluorescence was observed in biofilms formed by *S. aureus* alone. Despite this very modest phenotype, vancomycin was able to diffuse throughout the biofilm and reach all of the cells growing within the biofilm. Similarly, although the intrinsic fluorescence only produced a weak signal, delafloxacin was not inhibited by either single or polymicrobial biofilms. With the possible exception of vancomycin, the increased tolerance does not appear to be due to limited penetration of the antibiotic through the biofilm matrix.

Vancomycin Binding in Planktonic Cultures Is Not Inhibited by Matrix Coating

Confocal imaging revealed ConA binding *S. aureus* within polymicrobial cultures. To determine whether this coating was enough to inhibit antibiotics from accessing the cell, flow cytometry was used to measure the amount of antibiotics able to bind to the bacteria. Vancomycin was found to bind similarly to *S. aureus* cells regardless of whether they were grown in monomicrobial cultures or polymicrobial cultures (**Figure 4**). To confirm that the growth to mid-exponential phase was long enough for matrix coating to occur, polymicrobial cultures were stained with ConA. Matrix coating did occur during this time as indicated by the fluorescence associated with *S. aureus* cells in polymicrobial cultures. Unfortunately, the intrinsic fluorescence of delafloxacin was too weak for analysis and could not be properly assessed. Nevertheless, it is clear that despite coating of bacterial cells, vancomycin was still able to bind to *S. aureus*, and physical inhibition of the antibiotic is not the reason for increased tolerance.

Increased Antibiotic Tolerance Within *S. aureus* and *C. albicans* Co-cultures Is Not Affected by Secreted Products

Secreted *C. albicans* products larger than 3,000 MW were concentrated and added to cultures prior to antibiotic challenge to examine whether a specific virulence factor or biomolecule was influencing tolerance within *S. aureus*. After an incubation period, cultures were challenged with rifampicin. Cultures containing concentrated supernatant showed no difference in antibiotic tolerance compared to cultures incubated without the added supernatant (**Figure 5A**).

Previously, farnesol was shown to influence antibiotic tolerance (Jabra-Rizk et al., 2006; Kong et al., 2017). According to recent work, at high concentrations (100–150 μM), farnesol appears to enhance antibiotic effectiveness. Conversely, lower concentrations (40 μM) of farnesol appear to result in increased antibiotic tolerance. Therefore, we tested the possibility that increased tolerance is from farnesol secretion by *C. albicans.* Following the addition of farnesol (40 μM), no effect on antibiotic tolerance was observed when cultures were challenged with rifampicin (**Figure 5B**).

We considered the possibility that secreted products smaller than 3,000 MW were being excluded from these kill assays. To confirm previous findings, cultures were grown in spent media prior to antibiotic challenge. Growth in spent *C. albicans* media increased tolerance within *S. aureus,* however, growth in spent *S. aureus* media also increased tolerance to a similar extent

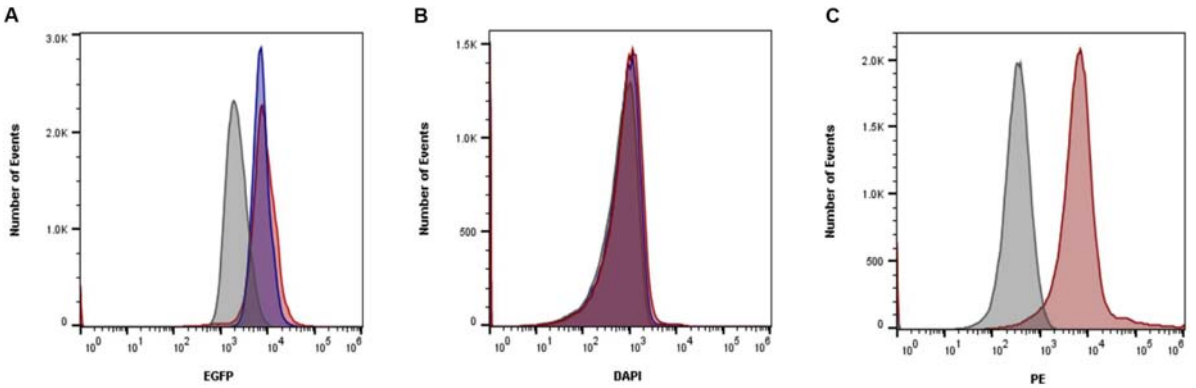

FIGURE 4 | Matrix coating does not inhibit vancomycin binding. **(A)** Vancomycin BODIPY FL conjugate was added to planktonic cells in either polymicrobial (red) or monomicrobial (blue) cultures. Vancomycin was able to bind *S. aureus* similarly in both conditions. Unstained cells were included as a control (gray). **(B)** Fluorescence from delafloxacin either in polymicrobial (red) or monomicrobial (blue) cultures was unable to be differentiated from unstained cells (gray) due to the weak signal produced. **(C)** To ensure matrix coating occurred, ConA was added to polymicrobial (red) cultures and compared to unstained polymicrobial cultures (gray). Data is representative of three independent replicates.

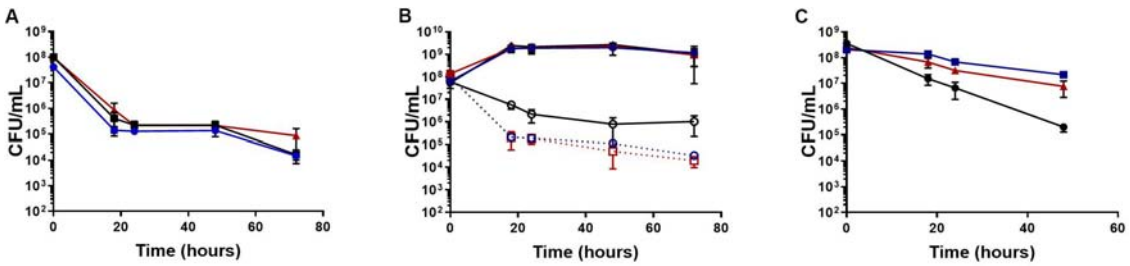

FIGURE 5 | Products secreted by *C. albicans* are not responsible for increased tolerance. **(A)** Planktonic cultures were grown to mid-exponential phase in TSB (blue) with the addition of concentrated *C. albicans* (red) or *S. aureus* (black) secreted products larger than 3000 MW and subsequently challenged with rifampicin. No change in tolerance was observed when compared to the control. **(B)** HG003 (solid blue line) showed no growth defect in the presence of farnesol (black solid line) or in the presence of *C. albicans* (solid red line). The presence of farnesol did not increase tolerance to rifampicin (dashed black) compared to *S. aureus* in monomicrobial cultures (dashed blue line). *S. aureus* grown in the presence of *C. albicans* (dashed red line) increased survival by a log. **(C)** Planktonic *S. aureus* cultures were grown to mid-exponential phase in TSB (black), in spent *S. aureus* media (blue), or in spent *C. albicans* media (red). Cultures were challenged with rifampicin and surviving bacteria were enumerated over 48 h. Growth in both *S. aureus* and *C. albicans* spent supernatant increased survival following antibiotic challenge. All experiments were performed in biological triplicate and error bars represent standard deviation.

(**Figure 5C**). These results cast doubt on the ability of secreted *C. albicans* products to increase antibiotic tolerance. Instead, the increase in tolerance in both environments suggests that a common cause, such as nutrient depletion, is responsible for increased tolerance.

Polymicrobial Cultures Consume Glucose at an Increased Rate, Leading to Lower Intracellular ATP Concentrations

Glucose, a preferred source of carbon for *S. aureus*, serves as the major substrate for glycolysis. This leads to NADH generation and subsequent ATP synthesis. Glucose concentration was measured over time to determine if a polymicrobial culture could deplete available glucose at an increased rate. As one would expect, glucose was consumed faster in the polymicrobial culture than the *S. aureus* monoculture (**Figure 6**).

To confirm that the lower concentrations of extracellular glucose affect the energy status of bacterial cells, the intracellular ATP in *S. aureus* from single and mixed cultures was measured. Previous work demonstrated that antibiotic tolerance is increased when intracellular ATP is depleted (Conlon et al., 2016). During late exponential phase, *S. aureus* cells from mixed cultures exhibited lower intracellular ATP concentrations compared to *S. aureus* from single cultures (**Figure 7**). Moreover, membrane potential is closely linked with the energy status of the cell, and therefore it is likely altered in polymicrobial cultures. *S. aureus* cells grown in the presence of *C. albicans* exhibited a reduced membrane potential compared to *S. aureus* monocultures (**Figure 8**). This indicates that polymicrobial cultures consume nutrients more rapidly than monomicrobial cultures, resulting in lower intracellular ATP and membrane potential.

Cells in Polymicrobial Biofilms Show a Decrease in Metabolic Gene Activity

Recent work has implicated an association between the TCA cycle and membrane potential and persister cell formation in

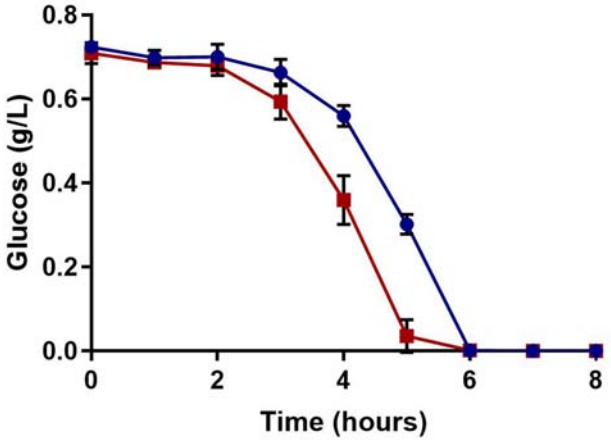

FIGURE 6 | Extracellular glucose availability. Glucose concentrations were measured over time. Glucose was more rapidly consumed in polymicrobial cultures (red) compared to *S. aureus* monocultures (blue); both cultures completely exhausted the glucose in the media by 6 h. Experiments were performed in triplicate and error bars represent standard deviation.

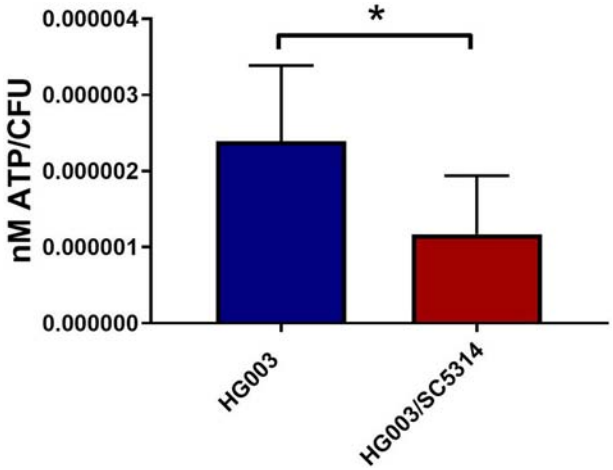

FIGURE 7 | *Staphylococcus aureus* grown in polymicrobial cultures has lower intracellular ATP. Planktonic cultures were grown to late exponential phase, pelleted and washed, and intracellular ATP was measured. Bacterial numbers were determined by standard serial dilution technique and ATP concentrations were normalized to CFU. Data is represented by the mean of six independent replicates and error bars represent standard deviation. Significance was determined using a *t*-test (*$p < 0.05$).

S. aureus (Wang et al., 2018; Zalis et al., 2019). To examine whether a similar mechanism was occurring in polymicrobial cultures, TCA cycle activity was measured using a promoter-*gfp* fusion construct, P*fumC:gfp*. In the presence of *C. albicans*, fluorescence was notably lower over a period of 22 h (**Figure 9**). In order to assess if this effect was from a generalized reduction in transcription or specific to genes in central metabolism, P*spa:gfp* was used as a control reporter. The *spa* gene encodes the virulence factor, protein A. The *spa* reporter had no difference between *S. aureus* cells grown alone compared to those cells grown in a polymicrobial culture, thus indicating decreased transcription was specific to metabolic processes.

DISCUSSION

It is estimated that fifty percent of all infections involve biofilms (Wolcott et al., 2010). Biofilm infections are notoriously difficult to eradicate completely, despite being caused primarily by drug-susceptible pathogens (Monack et al., 2004; Lewis, 2010; Conlon, 2014). Further complications arise when biofilms involve more than one organism, resulting in increased mortality (Gabrilska and Rumbaugh, 2015). Reasons for this increased mortality remain unclear but a number of studies have focused on individual antibiotic treatment as well as specific reasons for therapy failure. Increased antimicrobial resistance has been observed for a limited number of antibiotics (Harriott and Noverr, 2009), but this fails to explain recurring infections caused by drug-susceptible organisms. Our data provide an explanation for multi-drug tolerance by a broad acting energy-dependent mechanism. This is in accordance with recent work published on the mechanism of persister formation in *S. aureus* (Conlon et al., 2016; Wang et al., 2018; Zalis et al., 2019).

Polymicrobial biofilms were consistently more tolerant to antibiotics with the exception of vancomycin and gentamicin. This contradicts other findings, where the presence of *C. albicans* increased tolerance to both of these antibiotics (Singh et al., 2010; Perez et al., 2014; Li et al., 2015; Kong et al., 2016). This does not mean that there is no difference, and may be a result of little to no killing observed in either the monomicrobial or polymicrobial biofilms challenged with these antibiotics. Higher concentrations of antibiotics may show results similar to previously published work. However, a more interesting phenomena demonstrated here is that antibiotic diffusion through the biofilm did not appear to be a significant cause of increased antibiotic tolerance within the biofilm. In most cases, there was no significant difference between the zone of inhibition following diffusion through a polymicrobial or monomicrobial biofilm. Vancomycin diffusion was variable between replicates with one assay exhibiting no diffusion and the other replicates having impeded diffusion. The possibility exists that vancomycin is simply defusing through the biofilm at a slower rate than the other antibiotics. Confocal analysis also provided evidence that delafloxacin was not impeded by biofilm matrix. While the intrinsic fluorescent signal was faint, it is clearly present in the deeper biofilm layers.

Further support that physical inhibition is not the primary mechanism for increased tolerance is provided by experiments performed in a planktonic setting. It could be assumed that if physical inhibition was the primary mechanism for increased tolerance, there would be little difference in tolerance to non-cell wall acting antibiotics in a planktonic environment. However, the large increases in tolerance were consistent across all classes of antibiotics used, indicating that physical inhibition is not a likely explanation for multidrug tolerance. Further evidence against physical inhibition was provided by flow cytometry analysis. While the fluorescence from delafloxacin was too weak to be

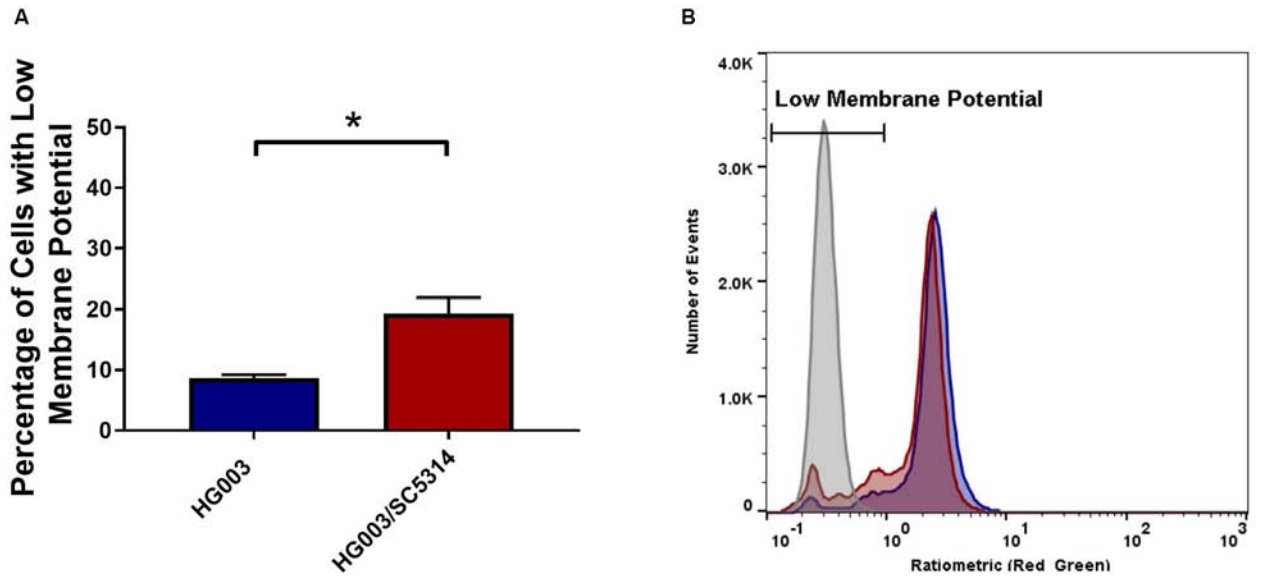

FIGURE 8 | The presence of *C. albicans* decreases membrane potential in *S. aureus* cells. **(A)** Membrane potential was measured during mid-exponential phase in *S. aureus* either grown alone (blue) or in the presence of *C. albicans* (red). 1×10^6 cells in PBS were stained with $DiOC_2(3)$ for 30 min and analyzed by flow cytometry. **(B)** Carbonyl cyanide *m-chlorophenylhydrazone* (CCCP) was used to dissipate membrane potential (gray) and was used to gate low membrane potential cells. The mean ± SD is shown, $n = 6$ for the graph on the left. The figure on the right is representative of six independent replicates. Significance was determined using a *t*-test ($^*p < 0.05$).

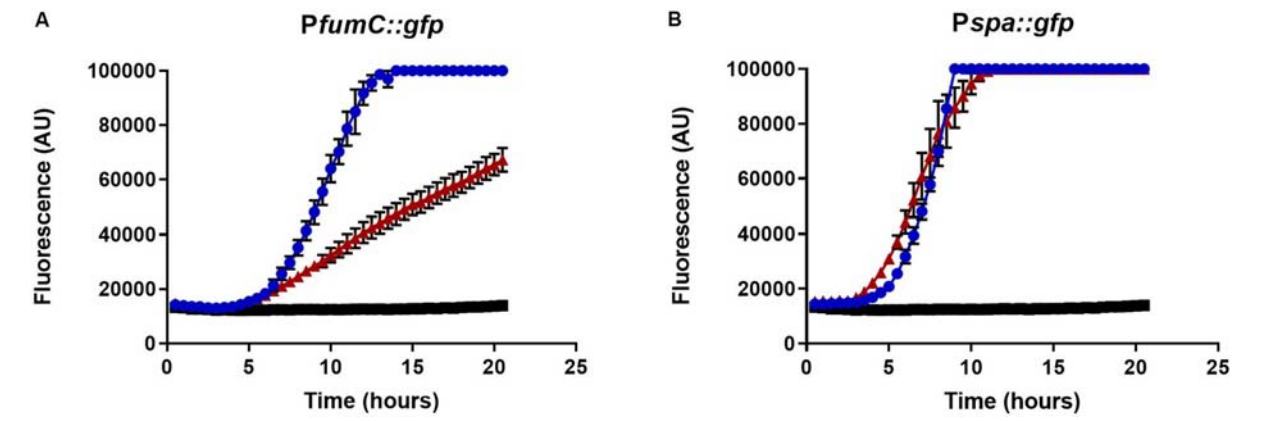

FIGURE 9 | Fumarase C Expression. GFP expression of P*fumC:gfp* **(A)** and P*spa:gfp* **(B)** was measured over time using a Biotek microplate reader. Overnight cultures of *S. aureus* (1:100) and *C. albicans* (1:50) were diluted in MHB in a microtiter plate. *C. albicans* decreased expression of the TCA cycle gene, fumarase (red) compared to expression observed when *S. aureus* was grown alone (blue). This effect was specific to fumarase and not the result of a generalized reduction in *S. aureus* transcription as indicated by the P*spa:gfp* control. *C. albicans* did not affect fluorescence outside of gene expression (black). Experiments were performed in biological triplicate; error bars represent standard deviation.

detected with our flow cytometer, vancomycin was clearly not inhibited by matrix coating from *C. albicans*.

Previous work has found the *C. albicans* quorum sensing molecule, farnesol, may both increase and decrease antibiotic susceptibility depending on its concentration (Jabra-Rizk et al., 2006; Kong et al., 2017). The effects of secreted products, including farnesol, on antibiotic tolerance were tested. Neither concentrated *C. albicans* nor *S. aureus* supernatant affected tolerance, indicating that extracellular byproducts larger than 3000 MW are not influencing antibiotic tolerance in *S. aureus*. However, this still leaves the possibility of smaller molecules influencing the bacteria.

Small products other than farnesol were further investigated by growing cultures in the presence of spent media. Growth in *C. albicans* conditioned media did increase antibiotic tolerance, however, the same phenotype was observed when grown in spent *S. aureus* media. Unexpectedly, the increase on antibiotic tolerance does not appear to be specific to a product secreted by *C. albicans*, rather, nutrient exhaustion was a more likely explanation for the observed increase in antibiotic tolerance.

Recent work on the mechanism of persister formation has implicated decreased intracellular ATP and membrane potential with an increase in antibiotic tolerance (Conlon et al., 2016; Shan et al., 2017; Wang et al., 2018; Zalis et al., 2019). Results from the spent media assay suggest that the increased tolerance in polymicrobial cultures can be explained by a similar mechanism. It follows that if *C. albicans* is decreasing available nutrients within the biofilm, *S. aureus* cells will have to compete for the same nutrients. Those cells, which are unable to find adequate nutrients will create a population of *S. aureus* cells in a low energy state, leading to an increase in tolerance to antibiotics with active targets. Available glucose was depleted faster in polymicrobial cultures and, fittingly, both ATP and membrane potential were lower in *S. aureus* cells grown in a mixed culture compared to monocultures. A specific mechanism with the TCA cycle was recently suggested (Wang et al., 2018; Zalis et al., 2019), and results with the TCA cycle reporter, P*fumC:gfp,* support those observations. Together these results demonstrate a decrease in *S. aureus* metabolism as a direct result of nutrient depletion by *C. albicans*.

Metabolism is becoming a focal point in the investigation of chronic *S. aureus* infections. While glycolysis is required for initial abscess formation in mice, upon maturation of the abscess glucose concentrations become a limiting factor (Richardson et al., 2015; Vitko et al., 2015; Thurlow et al., 2018). Similarly, during initial stages of biofilm formation, glucose is likely readily available and preferentially consumed. Later on in the process, the biofilm becomes a glucose-limited environment before subsequent dispersal of the biofilm (Boles and Horswill, 2008; Huynh et al., 2012). These examples are niches where antibiotic treatment of *S. aureus* is likely to fail. Furthermore, these niches often lead to chronic infections that the immune system is unable to manage (Leid et al., 2002; Jesaitis et al., 2003; Vuong et al., 2004; Cheng et al., 2011). Nutrient depletion leading to an antibiotic tolerant state may hold broader implications with parallels in chronic infections with other microorganisms.

DATA AVAILABILITY STATEMENT

All datasets generated for this study are included in the article/**Supplementary Material**.

AUTHOR CONTRIBUTIONS

DN, BL, and AN contributed to the conception and design of the study. DN and AN performed the statistical analysis. DN wrote the first draft of the manuscript. DN, SS, BL, and AN wrote sections of the manuscript. All authors performed the experiments, generated data appearing in the manuscript, contributed to the revision of the manuscript, and read and approved the submitted version.

FUNDING

This work was funded by National Center for Research Resources (5P20RR016469) and the National Institute for General Medical Science (8P20GM103427). Funding for this work was also provided by the Nebraska EPSCoR Undergraduate Research Experience at Small Colleges and Universities program and the Nebraska Research Initiative for equipment used in this project. Funding for the open access publication fees were provided by UNK Biology Department.

ACKNOWLEDGMENTS

We would like to thank Kim Lewis, Northeastern University, for the P*fumC*:*gfp* and P*spa:gfp* plasmids.

SUPPLEMENTARY MATERIAL

The Supplementary Material for this article can be found online at: https://www.frontiersin.org/articles/10.3389/fmicb.2019.02803/full#supplementary-material

FIGURE S1 | Increased antibiotic tolerance associated with polymicrobial cultures are not strain or species specific. Planktonic cultures were grown to early to mid-exponential phase in TSB and challenged with vancomycin (100× MIC), the surviving bacteria were enumerated over 72 h by plating on TSA containing amphotericin B (25 μg/mL). The presence of *C. albicans* increases *S. aureus* UAMS-1 **(A)**, *S. aureus* JE2 **(B)**, and *S. epidermidis* 1457 **(C)** (red) antibiotic tolerance compared to *S. aureus* monocultures (blue). Experiment was performed in biological triplicate and error bars represent standard deviation.

REFERENCES

Amato, S. M., and Brynildsen, M. P. (2014). Nutrient transitions are a source of persisters in *Escherichia coli* biofilms. *PLoS One* 9:e93110. doi: 10.1371/journal.pone.0093110

Boles, B. R., and Horswill, A. R. (2008). Agr-mediated dispersal of *Staphylococcus aureus* biofilms. *PLoS Pathog.* 4:e1000052. doi: 10.1371/journal.ppat.1000052

Cheng, A. G., DeDent, A. C., Schneewind, O., and Missiakas, D. (2011). A play in four acts: *Staphylococcus aureus* abscess formation. *Trends Microbiol.* 19, 225–232. doi: 10.1016/j.tim.2011.01.007

Cheung, A. L., Nast, C. C., and Bayer, A. S. (1998). Selective activation of sar promoters with the use of green fluorescent protein transcriptional fusions as the detection system in the rabbit endocarditis model. *Infect. Immun.* 66, 5988–5993.

Conlon, B. P. (2014). *Staphylococcus aureus* chronic and relapsing infections: evidence of a role for persister cells: an investigation of persister cells, their formation and their role in *S. aureus* disease. *Bioessays* 36, 991–996. doi: 10.1002/bies.201400080

Conlon, B. P., Rowe, S. E., Gandt, A. B., Nuxoll, A. S., Donegan, N. P., Zalis, E. A., et al. (2016). Persister formation in *Staphylococcus aureus* is associated with ATP depletion. *Nat. Microbiol.* 1:16051. doi: 10.1038/nmicrobiol.2016.51

Ericson, J. E., Popoola, V. O., Smith, P. B., Benjamin, D. K., Fowler, V. G., Benjamin, D. K. Jr., et al. (2015). Burden of invasive *Staphylococcus aureus* infections in hospitalized infants. *JAMA Pediatr.* 169, 1105–1111. doi: 10.1001/jamapediatrics.2015.2380

Fengcai, S., Di, X., Qianpeng, H., Hongke, Z., and Yiyu, D. (2015). [Microbial characteristics in culture-positive sepsis and risk factors of polymicrobial infection in ICU]. *Zhonghua Wei Zhong Bing Ji Jiu Yi Xue* 27, 718–723.

Gabrilska, R. A., and Rumbaugh, K. P. (2015). Biofilm models of polymicrobial infection. *Future Microbiol.* 10, 1997–2015. doi: 10.2217/fmb.15.109

Gillum, A. M., Tsay, E. Y., and Kirsch, D. R. (1984). Isolation of the *Candida albicans* gene for orotidine-5′-phosphate decarboxylase by complementation of *S. cerevisiae* ura3 and E. coli pyrF mutations. *Mol. Gen. Genet.* 198, 179–182. doi: 10.1007/bf00328721

Goetghebeur, M., Landry, P. A., Han, D., and Vicente, C. (2007). Methicillin-resistant *Staphylococcus aureus*: a public health issue with economic consequences. *Can. J. Infect. Dis. Med. Microbiol.* 18, 27–34.

Haley, K. P., and Skaar, E. P. (2012). A battle for iron: host sequestration and *Staphylococcus aureus* acquisition. *Microbes Infect.* 14, 217–227. doi: 10.1016/j.micinf.2011.11.001

Halsey, C. R., Lei, S., Wax, J., Lehman, M. K., Nuxoll, A. S., Steinke, L., et al. (2016). Amino acid catabolism in *Staphylococcus aureus* and the function of carbon catabolite repression. *mBio* 8:e1434-16.

Harriott, M. M., and Noverr, M. C. (2009). *Candida albicans* and *Staphylococcus aureus* form polymicrobial biofilms: effects on antimicrobial resistance. *Antimicrob. Agents Chemother.* 53, 3914–3922. doi: 10.1128/AAC.00657-09

Harriott, M. M., and Noverr, M. C. (2010). Ability of *Candida albicans* mutants to induce *Staphylococcus aureus* vancomycin resistance during polymicrobial biofilm formation. *Antimicrob. Agents Chemother.* 54, 3746–3755. doi: 10.1128/AAC.00573-10

Harriott, M. M., and Noverr, M. C. (2011). Importance of *Candida*-bacterial polymicrobial biofilms in disease. *Trends Microbiol.* 19, 557–563. doi: 10.1016/j.tim.2011.07.004

Hassoun, A., Linden, P. K., and Friedman, B. (2017). Incidence, prevalence, and management of MRSA bacteremia across patient populations-a review of recent developments in MRSA management and treatment. *Crit. Care* 21:211. doi: 10.1186/s13054-017-1801-3

Herbert, S., Ziebandt, A. K., Ohlsen, K., Schafer, T., Hecker, M., Albrecht, D., et al. (2010). Repair of global regulators in *Staphylococcus aureus* 8325 and comparative analysis with other clinical isolates. *Infect. Immun.* 78, 2877–2889. doi: 10.1128/IAI.00088-10

Huynh, T. T., McDougald, D., Klebensberger, J., Al Qarni, B., Barraud, N., Rice, S. A., et al. (2012). Glucose starvation-induced dispersal of *Pseudomonas aeruginosa* biofilms is cAMP and energy dependent. *PLoS One* 7:e42874. doi: 10.1371/journal.pone.0042874

Jabra-Rizk, M. A., Meiller, T. F., James, C. E., and Shirtliff, M. E. (2006). Effect of farnesol on *Staphylococcus aureus* biofilm formation and antimicrobial susceptibility. *Antimicrob. Agents Chemother.* 50, 1463–1469. doi: 10.1128/AAC.50.4.1463-1469.2006

Jesaitis, A. J., Franklin, M. J., Berglund, D., Sasaki, M., Lord, C. I., Bleazard, J. B., et al. (2003). Compromised host defense on *Pseudomonas aeruginosa* biofilms: characterization of neutrophil and biofilm interactions. *J. Immunol.* 171, 4329–4339. doi: 10.4049/jimmunol.171.8.4329

Kelly, B., and O'Neill, L. A. (2015). Metabolic reprogramming in macrophages and dendritic cells in innate immunity. *Cell Res.* 25, 771–784. doi: 10.1038/cr.2015.68

Koch, A. M., Nilsen, R. M., Dalheim, A., Cox, R. J., and Harthug, S. (2015a). Need for more targeted measures - only less severe hospital-associated infections declined after introduction of an infection control program. *J. Infect. Public Health* 8, 282–290. doi: 10.1016/j.jiph.2014.11.001

Koch, A. M., Nilsen, R. M., Eriksen, H. M., Cox, R. J., and Harthug, S. (2015b). Mortality related to hospital-associated infections in a tertiary hospital; repeated cross-sectional studies between 2004-2011. *Antimicrob. Resist. Infect. Control* 4:57. doi: 10.1186/s13756-015-0097-9

Kong, E. F., Tsui, C., Kucharikova, S., Andes, D., Van Dijck, P., and Jabra-Rizk, M. A. (2016). Commensal protection of *Staphylococcus aureus* against antimicrobials by *Candida albicans* biofilm matrix. *mBio* 7:e1365-16. doi: 10.1128/mBio.01365-16

Kong, E. F., Tsui, C., Kucharikova, S., Van Dijck, P., and Jabra-Rizk, M. A. (2017). Modulation of *Staphylococcus aureus* response to antimicrobials by the *Candida albicans* quorum sensing molecule farnesol. *Antimicrob. Agents Chemother.* 61:e1573-17. doi: 10.1128/AAC.01573-17

Leid, J. G., Shirtliff, M. E., Costerton, J. W., and Stoodley, A. P. (2002). Human leukocytes adhere to, penetrate, and respond to *Staphylococcus aureus* biofilms. *Infect. Immun.* 70, 6339–6345. doi: 10.1128/iai.70.11.6339-6345.2002

Lewis, K. (2010). Persister cells. *Annu. Rev. Microbiol.* 64, 357–372. doi: 10.1146/annurev.micro.112408.134306

Li, H., Zhang, C., Liu, P., Liu, W., Gao, Y., and Sun, S. (2015). In vitro interactions between fluconazole and minocycline against mixed cultures of *Candida albicans* and *Staphylococcus aureus*. *J. Microbiol. Immunol. Infect.* 48, 655–661. doi: 10.1016/j.jmii.2014.03.010

Lin, J. N., Lai, C. H., Chen, Y. H., Chang, L. L., Lu, P. L., Tsai, S. S., et al. (2010). Characteristics and outcomes of polymicrobial bloodstream infections in the emergency department: a matched case-control study. *Acad. Emerg. Med.* 17, 1072–1079. doi: 10.1111/j.1553-2712.2010.00871.x

Maisonneuve, E., Castro-Camargo, M., and Gerdes, K. (2013). (p)ppGpp controls bacterial persistence by stochastic induction of toxin-antitoxin activity. *Cell* 154, 1140–1150. doi: 10.1016/j.cell.2013.07.048

McKenzie, F. E. (2006). Case mortality in polymicrobial bloodstream infections. *J. Clin. Epidemiol.* 59, 760–761. doi: 10.1016/j.jclinepi.2005.12.009

Monack, D. M., Mueller, A., and Falkow, S. (2004). Persistent bacterial infections: the interface of the pathogen and the host immune system. *Nat. Rev. Microbiol.* 2, 747–765. doi: 10.1038/nrmicro955

Odds, F. C., Brown, A. J., and Gow, N. A. (2004). *Candida albicans* genome sequence: a platform for genomics in the absence of genetics. *Genome Biol.* 5:230. doi: 10.1186/gb-2004-5-7-230

Pereira, P. M., Filipe, S. R., Tomasz, A., and Pinho, M. G. (2007). Fluorescence imaging microscopy shows decreased access of vancomycin to cell wall synthetic sites in vancomycin-resistant *Staphylococcus aureus*. *Antimicrob. Agents Chemother.* 51, 3627–3633. doi: 10.1128/aac.00431-07

Perez, A. C., Pang, B., King, L. B., Tan, L., Murrah, K. A., Reimche, J. L., et al. (2014). Residence of *Streptococcus pneumoniae* and *Moraxella catarrhalis* within polymicrobial biofilm promotes antibiotic resistance and bacterial persistence in vivo. *Pathog. Dis.* 70, 280–288. doi: 10.1111/2049-632X.12129

Perlroth, J., Choi, B., and Spellberg, B. (2007). Nosocomial fungal infections: epidemiology, diagnosis, and treatment. *Med. Mycol.* 45, 321–346. doi: 10.1080/13693780701218689

Richardson, A. R., Somerville, G. A., and Sonenshein, A. L. (2015). Regulating the intersection of metabolism and pathogenesis in gram-positive bacteria. *Microbiol. Spectr.* 3. doi: 10.1128/microbiolspec.MBP-0004-2014

Royo-Cebrecos, C., Gudiol, C., Ardanuy, C., Pomares, H., Calvo, M., and Carratala, J. (2017). A fresh look at polymicrobial bloodstream infection in cancer patients. *PLoS One* 12:e0185768. doi: 10.1371/journal.pone.0185768

Shan, Y., Brown Gandt, A., Rowe, S. E., Deisinger, J. P., Conlon, B. P., and Lewis, K. (2017). ATP-dependent persister formation in *Escherichia coli*. *mBio* 8:e2267-16. doi: 10.1128/mBio.02267-16

Singh, R., Ray, P., Das, A., and Sharma, M. (2010). Penetration of antibiotics through *Staphylococcus aureus* and *Staphylococcus epidermidis* biofilms. *J. Antimicrob. Chemother.* 65, 1955–1958. doi: 10.1093/jac/dkq257

Spahich, N. A., Vitko, N. P., Thurlow, L. R., Temple, B., and Richardson, A. R. (2016). *Staphylococcus aureus* lactate- and malate-quinone oxidoreductases contribute to nitric oxide resistance and virulence. *Mol. Microbiol.* 100, 759–773. doi: 10.1111/mmi.13347

Thurlow, L. R., Joshi, G. S., and Richardson, A. R. (2018). Peroxisome proliferator-activated receptor gamma is essential for the resolution of *Staphylococcus aureus* skin infections. *Cell Host Microbe* 24, 261.e4–270.e4. doi: 10.1016/j.chom.2018.07.001

Tong, S. Y., Davis, J. S., Eichenberger, E., Holland, T. L., and Fowler, V. G. Jr. (2015). *Staphylococcus aureus* infections: epidemiology, pathophysiology, clinical manifestations, and management. *Clin. Microbiol. Rev.* 28, 603–661. doi: 10.1128/CMR.00134-14

Vitko, N. P., Spahich, N. A., and Richardson, A. R. (2015). Glycolytic dependency of high-level nitric oxide resistance and virulence in *Staphylococcus aureus*. *mBio* 6:e00045-15. doi: 10.1128/mBio.00045-15

Vuong, C., Voyich, J. M., Fischer, E. R., Braughton, K. R., Whitney, A. R., DeLeo, F. R., et al. (2004). Polysaccharide intercellular adhesin (PIA) protects *Staphylococcus epidermidis* against major components of the human innate immune system. *Cell Microbiol.* 6, 269–275. doi: 10.1046/j.1462-5822.2004.00367.x

Wang, Y., Bojer, M. S., George, S. E., Wang, Z., Jensen, P. R., Wolz, C., et al. (2018). Inactivation of TCA cycle enhances *Staphylococcus aureus* persister cell formation in stationary phase. *Sci. Rep.* 8:10849. doi: 10.1038/s41598-018-29123-0

Wolcott, R. D., Rhoads, D. D., Bennett, M. E., Wolcott, B. M., Gogokhia, L., Costerton, J. W., et al. (2010). Chronic wounds and the medical biofilm paradigm. *J. Wound Care* 19, 45–46.

Zalis, E. A., Nuxoll, A. S., Manuse, S., Clair, G., Radlinski, L. C., Conlon, B. P., et al. (2019). Stochastic variation in expression of the tricarboxylic acid cycle produces persister cells. *mBio* 10:e1930-19. doi: 10.1128/mBio.01930-19

Zarb, P., Coignard, B., Griskeviciene, J., Muller, A., Vankerckhoven, V., Weist, K., et al. (2012). The European centre for disease prevention and control (ECDC) pilot point prevalence survey of healthcare-associated infections and antimicrobial use. *Euro Surveill.* 17:20316.

Conflict of Interest: The authors declare that the research was conducted in the absence of any commercial or financial relationships that could be construed as a potential conflict of interest.

frontiers in Microbiology

ORIGINAL RESEARCH
published: 15 January 2020
doi: 10.3389/fmicb.2019.03006

Moraxella catarrhalis Promotes Stable Polymicrobial Biofilms With the Major Otopathogens

Kirsten L. Bair[1] *and Anthony A. Campagnari*[1,2]*

[1] Department of Microbiology and Immunology, Jacobs School of Medicine and Biomedical Sciences, University at Buffalo, State University of New York, Buffalo, NY, United States, [2] The Witebsky Center for Microbial Pathogenesis and Immunology, University at Buffalo, State University of New York, Buffalo, NY, United States

Otitis media (OM) is a prevalent pediatric infection characterized by painful inflammation of the middle ear. The Gram-negative diplococcus *Moraxella catarrhalis* is a commensal of the nasopharynx and one of three leading causative agents of OM. The most recent work on this multifaceted disease indicates that biofilms and polymicrobial infections play a pivotal role in recurrent and chronic OM, which are difficult to eradicate using standard antibiotic protocols. Although there have been significant advances in OM research, the actual bacterial and viral interactions leading to pathogenesis remain largely uncharacterized. However, colonization and persistence in the nasopharynx is clearly an essential first step. In this study, we assessed the role *M. catarrhalis* plays in the co-colonization and persistence of the other major otopathogens, *Streptococcus pneumoniae* and non-typeable *Haemophilus influenzae* (NTHi). We characterized both monomicrobial and polymicrobial biofilms using an *in vitro* nasopharyngeal colonization model. Biofilm assays were designed to mimic the nasopharynx and bacterial persistence was quantified over time. NTHi showed a steady and significant decline in viability over 20–48 h when this organism was in a dual species biofilm with *S. pneumoniae*. However, when *M. catarrhalis* was present in the polymicrobial biofilm NTHi survived for 48 h at 10^7 CFU per mL. In addition, an isogenic *M. catarrhalis* catalase-deficient mutant was also fully capable of protecting NTHi from the bactericidal activity of *S. pneumoniae* in a polymicrobial biofilm. Our results show that *M. catarrhalis* promotes a favorable environment for stable polymicrobial biofilms by enhancing the survival of NTHi in the presence of *S. pneumoniae*. These data suggest that colonization with *M. catarrhalis* promotes stable co-colonization with other otopathogens.

Keywords: otitis media, biofilm, polymicrobial, *Moraxella catarrhalis*, *Streptococcus pneumoniae*, non-typeable *Haemophilus influenzae*

OPEN ACCESS

Edited by:
Giovanna Batoni, University of Pisa, Italy

Reviewed by:
Kristian Riesbeck, Lund University, Sweden
Rosalia Cavaliere, University of Technology Sydney, Australia

***Correspondence:**
Anthony A. Campagnari
aac@buffalo.edu

Specialty section:
This article was submitted to Antimicrobials, Resistance and Chemotherapy, a section of the journal Frontiers in Microbiology

Received: *24 September 2019*
Accepted: *13 December 2019*
Published: *15 January 2020*

Citation:
Bair KL and Campagnari AA (2020) Moraxella catarrhalis Promotes Stable Polymicrobial Biofilms With the Major Otopathogens. Front. Microbiol. 10:3006. doi: 10.3389/fmicb.2019.03006

INTRODUCTION

There are more than 700 million cases of acute otitis media (AOM) diagnosed globally each year, with 50% of affected children under 5 years of age (Monasta et al., 2012). *Moraxella catarrhalis*, non-typeable *Haemophilus influenzae* (NTHi) and *Streptococcus pneumoniae* cause approximately 95% of AOM cases creating an incredible economic burden on healthcare

systems (Broides et al., 2009). In the United States, it is estimated that AOM is responsible for 4.3 billion dollars in health-related costs (Tong et al., 2018). In addition to being the most common reason for doctor's office visits among children, AOM is also currently the most common reason for antibiotic use in the pediatric population. Recent studies have shown antibiotic resistance and decreased sensitivity developing among the major otopathogens (Pichichero, 2000a; Zielnik-Jurkiewicz and Bielicka, 2015; Sillanpaa et al., 2016; Korona-Glowniak et al., 2018). Further, the polymicrobial biofilms associated with AOM are incredibly resistant and difficult to treat using classic antibiotic protocols (Pichichero, 2000b; Leibovitz et al., 2003; Libson et al., 2005; Asher et al., 2008; Leibovitz, 2008; Korona-Glowniak et al., 2018). This is a result of conferred β-lactamase protection, quiescent bacteria within biofilms, poor antibiotic penetration and persister cells. When taken in combination with the continued prevalence of AOM in the post-vaccine era, these challenges demand novel preventative and treatment strategies.

Because all of these otopathogens can colonize asymptomatically, the interactions that occur in the nasopharynx that prevent or promote co-colonization play an important role in the steps that eventually lead to pathogenesis. Thus, we focused our studies on a more thorough evaluation of the possible events that occur during nasopharyngeal colonization. Providing a better understanding of the bacterial interactions that occur between the three primary otopathogens could lead to novel strategies for the prevention and treatment of AOM (Armbruster and Swords, 2010; Murphy, 2015).

To date, some of the dual species interactions of otopathogens have been characterized *in vitro* or *in vivo*. However, the ability to compare the three species in a single system has been limited by animal models that are less than ideal for the strict human pathogen *M. catarrhalis*. We have extended studies on these otopathogens by employing an *in vitro* nasopharyngeal colonization model adapted from previous studies originally designed for *S. pneumoniae* (Marks et al., 2012; Chao et al., 2017; Reddinger et al., 2018). The model mimics the conditions of the human nasopharynx including considerations for nasopharyngeal temperature, nutrient availability, aeration, and epithelial attachment.

Using this modified *in vitro* nasopharyngeal colonization model we assessed co-colonization dynamics of each otopathogen in dual species. Further, we analyzed interactions of all three otopathogens in triple species biofilms which have not been previously studied. Our results indicate that *M. catarrhalis* is able to promote survival of NTHi even in the presence of *S. pneumoniae* in triple species biofilms like those that have been previously shown to colonize the human nasopharynx (Hoa et al., 2009; Casey et al., 2010; Palmu et al., 2019).

MATERIALS AND METHODS

Bacterial Strains and Culture Methods

Moraxella catarrhalis strain 7169 is a clinical middle ear isolate (Faden et al., 1997). Minimally passaged planktonic *M. catarrhalis* cultures were grown at 37°C, 180 RPM, aerobically in chemically defined pneumococcal growth media (CDM) as previously described (van de Rijn and Kessler, 1980). NTHi strain 86-028NP is a clinical isolate from a pediatric patient who underwent a tympanostomy for chronic otitis media (OM) (Kennedy et al., 2000). NTHi cultures were grow at 37°C, 180 RPM, aerobically in CDM. *S. pneumoniae* EF3030 is a serotype 19F OM isolate that was grown statically and anaerobically in CDM at 37°C (Andersson et al., 1983). The co-infection strains *M. catarrhalis* 11-01-125, *S. pneumoniae* 11-01-125 and NTHi 11-01-125 were isolated from the middle ear fluid of a pediatric patient during a polymicrobial infection and generously provided by Michael Pichichero, MD (Rochester, NY, United States). Each species was grown as outlined above. These isolates were maintained for long term storage at −80°C.

Static Biofilms and Time Course Assay

Stationary *in vitro* biofilms were grown in 24-well plates on a monolayer of NCI-H292 bronchial carcinoma cells (ATCC CCL-1848) as previously described (van Schilfgaarde et al., 1995). Planktonic cultures were grown to an OD_{600} of ∼0.2 (∼10^7 CFU per mL). *M. catarrhalis* and NTHi were used at this concentration whereas *S. pneumoniae* was diluted 1:100 prior to seeding (∼10^4 CFU per mL). These inocula were used for the studies in **Figures 1B,C**, **2**. For the data shown in **Figure 3**, all three otopathogens were used at a starting inoculum of ∼10^4 CFU per mL. Wells received 350 μL of each culture during seeding of either monomicrobial, dual species or triple species biofilms and CDM was added to a final volume of 1050 μL. Biofilms were incubated statically at 34°C and 5% CO_2. Media changes were completed at 4, 20, and 28 h post-seeding by replacing all spent media with 1 mL fresh CDM. Biofilm formation was quantified at 0, 4, 20, 24, and 48 h by carefully removing the supernatant and any planktonic or loosely attached bacteria and resuspending the biofilm in PBS via physical disruption with a pipette tip. Dilution plating onto selective media was utilized for CFU enumeration of *M. catarrhalis* (Mueller–Hinton agar + vancomycin at 3 mg per mL), *S. pneumoniae* (Blood agar + gentamicin at 4 mg per mL), and NTHi (Chocolate agar + clarithromycin at 2 mg per mL) at each time point. Plates were incubated for 24 h at 37°C and 5% CO_2.

Transwell Assay

Dual species *S. pneumoniae* EF3030 and NTHi 86-028NP biofilms were grown in 24-well plates on a fixed H292 cell monolayer. NTHi 86-028NP and *S. pneumoniae* EF3030 planktonic cultures were grown to an OD_{600} of ∼0.2 and diluted 1:100 for a seeding concentration of ∼10^5 CFU per mL and 350 μL of the 1:100 culture dilution was used for seeding. A transwell insert was added to each well [0.4 μm PET cell-culture 24-well adapted insert (Corning Inc., Corning, NY, United States)]. Transwell inserts of the treated wells received 350 μL of *M. catarrhalis* 7169 prepared for seeding as discussed previously, and control wells were seeded with 350 μL CDM. Media changes were completed at 4, 20, and 28 h post-seeding by replacing the spent media in the well and in the transwell insert separately. At 24 and 48 h the spent media was removed and the inserts were placed into a sterile 24 well plate. The biofilms in the

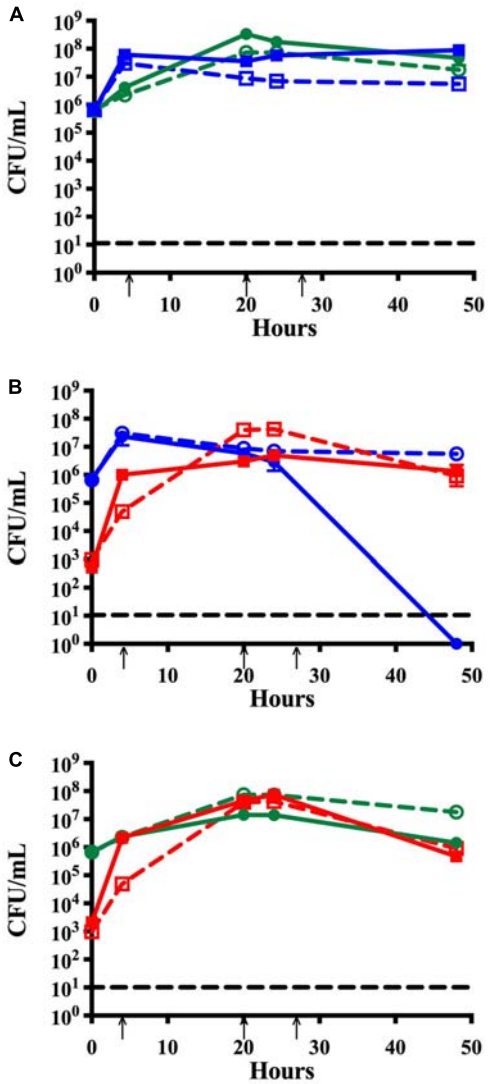

FIGURE 1 | Time course assay analyzing monomicrobial and dual species biofilms *in vitro*. Bacteria were grown in monomicrobial (dashed) or dual species (solid) biofilms and maintained with media changes (black arrows) for 48 h. **(A)** NTHi86-028 NP (blue) and *M. catarrhalis* 7169 (green) monomicrobial and dual species biofilms. **(B)** NTHi86-028 NP (blue) and *S. pneumoniae* EF3030 (red) monomicrobial and dual species biofilms. **(C)** *M. catarrhalis* 7169 (green) and *S. pneumoniae* EF3030 (red) monomicrobial and dual species biofilms. Black dashed line indicates the limit of CFU detection. Each symbol and error bar represent the mean CFU per mL and standard deviation (SD) of biofilms at the respective time point. Data presented are from three independent assays with a minimum of two biologic replicates per assay.

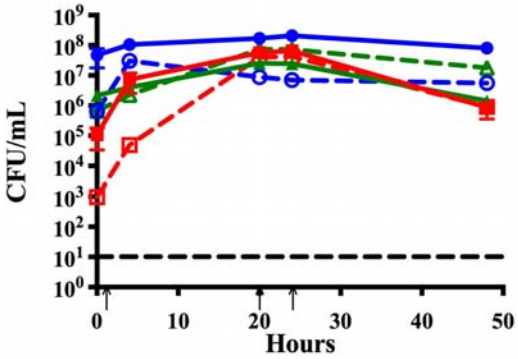

FIGURE 2 | Time course assay analyzing monomicrobial and triple species biofilms *in vitro*. Bacteria were grown in monomicrobial (dashed) or triple species biofilms (solid). Biofilms were seeded simultaneously and maintained with media changes (black arrows) for 48 h. NTHi86-028 NP (blue), *M. catarrhalis* 7169 (green), and *S. pneumoniae* EF3030 (red) monomicrobial and triple species biofilms. Black dashed line indicates the limit of CFU detection. Each symbol and error bar represent the mean CFU per mL and standard deviation (SD) of biofilms at the respective time point. Data presented are from three independent assays with a minimum of two biologic replicates per assay.

bottom of the 24-well plate and biofilms in the insert were each harvested in 1 mL PBS and dilution plated onto selective media for CFU enumeration as described above.

Catalase Mutant Formation

The *M. catarrhalis* catalase mutant 7169ΔkatSpec1 was constructed in 7169 using the SOE-PCR technique to construct an insertion/deletion mutation (Thornton, 2016). In brief, amplicons containing 1350 nucleotides (nt) of genomic 7169 DNA upstream (using primers 2865/2868, **Table 1**) and 1364 nt downstream (using primers 2869/2864, **Table 1**) of *katA* were amplified using the non-A-tailing high-fidelity polymerase PFU (Agilent Technologies, Santa Clara, CA, United States). A third 895 nt amplicon was generated using primers 2870 and 2871 designed to flank the spectinomycin resistance cassette using pSpec as the template (Whitby et al., 1998; Plamondon et al., 2007). The 5′ region of primers 2868 and 2869 contained 20 nucleotides of homology to the primers 2870 and 2871 to allow for overlap and priming to give the final product containing the spectinomycin resistance cassette inserted within a 150 nt deletion internal to the *katA* coding region. This was accomplished by a final PCR reaction using primers 2864 and 2865 and the three purified amplicons Qiagen MinElute Reaction Cleanup Kit (Qiagen, Germantown, MD, United States). The resulting 3609 nt amplicon, containing the insertionally inactivated *katA*, was purified Qiagen MinElute Reaction Cleanup Kit and used to mutagenize 7169 by natural transformation, as described (Furano and Campagnari, 2003). Transformants were selected following overnight growth on Mueller–Hinton agar plates containing 15 μg per ml spectinomycin. Chromosomal DNA from transformant 7169ΔkatSpec1 was isolated and subjected to PCR analysis (with primers 2874 and 2875 designed to flank the site of homologous recombination) and sequence analysis confirmed the integration of the inactivated *katA* construct into the 7169 genome. We further confirmed the functional inactivation using a qualitative catalase test. A sterile inoculating needle was used to transfer a single colony into a droplet of 3% hydrogen peroxide. A negative test is indicated by the lack of O_2 production, which is a product of hydrogen peroxide catalysis by catalase.

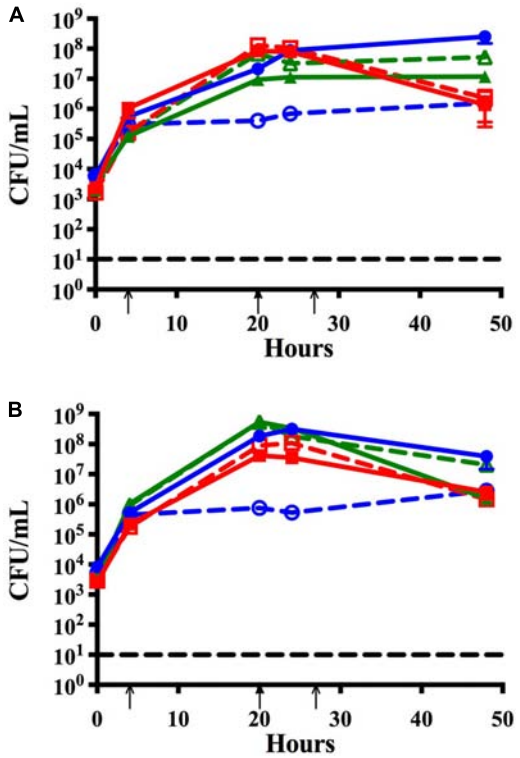

FIGURE 3 | Time course assay to assess the effects of lower seeding concentrations and address strain specificity by analyzing trends of co-infection isolates. Bacteria seeded simultaneously at a lower concentration (~10^5 CFU per mL) and maintained with media changes (black arrows) for 48 h in monomicrobial (dashed) or triple species (solid) biofilms. Each symbol and error bar represent the mean CFU per mL and standard deviation (SD) of biofilms at the respective time point. Data presented are from three independent assays with a minimum of two biologic replicates per assay. Black dashed line indicates the limit of CFU detection. **(A)** NTHi86-028 NP (blue), *M. catarrhalis* 7169 (green), and *S. pneumoniae* EF3030 (red) monomicrobial and triple species biofilms. **(B)** NTHi 11-01-125 (blue), *M. catarrhalis* 11-01-125 (green) and *S. pneumoniae* 11-01-125 (red) monomicrobial and triple species biofilms.

TABLE 1 | Nucleotide sequences of oligonucleotide primers used for PCR-based mutagenesis.

Primer	Sequence (5′–3′)
2864	ACCGATGCCGAAATGGTCTT
2865	TTTGCTGCACAGTTTACCGC
2868	CTCCTCACTATTTTGATTAGACCTGATGAAACGCCTCTGG
2869	GAAAACAATAAACCCTTGCCCGATGCCGAAGCTGAAATG
2870	CCAGAGGCGTTTCATCAGGTCTAATCAAAATAGTGAGGAG
2871	CATTTCAGCTTCGGCATCGGGCAAGGGTTTATTGTTTTC
2874	AAACTTCCCACATGCAACGC
2875	CAACTAGAAGCACCGCCTCA

Statistical Analyses

Student's *t*-tests were used to compare the CFUs per mL of NTHi and *S. pneumoniae* exposed to *M. catarrhalis* or CDM in the filter well experiments. In addition, log transformed values of NTHi in the transwell assay (CDM treated, WT treated and catalase mutant treated) were checked for normal distribution using the Shapiro–Wilk test. Normally distributed data sets were analyzed by one-way ANOVA with Dunnett's multiple comparison test. Alternatively, data sets that did not pass the Shapiro–Wilk test were analyzed using the non-parametric Kruskal–Wallis with Dunn's multiple comparison test. All *P*-values were derived using a 95% confidence interval. The statistical analysis was performed with Prism 8 from GraphPad Software, Inc. (La Jolla, CA, United States).

RESULTS

Moraxella catarrhalis Promotes the Growth of NTHi in Dual Species Biofilms *in vitro*

Previous studies have shown that colonization with *M. catarrhalis* occurs very early in life and *M. catarrhalis* is more likely to be present in polymicrobial AOM than infections resulting from a single bacterial species (Broides et al., 2009). Using our *in vitro* nasopharyngeal colonization model we assessed the relationship between *M. catarrhalis* and NTHi biofilms in physiologically relevant conditions. Biofilm formation was quantified over time via CFU enumeration. **Figure 1A**, shows that NTHi forms a slightly more robust biofilm, ~1 log greater, in dual species biofilms with *M. catarrhalis* than in monomicrobial biofilms which is consistent with previously reported data (Mokrzan et al., 2018). This is a statistically significant increase in viable NTHi at 48 h as compared to NTHi grown in monomicrobial biofilms (**Supplementary Figure S1A**).

NTHi Is Unable to Persist in Biofilms With *S. pneumoniae*

Although *S. pneumoniae* and NTHi each have a very high prevalence in OM individually, they are isolated together far less frequently (Casey et al., 2010). This is not surprising as previous studies have shown that peroxide production by planktonic *S. pneumoniae* elicits bactericidal effects on NTHi *in vitro* (Pericone et al., 2000). As recurrent OM is often considered a polymicrobial biofilm-associated disease, we performed studies to assess the relationship between these otopathogens in a dual species biofilm using our *in vitro* nasopharyngeal colonization model. **Figure 1B** shows that although NTHi can co-exist with *S. pneumoniae* for the initial 24 h, there is a rapid decline in NTHi viability to undetectable levels by 48 h. Based on these data, we concluded that NTHi and *S. pneumoniae* are unable to persist for extended periods in our *in vitro* model system.

Moraxella catarrhalis and *S. pneumoniae* Form Dual Species Biofilms *in vitro*

To determine if the *S. pneumoniae* bactericidal activity versus NTHi was also elicited against *M. catarrhalis*, we assessed the compatibility of these bacteria in biofilms using our *in vitro*

model system. In contrast to the NTHi data, *M. catarrhalis* viability in dual species biofilms with *S. pneumoniae* remained consistent with the monomicrobial biofilm control (**Figure 1C**). At 48 h both species were present in the biofilm at $\sim 10^6$ CFU per mL indicating that *M. catarrhalis* and *S. pneumoniae* can co-exist and persist in our model system *in vitro*. These data are consistent with previous *in vivo* studies suggesting that *M. catarrhalis* is capable of coping with the environmental stresses induced by *S. pneumoniae* in mixed species biofilms (Perez et al., 2014).

Moraxella catarrhalis Promotes the Survival of NTHi in Polymicrobial Biofilms With *S. pneumoniae*

As chronic or recurrent OM is considered a biofilm-associated disease, we further assessed the ability of these three otopathogens to co-exist and persist in a polymicrobial biofilm. **Figure 2** demonstrates that NTHi is now fully capable of surviving and persisting in this triple species biofilm even in the presence of *S. pneumoniae*. The survival of NTHi at 48 h was stastically significant as compared to NTHi in dual species with *S. pneumoniae* (**Supplementary Figure S1**). It appears that the presence of *M. catarrhalis* in these polymicrobial biofilms provides some form of protection from the bactericidal effects of *S. pneumoniae*. Further, at 48 h NTHi forms the most robust biofilms of all three otopathogens as quantified by CFU per mL.

Based on previous work done by Chao et al. (2017) we inoculated *S. pneumoniae* in all the previously mentioned time course assays at a lower seeding concentration to facilitate the analysis of bacterial-bacterial interactions. To ensure that our triple species data was not affected by lower seeding concentration, we completed a time course assay where all three otopathogens were diluted 1:100 and seeded simultaneously at approximately equivalent concentrations ($\sim 10^4$ CFU per mL). **Figure 3A** confirms that the starting inocula had no effect on the establishment of polymicrobial biofilms and also confirms that the lower inoculum of *M. catarrhalis* was still able to protect NTHi from the bactericidal effects of the pneumococci.

Multiple *M. catarrhalis* Clinical Isolates Protect NTHi in Polymicrobial Biofilms Containing *S. pneumoniae*

We further assessed the strain specificity of the protective effect by testing co-infection strains that were simultaneously isolated from the middle ear fluid of a pediatric patient during a middle ear infection. Data collected from the co-infection strains demonstrated that NTHi was able to persist within the triple species biofilm and that protection by *M. catarrhalis* is not strain specific (**Figure 3B**).

Cell to Cell Contact Is Not Required to Protect NTHi From the Bactericidal Effects of *S. pneumoniae*

As one of the classic characteristics of bacterial biofilms is close contact at the cellular level, we utilized a transwell insert in our *in vitro* model system to physically isolate *M. catarrhalis* biofilms. Briefly, dual species *S. pneumoniae* and NTHi biofilms were seeded in 24-well plates on fixed H292 cell monolayers as described and transwell inserts were added to each well. *M. catarrhalis* was seeded into the inserts of the experimental wells and media alone was added to the control wells. Bacterial viability was assessed at 24 and 48 h as previously stated. **Figure 4A** shows that NTHi viability had a modest but significant decrease ($\sim$1 log) at 24 h in the media treated controls as compared to the *M. catarrhalis* treated wells. This trend is even more apparent at 48 h, which shows that NTHi viability in the control wells was decreased by $\sim 10^3$ CFU/mL compared with the *M. catarrhalis* exposed dual species biofilms which actually showed an increase in NTHi bacterial persistence to $\sim 10^7$ CFU per mL (**Figure 4B**). These results demonstrate that *M. catarrhalis* can promote the survival and persistence of NTHi in the presence of *S. pneumoniae* and that this protective effect does not require direct contact. These data suggest that there is a factor(s) secreted or released into the supernatant that directly or indirectly confers protection to NTHi.

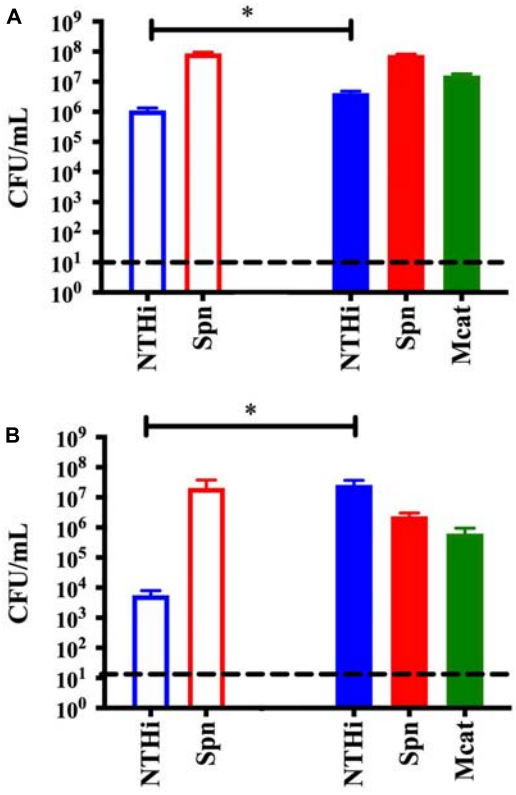

FIGURE 4 | Transwell assay to assess protection without cell to cell contact. Dual species *S. pneumoniae* EF3030 (Spn) and NTHi 86-028 NP (NTHi) biofilms were seeded in 24-well plates on a fixed H292 cell monolayer. To the filter inserts, approximately 10^5 CFU per mL *M. catarrhalis* 7169 (solid) or CDM (open) was added. Protection was assessed at **(A)** 24 h and **(B)** 48 h where bars represent the mean and SD of three independent assays with a minimum of four technical replicates. *P*-value of 0.05 was considered significant and indicated by asterisk (*).

Moraxella catarrhalis Catalase Production Is Not the Only Mechanism Involved in Protecting NTHi From Pneumococcal Hydrogen Peroxide

Previous studies have shown that the bactericidal effects of *S. pneumoniae* hydrogen peroxide production on NTHi can be reversed by the addition of catalase (Pericone et al., 2000). Although NTHi produces catalase, the activity *in vitro* is considered quite low (Pericone et al., 2000) and this likely explains why it is not protective in our model system (**Figure 1B**). However, *M. catarrhalis* does produce a highly active catalase and this has been previously shown to neutralize the effects of *S. pneumoniae* hydrogen peroxide in planktonic cultures *in vitro* (Pericone et al., 2000). Based on this previous report, we constructed an isogenic catalase mutant in the *M. catarrhalis* 7169 (Mcat7169ΔkatASpec1) and confirmed this mutant was defective in catalase production (data not shown). This Mcat7169ΔkatASpec1 construct was assessed for protective activity in the transwell assay versus the wild-type Mcat7169 at 24 h (**Figure 5A**) and 48 h (**Figure 5B**). These results show that the Mcat7169ΔkatASpec1 mutant was able to confer protection of NTHi to the same extent as the wild type Mcat7169 at both time points. Given the previous reports, these results were somewhat surprising suggesting that catalase is not solely responsible for the protective effect seen in these polymicrobial biofilms using our model system.

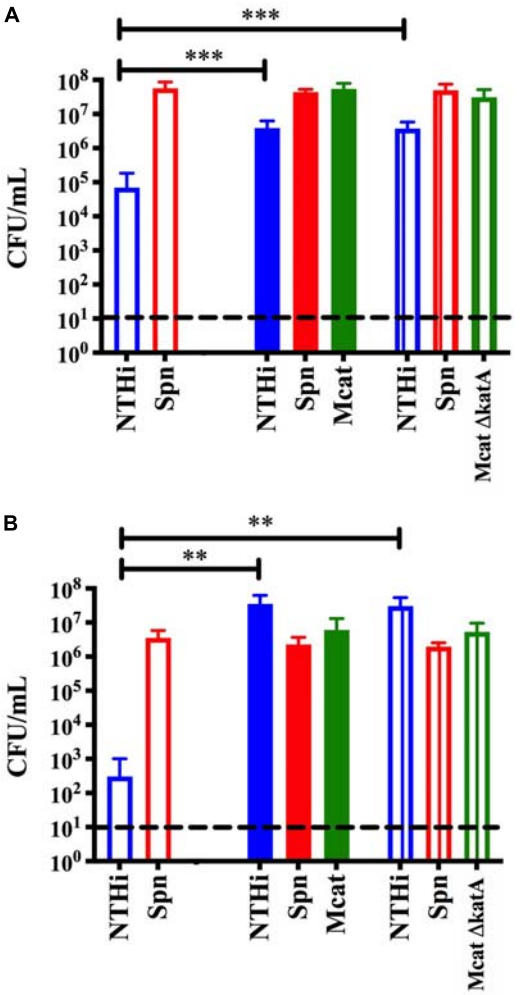

FIGURE 5 | Transwell assay to assess the protective capacity of a *M. catarrhalis* catalase mutant. Dual species *S. pneumoniae* (SpnEF3030) and NTHi 86-028 NP (NTHi86028) biofilms were seeded in 24-well plates on a fixed H292 cell monolayer. To the transwell inserts, approximately 10^5 CFU per mL *M. catarrhalis* 7169 (solid), Mcat7169 ΔkatASpec1 (vertical stripes) or CDM (open) was added. Protection was assessed at **(A)** 24 h and statistical analysis was performed using a one-way ANOVA and Dunnett's multiple comparison test of log transformed CFU per mL **(B)** and 48 h and statistical analysis was performed on log transformed CFU per mL using the Kruskal–Wallis with Dunn's multiple comparison test. Bars represent the mean and standard deviation of three independent assays with a minimum of two technical replicates. *P*-value of <0.01 denoted ** and *P*-value of <0.001 denoted ***.

DISCUSSION

The current model for OM pathogenesis is based on the concept that commensal bacteria colonize the nasopharynx of children very early in life and provide a reservoir for invasive diseases including AOM, sinusitis, and bacterial pneumonia. Although the mechanism of transition from colonization to opportunistic infection is not fully understood, it is widely accepted that changes in the host during a viral upper respiratory infection are linked to the subsequent onset of AOM (Heikkinen and Chonmaitree, 2003; Chonmaitree et al., 2008, 2016; Nokso-Koivisto et al., 2015). Based on this model, biofilms associated with colonization of otopathogens in the nasopharynx play a fundamental role in pathogenesis and are thus a primary target for preventative strategies.

While little is known about the transition from asymptomatic colonization to active infection, even less is known about how polymicrobial communities play a role in this transition. Using a model designed to mimic the environment of the nasopharynx we assessed the three primary otopathogens in dual species and triple species biofilms *in vitro*. To date, some of the dual species interactions have been characterized, but with contrasting results. For example, *S. pneumoniae* hydrogen peroxide production has been shown to have bactericidal effects on the other respiratory tract pathogens in planktonic cultures, in addition to being cytotoxic to the respiratory epithelial cells (Pericone et al., 2000). Likewise, *S. pneumoniae* produces neuraminidase which has the potential to remove sialic acid residues from other bacterial species exposing them to the host immune system. However, despite the many *S. pneumoniae* virulence factors cited, Perez et al. (2014) reported that *S. pneumoniae* increased colonization of *M. catarrhalis in vivo*. The same study also demonstrated that *M. catarrhalis* is able to confer

β-lactamase protection to *S. pneumoniae* and conversely *S. pneumoniae* is able to provide *M. catarrhalis* with macrolide resistance. Based on the current literature, many questions remain relating to the potential synergism or antagonistic co-colonization of these two respiratory pathogens. The data presented in this study confirm that *M. catarrhalis* is in fact able to co-colonize in dual species biofilms with *S. pneumoniae in vitro*.

The multivalent pneumococcal conjugate vaccine and the *Haemophilus influenzae* type b vaccine have changed the landscape of nasopharyngeal colonization (Cohen et al., 2006; Revai et al., 2006; Dagan, 2009). Despite the success of these vaccines, NTHi strains and non-vaccine serotypes of *S. pneumoniae* remain a prominent cause of AOM. One of the few studies on the interactions of *S. pneumoniae* and NTHi suggests that NTHi can also confer β-lactamase-dependent antibiotic resistance and promote biofilm formation, and thus increase persistence, *in vivo* (Weimer et al., 2010, 2011). When studied *in vitro*, the interactions between *S. pneumoniae* and NTHi were reported to be cell density dependent and required the down regulation of pneumococcal genes regulating autolysis and fratricide (Hong et al., 2014). Our results indicate that *S. pneumoniae* is bactericidal to NTHi in dual species biofilms despite seeding at a relatively low concentration of *S. pneumoniae* to limit cytotoxicity. After approximately 24 h of biofilm growth, NTHi began to decline as a result of *S. pneumoniae* virulence.

We were also able to confirm that *M. catarrhalis* and NTHi successfully co-colonize in dual species biofilms as previously reported (Armbruster et al., 2010). Additionally, in our dual species model *M. catarrhalis* is able to promote the biofilm formation of NTHi supporting recently published work by Mokrzan et al. (2018). These observations have important implications because prolonged nasopharyngeal carriage subsequently increases the potential for transition to disease.

The nasopharynx is a polymicrobial environment. Multiple studies have shown that *S. pneumoniae*, *M. catarrhalis* and NTHi can simultaneously occupy this mucosal niche; however, very little is known about the bacterial interactions that occur between these species and the possible role these play in the pathogenesis of AOM (Hoa et al., 2009; Casey et al., 2010; Palmu et al., 2019). As mentioned previously, studies have shown that *M. catarrhalis* is more likely to be found in polymicrobial AOM infections than from a single-species infection (Broides et al., 2009). Additionally, colonization with *M. catarrhalis* happens very early in life, which is in part why *M. catarrhalis* is more frequently seen in children experiencing their first AOM episode as opposed to those with recurrent infections (Broides et al., 2009). These two qualities suggest that *M. catarrhalis* may be one of the first bacteria-bacteria interactions and a major factor in the subsequent colonization of other bacterial species. To test the possibility that *M. catarrhalis* may be important in polymicrobial colonization, we analyzed all three bacterial species in our colonization model *in vitro*. Our data confirmed that all three otopathogens were able to form a mixed species biofilm in our model system. More importantly, the presence of *M. catarrhalis* was essential for NTHi to survive the bactericidal effects of *S. pneumoniae*. This phenomenon, which appears to be "protective" for NTHi, has not been documented to date and provides novel insight into nasopharyngeal co-colonization and subsequently polymicrobial infection pathogenesis.

To explore the mechanism of protection we first considered the physical properties of the biofilms. We addressed the possibility that biofilm architecture was involved in shielding NTHi from *S. pneumoniae* or that cell to cell contact was required. We utilized a transwell assay which physically separated *M. catarrhalis* biofilms from NTHi and *S. pneumoniae* dual species biofilms, but allowed for the exchange of components in the supernatant. We found that physical contact is not necessary for *M. catarrhalis* to confer protection. These data suggest that a secreted or released factor(s) is responsible for the observed protective effect. We considered the known bactericidal effects of *S. pneumoniae* hydrogen peroxide production and hypothesized that catalase production may play a role in this process (Pericone et al., 2000). To test this, we constructed a catalase mutant in the *M. catarrhalis* 7169 background (Mcat7169ΔkatASpec1) and assessed its protective capacity in the transwell assay. The mutant had a phenotype similar to the wild-type demonstrating that catalase production by *M. catarrhalis* was not essential for protection. It is possible that Mcat7169ΔkatASpec1 was able to compensate using other mechanisms for coping with oxidative stress. Our initial results do not indicate a clear mechanism of protection, but they do suggest that it is reliant on a secreted or released factor(s) that is not catalase and is not dependent on physical or architectural characteristics of polymicrobial biofilms.

Future studies aim to use a more global approach to analyze the transcriptome of *M. catarrhalis* monomicrobial biofilms versus *M. catarrhalis* polymicrobial biofilms to parse out genes that are important in the polymicrobial environment and thus potentially important for the protective effect. The cumulative ability of these otopathogens to form polymicrobial biofilms, persist, and resist antibiotics has major implications in AOM epidemiology and pathogenesis. The mechanism of protection could provide a target for minimizing polymicrobial biofilms of the nasopharynx.

DATA AVAILABILITY STATEMENT

The raw data supporting the conclusions of this article will be made available by the authors, without undue reservation, to any qualified researcher.

AUTHOR CONTRIBUTIONS

KB performed all the aforementioned experimentation. KB and AC contributed to the conception of the experimental design and preparation of the manuscript.

FUNDING

This work was supported by NIH R01DC014576 and NIH R01DC013554, awarded to AC.

ACKNOWLEDGMENTS

We would like to thank Lisa Hansen and Shauna Sauberan for technical assistance, Mary Canty and Chelsie Armbruster for guidance with statistical analyses, and Nicole Luke-Marshall for editorial insight.

SUPPLEMENTARY MATERIAL

The Supplementary Material for this article can be found online at: https://www.frontiersin.org/articles/10.3389/fmicb.2019.03006/full#supplementary-material

FIGURE S1 | A 48 h survival assessment. Bacterial species were statistically analyzed under each polymicrobial growth condition as compared to the monomicrobial control. Bars represent the mean and SD of minimally three independent assays. **(A)** NTHi, **(B)** *S. pneumoniae*, and **(C)** *M. catarrhalis* growth conditions were log transformed and analysis was completed using a student's *t*-test or a Mann–Whitney test based on the Shapiro–Wilk test for normality. *P*-value of <0.05 denoted *, <0.01 denoted **, and <0.001 denoted ***.

REFERENCES

Andersson, B., Dahmen, J., Frejd, T., Leffler, H., Magnusson, G., Noori, G., et al. (1983). Identification of an active disaccharide unit of a glycoconjugate receptor for pneumococci attaching to human pharyngeal epithelial cells. *J. Exp. Med.* 158, 559–570. doi: 10.1084/jem.158.2.559

Armbruster, C. E., Hong, W., Pang, B., Weimer, K. E., Juneau, R. A., Turner, J., et al. (2010). Indirect pathogenicity of *Haemophilus influenzae* and *Moraxella catarrhalis* in polymicrobial otitis media occurs via interspecies quorum signaling. *mBio* 1:e0010210. doi: 10.1128/mBio.00102-10

Armbruster, C. E., and Swords, W. E. (2010). Interspecies bacterial communication as a target for therapy in otitis media. *Expert Rev. Anti Infect Ther.* 8, 1067–1070. doi: 10.1586/eri.10.109

Asher, E., Dagan, R., Greenberg, D., Givon-Lavi, N., Libson, S., Porat, N., et al. (2008). Persistence of pathogens despite clinical improvement in antibiotic-treated acute otitis media is associated with clinical and bacteriologic relapse. *Pediatr. Infect. Dis. J.* 27, 296–301. doi: 10.1097/INF.0b013e31815ed79c

Broides, A., Dagan, R., Greenberg, D., Givon-Lavi, N., and Leibovitz, E. (2009). Acute otitis media caused by *Moraxella catarrhalis*: epidemiologic and clinical characteristics. *Clin. Infect. Dis.* 49, 1641–1647. doi: 10.1086/647933

Casey, J. R., Adlowitz, D. G., and Pichichero, M. E. (2010). New patterns in the otopathogens causing acute otitis media six to eight years after introduction of pneumococcal conjugate vaccine. *Pediatr. Infect. Dis. J.* 29, 304–309. doi: 10.1097/INF.0b013e3181c1bc48

Chao, Y., Bergenfelz, C., and Hakansson, A. P. (2017). *In vitro* and *in vivo* biofilm formation by pathogenic streptococci. *Methods Mol. Biol.* 1535, 285–299. doi: 10.1007/978-1-4939-6673-8_19

Chonmaitree, T., Revai, K., Grady, J. J., Clos, A., Patel, J. A., Nair, S., et al. (2008). Viral upper respiratory tract infection and otitis media complication in young children. *Clin. Infect. Dis.* 46, 815–823. doi: 10.1086/528685

Chonmaitree, T., Trujillo, R., Jennings, K., Alvarez-Fernandez, P., Patel, J. A., Loeffelholz, M. J., et al. (2016). Acute otitis media and other complications of viral respiratory infection. *Pediatrics* 137:e20153555. doi: 10.1542/peds.2015-3555

Cohen, R., Levy, C., de La Rocque, F., Gelbert, N., Wollner, A., Fritzell, B., et al. (2006). Impact of pneumococcal conjugate vaccine and of reduction of antibiotic use on nasopharyngeal carriage of nonsusceptible pneumococci in children with acute otitis media. *Pediatr. Infect. Dis. J.* 25, 1001–1007. doi: 10.1097/01.inf.0000243163.85163.a8

Dagan, R. (2009). Impact of pneumococcal conjugate vaccine on infections caused by antibiotic-resistant Streptococcus pneumoniae. *Clin. Microbiol. Infect.* 15(Suppl. 3), 16–20. doi: 10.1111/j.1469-0691.2009.02726.x

Faden, H., Duffy, L., Wasielewski, R., Wolf, J., Krystofik, D., and Tung, Y. (1997). Relationship between nasopharyngeal colonization and the development of otitis media in children. Tonawanda/Williamsville Pediatrics. *J. Infect. Dis.* 175, 1440–1445. doi: 10.1086/516477

Furano, K., and Campagnari, A. A. (2003). Inactivation of the *Moraxella catarrhalis* 7169 ferric uptake regulator increases susceptibility to the bactericidal activity of normal human sera. *Infect. Immun.* 71, 1843–1848. doi: 10.1128/iai.71.4.1843-1848.2003

Heikkinen, T., and Chonmaitree, T. (2003). Importance of respiratory viruses in acute otitis media. *Clin. Microbiol. Rev.* 16, 230–241. doi: 10.1128/cmr.16.2.230-241.2003

Hoa, M., Tomovic, S., Nistico, L., Hall-Stoodley, L., Stoodley, P., Sachdeva, L., et al. (2009). Identification of adenoid biofilms with middle ear pathogens in otitis-prone children utilizing SEM and FISH. *Int. J. Pediatr. Otorhinolaryngol.* 73, 1242–1248. doi: 10.1016/j.ijporl.2009.05.016

Hong, W., Khampang, P., Erbe, C., Kumar, S., Taylor, S. R., and Kerschner, J. E. (2014). Nontypeable *Haemophilus influenzae* inhibits autolysis and fratricide of *Streptococcus pneumoniae* in vitro. *Microbes Infect.* 16, 203–213. doi: 10.1016/j.micinf.2013.11.006

Kennedy, B. J., Novotny, L. A., Jurcisek, J. A., Lobet, Y., and Bakaletz, L. O. (2000). Passive transfer of antiserum specific for immunogens derived from a nontypeable *Haemophilus influenzae* adhesin and lipoprotein D prevents otitis media after heterologous challenge. *Infect. Immun.* 68, 2756–2765. doi: 10.1128/iai.68.5.2756-2765.2000

Korona-Glowniak, I., Zychowski, P., Siwiec, R., Mazur, E., Niedzielska, G., and Malm, A. (2018). Resistant *Streptococcus pneumoniae* strains in children with acute otitis media- high risk of persistent colonization after treatment. *BMC Infect. Dis.* 18:478. doi: 10.1186/s12879-018-3398-9

Leibovitz, E. (2008). Complicated otitis media and its implications. *Vaccine* 26(Suppl. 7), G16–G19. doi: 10.1016/j.vaccine.2008.11.008

Leibovitz, E., Greenberg, D., Piglansky, L., Raiz, S., Porat, N., Press, J., et al. (2003). Recurrent acute otitis media occurring within one month from completion of antibiotic therapy: relationship to the original pathogen. *Pediatr. Infect. Dis. J.* 22, 209–216.

Libson, S., Dagan, R., Greenberg, D., Porat, N., Trepler, R., Leiberman, A., et al. (2005). Nasopharyngeal carriage of *Streptococcus pneumoniae* at the completion of successful antibiotic treatment of acute otitis media predisposes to early clinical recurrence. *J. Infect. Dis.* 191, 1869–1875. doi: 10.1086/429918

Marks, L. R., Parameswaran, G. I., and Hakansson, A. P. (2012). Pneumococcal interactions with epithelial cells are crucial for optimal biofilm formation and colonization in vitro and in vivo. *Infect. Immun.* 80, 2744–2760. doi: 10.1128/IAI.00488-12

Mokrzan, E. M., Novotny, L. A., Brockman, K. L., and Bakaletz, L. O. (2018). Antibodies against the majority subunit (PilA) of the Type IV pilus of nontypeable *Haemophilus influenzae* disperse *Moraxella catarrhalis* from a dual-species biofilm. *mBio* 9:e02423–18. doi: 10.1128/mBio.02423-18

Monasta, L., Ronfani, L., Marchetti, F., Montico, M., Vecchi Brumatti, L., Bavcar, A., et al. (2012). Burden of disease caused by otitis media: systematic review and global estimates. *PLoS One* 7:e36226. doi: 10.1371/journal.pone.0036226

Murphy, T. F. (2015). Vaccines for nontypeable *Haemophilus influenzae*: the future is now. *Clin. Vaccine Immunol.* 22, 459–466. doi: 10.1128/cvi.00089-15

Nokso-Koivisto, J., Marom, T., and Chonmaitree, T. (2015). Importance of viruses in acute otitis media. *Curr. Opin. Pediatr.* 27, 110–115. doi: 10.1097/MOP.0000000000000184

Palmu, A. A., Ware, R. S., Lambert, S. B., Sarna, M., Bialasiewicz, S., Seib, K. L., et al. (2019). Nasal swab bacteriology by PCR during the first 24-months of life: a prospective birth cohort study. *Pediatr. Pulmonol.* 54, 289–296. doi: 10.1002/ppul.24231

Perez, A. C., Pang, B., King, L. B., Tan, L., Murrah, K. A., Reimche, J. L., et al. (2014). Residence of *Streptococcus pneumoniae* and *Moraxella catarrhalis* within polymicrobial biofilm promotes antibiotic resistance and bacterial persistence in vivo. *Pathog. Dis.* 70, 280–288. doi: 10.1111/2049-632X.12129

Pericone, C. D., Overweg, K., Hermans, P. W., and Weiser, J. N. (2000). Inhibitory and bactericidal effects of hydrogen peroxide production by *Streptococcus pneumoniae* on other inhabitants of the upper respiratory tract. *Infect. Immun.* 68, 3990–3997. doi: 10.1128/iai.68.7.3990-3997.2000

Pichichero, M. E. (2000a). Acute otitis media: part II. Treatment in an era of increasing antibiotic resistance. *Am. Fam. Phys.* 61, 2410–2416.

Pichichero, M. E. (2000b). Recurrent and persistent otitis media. *Pediatr. Infect. Dis. J.* 19, 911–916. doi: 10.1097/00006454-200009000-00034

Plamondon, P., Luke, N. R., and Campagnari, A. A. (2007). Identification of a novel two-partner secretion locus in *Moraxella catarrhalis*. *Infect. Immun.* 75, 2929–2936. doi: 10.1128/iai.00396-07

Reddinger, R. M., Luke-Marshall, N. R., Sauberan, S. L., Hakansson, A. P., and Campagnari, A. A. (2018). Streptococcus pneumoniae modulates staphylococcus aureus biofilm dispersion and the transition from colonization to invasive disease. *mBio* 9:e02089–17. doi: 10.1128/mBio.02089-17

Revai, K., McCormick, D. P., Patel, J., Grady, J. J., Saeed, K., and Chonmaitree, T. (2006). Effect of pneumococcal conjugate vaccine on nasopharyngeal bacterial colonization during acute otitis media. *Pediatrics* 117, 1823–1829. doi: 10.1542/peds.2005-1983

Sillanpaa, S., Sipila, M., Hyoty, H., Rautiainen, M., and Laranne, J. (2016). Antibiotic resistance in pathogens causing acute otitis media in Finnish children. *Int. J. Pediatr. Otorhinolaryngol.* 85, 91–94. doi: 10.1016/j.ijporl.2016.03.037

Thornton, J. A. (2016). Splicing by overlap extension PCR to obtain hybrid DNA products. *Methods Mol. Biol.* 1373, 43–49. doi: 10.1007/7651_2014_182

Tong, S., Amand, C., Kieffer, A., and Kyaw, M. H. (2018). Trends in healthcare utilization and costs associated with acute otitis media in the United States during 2008-2014. *BMC Health Serv. Res.* 18:318. doi: 10.1186/s12913-018-3139-1

van de Rijn, I., and Kessler, R. E. (1980). Growth characteristics of group a streptococci in a new chemically defined medium. *Infect. Immun.* 27, 444–448.

van Schilfgaarde, M., van Alphen, L., Eijk, P., Everts, V., and Dankert, J. (1995). Paracytosis of *Haemophilus influenzae* through cell layers of NCI-H292 lung epithelial cells. *Infect. Immun.* 63, 4729–4737.

Weimer, K. E., Armbruster, C. E., Juneau, R. A., Hong, W., Pang, B., and Swords, W. E. (2010). Coinfection with *Haemophilus influenzae* promotes pneumococcal biofilm formation during experimental otitis media and impedes the progression of pneumococcal disease. *J. Infect. Dis.* 202, 1068–1075. doi: 10.1086/656046

Weimer, K. E., Juneau, R. A., Murrah, K. A., Pang, B., Armbruster, C. E., Richardson, S. H., et al. (2011). Divergent mechanisms for passive pneumococcal resistance to beta-lactam antibiotics in the presence of *Haemophilus influenzae*. *J. Infect. Dis.* 203, 549–555. doi: 10.1093/infdis/jiq087

Whitby, P. W., Morton, D. J., and Stull, T. L. (1998). Construction of antibiotic resistance cassettes with multiple paired restriction sites for insertional mutagenesis of *Haemophilus influenzae*. *FEMS Microbiol. Lett.* 158, 57–60. doi: 10.1016/s0378-1097(97)00500-4

Zielnik-Jurkiewicz, B., and Bielicka, A. (2015). Antibiotic resistance of *Streptococcus pneumoniae* in children with acute otitis media treatment failure. *Int. J. Pediatr. Otorhinolaryngol.* 79, 2129–2133. doi: 10.1016/j.ijporl.2015.09.030

Conflict of Interest: The authors declare that the research was conducted in the absence of any commercial or financial relationships that could be construed as a potential conflict of interest.

frontiers in Microbiology

ORIGINAL RESEARCH
published: 15 January 2020
doi: 10.3389/fmicb.2019.02977

Antimicrobial Activity of Clinically Isolated Bacterial Species Against *Staphylococcus aureus*

*Britney L. Hardy[1], Garima Bansal[1], Katharine H. Hewlett[1], Arshia Arora[1], Scott D. Schaffer[1], Edwin Kamau[2,3], Jason W. Bennett[4,5] and D. Scott Merrell[1,5]**

[1] Department of Microbiology and Immunology, F. Edward Hébert School of Medicine, Uniformed Services University of the Health Sciences, Bethesda, MD, United States, [2] Department of Clinical Microbiology, Walter Reed National Military Medical Center, Bethesda, MD, United States, [3] U.S. Military HIV Research Program, Walter Reed Army Institute of Research, Silver Spring, MD, United States, [4] Multidrug-Resistant Organism Repository and Surveillance Network, Walter Reed Army Institute of Research, Silver Spring, MD, United States, [5] Department of Medicine, F. Edward Hébert School of Medicine, Uniformed Services University of the Health Sciences, Bethesda, MD, United States

OPEN ACCESS

Edited by:
Giuseppantonio Maisetta, University of Pisa, Italy

Reviewed by:
Bernhard Krismer, University of Tübingen, Germany
Karl Hassan, University of Newcastle, Australia

***Correspondence:**
D. Scott Merrell
douglas.merrell@usuhs.edu;
dmerrell@usuhs.mil

Specialty section:
This article was submitted to Antimicrobials, Resistance and Chemotherapy, a section of the journal Frontiers in Microbiology

Received: *13 August 2019*
Accepted: *10 December 2019*
Published: *15 January 2020*

Citation:
Hardy BL, Bansal G, Hewlett KH, Arora A, Schaffer SD, Kamau E, Bennett JW and Merrell DS (2020) Antimicrobial Activity of Clinically Isolated Bacterial Species Against Staphylococcus aureus. Front. Microbiol. 10:2977. doi: 10.3389/fmicb.2019.02977

Bacteria often exist in polymicrobial communities where they compete for limited resources. Intrinsic to this competition is the ability of some species to inhibit or kill their competitors. This phenomenon is pervasive throughout the human body where commensal bacteria block the colonization of incoming microorganisms. In this regard, molecular epidemiological and microbiota-based studies suggest that species-specific interactions play a critical role in the prevention of nasal colonization of the opportunistic pathogen *Staphylococcus aureus*. Despite this, *S. aureus* exists as part of the microbiota of ∼25% of the population, suggesting that the interplay between *S. aureus* and commensals can be complex. Microbiota studies indicate that several bacterial genera are negatively correlated with *S. aureus* colonization. While these studies paint a broad overview of bacterial presence, they often fail to identify individual species-specific interactions; a greater insight in this area could aid the development of novel antimicrobials. As a proof of concept study designed to identify individual bacterial species that possess anti-*S. aureus* activity, we screened a small collection of clinical isolates from the Walter Reed National Military Medical Center for the ability to inhibit multiple *S. aureus* strains. We found that the majority of the isolates (82%) inhibited at least one *S. aureus* strain; 23% inhibited all *S. aureus* strains tested. In total, seven isolates mediated inhibitory activity that was independent of physical contact with *S. aureus*, and seven isolates mediated bactericidal activity. 16S rRNA based-sequencing revealed that the inhibitory isolates belonged to the *Acinetobacter*, *Agromyces*, *Corynebacterium*, *Microbacteria*, *Mycobacterium,* and *Staphylococcus* genera. Unexpectedly, these included seven distinct *Acinetobacter baumannii* isolates, all of which showed heterogeneous degrees of anti-*S. aureus* activity. Defined mechanistic studies on specific isolates revealed that the inhibitory activity was retained in conditioned cell free medium (CCFM) derived from the isolates. Furthermore, CCFM obtained from *S. saprophyticus* significantly decreased mortality of *S. aureus*-infected

Galleria mellonella caterpillars. While future studies will seek to define the molecular mechanisms of the inhibitory activities, our current findings support the study of polymicrobial interactions as a strategy to understand bacterial competition and to identify novel therapeutics against *S. aureus* and other pathogens.

Keywords: *Staphylococcus aureus*, MRSA, polymicrobial interactions, bacterial interaction, clinical isolates

INTRODUCTION

Staphylococcus aureus is an opportunistic pathogen that, due to its ability to quickly adapt to harsh conditions and evade the host's immune system, can colonize virtually any niche throughout the human body. *S. aureus* causes a variety of diseases, most frequently skin and soft tissue infections, but also systemic and toxin-mediated disease (Otto, 2010). To further exacerbate matters, numerous *S. aureus* strains are resistant to multiple antibiotics, which subsequently makes treatment more difficult. Even amongst otherwise healthy individuals, the lack of appropriate treatment often leads to more severe morbidity and higher mortality rates (Lowy, 2003). Accordingly, methicillin-resistant *S. aureus* (MRSA)-mediated disease was responsible for approximately 10,000 deaths from 2005 to 2013 in the United States (Klevens et al., 2007). Furthermore, the worldwide pervasiveness of multidrug-resistant *S. aureus* strains has led the World Health Organization to designate MRSA as a "high" threat to the global population (WHO, 2017).

Despite the propensity to cause significant morbidity and mortality, *S. aureus* exists as a part of the microbiota of approximately one-quarter of the population (Sakr et al., 2018); however, colonized individuals are more likely to develop *S. aureus*-mediated disease (Kluytmans and Wertheim, 2005). In thinking about the dynamics of colonization of the host, *S. aureus* must interact and compete with the other resident flora as a means to establish itself as a part of the microbiota of a particular niche (Burian et al., 2017). This is undoubtedly a complicated process. However, even the vast amount of currently available microbiota data has not substantially increased our current understanding of the molecular mechanisms underlying the complex interactions between resident flora and incoming pathogens like *S. aureus*. It is well-established that commensal microbes play a critical role in decreasing and preventing pathogen colonization. A well-known example of this can be found with the ability of fecal transplants from healthy donors to treat patients with recurrent *Clostridium difficile* infections; restoration of the normal gastrointestinal microbiota eliminates and prevents *C. difficile* colonization (Buffie et al., 2015).

The ability of commensal bacteria to block pathogen colonization is true at other anatomical locations as well. *S. aureus* nasal colonization in particular is greatly dependent on molecular interactions with the nasal flora (Brugger et al., 2016; Sakr et al., 2018). Indeed, the nasal cavity is a high salinity and nutrient scarce niche where resident and incoming bacteria compete for limited resources and space in a type of "bacterial warfare" (Krismer et al., 2014). These interactions are often species-specific, and commensal bacterial have been found to use a variety of mechanisms to block pathogen colonization, including the production and secretion of toxic compounds that directly kill or inhibit competitors. For example, various species from within the *Streptococcus* and *Corynebacterium* genera are inversely correlated with the presence of *S. aureus* in the nasal cavity or have been found to directly antagonize *S. aureus* (Lemon et al., 2010; Bomar et al., 2016). Even other members of the *Staphylococcus* genus have been found to negatively impact *S. aureus* viability; several coagulase-negative *Staphylococcus* (CoNS) species have evolved mechanisms to inhibit *S. aureus* colonization. Specifically, some *S. epidermidis* strains secrete a serine protease that is capable of disrupting *S. aureus* biofilm formation and blocking nasal colonization (Iwase et al., 2010). *S. hominis* and *S. epidermidis* both secrete strain-specific antimicrobial peptides that have potent selective bactericidal activity against *S. aureus* (Nakatsuji et al., 2017). Moreover, lugdunin, a novel cyclic peptide antibiotic produced by *S. lugdunensis,* has bactericidal properties against several Gram-positive pathogens, including *S. aureus*, and can prevent *S. aureus* nasal colonization (Zipperer et al., 2016). It is clear that within the context of the human nose, there is a selective pressure, even amongst closely related commensal species, to block or eliminate *S. aureus*.

Despite recent advancements detailing the negative molecular interactions that occur between *S. aureus* and the resident nasal flora, little is known about *S. aureus* interactions with bacteria isolated from other anatomical locations. Given this deficit and the fact that *S. aureus* can colonize the human body virtually ubiquitously, as a proof of concept study we set out to characterize *S. aureus* interactions with clinical bacterial isolates obtained from a variety of body sites from a diverse patient population at the Walter Reed National Military Medical Center. Herein, we show that the majority (82%, 28/34) of clinical isolates possessed some degree of *in vitro* anti-*S. aureus* activity when tested against multiple strains of *S. aureus*, including MRSA. Moreover, eight clinical isolates showed anti-*S. aureus* activity against all tested strains. Several of the clinical isolates that belonged to the *Staphylococcus* and *Corynebacterium* genera mediated contact-independent inhibitory activity against *S. aureus*. Furthermore, a portion of the clinical isolates (7/28) showed bactericidal activity against *S. aureus*. Unexpectedly, *Acinetobacter baumannii* isolates represented the most commonly identified species that produced heterogenous strain-specific anti-*S. aureus* activity. Finally, analysis of conditioned cell free medium (CCFM) from several isolates revealed that inhibitory activity was often

present in the CCFM. Furthermore, CCFM derived from *S. saprophyticus* was able to reduce mortality of *S. aureus*-infected *Galleria mellonella* caterpillars. These findings suggest that *S. aureus* interactions with other bacteria are far more multifaceted than previously recognized, and strongly support the study of these interactions at the molecular level as a means to reveal novel *S. aureus* molecular targets or therapeutics.

MATERIALS AND METHODS

Strains, Culture and Bacterial Interaction Assays

All deidentified clinical isolates were obtained as a part of a memorandum of understanding (MOU) between the Uniformed Services University of the Health Sciences (USU) and the Walter Reed National Military Medical Center (WRNMMC), Department of Clinical Microbiology. The described studies represent research Not Involving Human Subjects since all isolates were obtained from discarded clinical microbiology plates that contained samples that were obtained during routine diagnostic testing and treatment of WRNMMC patients. Both USU and WRNMMC agree and acknowledge that the activities and projects pursued under the MOU complied with the applicable rules and regulations governing human subjects research within the Department of Defense; the Institutional Review Board at WRNMMC was the IRB of record for the collection of all patient samples. Strains were maintained as −80°C freezer stocks and were cultured under the following conditions unless otherwise noted: Clinical isolates were streaked from frozen glycerol stocks on Brain Heart Infusion (BHI) agar (Becton Dickinson) supplemented with 1% $Tween_{80}$ (BHIT, Sigma-Aldrich). *S. aureus* strains were streaked from glycerol stocks on BHI agar. Each isolate was incubated overnight at 37°C. Bacterial interaction assays were performed as previously described (Yan et al., 2013; Hardy et al., 2019). Briefly, 40 mg of *S. aureus* or a clinical isolate was directly harvested from an agar plate with a sterile inoculating loop and then re-suspended in 200 μL of sterile saline solution (Fisher Chemicals). Eight microliters of the *S. aureus* cell suspension was inoculated into 15 mL of sterile BHIT agar that had been cooled to 55°C; inoculated agar was poured into a sterile petri dish, and allowed to solidify under sterile conditions. Next, 25 μL of a clinical isolate cell suspension was spotted onto the center of an agar dish (one clinical isolate per a *S. aureus*-seeded agar plate), and was allowed to dry for 40 min under sterile conditions. The resulting plates were incubated at 28°C, and the formation of a zone of clearance (ZOC) was visually assessed at 24, 72, and 120 h. Images of the ZOC were taken with an Amersham Imager 680 (General Electric). The ZOC was defined as the distance between the edge of the clinical isolate spot and the visible edge of the clearance ring. To measure ZOC length, images were analyzed using ImageJ software (NCBI). Each clinical isolate was assessed in three independent biological replicates against *S. aureus* strains 2014.N, LAC, and Mu50 (**Table 1**).

DNA Extraction, Amplification, Cloning, and 16S rRNA Gene Sequencing

All clinical isolates that possessed anti-*S. aureus* activity (28/34) were streaked from frozen glycerol stocks on BHIT agar and incubated overnight at 37°C. Single colonies of each isolate were subcultured in 2 mL of BHIT broth and incubated at 37°C with shaking for 24–48 h. Overnight broth cultures were pelleted by centrifugation and re-suspended in 0.2 mL of Phosphate Buffer Solution (PBS, Fisher Chemicals). Cell suspensions were lysed in a Bullet Blender Homogenizer for 5 min by mechanical disruption in bead-beater tubes that contained 0.1 mm sterile glass beads. Genomic DNA was extracted from lysed cells suspensions with the Wizard Genomic DNA Purification Kit (Promega) according to the manufacturer's instructions.

Purified genomic DNA from each sample was subjected to PCR amplification of the 16S rRNA gene using the 8F (5′ AGAGTTTGATCCTGGCTCAG 3′) and 1492R (5′ GGTTACCTTGTTACGACTT 3′) primers. PCR mixtures (25 μL) contained 5X Phusion HF buffer, 200 mM of each dNTP, 0.5 μM of each primer, and 0.02 U/μL of Phusion DNA polymerase. PCR amplification was performed with the following reaction conditions: 98°C for 30 s, 30 cycles of 98°C for 5 s, 51°C for 30 s, 72°C for 1 min 30 s, with a final elongation step of 72°C for 5 min. The PCR amplified products were visualized on a 1% agarose gel to confirm the presence of an approximately 1,500 base pair band.

PCR products were purified using the QIAquick PCR purification kit according to the manufacturer's instructions. Purified PCR products were polyadenylated utilizing the A-tailing procedure; reaction components (10 μL), including PCR-amplified DNA, 10X ThermoPol Buffer, 1mM dATP, and Taq DNA Polymerase, were incubated at 70°C for 30 min. A-tailed PCR products were subsequently cloned into the pGEM-T Easy vector according to the manufacturer's instructions (Promega). Ligation products were transformed into *E. coli* TOP10 $CaCl_2$ chemically competent cells. Transformants with the desired insert were isolated via "blue/white" selection on LB (Luria-Bertani) agar supplemented with ampicillin (100 μg/mL), X-gal (40 μg/mL) and IPTG (1 μM). To confirm the presence of the correct insert, colony PCR was performed on at least five white colonies per transformation using the GoTaq Green Master Mix (Promega) and pGEM-T Easy specific T7 (5′ GGGTTTTCCCAGTCACGA 3′) and SP6 (5′ GCACCCCAGGCTTTACAC 3′) primers with the following PCR conditions: 95°C for 3 min, 30 cycles of 95°C for 30 s, 45°C for 30 s, 72°C for 1 min 30 s, with a final elongation step of 72°C for 5 min. White colonies that contained the correct insert were cultured overnight in LB Broth plus ampicillin (100 μg/mL) with shaking. Plasmids were purified using QIAprep Spin Miniprep Kit (Qiagen) according to the manufacturer's instructions and then used for sequencing.

As previously described (Johnson et al., 2016), to ensure near full-length coverage of the 16S rRNA gene, six individual sequencing reactions were performed on purified plasmids using the following primers: T7, SP6, 8F, 1492R, 515F (5′ GTGYCAGCMGCCGCGGTA 3′), and 806R (5′

TABLE 1 | Clinical isolates and *S. aureus* strains assayed.

Strain	Lab strain designation	Origin	Accession #	Year isolated	Anti-*S. aureus* activity$_4$			Contact dependent vs. Independent	Bactericidal vs. Bacteriostatic	References
					2014.N	LAC	Mu50			
***Staphylococcus aureus* test strains**										
S. aureus LAC	DSM1485	Blood	NC_002758.2	2005		N/A		N/A	N/A	Voyich et al. (2005)
S. aureus 2014.N	DSM1416	Nose	N/A	2012		N/A		N/A	N/A	Hardy et al. (2019)
S. aureus Mu50	DSM1633	Abscess	NC_002758.2	1997		N/A		N/A	N/A	Kuroda et al. (2001)
***Acinetobacter* clinical isolates**										
A. baumannii-1	DSM1675	Wound	MN175920	2016	Strong	Weak	Weak	Dependent$_1$	Bactericidal$_1$	This Study
A. baumannii-2	DSM1676	Wound	MN175921	2016	Strong	Weak	None	Dependent$_1$	Bacteriostatic$_1$	This Study
A. baumannii-3	DSM1923	Wound	MN175922	2016	Strong	Weak	Weak	Dependent$_1$	Bacteriostatic$_1$	This Study
A. baumannii-4	DSM1924	Wound	MN175925	2016	None	Weak	Weak	Not Tested	Not Tested	This Study
A. baumannii-5	DSM1917	Blood	MN175926	2016	None	Weak	Strong	Dependent$_3$	Not Tested*	This Study
A. baumannii-6	DSM1762	Wound	MN175924	2016	None	Weak	Strong	Dependent$_3$	Bactericidal$_3$	This Study
A. baumannii-7	DSM1918	Wound	MN175923	2016	None	Weak	Weak	Not Tested	Not Tested	This Study
***Corynebacterium* clinical isolates**										
C. amycolatum-1	DSM1914	Nasal	MN175942	2016	Weak	None	None	Not Tested	Not Tested	This Study
C. amycolatum-2	DSM1567	Nasal	MN175937	2016	Weak	None	Strong	Independent$_3$	Bactericidal$_3$	This Study
C. aurimucosum-1	DSM1560	Urine	MN175936	2016	Strong	None	Weak	Independent$_1$	Bacteriostatic$_1$	This Study
C. aurimucosum-2	DSM1678	Wound	MN175938	2016	Weak	None	Strong	Independent$_3$	Bacteriostatic$_3$	This Study
C. aurimucosum-3	DSM1912	Wound	MN175945	2016	None	None	Strong	Dependent$_3$	Not Tested*	This Study
C. aurimucosum-4	DSM1913	Wound	MN175932	2016	None	None	Weak	Not Tested	Not Tested	This Study
C. jeikeium	DSM1915	Would	MN175945	2016	None	Weak	None	Not Tested	Not Tested	This Study
C. striatum-1	DSM1564	Wound	MN175927	2016	Weak	None	Weak	Not Tested	Not Tested	This Study
C. striatum-2	DSM1566	Blood	MN175947	2016	Strong	None	None	Independent$_1$	Bacteriostatic$_1$	This Study
C. tuberculostearicum	DSM1925	Nasal	MN175944	2016	None	None	Weak	Not Tested	Not Tested	This Study
***Microbacterium* clinical isolates**										
M. paraoxydans-1	DSM1919	Nasal	MN175940	2016	None	Weak	Weak	Not Tested	Not Tested	This Study
M. paraoxydans-2	DSM1920	Wound	MN175935	2016	None	Weak	Weak	Not Tested	Not Tested	This Study
***Staphylococcus* clinical isolates**										
S. epidermidis-1	DSM1679	Would	MN175939	2016	Strong	Strong	Weak	Independent$_1$	Bacteriostatic$_1$	This Study
S. epidermidis-2	DSM1759	Wound	MN175929	2016	Strong	Strong	Weak	Dependent$_1$	Bactericidal$_1$	This Study
S. epidermidis-3	DSM1760	Wound	MN175930	2016	Strong	Strong	Weak	Independent$_1$	Bactericidal$_1$	This Study
S. epidermidis-4	DSM1922	Wound	MN175931	2016	Strong	Strong	Weak	Dependent$_1$	Bactericidal$_1$	This Study$_1$
S. epidermidis-5	DSM1761	Nasal	MN175933	2016	Weak	Weak	None	Not Tested	Not Tested	This Study
S. hominis	DSM1916	Wound	MN175934	2016	Strong	Strong	Weak	Dependent$_1$	Bactericidal$_1$	This Study
S. saprophyticus	DSM1655	Urine	MN175941	2016	Weak	Strong	Weak	Independent$_2$	Bactericidal$_2$	This Study
Other clinical isolates										
Agromyces sp. 3098BRRJ	DSM1921	Wound	MN175928	2016	None	None	Weak	Not Tested	Not Tested	This Study
Mycobacterium yunnanensis	DSM1677	Wound	MN175946	2016	Strong	None	Weak	Dependent$_1$	Bacteriostatic$_1$	This Study

Subscript "1" indicates assay was tested against S. aureus 2014.N. Subscript "2" indicates assay was tested against S. aureus LAC. Subscript "3" indicates assay was tested against S. aureus Mu50. Subscript "4" indicates strong anti-S. aureus activity defined as follows: ZOC was completely transparent, ≥2 mm, and a defined edge at 72 h. Weak anti-S. aureus was defined as follows: ZOC was not completely transparent, with a hazy and undefined edge at 72 h. None indicates a ZOC was not present at 72 h. A "" indicates that the ZOC was too small to perform Bactericidal vs. Bacteriostatic assays. "N/A" denotes information that was unavailable or not applicable.*

AGAGTTTGATCCTGGCTCAG 3′). Sequence reads were manually assembled into a double stranded near full length 16S rRNA gene sequence, and taxonomic information was assigned after comparison with other 16S rRNA gene sequences in the Ribosomal Database Project (RDP)[1] and GenBank[2] using the Basic Local Alignment Search Tool (BLAST). The 16S rRNA gene sequences of all the strains speciated in this study were deposited in GenBank and assigned accession numbers. Strain descriptions, species identification, and accession numbers can be found in **Table 1**.

Contact-Dependent Assays

Strongly inhibitory clinical isolates were defined as follows: a ZOC that was visibly transparent, at least 2 mm in length,

[1]http://rdp.cme.msu.edu

[2]https://blast.ncbi.nlm.nih.gov

and with a defined edge. These isolates (17/28) were assayed to determine if anti-*S. aureus* activity was dependent on direct physical contact between the bacteria; in each case, the activity of each clinical isolate was tested against the *S. aureus* strain for which the strongest ZOC was obtained in the absence of a filter disk. A sterile 0.2 μm filter disk was placed on top of the BHIT agar that had been seeded with *S. aureus*; each clinical isolate was then individually spotted on top of the filter disk so that none of the cell suspension physically touched the *S. aureus* seeded agar plate. Plates were incubated at 28°C and were visually assessed at 24, 72, and 120 h for the absence or presence of a ZOC. The absence of a ZOC in the presence of a filter disk indicates that physical contact is necessary for anti-*S. aureus* activity against the corresponding most sensitive *S. aureus* strain. Clinical isolates were assessed in three independent biological replicates.

Recovery of *S. aureus* From ZOC

To determine if anti-*S. aureus* activity was bacteriostatic (growth inhibition) or bactericidal (killing), *S. aureus* survival and growth was monitored as compared to the original inoculum. Immediately after the plates solidified and before a clinical isolate was spotted, five-milligram punches of *S. aureus*-seeded agar were taken with a sterile pipette tip as a means to enumerate *S. aureus* colony forming units (CFU) present at T0. Bacterial interaction assays were performed with 15/28 strongly inhibitory clinical isolates as described above. Two isolates that produced a defined and transparent ZOC, but exactly 2 mm in length, were excluded from these experiments as the ZOC produced against *S. aureus* was too small to accurately extract agar punches. Each strongly inhibitory clinical isolate was tested against the *S. aureus* strain for which the strongest ZOC was produced. After 48 h (T48) of incubation at 28°C, five-milligram punches of agar directly adjacent to the clinical isolate spot (Inside ZOC) or at the edge of the petri dish (Outside ZOC) were again taken with a sterile pipette tip. To determine the number of *S. aureus* CFU present in an agar punch, punches were resuspended in 1 mL of BHI broth and heated to 55°C for 10 min. 10-fold serial dilutions of each suspension were prepared in PBS and then plated on Mannitol Salt Agar (MSA, Criterion). Plates were incubated at 37°C overnight, and recovered colonies were quantified. The number of CFU present in the 1 mL original suspension was calculated, and the fold change from T0 was calculated as follows: (Number of CFU present Inside or Outside ZOC at T48/Number of CFU present at T0). Fold change values less than 1 indicate bactericidal activity; *S. aureus* CFU recovered in an agar punch at T48 was less than the *S. aureus* CFU recovered in an agar punch at T0. Contact-dependent experiments were completed in three independent biological replicates.

Conditioned Cell Free Medium (CCFM) Preparation and Disk Diffusion Assays

Clinical isolates that produced contact-independent bactericidal anti-*S. aureus* activity (*C. amy*-2, *S. sap*, and *S. epi*-3) were independently cultured in 10 mL BHIT broth overnight at 37°C with shaking at 190 rpm. Cultures were pelleted by centrifugation, and the supernatant was filter sterilized with a.2 μm filter (Corning). One-milliliter of sterile supernatant was retained, and the remaining supernatant was concentrated (50X) with ammonium sulfate precipitation as previously described (Hardy et al., 2019). For heat-treatments, 50 μL aliquots of unconcentrated or 50X CCFM were incubated at 90°C for 10 min, then allowed to cool. For the disk diffusion assays, the *S. aureus* strain that was most sensitive to the corresponding inhibitory activity (*C. amy*-2/Mu50, *S. sap*/LAC, and *S. epi*-3/LAC) was cultured on BHI agar overnight at 37°C. The following day, the plate-grown cells were recovered and diluted to 1×10^8 cells/ml (OD_{600} 0.1) in BHI broth. A sterile swab was then used to spread the *S. aureus* cell suspension on BHIT agar as a lawn. The plate was allowed to dry in a laminar flow hood for 30 min. Next, a sterile 5 mm diffusion disk was placed on top of the *S. aureus* lawn, and 50 μL of unconcentrated CCFM or 50X CCFM was inoculated onto the disk. Plates were incubated at 28°C, and images were taken after 72 h of incubation. Disk diffusion assays were conducted in three independent biological replicates.

S. aureus Infection and CCFM Treatment of *Galleria mellonella* Caterpillars

Staphylococcus aureus strains 2014.N, Mu50, and LAC were cultured overnight on BHI agar at 37°C. The following day, *S. aureus* cells were recovered and diluted to 1×10^8 cells/ml (OD_{600} 0.1) in PBS. Total CFU were then further adjusted to obtain the required doses; i.e., 10^7 CFU or 10^6 CFU in 5 μL of PBS + 0.01% bromophenol dye. For infections, *Galleria mellonella* caterpillars (Vanderhorst Wholesale Inc) were utilized within 1 day of receipt. Caterpillars between 200 and 300 mg were chosen for infection. The injections were carried out as described previously (Desbois and Coote, 2011) with minor adaptations. Briefly, 5 μL of inoculum that contained 10^7 or 10^6 total CFU of *S. aureus* was injected into the last left proleg using a 10 μL glass syringe (Hamilton) fitted with a 31G needle. For caterpillars that were treated with CCFM, the caterpillars were maintained at room temperature for 1 h following the *S. aureus* injection, then refrigerated at 4°C for 12 min and then injected with 5 μL of freshly prepared 50X CCFM from *S. sap* or *S. epi*-3 (treated) or 50X concentrated BHIT (sham treated). These injections were into the last right proleg. All caterpillars were incubated at 37°C, and survival was monitored over 120 h. Untouched, and PBS injected caterpillars were included as controls. Data found in **Figures 7A,B** represent two completely independent biological replicates (n = 15 caterpillars) performed with different batches of caterpillars. Data found in **Figure 7C** represent a single batch of caterpillars, but two independently derived batches of CCFM (n = 15 caterpillars)/CCFM preparation. Kaplan–Meier survival curves were compared between groups using the Mantel–Cox test with Holm's correction for multiple comparisons (excluding Untouched and PBS negative controls). An alpha value of 0.05 was considered statistically significant.

RESULTS

Activity of Clinical Bacterial Isolates Against *S. aureus*

Polymicrobial interactions within the human host are complex and dynamic. Numerous studies have shown that several genera that inhabit the skin and nasal cavity prevent the colonization of opportunistic pathogens (Jarraud et al., 2002; Bomar et al., 2016). However, these studies often focus on specific anatomical locations and do not represent the host as one environmental niche. Given this, we questioned whether bacterial species isolated from a diverse patient population and a variety of body sites would display antagonistic interactions against *S. aureus*. To this end, we obtained a collection of clinical isolates (**Table 1**) from the WRNMMC Clinical Microbiology Lab and assayed *in vitro* anti-*S. aureus* activity utilizing a bacterial interaction assay (Hardy et al., 2019). As prior studies have shown that antagonistic polymicrobial interactions are often strain-specific and because we previously showed that *Corynebacterium pseudodiphtheriticum*, a common skin and nasal commensal microbe, mediates heterotypic bactericidal activity against specific *S. aureus* strains (Hardy et al., 2019), we assayed anti-*S. aureus* activity against three phenotypically different *S. aureus* strains: *S. aureus* LAC (Community-Acquired, MRSA), *S. aureus* Mu50 (Hospital-Acquired, MRSA) and 2014.N (Methicillin-Sensitive *S. aureus*), a recently acquired nasal isolate (**Table 1**). To this end, 34 individual clinical isolates were assessed against each *S. aureus* strain in the bacterial interaction assays; appearance of a visible zone of clearance (ZOC) around the clinical isolate was considered a positive indicator of anti-*S. aureus* activity. While we found that six clinical isolates showed no anti-*S. aureus* activity, the majority (28/34, 82%) of tested clinical isolates possessed inhibitory activity against at least one of the *S. aureus* strains (**Figure 1A**). Furthermore, eight of the clinical isolates were able to inhibit the growth of all tested *S. aureus* strains. As expected, many of the clinical isolates mediated inhibitory activity in a *S. aureus* strain-specific manner: three clinical isolates only inhibited 2014.N, five only inhibited Mu50, and two only inhibited LAC (**Figure 1A**).

The species of the 28 isolates that exhibited anti-*S.aureus* activity were next identified via cloning and sequencing of the 16S rRNA gene; sequences were deposited into GenBank and accession numbers are available in **Table 1**. Analysis of the species information combined with the bacterial interaction assays revealed several types of ZOCs that developed over time (**Figure 1B**). For example, co-incubation of *Corynebacterium aurimucosum* (*C. aur*-1) or *Mycobacterium yunnanensis* (*M. yun*) with *S. aureus* 2014.N or Mu50 resulted in a diffused and moderately sized ZOC; a ZOC did not develop upon co-incubation with *S. aureus* LAC for either clinical isolate (**Figure 1B**). In contrast, co-incubation of *Staphylococcus saprophyticus* (*S. sap*) with *S. aureus* LAC resulted in a defined and transparent ZOC, while only a modest and hazy ZOC was produced against *S. aureus* 2014.N and Mu50.

Temporal quantification of ZOC length additionally revealed distinct patterns of interactions between each clinical isolate and each *S. aureus* strain. For the majority of the isolates, the ZOC length either remained constant or increased over time (**Figure 2A**). In support of the literature that suggests that some members of the *Corynebacterium* genus promote negative interactions with *S. aureus* (Yan et al., 2013; Hardy et al., 2019), numerous inhibitory isolates were speciated to be members of the *Corynebacterium* genus. These isolates tended to show anti-*S. aureus* activity selectively against strains 2014.N and Mu50; only one *Corynebacterium* isolate, *C. jeikeium* (*C. jei*), inhibited *S. aureus* LAC growth, but neither 2014.N or Mu50. Previous reports have also shown that several CoNS prevent *S. aureus* colonization by inhibiting growth or by direct killing (Iwase et al., 2010; Zipperer et al., 2016; Nakatsuji et al., 2017). In support of this, numerous Staphylococcal isolates were identified and possessed activity against *S. aureus*. These isolates generally mediated robust activity against *S. aureus* 2014.N and LAC, but only modest anti-*S. aureus* activity against Mu50 (**Figures 2A,B**). For example, *Staphylococcus epidermidis* (*S. epi*-1) and *S. hominis* (*S. hom*) produced defined and transparent ZOCs against 2014.N and LAC, but a comparatively small ZOC was produced against Mu50. Taken together, these results support the current hypothesis that antagonistic interactions with *S. aureus* are often strain-specific. As it would account for the differences in sensitivity amongst the various *S. aureus* strains, this may indicate that the *S. aureus* molecular target(s) of each inhibitory isolate is strain-specific and/or differentially expressed between the various *S. aureus* strains.

In addition to the expected members of the *Corynebacterium* and *Staphylococcus* genera, several clinical isolates that are not typically associated with the human microbiota were found to have anti-*S. aureus* activity. For example, there are few reports of the clinical isolation of *Microbacterium* species (Laffineur et al., 2003). However, *M. paraoxydans*, a pathogen of various fish species (Soto-Rodriguez et al., 2013), was recovered from two separate patients and both isolates possessed anti-*S. aureus* activity against strains LAC and Mu50 (**Figure 2A**). Similarly, *Agromyces*, a common soil microbe, also mediated anti-*S. aureus* activity against Mu50 (**Figure 2A**). These data indicate that antagonistic interactions with *S. aureus* are not limited to conventional members of the human microbiota that would have been under evolutionary pressure to evolve mechanisms to compete with *S. aureus*.

Heterotypic Inhibitory Activity of *A. baumannii* Against *S. aureus*

While *Acinetobacter baumannii* and *S. aureus* have been frequently co-isolated from wounds (Furuno et al., 2008; Castellanos et al., 2019), to our knowledge there is no published evidence that *A. baumannii* possesses any inhibitory activity against *S. aureus*. Thus, we were surprised that *A. baumannii* isolates represented ∼20% (7/34) of the clinical isolates that showed anti-*S. aureus* activity (**Figures 2A**, **3**). Though not certain, this large representation of *A. baumannii* clinical isolates may be a result of the "wounded warrior" patient population that is often treated at WRNMMC. Of the seven *A. baumannii*

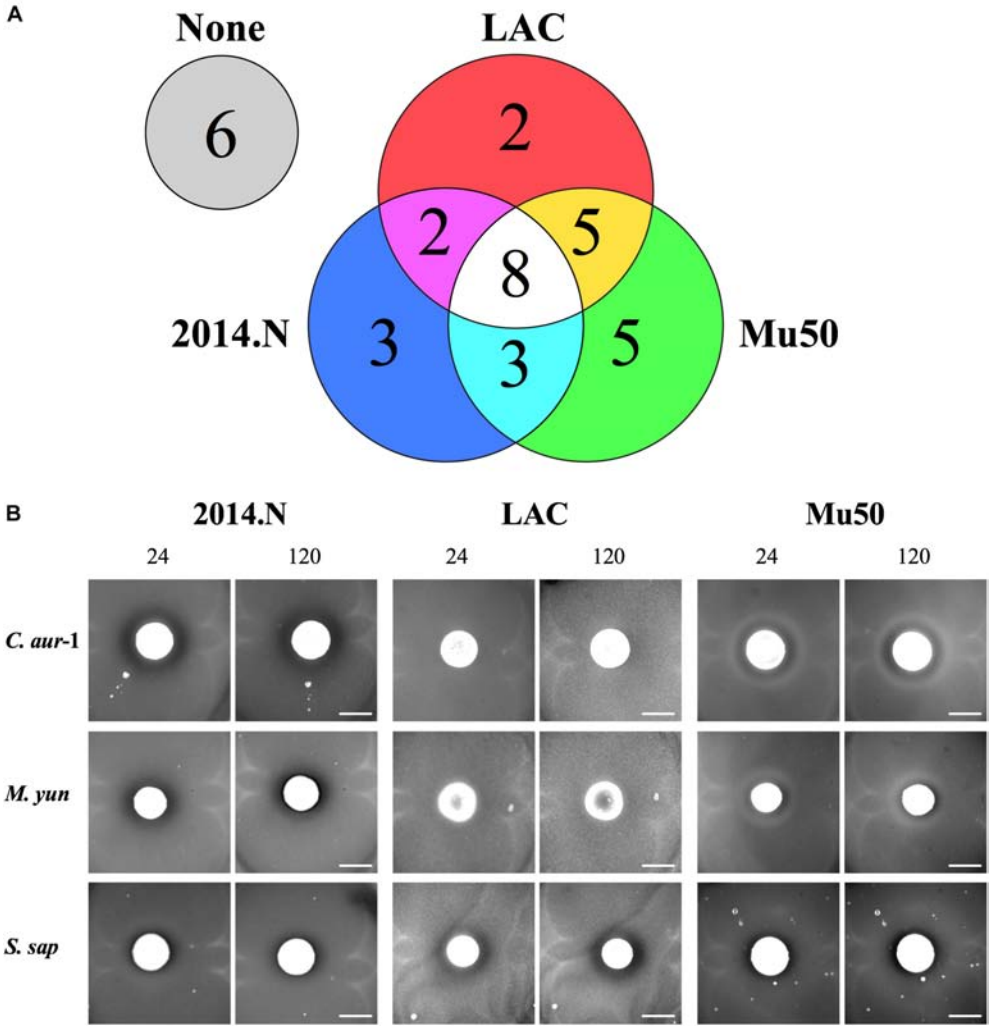

FIGURE 1 | Bacterial species isolated from patients at the Walter Reed National Military Medical Center inhibit *Staphylococcus aureus* growth. **(A)** Venn Diagram of anti-*S. aureus* activity: thirty-four clinical isolates were screened for anti-*S. aureus* activity in an *in vitro* bacterial interaction assays against *S. aureus* strains 2014.N, LAC and Mu50. 28/34 isolates tested possessed anti-*S. aureus* activity against at least one *S. aureus* strain. 6/34 possessed no activity against *S. aureus*. 8/34 inhibited growth of all *S. aureus* strains tested while the remaining 20 strains showed activity against one or two of the *S. aureus* strains as indicated in the Venn Diagram. **(B)** Representative Bacterial Interaction Assays: *C. aurimucosum* (*C. aur*-1), *M. yunnanensis* (*M. yun*), or *S. saprophyticus* (*S. sap*) were spotted onto an agar plate that had been seeded with the indicated *S. aureus* strains (2014.N, LAC, or Mu50). Plates were incubated at 28°C, and images were taken at 24, 72, and 120 h (24 and 120 h images are shown). Images are representative of three independent biological replicates. Scale bar = 10 mm and is the same in the corresponding 24 h and 120 images; in some cases the 120 h spots appear larger than the 24 h spots due to growth of the bacteria within the spots.

isolates, two (*A. bau*-1 and *A. bau*-3) possessed inhibitory activity against all tested *S. aureus* strains. The remaining five *A. baumannii* mediated anti-*S. aureus* activity against at least two strains (**Figure 2A**).

The type of ZOC produced by *A. baumannii* varied and was largely dependent on the *S. aureus* strain being tested. For example, *A. bau*-2 produced a large and defined ZOC against 2014.N, a large and hazy ZOC against LAC, and no ZOC against Mu50 (**Figure 3**). In contrast, *A. bau*-6 produced a moderately sized and very defined ZOC against Mu50, a small and hazy ZOC against LAC, and no ZOC against 2014.N. Taken together, these data indicate that *A. baumannii* possesses heterogeneous strain-specific anti-*S. aureus* activity. This may in turn indicate that *A. baumannii* utilizes multiple independently evolved mechanisms to compete with *S. aureus* or that the target(s) of anti-*S. aureus* activity are differentially expressed between *S. aureus* strains.

Characterization of Contact-Dependent and Bactericidal Anti-*S. aureus* Activity

Commensal bacteria utilize a wide variety of molecular mechanisms to compete with other microbes; these include both contact dependent and independent mechanisms (Brugger et al., 2016). Thus, we sought to determine whether the observed anti-*S. aureus* activity of the clinical isolates required physical

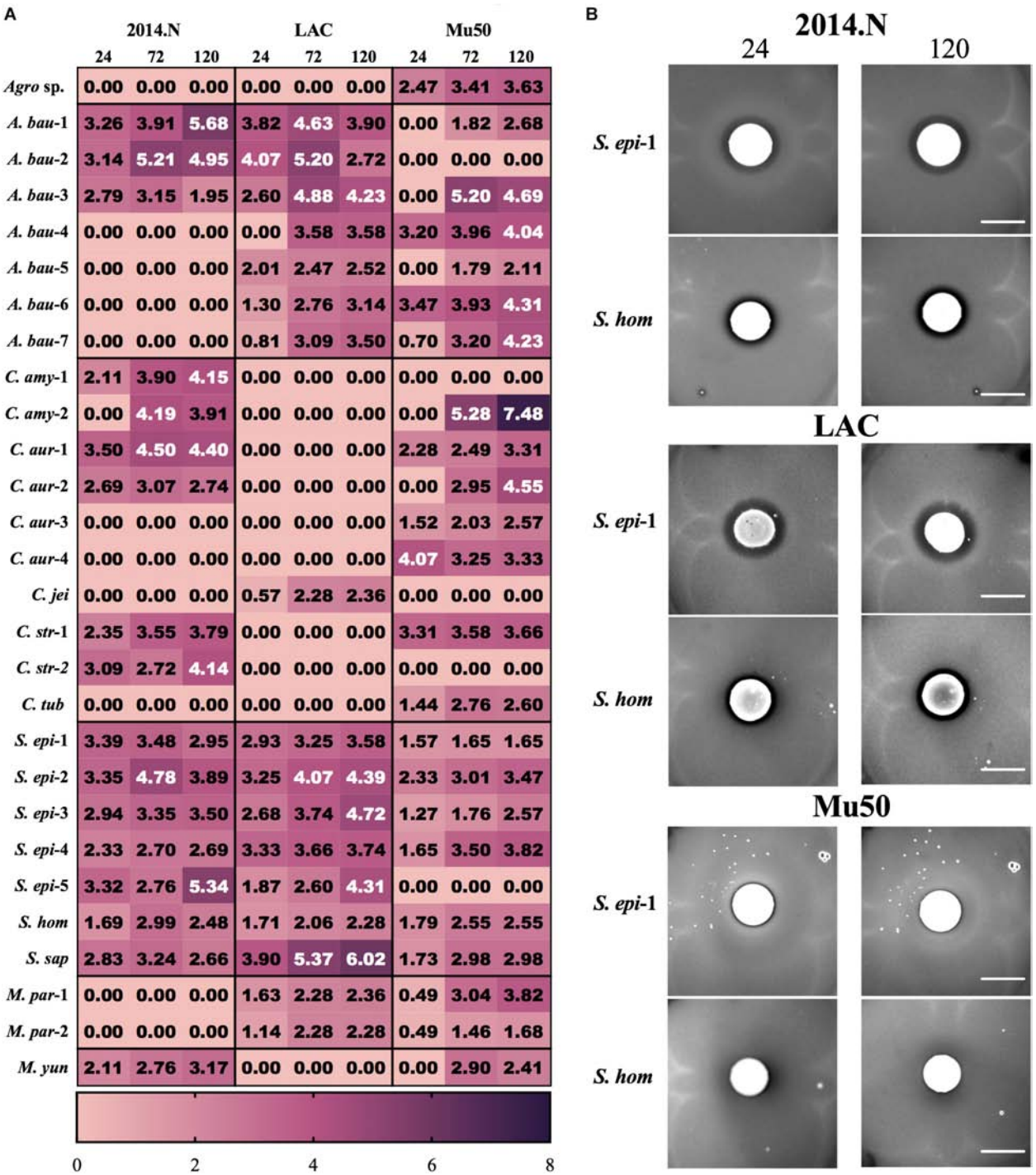

FIGURE 2 | Clinical isolates mediate strain-specific anti-*S. aureus* activity. **(A)** Heat map showing the activity of the indicated clinical isolate against the indicated *S. aureus* strains: The Zone of Clearance (ZOC) was defined as the distance between the edge of the clinical isolate spot to the visible edge of the *S. aureus* ring of clearance. The ZOC was measured using ImageJ software (NCBI) and each value within a box represents the arithmetic mean (in millimeters) of three independent biological replicates measured temporally (24, 72, and 120 h). Clinical isolate species names have been abbreviated as follows: *C. aurimucosum* (*C. aur*), *C. striatum* (*C. str*), *C. amycolatum* (*C. amy*), *C. jeikeium* (*C. jei*), *C. tuberculostearicum* (*C. tub*), *S. epidermidis* (*S. epi*), *S. saprophyticus* (*S. sap*), *S. hominis* (*S. hom*), *A. baumannii* (*A. bau*), *M. paraoxydans* (*M. par*), *M. yunnanensis* (*M. yun*), and *Agromyces* sp. 3098BRRJ (*Agro* sp.). Additionally, a number preceded by a – is used to indicate an independent isolate of the indicated species. **(B)** Example of strain-specific activity: *S. epidermidis* (*S. epi*-1) and *S. hominis* (*S. hom*) were co-incubated with agar plates seeded with *S. aureus* strains 2014.N, LAC or Mu50. Images of the ZOC were taken after 24 and 120 h of incubation at 28°C and are representative of three independent biological replicates. Scale bar = 10 mm and is the same in the corresponding 24 h and 120 images; in some cases the 120 h spots appear larger than the 24 h spots due to growth of the bacteria within the spots.

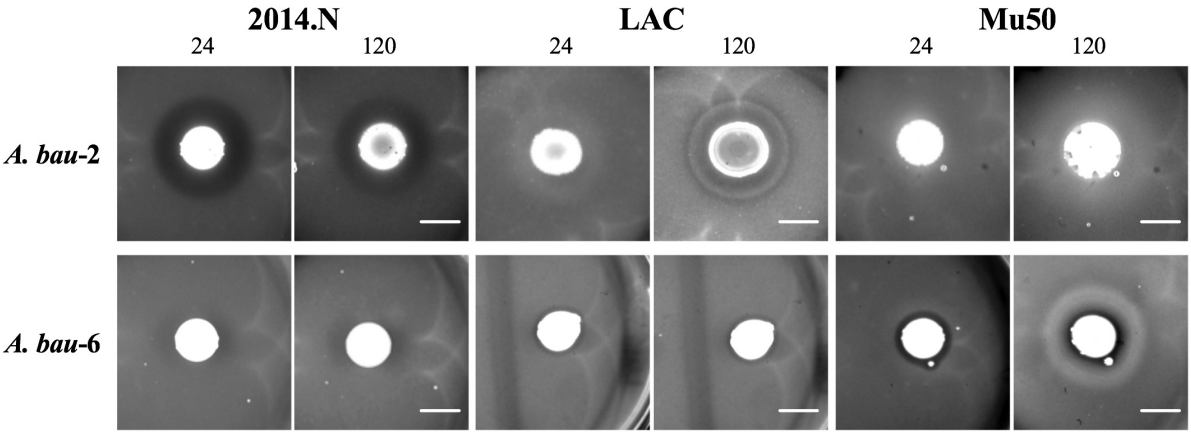

FIGURE 3 | Independent *Acinetobacter baumannii* isolates produce strain-specific anti-*S. aureus* activity. Individual *A. baumannii* (*A. bau*-2 and *A. bau*-6) isolates were spotted onto an agar plate that had been seeded with various *S. aureus* strains (2014.N, LAC, or Mu50). Plates were incubated at 28°C, and images were taken at 24, 72, and 120 h (24 and 120 h images are shown). Images are representative of three independent biological replicates. Scale bar = 10 mm and is the same in the corresponding 24 h and 120 images; in some cases the 120 h spots appear larger than the 24 h spots due to growth of the bacteria within the spots.

bacterial interaction. Of the 28 strains that displayed activity, we focused our efforts on the 17 clinical isolates that showed strong inhibitory activity; these strains produced a defined and transparent ZOC against *S. aureus* that was greater than or equal to 2 mm. To this end, bacterial interaction assays were repeated, but the clinical isolate was separated from the *S. aureus* seeded agar with a 0.2 μm filter disk. A ZOC still formed for 41% (7/17) of the tested clinical isolates (**Figure 4A**), indicating that anti-*S. aureus* activity was contact-independent. The clinical isolates that mediated contact-independent anti-*S. aureus* activity were restricted to the *Staphylococcus* and *Corynebacterium* genera (**Figure 4B** and data not shown). For example, two independently recovered *S. epidermidis* isolates (*S. epi*-1 and *S. epi*-3) and *S. saprophyticus* (*S. sap*) mediated robust contact-independent inhibitory activity (**Figure 4B** and data not shown). In addition, four *Corynebacterium* species (*C. amy*-2, *C. aur*-1, *C. aur-2,* and *C. str*-1) produced moderate inhibitory activity in the presence of a filter disk (**Figure 4B** and data not shown). Taken together, these data indicate that the various isolates can use both contact-dependent and contact-independent mechanisms as a means to inhibit *S. aureus* growth.

Commensal bacteria can compete with other bacteria using mechanisms that either inhibit bacterial growth (bacteriostatic) or directly kill (bactericidal) the competitor. To further characterize the anti-*S. aureus* activities of the strongly inhibitory clinical isolates, the number of *S. aureus* CFU were determined from within the ZOC, directly adjacent to the clinical isolate spot (Inside ZOC), and outside of the ZOC, on the edge of the petri dish (Outside ZOC), after 48 h (T48) of incubation. These numbers were then compared to the number of *S. aureus* CFU seeded within a comparable area of the agar plate at the initiation of the experiment (T0). Of the 17 strongly inhibitory isolates, 15 developed a ZOC that was large enough (greater than 2 mm) to take accurate agar punches that fell fully within the ZOC. Of these 15 isolates, 7 mediated bactericidal activity against *S. aureus*. Most of these isolates belonged to the *Staphylococcus* genus (4/7), followed by *A. baumannii* (2/7), and *Corynebacterium* (1/7, **Figure 5**). Combined with the contact dependence assays, a total of 3 clinical isolates (*C. amy*-2, *S. sap*, and *S. epi*-3) produced anti-*S. aureus* activity that was independent of direct contact and was also bactericidal. This strongly suggests that these isolates directly kill *S. aureus* via the secretion of toxic compound(s).

Basic Mechanistic Characterization of Contact-Independent Bactericidal Activity

We hypothesized that clinical isolates that produced contact-independent bactericidal anti-*S. aureus* activity would do so via a secreted compound(s) that would be present in culture supernatants. To test this hypothesis, *C. amy*-2, *S. sap*, and *S. epi*-3 were independently cultured in BHIT broth, and sterile conditioned cell free medium (CCFM) was prepared. Unconcentrated CCFM and 50X concentrated CCFM were then tested in a disk diffusion assay (**Figure 6** and data not shown) against the *S. aureus* strain for which they showed the most robust bactericidal activity (*C. amy*-2/Mu50, *S. sap*/LAC, and *S. epi*-3/LAC). Each of the 50X concentrated CCFM samples produced a ZOC against the tested *S. aureus* strain (**Figure 6**). In addition, unconcentrated CCFM derived from *S. sap* and *S. epi*-3 produced a small ZOC against *S. aureus* LAC (data not shown). To determine the thermostability of the compound(s) found in the concentrated CCFM, aliquots of CCFM were also subjected to heat treatment prior to testing for anti-*S. aureus* activity. In all cases anti-*S. aureus* activity was maintained after heat treatment (**Figure 6**).

To examine the therapeutic potential of the compound(s) found within the CCFM, we next examined the ability of CCFM to rescue *S. aureus*-infected *Galleria mellonella* caterpillars. *G. mellonella* have been established as a simple infection model for several pathogens, including *S. aureus*

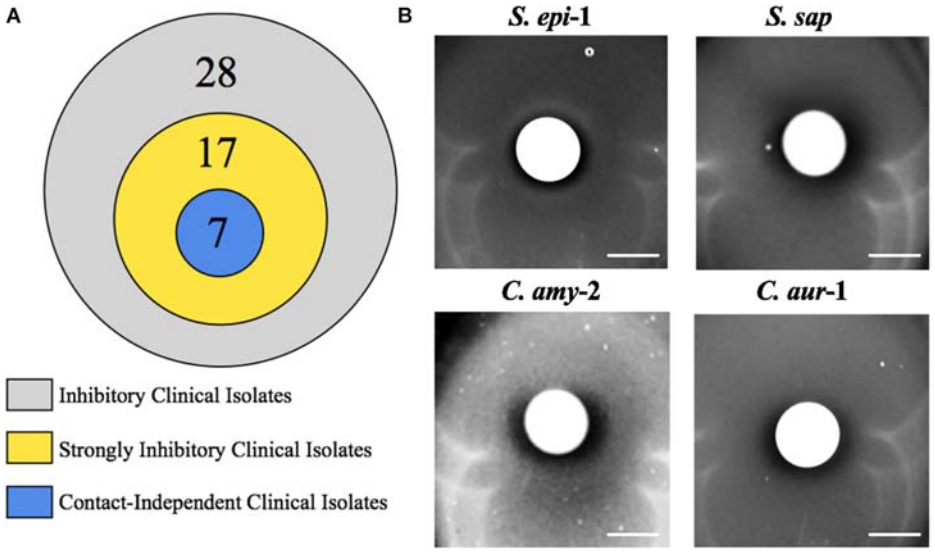

FIGURE 4 | Select clinical isolates mediate contact-independent anti-*S. aureus* activity. **(A)** Strongly inhibitory clinical isolates (17/28) were defined as follows: visibly transparent ZOC of at least 2 mm with a defined edge. **(B)** A 0.2 μm filter was placed on top of BHIT agar plates seeded with *S. aureus* (*S. epi*-1 and *S. sap* were incubated with *S. aureus* LAC, *C. amy*-2 was incubated with *S. aureus* Mu50, and *C. aur*-1 was incubated with *S. aureus* 2014.N). A clinical isolate (as described above) was then spotted on top of the filter paper such that the clinical isolate and the *S. aureus* seeded agar plate were physically separated. Images of the ZOC were taken after 120 h of incubation at 28°C. Images are representative of three independent biological replicates. Scale bar = 10 mm.

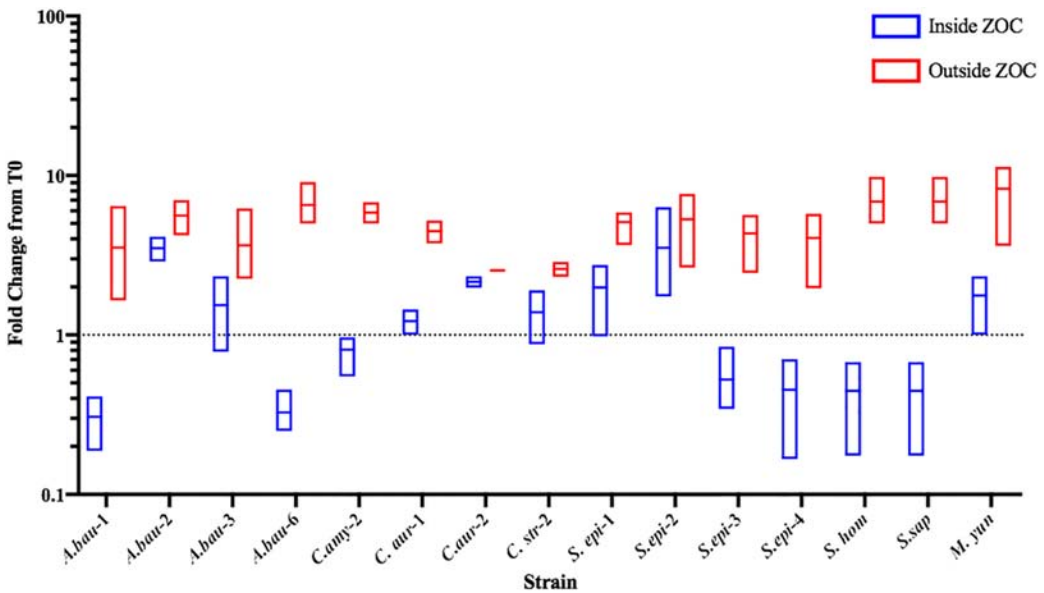

FIGURE 5 | Select clinical isolates mediate bacteriostatic or bactericidal activity against *S. aureus*. The number of *S. aureus* CFU seeded within the agar (T0) was compared to the number of *S. aureus* found after 48 h of incubation. *S. aureus* CFU numbers were determined from directly adjacent to the clinical isolate spot (Inside ZOC) or from outside the ZOC and the fold change from T0 was calculated. Each box represents the data from three independent biological replicates; the horizontal line is plotted at the arithmetic mean and the length of the box represents the range. A dotted line is indicated at 1, which would represent a purely bacteriostatic interaction where the numbers of *S. aureus* at T0 and T48 were unchanged. Values below the line indicate a decrease in *S. aureus* at the 48-h time point, which indicates bactericidal activity.

(Desbois and Coote, 2011; Tsai et al., 2016), and have also been used to test the efficacy of antimicrobials (Desbois and Coote, 2011). Despite the usefulness of this model, little is understood about the relative virulence of different *S. aureus* strains in *G. mellonella*. We previously found that *in vitro* gene expression of important virulence factors broadly varied amongst *S. aureus* strains 2014.N, LAC, and Mu50; 2014.N expresses the highest levels followed by LAC and then Mu50 (Hardy et al., 2019).

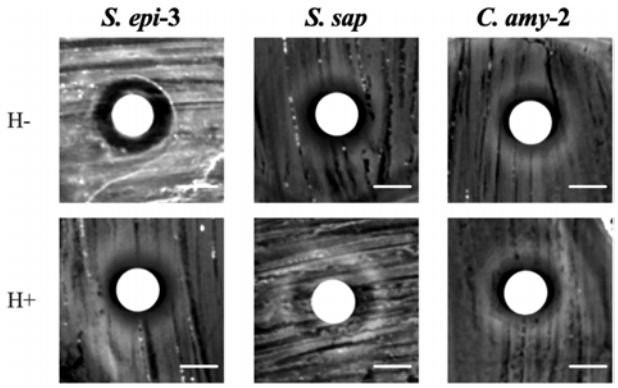

FIGURE 6 | Anti-*S. aureus* activity is retained in Conditioned Cell Free Medium. *S. aureus* strains LAC or Mu50 were spread on the BHI agar surface and a sterile disk was placed in the center of the plate. Fifty μl of concentrated CCFM prepared from *C. amy*-2; (incubated with Mu50), *S. sap* (incubated with LAC), and *S. epi*-3 (incubated with LAC) that was Heat-Treated (H+) or maintained at room temperature (H–) prior to use was inoculated onto the disk and allowed to dry. Images of the ZOC were taken after 72 h of incubation. Images are representative of three independent biological replicates. Scale bar = 10 mm.

Thus, we first tested the ability of these various strains to induce *G. mellonella* mortality at various doses. The overall virulence in this model revealed that LAC induced the highest level of death, followed by 2014.N and Mu50. Indeed, infection with LAC or 2014.N killed significantly more *G. mellonella* than Mu50 at the tested doses (**Figures 7A,B**). These data support the notion that though *in vitro* defined virulence factor expression profiles may be helpful, they do not always directly correlate with virulence in every *in vivo* model.

To examine the therapeutic potential of the compound(s) found within the CCFM, we next tested the ability of CCFM to rescue *S. aureus*-infected *G. mellonella*. As we found Mu50 to be essentially avirulent in this model (**Figures 7A,B**), we focused our efforts on CCFM derived from *S. sap* and *S. epi*-3, which was most active against *S. aureus* LAC (**Figure 2A**). Treatment with *S. sap* CCFM, but not *S. epi*-3 CCFM, 1-h post infection with 10^6 *S. aureus* LAC significantly reduced mortality of infected *G. mellonella* compared to sham treated controls (**Figure 7C**). Taken together, our results indicate that anti-*S. aureus* activity mediated by the various bacterial species is diverse and suggest that secreted compound(s) derived from *S. saprophyticus* may have possible future therapeutic value.

DISCUSSION

Humans serve as an incredibly complicated and dynamic environmental niche for microorganisms. Our understanding of this fact has been greatly enhanced by the Human Microbiome Project, which has revealed that most anatomical locations are colonized with dozens, if not hundreds of bacterial species that must compete with each other for limited nutrients (Turnbaugh et al., 2007). While large microbiota-based epidemiological studies have identified the presence of these microbes, they often fail to elucidate the molecular interactions that occur between the resident flora and how these interactions may impact incoming pathogens. In addition, interactions with opportunistic pathogens are difficult to study in particular as the factors that promote commensalism vs. pathogenesis are often ill-defined. This is especially true for *S. aureus*, which asymptotically colonizes one-quarter of the population at any given time (Kluytmans and Wertheim, 2005; Wertheim et al., 2005), while simultaneously maintaining the ability to cause severe disease. It is well-established that the composition of the host microbiota heavily influences *S. aureus* carriage (Burian et al., 2017). This is particularly true in the nasal cavity, which serves as a primary reservoir for *S. aureus* colonization (Sakr et al., 2018). As such, many microbiota studies have focused on *S. aureus* interactions with the nasal flora. However, little is known about how *S. aureus* may interact with bacteria commonly found at other anatomical sites. Thus, in a proof of concept study we set out to characterize the basic interactions of *S. aureus* with bacterial isolates obtained from various sites (wound, blood, urine, and the nasal cavity) from patients at the WRNMMC. By taking a reductionist approach, we found that the majority of clinical isolates we screened displayed some form of *in vitro* anti-*S. aureus* activity.

En masse, *in vitro* bacterial interaction assays against three phenotypically different *S. aureus* strains revealed that the majority of tested clinical isolates were able to inhibit *S. aureus* to some degree (**Figure 1**, **2**). Most of the inhibitory isolates were members of the *Corynebacterium* genera (10/28), which supports well-established findings that show that the *Corynebacterium* genus heavily impacts *S. aureus* colonization and viability (Yan et al., 2013; Hardy et al., 2019). For example, we previously showed that *C. pseudodiphtheriticum*, an important community determinant of *S. aureus* nasal colonization, mediates potent strain-specific bactericidal activity against *S. aureus* via production of a secreted factor(s) (Hardy et al., 2019). The results described herein indicate that related *Corynebacterium* species (*C. aurimucosum*, *C. amycolatum*, *C. striatum*, *C. jeikeium*, and *C. tuberculostearicum*) also possess some level of anti-*S. aureus activity*. Despite this finding, it is not possible to generalize that all *Corynebacterium* species negatively impact *S. aureus*. For example, *C. accolens* has been shown to actually promote *S. aureus* nasal colonization by reducing competition from other opportunistic pathogens (Yan et al., 2013; Bomar et al., 2016). In our screen, *C. accolens* possessed no anti-*S. aureus* activity (**Figure 1A**). In addition, recent work from Stubbendieck et al. (2019) showed that some *Corynebacterium* species can inhibit CoNS growth through the production of siderophores that enable these species to out-compete the CoNS for available iron, and thusly influence *S. aureus* viability. Therefore, individual *Corynebacterium* species appear to have evolved independent mechanisms that allow them to either cooperate or compete with *S. aureus*. Overall, our results combined with the growing body of literature suggest that the relationships observed in microbiota-based studies can be translated into *in vitro* phenotypes, and that the *Corynebacterium* genus in particular greatly impacts *S. aureus* viability and thusly colonization.

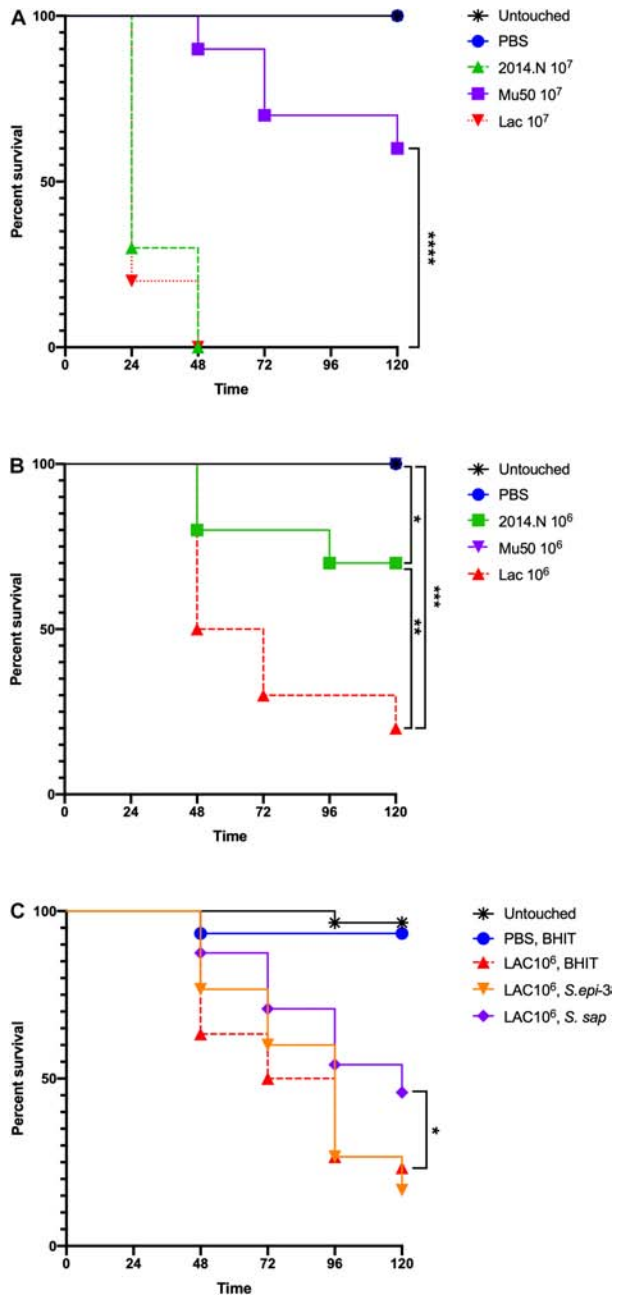

FIGURE 7 | *Staphylococcus aureus*-infected *Galleria mellonella*. *Galleria mellonella* caterpillars were divided into the indicated groups and were monitored for survival over 120 h at 37°C after the indicated inoculations. **(A,B)** Untouched and PBS injected *Galleria* served as negative controls and the indicated doses of 2014.N, LAC and Mu50 were tested. **(C)** For the treatment experiments, untouched caterpillars were maintained. Additionally, PBS injected caterpillars were treated 1-h post *S. aureus* infection with CCFM prepared from BHIT in which no bacteria had been cultured to ensure no effect of dual injection on survival. Caterpillars that were injected with 10^6 CFU of *S. aureus* strain LAC were treated 1-h post infection with BHIT CCFM (sham treatment) or *S. epi*-3 or *S. sap* derived CCFM. Kaplan-Meier survival curves were compared (excluding negative controls) using the Mantel–Cox test with Holm's correction for multiple comparisons. In **(A,B)**, the three *S. aureus* strains were compared to identify statistically significant differences *(Continued)*

FIGURE 7 | Continued
in Galleria mortality; untouched and PBS dosed caterpillars were not included in the comparisons. In **(A)**, Mu50 was significantly different than both 2014.N and LAC. In **(B)**, significant differences between the various groups are indicated. In **(C)**, BHIT treated caterpillars were compared to CCFM treated (*S. epi*-3 or *S. sap*) Galleria to identify difference; only *S. sap* was significantly different. Asterisks signifying the *P* value as follows: $*P < 0.05$; $**P < 0.01$; $***P < 0.001$; $****P < 0.0001$.

Culture independent-identification methods have revealed that wound infections, rather than being caused by a single species, are often polymicrobial in nature (Bowler et al., 2001; Peters et al., 2012; Tay et al., 2016). Moreover, microbiota-based studies have shown that wounds that are infected with multiple bacterial species tend to have worse outcomes as compared to wounds that are infected with a single species (Dalton et al., 2011; Pastar et al., 2013). It is worth noting that bacteria within wounds have to compete for resources and must contend with the host's immune system. To aid these processes, bacteria that commonly infect wounds have evolved multiple mechanisms that help in these responses. For example, *Pseudomonas aeruginosa* and *S. aureus* are often co-isolated from wounds (Giacometti et al., 2000; Dowd et al., 2008). *P. aeruginosa* has been found to limit *S. aureus* growth by sensing the presence of *S. aureus* peptidoglycan (Korgaonkar et al., 2013; Pastar et al., 2013). *P. aeruginosa* responds by producing pyocyanin and elastase; both of these molecules have anti-*S. aureus* properties (Korgaonkar et al., 2013). Similarly, *S. aureus* and *A. baumannii* are also commonly co-isolated from wounds. However, to our knowledge there are no published reports of cooperative or competitive interactions between these two species. Thus, we were surprised that our initial screen revealed that *A. baumannii* was the most frequently isolated species possessing anti-*S. aureus* activity (7/28, **Figures 2**, **3**). Moreover, the various *A. baumannii* isolates displayed a wide range of anti-*S. aureus* activities that were dependent upon both the *A. baumannii* and *S. aureus* strains. Future studies that seek to understand these interactions at a molecular level will be of great interest.

In thinking about the types of inhibition that we observed, contact-dependent inhibition can be mediated by variety of different mechanisms. For example, Type VI Secretion Systems (T6SS), which are found in many Gram-negative species, require physical contact and involve injection of toxic compounds directly into competitor cells (Coulthurst, 2019). Similarly, though mechanistically divergent from the T6SS, the Esx secretion pathway, which is broadly distributed amongst Gram-positive bacteria, also requires physical contact between competing bacterial species to mediate growth inhibition via toxic compounds (Whitney et al., 2017). In both these examples, only target cells that are physically touching the inhibitory cells are negatively impacted. In contrast contact-independent growth inhibition is typically mediated by toxic compounds that are synthesized and then secreted by the inhibitory species as a means to kill/prevent the growth of a competitor; no cell-to-cell contact between the two species is required. This approach is a common mechanism that is used by various microbes across

multiple ecological niches and these compounds can include bacteriocins, secondary metabolites, and other small molecules (Zipperer et al., 2016; Terra et al., 2018). Finally, it is worth noting that some antagonistic interactions are more complex and can involve both contact-independent and dependent mechanisms. For example, initial physical contact between *Streptococcus pneumoniae* and *S. aureus* induces *S. pneumoniae* to generate and secrete hydrogen peroxide that can then kill *S. aureus* (Khan et al., 2016; Wu et al., 2019). Similarly, *P. aeruginosa* can physically senses *S. aureus*, which leads to global changes in transcription, resulting in the secretion of multiple compounds that have anti *S. aureus* activity (Korgaonkar et al., 2013; Filkins et al., 2015). Thus, of the 10 strongly inhibitory clinical isolates that produced a ZOC against *S. aureus* that was dependent on direct contact (**Figure 4**), some of these may require initial physical contact with *S. aureus* as a way to stimulate production of a toxic compound(s) or a secondary metabolite into the surrounding agar that can alter the pH or other environmental conditions in such a way as to impact *S. aureus* viability in that region. Undoubtedly, various species and strains utilize a diverse number of mechanisms to inhibit *S. aureus*.

Recently, there has been a renewed interest in the use of bacterial-derived compounds as novel therapeutics to treat highly drug resistant infections. Indeed, these compounds are potentially even more valuable because of the dearth of new antibiotics that are entering the market for human use. Our studies identified several isolates that inhibited *S. aureus* growth independent of physical contact, presumably through the activity of a secreted and diffusible compound(s) (**Figures 1**, **4**). These isolates exclusively belonged to the *Corynebacterium* and *Staphylococcus* genera. Given that *Corynebacterium* and *Staphylococcus* are the primary genera that have been found to inhibit *S. aureus* growth on the skin and within the nasal cavity, it is clear that there appears to be a selective pressure for members of these genera to compete with *S. aureus*. It is worth noting that a portion of the identified isolates mediated killing activity (**Figure 5**); *S. epidermidis* represented the majority of the isolates that mediated bactericidal activity. This finding is likely not unexpected given that *S. epidermidis*, a common member of the human microbiota, has been found to actively compete with *S. aureus* by a variety of mechanisms: production of *S. aureus*-specific anti-microbial peptides, production of anti-biofilm compounds, and rapid and efficient nutrient acquisition (Lina et al., 2003; Iwase et al., 2010; Nakatsuji et al., 2017).

While the finding that *S. epidermidis* inhibits *S. aureus* is not surprising, to our knowledge our results are the first to show that *Staphylococcus saprophyticus* has anti-*S. aureus* activity (**Figures 4–6**). Moreover, we observed that treatment with *S. saprophyticus* CCFM was able to rescue survival of *S. aureus*-infected *G. mellonella* caterpillars (**Figure 7C**). *S. saprophyticus* is the second most common cause of bacterial urinary tract infections (UTIs) and is not associated with the healthy urinary tract (Marrie et al., 1982). Thus, *S. saprophyticus* presumably must out-compete normal urinary tract flora during the process of colonization and ultimate disease causation. Given that *S. aureus* can also infrequently colonize the urinary tract and cause UTIs, it's interesting to speculate that *S. saprophyticus* has evolved to kill *S. aureus* as a means to prevent competition for this niche.

We note that secreted bactericidal compound(s) from some of the characterized isolates may have the potential to be developed for use as novel therapeutics to treat or prevent *S. aureus*-mediated infection. This ascertain is supported by the fact that anti-*S. aureus* activity was retained in CCFM from the three tested isolates (**Figure 6**), suggesting that these species negatively impact *S. aureus* viability most likely through the secretion of a toxic compound(s). Thought the nature of these compound(s) are unclear, they may include compounds like lantibiotics (McAuliffe et al., 2001), which are peptide antibiotics that are produced by a broad range of Gram-positive bacteria, including *Staphylococcus*. Genes that code for lantibiotics are often located on plasmids and other mobile genetic elements, and have a wide range of target-species specificity. Lantibiotics from closely related Staphylococcal species, such as epidermin (Götz et al., 2014), have been found to have potent inhibitory activity against *S. aureus*, including MRSA. It is possible that the anti-*S. aureus* activity we observed from *S. saprophyticus*, and the other Staphylococcal tested species, is the result of a lantibiotic that maintains potent inhibitory properties. Combined, our results indicate that many Staphylococcal species have evolved strategies to compete with *S. aureus*.

While this work was designed as a proof of concept study to explore the extent of anti-*S. aureus* activity exhibited by various microbes, we acknowledge that there are limitations to the study. For example, while the patient population at WRMMC is fairly diverse, given that many of the patients are soldiers that may have incurred traumatic injuries during the course of their service, a substantial proportion of isolates were obtained from wounds; this undoubtedly affected the types of species of bacteria that we ultimately screened. In addition, while this study described the basic molecular mechanisms of these interactions, a more detailed study will be required to clearly identify specific compounds and/or mechanisms of action that are responsible for anti-*S. aureus* activity.

In summary, this proof of concept study indicates that multiple bacterial species possess strain-specific anti-*S. aureus* activity when co-cultured in a bacterial interaction assay. This study further highlights the multifarious nature of polymicrobial interactions, which remain poorly understood. Furthermore, this work expands upon the growing body of literature that supports that the study of 'bacterial warfare' and the toxic compounds created by microbes as a means to compete with one another may be a 'next best option' for the identification of novel therapeutics that will help in overcoming the significant increase in antimicrobial resistance that threatens the health and wellbeing of the population (Zipperer et al., 2016; Nakatsuji et al., 2017; Stubbendieck et al., 2019). As such, we hypothesize that several of the inhibitory isolates identified in this study may produce toxic compounds that have the potential to be used as novel therapeutics or intervention strategies. Our future work will pursue elucidation of the molecular mechanism by which

both *A. baumannii* and *S. saprophyticus* inhibit *S. aureus*. Overall, our findings support the continued study of polymicrobial interactions as a means to identify novel therapeutics and/or molecular targets of *S. aureus* and other pathogens.

DATA AVAILABILITY STATEMENT

The datasets generated for this study can be found in the NCBI, GenBank, MN175920–MN175947.

AUTHOR CONTRIBUTIONS

BH and DM designed the research study. EK and JB provided the clinical bacterial isolates utilized in all experiments. BH, GB, KH, AA, and SS performed the experiments. BH, GB, and DM analyzed the data. BH wrote the manuscript. All authors contributed substantially to revisions and approved the final manuscript.

FUNDING

This study was supported by a U.S. Department of Defense Program project grant (HT9404-12-1-0019) and a Military Infectious Diseases Research Program award (#HU0001-15-2-0031).

ACKNOWLEDGMENTS

We would like to thank the members of Clinical Microbiology, Walter Reed National Military Medical Center for collecting the clinical isolates used in this study, the Uniformed Services University of the Health Sciences Infectious Disease Clinical Research Program for providing *S. aureus* strain 2014.N, and Emad Elassal and Michael Otto for providing *S. aureus* strains Mu50 and LAC, respectively. The contents of this manuscript are solely those of the authors and do not reflect the views of the Uniformed Services University of the Health Sciences, the Department of Defense, or the United States Government.

REFERENCES

Bomar, L., Brugger, S. D., Yost, B. H., Davies, S. S., and Lemon, K. P. (2016). *Corynebacterium accolens* releases antipneumococcal free fatty acids from human nostril and skin surface triacylglycerols. *mBio* 7:e1725-15. doi: 10.1128/mBio.01725-15

Bowler, P. G., Duerden, B. I., and Armstrong, D. G. (2001). Wound microbiology and associated approaches to wound management. *Clin. Microbiol. Rev.* 14, 244–269. doi: 10.1128/cmr.14.2.244-269.2001

Brugger, S. D., Bomar, L., and Lemon, K. P. (2016). Commensal–Pathogen interactions along the human nasal passages. *PLoS Pathog.* 12:e1005633. doi: 10.1371/journal.ppat.1005633

Buffie, C. G., Bucci, V., Stein, R. R., McKenney, P. T., Ling, L., Gobourne, A., et al. (2015). Precision microbiome reconstitution restores bile acid mediated resistance to *Clostridium difficile*. *Nature* 517, 205–208. doi: 10.1038/nature13828

Burian, M., Bitschar, K., Dylus, B., Peschel, A., and Schittek, B. (2017). The protective effect of microbiota on *S. aureus* skin colonization depends on the integrity of the epithelial barrier. *J. Investig. Dermatol.* 137, 976–979. doi: 10.1016/j.jid.2016.11.024

Castellanos, N., Nakanouchi, J., Yüzen, D. I., Fung, S., Fernandez, J. S., Barberis, C., et al. (2019). A study on *Acinetobacter baumannii* and *Staphylococcus aureus* strains recovered from the same infection site of a diabetic patient. *Curr. Microbiol.* 76, 842–847. doi: 10.1007/s00284-019-01696-7

Coulthurst, S. (2019). The type VI secretion system: a versatile bacterial weapon. *Microbiology* 165, 503–515. doi: 10.1099/mic.0.000789

Dalton, T., Dowd, S. E., Wolcott, R. D., Sun, Y., Watters, C., Griswold, J. A., et al. (2011). An in vivo polymicrobial biofilm wound infection model to study interspecies interactions. *PLoS One* 6:e27317. doi: 10.1371/journal.pone.0027317

Desbois, A. P., and Coote, P. J. (2011). Wax moth larva (*Galleria mellonella*): an in vivo model for assessing the efficacy of antistaphylococcal agents. *J. Antimicrob. Chemother.* 66, 1785–1790. doi: 10.1093/jac/dkr198

Dowd, S. E., Sun, Y., Secor, P. R., Rhoads, D. D., Wolcott, B. M., James, G. A., et al. (2008). Survey of bacterial diversity in chronic wounds using pyrosequencing, DGGE, and full ribosome shotgun sequencing. *BMC Microbiol.* 8:43. doi: 10.1186/1471-2180-8-43

Filkins, L. M., Graber, J. A., Olson, D. G., Dolben, E. L., Lynd, L. R., Bhuju, S., et al. (2015). Coculture of *Staphylococcus aureus* with *Pseudomonas aeruginosa* Drives *S. aureus* towards fermentative metabolism and reduced viability in a cystic fibrosis model. *J. Bacteriol.* 197, 2252–2264. doi: 10.1128/JB.00059-15

Furuno, J. P., Hebden, J. N., Standiford, H. C., Perencevich, E. N., Miller, R. R., Moore, A. C., et al. (2008). Prevalence of methicillin-resistant *Staphylococcus aureus* and *Acinetobacter baumannii* in a long-term acute care facility. *Am. J. Infect. Control* 36, 468–471. doi: 10.1016/j.ajic.2008.01.003

Giacometti, A., Cirioni, O., Schimizzi, A. M., Del Prete, M. S., Barchiesi, F., D'Errico, M. M., et al. (2000). Epidemiology and microbiology of surgical wound infections. *J. Clin. Microbiol.* 38, 918–922.

Götz, F., Perconti, S., Popella, P., Werner, R., and Schlag, M. (2014). Epidermin and gallidermin: staphylococcal lantibiotics. *Int. J. Med. Microbiol.* 304, 63–71. doi: 10.1016/j.ijmm.2013.08.012

Hardy, B. L., Dickey, S. W., Plaut, R. D., Riggins, D. P., Stibitz, S., Otto, M., et al. (2019). *Corynebacterium pseudodiphtheriticum* exploits *Staphylococcus aureus* virulence components in a novel polymicrobial defense strategy. *mBio* 10:e2491-18. doi: 10.1128/mBio.02491-18

Iwase, T., Uehara, Y., Shinji, H., Tajima, A., Seo, H., Takada, K., et al. (2010). *Staphylococcus epidermidis* Esp inhibits *Staphylococcus aureus* biofilm formation and nasal colonization. *Nature* 465, 346–349. doi: 10.1038/nature09074

Jarraud, S., Mougel, C., Thioulouse, J., Lina, G., Meugnier, H., Forey, F., et al. (2002). Relationships between *Staphylococcus aureus* genetic background, virulence factors, *agr* Groups (Alleles), and human disease. *Infect. Immun.* 70, 631–641. doi: 10.1128/iai.70.2.631-641.2002

Johnson, R. C., Ellis, M. W., Schlett, C. D., Millar, E. V., LaBreck, P. T., Mor, D., et al. (2016). Bacterial etiology and risk factors associated with cellulitis and purulent skin abscesses in military trainees. *PLoS One.* 11:e0165491. doi: 10.1371/journal.pone.0165491

Khan, F., Wu, X., Matzkin, G. L., Khan, M. A., Sakai, F., and Vidal, J. E. (2016). *Streptococcus pneumoniae* eradicates preformed *Staphylococcus aureus* biofilms through a mechanism requiring physical contact. *Front. Cell. Infect. Microbiol.* 6:104. doi: 10.3389/fcimb.2016.00104

Klevens, R., Morrison, M. A., Nadle, J., Petit, S., Gershman, K., Ray, S., et al. (2007). Invasive methicillin-resistant *Staphylococcus aureus* infections in the United States. *JAMA* 298, 1763–1771.

Kluytmans, J. A. J. W., and Wertheim, H. F. L. (2005). Nasal carriage of *Staphylococcus aureus* and prevention of nosocomial infections. *Infection* 33, 3–8. doi: 10.1007/s15010-005-4012-9

Korgaonkar, A., Trivedi, U., Rumbaugh, K. P., and Whiteley, M. (2013). Community surveillance enhances *Pseudomonas aeruginosa* virulence during polymicrobial infection. *Proc. Natl. Acad. Sci. U.S.A.* 110, 1059–1064. doi: 10.1073/pnas.1214550110

Krismer, B., Liebeke, M., Janek, D., Nega, M., Rautenberg, M., Hornig, G., et al. (2014). Nutrient limitation governs *Staphylococcus aureus* metabolism and

niche adaptation in the human nose. *PLoS Pathog.* 10:e1003862. doi: 10.1371/journal.ppat.1003862

Kuroda, M., Ohta, T., Uchiyama, I., Baba, T., Yuzawa, H., Kobayashi, I., et al. (2001). Whole genome sequencing of meticillin-resistant *Staphylococcus aureus*. *Lancet* 357, 1225–1240. doi: 10.1016/s0140-6736(00)04403-2

Laffineur, K., Avesani, V., Cornu, G., Charlier, J., Janssens, M., Wauters, G., et al. (2003). Bacteremia due to a novel *Microbacterium* species in a patient with leukemia and description of *Microbacterium paraoxydans* sp. nov. *J. Clin. Microbiol.* 41, 2242–2246. doi: 10.1128/jcm.41.5.2242-2246.2003

Lemon, K. P., Klepac-Ceraj, V., Schiffer, H. K., Brodie, E. L., Lynch, S. V., and Kolter, R. (2010). Comparative analyses of the bacterial microbiota of the human nostril and oropharynx. *mBio* 1:e0129-10. doi: 10.1128/mBio.00129-10

Lina, G., Boutite, F., Tristan, A., Bes, M., Etienne, J., and Vandenesch, F. (2003). Bacterial competition for human nasal cavity colonization: role of staphylococcal *agr* alleles. *Appl. Environ. Microbiol.* 69, 18–23. doi: 10.1128/aem.69.1.18-23.2003

Lowy, F. D. (2003). Antimicrobial resistance: the example of *Staphylococcus aureus*. *J. Clin. Investig.* 111, 1265–1273. doi: 10.1172/jci200318535

Marrie, T. J., Kwan, C., Noble, M. A., West, A., and Duffield, L. (1982). *Staphylococcus saprophyticus* as a cause of urinary tract infections. *J. Clin. Microbiol.* 16, 427–431.

McAuliffe, O., Ross, R. P., and Hill, C. (2001). Lantibiotics: structure, biosynthesis and mode of action. *FEMS Microbiol. Rev.* 25, 285–308. doi: 10.1016/s0168-6445(00)00065-6

Nakatsuji, T., Chen, T. H., Narala, S., Chun, K. A., Two, A. M., Yun, T., et al. (2017). Antimicrobials from human skin commensal bacteria protect against *Staphylococcus aureus* and are deficient in atopic dermatitis. *Sci. Transl. Med.* 9:eaah4680. doi: 10.1126/scitranslmed.aah4680

Otto, M. (2010). Basis of virulence in community-associated methicillin-resistant *Staphylococcus aureus*. *Annu. Rev. Microbiol.* 64, 143–162. doi: 10.1146/annurev.micro.112408.134309

Pastar, I., Nusbaum, A. G., Gil, J., Patel, S. B., Chen, J., Valdes, J., et al. (2013). Interactions of methicillin resistant *Staphylococcus aureus* USA300 and *Pseudomonas aeruginosa* in polymicrobial wound infection. *PLoS One* 8:e56846. doi: 10.1371/journal.pone.0056846

Peters, B. M., Jabra-Rizk, M. A., O'May, G. A., Costerton, J. W., and Shirtliff, M. E. (2012). Polymicrobial interactions: impact on pathogenesis and human disease. *Clin. Microbiol. Rev.* 25, 193–213. doi: 10.1128/cmr.00013-11

Sakr, A., Brégeon, F., Mège, J.-L., Rolain, J.-M., and Blin, O. (2018). *Staphylococcus aureus* nasal colonization: an update on mechanisms, epidemiology, risk factors, and subsequent infections. *Front. Microbiol.* 9:2419. doi: 10.3389/fmicb.2018.02419

Soto-Rodriguez, S. A., Cabanillas-Ramos, J., Alcaraz, U., Gomez-Gil, B., and Romalde, J. L. (2013). Identification and virulence of *Aeromonas dhakensis*, *Pseudomonas mosselii* and *Microbacterium paraoxydans* isolated from Nile tilapia, *Oreochromis niloticus*, cultivated in Mexico. *J. Appl. Microbiol.* 115, 654–662. doi: 10.1111/jam.12280

Stubbendieck, R. M., May, D. S., Chevrette, M. G., Temkin, M. I., Wendt-Pienkowski, E., Cagnazzo, J., et al. (2019). Competition among nasal bacteria suggests a role for siderophore-mediated interactions in shaping the human nasal microbiota. *Appl. Environ. Microbiol.* 85, e2406–e2418. doi: 10.1128/AEM.02406-18

Tay, W. H., Chong, K. K. L., and Kline, K. A. (2016). Polymicrobial–host interactions during infection. *J. Mol. Biol.* 428, 3355–3371. doi: 10.1016/j.jmb.2016.05.006

Terra, L., Dyson, P. J., Hitchings, M. D., Thomas, L., Abdelhameed, A., Banat, I. M., et al. (2018). A novel alkaliphilic *Streptomyces* inhibits ESKAPE pathogens. *Front. Microbiol.* 9:2458. doi: 10.3389/fmicb.2018.02458

Tsai, C. J.-Y., Loh, J. M. S., and Proft, T. (2016). *Galleria mellonella* infection models for the study of bacterial diseases and for antimicrobial drug testing. *Virulence* 7, 214–229. doi: 10.1080/21505594.2015.1135289

Turnbaugh, P. J., Ley, R. E., Hamady, M., Fraser-Liggett, C. M., Knight, R., and Gordon, J. I. (2007). The human microbiome project. *Nature* 449, 804–810.

Voyich, J. M., Braughton, K. R., Sturdevant, D. E., Whitney, A. R., Saïd-Salim, B., Porcella, S. F., et al. (2005). Insights into Mechanisms Used by *Staphylococcus aureus* to Avoid Destruction by Human Neutrophils. *J. Immunol.* 175, 3907–3919. doi: 10.4049/jimmunol.175.6.3907

Wertheim, H. F. L., Melles, D. C., Vos, M. C., van Leeuwen, W., van Belkum, A., Verbrugh, H. A., et al. (2005). The role of nasal carriage in *Staphylococcus aureus* infections. *Lancet Infect. Dis.* 5, 751–762.

Whitney, J. C., Peterson, S. B., Kim, J., Pazos, M., Verster, A. J., Radey, M. C., et al. (2017). A broadly distributed toxin family mediates contact-dependent antagonism between gram-positive bacteria. *eLife* 6:e26938. doi: 10.7554/eLife.26938

WHO, (2017). Global Priority List of Antibiotic-Resistant Bacteria To Guide Research, Discovery, And Development Of New Antibiotics. Available at: https://www.who.int/medicines/publications/WHO-PPL-Short_Summary_25Feb-ET_NM_WHO.pdf

Wu, X., Gordon, O., Jiang, W., Antezana, B. S., Angulo-Zamudio, U. A., del Rio, C., et al. (2019). Interaction between *Streptococcus pneumoniae* and *Staphylococcus aureus* generates OH radicals that rapidly kill *Staphylococcus aureus* strains. *J. Bacteriol.* 201:e0474-19. doi: 10.1128/JB.00474-19

Yan, M., Pamp, S. J., Fukuyama, J., Hwang, P. H., Cho, D.-Y., Holmes, S., et al. (2013). Nasal microenvironments and interspecific interactions influence nasal microbiota complexity and *S. aureus carriage*. *Cell Host Microbe* 14, 631–640. doi: 10.1016/j.chom.2013.11.005

Zipperer, A., Konnerth, M. C., Laux, C., Berscheid, A., Janek, D., Weidenmaier, C., et al. (2016). Human commensals producing a novel antibiotic impair pathogen colonization. *Nature* 535, 511–516. doi: 10.1038/nature18634

Conflict of Interest: The authors declare that the research was conducted in the absence of any commercial or financial relationships that could be construed as a potential conflict of interest.

frontiers in Microbiology

ORIGINAL RESEARCH
published: 17 January 2020
doi: 10.3389/fmicb.2019.03028

A Human Lung-Associated *Streptomyces* sp. TR1341 Produces Various Secondary Metabolites Responsible for Virulence, Cytotoxicity and Modulation of Immune Response

*Andrej Herbrík[1], Erika Corretto[2], Alica Chroňáková[2], Helena Langhansová[3], Petra Petrásková[1], Jiří Hrdý[1], Matouš Čihák[1], Václav Krištůfek[2], Jan Bobek[1,4], Miroslav Petříček[1] and Kateřina Petříčková[1,3]**

[1] Institute of Immunology and Microbiology, 1st Faculty of Medicine, Charles University, Prague, Czechia, [2] Institute of Soil Biology, Biology Centre Academy of Sciences of the Czech Republic, České Budějovice, Czechia, [3] Faculty of Science, University of South Bohemia, České Budějovice, Czechia, [4] Department of Chemistry, Faculty of Science, Jan Evangelista Purkyně University in Ústí nad Labem, Ústí nad Labem, Czechia

OPEN ACCESS

Edited by:
Giuseppantonio Maisetta, University of Pisa, Italy

Reviewed by:
Min Yue, Zhejiang University, China
Jintae Lee, Yeungnam University, South Korea

***Correspondence:**
Kateřina Petříčková
katerina.petrickova@lf1.cuni.cz

Specialty section:
This article was submitted to Microbial Physiology and Metabolism, a section of the journal Frontiers in Microbiology

Received: *05 September 2019*
Accepted: *17 December 2019*
Published: *17 January 2020*

Citation:
Herbrík A, Corretto E, Chroňáková A, Langhansová H, Petrásková P, Hrdý J, Čihák M, Krištůfek V, Bobek J, Petříček M and Petříčková K (2020) A Human Lung-Associated Streptomyces sp. TR1341 Produces Various Secondary Metabolites Responsible for Virulence, Cytotoxicity and Modulation of Immune Response. Front. Microbiol. 10:3028. doi: 10.3389/fmicb.2019.03028

Streptomycetes, typical soil dwellers, can be detected as common colonizers of human bodies, especially the skin, the respiratory tract, the guts and the genital tract using molecular techniques. However, their clinical manifestations and isolations are rare. Recently they were discussed as possible "coaches" of the human immune system in connection with certain immune disorders and cancer. This work aimed for the characterization and evaluation of genetic adaptations of a human-associated strain *Streptomyces* sp. TR1341. The strain was isolated from sputum of a senior male patient with a history of lung and kidney TB, recurrent respiratory infections and COPD. It manifested remarkably broad biological activities (antibacterial, antifungal, beta-hemolytic, etc.). We found that, by producing specific secondary metabolites, it is able to modulate host immune responses and the niche itself, which increase its chances for long-term survival in the human tissue. The work shows possible adaptations or predispositions of formerly soil microorganism to survive in human tissue successfully. The strain produces two structural groups of cytotoxic compounds: 28-carbon cytolytic polyenes of the filipin type and actinomycin X2. Additionally, we summarize and present data about streptomycete-related human infections known so far.

Keywords: *Streptomyces*, human pneumonia, pathogenicity, secondary metabolites, hemolysis, actinomycin, cytolytic polyenes

INTRODUCTION

Streptomycetes are commonly reported as soil bacteria with a life-style similar to fungi (Chater and Hopwood, 1993). Though indisputably based in soil, they can inhabit many more habitats including soil-like substrates (bat guano, tertiary sediments, and sea sediments), sea water and extreme habitats (arid, hypersaline or heavy metals-polluted biotopes, extreme temperatures, etc.) (Kampfer et al., 2014). Recently, numerous works report their

important symbiotic relationships with plants and animals (Kaltenpoth et al., 2005; Behie et al., 2016). In some cases, they develop tight bonds with the host as it is documented in leaf-cutting (Haeder et al., 2009), but also other families of ants (Liu et al., 2018), and in the digging wasps. The wasp females form specific cultivation organs in their antennae to grow streptomycetes that in return produce antifungals protecting their offspring from deadly fungal diseases (Kaltenpoth et al., 2005; Nechitaylo et al., 2014). A recent work describes the first clearly documented case of their mutualism with vertebrates, sea turtles (Sarmiento-Ramirez et al., 2014). In almost all reported cases the streptomycetes protect the host or its food resources from pathogenic fungi.

In contrast, *Streptomyces* interaction with human seems to be marginal, or maybe neglected until recent days. Their ability to produce a plethora of secondary metabolites specifically targeted to human or mammalian cells is well known. Some of these have already been applied in human medicine as immunomodulators (rapamycin, tacrolimus) (Bolourian and Mojtahedi, 2018a) and cancerostatics (mitomycin C, bleomycin, actinomycin, doxorubicin and many others) (Olano et al., 2009). Despite this, only limited data report direct colonization of human bodies by streptomycetes. These include mainly endemic human streptomycetomas caused by *S. somaliensis* and *S. sudanensis* and rarely by other species in sub-Saharan Africa and India (Martin et al., 2004; van de Sande, 2013; Verma and Jha, 2019). It should be noted that even in the case of these "well-established" streptomycete pathogens, no specific virulence factors were recognized, and nothing is known about the molecular mechanisms of their pathogenicity. *S. somaliensis* has a remarkably small genome: 5.7 Mb compared to an average size of 7–10 Mbp of other streptomycetes. A reduced genome is a trend typical for obligatory, mostly intracellular pathogens (Kirby et al., 2012). In general, streptomycetes cause suppurative granulomatous tissue changes. The infection starts from the surface skin structures. If untreated, it proceeds to muscles, bones and may even spread via the lymphatic system or blood and cause a systemic disease. Compared to similar, fungi-originated, mycetomas, the actinomycetomas progress more rapidly and affect the deep bone structures in a short time. However, the antibiotic long-term treatment is quite successful (Relhan et al., 2017). Certain respiratory diseases (e.g., farmer's lung disease) have been associated with inhalation of actinomycete spores, together with spores of fungi (Roussel et al., 2005; Cano-Jimenez et al., 2016). As streptomycete spores are significantly smaller than those of fungi (1.2–2.5 μm vs. 2.5–10 μm), they are extremely likely to reach the alveoli, which may elicit potential risk for exposed residents (Awad and Farag, 1999). Streptomycetes are often mentioned as etiologic agents of inflammatory diseases originated from water-damaged houses. The study of Huttunen et al. (2003) proves them to be one of the top microbial producers of pro-inflammatory and cytotoxic compounds in wet buildings. Scarce reports bring information of other infections of human manifested mainly as pulmonary infections, bacteremias and different organs abscesses (Kapadia et al., 2007) – see **Supplementary Table S1** for details. Typical patients are immunocompromised, undergoing cancer therapy, etc., but also infections of immunocompetent people are reported (Yacoub et al., 2014).

For a long time, the presence of streptomycetes in healthy human microbiome remained neglected, though it was clearly reported in various animals. We suppose that their colonization of human tissues was and still is underestimated due to the lack of selective streptomycete cultivation techniques, their low growth rates and the generally accepted opinion of clinical microbiologist to view them as an air-born contamination. However, recent molecular data on the human microbiome confirm that they are present in the healthy skin (Gallo and Hooper, 2012), the gastro-intestinal tract (Bolourian and Mojtahedi, 2018b), the respiratory tract (Huang et al., 2015), and surprisingly also in the uterus (Collado et al., 2016). The major resource, whether ingested or inhaled, is soil, the contact with which is often mentioned as an important factor of human health (Sing and Sing, 2010). This makes them one of the hottest candidates as control agents of the developing microbial communities and coaches of the host immune system (Bolourian and Mojtahedi, 2018a,b). In fact, their huge variability of metabolite structures and activities must originate from broad interactions with various organisms, tissues and cells. They were recently also mentioned in connection to the suspected communication of gut microbiota with other organs, the gut-brain and gut-lung axes (Engevik and Versalovic, 2017; Bolourian and Mojtahedi, 2018b). Next, substantial changes in their abundance correlate with certain diseases or treatments (Huang et al., 2015; Wu et al., 2017; Silva et al., 2018). And last, we should also note that human guts contain considerably lower counts of streptomycetes than we can see in other, even closely related animals (Bolourian and Mojtahedi, 2018a). This was mentioned in connection to the typically cooked human diet, which destroys their important source – the soil particles-contaminated raw food. If we accept the theory of streptomycetes as one of the immune system coaches, their substantial reduction in human guts may correlate with the high incidence of the inflammatory bowel disease and gut cancer, almost unknown in animals (Rea et al., 2018). Taking all the recorded data together, the question arises: Can we consider streptomycetes to be friends or foes?

This work presents the characterization of *Streptomyces* sp. TR1341 strain isolated from the sputum of a patient with a history of multiple-organ TB, repeated respiratory infections and COPD. The patient was a senior man, living in the region with dust-polluted air. The strain was selected from our collection of about 80 strains of human specimen-originated streptomycetes due to a wide range of activities: from hemolysis to growth-inhibiting activities against both fungi and bacteria and other. We aimed to identify its specific genetic or metabolic features allowing it to colonize human tissues successfully. These human-adapted strains, in general, may serve as a great source of novel bioactive compounds specifically designed to modulate human cells behavior, e.g., suppressing the action of the immune cells to eliminate them. Moreover, they may substantially alter the behavior of the common microbiota and pathogens by targeted antibiotic

activities or quorum quenching mechanisms (Park et al., 2005; Stubbendieck et al., 2016).

MATERIALS AND METHODS

Cultivation Media and Microbial Strains

The streptomycete strain was cultivated in mannitol-soya (MS) agar without $CaCl_2$ (Hobbs et al., 1989), Oatmeal agar (HiMedia) or standard Columbia blood agar with sheep blood (Oxoid) at 28°C. Pathogenic bacteria were cultivated in the Columbia blood agar in 37°C. Streptomycete liquid cultures for metabolite extractions were cultivated in standard GYM medium (Ochi, 1987), 200 rpm, 28°C.

Following microbial species were used in the activity assays: *Candida albicans* CCM 8186, *Staphylococcus aureus* DSM 346, *Bacillus subtilis* CCM 1718, *Streptococcus pneumoniae* CCM 4424, *Escherichia coli* DSM 682, *Klebsiella pneumoniae* DSM 681, and *Pseudomonas aeruginosa* DSM 50071 from the culture stock of the Institute of Immunology and Microbiology, 1st Faculty of Medicine, Charles University. *Staphylococcus aureus* MRSA, *Moraxella catarrhalis,* and *Neisseria pharyngis* were clinical isolates isolated in the Laboratory of Clinical Microbiology, General Teaching Hospital, Prague. *Saccharomyces cerevisiae* CCM 8191 and *Fusarium oxysporum* BCCO 20_0605 strains were provided from culture stock of Biology Centre Collection of Organisms (BCCO) at Institute of Soil Biology.

Genome Sequencing and Assembly

DNA was extracted following the instructions of the Wizard Genomic DNA purification kit by Promega. An additional second centrifugation step was performed before resuspending the DNA. The sequencing of *Streptomyces* sp. TR1341 genome was performed by the Laboratory of Environmental Microbiology at the Institute of Microbiology, CAS, Prague. The library was prepared using the TruSeq PCR free LT library preparation kit (Illumina) and quantified with the KAPA library quantification kit (Roche). The library was sequenced using the Illumina MiSeq platform (Reagent kit v2, paired-end, 300 bp). Bowtie2 was used to screen for PhiX contamination (Langmead and Salzberg, 2012). Subsequently, reads quality was improved using Trimmomatic-0.36 (Bolger et al., 2014). Overlapping reads were merged using FLASH (Magoc and Salzberg, 2011). SPAdes 3.10.1 was used for assembly (Bankevich et al., 2012). The quality of the draft genome was assessed with QUAST (Gurevich et al., 2013) and Qualimap2 (Okonechnikov et al., 2016).

Phylogenetic Analyses

Maximum likelihood phylogenetic tree of the 16S rRNA gene was calculated in RAxML-NG (Kozlov et al., 2019) with the GTR + F0 + G model: general time reversible model, optimized base frequencies by maximum-likelihood, gamma distribution and bootstrap 100. The 16S rRNA gene sequences of closely related strains were obtained from the NCBI database and are summarized in **Supplementary Table S2**. In addition, autoMLST (Alanjary et al., 2019) was used to perform the multi-locus taxonomy analysis using 85 single copy housekeeping genes (**Supplementary Table S3**).

Hemolysis Assay

To assay the hemolysis, streptomycetes were inoculated from a sporulated culture on the MS agar onto the Columbia Blood agar. Development of hemolytic zones was observed in 2–5 days of cultivation at 28°C. The hemolysis type was evaluated according to the standard ASM guide (Blood Agar Plates and Hemolysis Protocols)[1]: β-hemolysis (complete hemolysis) was defined as a complete lysis of red blood cells in the media around and under the colonies, the area appeared lightened (yellow) and transparent. Green or brown discoloration in the medium surrounding the colony, caused by the reduction of the red blood cell hemoglobin to methemoglobin, was assigned as α-hemolysis.

Antibiotic Susceptibility Testing

The streptomycete strain was characterized for susceptibility to set of 21 antibiotics using a disk diffusion assay as follows (modification of Kirby-Bauer disk diffusion method). The antibiotic disks contained following antibiotics: amikacin 30, amoxicillin 25, amoxicillin + clavulanic acid 20 + 10, ampicillin 10, azithromycin 15, cefazolin 30, ceftriaxone 30, ciprofloxacin 5, clarithromycin 15, doxycycline 30, erythromycin 15, gentamicin 10, chloramphenicol 30, minocycline 30, ofloxacin 5, penicillin 6, rifampicin 5, streptomycin 10, tetracycline 30, trimethoprim-sulfamethoxazole 1.25 + 23.75, vancomycin 30. The numbers indicate amount of the antibiotics in μg per disk.

First, isolate was grown on Oat Meal agar (HiMedia Laboratories, India) for 14 days at 28°C, then spore suspension of an isolate was prepared in sterile tap water (McFarland density scale of 0.5) and 200 μL of spore suspension isolate was spread on the Mueller Hinton plates (Dulab, Czechia). Filter paper disks, containing selected antibiotics (Bio-Rad Laboratories, Hercules, CA, United States) were placed immediately after drying (no later than 15 min after plating) on the plates in triplicates. Inhibition zones were measured after 24 h of growth at 28°C. Simultaneously, *Staphylococcus aureus* DSM 346 was analyzed as internal quality control. Evaluation was done according to EUCAST guidelines for aerobic actinomycetes (e.g., *Corynebacterium*, *Nocardia*) or based on arbitrary breakpoints according to zone size distributions amongst strains in our collection (Adámkova V., personal communication).

Cocultures With Pathogens

Due to the slower growth of streptomycetes, TR1341 was inoculated 48 h in advance and cultivated at 28°C. The pathogen line in a T-shape was added afterward. The vegetative growth of streptomycetes was already obvious, though they were usually not forming aerial mycelia yet. The bacteria were cocultured for next 1–2 days at 37°C and their interactions were observed.

[1]https://www.asm.org/getattachment/7ec0de2b-bb16-4f6e-ba07-2aea25a43e76/protocol-2885.pdf

Cocultures With Human Macrophages

Human monocyte cell line THP-1 (purchased from the American Type Culture Collection, ATCC® TIB-202™) was cultured in the RPMI-1640 medium supplemented with 10% fetal calf serum (FCS), L-glutamine (292 μg/ml), penicillin G (100 U/ml), streptomycin (100 μg/ml; all from Biowest) and 50 μM mercaptoethanol (Sigma-Aldrich). Cells were cultured at 37°C in 5% CO_2 and 95% air in a humidified incubator and passaged twice a week.

For the coculture experiments, the cells were resuspended in PBS with 1% FCS in concentration of 1×10^6 cells per ml. Aliquots of 100 μl (10^5 cells) were mixed with 10 μl of streptomycete spore suspension containing 10^6 spores. In the negative control the same volume of PBS with 1% FCS was used instead of the spores, in the positive control 10 μl PMA (phorbol 12-myristate 13-acetate) was used to activate monocytes. The activation of THP-1 was performed using the FagoFlowEx® kit (Sigma) according to manufacturer's protocol. The cells were cocultured for 30 and 90 min at 37°C. Just before the flow cytometry analysis, the cells were washed once in PBS with 1% FCS and 1 μl of propidium iodide (PI, 50 μg/ml) was added to stain dead cells (monitoring of cytotoxicity). Respiratory burst of THP-1 cells was measured as the fluorescence of rhodamine 123 detected in 525 nm channel in BD FACS Canto II flow cytometer and analyzed using BD FACS Diva software. Data are expressed as average ($n = 3$) proportion of dead cells, dead but activated cells, neither activated nor dead cells and live activated cells. To compare the differences between control (PBS) and treated (TR1341) groups, two-way analysis of variance (ANOVA) followed by Bonferroni *post hoc* test in GraphPad Prism, version 5.0 was used. $P \leq 0.05$ was considered as the level of statistical significance.

For the analysis of the coculture effect on the TR1341 secondary metabolome, the TR1341 spores (10^8 cells/ml, 0.5 ml) were subjected to 10 min 55°C heat shock to induce their germination and transferred to 30 ml of RPMI-1640 media without antibiotics in a baffled Erlenmeyer flask. After 6 h of cultivation at 28°C, 200 rpm, 50 ml of RPMI-1640 with or without THP-1 cells (10^5 cells/ml) and the cultivation continued for another 48 h. 8 ml of the culture was used as a seed to inoculate 80 ml of GYM. Fermentation in GYM continued in standard conditions for 3 days and secondary metabolites were extracted.

Extraction of Secondary Metabolites

Secondary metabolites were extracted after 3 days of cultivation in 80 ml of GYM media in 500 ml baffled Erlenmeyer flask at 28°C, 200 rpm. The 8 ml inoculum for the fermentation culture was grown for 2 days under the same conditions. Two techniques were used to extract the secondary metabolites: SPE columns and organic solvent extraction. SPE columns were used solely for pilot extraction for analytical reasons. Subsequent organic solvent extraction provided sufficient extract amounts for the activity assays.

Pilot screening of the secondary metabolites production was done using SPE columns small-scale isolation using Oasis HLB 3cc 60 mg cartridge (hydrophilic-lipophilic balanced sorbent, Waters, United States) as described previously (Cihak et al., 2017).

Medium scale extraction was performed as liquid phase extraction using organic solvents. The 3 days fermentation culture (80 ml) was spun down: the medium and the cell pellet were processed separately. The cells were extracted with 1/2 volume of acetone for 30 min at 4°C, in a reciprocal shaker, and 250 rpm. The organic fraction was evaporated under 140 mbar pressure at 37°C. The rest of the liquid was extracted with 8 ml of ethylacetate using the same extraction conditions. NaCl was added in the post-fermentation media to 5M concentration and it was extracted with 1/3 volume of ethylacetate, the same conditions as above. Both ethylacetate extracts were combined, dried and dissolved in 200 μl of chloroform.

LC Analysis of the Extracts

The pilot TLC fractionation of the extracts was performed using Silica gel TLC plates with 254 nm fluorescence indicator (Sigma-Aldrich, St. Louis, MO, United States). Ten μl of an extract were applied and developed in benzene: acetone (3: 2). The plates were recorded under short- and long-wavelength UV illumination (254 and 366 nm). LC-MS analysis was performed as described by Cihak et al. (2017).

Bioactivities of the Metabolic Extracts

Hemolytic activity was assayed using standard Columbia blood agar. Ten μl of the culture metabolic extract dissolved in chloroform were dropped on the blood agar and let air-dry. The same amount of the pure chloroform was used as a negative control. The plate was incubated overnight at 37°C.

For the antibacterial and antifungal activity assays of the extracts, 10 μl was fractionated using TLC. The TLC plate was air-dried and printed on top of the blood agar previously covered with a cell suspension of the selected target microorganism as listed in Methods (McFarland density scale of 0.5). The TLC plate was left attached for 15 min to allow diffusion of the active compounds into the agar, removed and the plate was incubated overnight at 37°C for the development of the growth inhibition zones.

The cytotoxicity of the extracts was assayed using the THP-1 human monocyte cell line. For the human cell assays the streptomycete metabolic extracts were dissolved in DMSO. The concentration of the THP-1 cells used in the assay was 10^6 cells/ml in RPMI-1640 with antibiotics. Final dilution of the extracts in the assay ranged from 1:500 to 1:50,000. The cells were cultured for 24 h at 37°C and 5.7% CO_2. DMSO served as a negative control. Trypan Blue was used to stain and count the dead cells after the incubation.

The immunomodulatory effect of the extracts was assayed as their effect on THP-1 activation measured as production of the pro-inflammatory IL-1β by ELISA kit (Human IL-1beta Uncoated ELISA Kit, Invitrogen) according to the manufacturer's recommendation. Non-lethal concentrations of the extract were used based on the cytotoxicity assays results. Results are

presented as a mean of three independent experiments with standard error mean. *T*-test was employed to evaluate statistically significant differences between groups.

Disruption of the Filipin Gene Cluster

Genomic DNA of streptomycetes was isolated using the Wizard Genomic DNA Extraction Kit (Promega) using standard manufacturer's protocol for Gram-positive bacteria. For the disruption of the putative filipin gene cluster, the pGM160 plasmid with the temperature—sensitive replication was used (Muth et al., 1989). The disruption cassette contained the spectinomycin-resistance gene with conjugative *oriT* of the pIJ778 plasmid (Gust et al., 2004) surrounded by two arms homologous to the regions upstream and downstream of the five PKS I-encoding genes of the filipin cluster. The left arm (1050 bp) was amplified by PCR using FIL1L (5′-CAGCATGTTGGTGGTGGTCT-3′) and FIL1R (5′-CTCGACCATTTGCACTCCAC-3′) primers. The right arm (1299 bp) was amplified using FILCRO1L (5′-CTTTACGAAATCGGCGAGA-3′) and FILCRO1R (5′-GCTCGGACATGACTCTCCTT-3′) primers. The scheme of the insertion cassette is shown in Results. The cassette was cloned in the pGM160 vector and the resulting pFILDIS was introduced in *E. coli* ET12567/pUZ8002 by electroporation. From the resulting strain the construct was inserted in TR1341 by conjugation as described by Gust et al. (2004). The presence of the plasmid was checked by PCR using the FIL1L and spec200 (5′-ATTTTGCCAAAGGGTTCGTG-3′) primers and next using spec1300 (5′-TCACCAAGGTAGTCGGCAAA-3′) and FILCRO1R. Both spec primers anneal inside the spectinomycin resistance region of the cassette. The recombinant strain was cultured in YEME media supplemented with spectinomycin (400 μg/ml) in a rotary shaker at 28°C to late exponential phase and then the cultivation continued in the non-permissive temperature of 39°C. The culture was plated in serial dilutions on the MS plates with spectinomycin and MS plates with thiostrepton. Already after 2 days of non-permissive culture only $spec^R$ $thio^S$ colonies were found, indicating for the double crossing-over. The mutant colonies were checked using PCR with FIL1F – spec200 primers and spec1300 – FILCRO1R – both with positive band of a proper size and FIL1F – FILwtR (5′-GCGGTACGTCGGTGATCG-3′) and FILwtF (5′-TACTCGATGCTGGAGGACCA-3′) with no band formed in the disruption mutant. Both FILwt primers map within the deleted region of the filipin gene cluster. The parental *wt* strain was used as a control with no bands with spec primers and proper band size with FILwt primers.

RESULTS

Strain Isolation and Identification

The strain was isolated in the District Hospital in Pribram, Czech Republic, 2008, from sputum of an 81-year old male patient with previous history of lung and kidney TB. The patient's medical records also report ischemic heart disease, hypertension, gastroduodenal ulcer, lung fibrosis, COPD and repeated infections of the respiratory tract. He lived in a region with a high air pollution and died 4 years later due to the secondary liver cancer combined with pneumonia.

The sputum was subjected to selective cultivation for mycobacteria due to the suspected tuberculosis by a standard procedure (decontaminated sputum). This eliminated majority of microbiota with only mycobacteria resistant enough to the harsh treatment. To certain extent, streptomycetes can survive it as well, though with much lower rates. So, the streptomycetes can be isolated only from heavily colonized specimen. The strain was deposited in the collection of the National Reference Laboratory for Pathogenic Actinomycetes in the Local Hospital in Trutnov, Czech Republic, and kindly provided for our research.

The only organism cultivated from the sputum had a typical filamentous appearance and grew in streptomycete-like colonies with gray-pigmented spores and yellow pigment produced to the culture media. The analysis of the 16S rRNA gene using EzTaxon (Chun et al., 2007) revealed *Streptomyces costaricanus* NBRC100773 as the closest match (1480/1480, 100%) – see **Figure 1**. AutoMLST (Alanjary et al., 2019) was used to perform the multi-locus taxonomy analysis using 86 single copy housekeeping genes (**Supplementary Table S3** and **Supplementary Figure S1**). Both phylogenetic trees (**Figure 1** and **Supplementary Figure S1**) suggest that *Streptomyces* sp. TR1341 belongs to the *Streptomyces murinus* group (clade 12 of family *Streptomycetaceae*), together with *S. griseofuscus* and *S. costaricanus* (Labeda et al., 2012)[2]. It is quite distant from plant and human pathogenic strains like *S. scabiei*, *S. sudanensis,* and *S. somaliensis* (**Figure 1**).

Streptomyces sp. TR1341 showed susceptibility to aminoglycosides, macrolides, vancomycin, 2nd generation of tetracyclines, chloramphenicol and aminopenicillin augmented with β-lactamase inhibitor. On the other hand, strain TR1341 was resistant to penicillin, ampicillin, cephalosporins, quinolones, rifampicin, tetracycline and trimethoprim with sulfamethoxazole (**Supplementary Table S4**).

The genomic data have been deposited under the following accession numbers: BioProject PRJNA558635, BioSample SAMN12496210, SRA SRR9903270 and WGS VSDL00000000.

Hemolytic Activity

The TR1341 strain possesses strong β-hemolytic activity (i.e., causing complete hemolysis) that can be observed using Columbia Blood Agar plates already after 48 h of cultivation at 28°C (**Figure 2A**). The activity is not so common in soil-originated strains of streptomycetes, though the exact rates have not been studied yet. A pilot screening of our collection of 102 human-associated strains revealed 77.5% of β-hemolytic strains, but only 56% among 184 soil-originated strains (data not shown). The hemolysis is considered to be one of the virulence factors of pathogens and typically results from the action of protein hemolysins of various types (Vandenesch et al., 2012).

[2]https://link.springer.com/article/10.1007%2Fs10482-016-0824-0#Sec3

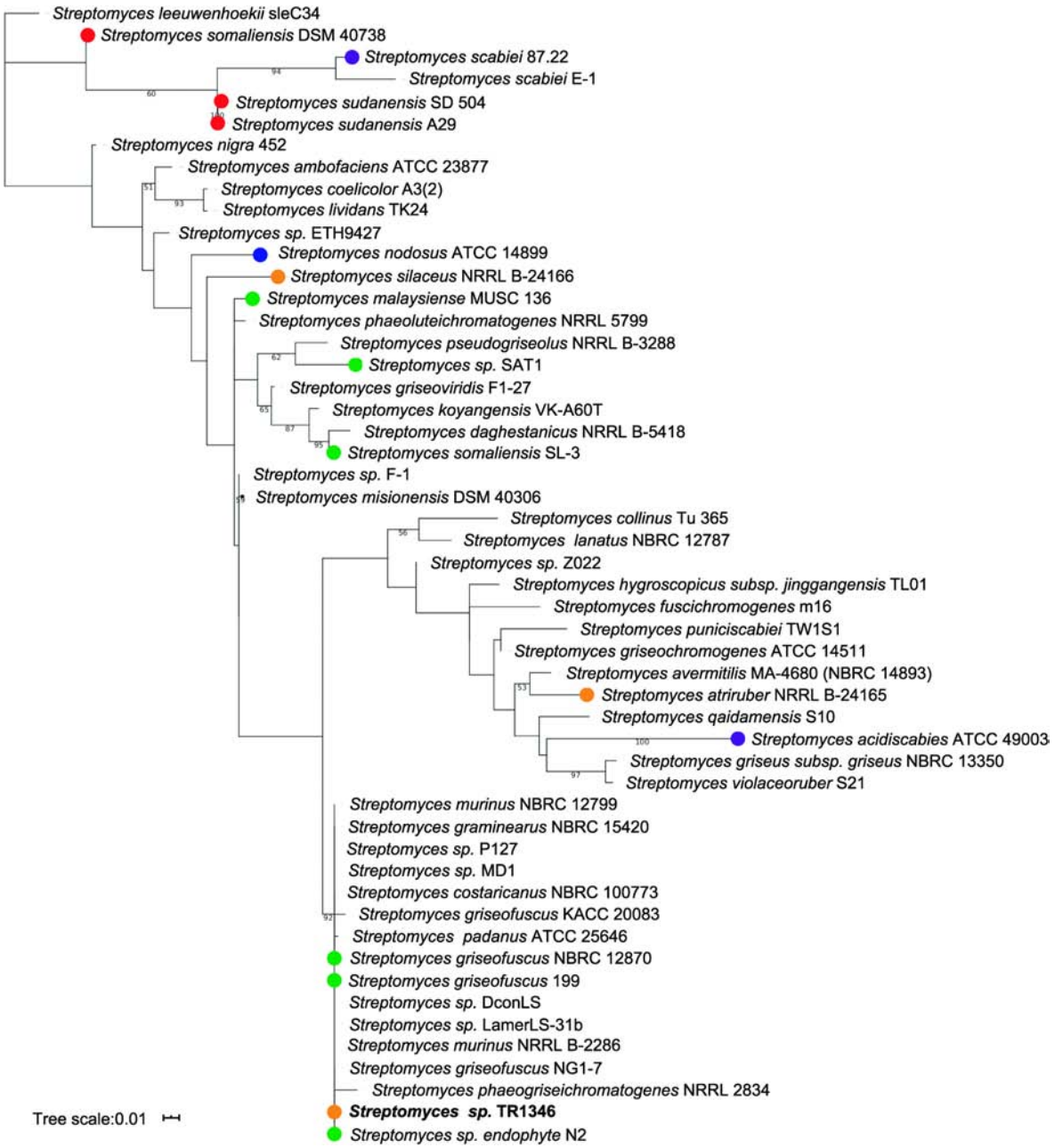

FIGURE 1 | Maximum likelihood phylogenetic tree based on 16S rRNA gene. Only bootstrap values higher than 50 are shown. *Streptomyces* strains marked with dots were isolated from water (blue) or are plant associated (green), plant pathogens (purple), animal associated (orange) or human pathogens (red); all other strain were either isolated from soil or their isolation source could not be found in literature.

As the soil-originated, α-hemolytic (i.e., viridating, incompletely hemolytic) *S. coelicolor* A3(2) type strain, the genome of TR1341 contains 4 putative homologs of known hemolysin genes (**Table 1**). Of these, SCO1782 is implicated in the α-hemolysis in *S. coelicolor* M145 (Rajesh et al., 2013). These genes seem to cluster with other putative genes that could play a role in the organism survival in the host tissue or even in intracellular parasitism. As an example we can mention ABC-transporter genes specific for $Fe3^{+}$-siderophore just next to the SCO1782 homolog in TR1341 (see **Table 1** for details and references).

Production of Siderophores

Siderophores are commonly produced by all bacteria: free-living, commensal and pathogenic. Iron is considered an essential element. However, it is not always freely available. For instance, concentrations of free ferric cations in human tissues are extremely low. Successful colonizers must develop efficient

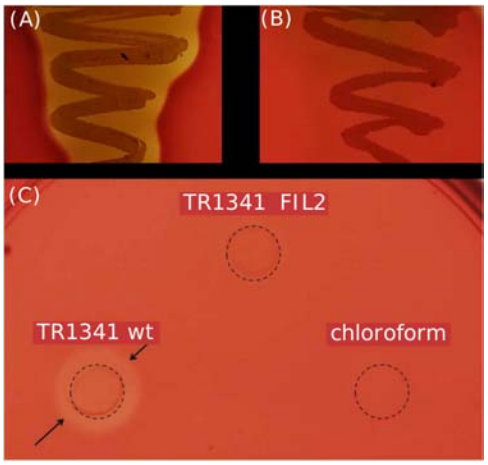

FIGURE 2 | β-hemolytic features of *S. sp.* TR1341. **(A)** β-hemolysis of TR1341 wt colonies in a standard blood agar plate, 3 days incubation in 28°C. **(B)** Disruption of the filipin/fungichromin production in TR1341ΔFIL2 causes complete loss of β-hemolysis. Grown for 4 days at 28°C in blood agar. **(C)** Production of hemolytic secondary metabolites by the strain (TR1341 *wt*) – extracted from 3-days old culture grown in GYM media by acetone/ethylacetate liquid phase extraction. The amount of extract applied (10 μl) corresponds to 4 ml of original culture. Dashed circle indicates the extract drop border, the arrows show the hemolytic zone. TR1341ΔFIL2 is the extract of filipin-deficient mutant of TR1341, chloroform stands for the negative control (the solvent only). Photographed after 16 h incubation at 28°C.

systems of Iron acquisition, where to seize the entire iron-chelating complexes of the host seems beneficial (Miethke and Marahiel, 2007). Genes putatively encoding such factors can be found in the close vicinity of the β-hemolytic gene homolog SCO1782 (**Table 1**).

Filipin-Like Biosynthetic Gene Cluster Is Encoded in the Genome

The putative hemolysin genes described above can be identified in majority of available streptomycete genomes, too, disregarding their hemolytic activity (data not shown). No homologs of genes encoding typical β-hemolysis-causing hemolysins, such as streptolysins of the group A streptococci (Molloy et al., 2011), are present. Because if this, we speculated that the activity may not be caused by a protein factor, but a secondary metabolite. It has been well documented in the literature that certain polyene secondary metabolites of actinomycetes and fungi show hemolytic or general cytolytic properties: filipin- or pentamycin-type compounds with smaller rings and amphotericin- or candicidin-like compounds with larger rings. The smaller compounds cause quite harsh damage to the erythrocyte membranes, whereas the larger make subtler changes depending on many other factors. All these compounds are fungicidal and those with lower toxicity are used in clinical medicine – amphotericin B, nystatin A1, pentamycin – as crucial anti-fungal and anti-protozoal agents (Knopik-Skrocka and Bielawski, 2002).

Scanning of the TR1341 genome revealed a putative gene cluster encoding filipin-type of pentaene compounds. All biosynthetic genes are similar to those of the known filipin producers *S. filipinensis* (Payero et al., 2015) and *S. avermitilis* (Vicente et al., 2014). The PKS I-encoding genes A1-A5 resemble those of filipin and encodes a 28-carbon macrolactone ring typical for filipin, fungichromin, antifungalmycin or thailandin. Genes B, C, D, E, G, and H encode chain-tailoring enzymes (**Figure 3**). The cluster encodes the same three regulatory genes as in *S. filipensis*: FilR, a SARP-LAL regulator; FilF, a regulator from the PAS-LuxR family, which is involved in the regulation of virulence factors in pathogenic actinobacteria (Ryan et al., 2015) and finally FilI, a PadR family transriptional regulator (Santos et al., 2012; Vicente et al., 2014). An extra, perhaps incomplete, ORF encodes a short protein with another PAS domain.

The TR1341 Strain Produces Filipin III and Fungichromin

The strain was cultured in GYM liquid media and extraction of secondary metabolites was done following two methods: using solid phase extraction (SPE) 3 ml columns; liquid phase extraction using acetone and ethylacetate sequentially for the mycelia and ethylacetate only for the post-fermentation media. The extract was analyzed using UHPLC-MS. Both extracts contain two polyene compounds: filipin III and fungichromin in concordance with the genetic information (**Figure 4**). The extract itself showed β-hemolytic features: a quantity corresponding to 4 ml of initial culture formed a clear hemolytic spot on the blood agar plate after incubation at 37°C for 12 h (**Figure 2C**).

Gene Bank Accession numbers of homologous proteins given in brackets. The last column of the table shows genes that are encoded in the close vicinity of the putative hemolysin genes and may play roles in the bacteria survival in the host tissue.

28-Carbon Polyenes Are the Only Factors Causing β-Hemolysis of TR1341

To verify the hemolytic activity of filipin and fungichromin in the TR1341 extract, a mutant strain unable to synthesize this type of compounds was designed. The entire region encoding all 5 PKS I genes was replaced with a cassette harboring the spectinomycin resistance gene (*aadA*) originated from the pIJ778 vector of the streptomycete Lambda Red system (Gust et al., 2004) using a temperature-sensitive pGM160 replicon (see in section Materials and Methods). Thio^R and spec^R recombinant colonies of putative filipin mutants were checked using PCR for a proper replacement (see Materials and Methods for details). The selected clone was designated as TR1341ΔFIL2. In order to exclude any contamination with the wt parent, the strain spores were collected and plated to grow in single colonies in MS media. A single spore (single colony) offspring was used in following experiments.

All the mutant colonies completely lost the β-hemolytic features (**Figure 2B**). However, incomplete hemolysis (viridation), seen as a greenish halo around the colonies was retained.

The TR1341ΔFIL2 mutant clones was subjected to regular fermentation. The extract was analyzed with UHPLC-MS and revealed no production of any of the cytolytic polyene

TABLE 1 | Putative hemolysin genes in TR1341 genome and their homologs in *S. coelicolor* A3(2) genome (NC_003888.3).

TR1341 ORF	*S. coelicolor* homolog	Similar to	Surrounding genes relevant to putative survival in the host
FSY75_36865	SCO1782	**Bifunctional tRNA methyl-transferase/TlyA hemolysin** of *Mycobacterium tuberculosis* (AQO55200.1) and *Brachyspira* (former *Treponema) hyodysenteriae* (APP13931.1)	$Fe3^{+}$-siderophore ABC-type transporter (Rahman et al., 2010; Forrellad et al., 2013; Rahman et al., 2015)
FSY75_17865	SCO2534	**HlyC/CorC family magnesium and cobalt efflux protein – TlyC family**: hemolysin C of *Brachyspira hyodysenteriae* (ACN83901.1) and Co^{2+}-resistance protein CorC of *Salmonella typhimurium* (TKE78380.1), TlyC hemolysin of *Rickettsia prowazekii (*CAA72456.1)	Adenosine deaminase (Lee and Yilmaz, 2018) Methalo beta-lactamase (Somboro et al., 2018) Heat shock-inducible repressor and DnaJ chaperone (Forrellad et al., 2013)
FSY75_04245	SCO3882	**HylA/YidD**, *Aeromonas hydrophila* **β-hemolysin** (WP_011707926.1)	Thioredoxin, thioredoxin reductase (May et al., 2019)
FSY75_26430	SCO4978	**YqfA family hemolysin III family**, e.g., *Escherichia coli* (ANK03204.1)	Aspartate aminotransferase (Wang et al., 2016) Phosphoenolypyruvate carboxykinase (Forrellad et al., 2013) Thymidylate kinase (Challacombe et al., 2014)

Gene Bank Accession numbers of homologous proteins given in brackets. The last column of the table shows genes that are encoded in the close vicinity of the putative hemolysin genes and may play roles in the bacteria survival in the host tissue. Protein family names are shown in bold.

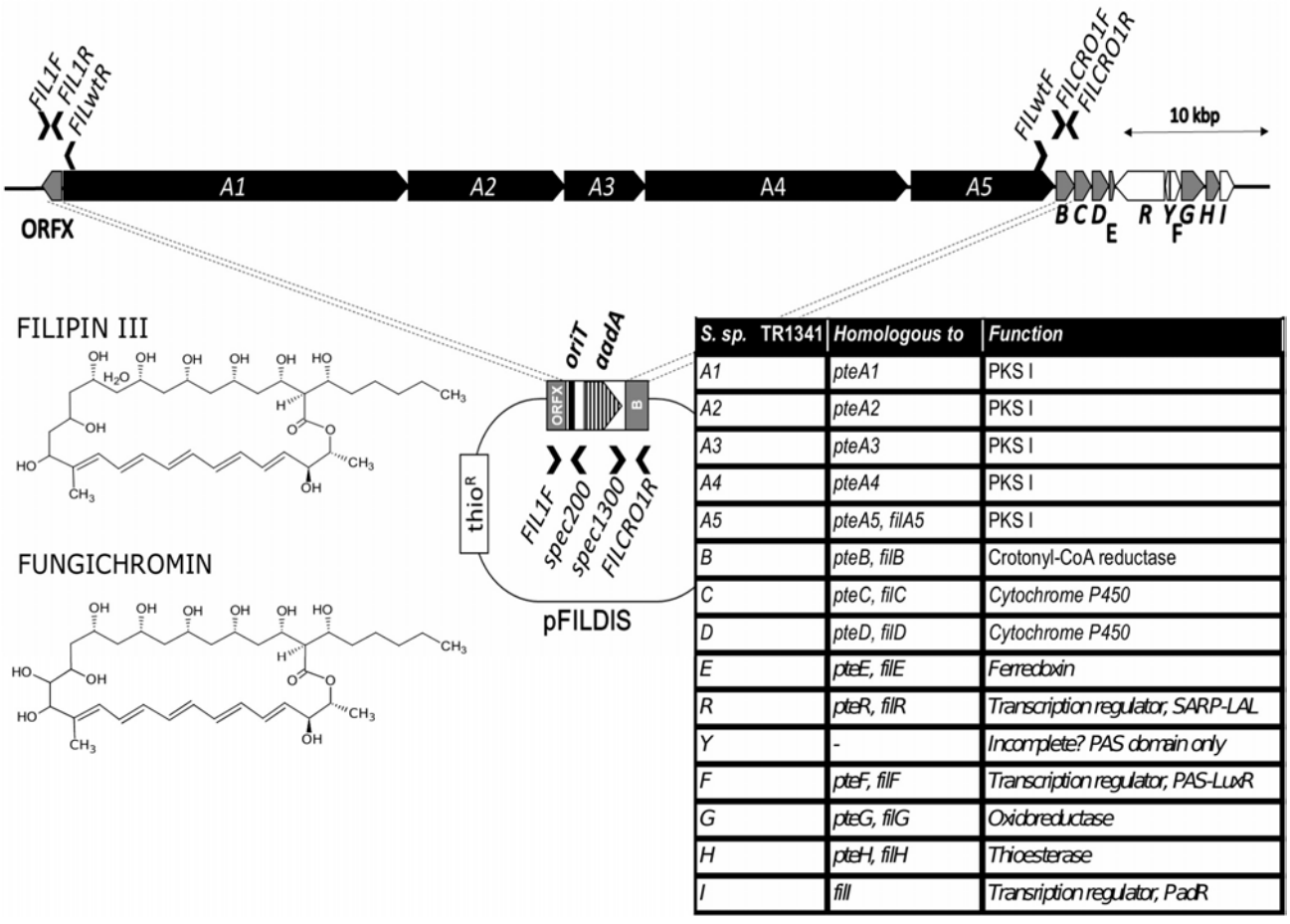

S. sp. TR1341	Homologous to	Function
A1	pteA1	PKS I
A2	pteA2	PKS I
A3	pteA3	PKS I
A4	pteA4	PKS I
A5	pteA5, filA5	PKS I
B	pteB, filB	Crotonyl-CoA reductase
C	pteC, filC	Cytochrome P450
D	pteD, filD	Cytochrome P450
E	pteE, filE	Ferredoxin
R	pteR, filR	Transcription regulator, SARP-LAL
Y	-	Incomplete? PAS domain only
F	pteF, filF	Transcription regulator, PAS-LuxR
G	pteG, filG	Oxidoreductase
H	pteH, filH	Thioesterase
I	filI	Transription regulator, PadR

FIGURE 3 | Filipin biosynthetic gene cluster of TR1341. The PKS I genes shown in black, tailoring genes in gray, regulatory in white. The gene annotation indicated in the table on the right and both compounds produced shown on the left. The PKSI genes disruption scheme shown in the middle A1-A5 genes replaced with the *aadA* spectinomycin resistance gene in TR1341 ΔFIL2. Primers used to verify the gene disruption indicated by black arrows.

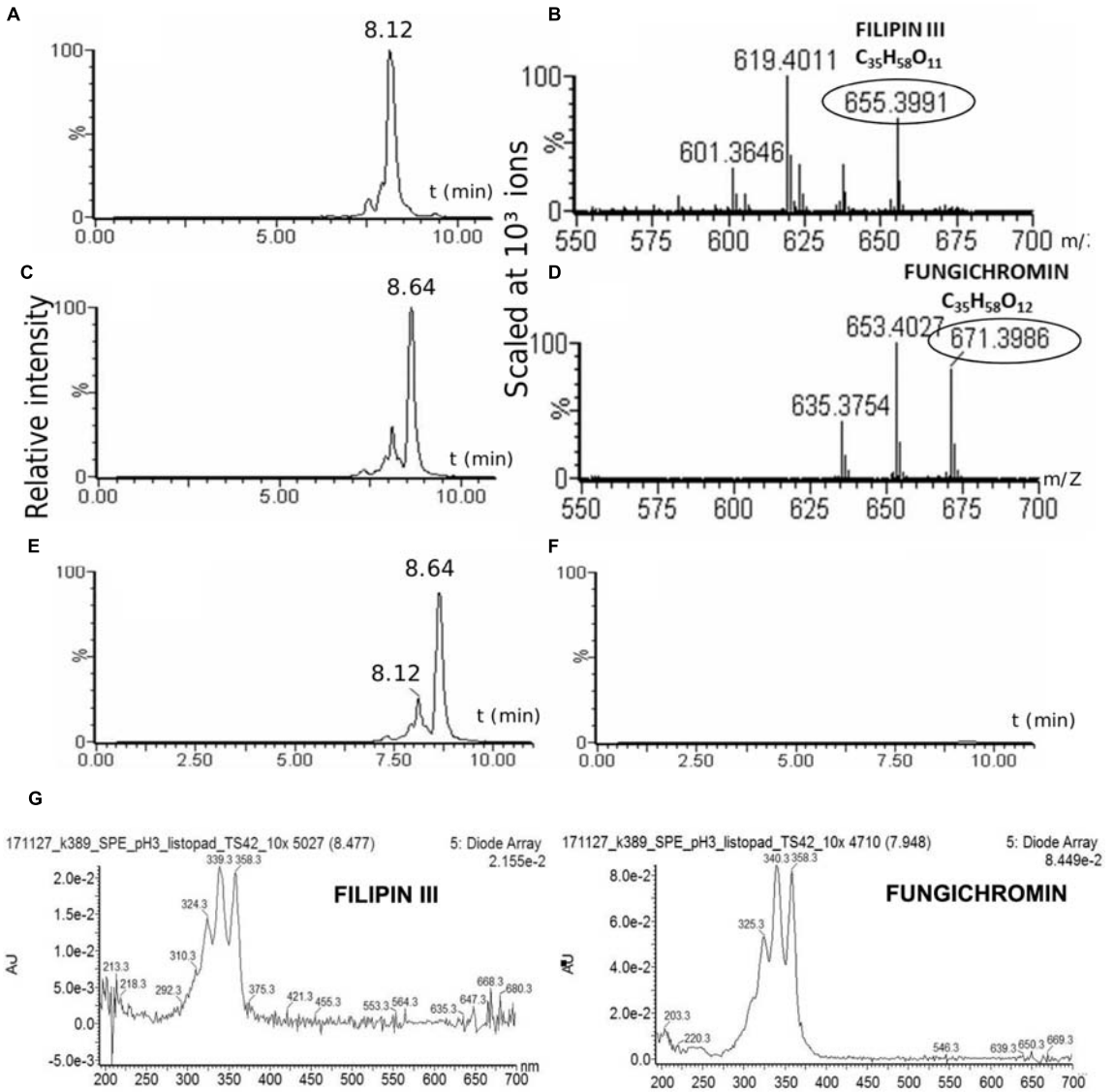

FIGURE 4 | Production of cytolytic polyenes by TR1341. LC-MS analysis of the TR1341 extract of secondary metabolites: Filipin III **(A)** and fungichromin **(C)** peaks and corresponding MS analyses **(B,D)**. Disruption of the filipin III and fungichromin production in the TR1341 ΔFIL2 mutant: **(E)** *wt* chromatogram, **(F)** mutant chromatogram. The absorption spectra of compounds correspond to the standards of both polyenes – 5 conjugated double bonds (Castanho et al., 1992) **(G).**

macrolactones. The extract was assayed for the β-hemolytic activity together with the extract of the parental *wt* TR1341 strain. The hemolytic activity of the extract completely disappeared after disruption of filipin and fungichromin production (**Figure 2C**). This means that the hemolytic features of the strain are caused solely by the production of low-molecular weight hemolysins, the polyene secondary metabolites, and not by any other protein-type hemolysins putatively encoded in the genome.

TR1341 Influences Growth and Virulence of Human Pathogens

In order to check the antibiotic activities of TR1341, first, the T-shape co-inoculation of TR1341 with selected human pathogens was performed and the appearance of a growth-inhibiting zone around TR1341 was recorded. The results are summarized in **Table 2** and **Figure 5**. Next, the metabolic extracts of TR1341 and the TR1341 ΔFIL2 mutant were fractionated by TLC and the chromatographic plate was directly "printed" on the top of a blood agar plate inoculated with the pathogens.

The TLC fractionation-based assay of the wt and mutant has shown that TR1341 produces at least two bioactive compounds: the fungicidal one with hemolytic features and an antibacterial compound. For the fungicidal activities, only the macrolactone polyenes of filipin and fungichromin are responsible. The activity completely disappears in the TR1341 ΔFIL2 mutant. Antibacterial activity has a different retention factor using the TLC system and has quite a wide spectrum of activities – it

TABLE 2 | Antibiotic activities of the TR1341 strain and the filipin/fungichromin mutant TR1341ΔFIL2.

Pathogen	Growth inhibition		Other effects
	wt	TR1341ΔFIL2	
Candida albicans CCM 8186	+	−	−
Sacharomyces cerevisiae CCM 8191	+	−	−
Fusarium sp. BCCO 20_0605	+	−	−
Staphylococcus aureus DSM 346	++	++	Hemolysis induced (only in the wt)
Staph. aureus MRSA (clinical)	+	+	n.d.
Bacillus subtilis CCM 1718	+	+	−
Streptococcus pneumoniae CCM 4424	+	++	Formation of a capsule inhibited
Moraxella catarrhalis (clinical)	+	+	−
Neisseria pharyngis (clinical)	+	++	−
Escherichia coli DSM 682	−	−	−
Klebsiella pneumoniae DSM 681	−	−	−
Pseudomonas aeruginosa DSM 50071	−	−	Hemolysis induced (only in the wt)

Growth inhibition zone of the pathogen indicated: "+": a small inhibitory zone < 8 mm; "++": a big inhibitory zone > = 8 mm; "−": no growth inhibition; n.d., not defined. Other effects on the growth and characteristics given in the last column. For a typical picture see the ***Supplementary Figure S2****.*

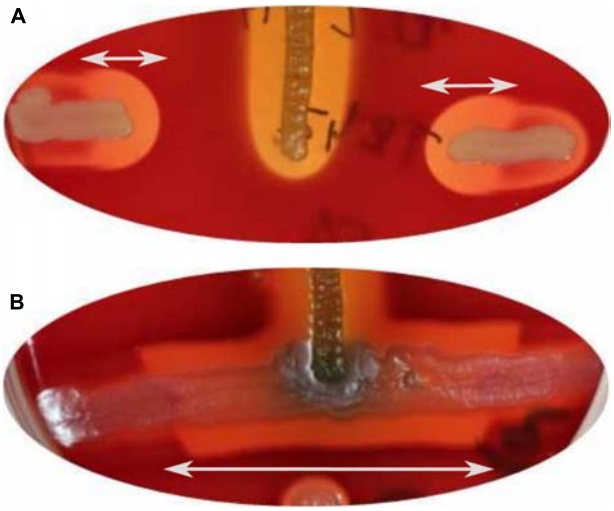

FIGURE 5 | Interactions of TR1341 with human bacterial pathogens *in vivo*. Vertical line = TR1341, horizontal line inoculated in a T-shape to touch the TR1341 inoculation = the pathogen. **(A)** *Staphylococcus aureus:* Growth inhibitory zone + induction of β-hemolysis by TR1341 (white arrows). **(B)** *Pseudomonas aeruginosa:* Induction of β-hemolysis (white arrows), motility and colored secondary metabolites production in *Pseudomonas* in the close vicinity of TR1341.

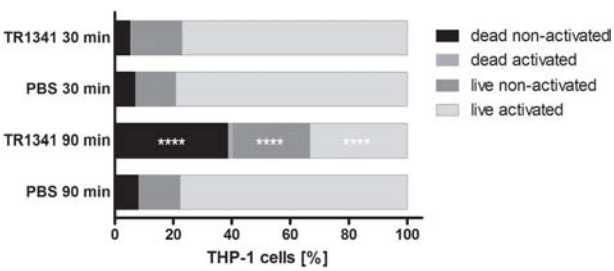

FIGURE 6 | *In vivo* influence of TR1341 spores on human THP-1 monocytes after 30 and 90 min of coculture. Data are expressed as an average (n = 3) proportion of dead cells, dead but activated cells, neither activated nor dead cells and live activated cells. Control cells were cultivated in PBS only. ****$P \leq 0.0001$ (two-way ANOVA).

acts against all assayed Gram-positives, including methicillin-resistant *Staphylococcus aureus* (MRSA), but also against some Gram-negatives (*Moraxella* and *Neisseria*). The compound(s) identification will be our future aim, as it targets clinically relevant human pathogens. Interestingly, the antibacterial activity against some microbes (*S. aureus, S. pneumoniae, N. pharyngis*) raised in the TR1341ΔFIL2 mutant compared to the *wt*, but remained the same against all others (**Supplementary Figure S2**). The mutant also loses the ability of the wt (**Figure 5** and **Table 2**) to induce the hemolysis in *S. aureus* and *P. aeruginosa*, but the capsule-suppressing effect on *S. pneumoniae* is retained.

Human Cells-Targeted Activities of TR1341

The interactions of TR1341 with human cells was first assayed *in vivo*, using coculture of the strain spores with human monocyte cell line THP-1 (ratio 10: 1 = spores: macrophages). The viability and activation of THP-1 was assayed after 30 and 90 min of coculture as described in Section "Materials and Methods." There was no effect neither in activation nor in survival of the THP-1 after 30 min coculture. But after 90 min, compared to PBS, a substantial drop in viability was obvious in the coculture with TR1341 spores – around 40% dead cells compared to about 8% in the controls. Also, number of viable, but not activated cells was significantly higher in the coculture: Above 26% compared to approx. 14% in the controls, suggesting the slight immunosuppressive effect of the germinating spores (**Figure 6**).

Next, the immunomodulatory effect of the metabolic extracts originated from the 3-days old stationary cultures was assayed for the cytotoxicity to THP-1. The experiment showed quite high level of cytotoxicity of the GYM media-derived culture with only 7% surviving cells in average in the 1: 10,000 dilution of the extract, and 64% in 1:50,000 dilution (compared to the control 88%, p = 0.001 and p = 0.0292, respectively). For the

pro-inflammatory activity assays, measured as activation of IL-1β production in comparison with control, dilution of 1: 10,000 ($p = 0.0362$), 1: 50,000 ($p = 0.0038$) and 1: 100,000 ($p = 0.0714$) were used and the cells were simultaneously stimulated by LPS. The TR1341 extract caused a strong pro-inflammatory effect: the effect was concentration-dependent, dropping with the extract dilution, and statistically significant for the two lower dilutions of 1: 10,000 and 1: 50,000 (**Figure 7A**).

In the last experiment, we assayed whether the previous contact with THP-1 human cells may change secondary metabolome bioactivities in TR1341. The streptomycete early exponential phase mycelia were cocultured with THP-1 in the RPMI-1640 media for 6 hrs. The culture was used as seed culture in standard GYM fermentation. In a control, only RPMI-1640 media without THP-1 was used to assess the impact of the rich tissue culture media itself on the streptomycete metabolism. The extracts were prepared as in the previous experiment and assayed the same way. The cytotoxicity of the extracts was ten times lower then after the standard fermentation: 1: 10,000 diluted extract had no effect on the cell viability; 1: 5,000 diluted extracts reduced viability to 50% in the coculture experiment ($p = 0.0019$), but had no effect in the control (84% viable, $p = 0.3794$). The same dilution was used to assess the effect of the extracts on the IL-1β production. Despite the drop in the percentage of alive cells, the overall production of IL-1β was more than seven times higher ($p = 0.0099$). This means that TR1341 cells boost its pro-inflammatory effect upon the contact with human cells (**Figure 7B**).

We hypothesized that the high cytotoxicity of the TR1341 extracts originates in the production of the cytolytic polyenes. That is why the cytotoxicity of the TR1341ΔFIL2 was assessed, too. Surprisingly, it was even an order higher than in wt. As the genome of TR1341 contains a putative gene cluster encoding another highly cytotoxic compound, actinomycin (data not shown), we analyzed the *wt* and mutant extracts for the presence of any actinomycin derivative. Actinomycin X2 was, in concordance with the genetic data, detected in both extracts by LC-MS, but the peak relative intensity was approximately 5.4 times higher in the extract of the filipin mutant TR1341ΔFIL2 than in *wt* (**Figure 8**). Comparison of the peak areas in HPLC chromatogram confirms 3.8 times higher production of actinomycin X2 in the filipin mutant. This finding can well explain the high cytotoxicity of the mutant extract and may also cause stronger antibacterial activity of the mutant extract (Sharma and Manhas, 2019).

DISCUSSION

In this study, we attempted to assess what factors may predetermine a streptomycete strain to colonize human tissues successfully and, perhaps, to become pathogenic. Such data are completely missing, even in the case of the well-recognized pathogens, *S. somaliensis* and *S. sudanensis*. Many factors may play a role in human non-mycetoma opportunistic infections: the individual strain metabolic characteristics – character of hydrolytic enzymes and bioactive secondary metabolites, the host immune system status or superinfection by other microbes (Verma and Jha, 2019). The **Supplementary Table S1** summarizes all clinical cases of non-mycetoma human infections described in the literature up to date.

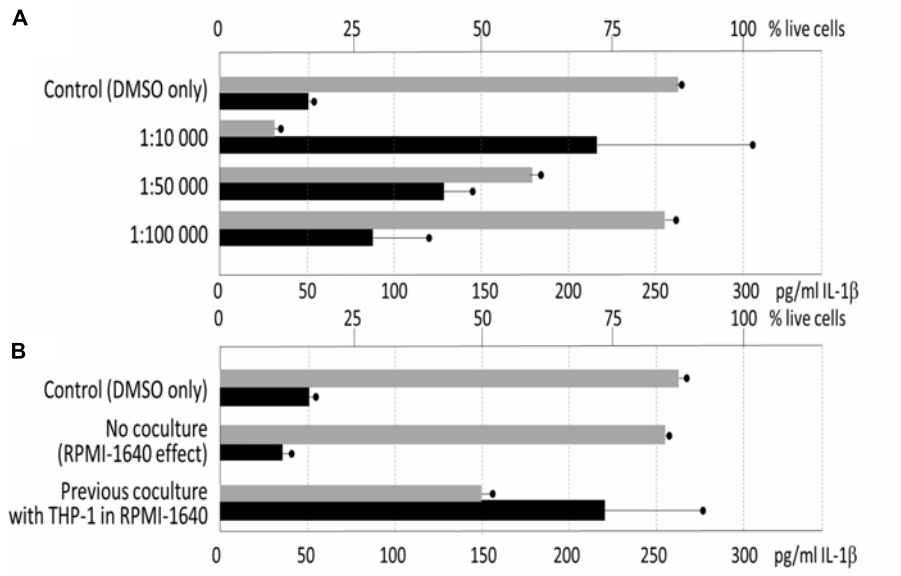

FIGURE 7 | Influence of TR1341 extracts on THP-1 human macrophages. Viability of the cells indicated by gray rectangles (top axis scale), pro-inflammatory activation of the cells measured as IL-1β release indicated by black rectangles (bottom axis). In all the assays THP-1 were activated by LPS. **(A)** Standard fermentation in GYM media – effect of extract dilution (dilution indicated on the *Y* axis). Control = cells + LPS + DMSO. **(B)** Effect of preculture of TR1341 with THP-1 prior to fermentation on production of pro-inflammatory and cytotoxic compounds. Control as above, extracts diluted 1:5,000.

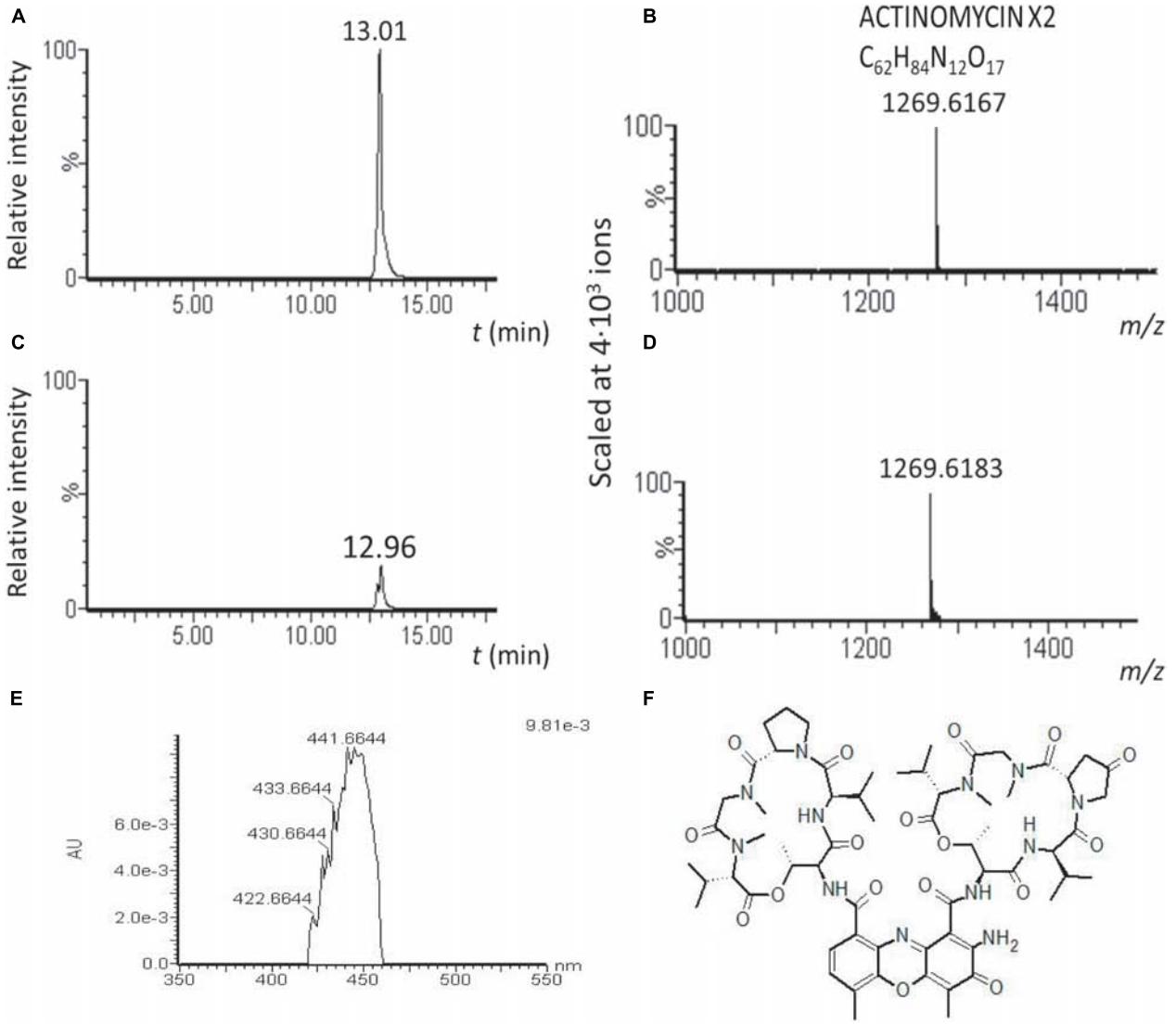

FIGURE 8 | Actinomycin X2 production is substantially augmented in the TR1341 ΔFIL2 mutant. LC-MS analysis of the acetone/ethylacetate extracts of *wt* and filipin mutant grown under standard conditions in GYM. Relative intensity of the actinomycin X2 signal in the TR1341 ΔFIL2 mutant **(A)** is approximately 5 times higher than in the wt **(C)**. The molecular mass of the corresponding peaks is given in **(B,D)**. Absorption spectrum of the compound **(E)** corresponds to that of actinomycin X2 **(F)** (Furukawa et al., 1968).

Almost 30 years ago McNeil et al. (1990) postulated that streptomycetes should be considered as potential pathogens to humans, having a role in primary pulmonary and cutaneous infections in some patients. Additionally, they recognized streptomycetes as the fourth most common isolate from clinical specimens among aerobic actinomycetes (following *Nocardia asteroides*, *Actinomadura madurae*, and *N. brasiliensis*) and underlined the importance to be further studied by clinical microbiologists. By inspecting the previous studies, we found, that the human non-mycetoma streptomycete infections are not linked to particular species (**Supplementary Table S1**), even though the set of 28 streptomycete clinical isolates mainly from sputum and wounds in the Mc Neil's work was biochemically characterized as a single species: *S. griseus*. However, we should take in account that all the early taxonomic data, based solely on biochemical characteristics of the strains, might be quite misleading. The available data indicate that diverse streptomycetes from the nearby environment can colonize human body and potentially cause infection. The *Streptomyces* sp. TR1341 strain was selected from the collection of human-associated streptomycete isolates for further characterization mostly due to its most complex bioactive compounds production and strong β-hemolytic features. According to phylogenetic analyses, the pneumonia-associated strain is closely related to *Streptomyces costaricanus* NBRC100773 by 16S rRNA taxonomy and belongs to the *S. murinus* group by autoMLST multi-locus taxonomy. None of the closely related strains has been linked to human infection, though some were reported as plant-associated

(**Figure 1** and **Supplementary Figure S1**). Strain showed typical streptomycete antibiotic susceptibility profile: it was susceptible to aminoglycosides, macrolides, and additionally to minocycline, vancomycin, and amoxicillin augmented by clavulanic acid and resistant to cephalosporins, quinolones, rifampicin, tetracycline, chloramphenicol and penicillins. However, it was resistant to trimethoprim-sulfamethoxazole (cotrimoxazole, COX), showing completely no inhibition zone. This is not so often among streptomycetes, being previously observed only in streptomycete isolate from lung nodule (Kapadia et al., 2007), in *Streptomyces cacaoi* isolated from scalp abscess (Pellegrini et al., 2012), and in 29% of clinical streptomycete isolates of the study of McNeil (McNeil et al., 1990). Interestingly, the patient had been treated with COX a few years prior to the strain isolation.

We hypothesize, that one of the characteristics significant for successful colonization of human tissue by certain streptomycetes is their secondary metabolites repertoire. Though taxonomically related, the family of *Streptomycetaceae* varies greatly in the secondary metabolites produced by individual species or even strains of a single species. About 2/3 of their linear genomes encodes adaptive functions: secondary metabolites, extracellular enzymes, resistance genes, etc., which can be easily exchanged in the bacterial communities by means of horizontal gene transfer (Egan et al., 2001; Barka et al., 2016). The secondary metabolites produced may not have only positive impacts on the putative hosts, as mentioned in connection to streptomycetes as a members of healthy human microbiota. Many strains produce cytotoxic or cytolytic compounds (Knopik-Skrocka and Bielawski, 2002), or compounds able to slow down or stop the host immune response, cell division, etc. (e.g., (Striz et al., 2008; Petrickova et al., 2014). People in regular contact with the soil dust (miners, farmers) as well as inhabitants of cities with high air pollution and water-damaged houses are the most exposed. Minor immune system disorders or the altered mucosa and skin fitness or superinfection may be the major factors of the successful colonization or even progression to disease.

Our data show that the predispositions of the TR1341 strain encompass the production of β-hemolytic compounds with fungicide activity (filipin and fungichromin) and the production of another highly cytotoxic compound, actinomycin X2. Both can have a deadly impact on any human cell (Knopik-Skrocka and Bielawski, 2002; Liu et al., 2016). We have proven that the only β-hemolytic factor of the TR1341 strain are polyene compounds of the filipin group. Moreover, the genomes of streptomycetes, including TR1341 and the type soil strain *S. coelicolor* A3(2) contain at least 4 putative genes homologous to protein hemolysins genes of human or animal pathogens. One of these is essential for the incomplete α-hemolysis of *S. coelicolor* (**Table 1**). The disruption of the filipin/fungichromin gene cluster in TR1341 destroyed the β-hemolytic features of the strain entirely, leaving just the α-hemolytic features. As expected, together with the loss of hemolysis, the mutant strain lost also its fungicidal activities. However, the antibacterial activity remained the same or was even stronger in the mutant than in the *wt* (the wild type is active against various Gram-positive and Gram-negative bacteria – see **Table 2**). To explain these unexpected results, we have compared the *wt* and mutant metabolic profile that documented substantially higher production of actinomycin X2 in the filipin mutant compared to the *wt*. As both metabolic pathways do not share the same precursors, this may be due to the better supply of energy (ATP) and cofactors (NADH, NADPH) for the actinomycin biosynthetic machinery after depletion of the competing filipin pathway. The actinomycin X2 also has antibacterial features that may explain the higher antibacterial activity of the mutant extract, too.

The hemolytic effect of the strain *in vivo* is stronger than that of its metabolic extract. The finding may have several reasons. It is well documented that the production of secondary metabolites is coregulated by global regulators with morphogenesis (Hou et al., 2018; Wang et al., 2018). Since the extractions were performed from liquid cultures where the streptomycete cells often do not undergo standard morphological differentiation, the overall secondary metabolism rates may be reduced. Next, filipin-type polyenes are prone to oxidations and subsequent loss of the bioactivity (Tingstad and Garrett, 1960), so they may be partially degraded during the extraction. The appearance of hemolytic zones caused by the culture and its extract is slightly different. Production of the putative α-hemolysin (SCO1782) homolog may contribute to the discoloration of the zone by hemoglobin degradation (Rajesh et al., 2013) *in vivo*.

Disruption of the polyene production stops the CAMP test-like induction of hemolysis in other pathogens (*S. aureus, P. aeruginosa*) by TR1341 in the coculture assays. We can expect that larger and clearer hemolytic zones around the β-hemolytic pathogens originate from the secretion of the cytolytic polyenes from the TR1341 wt mycelia into the agar media. On the other hand, polyene-less mutant still suppresses formation of the capsule in the *S. pneumoniae*. Of the possible mechanisms, which might be involved in the suppression, production of extracellular capsule-degrading enzymes or quorum quenching mechanisms should be considered.

Next, we assayed immunomodulatory impacts of the interaction of human THP-1 macrophage cells with germinating spores. The germinating spores can be considered as the first active cells that the human mucosa immune cells encounter and react to when they are inhaled. We have shown in *in vitro* experiments that human macrophages viability and ability to activate the proper response to an invader are significantly reduced by their contact with the TR1341 germinating spores. Additionally, we have monitored the effect of secondary metabolites produced by stationary TR1341 cultures on viability and pro-inflammatory response of THP-1. The extracts of the late culture showed high cytotoxicity that we first ascribed to the production of the cytolytic polyenes. However, the extract of the polyene non-producing mutant had the cytotoxic effects even 10 times higher, though it obviously lost hemolytic activities. Detailed comparison of LC-MS data of both strains revealed a substantial elevation of the actinomycin X2 production, another highly cytotoxic compound. Disregarding the cytotoxicity of the wt extract, in sub-cytotoxic dilutions, it stimulated the pro-inflammatory response of THP-1. The late, stationary cultures used for the metabolite extractions may mimic microcolonies putatively formed in the host tissue after successful colonization.

The data presented in this work cannot be considered as a proof of a direct link between the patient's symptoms of relapsing atypical pneumonias and colonization of his lungs by *Streptomyces* sp. TR1341, though no other facultative or obligatory pathogens were found in the sputum. In order to assess the facultative pathogenicity of the strain, at least an animal (mouse) model of lung colonization/infection should be used, which we would like to do in the near future. However, we should mention that production of similar metabolites (antifungal and cytolytic polyenes, actinomycins and cytotoxic compounds) was often reported in actinomycetes associated with animals and plants: Filipins are produced by mutualistic actinomycetes of brown algae (Parrot et al., 2019) and water caltrop plant (Kim et al., 2012), larger candicidins by symbionts of ants (Haeder et al., 2009; Barke et al., 2010; McLean et al., 2016), sceliphrolactam by digger wasps symbionts (Oh et al., 2011; Poulsen et al., 2011) and linear micangymicins by actinomycetes associated with southern pine beetles (Oh et al., 2009). Similarly, actinomycins production is often associated with ants actinomycete symbionts (Schoenian et al., 2011; Boya et al., 2017), where also cancerostatic antimycins frequently appear (Poulsen et al., 2011; Seipke et al., 2011; McLean et al., 2016). This supports our hypothesis that human-associated streptomycetes may benefit from production of these compounds, too.

CONCLUSION

This work documents several genetic adaptations that could help *Streptomyces* sp. TR1341 and perhaps also other human-associated streptomycetes to colonize the evolutionary new niche, the human tissue. First, it is a production of cytolytic or hemolytic polyenes, which allows the streptomycete not only to lyse human cells for nutrition, but also to conquer fungi. Second, it produces highly cytotoxic actinomycin X2. Third, the strain germinating spores can suppress the immune response of the human macrophages *in vitro*. The mechanism remains still unclear. Though the production of secondary metabolites is typical for stationary growth phases, small amounts of secondary metabolites can be detected already during the spore germination in *S. coelicolor* (Cihak et al., 2017). The observed suppression of THP-1 activation thus may originate from both direct interaction of TR1341 with macrophages and production of some bioactive compounds. Such activity would be quite beneficial for the streptomycete in the early phase of human lung tissue colonization as it could protect the spores and young mycelia from the attack of innate immune cells. Fourth, in contrast to the germinating spores, the stationary cultures of TR1341 produce secondary metabolites with pro-inflammatory and cytotoxic features. This feature becomes even stronger upon contact with human macrophages. Inflammatory processes are associated with destruction of the host tissue that may certainly provide the intruder with nutrients from the lysing host cells. Taking all the data together, we think that the crucial factors of pathogenicity in streptomycetes originate from their secondary metabolism. "Suitable" biosynthetic gene clusters may be easily spread by mechanisms of horizontal gene transfer in soil or other biotopes (Shintani et al., 2014; McDonald and Currie, 2017). This may explain why non-actinomycetoma streptomycete infections are reported even in taxonomically distant strains.

DATA AVAILABILITY STATEMENT

The datasets generated for this study can be found in the genomic NCBI: BioProject PRJNA558635, BioSample SAMN12496210, SRA SRR9903270 and WGS VSDL00000000.

AUTHOR CONTRIBUTIONS

AH made the genetic manipulations with the streptomycete strain, performed fermentations and cocultures with human cells, prepared the metabolic extracts, and performed cytotoxicity and immunomodulatory effects assays of the extracts. EC performed the phylogenetic analyses, analyzed the genomic data and made the hemolysis and growth-inhibitory activities assays *in vivo*. AC supervised the phylogenetic analyses and analyzed the data, performed the genome sequencing, and participated in the manuscript preparation. HL, PP, and JH assayed the human cells-targeted activities. HL designed and performed the *in vivo* cocultures and evaluated their effects. PP, JH, and AH designed and performed the experiments to assess immunomodulatory features of metabolic extracts and their cytotoxicity. JH and HL evaluated the human cells-related experiments data and participated in the manuscript preparation. MČ performed and evaluated the LC-MS experiments. VK made the strain taxonomic and morphologic characterization. JB was involved in the growth-inhibitory activities *in vivo* and in evaluation of the strain interactions with pathogenic microbes. MP made the overall design of extraction experiments and evaluated the data. KP planned the experiments, participated in the activity screenings, analyzed and interpreted the data, made the literature review on streptomycete-related human infections, and prepared the manuscript.

FUNDING

This work was supported by the Czech Health Research Council project No. 17-30091A.

ACKNOWLEDGMENTS

We would like to acknowledge Josef Scharfen of the National Reference Laboratory for Pathogenic Actinomycetes, Trutnov, Czech Republic, for providing the strain for the study and Petr Ježek of the District Hospital in Příbram, Czech Republic, for the clinical microbiology consultations and isolation of the strain, and Václava Adámková, Antibiotic Center of the General Teaching Hospital, Prague, Czech Republic, for her guidance in antibiotic susceptibility tests evaluation. We would like to thank to Dr. Engy Ahmed (BC, ISB) for providing the strain of *Fusarium oxysporum* BCCO 20_0605 for bioassays. Next, we

would also like to thank to our technical staff Tomáš Chrudimský, Petra Benešková, Martina Petrlíková, Petr Pospíchal, and Zuzana Žlábková for assistance with the experiments and to Zdeněk Kameník of the Institute of Microbiology, CAS, Prague, Czech Republic, for providing the LC-MS instrumentation for the study.

SUPPLEMENTARY MATERIAL

The Supplementary Material for this article can be found online at: https://www.frontiersin.org/articles/10.3389/fmicb.2019.03028/full#supplementary-material

REFERENCES

Alanjary, M., Steinke, K., and Ziemert, N. (2019). AutoMLST: an automated web server for generating multi-locus species trees highlighting natural product potential. *Nucleic Acids Res.* 47, W276–W282. doi: 10.1093/nar/gkz282

Awad, A. H. A., and Farag, S. A. (1999). An indoor bio-contaminants air quality. *Int. J. Environ. Health Res.* 9, 313–319. doi: 10.1080/09603129973100

Bankevich, A., Nurk, S., Antipov, D., Gurevich, A. A., Dvorkin, M., Kulikov, A. S., et al. (2012). SPAdes: a new genome assembly algorithm and its applications to single-cell sequencing. *J. Comput. Biol.* 19, 455–477. doi: 10.1089/cmb.2012.0021

Barka, E. A., Vatsa, P., Sanchez, L., Gaveau-Vaillant, N., Jacquard, C., Meier-Kolthoff, J. P., et al. (2016). Taxonomy, physiology, and natural products of *Actinobacteria*. *Microbiol. Mol. Biol. Rev.* 80, 1–43. doi: 10.1128/MMBR.00019-15

Barke, J., Seipke, R. F., Gruschow, S., Heavens, D., Drou, N., Bibb, M. J., et al. (2010). A mixed community of actinomycetes produce multiple antibiotics for the fungus farming ant *Acromyrmex octospinosus*. *BMC Biol.* 8:109. doi: 10.1186/1741-7007-8-109

Behie, S. W., Bonet, B., Zacharia, V. M., McClung, D. J., and Traxler, M. F. (2016). Molecules to ecosystems: actinomycete natural products *in situ*. *Front. Microbiol.* 7:2149. doi: 10.3389/fmicb.2016.02149

Bolger, A. M., Lohse, M., and Usadel, B. (2014). Trimmomatic: a flexible trimmer for Illumina sequence data. *Bioinformatics* 30, 2114–2120. doi: 10.1093/bioinformatics/btu170

Bolourian, A., and Mojtahedi, Z. (2018a). Immunosuppressants produced by *Streptomyces*: evolution, hygiene hypothesis, tumour rapalog resistance and probiotics. *Environ. Microbiol. Rep.* 10, 123–126. doi: 10.1111/1758-2229.12617

Bolourian, A., and Mojtahedi, Z. (2018b). *Streptomyces*, shared microbiome member of soil and gut, as 'old friends' against colon cancer. *FEMS Microbiol. Ecol.* 94:fiy120. doi: 10.1093/femsec/fiy120

Boya, C. A., Fernandez-Marin, H., Mejia, L. C., Spadafora, C., Dorrestein, P. C., and Gutierrez, M. (2017). Imaging mass spectrometry and MS/MS molecular networking reveals chemical interactions among cuticular bacteria and pathogenic fungi associated with fungus-growing ants. *Sci. Rep.* 7:5604. doi: 10.1038/s41598-017-05515-6

Cano-Jimenez, E., Acuna, A., Botana, M. I., Hermida, T., Gonzalez, M. G., Leiro, V., et al. (2016). Farmer's lung disease. A review. *Arch. Bronconeumol.* 52, 321–328. doi: 10.1016/j.arbres.2015.12.001

Castanho, M. A., Coutinho, A., and Prieto, M. J. (1992). Absorption and fluorescence spectra of polyene antibiotics in the presence of cholesterol. *J. Biol. Chem.* 267, 204–209.

Challacombe, J. F., Stubben, C. J., Klimko, C. P., Welkos, S. L., Kern, S. J., Bozue, J. A., et al. (2014). Interrogation of the *Burkholderia pseudomallei* genome to address differential virulence among isolates. *PLoS One* 9:e115951. doi: 10.1371/journal.pone.0115951

Chater, K. F., and Hopwood, D. A. (1993). "*Streptomyces*," in *Bacillus subtilis and Other Gram-Positive Bacteria. Biochemistry, Physiology, and Molecular Genetics*, eds A. L. Sonenshein, J. A. Hoch, and R. Losick, (Washington, DC: American Society for Microbiology), 83–100.

Chun, J., Lee, J. H., Jung, Y., Kim, M., Kim, S., Kim, B. K., et al. (2007). EzTaxon: a web-based tool for the identification of prokaryotes based on 16S ribosomal RNA gene sequences. *Int. J. Syst. Evol. Microbiol.* 57, 2259–2261.

Cihak, M., Kamenik, Z., Smidova, K., Bergman, N., Benada, O., Kofronova, O., et al. (2017). Secondary metabolites produced during the germination of *Streptomyces coelicolor*. *Front. Microbiol.* 8:2495. doi: 10.3389/fmicb.2017.02495

Collado, M. C., Rautava, S., Aakko, J., Isolauri, E., and Salminen, S. (2016). Human gut colonisation may be initiated in utero by distinct microbial communities in the placenta and amniotic fluid. *Sci. Rep.* 6:23129. doi: 10.1038/srep23129

Egan, S., Wiener, P., Kallifidas, D., and Wellington, E. M. (2001). Phylogeny of *Streptomyces* species and evidence for horizontal transfer of entire and partial antibiotic gene clusters. *Antonie Van Leeuwenhoek* 79, 127–133. doi: 10.1023/A:1010296220929

Engevik, M. A., and Versalovic, J. (2017). Biochemical features of beneficial microbes: foundations for therapeutic microbiology. *Microbiol. Spectr.* 5:BAD-0012-2016. doi: 10.1128/microbiolspec.BAD-0012-2016

Forrellad, M. A., Klepp, L. I., Gioffre, A., Sabio y Garcia, J., Morbidoni, H. R., de la Paz Santangelo, M., et al. (2013). Virulence factors of the *Mycobacterium tuberculosis* complex. *Virulence* 4, 3–66. doi: 10.4161/viru.22329

Furukawa, M., Inoue, A., and Asano, K. (1968). Chemical studies on actinomycin S. II. Chemical structures of actinomycin S2 and S3. *J. Antibiot.* 21, 568–570. doi: 10.7164/antibiotics.21.568

Gallo, R. L., and Hooper, L. V. (2012). Epithelial antimicrobial defence of the skin and intestine. *Nat. Rev. Immunol.* 12, 503–516. doi: 10.1038/nri3228

Gurevich, A., Saveliev, V., Vyahhi, N., and Tesler, G. (2013). QUAST: quality assessment tool for genome assemblies. *Bioinformatics* 29, 1072–1075. doi: 10.1093/bioinformatics/btt086

Gust, B., Chandra, G., Jakimowicz, D., Yuqing, T., Bruton, C. J., and Chater, K. F. (2004). Lambda red-mediated genetic manipulation of antibiotic-producing *Streptomyces*. *Adv. Appl. Microbiol.* 54, 107–128.

Haeder, S., Wirth, R., Herz, H., and Spiteller, D. (2009). Candicidin-producing *Streptomyces* support leaf-cutting ants to protect their fungus garden against the pathogenic fungus *Escovopsis*. *Proc. Natl. Acad. Sci. U.S.A.* 106, 4742–4746. doi: 10.1073/pnas.0812082106

Hobbs, G., Frazer, C. M., Gardner, D. C. J., Cullum, J. A., and Oliver, S. G. (1989). Dispersed growth of *Streptomyces* in liquid culture. *Appl. Microbiol. Biotechnol.* 31, 272–277. doi: 10.1007/BF00258408

Hou, B. B., Tao, L. Y., Zhu, X. Y., Wu, W., Guo, M. J., Ye, J., et al. (2018). Global regulator BldA regulates morphological differentiation and lincomycin production in *Streptomyces lincolnensis*. *Appl. Microbiol. Biotechnol.* 102, 4101–4115. doi: 10.1007/s00253-018-8900-1

Huang, Y. J., Nariya, S., Harris, J. M., Lynch, S. V., Choy, D. F., Arron, J. R., et al. (2015). The airway microbiome in patients with severe asthma: associations with disease features and severity. *J. Allergy Clin. Immunol.* 136, 874–884. doi: 10.1016/j.jaci.2015.05.044

Huttunen, K., Hyvarinen, A., Nevalainen, A., Komulainen, H., and Hirvonen, M. R. (2003). Production of proinflammatory mediators by indoor air bacteria and fungal spores in mouse and human cell lines. *Environ. Health Perspect.* 111, 85–92. doi: 10.1289/ehp.5478

Kaltenpoth, M., Gottler, W., Herzner, G., and Strohm, E. (2005). Symbiotic bacteria protect wasp larvae from fungal infestation. *Curr. Biol.* 15, 475–479. doi: 10.1016/j.cub.2004.12.084

Kampfer, P., Glaeser, S. P., Parkes, L., Van Keulen, G., and Dyson, P. (2014). "The Family *Streptomycetaceae*," in *The Prokaryotes: Actinobacteria*, eds E. Rosenberg, E. F. DeLong, S. Lory, E. Stackebrandt, and F. Thompson, (Berlin: Springer).

Kapadia, M., Rolston, K. V. I., and Han, X. Y. (2007). Invasive *Streptomyces* infections - Six cases and literature review. *Am. J. Clin. Pathol.* 127, 619–624. doi: 10.1309/QJEBXP0BCGR54L15

Kim, J. D., Han, J. W., Hwang, I. C., Lee, D., and Kim, B. S. (2012). Identification and biocontrol efficacy of *Streptomyces miharaensis* producing filipin III against *Fusarium wilt*. *J. Basic Microbiol.* 52, 150–159. doi: 10.1002/jobm.201100134

Kirby, R., Sangal, V., Tucker, N. P., Zakrzewska-Czerwinska, J., Wierzbicka, K., Herron, P. R., et al. (2012). Draft genome sequence of the human pathogen *Streptomyces somaliensis*, a significant cause of actinomycetoma. *J. Bacteriol.* 194, 3544–3545. doi: 10.1128/JB.00534-12

Knopik-Skrocka, A., and Bielawski, J. (2002). The mechanism of the hemolytic activity of polyene antibiotics. *Cell. Mol. Biol. Lett.* 7, 31–48.

Kozlov, A. M., Darriba, D., Flouri, T., Morel, B., and Stamatakis, A. (2019). RAxML-NG: a fast, scalable and user-friendly tool for maximum likelihood phylogenetic inference. *Bioinformatics* 35, 4453–4455. doi: 10.1093/bioinformatics/btz305

Labeda, D. P., Goodfellow, M., Brown, R., Ward, A. C., Lanoot, B., Vanncanneyt, M., et al. (2012). Phylogenetic study of the species within the family *Streptomycetaceae*. *Antonie Van Leeuwenhoek* 101, 73–104.

Langmead, B., and Salzberg, S. L. (2012). Fast gapped-read alignment with Bowtie 2. *Nat. Methods* 9, 357–359. doi: 10.1038/nmeth.1923

Lee, J. S., and Yilmaz, O. (2018). Unfolding role of a danger molecule adenosine signaling in modulation of microbial infection and host cell response. *Int. J. Mol. Sci.* 19:E199. doi: 10.3390/ijms19010199

Liu, C. X., Han, C. Y., Jiang, S. W., Zhao, X. L., Tian, Y. Y., Yan, K., et al. (2018). *Streptomyces lasii* sp nov., a novel actinomycete with antifungal activity isolated from the head of an ant (*Lasius flavus*). *Curr. Microbiol.* 75, 353–358. doi: 10.1007/s00284-017-1388-6

Liu, J., Xie, S., Wu, Y., Xu, M., Ao, C., Wang, W., et al. (2016). Apoptosis of human prostate cancer cells induced by marine actinomycin X2 through the mTOR pathway compounded by MiRNA144. *Anticancer Drugs* 27, 156–163. doi: 10.1097/CAD.0000000000000309

Magoc, T., and Salzberg, S. L. (2011). FLASH: fast length adjustment of short reads to improve genome assemblies. *Bioinformatics* 27, 2957–2963. doi: 10.1093/bioinformatics/btr507

Martin, M. C., Manteca, A., Castillo, M. L., Vazquez, F., and Mendez, F. J. (2004). *Streptomyces albus* isolated from a human actinomycetoma and characterized by molecular techniques. *J. Clin. Microbiol.* 42, 5957–5960. doi: 10.1128/JCM.42.12.5957-5960.2004

May, H. C., Yu, J. J., Zhang, H., Wang, Y., Cap, A. P., Chambers, J. P., et al. (2019). Thioredoxin-A is a virulence factor and mediator of the type IV pilus system in *Acinetobacter baumannii*. *PLoS One* 14:e0218505. doi: 10.1371/journal.pone.0218505

McDonald, B. R., and Currie, C. R. (2017). Lateral gene transfer dynamics in the ancient bacterial genus *Streptomyces*. *mBio* 8:e00644-17. doi: 10.1128/mBio.00644-17

McLean, T. C., Hoskisson, P. A., and Seipke, R. F. (2016). Coordinate regulation of antimycin and candicidin biosynthesis. *mSphere* 1:e00305-16.

McNeil, M. M., Brown, J. M., Jarvis, W. R., and Ajello, L. (1990). Comparison of species distribution and antimicrobial susceptibility of aerobic actinomycetes from clinical specimens. *Rev. Inf. Dis.* 12, 778–783.

Miethke, M., and Marahiel, M. A. (2007). Siderophore-based iron acquisition and pathogen control. *Microbiol. Mol. Biol. Rev.* 71, 413–451.

Molloy, E. M., Cotter, P. D., Hill, C., Mitchell, D. A., and Ross, R. P. (2011). Streptolysin S-like virulence factors: the continuing sagA. *Nat. Rev. Microbiol.* 9, 670–681. doi: 10.1038/nrmicro2624

Muth, G., Nusbaumer, B., Wohlleben, W., and Puhler, A. (1989). A vector system with temperature-sensitive replication for gene disruption and mutational cloning in streptomycetes. *Mol. Gen. Genet.* 219, 341–348. doi: 10.1007/Bf00259605

Nechitaylo, T. Y., Westermann, M., and Kaltenpoth, M. (2014). Cultivation reveals physiological diversity among defensive *'Streptomyces philanthi'* symbionts of beewolf digger wasps (*Hymenoptera, Crabronidae*). *BMC Microbiol.* 14:202. doi: 10.1186/s12866-014-0202-x

Ochi, K. (1987). Metabolic initiation of differentiation and secondary metabolism by *Streptomyces griseus*: significance of the stringent response (ppGpp) and GTP content in relation to A factor. *J. Bacteriol.* 169, 3608–3616. doi: 10.1128/jb.169.8.3608-3616.1987

Oh, D. C., Poulsen, M., Currie, C. R., and Clardy, J. (2011). Sceliphrolactam, a polyene macrocyclic lactam from a wasp-associated *Streptomyces* sp. *Org. Lett.* 13, 752–755. doi: 10.1021/ol102991d

Oh, D. C., Scott, J. J., Currie, C. R., and Clardy, J. (2009). Mycangimycin, a polyene peroxide from a mutualist *Streptomyces* sp. *Org. Lett.* 11, 633–636. doi: 10.1021/ol802709x

Okonechnikov, K., Conesa, A., and Garcia-Alcalde, F. (2016). Qualimap 2: advanced multi-sample quality control for high-throughput sequencing data. *Bioinformatics* 32, 292–294. doi: 10.1093/bioinformatics/btv566

Olano, C., Mendez, C., and Salas, J. A. (2009). Antitumor compounds from actinomycetes: from gene clusters to new derivatives by combinatorial biosynthesis. *Nat. Prod. Rep.* 26, 628–660. doi: 10.1039/b822528a

Park, S. Y., Kang, H. O., Jang, H. S., Lee, J. K., Koo, B. T., and Yum, D. Y. (2005). Identification of extracellular N-acylhomoserine lactone acylase from a *Streptomyces* sp. and its application to quorum quenching. *Appl. Environ. Microbiol.* 71, 2632–2641. doi: 10.1128/AEM.71.5.2632-2641.2005

Parrot, D., Blumel, M., Utermann, C., Chianese, G., Krause, S., Kovalev, A., et al. (2019). Mapping the surface microbiome and metabolome of brown seaweed *Fucus vesiculosus* by amplicon sequencing, integrated metabolomics and imaging techniques. *Sci. Rep.* 9:1061. doi: 10.1038/s41598-018-37914-8

Payero, T. D., Vicente, C. M., Rumbero, A., Barreales, E. G., Santos-Aberturas, J., de Pedro, A., et al. (2015). Functional analysis of filipin tailoring genes from *Streptomyces filipinensis* reveals alternative routes in filipin III biosynthesis and yields bioactive derivatives. *Microb. Cell Fact.* 14:114. doi: 10.1186/s12934-015-0307-4

Pellegrini, G. J. Jr., Graziano, J. C., Ragunathan, L., Bhat, M. A., Hemashettar, B. M., and Brown, J. M. (2012). Scalp abscess due to *Streptomyces cacaoi* subsp. *cacaoi*, first report in a human infection. *J. Clin. Microbiol.* 50, 1484–1486. doi: 10.1128/JCM.06372-11

Petrickova, K., Pospisil, S., Kuzma, M., Tylova, T., Jagr, M., Tomek, P., et al. (2014). Biosynthesis of colabomycin E, a new manumycin-family metabolite, involves an unusual chain-length factor. *Chembiochem* 15, 1334–1345. doi: 10.1002/cbic.201400068

Poulsen, M., Oh, D. C., Clardy, J., and Currie, C. R. (2011). Chemical analyses of wasp-associated *Streptomyces* bacteria reveal a prolific potential for natural products discovery. *PLoS One* 6:e16763. doi: 10.1371/journal.pone.0016763

Rahman, A., Srivastava, S. S., Sneh, A., Ahmed, N., and Krishnasastry, M. V. (2010). Molecular characterization of *tlyA* gene product, Rv1694 of *Mycobacterium tuberculosis*: a non-conventional hemolysin and a ribosomal RNA methyl transferase. *BMC Biochem.* 11:35. doi: 10.1186/1471-2091-11-35

Rahman, M. A., Sobia, P., Dwivedi, V. P., Bhawsar, A., Singh, D. K., Sharma, P., et al. (2015). *Mycobacterium tuberculosis* TlyA protein negatively regulates T helper (Th) 1 and Th17 differentiation and promotes tuberculosis pathogenesis. *J. Biol. Chem.* 290, 14407–14417. doi: 10.1074/jbc.M115.653600

Rajesh, T., Jeon, J. M., Kim, Y. H., Kim, H. J., Yi da, H., Park, S. H., et al. (2013). Functional analysis of the gene SCO1782 encoding *Streptomyces* hemolysin (S-hemolysin) in *Streptomyces coelicolor* M145. *Toxicon* 71, 159–165. doi: 10.1016/j.toxicon.2013.05.023

Rea, D., Coppola, G., Palma, G., Barbieri, A., Luciano, A., Del Prete, P., et al. (2018). Microbiota effects on cancer: from risks to therapies. *Oncotarget* 9, 17915–17927. doi: 10.18632/oncotarget.24681

Relhan, V., Mahajan, K., Agarwal, P., and Garg, V. K. (2017). Mycetoma: an update. *Indian J. Dermatol.* 62, 332–340. doi: 10.4103/ijd.IJD_476_16

Roussel, S., Reboux, G., Dalphin, J. C., Pernet, D., Laplante, J. J., Millon, L., et al. (2005). Farmer's lung disease and microbiological composition of hay: a case-control study. *Mycopathologia* 160, 273–279.

Ryan, R. P., An, S. Q., Allan, J. H., McCarthy, Y., and Dow, J. M. (2015). The DSF family of cell-cell signals: an expanding class of bacterial virulence regulators. *PLoS Pathog.* 11:e1004986. doi: 10.1371/journal.ppat.1004986

Santos, C. L., Correia-Neves, M., Moradas-Ferreira, P., and Mendes, M. V. (2012). A walk into the LuxR regulators of *Actinobacteria*: phylogenomic distribution and functional diversity. *PLoS One* 7:e46758. doi: 10.1371/journal.pone.0046758

Sarmiento-Ramirez, J. M., van der Voort, M., Raaijmakers, J. M., and Dieguez-Uribeondo, J. (2014). Unravelling the microbiome of eggs of the endangered sea turtle *Eretmochelys imbricata* identifies bacteria with activity against the emerging pathogen *Fusarium falciforme*. *PLoS One* 9:e95206. doi: 10.1371/journal.pone.0095206

Schoenian, I., Spiteller, M., Ghaste, M., Wirth, R., Herz, H., and Spiteller, D. (2011). Chemical basis of the synergism and antagonism in microbial communities in the nests of leaf-cutting ants. *Proc. Natl. Acad. Sci. U.S.A.* 108, 1955–1960. doi: 10.1073/pnas.1008441108

Seipke, R. F., Barke, J., Brearley, C., Hill, L., Yu, D. W., Goss, R. J., et al. (2011). A single *Streptomyces* symbiont makes multiple antifungals to support the fungus farming ant *Acromyrmex octospinosus*. *PLoS One* 6:e22028. doi: 10.1371/journal.pone.0022028

Sharma, M., and Manhas, R. K. (2019). Purification and characterization of actinomycins from *Streptomyces* strain M7 active against methicillin resistant

Staphylococcus aureus and vancomycin resistant *Enterococcus*. *BMC Microbiol.* 19:44. doi: 10.1186/s12866-019-1405-y

Shintani, M., Matsui, K., Inoue, J., Hosoyama, A., Ohji, S., Yamazoe, A., et al. (2014). Single-cell analyses revealed transfer ranges of IncP-1, IncP-7, and IncP-9 plasmids in a soil bacterial community. *Appl. Environ. Microbiol.* 80, 138–145. doi: 10.1128/AEM.02571-13

Silva, P. E. S., Reis, M. P., Avila, M. P., Dias, M. F., Costa, P. S., Suhadolnik, M. L. S., et al. (2018). Insights into the skin microbiome dynamics of leprosy patients during multi-drug therapy and in healthy individuals from Brazil. *Sci. Rep.* 8:8783. doi: 10.1038/s41598-018-27074-0

Sing, D., and Sing, C. F. (2010). Impact of direct soil exposures from airborne dust and geophagy on human health. *Int. J. Environ. Res. Publ. Health* 7, 1205–1223. doi: 10.3390/ijerph7031205

Somboro, A. M., Osei Sekyere, J., Amoako, D. G., Essack, S. Y., and Bester, L. A. (2018). Diversity and proliferation of metallo-beta-lactamases: a clarion call for clinically effective metallo-beta-lactamase inhibitors. *Appl. Environ. Microbiol.* 84:e00698-18. doi: 10.1128/AEM.00698-18

Striz, I., Krasna, E., Petrickova, K., Brabcova, E., Kolesar, L., Slavcev, A., et al. (2008). Manumycin and asukamycin inhibition of IL-1beta and IL-18 release from human macrophages by caspase-1 blocking. *Allergy* 63, 142–143.

Stubbendieck, R. M., Vargas-Bautista, C., and Straight, P. D. (2016). Bacterial communities: interactions to scale. *Front. Microbiol.* 7:1234. doi: 10.3389/fmicb.2016.01234

Tingstad, J. E., and Garrett, E. R. (1960). Studies on the stability of filipin.1. Thermal degradation in the presence of air. *J. Am. Pharm. Assoc.* 49, 352–355. doi: 10.1002/jps.3030490607

van de Sande, W. W. J. (2013). Global burden of human mycetoma: a systematic review and meta-analysis. *PLoS Negl. Trop. Dis.* 7:e2550. doi: 10.1371/journal.pntd.0002550

Vandenesch, F., Lina, G., and Henry, T. (2012). *Staphylococcus aureus* hemolysins, bi-component leukocidins, and cytolytic peptides: a redundant arsenal of membrane-damaging virulence factors? *Front. Cell. Infect. Microbiol.* 2:12. doi: 10.3389/fcimb.2012.00012

Verma, P., and Jha, A. (2019). Mycetoma: reviewing a neglected disease. *Clin. Exp. Dermatol.* 44, 123–129. doi: 10.1111/ced.13642

Vicente, C. M., Santos-Aberturas, J., Payero, T. D., Barreales, E. G., de Pedro, A., and Aparicio, J. F. (2014). PAS-LuxR transcriptional control of filipin biosynthesis in *S. avermitilis*. *Appl. Microbiol. Biotechnol.* 98, 9311–9324. doi: 10.1007/s00253-014-5998-7

Wang, J., Xu, J., Luo, S., Ma, Z., Bechthold, A., and Yu, X. P. (2018). AdpAsd, a positive regulator for morphological development and toyocamycin biosynthesis in *Streptomyces diastatochromogenes* 1628. *Curr. Microbiol.* 75, 1345–1351.

Wang, R., Zhang, M., Liu, H., Xu, J., Yu, J., He, F., et al. (2016). PsAAT3, an oomycete-specific aspartate aminotransferase, is required for full pathogenicity of the oomycete pathogen *Phytophthora sojae*. *Fungal Biol.* 120, 620–630. doi: 10.1016/j.funbio.2016.01.005

Wu, X., Chen, J., Xu, M., Zhu, D., Wang, X., Chen, Y., et al. (2017). 16S rDNA analysis of periodontal plaque in chronic obstructive pulmonary disease and periodontitis patients. *J. Oral Microbiol.* 9:1324725. doi: 10.1080/20002297.2017.1324725

Yacoub, A. T., Velez, A. P., Khwaja, S. I., Sandin, R. L., and Greene, J. (2014). *Streptomyces* pneumonia in an immunocompromised patient: a case report and a review of literature. *Inf. Dis. Clin. Pract.* 22, e113–e115. doi: 10.1097/IPC.0000000000000172

Conflict of Interest: The authors declare that the research was conducted in the absence of any commercial or financial relationships that could be construed as a potential conflict of interest.

frontiers in Microbiology

ORIGINAL RESEARCH
published: 26 February 2020
doi: 10.3389/fmicb.2020.00291

A Simple Polymicrobial Biofilm Keratinocyte Colonization Model for Exploring Interactions Between Commensals, Pathogens and Antimicrobials

Elena Jordana-Lluch[1†], Vanina Garcia[1], Alexander D. H. Kingdon[1], Nishant Singh[2], Cameron Alexander[2], Paul Williams[1] and Kim R. Hardie[1]*

[1] Centre for Biomolecular Sciences, School of Life Sciences, University of Nottingham, Nottingham, United Kingdom, [2] School of Pharmacy, University of Nottingham, Nottingham, United Kingdom

OPEN ACCESS

Edited by:
Giuseppantonio Maisetta, University of Pisa, Italy

Reviewed by:
Bastiaan P. Krom, Vrije Universiteit Amsterdam, Netherlands
Wolf-Rainer Abraham, Helmholtz Association of German Research Centres (HZ), Germany

***Correspondence:**
Kim R. Hardie
kim.hardie@nottingham.ac.uk

†Present address:
Elena Jordana-Lluch, Balearic Islands Health Research Institute (IdISBa), Palma de Mallorca, Spain

Specialty section:
This article was submitted to Antimicrobials, Resistance and Chemotherapy, a section of the journal Frontiers in Microbiology

Received: 17 December 2019
Accepted: 10 February 2020
Published: 26 February 2020

Citation:
Jordana-Lluch E, Garcia V, Kingdon ADH, Singh N, Alexander C, Williams P and Hardie KR (2020) A Simple Polymicrobial Biofilm Keratinocyte Colonization Model for Exploring Interactions Between Commensals, Pathogens and Antimicrobials. Front. Microbiol. 11:291. doi: 10.3389/fmicb.2020.00291

Skin offers protection against external insults, with the skin microbiota playing a crucial defensive role against pathogens that gain access when the skin barrier is breached. Linkages between skin microbes, biofilms and disease have not been well established although single-species biofilm formation by skin microbiota *in vitro* has been extensively studied. Consequently, the purpose of this work was to optimize and validate a simple polymicrobial biofilm keratinocyte model for investigating commensal, pathogen and keratinocyte interactions and for evaluating therapeutic agents or health promoting interventions. The model incorporates the commensals (*Staphylococcus epidermidis* and *Micrococcus luteus*) and pathogens (*Staphylococcus aureus* and *Pseudomonas aeruginosa*) which form robust polymicrobial biofilms on immortalized keratinocytes (HaCat cells). We observed that the commensals reduce the damage caused to the keratinocyte monolayer by either pathogen. When the commensals were combined with *P. aeruginosa* and *S. aureus*, much thinner biofilms were observed than those formed by the pathogens alone. When *P. aeruginosa* was inoculated with *S. epidermidis* in the presence or absence of *M. luteus*, the commensals formed a layer between the keratinocytes and pathogen. Although *S. aureus* completely inhibited the growth of *M. luteus* in dual-species biofilms, inclusion of *S. epidermidis* in triple or quadruple species biofilms, enabled *M. luteus* to retain viability. Using this polymicrobial biofilm keratinocyte model, we demonstrate that a quorum sensing (QS) deficient *S. aureus agr* mutant, in contrast to the parent, failed to damage the keratinocyte monolayer unless supplied with the exogenous cognate autoinducing peptide. In addition, we show that treatment of the polymicrobial keratinocyte model with nanoparticles containing an inhibitor of the PQS QS system reduced biofilm thickness and *P. aeruginosa* localization in mono- and polymicrobial biofilms.

Keywords: polymicrobial biofilm, skin infections, *Pseudomonas aeruginosa*, *Staphylococcus*, *Micrococcus luteus*, quorum sensing, keratinocyte, antimicrobial

INTRODUCTION

Skin is the largest organ of the body and functions as a physical barrier against external insults, such as toxins or pathogenic microorganisms (Parlet et al., 2019). Skin is principally composed of an epidermis and underlying dermis with keratinocytes constituting 90–95% of the upper epidermal layer nearest to the colonizing microbiota. Depending on their differentiation state, keratinocytes are arranged in stratified layers and are potent sources of antimicrobial peptides and cytokine/chemokine signals. Keratinocytes orchestrate the formation of the stratum corneum which physically separates the viable layers of the cutaneous epithelium from surface microbes. The stratum corneum is a waxy waterproof composite containing flattened corneocytes and interlocking keratinocyte-derived lipids and granules that forms a tight mechanical barrier. Despite this seemingly inhospitable niche that is acidic, lipid dense and lacking in nutrients, direct contact with the environment results in skin becoming colonized by a diverse community of bacteria, fungi, viruses and mites, for which the skin offers a variety of stable niches with different environmental conditions and nutrients (Grice and Segre, 2011; Brandwein et al., 2016; Byrd et al., 2018; Erin Chen et al., 2018). Skin also acts as an immunological barrier that distinguishes between commensals and harmful microbes (Negrini et al., 2014). The commensal microbiota play an important role by "educating" the innate immune system to mount a response against antigens produced by pathogens, but not by commensals (Leech et al., 2019). Furthermore, commensals secrete proteins and other metabolites that modulate the virulence of pathogens or give the commensals a selective advantage to outcompete the pathogens (Cogen et al., 2008; Grice and Segre, 2011; Chen and Tsao, 2013; Bosko, 2019; Parlet et al., 2019). For instance, *Staphylococcus epidermidis* autoinducing peptide (AIP) signal molecules inhibit the *Staphylococcus aureus agr* system and hence exotoxin production (Otto et al., 2001) whereas *Micrococcus luteus* enhances *S. aureus* pathogenesis (Boldock et al., 2018).

Skin damage facilitates the entry of pathogenic bacteria resulting in an infected wound. Chronic wound infections, cost the United Kingdom healthcare service over £1 billion per year (Percival et al., 2012). Due to their links with predisposing conditions including diabetes and obesity, such chronic wound infections are increasing in prevalence. Infected surgical wounds increase the average hospital stay by 10.2 days compared with those that heal without complications. Extended periods of bacterial colonization in patients receiving antibiotics also create selection pressures that may allow resistant pathogens to emerge, impairing treatment and further delaying healing (Bowler et al., 2001).

The chronicity of wound infections is linked to biofilm formation because the extracellular matrix protects bacteria against host defenses and antimicrobial agents (Snyder et al., 2017). Biofilm related persistent infections account for 65–80% of all infections (Macià et al., 2014). Furthermore, such biofilms tend to be polymicrobial, which worsens prognosis (Peters et al., 2012). *Staphylococcus aureus* and *Pseudomonas aeruginosa* commonly infect chronic wounds and are often isolated from the same infection site (Deleon et al., 2014; Serra et al., 2015). Both species have developed intricate regulatory networks to achieve evasion, counter-inhibition and suppression of the other bacterial species to enable them to co-exist in the same niche (Hotterbeekx et al., 2017). Furthermore, the growth of the two pathogens together can offer mutual benefit through increased biofilm production, gentamicin tolerance and more severe infection (Deleon et al., 2014).

The regulation of biofilm development is complex, involving diverse transcriptional and post-transcriptional mechanisms. These include the population density dependent cell-cell communication network known as quorum sensing (QS) (Atkinson and Williams, 2009). The QS network of *P. aeruginosa* integrates three systems, *las*, *rhl*, and *pqs* (Lee et al., 2013), whereas *S. aureus* employs the accessory gene regulator (*agr)* QS system (Gordon et al., 2013; Bronesky et al., 2016). QS regulates the expression of diverse virulence genes (Njoroge and Sperandio, 2009), and thus QS inhibition has been widely investigated as an alternative to antibiotics to tackle specific pathogens given that interference with signaling would allow attenuation of virulence without compromising bacterial viability, thereby reducing the likely selection of resistance (Njoroge and Sperandio, 2009; Romero et al., 2012; Soukarieh et al., 2018; Shaaban et al., 2019). A notable added benefit is that QS inhibition may reduce biofilm maturation such that susceptibility to antibiotics and host defenses is enhanced. Recently, the usefulness of encapsulating a quorum sensing inhibitor (QSI) targeting the PqsR receptor of *P. aeruginosa* has been demonstrated (Singh et al., 2019). In an alginate nanoparticle delivery system, the QSI reduced *P. aeruginosa* biofilm development on keratinocytes, and when delivered in combination with an antibiotic and fully cleared *P. aeruginosa* biofilms in an *ex vivo* pig skin model (Singh et al., 2019).

Several *in vitro* models describing polymicrobial biofilms, including those pathogens most relevant to skin infections, have been developed (Coenye and Nelis, 2010; Negrini et al., 2014). The main drawback of these models is the lack of a host component (Ganesh et al., 2015; Roberts et al., 2015). *In vivo* (mice or porcine) models allow long term infection and mimic the chronicity of wounds (Ganesh et al., 2015). However, these models suffer from ethical limitations, especially when high-throughput analysis to test several anti-biofilm compounds needs to be performed. Thus, a simple, robust 2D polymicrobial model of skin infection that would facilitate the investigation of the interactions between skin colonizing bacteria (both commensal and pathogen) and to validate interventions, such as the impact of a QSI (Singh et al., 2019) is highly desirable. Here, we describe and validate a proof of concept model incorporating both commensals (*S. epidermidis* and *Micrococcus luteus*) and pathogens (*S. aureus* and *P. aeruginosa*) using HaCat cells (immortalized keratinocytes) as the model "skin" substrate. This simple skin model is shown to be useful for investigating commensal, pathogen and keratinocyte interactions and for evaluating therapeutic agents or health promoting interventions. We exemplify this by evaluating the impact of mutating the *S. aureus agr* QS system or delivering an

anti-pseudomonal QSI nanoparticle on the polymicrobial biofilm and keratinocyte community.

MATERIALS AND METHODS

Bacterial Strains and Growth Conditions

The bacterial strains, plasmids and antibiotics used are listed in **Table 1**. All bacteria were grown at 37°C in LB (*P. aeruginosa*) or BHI (*S. aureus*, *S. epidermidis*, and *M. luteus*), and shaken at 200 rpm when required. Plasmids including pSB2019 (carrying GFP protein) (Qazi et al., 2001) was transformed into the group I *agr S. aureus* strain SH1000 (Doherty et al., 2006) and *S. epidermidis* 1457 (Galac et al., 2017) as described elsewhere (Monk et al., 2012). *S. aureus* SH1000 Δ*agr* was constructed by transducing the Δ*agr*:*tetM* cassette from strain RN6911 (Novick et al., 1993) using phage phi ϕ11 as described previously (McVicker et al., 2018).

2D Infection Model

HaCat Cells

Immortalized keratinocytes (HaCat, Culture Cell Lines, CLS Gmbh) were used as the "skin" substrate for the infection model. Cells were expanded in T75 flasks (Corning), in RPMI-1640 with phenol red supplemented with 10% v/v heat-inactivated foetal bovine serum (FBS), 1% v/v L-glutamine (200 mM) and 1% v/v penicillin (10,000 units/mL)/streptomycin (10 mg/mL) until 80% confluent. After removing the growth medium, cells were trypsinised using 7 ml of a solution containing 0.5 g/L trypsin/0.02 g/L EDTA. Trypsinization was stopped by adding 7 ml of heat-inactivated FBS. Cells were pelleted (5 min, 300 × *g*) and resuspended in 2 mL of RPMI supplemented with phenol red and seeded at 45,000 cells/cm^2 in an eight well micro-slide Ibitreat chamber (ibidi, GmbH, Martinsried, Germany). When 100% confluent (approximately 90,000 cells/cm^2), cells were washed three times by adding/removing 300 μL of Dulbecco's Phosphate Buffered Saline (DPBS), prior to infection. HaCat cells were stained using either CellTracker (deep red) before infection or CellMask (deep red) prior to confocal imaging (both from Thermo Fisher Scientific), following the manufacturer's instructions.

Bacteria

Separate overnight cultures of *S. aureus*, *S. epidermidis*, and *M. luteus* (day 1 of infection) were diluted 1:10 with fresh BHI (for both staphylococcal species) or 1:5 (for *M. luteus*) and further incubated at 37°C, 200 rpm until an OD_{600} 1–1.5. For *P. aeruginosa* (day 2 of infection), the overnight culture was diluted 1:5 with fresh LB and further incubated (37°C, 200 rpm) until an OD_{600} 0.8–1 was reached. For all bacteria, 1 ml of culture was pelleted for 1 min at 13,000 rpm and washed with Phosphate Buffered Saline (PBS, pH7.4). The cultures were subsequently resuspended in RPMI-1640 without phenol red to an OD_{600} 0.01 in a final volume of 5 mL and further diluted 1:1,000. *S. aureus* and *P. aeruginosa* were further diluted to reach a 1:10,000 and 1:100,000 dilution, respectively. For the polymicrobial studies, the volume required to obtain an OD_{600} 0.01 for each bacterial species was added together, adjusting the volume of RPMI accordingly and further diluted as above. A total of 150 μL were added to each well containing confluent HaCat cells (day 1 of infection) or HaCat cells and the Gram-positive bacteria (day 2 of infection), setting up 2 repeats per condition. Infected cells were incubated at 37°C, with 5% v/v CO_2 and 95% humidity. Planktonic cells and growth medium were carefully removed and 100 μl of PBS were added to each well to avoid desiccation during confocal imaging (CLSM, LSM 700 Carl Zeiss, Germany).

Image Analysis

An average of 4–5 Z-stack images per well (8–10 per condition) were taken. Biomass, average thickness and surface area of the biofilms were quantified using COMSTAT2 software (Heydorn et al., 2000), applying automatic thresholding (Otsu's method) and without connected volume filtering. Three biofilm parameters were analyzed. bio-volume (which represents the overall volume of the biofilm and provides an estimate of its biomass), average thickness (which provides a measure of the spatial size of the biofilm) and surface area (which calculated the area of the biomass surface exposed to the environment). A total of four independent experiments, with eight images per condition were analyzed.

Statistical Analysis

GraphPad Prism 7 software was used for graphical representation and statistical analysis. Quantitative variables were compared using a ratio paired two-tailed Student's t. p-values < 0.05 were considered statistically significant.

Biofilm Bacterial Viable Counts

Biofilms were prepared in 96 well plates by adding 200 μl of the diluted cultures prepared as outlined above and incubated for a

TABLE 1 | Strains used in this study.

Microorganism	Strain	Plasmid	Antibiotic resistance	References
Micrococcus luteus	2665		Furazolidone, Nalidixic acid, Colistin (all at 10 μg/ml)	Rokem et al., 2011
Staphylococcus epidermidis	1457		Nalidixic acid, Colistin (all at 10 μg/ml)	Galac et al., 2017
Staphylococcus epidermidis	1457	pSB2019-gfp	Chloramphenicol, Nalidixic acid, Colistin (all at 10 μg/ml)	This study
Staphylococcus aureus	SH1000	pSB2019-gfp	Chloramphenicol, Nalidixic acid, Colistin (all at 10 μg/ml)	This study
Staphylococcus aureus	SH1000	pmKAT	Erythromycin (20 μg/ml) Nalidixic acid, Colistin (both at 10 μg/ml)	This study
Staphylococcus aureus Δ*agr*	SH1000		Tetracycline, Nalidixic acid, Colistin (all at 10 μg/ml)	This study
Pseudomonas aeruginosa	PAO1-Nottingham	pME6032-mCherry	Tetracycline (125 μg/ml)	Heeb et al., 2000; Ortori et al., 2011

total of 40 h (but where included, *P. aeruginosa* was added after 20 h incubation). Biofilms were disrupted by sonication for 5 min and thoroughly resuspended by pipetting. Thirty microlitres of resuspended biofilm were added to 270 µl PBS in a 96 well plate and diluted up to 10^{-8}. Five microliters were plated onto agar containing the appropriate antibiotics to selectively count each microorganism (**Table 1**). Nalidixic acid combined with colistin was used to inhibit the growth of *P. aeruginosa*. Viable counts were performed after 24 h (48 h for *M. luteus*).

16S rRNA Fluorescence *in situ* Hybridization (FISH)

Bacteria were identified using the protocol described by Pihl et al. (2010a) with some modifications. A pan-bacteria probe [5′-HyLite 488-GCTGCCTCCCGTAGGAGT-3′ (Malic et al., 2009)] was used to detect the four microorganisms included in the model. *P. aeruginosa* and *S. aureus* were further identified by the specific probes [5′ Hylite 555-GGTAACCGTCCCCCTTGC-3′ (Pihl et al., 2010b) and 5′ ATTO 647-GAAGCAAGCTTCTCGTCCG-3′ (Lawson et al., 2011), respectively]. After carefully removing the supernatant from the Ibitreat chamber, biofilms were fixed with 4% v/v paraformaldehyde in PBS (pH 7.4) overnight at 4°C before being washed with cold sterile PBS. Bacterial biofilm cells were permeabilized using lysozyme (7 mg/mL) in 100 mM of Tris–HCl, pH 7.5, and 5 mM EDTA for 15 min at 37°C followed by lysostaphin (0.1 mg/mL) in 10 mM Tris–HCl, pH 7.5, for 5 min at 37°C. Biofilms were washed with ultrapure water and dehydrated with 50, 80, and 99% ethanol for 3 min, respectively. Wells were inoculated with 250 µL of freshly prepared hybridization buffer [0.9 M NaCl, 20 mM Tris–HCl buffer, pH 7.5, with 0.01% w/v sodium dodecyl sulphate (SDS) and 25% v/v formamide containing 50 ng/mL of the oligonucleotide probes (Eurogentec)] and incubated at 47°C for 90 min in a humid chamber. After hybridization, the Ibitreat chambers were incubated with washing buffer (20 mM Tris–HCl buffer, pH 7.5, 0.01% w/v SDS and 149 mM NaCl) for 15 min at 47°C, and then rinsed with ultrapure water.

Measurement of Monolayer Integrity

Z-stack images of the HaCaT cells grown under different conditions stained with CellMask or CellTracker were captured using confocal fluorescence microscopy. Total fluorescence of the monolayer was used as an indirect way of measuring monolayer integrity. FIJI (free software) (Schindelin et al., 2012) enabled combination of all the slices of the Z-stack into a single plane (Z-project) in order to measure the total fluorescence emitted by the HaCat cells. Mean values of all the images taken per condition (8–10) were calculated and presented as the percentage of fluorescence compared with the HaCat control (100% fluorescence).

Quorum Sensing Activation and Inhibition

AIP-1 was synthesized as previously described (Murray et al., 2014) and used to supplement *S. aureus* SH1000 Δ*agr* cultures by adding to the growth medium at a final concentration of 1 µM. ALG_{QSI} nanoparticles (Singh et al., 2019) containing 4 µg/mL of 3-amino-7-chloro-2-n-nonyl-4(3*H*)-quinazolinone (3-NH_2-7Cl-C9-QZN) (Ilangovan et al., 2013) were added to a final concentration of 300 µg/mL at day 2 of infection, and inoculated with *P. aeruginosa*.

RESULTS

Development and Validation of a Polymicrobial Biofilm Keratinocyte Colonization Model

To achieve co-culture of keratinocytes with more than one bacterial species, it was necessary to optimize the (i) bacterial inoculum size, (ii) timing of inoculation, and (iii) duration of co-incubation. The inoculum added to the keratinocytes (multiplicity of infection, MOI) was kept low with the aim of maintaining a healthy cell monolayer beneath the polymicrobial biofilm. To verify monolayer integrity, HaCat cells were monitored for 40 h post-inoculation with bacteria. **Figure 1** illustrates the stages involved in establishing a polymicrobial species biofilm on the keratinocyte monolayer.

The commensals *S. epidermidis* and *M. luteus* were selected for this study due to their abundance in the healthy skin microbiota (van Rensburg et al., 2015), and similar nutritional requirements (Madigan et al., 2006). *S. aureus* and *P. aeruginosa* were chosen as representative pathogens based on their medical importance since they commonly cause skin and wound infections (Deleon et al., 2014; Serra et al., 2015). To monitor the formation of biofilms, both *S. aureus* and *P. aeruginosa* were engineered to produce a fluorescent protein by introducing a plasmid carrying the genes for either Green Fluorescent Protein (GFP) or mCherry (**Table 1** and **Figure 1B**). The commensals were not tagged. The keratinocytes were routinely stained with

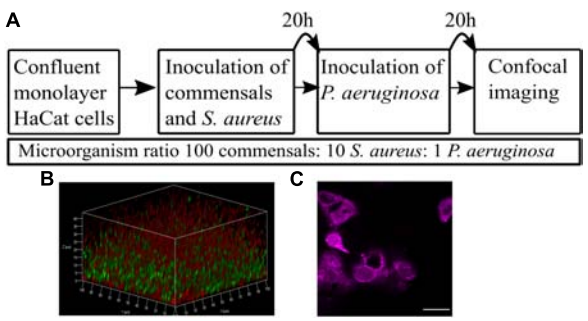

FIGURE 1 | Overview of the keratinocyte polymicrobial colonization model. **(A)** The steps required to establish polymicrobial colonization of keratinocytes. **(B)** 3D projection of a dual species biofilm (red: *P. aeruginosa*-mCherry, green: *S. aureus*-GFP) set up as described in panel **A**. **(C)** Visualization of the HaCat monolayer beneath the dual species polymicrobial biofilm shown in panel **B**. Keratinocytes were stained with CellTracker and imaged with 63 × magnification. Scale bar indicates 20 µm.

CellTracker or CellMask to assess and quantify monolayer integrity (**Figures 1C**, **2A**).

Commensal cultures were adjusted to approximately 3×10^3 cfu/mL before inoculating the HaCat cell monolayer (corresponding to a final MOI = 0.005 bacteria:keratinocyte). This commensal load permitted biofilm formation without compromising HaCat cell health during the 40 h infection period (**Figure 2B** and **Supplementary Figure S1O**).

Little information is available with respect to the likely ratio of commensals to pathogens during the early stages of an infection. However, on healthy skin, the microbiota range from 10^2–10^6 cfu/cm^2 (Egert and Simmering, 2016). For *P. aeruginosa*, an infecting dose for wounded skin has been reported to be ∼1,000 cfu (Leggett et al., 2012). For *S. aureus*, the infective dose was reported to be 100,000 cfu when ingestion was the route of infection (Leggett et al., 2012), but lower when the pathogen was administered topically. Thus, we assumed that the number of pathogen cells would be lower than the number of commensal cells. For the initial HaCat cell colonization, the commensal inoculum consisted of *S. epidermidis* or *M. luteus* cultures at OD_{600} 0.01 diluted 1/1000 to give a final bacterial cell number of $\sim 3 \times 10^3$ cfu/mL in supplemented RPMI without antibiotics or phenol red. The commensals were mixed with a range of (i) *S. aureus* cells (10-fold and 50-fold dilutions of 3×10^3 cfu/ml) or (ii) *P. aeruginosa* cells (10-fold, 50-fold, and 100-fold dilutions of 3×10^3 cfu/ml). Both biofilm formation and HaCat health post-inoculation were monitored by confocal imaging to determine the conditions best suited for the final polymicrobial model. For *S. aureus*, the 50- and 100-fold culture dilutions did not form reproducible biofilms (data not shown). In contrast, HaCat monolayer inoculation with the 10-fold dilution of an *S. aureus* culture supported reproducible biofilm formation, although it should be noted that an ∼70% reduction in the HaCat cell monolayer integrity (calculated by measuring fluorescence as described in the Methods) was observed during the later stages (after 40 h) of colonization (**Figures 2E,I** and **Supplementary Figure S1E**). For *P. aeruginosa*, inoculation with 10- and 50-fold dilutions of culture caused complete destruction of the HaCat cells (data not shown), whereas the 100-fold dilution formed a robust biofilm while maintaining ∼10% of the HaCat monolayer integrity (**Figures 2C,I** and **Supplementary Figure S1A**).

The final bacterial ratios chosen were: 100:10:1 for commensals: *S. aureus*: *P. aeruginosa*. By pre-colonizing the HaCat cells for 20 h with commensals (and *S. aureus* if required) prior to inoculation with *P. aeruginosa* (**Figure 1A**), robust polymicrobial biofilms formed (**Figure 3** and **Supplementary Figure S1K**). When quantified using COMSTAT2 for biovolume, thickness and surface area (**Figure 4** and **Supplementary Figure S2**), the same trends were observed for each biofilm parameter quantified, confirming the stability and reproducibility of the model, although intrinsic biological variability between experiments meant that statistical significance was not always evident. However, the conditions used enabled the keratinocytes to maintain a monolayer when both pathogens were present (**Figure 2H** and **Supplementary Figure S1K**). The relative disruption of the HaCat monolayer could also be quantified following staining with CellTracker deep red (**Figure 2I**).

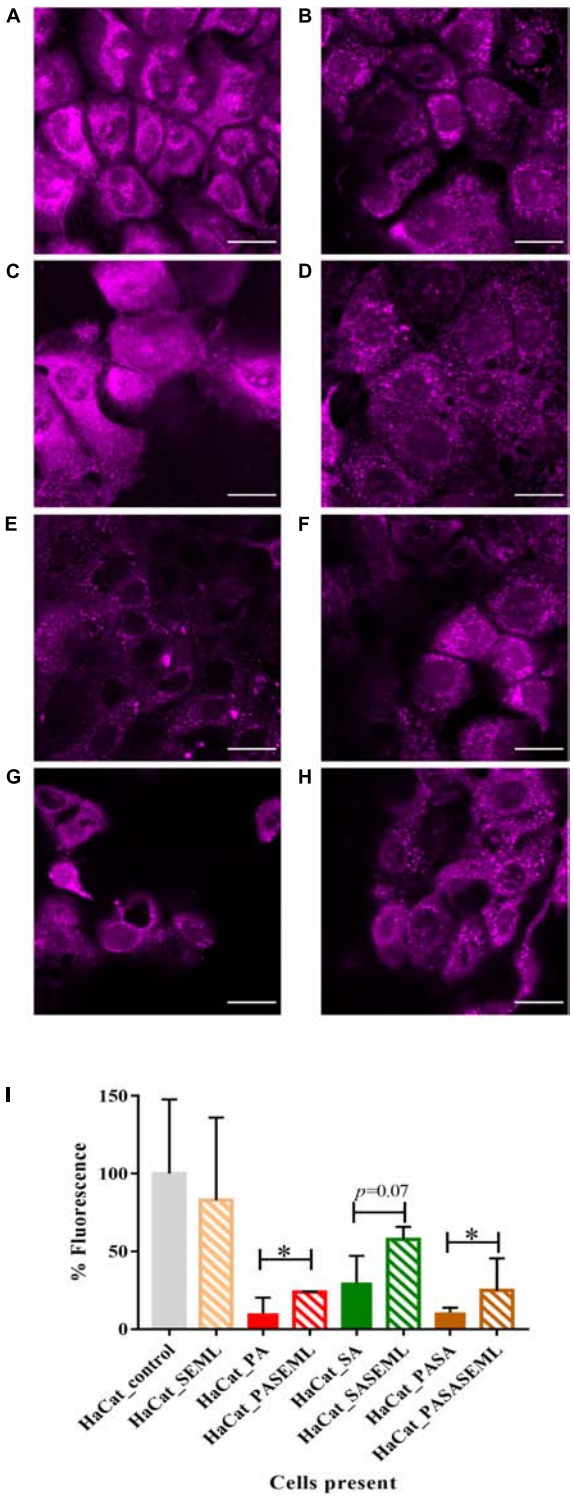

FIGURE 2 | Commensals aid maintenance of monolayer integrity during pathogen colonization. HaCat monolayers were stained with CellTracker deep red prior to incubation with commensals and/or *S. aureus* for 40 h. Where present, *P. aeruginosa* was included for the final 20 h of the incubation. Bacterial inoculation ratios were as described in **Figure 1**, and images taken at 63 × magnification. Scale bar indicates 20 μm. HaCat cells were inoculated

(Continued)

FIGURE 2 | Continued
with **(A)** no bacteria; **(B)** commensals *S. epidermidis* and *M. luteus;* **(C)** *P. aeruginosa;* **(D)** *P. aeruginosa* and commensals; **(E)** *S. aureus;* **(F)** *S. aureus* and commensals; **(G)** *P. aeruginosa* and *S. aureus;* **(H)** HaCat *P. aeruginosa* and *S. aureus* and commensals. HaCat cells are shown as a representative single plane. **(I)** Quantification of HaCat monolayer integrity by measuring the total fluorescence of the z-stack HaCat cells using ImageJ (8–10 Z-stack images analyzed per condition, two experiments), and plotted as percentage of the HaCat only control. SE: *S. epidermidis*; ML: *M. luteus*; SA: *S. aureus*; PA: *P. aeruginosa.* **p*-value < 0.05.

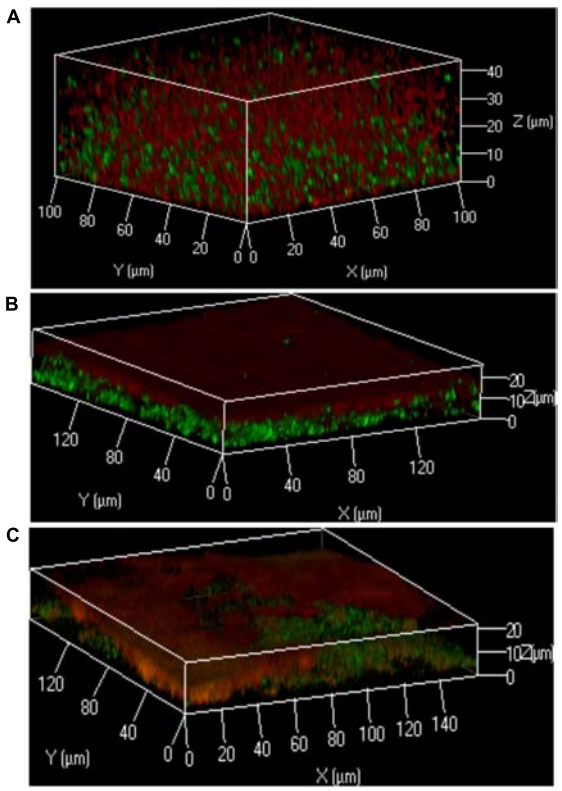

FIGURE 3 | Localization of bacteria within the polymicrobial keratinocyte colonization model is species dependent. Using the protocol outlined in **Figure 1**, either *S. aureus, S. epidermidis* or *M. luteus* was combined with *P. aeruginosa* to form a polymicrobial biofilm on top of a HaCat monolayer. 3D reconstructions of the polymicrobial biofilms are shown using 40 × magnification. HaCat cells were not stained. **(A)** Dual species intercalated biofilm of *S. aureus* (GFP tagged, green) combined with *P. aeruginosa* (mCherry tagged, red). **(B)** Dual species layered biofilm of *S. epidermidis* (GFP tagged, green) with *P. aeruginosa* (mCherry tagged, red). **(C)** Triple species biofilm containing a layer of *M. luteus* intercalated with *S. epidermidis* between *P. aeruginosa* (above) and the keratinocyte monolayer (below). Bacteria were detected by FISH using pan-bacterial (green) and *Pseudomonas*-specific (red) probes.

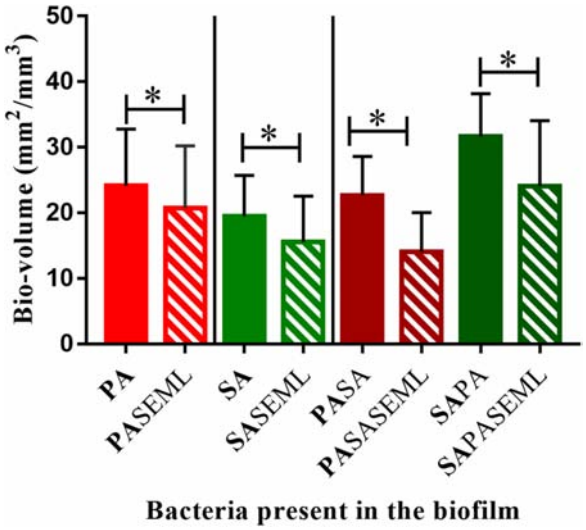

FIGURE 4 | Commensals reduce biofilm biomass for both *S. aureus* and *P. aeruginosa* individually and when co-inoculated. The HaCat monolayer was inoculated with the indicated bacterial species and incubated for 40 h (*S. aureus*, commensals) or 20 h (*P. aeruginosa*) as outlined in **Figure 1**. The biofilm biomass was calculated using ImageJ. SE: *S. epidermidis*; ML: *M. luteus*; SA: *S. aureus*; PA: *P. aeruginosa.* Bold font indicates the bacterial species quantified. **p*-value < 0.05. Images of the biofilms and HaCat monolayer are shown in **Supplementary Figure S1**, and average thickness and surface area are shown in **Supplementary Figure S2**.

Commensals Protect HaCat Cells From Pathogen Damage

To determine whether the commensals protected the HaCat cells from pathogen-mediated damage, the eukaryotic cells were stained using CellTracker deep red to visualize and quantify monolayer disruption (**Figure 2**). The penetration of CellTracker into all cellular compartments was observed in the HaCat control (**Figure 2A**). When the commensals were present (**Figure 2B**), similar cell staining was observed, indicating minimal disruption of the monolayer. Conversely, *P. aeruginosa* (**Figure 2C**) or *S. aureus* (**Figure 2E**) alone, or in combination (**Figure 2G**) disrupted the HaCat monolayer as shown by the reduction in the fluorescence of HaCat nuclei indicative of cell death. Interestingly, when the commensals were applied in combination with one or both pathogens, less eukaryotic cell damage was apparent (**Figures 2D,F,H**). To quantify these observations, the total fluorescence from HaCat cells was measured and averaged for two independent experiments (eight images each). By representing the monolayer integrity as a percentage of fluorescence relative to the HaCat control (**Figure 2I**), the commensals confer a significant level of protection of the keratinocytes from damage by either or both of the pathogens. In agreement with this, analysis of the polymicrobial biofilm biovolume revealed that the presence of the commensals significantly reduced the biofilm biovolume, thickness and surface coverage (**Figure 4** and **Supplementary Figure S2**).

Bacterial Localization Within 2D Polymicrobial Biofilms Is Species Dependent

In the keratinocyte colonization model, *S. epidermidis* and *S. aureus* showed different biofilm localization patterns when co-cultured with *P. aeruginosa* (**Figure 3**). Both staphylococcal species were grown for 20 h to establish their colonization of

the HaCat monolayer prior to inoculation with *Pseudomonas*. Incubation was subsequently continued for a further 20 h. The microcolonies of *S. aureus* intercalated with those of *P. aeruginosa* whereas *P. aeruginosa* formed a layer on top of the *S. epidermidis* biofilm (compare **Figures 3A,B**). In addition, the thickness of the *P. aeruginosa*/*S. epidermidis* biofilm was ∼50% less than the *P. aeruginosa*/*S. aureus* biofilm (**Figures 3A,B**). The other commensal chosen for this study, *M. luteus*, behaved similarly to *S. epidermidis* by combining with the latter to form a layer between *P. aeruginosa* and the keratinocytes (**Figure 3C**). In **Figure 3C**, FISH (*in situ* Fluorescent Hybridization) rather than a fluorescent protein was used to identify the bacteria. The pan-Bacterial probe (green) and *P. aeruginosa* specific probe (red) can be observed in differentiated layers (**Figure 3C**) where the upper orange layer corresponds to *P. aeruginosa* alone (as both green and red probes hybridized) and the bottom layer (green) indicates the location of the commensals. The absence of green fluorescent bacteria interspersed within the orange microcolonies suggests that both commensals are co-located in a separate biofilm layer.

Interspecies Interactions Are Detectable Within the Polymicrobial Biofilm Model

The differences in the relative localization of bacteria within the polymicrobial biofilm model could derive from interactions between the bacterial species that are competitive/inhibitory or synergistic/advantageous. To assess this, viable counts for each species were quantified after growing the bacteria in single or multi-species biofilms (**Figure 5**).

S. aureus, *S. epidermidis*, and *P. aeruginosa*, exhibited comparable viable counts, irrespective of whether they were grown in monoculture or in combination (**Figure 5**). In contrast, the viability of *M. luteus* was completely abolished by *S. aureus* in the dual biofilm (7-fold reduction, **Figure 5**). Interestingly, if *S. epidermidis* was present to form a triple species biofilm, *M. luteus* cfus were not reduced, which could support either an inhibitory effect of *S. epidermidis* upon *S. aureus* or synergy between *S. epidermidis* and *M. luteus* (**Figure 5**). Introducing *P. aeruginosa* into the polymicrobial biofilm after 20 h to create a quadruple-species biofilm, had little effect on the viability of the Gram positive bacteria already present.

The *S. aureus agr* QS System Contributes to HaCat Cell Damage

To demonstrate the utility of the assay for exploring the mechanisms underlying HaCat monolayer damage (**Figure 2E**), we investigated the role of the *S. aureus agr* QS system since it regulates the expression of multiple cytotoxins including alpha-hemolysin (Murray et al., 2014). An *S. aureus* QS-deficient Δ*agr* mutant was incorporated into the keratinocyte polymicrobial model in the absence or presence of the exogenous cognate QS signaling molecule, AIP-1. Keratinocytes were stained with CellMask to determine the extent of any cell damage (**Figure 6**). The HaCat cell damage caused by the wild type *S. aureus* strain is clearly apparent (compare **Figure 6A** with **Figure 6C**). In contrast, the HaCat monolayer was mostly intact and comparable with the uninfected control when the cells were infected with the *S. aureus*Δ*agr* mutant (compare **Figures 6C,E**). When the *S. aureus*Δ*agr* mutant was supplemented with exogenous AIP-1, the keratinocyte monolayer was disrupted and rounded (dying) cells were observed, demonstrating the QS-dependent nature of the damage to the eukaryotic cells (**Figure 6G**). The commensals did not damage the HaCat monolayer (**Figure 6B**) and reduced the damage caused by both the *S. aureus* WT and the Δ*agr* mutant provided with exogenous AIP (**Figures 6D,H**, respectively). Quantification of the HaCat cell fluorescence confirmed these observations (**Figure 6I**).

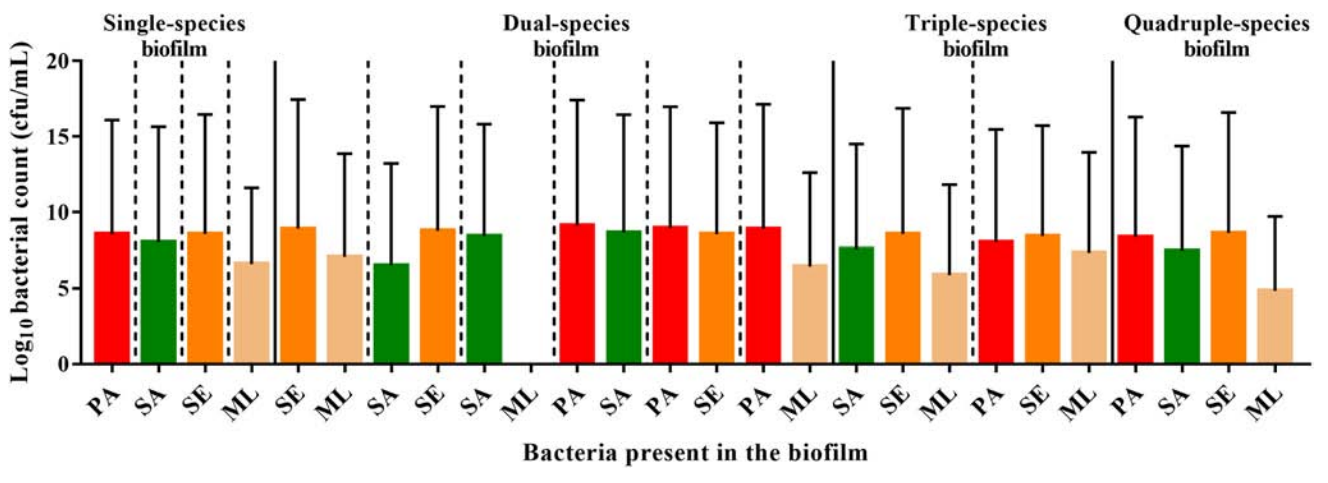

FIGURE 5 | Interspecies interactions are detectable within the polymicrobial biofilm. To form a single-species biofilm, each bacterial species was grown in wells in a 96 well plate. *S. aureus* and commensals were incubated for 40 h, while *P. aeruginosa* was incubated for 20 h before harvesting to determine the number of cfu. Polymicrobial biofilms were generated by incubating *S. aureus* and commensals together for 40 h in the combinations indicated. When *P. aeruginosa* was present, it was added after 20 h, and thus was only in combination with the others for 20 h. SE: *S. epidermidis*; ML: *M. luteus*; SA: *S. aureus*; PA: *P. aeruginosa*.

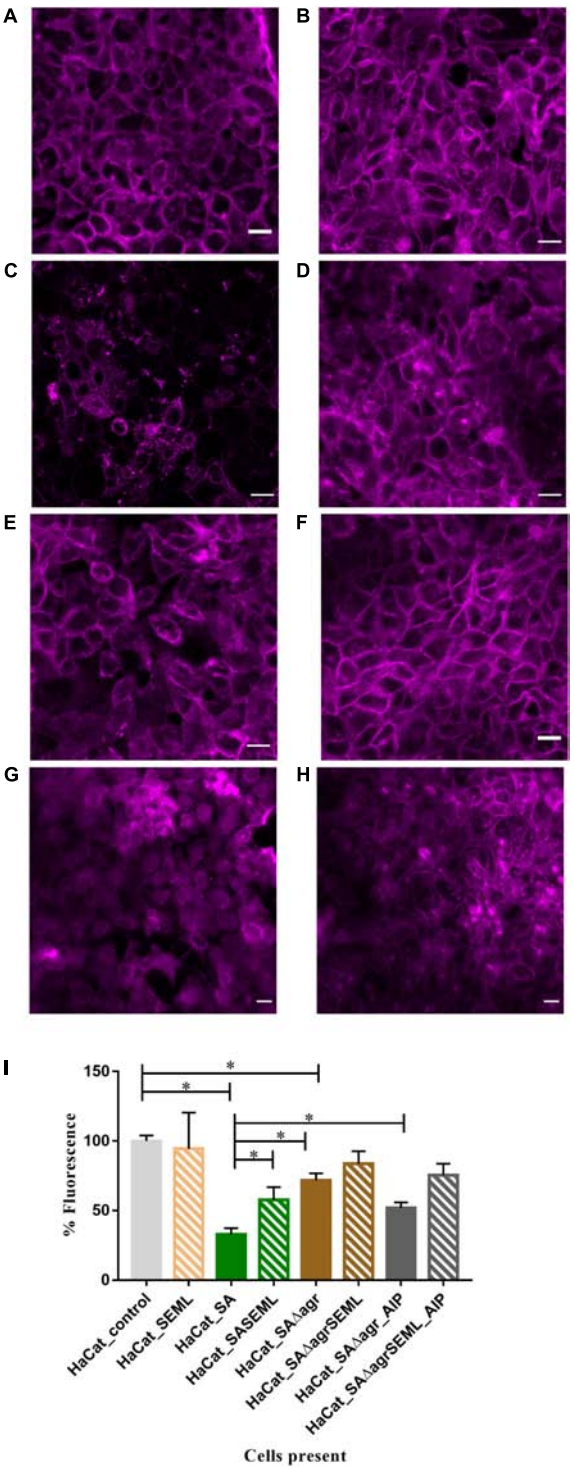

FIGURE 6 | The *S. aureus agr* QS system contributes to keratinocyte cell damage HaCat cells were incubated for 40 h after inoculation with **(A)** no bacteria; **(B)** commensals *S. epidermidis* and *M. luteus*; **(C)** *S. aureus* WT; **(D)** *S. aureus* WT and commensals *S. epidermidis* and *M. luteus*; **(E)** *S. aureus* Δ*agr*; **(F)** *S. aureus* Δ*agr* and commensals *S. epidermidis* and *M. luteus*; **(G)** *S. aureus* Δ*agr* supplemented with 100 nM of AIP-1; **(H)** *S. aureus* Δ*agr* and commensals *S. epidermidis* and *M. luteus* supplemented with 100 nM of AIP-1. HaCat cells are shown as a representative single plane. **(I)** Quantification of HaCat monolayer integrity by measuring the total fluorescence of the z-stack HaCat cells using ImageJ (8–10 Z-stack images analyzed per condition, two experiments) is shown as a percentage of the control lacking bacteria. **p*-value < 0.05. SA: *S. aureus*, SE: *S. epidermidis*; ML: *M. luteus*; AIP: autoinducing peptide. HaCat cells were stained with CellMask prior to confocal imaging. Scale bar indicates 20 μm. Images were taken at 40 × magnification.

A Nanoparticle Encapsulated PQS Inhibitor Reduces *P. aeruginosa* Colonization of the Keratinocyte Polymicrobial Biofilm Model

To exemplify the use of the keratinocyte polymicrobial biofilm model for evaluating anti-virulence agents, we explored the effectiveness of alginate nanoparticles (ALG_QSI) loaded with the *P. aeruginosa* PQS system anti-virulence agent, 3-NH_2-7Cl-C9-QZN. This was selected since we recently demonstrated that it was effective against monospecies *P. aeruginosa* biofilms in an *ex vivo* pig skin infection model (Singh et al., 2019). **Figure 7** and **Supplementary Figures S1, S3** show that the nanoparticles alone had no effect on *S. aureus* in monospecies biofilms or when co-colonizing with commensals. In contrast, the ALG_QSI nanoparticles reduced the *P. aeruginosa* biofilm in the presence and absence of commensals, and this was statistically significant (biovolume (*p*-value = 0.003), surface area (*p*-value = 0.0021); **Figure 7** and **Supplementary Figure S3**). Polymicrobial biofilms containing *P. aeruginosa* and *S. aureus* in the presence of commensals were further reduced by ALG_QSI, suggesting an additive effect of nanoparticles and commensals (**Figure 7** and compare **Supplementary Figures S1J,L**). Furthermore, the ALG_QSI nanoparticles affected the localization of *P. aeruginosa* with respect to *S aureus* (**Supplementary Figure S1** compare panels **I,J** and panels **K,L**).

DISCUSSION

Here, we describe the development, optimization and validation of a polymicrobial biofilm keratinocyte model combining commensals and pathogens. The methodology provides a protocol for investigating the impact of biofilms upon HaCat cell monolayers using confocal fluorescence microscopy to quantify monolayer integrity. The commensals were shown to reduce pathogen-mediated damage and help protect the integrity of the underlying keratinocyte monolayer. In addition, the model was used to exemplify (a) the impact of *S. aureus* AIP-mediated QS sensing, and (b) the effectiveness of a nanoparticle QSI delivery system targeting *P. aeruginosa*. The results obtained indicate that the model offers significant potential as a screening platform to assess interventions that reduce pathogen biofilms, promote healthy skin or aid healing as well as for investigating interactions that occur between commensals, pathogens and host keratinocytes (Egert and Simmering, 2016).

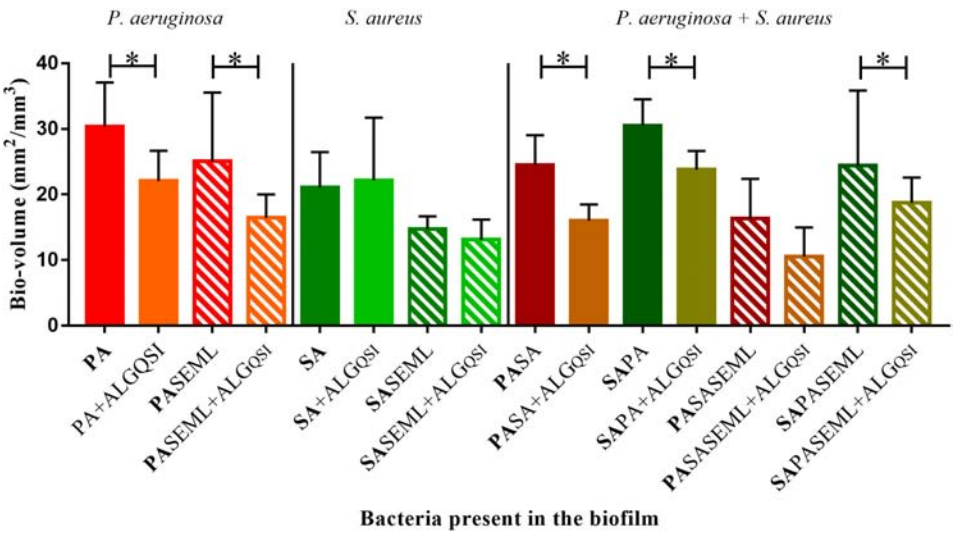

FIGURE 7 | The QSI inhibitor delivered in nanoparticles (ALG_{QSI}) reduced biofilm formation by *P. aeruginosa* alone and in polymicrobial biofilms. HaCat monolayers were inoculated with *S. aureus* (40 h growth) and *P. aeruginosa* (20 h growth) alone or together with commensals (as outlined in **Figure 1**) in the presence or absence of ALG_{QSI} nanoparticles. The biomass was quantified and plotted. SE: *S. epidermidis*; ML: *M. luteus*; SA: *S. aureus*; PA: *P. aeruginosa*. Bold font indicates the bacterial species quantified. **p*-value < 0.05. Not all the statistically significant values have been marked. Images of the biofilms and HaCat monolayer are shown in **Supplementary Figure S1**, and average thickness and surface area are shown in **Supplementary Figure S3**.

In co-cultures where *P. aeruginosa* has been reported to outcompete or largely inhibit staphylococcal growth (*S. aureus* or *S. epidermidis*), comparable numbers of both bacterial species co-inoculated at the same time have generally been used (Hotterbeekx et al., 2017; Bahamondez-Canas et al., 2019). However, this approach may be unrealistic, as infective doses vary (Leggett et al., 2012), and a relatively higher number of commensals are already present in the niche (Egert and Simmering, 2016). By assessing different ratios of commensals and pathogens and by adding *P. aeruginosa* 20 h later than either *S. aureus* or *S. epidermidis*, we were able to overcome *P. aeruginosa*-mediated inhibition. Both *P. aeruginosa* and *S. aureus* are capable of outcompeting *M. luteus* in co-culture (Malic et al., 2011). Consistent with this, *M. luteus* was not recovered when co-cultured with *S. aureus* but could be recovered if allowed to establish before inoculating *P. aeruginosa*. However, when *S. epidermidis* was included, *M. luteus* survived *S. aureus* mediated-inhibition, probably due to the inhibitory effect that *S. epidermidis* has upon the *agr* QS sytem of *S. aureus* (Otto et al., 2001; Chiu et al., 2017).

The ratio of *P. aeruginosa* to *S. aureus* in the inoculum did not inhibit the formation of, or localization within dual species biofilms on HaCAT monolayers (data not shown). *S. aureus* formed microcolonies interspersed throughout the *P. aeruginosa* biofilm, as previously observed (Yang et al., 2011). However, the inoculum ratios influenced the geography of biofilms formed by *S. epidermidis* and *P. aeruginosa*. While it has been previously reported that *P. aeruginosa* outcompetes and reduces *S. epidermidis* biofilms, either when both bacteria were inoculated at the same time or when *P. aeruginosa* was added to an established *S. epidermidis* biofilm (Pihl et al., 2010b), inoculating *P. aeruginosa* at a lower cell density resulted in the formation of a biofilm consisting of two distinct layers that was ∼50% thinner than the *P. aeruginosa*/*S. aureus* mixed biofilm (compare **Figures 3A,B**).

In common with all simple experimental models and the nature of the data that can be collected from them, that described here has limitations. For example, the colony counts to enumerate viable bacteria in the biofilms may be underestimates due to microbial aggregation. To minimize this, a sonication step was incorporated (Azeredo et al., 2017). Ideally, the commensals would be labeled with fluorescent proteins with complementary emissions to avoid the washing steps required by FISH since extensive washing can disrupt biofilms. Further development of the model will also require alternative methods for assessing keratinocyte monolayer disruption and HaCat cell viability since the fluorescent stains employed offer only indirect quantification. Most of the assays available for evaluating eukaryotic cell viability can also be used for assessing bacterial viability (e.g. Alamar blue) and so are not compatible with the model. The lactate dehydrogenase assay (Koeva et al., 2017) was evaluated during the development of the current model, however, inconsistent results were obtained (data not shown) that were attributed to the complexity of the system. Direct assessment of keratinocyte viability may be possible by analysis of mRNA (Lemaître et al., 2004), however, this would be lengthy and expensive, and thus not be suitable for high-throughput screening. Since only laboratory strains were evaluated, the behavior of fresh clinical strains should be investigated.

A major limitation of the model presented that is inherent to any *in vitro* assay, is that it lacks an active host immune system or blood supply, thus it does not fully represent the *in vivo* situation (Ganesh et al., 2015; Roberts et al., 2015). Although *in vivo* models are more realistic in terms of host-biofilm interactions,

they have ethical and feasibility considerations. *In vitro* models are invaluable for the preliminary testing of novel antimicrobial compounds and an irreplaceable first step for the study of the mechanisms of intercellular interactions. However, it would be desirable to corroborate the interactions described here in an *in vivo* infection model (Roberts et al., 2015).

The intricate interplay between *S. aureus* and *P. aeruginosa* (Hotterbeekx et al., 2017) likely drives the reduction of biofilm observed most markedly in the presence of commensals. However, investigation of the underlying molecular mechanisms involved remains to be undertaken. In support of our observations, *S. epidermidis* can inhibit *S. aureus* survival (Chiu et al., 2017) and *agr*-dependent QS (Otto et al., 2001). In line with this hypothesis, we report reduced keratinocyte damage using the *S. aureus*Δ*agr* mutant. This observation is supported by the previous study that described a timing dependent attenuation of cytotoxicity in ArgC mutants that produce reduced levels of AIP and suggested a survival advantage during infection by promoting colonization while restricting unnecessary overproduction of exotoxins (Sloan et al., 2019). Current studies are underway to identify the bacterial factors that contribute to the development of the polymicrobial biofilms described in the keratinocyte model presented here.

The polymicrobial keratinocyte colonization model assay was also used to assess the effectiveness of a novel *P. aeruginosa* QSI (Ilangovan et al., 2013) delivered via alginate nanoparticle encapsulation (ALG_QSI) (Singh et al., 2019). As expected, ALG_QSI reduced *P. aeruginosa* biofilm formation in monoculture. The less marked reduction compared to our previous study (Singh et al., 2019), likely reflects the shorter incubation of the bacteria with the keratinocytes. Given that the maximum reduction of pathogen biofilm occurred when the ALG_QSI was combined with the commensals, further work is required to determine whether this delivery system has any potential for treating wound infections.

In summary, we have developed a stable and reproducible keratinocyte colonization model that combines commensals and pathogens. The model can be easily adapted to study the effect of single bacterial species on HaCat cells (Singh et al., 2019) or modified by adding other commensals such as *Corynebacterium* spp., that are abundant in the skin microbiota. Alternatively it could be adapted for certain skin environments where different microbiome composition driven by skin characteristics occur (oily, moist, dry) by incorporating the most relevant bacteria or fungi (Grice and Segre, 2011). Furthermore, we have demonstrated that the ratio between bacterial species and the timing of inoculation of a polymicrobial biofilm can affect the outcome. Thus, closely mimicking the bacterial cell numbers found in a real scenario would be recommended. In the future, it will be interesting to conduct further experiments to unravel the underlying protective mechanisms that commensals provide to HaCat cells during early stage colonization by pathogens. The results obtained indicate that the model offers significant potential as a screening platform to assess interventions that reduce pathogen biofilms, promote healthy skin or aid healing as well as for investigating interactions that occur between commensals, pathogens and host keratinocytes (Egert and Simmering, 2016).

DATA AVAILABILITY STATEMENT

All datasets generated for this study are included in the article/**Supplementary Material**.

AUTHOR CONTRIBUTIONS

EJ-L, VG, AK, KH, and PW designed the experiments. EJ-L, VG, and AK performed the experiments and analyzed the data. NS developed the ALG_{QSI} nanoparticles. EJ-L, KH, and PW wrote the manuscript. EJ-L, VG, AK, NS, CA, KH, and PW critically reviewed the manuscript.

FUNDING

This work was supported by the Unilever, the EMPIR program co-financed by the Participating States and the European Union (grant ref. 15HLT01 MetVBadBugs) and Medical Research Council, United Kingdom (grant no. MR/N010477/1). AK was funded via a Wellcome Trust Doctoral Training Program (Antimicrobials and Antimicrobial Resistance) (grant no. 108876/B/15/Z). NS was funded by the Engineering and Physical Sciences Research Council (EPSRC) (grant nos. EP/N006615/1, EP/K005138/1, and EP/N03371X/1).

ACKNOWLEDGMENTS

We thank Rupak Mitra (Unilever R&D, Bangalore) for his support in progressing this work, Alex Truman for 3-NH_2-7Cl-C9-QZN synthesis and Ewan Murray for the construction of the *S. aureus* SH1000 Δ*agr* strain.

SUPPLEMENTARY MATERIAL

The Supplementary Material for this article can be found online at: https://www.frontiersin.org/articles/10.3389/fmicb.2020.00291/full#supplementary-material

REFERENCES

Atkinson, S., and Williams, P. (2009). Quorum sensing and social networking in the microbial world. *J. R. Soc. Interface* 6, 959–978. doi: 10.1098/rsif.2009.0203

Azeredo, J., Azevedo, N. F., Briandet, R., Cerca, N., Coenye, T., Costa, A. R., et al. (2017). Critical review on biofilm methods. *Crit. Rev. Microbiol.* 43, 313–351. doi: 10.1080/1040841X.2016.1208146

Bahamondez-Canas, T. F., Heersema, L. A., and Smyth, H. D. C. (2019). Current status of *in vitro* models and assays for susceptibility testing for

wound biofilm infections. *Biomedicines* 7:34. doi: 10.3390/biomedicines7020034

Boldock, E., Surewaard, B. G. J., Shamarina, D., Na, M., Fei, Y., Ali, A., et al. (2018). Human skin commensals augment *Staphylococcus aureus* pathogenesis. *Nat. Microbiol.* 3, 881–890. doi: 10.1038/s41564-018-0198-3

Bosko, C. A. (2019). Skin barrier insights: from bricks and mortar to molecules and microbes. *J. Drugs Dermatol.* 18, s63–s67.

Bowler, P. G., Duerden, B. I., and Armstrong, D. G. (2001). Wound microbiology and associated approaches to wound management. *Clin. Microbiol. Rev.* 14, 244–269. doi: 10.1128/CMR.14.2.244-269.2001

Brandwein, M., Steinberg, D., and Meshner, S. (2016). Microbial biofilms and the human skin microbiome. *NPJ Biofilms Microbiomes* 2:3. doi: 10.1038/s41522-016-0004-z

Bronesky, D., Wu, Z., Marzi, S., Walter, P., Geissmann, T., Moreau, K., et al. (2016). *Staphylococcus aureus* RNAIII and its regulon link quorum sensing, stress responses, metabolic adaptation, and regulation of virulence gene expression. *Annu. Rev. Microbiol.* 70, 299–316. doi: 10.1146/annurev-micro-102215-095708

Byrd, A. L., Belkaid, Y., and Segre, J. A. (2018). The human skin microbiome. *Nat. Rev. Microbiol.* 16, 143–155. doi: 10.1038/nrmicro.2017.157

Chen, Y. E., and Tsao, H. (2013). The skin microbiome: current perspectives and future challenges. *J. Am. Acad. Dermatol.* 69, 143–155. doi: 10.1016/j.jaad.2013.01.016

Chiu, L., Bazin, T., Truchetet, M.-E., Schaeverbeke, T., Delhaes, L., and Pradeu, T. (2017). Protective microbiota: from localized to long-reaching co-immunity. *Front. Immunol.* 8:1678. doi: 10.3389/fimmu.2017.01678

Coenye, T., and Nelis, H. J. (2010). *In vitro* and *in vivo* model systems to study microbial biofilm formation. *J. Microbiol. Methods* 83, 89–105. doi: 10.1016/j.mimet.2010.08.018

Cogen, A. L., Nizet, V., and Gallo, R. L. (2008). Skin microbiota: a source of disease or defence? *Br. J. Dermatol.* 158, 442–455. doi: 10.1111/j.1365-2133.2008.08437.x

Deleon, S., Clinton, A., Fowler, H., Everett, J., Horswill, A. R., and Rumbaugh, K. P. (2014). Synergistic interactions of *Pseudomonas aeruginosa* and *Staphylococcus aureus* in an *in vitro* wound model. *Infect. Immun.* 82, 4718–4728.

Doherty, N., Holden, M. T. G., Qazi, S. N., Williams, P., and Winzer, K. (2006). Functional analysis of *luxS* in *Staphylococcus aureus* reveals a role in metabolism but not quorum sensing. *J. Bacteriol.* 188, 2885–2897. doi: 10.1128/JB.188.8.2885-2897.2006

Egert, M., and Simmering, R. (2016). The microbiota of the human skin. *Adv. Exp. Med. Biol.* 902, 61–81. doi: 10.1007/978-3-319-31248-4_5

Erin Chen, Y., Fischbach, M. A., and Belkaid, Y. (2018). Skin microbiota-host interactions. *Nature* 553, 427–436. doi: 10.1038/nature25177

Galac, M. R., Stam, J., Maybank, R., Hinkle, M., Mack, D., Rohde, H., et al. (2017). Complete genome sequence of *Staphylococcus epidermidis* 1457. *Genome Announc.* 5:e00450-17.

Ganesh, K., Sinha, M., Mathew-Steiner, S. S., Das, A., Roy, S., and Sen, C. K. (2015). Chronic wound biofilm model. *Adv. Wound Care* 4, 382–388. doi: 10.1089/wound.2014.0587

Gordon, C. P., Williams, P., and Chan, W. C. (2013). Attenuating *Staphylococcus aureus* virulence gene regulation: a medicinal chemistry perspective. *J. Med. Chem.* 56, 1389–1404. doi: 10.1021/jm3014635

Grice, E. A., and Segre, J. A. (2011). The skin microbiome. *Nat. Rev. Microbiol.* 9, 244–253. doi: 10.1038/nrmicro2537

Heeb, S., Itoh, Y., Nishijyo, T., Schnider, U., Keel, C., Wade, J., et al. (2000). Small, stable shuttle vectors based on the minimal pVS1 replicon for use in gram-negative, plant-associated bacteria. *Mol. Plant Microbe Interact.* 13, 232–237. doi: 10.1094/MPMI.2000.13.2.232

Heydorn, A., Nielsen, A. T., Hentzer, M., Sternberg, C., Givskov, M., Ersboll, B. K., et al. (2000). Quantification of biofilm structures by the novel computer program COMSTAT. *Microbiology* 146, 2395–2407. doi: 10.1099/00221287-146-10-2395

Hotterbeekx, A., Kumar-singh, S., Goossens, H., and Maddocks, S. (2017). In vivo and in vitro interactions between *Pseudomonas aeruginosa* and *Staphylococcus* spp. *Front. Cell. Infect. Microbiol.* 7:106. doi: 10.3389/fcimb.2017.00106

Ilangovan, A., Fletcher, M., Rampioni, G., Pustelny, C., Rumbaugh, K., Heeb, S., et al. (2013). Structural basis for native agonist and synthetic inhibitor recognition by the *Pseudomonas aeruginosa* quorum sensing regulator *PqsR* (*MvfR*). *PLoS Pathog.* 9:e1003508. doi: 10.1371/journal.ppat.1003508

Koeva, M., Gutu, A. D., Hebert, W., Wager, J. D., Yonker, L. M., O'Toole, G. A., et al. (2017). An antipersister strategy for treatment of chronic *Pseudomonas aeruginosa* infections. *Antimicrob. Agents Chemother.* 61:e00987-17.

Lawson, T. S., Connally, R. E., Iredell, J. R., Vemulpad, S., and Piper, J. A. (2011). Detection of *Staphylococcus aureus* with a fluorescence *in situ* hybridization that does not require lysostaphin. *J. Clin. Lab. Anal.* 25, 142–147. doi: 10.1002/jcla.20448

Lee, J., Wu, J., Deng, Y., Wang, J., Wang, C., Wang, J., et al. (2013). A cell-cell communication signal integrates quorum sensing and stress response. *Nat. Chem. Biol.* 9, 339–343. doi: 10.1038/nchembio.1225

Leech, J. M., Dhariwala, M. O., Lowe, M. M., Chu, K., Merana, G. R., Cornuot, C., et al. (2019). Toxin-triggered interleukin-1 receptor signaling enables early-life discrimination of pathogenic versus commensal skin bacteria. *Cell Host Microbe* 26, 795–809.e5. doi: 10.1016/j.chom.2019.10.007

Leggett, H. C., Cornwallis, C. K., and West, S. A. (2012). Mechanisms of pathogenesis, infective dose and virulence in human parasites. *PLoS Pathog.* 8:e1002512. doi: 10.1371/journal.ppat.1002512

Lemaître, G., Lamartine, J., Pitaval, A., Vaigot, P., Garin, J., Bouet, S., et al. (2004). Expression profiling of genes and proteins in HaCaT keratinocytes: proliferating versus differentiated state. *J. Cell. Biochem.* 93, 1048–1062. doi: 10.1002/jcb.20212

Macià, M. D., Rojo-Molinero, E., and Oliver, A. (2014). Antimicrobial susceptibility testing in biofilm-growing bacteria. *Clin. Microbiol. Infect.* 20, 981–990. doi: 10.1111/1469-0691.12651

Madigan, M. T., Martinko, J. M., and Brock, T. D. (2006). *Brock Biology of Microorganisms*, 11th Edn. Upper Saddle River NJ: Pearson Prentice Hall.

Malic, S., Hill, K. E., Hayes, A., Percival, S. L., Thomas, D. W., and Williams, D. W. (2009). Detection and identification of specific bacteria in wound biofilms using peptide nucleic acid fluorescent *in situ* hybridization (PNA FISH). *Microbiology* 155, 2603–2611. doi: 10.1099/mic.0.028712-0

Malic, S., Hill, K. E., Playle, R., Thomas, D. W., and Williams, D. W. (2011). *In vitro* interaction of chronic wound bacteria in biofilms. *J. Wound Care* 20, 569–577. doi: 10.12968/jowc.2011.20.12.569

McVicker, G., Prajsnar, T. K., and Foster, S. J. (2018). Construction and use of *Staphylococcus aureus* strains to study within-host infection dynamics. *Methods Mol. Biol.* 1736, 17–27. doi: 10.1007/978-1-4939-7638-6_2

Monk, I. R., Shah, I. M., Xu, M., Tan, M.-W., and Foster, T. J. (2012). Transforming the untransformable: application of direct transformation to manipulate genetically *Staphylococcus aureus* and *Staphylococcus epidermidis*. *mBio* 3:e00277-11.

Murray, E. J., Crowley, R. C., Truman, A., Clarke, S. R., Cottam, J. A., Jadhav, G. P., et al. (2014). Targeting *Staphylococcus aureus* quorum sensing with nonpeptidic small molecule inhibitors. *J. Med. Chem.* 57, 2813–2819. doi: 10.1021/jm500215s

Negrini, T. C., Arthur, R. A., Waeiss, R. A., Carlosa, I. Z., and Srinivasan, M. (2014). Salivary epithelial cells as model to study immune response against cutaneous pathogens. *Clin. Transl. Sci.* 7, 48–51. doi: 10.1111/cts.12113

Njoroge, J., and Sperandio, V. (2009). Jamming bacterial communication: new approaches for the treatment of infectious diseases. *EMBO Mol. Med.* 1, 201–210. doi: 10.1002/emmm.200900032

Novick, R. P., Ross, H. F., Projan, S. J., Kornblum, J., Kreiswirth, B., and Moghazeh, S. (1993). Synthesis of staphylococcal virulence factors is controlled by a regulatory RNA molecule. *EMBO J.* 12, 3967–3975. doi: 10.1002/j.1460-2075.1993.tb06074.x

Ortori, C. A., Dubern, J.-F., Chhabra, S. R., Cámara, M., Hardie, K., Williams, P., et al. (2011). Simultaneous quantitative profiling of N-acyl-L-homoserine lactone and 2-alkyl-4(1H)-quinolone families of quorum-sensing signaling molecules using LC-MS/MS. *Anal. Bioanal. Chem.* 399, 839–850. doi: 10.1007/s00216-010-4341-0

Otto, M., Echner, H., Voelter, W., and Gotz, F. (2001). Pheromone cross-inhibition between *Staphylococcus aureus* and *Staphylococcus epidermidis*. *Infect. Immun.* 69, 1957–1960. doi: 10.1128/IAI.69.3.1957

Parlet, C. P., Brown, M. M., and Horswill, A. R. (2019). Commensal staphylococci influence *Staphylococcus aureus* skin colonization and disease. *Trends Microbiol.* 27, 497–507. doi: 10.1016/j.tim.2019.01.008

Percival, S. L., Hill, K. E., Williams, D. W., Hooper, S. J., Thomas, D. W., and Costerton, J. W. (2012). A review of the scientific evidence for biofilms in wounds. *Wound Repair. Regen.* 20, 647–657. doi: 10.1111/j.1524-475X.2012.00836.x

Peters, B. M., Jabra-rizk, M. A., Costerton, J. W., and Shirtliff, M. E. (2012). Polymicrobial interactions: impact on pathogenesis and human disease. *Clin. Microbiol. Rev.* 25, 193–213. doi: 10.1128/cmr.00013-11

Pihl, M., Chávez de Paz, L. E., Schmidtchen, A., Svensäter, G., and Davies, J. R. (2010a). Effects of clinical isolates of *Pseudomonas aeruginosa* on *Staphylococcus epidermidis* biofilm formation. *FEMS Immunol. Med. Microbiol.* 59, 504–512. doi: 10.1111/j.1574-695X.2010.00707.x

Pihl, M., Davies, J. R., Chávez de Paz, L. E., and Svensäter, G. (2010b). Differential effects of *Pseudomonas aeruginosa* on biofilm formation by different strains of *Staphylococcus epidermidis*. *FEMS Immunol. Med. Microbiol.* 59, 439–446. doi: 10.1111/j.1574-695X.2010.00697.x

Qazi, S. N. A., Counil, E., Morrissey, J., Rees, C. E. D., Cockayne, A., Winzer, K., et al. (2001). *agr* expression precedes escape of internalized *Staphylococcus aureus* from the host endosome. *Infect. Immun.* 69, 7074–7082. doi: 10.1128/IAI.69.11.7074-7082.2001

Roberts, A. E. L., Kragh, K. N., Bjarnsholt, T., and Diggle, S. P. (2015). The limitations of in vitro experimentation in understanding biofilms and chronic infection. *J. Mol. Biol.* 427, 3646–3661. doi: 10.1016/j.jmb.2015.09.002

Rokem, J. S., Vongsangnak, W., and Nielsen, J. (2011). Comparative metabolic capabilities for *Micrococcus luteus* NCTC 2665, the "Fleming" strain, and actinobacteria. *Biotechnol. Bioeng.* 108, 2770–2775. doi: 10.1002/bit.23212

Romero, M., Acuna, L., and Otero, A. (2012). Patents on quorum quenching: interfering with bacterial communication as a strategy to fight infections. *Recent Pat. Biotechnol.* 6, 2–12. doi: 10.2174/187220812799789208

Schindelin, J., Arganda-Carreras, I., Frise, E., Kaynig, V., Longair, M., Pietzsch, T., et al. (2012). Fiji: an open-source platform for biological-image analysis. *Nat. Methods* 9, 676–682. doi: 10.1038/nmeth.2019

Serra, R., Grande, R., Butrico, L., Rossi, A., Settimio, U. F., Caroleo, B., et al. (2015). Chronic wound infections: the role of *Pseudomonas aeruginosa* and *Staphylococcus aureus*. *Expert Rev. Anti Infect. Ther.* 13, 605–613. doi: 10.1586/14787210.2015.1023291

Shaaban, M., Elgaml, A., and Habib, E. S. E. (2019). Biotechnological applications of quorum sensing inhibition as novel therapeutic strategies for multidrug resistant pathogens. *Microb. Pathog.* 127, 138–143. doi: 10.1016/j.micpath.2018.11.043

Singh, N., Romero, M., Travanut, A., Monteiro, P. F., Jordana-Lluch, E., Hardie, K. R., et al. (2019). Dual bioresponsive antibiotic and quorum sensing inhibitor combination nanoparticles for treatment of *Pseudomonas aeruginosa* biofilms in vitro and ex vivo. *Biomater. Sci.* 7, 4099–4111. doi: 10.1039/c9bm00773c

Sloan, T. J., Murray, E., Yokoyama, M., Massey, R. C., Chan, W. C., Bonev, B. B., et al. (2019). Timing is everything: impact of naturally occurring *Staphylococcus aureus AgrC* cytoplasmic domain adaptive mutations on autoinduction. *J. Bacteriol.* 201:e00409-19.

Snyder, R. J., Bohn, G., Hanft, J., Harkless, L., Kim, P., Lavery, L., et al. (2017). Wound biofilm: current perspectives and strategies on biofilm disruption and treatments. *Wounds* 29, S1–S17.

Soukarieh, F., Williams, P., Stocks, M. J., and Cámara, M. (2018). *Pseudomonas aeruginosa* quorum sensing systems as drug discovery targets: current position and future perspectives. *J. Med. Chem.* 61, 10385–10402. doi: 10.1021/acs.jmedchem.8b00540

van Rensburg, J. J., Lin, H., Gao, X., Toh, E., Fortney, K. R., Ellinger, S., et al. (2015). The human skin microbiome associates with the outcome of and is influenced by bacterial infection. *mBio* 6:e01315-15.

Yang, L., Liu, Y., Markussen, T., Høiby, N., Tolker-Nielsen, T., and Molin, S. (2011). Pattern differentiation in co-culture biofilms formed by *Staphylococcus aureus* and *Pseudomonas aeruginosa*. *FEMS Immunol. Med. Microbiol.* 62, 339–347. doi: 10.1111/j.1574-695X.2011.00820.x

Conflict of Interest: The authors declare that the research was conducted in the absence of any commercial or financial relationships that could be construed as a potential conflict of interest.

frontiers in Microbiology

ORIGINAL RESEARCH
published: 30 April 2020
doi: 10.3389/fmicb.2020.00774

Inhibition of *Streptococcus mutans* Biofilm Formation and Virulence by *Lactobacillus plantarum* K41 Isolated From Traditional Sichuan Pickles

Guojian Zhang[1†], Miao Lu[2†], Rongmei Liu[3], Yuanyuan Tian[3], Viet Ha Vu[2], Yang Li[3], Bao Liu[3], Ariel Kushmaro[4], Yuqing Li[2] and Qun Sun[1,3]**

[1] Department of Food Science and Technology, College of Light Industry, Textile and Food Engineering, Sichuan University, Chengdu, China, [2] State Key Laboratory of Oral Diseases, National Clinical Research Center for Oral Diseases, Department of Cariology and Endodonics, West China Hospital of Stomatology, Sichuan University, Chengdu, China, [3] Key Laboratory of Bio-resources & Eco-environment of the Ministry of Education, College of Life Sciences, Sichuan University, Chengdu, China, [4] Avram and Stella Goldstein-Goren Department of Biotechnology Engineering, Ben-Gurion University of the Negev, Beersheba, Israel

OPEN ACCESS

Edited by:
Giovanna Batoni,
University of Pisa, Italy

Reviewed by:
Santosh Pandit,
Chalmers University of Technology, Sweden
Megan L. Falsetta,
University of Rochester, United States

***Correspondence:**
Yuqing Li
liyuqing@scu.edu.cn;
liyuqing13@163.com
Qun Sun
qunsun@scu.edu.cn

[†] These authors have contributed equally to this work

Specialty section:
This article was submitted to Microbial Physiology and Metabolism, a section of the journal Frontiers in Microbiology

Received: 03 February 2020
Accepted: 31 March 2020
Published: 30 April 2020

Citation:
Zhang G, Lu M, Liu R, Tian Y, Vu VH, Li Y, Liu B, Kushmaro A, Li Y and Sun Q (2020) Inhibition of Streptococcus mutans Biofilm Formation and Virulence by Lactobacillus plantarum K41 Isolated From Traditional Sichuan Pickles. Front. Microbiol. 11:774. doi: 10.3389/fmicb.2020.00774

Among cariogenic microbes, *Streptococcus mutans* is considered a major etiological pathogen of dental caries. *Lactobacilli* strains have been promoted as possible probiotic agents against *S. mutans*, although the inhibitory effect of *Lactobacilli* on caries has not yet been properly addressed. The objective of this study was to screen *Lactobacillus* strains found in traditional Sichuan pickles and to evaluate their antagonistic properties against *S. mutans in vitro* and *in vivo*. In the current study, we analyzed 54 *Lactobacillus* strains isolated from pickles and found that strain *L. plantarum* K41 showed the highest inhibitory effect on *S. mutans* growth as well as on the formation of exopolysaccharides (EPS) and biofilm *in vitro*. Scanning electron microscopy (SEM) and confocal laser scanning microscope (CLSM) revealed the reduction of both EPS and of the network-like structure in *S. mutans* biofilm when these bacteria were co-cultured with strain *L. plantarum* K41. Furthermore, when rats were treated with strain *L. plantarum* K41, there was a significant reduction in the incidence and severity of dental caries. Due to K41's origin in a high salinity environment, it showed a high tolerance to acids and salts. This may give this strain an advantage in harsh oral conditions. Results showed that *L. plantarum* K41 isolated from traditional Sichuan pickles effectively inhibited *S. mutans* biofilm formation and thus possesses a potential inhibitory effect on dental caries *in vivo*.

Keywords: *Streptococcus mutans*, *Lactobacillus plantarum*, sichuan pickles, antibacterial properties, dental caries

INTRODUCTION

Dental caries is a common biofilm-dependent oral disease in humans, which manifests itself as a progressive demineralization of calcareous tissues caused by the complicated interactions between acid-generating bacteria and fermentable carbohydrates (Bal et al., 2019). The burden of untreated dental caries is shifting from children to adults, and caries in permanent teeth is one of the most prevalent disease world-over (Kassebaum et al., 2015). According to the 4th National Oral Health

Survey of China 3-, 4-, and 5-years-old children, show the prevalence of dental caries of 50.8, 63.6, and 71.9%, respectively (Du et al., 2018). Dental biofilms are some of the most complex biofilm systems in nature. They are composed of multiple bacteria and fungi embedded in a matrix of polymers covering the surfaces of teeth (Xiao et al., 2012; Kidd and Fejerskov, 2016). Bacterial cells in the biofilm exhibit low metabolic activity, strong drug tolerance, and specific phenotype changes caused by the cell signaling or cross-species reciprocal protection (Yue et al., 2018). Previous studies have shown that *Streptococcus mutans* is an important oral cariogenic bacterium (He et al., 2013; Kulshrestha et al., 2016). Although it does not always dominate human dental plaque, in the presence of sucrose *S mutans* can assemble an insoluble exopolysaccharide (EPS). This EPS acts as a supportive framework for diffusion within the oral biofilm structure (Koo et al., 2013; Kim et al., 2015; Andre et al., 2017).

Currently, this cariogenic structure is eradicated mainly using non-specific mechanical removal such as tooth brushing and flossing, or by treatment with mouthwashes containing chlorhexidine (Gunsolley, 2010), essential oils (Van Leeuwen et al., 2011), or cetylpyridinium chloride (Haps et al., 2008). Fluoride washes are also used for the prevention of dental caries. In addition, natural substances such as tea catechins (Xu et al., 2012) and cranberry constituents (Koo et al., 2010), small molecules including dihydrofolate reductase (Zhang et al., 2015) and 7-epiclusianone (Murata et al., 2010), have also been characterized to show anti-plaque activities through unselective killing of oral microorganisms. However, few of them selectively eliminate cariogenic bacteria without disturbing the ecological balance of oral cavity. Therefore, novel therapies like probiotics (Kaye, 2017; Pahumunto et al., 2019) and glucansucrase inhibitors (Ito et al., 2011) have gained increasing attention for their antimicrobial activities in dental biofilm.

Probiotic microorganisms are living microbes that are beneficial to general health of hosts when taken in sufficient quantities. Delivery of probiotics to teeth as a paste or wash may concentrate the probiotic bacteria in the region of dental biofilm and thus may eradicate or diminish more pathogenic bacteria (Bosch et al., 2012; Fernandes et al., 2018). The most common strains found in commercial dental probiotic products include the genera *Lactobacillus* and *Bifidobacterium* (Sanders and Marco, 2010). However, both *in vitro* and clinical investigations of their effectiveness yielded ambiguous results with regards to their effects on *Lactobacillus* strains associated with caries (Fitzgerald et al., 1966; Tahmourespour and Kermanshahi, 2011; Hasslöf et al., 2013; Campus et al., 2014; Lin and Pan, 2014; Rodríguez et al., 2016).

Lactobacillus plantarum has been widely used in the preservation of cooked meat products (Vermeiren et al., 2004), condiments, and dairy products (Li et al., 2017). It exerts several beneficial effects, including immune system regulation, stabilization of the intestinal microbiota, and reducing cholesterol level (Vries et al., 2006). Furthermore, metabolic products of *L. plantarum*, including lactic acid and bacteriocin, have the antagonistic activities against adverse microorganisms (Zhu et al., 2014; Li et al., 2016). However, the inhibitory effect of *L. plantarum* on the control of caries has been only sparsely reported, and all the studies available to date were performed *in vitro* (Chun et al., 2013; Guo et al., 2016). Moreover, only a few studies have been performed on probiotics that can be added to daily foods directly. Therefore, an effort to control dental caries using probiotics is still necessary. Here, we propose exploring the anti-caries activity of *L. plantarum,* a bacterium that may be potentially supplemented in our daily diet.

Pickles are traditional fermented foods that are an integral part of the diet in the southwest of China due to their unique taste and beneficial functions. The numerous beneficial properties of pickles are conferred to them by the presence of microorganisms that contribute to the fermentation process. *L. plantarum* is one of the major contributors to these processes (Tian et al., 2013; Zhang et al., 2013). However, to date, no relevant reports have been published on the relationship between Sichuan pickles and oral health. We hypothesize that some *L. plantarum* strains in these pickles may be beneficial to the oral health by affecting the oral microbiome. We therefore undertook to evaluate the inhibitory effect of *L. plantarum* isolated from Sichuan pickles on dental caries both *in vitro* and *in vivo*.

MATERIALS AND METHODS

Bacterial Strains and Growth Conditions

A total of 14 samples of pickles, the traditional fermented products in China, were collected from different areas in Sichuan province. All the samples were cut into pieces and subjected to serial dilution using sterile saline (0.80 g/100 mL), then suitable dilutions were spread on to the deMan-Rogosa-Sharpe (MRS) agar plates and incubated at 37°C for 48 h (Vijayendra et al., 2009). We preliminarily selected 54 mucoid colonies according to their morphological characteristics, as they were expected to be lactic acid bacteria, which were then stored at −80°C. According to the growth inhibition assay against *S. mutans*, five strains that exerted antibacterial activities were chosen. DNA of these five strains was extracted using QIAamp DNA Mini Kit following the manufacturer's instruction and later subjected to polymerase chain reaction (PCR) using the universal primers of 27F and 1492R. According to their NCBI BLAST of 16S rDNA sequence, all these strains had the highest similarity to *L. plantarum*. The same results were obtained by matrix-assisted laser desorption ionization-time of flight mass spectrometry identification. The ABY-8 is a freeze-dried culture containing *Streptococcus thermophilic* and *Lactobacillus bulgaricus* used in yogurt fermentation.

All *Lactobacillus* strains and *S. thermophilic* were cultured in deMan-Rogosa-Sharpe (MRS) media. *S. mutans* UA159 was routinely grown in brain-heart infusion (BHI) medium (Difco, Detroit, MI, United States) in an anaerobic chamber (5% CO_2, 10% H_2, and 85% N_2) at 37°C. All bacteria were stored at −80°C in 50% glycerol. After overnight incubation at 37°C, bacterial suspensions of both *S. mutans* and *Lactobacillus* were diluted by 10-fold using fresh media and cultured for approximately 2 h till reaching an OD_{600} = 0.5 before use.

Growth Inhibition Assay

The antibacterial activities of *Lactobacillus* strains against *S. mutans* was quantified using a modified well-diffusion method (Lin and Pan, 2014). As shown in **Supplementary Figure S1**, 200 ml melted BHI agar medium held at about 45°C was inoculated with 20 μl well mixed bacterial suspension of *S. mutans*. The medium containing S. *mutans* was poured into plates quickly, then placed in Oxford cups (San Ai Si Scientific Instrument Co., Ltd., Yancheng, Jiangsu, China) for medium solidification. Oxford cups of 7.8 mm diameters were then filled with 200 μl bacterial suspension of *Lactobacillus* strains, or chlorhexidine acetate (0.02%, Madam Health pharmaceutical Co., Ltd., Shanghai, China) that was chosen as the positive control. The growth inhibition diameter was measured after incubation at 37°C for 24 h.

Biofilm Formation Assay

The inhibitory effect of *Lactobacillus* sp. on *S. mutans* biofilm formation was performed as previously reported (Soderling et al., 2011). In brief, both *Lactobacilli* strains and *S. mutans* were diluted by 50-fold in the corresponding medium supplemented with 1% (w/v) sucrose and 25 μl MES (Sigma, St. Louis, MO, United States). Then, the formation of *S. mutans* biofilm was evaluated in the absence or presence of *Lactobacillus* strains. *Lactobacilli* strains were also cultivated alone to establish mono-species biofilms. Dilution of *S. mutans* and *Lactobacillus* strains were mixed at equal ratios (chlorhexidine acetate was used as the positive control). Biofilms were formed in 24-multiwell plates in order to enable viable cells measurements, and on sterile glass slides for microscopic observation.

In order to measure the viable cells in the biofilms, the unattached cells were removed from the wells after anaerobic incubation at 37°C for 18∼24 h. The remaining cells adhering to the wells were washed three times and resuspended in 1 ml PBS buffer. The re-suspensions were then collected and cultured in BHI agar plates supplemented with 0.1% (m/m) bromocresol. The CFU of *S. mutans* and *Lactobacillus* strains were enumerated following a culture period of 48 h (Schwendicke et al., 2017).

Extracellular Polysaccharide Measurement

The "Anthrone-sulfuric acid method" was used to identify EPS production as previously described by Ren et al. (2016). After *Lactobacillus* strains and *S. mutans* were cultured to reach an OD_{600} = 0.5, *S. mutans* were diluted by 50-fold in BHI medium supplemented with 2% (w/v) sucrose. The bacterial suspensions of *Lactobacillus* strains were mixed with an equal volume of diluted *S. mutans* suspension. MRS medium was used as a control. After anaerobic incubation at 37°C for 24 h, the culture fluid was removed and replaced with 2 ml sterile PBS. The deposits were resuspended and washed three times with sterile PBS to remove the water-soluble EPS. Then, insoluble EPS was extracted using 1.0 M NaOH with agitation at 37°C for 2 h. EPS production was measured at the absorbance of 620 nm, and a standard curve was made using glucose.

Autoaggregation and Coaggregation Assay

An autoaggregation assay was carried out as follows. *Lactobacillus* cells resuspended in PBS were adjusted to an absorbance of 0.6 ± 0.02 at A_{600} (A_0); the absorbance (A_t) of the upper suspension was measured in the following 4 h. The result was calculated as: Autoaggregation (%) = $1 - (A_t/A_0) \times 100$, where A_t represents the absorbance at time t = 1, 2, 3 or 4 h.

For the coaggregation assay, equal volumes of *Lactobacillus* sp. and *S. mutans* were mixed, and the absorbance of the upper suspension was measured in the following 4 h. Coaggregation was calculated as follows: Coaggregation (%) = $(((A_0 + B_0)/2) - C_t)/((A_0 + B_0)/2) \times 100$, where A_0 and B_0 represent the initial absorbance of *Lactobacillus* sp. and *S. mutans*, and C_t represents the absorbance of the mixture measured at time t = 1, 2, 3 or 4 h.

Tolerance to Acids and Salts

To test the acid tolerance, *Lactobacillus* sp. was inoculated in MRS medium with a pH of 3∼6 in the treated group, and pH 7 in the control group. The salt tolerance was evaluated in MRS medium supplemented with NaCl 0.5%, 1.0%, 2.0%, 4.0%, and 8.0%, while the untreated MRS medium represented the control group, after incubation of *Lactobacillus* sp. at 37°C for 24 h. The survival rate was calculated as follows: survival rate (%) = treated group/control group × 100.

Minimum Inhibitory Concentration to Antibiotics

The minimum inhibitory concentration (MIC) of K41 against antibiotics was determined by the broth micro-dilution method using the standardized lactic acid bacteria susceptibility test medium (LSM), and *L. plantarum* ATCC 14917T was used as control (International Organization of Standardization/International Dairy Federation (ISO10932/Idf 223), 2010). The antibiotics concentrations in the plates were shown in **Supplementary Table S1**. The MIC was defined as the lowest concentration of the antibiotics that completely inhibited the growth of the tested strain. Each test was performed in triplicate.

Scanning Electron Microscope Observation

Scanning electron microscopy (SEM) observation was performed as previously described (Wu et al., 2015). Sterile glass slides were added to a 24-multiwell plate. Biofilms were grown on slides and incubated under anaerobic conditions at 37°C for 24 h. Glass slides were gently washed with PBS buffer twice and fixed with 2.5% glutaraldehyde overnight, then dehydrated in graded ethanol solutions (30%, 40%, 50%, 60%, 70%, 80%, 85%, 90%, 95%, 100%) for 15 min, dried in liquid CO_2, and sputter-coated with gold before observation (FEI, Hillsboro, OR, United States). SE mode was used for SEM evaluation, and the scanning parameter was set at 20.00 kV.

Confocal Laser Scanning Microscope Observation

Confocal laser scanning microscope (CLSM) observation was performed as previously described with some modification (Cheng et al., 2016). All biofilms were dyed with Alexa Fluor 647-labeled dextran conjugate (1 μM; Life Technologies, Grand Island, NY, United States) and cultured on glass slides away from light for 24 h. Glasses were washed twice and labeled with 40 μL SYTO 9 green fluorescent nucleic acid stain (2.5 μM; Life Technologies, Grand Island, NY, United States) for 15 min. Then glass slides with biofilms were examined using a Leica DMIRE2 CLSM (Leica, Wetzlar, Germany) under a 60 × oil immersion objective lens. Emission wavelength at 668 nm was used for the detection of the EPS stained by Fluor 647-labeled dextran conjugate, while 498 nm was used for bacteria stained by SYTO 9 green fluorescent nucleic acid stain. Each image series was generated using optical sectioning at each position. Three-dimensional reconstruction and quantification of EPS/bacteria biomass at each position of biofilm were performed using IMARIS 7.0.0 (Bitplane, Zurich, Switzerland).

Animals and Diet

The dosing experiments were performed on 28, 17-day-old females of specific-pathogen-free Sprague Dawley rats (Dashuo Inc., Chengdu, China), weighing 60 ± 5 g. The flow chart of the animal model is shown in **Figure 4A**. During the first 3 days, the rats were fed with a diet supplemented with 0.1% carbenicillin, 0.1% chloramphenicol, and water containing 4,000 U/ml penicillin. From the fifth day on, rats were fed with a diet no. 2000 (56% sucrose; Dashuo Inc.), and 10% sucrose was added into the drinking water with *ad libitum* access (Murata et al., 2010). At the age of 21 days, rats were infected with an overnight bacterial suspension of *S. mutans* UA159 (10^8 CFU/ml) administered orally for three consecutive days. At age 24 days, the infection was assessed, and rats were randomly divided into four groups (n = 8): group 1, Control (MRS medium); group 2, Chlorhexidine acetate (0.02%); group 3, K41 (10^8 CFU/ml); group 4, K41 alone (10^8 CFU/ml) mixed with ABY-8 (10^8 CFU/ml). Rat-molars were topical treated daily as mentioned above using oral swabs at a unified time of 20 s per quadrant for a period of 35 days (Beiraghi et al., 1990). Rats were weighed twice a week for the first 2 weeks and then once a week. After 5 weeks of treatment, the animals were sacrificed, and the maxillae and mandibles were aseptically removed. This study was reviewed and approved by the Ethics Committee of the College of Life Sciences, Sichuan University (No. 20191217001; Sichuan University, Chengdu, China).

Caries Scoring Assay

After flesh removal from around each tooth, the teeth were stained with 0.4% murexide solution for 12 h, then rinsed with distilled water (Han et al., 2017). Maxillary and mandibular molars were ground up along the mesiodistal sagittal plane using the rainbow technique (Super-Snap kit). Molar caries was evaluated and scored according to the Keyes' method using a stereoscopic microscope (Keyes, 1958). Caries scoring was established by two expert examiners, who carried out blind scorings as the jaws were mixed-up and randomly assigned to the examiners.

Micro-CT Analysis

The right halves of the maxilla of five rats in each group were scanned at 10 μM isotropic voxel resolution using a cone-beam Micro-CT system (SCANCO MEDICAL, Swiss). The scanning parameters were set at 70 kV and 200 μA. After scanning, three-dimensional images of the maxilla were reconstructed, and the enamel volume and mineral density of the first molars were analyzed.

Laser Fluorescence Intensity Assessment

DIAGNOdent pen, a new generation of laser fluorescence device, was used for caries detection and quantification of the left halves of maxilla and mandible of eight rats in each group. Smooth surfaces and occlusal surfaces of each tooth were scored using a DIAGNOdent pen (model 2190) fitted with a fissure probe (Mat. no. 1.002.6967, KaVo, Biberach, Germany) and a proximal probe (Mat. no. 1.002.6970, KaVo, Biberach, Germany) that emitted visible red laser at a wavelength of 655 nm. The DIAGNOdent pen was calibrated according to the manufacturer's guidelines with a ceramic standard (Rams and Alwaqyan, 2017). In all cases, the peak value was recorded as the final data for the surface. Every jaw had eight smooth surfaces and three occlusal surfaces to be assessed. These resulted in 112 smooth surfaces and 42 occlusal surfaces assessed in total. The readings of the DIAGNOdent pen in the smooth surfaces were the following: 0∼7, healthy tooth substance; 8∼15, beginning of the demineralization; ≥15, strong demineralization. The readings in the occlusal surfaces were the following: 0∼12, healthy tooth substance; 13∼24, beginning of the demineralization; ≥25, strong demineralization.

Statistical Analysis

Statistical analysis was performed using SPSS Statistics 17.0. Differences among groups were evaluated using one-way analysis of variance (ANOVA) with Duncan's multiple comparison test. Values are expressed as mean ± standard deviation (SD). A value of $P < 0.05$ was considered statistically significant.

RESULTS

Inhibitory Effect of *Lactobacillus* sp. on *S. mutans* Growth, Biofilm Formation, and EPS Production

A total of 54 *Lactobacillus* strains isolated from pickles were used to analyze their inhibitory effect on *S. mutans* growth. Six of the strains formed an inhibitory area around *S. mutans* (**Table 1**). According to the diameter of the inhibition area, the highest antimicrobial activity, 14.7 ± 1.5 mm, was observed for strain K41. This was slightly higher than the chlorhexidine acetate (14.2 ± 1.9 mm), indicating that K41 had the best inhibitory effect on the growth of *S. mutans*.

TABLE 1 | Effect of *Lactobacillus* strains on the growth of *Streptococcus mutans*.

Strains	Inhibition diameter (mm)	Strains	Inhibition diameter (mm)	Strains	Inhibition diameter (mm)
Control[a]	ND[b]	K36	ND	K91	ND
Chlorhexidine acetate (0.02%)	14.2 ± 1.9^{Ac}	K41	14.7 ± 1.5^{A}	K92	ND
K11	11.3 ± 4.9^{A}	K42	ND	K93	ND
K12	ND	K43	ND	K101	ND
K13	ND	K44	ND	K102	ND
K14	ND	K45	ND	K103	ND
K15	ND	K46	ND	K111	ND
K16	ND	K51	ND	K112	ND
K21	ND	K52	ND	K113	ND
K22	ND	K53	8.8 ± 1.0^{B}	K121	ND
K23	ND	K61	ND	K122	ND
K24	ND	K62	ND	K123	ND
K25	ND	K63	ND	K131	ND
K26	10.3 ± 1.5^{A}	K71	ND	K132	ND
K31	ND	K72	ND	K133	ND
K32	ND	K73	ND	K141	ND
K33	ND	K81	ND	K142	11.3 ± 1.2^{A}
K34	13.3 ± 1.0^{A}	K82	ND	K143	ND
K35	ND	K83	ND		

[a]*Control: deMan-Rogosa-Sharpe media.* [b]*ND: not detectable.* [c]*Values are expressed as mean ± SD of the inhibition diameter (mm). Results with different superscript capital letters are significantly different ($P < 0.05$).*

The inhibitory effect on *S. mutans* biofilm formation is illustrated in **Figure 1A**. Viable *S. mutans* cells in the chlorhexidine acetate group were significantly different from the control group ($P < 0.05$). *L. plantarum* K11 and K41 possessed a similar magnitude of bactericidal activity against *S. mutans,* their inhibition rates were 97.7 and 98.4%, respectively. Interestingly, the viability of the different *Lactobacillus* sp. in the biofilm was not significantly different ($P > 0.05$).

As shown in **Figure 1B** and **Supplementary Figure S4**, *L. plantarum* K26, K34 and K41, showed no significant differences with regards to EPS concentration. Furthermore, K41 showed a better inhibitory effect on EPS formation than K11 ($P < 0.05$). Therefore, *L. plantarum* K41 should be considered the strain with the best inhibitory effect on *S. mutans* growth, biofilm formation and EPS production, of *Lactobacillus* sp. perhaps indicating its potential benefit on the control of dental caries.

The Aggregation Ability and Tolerance of *Lactobacillus* sp. to Oral Condition

The autoaggregation ability of *Lactobacillus* is shown in **Figure 2A** and shows a significant difference among the five strains at 4 h. The best autoaggregation ability was K26 (35.1%), followed by K41 (31.0%). There was no significant difference in the remaining three strains ($P > 0.05$). The coaggregation with *S. mutans* increased during the first 4 h, and the difference among the five strains was small varying from 33.6 to 44.0% at 4 h (**Figure 2B**).

The survival rates of all strains were over 75% when the pH was 5∼6, but lower than 5% at pH 3 (**Figure 2C**). When the salinity was less than 4.0%, the survival rates of all five strains were greater than 70% (**Figure 2D**). According to the aggregation results and the tolerance to acids and salt, all tested strains had strong ability to survive in the harsh oral environment. Thus, due to its extensive bactericidal activity, *L. plantarum* K41 was chosen for the subsequent experiments.

The MIC distributions and breakpoints of K41 are presented in **Supplementary Table S2**. *L. plantarum* K41 was characterized as sensitive according to breakpoints proposed by the Clinical and Laboratory Standards Institute [CLSI] (2015) and European Food Safety Authority [EFSA] (2012).

Inhibitory Effect of *L. plantarum* K41 on *S. mutans* Biofilm Structure

Once it was determined at what point K41 exerted the best inhibitory effect on *S. mutans* biofilm formation, we investigated the structure of the biofilm when *S. mutans* was co-cultured with K41. The SEM micrograph in **Figure 3A** showed that UA159-species formed a compact biofilm covered by network-like structures, which were identified as EPS. The structure in UA159 biofilm, following the addition of K41, showed a looser biofilm when compared to UA159-species alone, and the amount of EPS was decreased. Moreover, K41-species biofilm showed the thinnest structure, and had few micro-colonies on the surface. CLSM results in **Figure 3B** and **Supplementary Figure S2A** confirmed that EPS in UA159 + K41 biofilm was less dense than UA159-species biofilm. Moreover, the biofilm formed by *S. mutans* UA159 was significantly thicker (65.0 μm) than that formed by *L. plantarum* K41 (18.0 μm) and by the mixed co-culture (40 μm) (**Figure 3C**). As shown in **Supplementary Figure S2B**, the EPS/bacterial ratio in UA159-species biofilm was greater

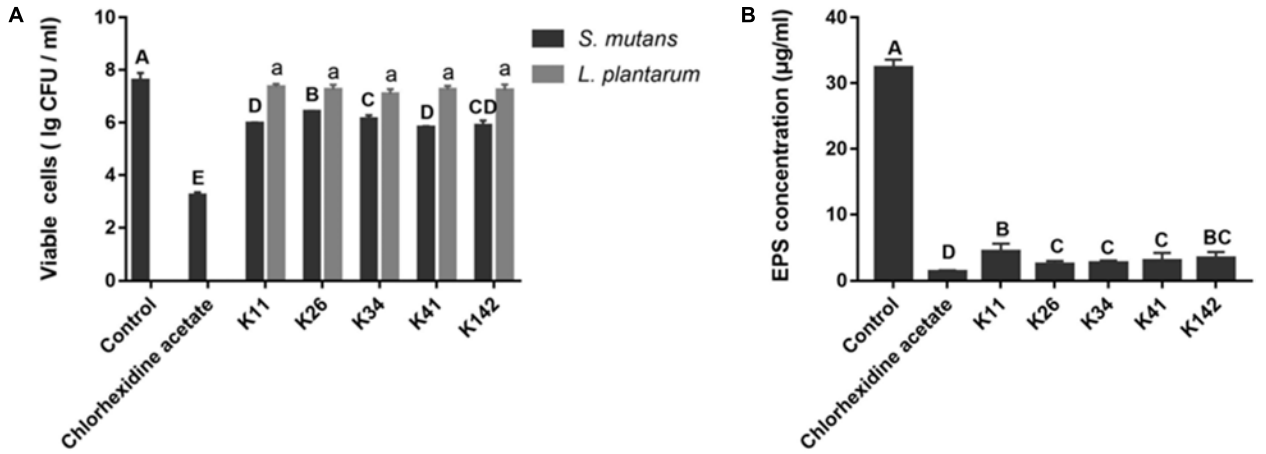

FIGURE 1 | Screening of potential probiotics with antagonistic properties against *S. mutans*. **(A)** Viable cells of *S. mutans* and *Lactobacillus* sp. in different biofilms. **(B)** EPS production by *S. mutans* in the presence of a bacterial suspension of *Lactobacillus* strains. Control: deMan-Rogosa-Sharpe media. Results with different letters are significantly different ($P < 0.05$).

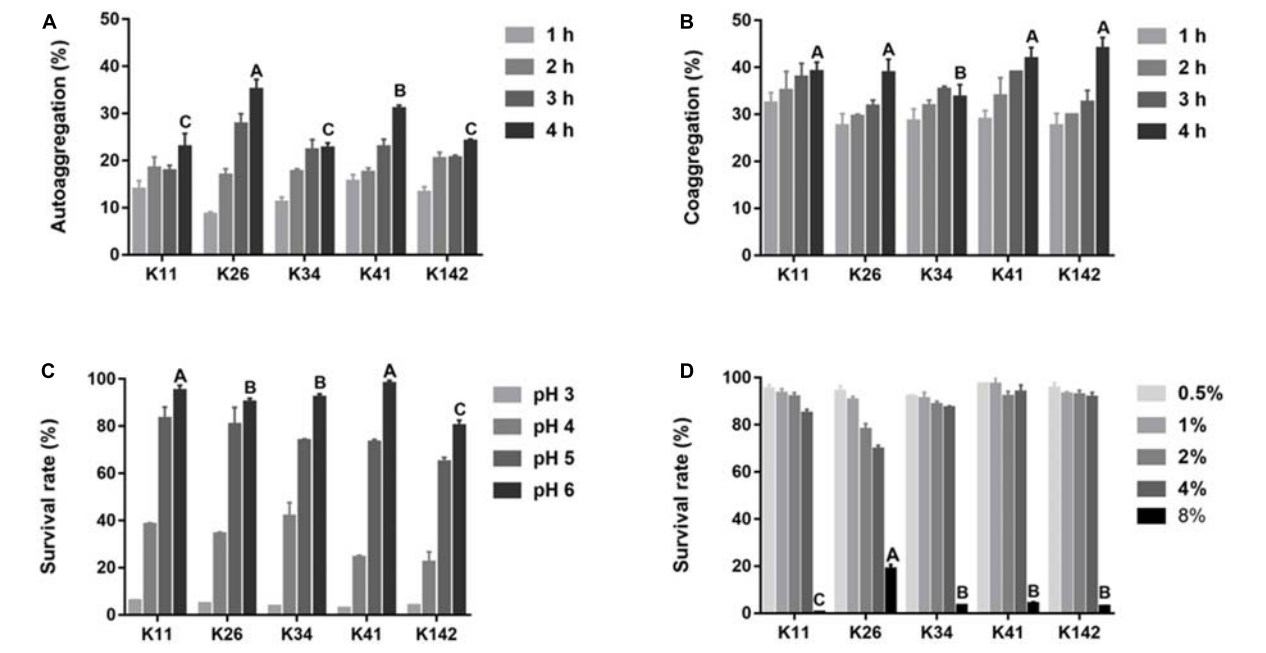

FIGURE 2 | Aggregation ability and tolerance to harsh oral condition of *L. plantarum*. **(A)** The ability of autoaggregation measured at 1, 2, 3, and 4 h. **(B)** Coaggregation of *Lactobacillus* sp. with *S. mutans* at 1, 2, 3, and 4 h. **(C)** *Lactobacillus* sp. survival rate in acid condition. **(D)** *Lactobacillus* sp. survival rate in salty condition. Control: deMan-Rogosa-Sharpe media. Values are expressed as the mean ± S.D. Results with different capital letters are significantly different ($P < 0.05$).

than in UA159 + K41 biofilm, suggesting that *L. plantarum* K41 exerted an inhibitory effect on EPS formation in biofilm.

Inhibitory Effect of *L. plantarum* K41on *S. mutans* Virulence *in vivo*

The rats remained in stable health throughout the entire experimental period. No significant weight gain or loss was observed in the treated groups (**Supplementary Figure S3**). Significant caries lesions were observed in all the untreated stained molars under stereoscopic microscopy (**Table 2**). Treatment with K41 significantly reduced the incidence and severity of smooth and sulcal caries compared with the negative control group ($P < 0.05$). The maxilla was reconstructed, and the three-dimensional images were performed in **Figure 4B**. The mean mineral density of the first molar enamel treated with K41 was higher than the one in the control group and lower than that in the positive control group (**Figure 4C**). In addition, the

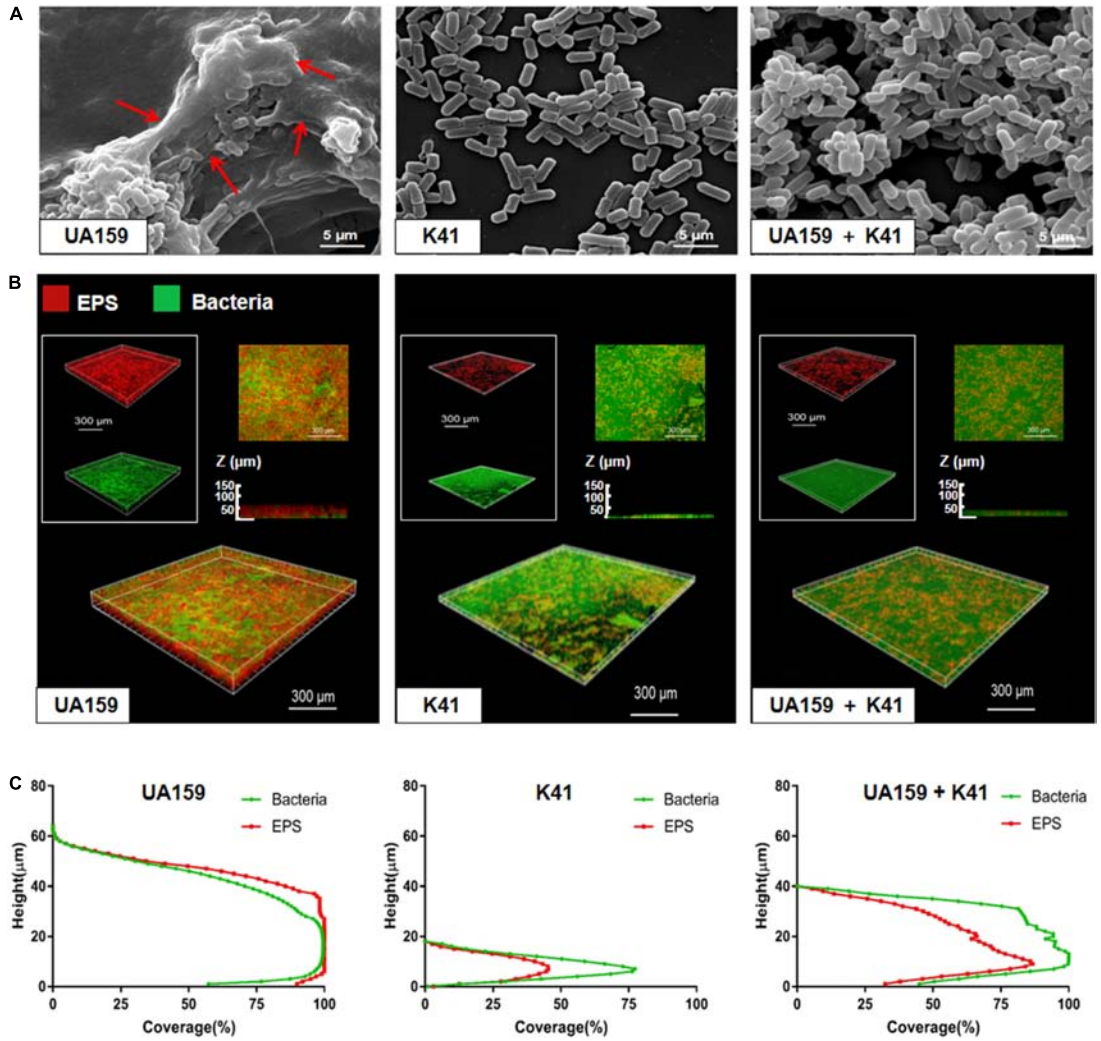

FIGURE 3 | Microscope imaging of *L. plantarum* K41 on the *S. mutans* biofilm formation. **(A)** Scanning electron microscopy (SEM) images of the structures of different biofilms. Images were taken at 20,000× magnification. **(B)** EPS (red) and bacteria (green) distribution in the double-labeled biofilm was observed by confocal laser scanning microscope (CLSM). **(C)** The distribution of bacteria and EPS at different heights. The three-dimensional reconstruction was performed by IMARIS 7.0.0. Images were taken at 60× magnification. Red arrows in **Figure 3A** were the network-like structures.

mean volume of the first molar enamel treated with K41 was larger than that of the molar treated with MRS medium and smaller compared to that of the molar treated with chlorhexidine acetate ($P < 0.05$) (**Figure 4D**). The condition of the smooth surfaces and occlusal surfaces of every jaw was recorded. The results are summarized in **Table 3**. The demineralization degree of the control group was more severe than the other three groups on both smooth and occlusal surfaces ($P < 0.01$), but no statistical difference was observed among chlorhexidine acetate (0.02%), K41 and K41 + ABY-8 group ($P > 0.01$).

DISCUSSION

Dental plaque biofilm is the ecological structure formed by a variety of microorganisms deposited on the tooth surface, and it is a key process leading to dental caries (Matsumoto et al., 2010). With the frequent exposure to dietary carbohydrate, the microbial community of plaque biofilm microbial population gradually shifts toward to cariogenic bacteria with characteristics of acidogenicity and acidurity (Bowen and Koo, 2011). Extensive investigations showed that *S. mutans* was the primary causative agent specifically found in the dental plaque (Aida et al., 2018; Jeong et al., 2018). Many probiotic solutions purportedly affecting *S. mutans* have been reported to treat dental caries (Soderling et al., 2011; Gruner et al., 2016; Schwendicke et al., 2017). Indeed in recent years, probiotic products such as probiotic powders or yogurts are becoming more and more popular as treatments for caries (Nadelman et al., 2017). Thus, it is possible that the daily application of probiotic microorganisms like *Lactobacillus* sp. through the consumption of fermented products will provide an important novel probiotic treatment for dental caries.

TABLE 2 | Effect of different treatments on the development of dental caries in rats (Keyes score).

Treatment	Smooth-surface caries	Sulcal-surface caries	Sulcal-surface severity (mean ± SD)		
			Ds[a]	Dm[b]	Dx[c]
Control[d]	55.4 ± 3.7[Af]	30.0 ± 3.6[A]	21.0 ± 2.5[A]	11.1 ± 3.4[A]	ND[e]
Chlorhexidine acetate (0.02%)	45.9 ± 3.4[B]	22.3 ± 2.3[B]	11.7 ± 2.4[B]	5.0 ± 2.6[B]	ND
K41	44.4 ± 4.6[B]	21.4 ± 4.1[B]	11.7 ± 3.5[B]	5.0 ± 1.3[B]	ND

[a]Ds: dentin exposed. [b]Dm: 3/4 of the dentin affected. [c]Dx: whole dentin affected. [d]Control: deMan-Rogosa-Sharpe media. [e]ND: not detectable. [f]Values followed by the same capital letter are not significantly different from each other.

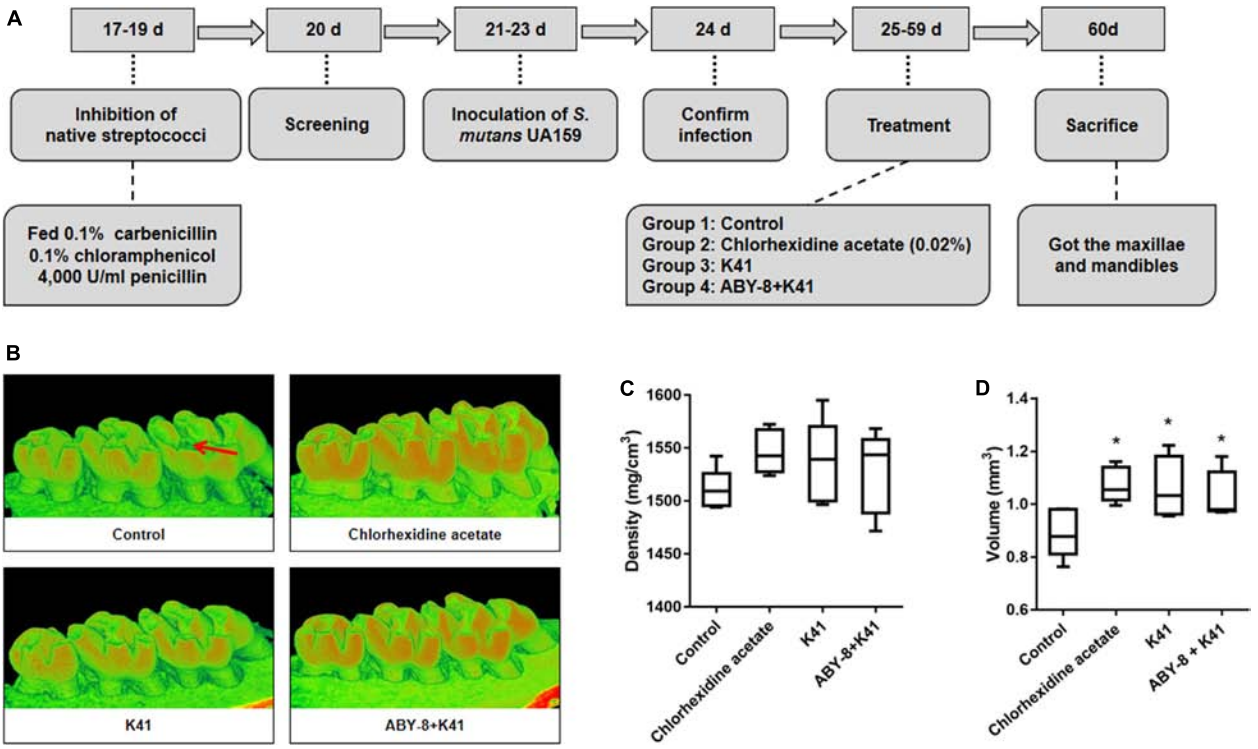

FIGURE 4 | The observation and enamel analysis of maxillary by Micro-CT. **(A)** Flow chart of animal model. **(B)** Three-dimensional images of the molar area (right column) of the left mandible. **(C)** Density of the first molar enamel. **(D)** Volume of the first molar enamel. Control: deMan-Rogosa-Sharpe media; ABY-8: a mixture culture of *S. thermophilic* and *L. bulgaricus*. "*": significant difference compared with control group ($P < 0.05$). Red arrows in **Figure 4B** were for tooth cavity. The red and green represented the degree of the mineralization, and the redder color means the higher degree of mineralization.

TABLE 3 | DIAGNOdent laser autofluorescence intensity on rat teeth.

Treatment	Smooth surface					Occlusal surface				
	Total[a]	H[b]	B[c]	S[d]	Mean Rank[e]	Total	H	B	S	Mean Rank
Control[f]	112	58	46	8	269.92[A]	42	11	19	12	105.60[A]
Chlorhexidine acetate (0.02%)	112	83	29	0	217.06[B]	42	24	18	0	68.07[B]
K41	112	88	20	4	209.66[B]	42	19	22	1	78.29[B]
K41 + ABY-8	112	92	17	3	201.36[B]	42	16	23	3	86.05[B]

[a]Total surface of each group. [b]Healthy tooth substance, read as 0~7 in smooth surfaces and 0~12 in occlusal surfaces. [c]Beginning of the demineralization, read as 8~15 in smooth surfaces and 13~24 in occlusal surfaces. [d]Strong demineralization, read as ≥15 in smooth surfaces and ≥25 in occlusal surfaces. [e]Statistically significant capital differences ($P < 0.05$) were observed between groups assessed. [f]Control: deMan-Rogosa-Sharpe media.

Although numerous studies have explored the potential benefit of probiotics to oral health (Campus et al., 2014; Lin and Pan, 2014), there is currently no standardized or comprehensive protocol for screening novel oral probiotics *in vitro*. Although it has been reported that probiotics inhibiting the growth of *S. mutans* it was thought that it did not necessarily control dental caries. Despite this the inhibition of biofilm formation by probiotics may well be relevant in the reduction of carinogenicity (Schwendicke et al., 2017). The main action of *Lactobacillus* sp. observed here was the inhibition of the formation of *S. mutans* biofilm and the reduction of the dental caries occurrence. In our study, the inhibitory rate of biofilm formation by *S. mutans* when co-cultured with *L. plantarum* K41 was 98.4%, which was similar to that of *W. cibaria CMU* of approximately 95% (Jang et al., 2016). Moreover, the inhibitory effect of *L. plantarum* K41 against *S. mutans* was higher than chlorhexidine acetate. In addition, the inhibitory rate in the formation of insoluble EPS by K41 was 90.7%, which was significantly higher than that for the previously reported *L. plantarum* K25 (21.44%) (Guo et al., 2016). Therefore, *L. plantarum* K41 provides an inhibitory effect on biofilm formation, indicating its potential beneficial effect in control of dental caries.

Lactobacillus sp. may provide a beneficial effect of reducing the occurrence of dental caries by having an inhibitory effect on biofilm formation *in vitro*. To be effective it must also be able to survive in the condition of the mouth (Jeong et al., 2018). Indeed, it is possible that *Lactobacillus paracasei* F19 had no long-term effect on the incidence of caries due to poor viability under the oral conditions over a long time (Hasslöf et al., 2013). Adhesion to epithelial cells and mucosal surfaces is the primary indicator of the effect of *Lactobacillus* sp. in maintaining oral health, and it is a multistep process involving the composition, structure and forces of interaction related to the intestinal epithelial cells or mucosal surfaces (Hagerman et al., 2010). In most cases, autoaggregation is beneficial for adhesion, and coaggregation with *S. mutans* may form a barrier to prevent the action of pathogenic microorganisms (Del et al., 2000; Lang et al., 2010). In our research, the coaggregation and autoaggregation rates at 4 h of *L. plantarum* K41 were 41.87 and 31.01%, respectively, which was similar to *L. plantarum* K25 as previously reported (Guo et al., 2016). Moreover, as harsh oral conditions due to the intake of low-acid or high-salt food, may affect the viability of probiotics the ability of K41 to withstand these conditions make it a candidate for probiotics. In view of horizontal gene transfer occurring in dental biofilms, the microbiological breakpoints of Clinical Laboratory Standards Institute [CLSI] (2015) and European Food Safety Authority [EFSA] (2012) indicate that the use of K41 in food is safe. Moreover, it has been reported that the antibiotics' resistance of the *Lactobacillus* strains used widely in fermentation processes is not likely to have the potential health threat to humans (Ma et al., 2017).

To further verify the inhibitory effect of *L. plantarum* K41 on dental caries, an animal model was established to examine whether K41 could reduce the incidence of caries. In a previous study, *L. paracasei* subsp. paracasei NTU 101 was found to be protective against the development of dental caries in rats (Lin and Pan, 2014), but no report is available to date with regards to the inhibitory effect of *L. plantarum* on dental caries in animal models. When compared with micro-CT, the process of laser fluorescence intensity assessment was simple and convenient and thus used here. This enabled the use of one half of the maxilla of five rats in each group for micro-CT analysis, while the other half and mandible of eight rats were used for the assessment of the degree of demineralization by laser fluorescence intensity assessment. According to the analysis of micro-CT, the density was not significantly different among the four groups ($P > 0.05$), perhaps due to the individual differences and sampling capacity. Moreover, caries scoring assay, which is widely used in the clinical examination of dental caries, was also used to detect the caries lesions. In our study, we found that caries lesions and demineralization degree in K41 group were significantly lower than those of control group, suggesting that K41 had also beneficial effect on the control of dental caries.

Recently, an increased interest in the application of probiotics for oral health has emerged, and the concept of using probiotics to prevent caries has been proposed (Isabelle and Teughels, 2015; Pahumunto et al., 2019). To date, probiotics have been added to some functional beverages, while fermented milk is considered to be the most widely food vehicle supplemented with probiotic bacteria due to its unique taste and high nutritional properties (Balthazar et al., 2017; Nadelman et al., 2017; Nadelman et al., 2019). Therefore, *L. plantarum* K41 shows a potential commercial value when added to dairy products.

However, the animal assay still has its limitations. Our animal assay missed evaluating the influence of *L. plantarum* K41 on lesions in dentin and root caries. Rat-molars were treated by *L. plantarum* K41 following *S. mutans* infection and were assessed, even if there was no gross morphological evidence of dental caries lesions. The colonization of the oral cavity by *Lactobacilli* requires a retentive niche (Caufield et al., 2005). Our animal assay could not prove the relationship of K41 with root caries. It was commonly accepted that *L. acidophilus* was dominant in deep caries samples (Martin et al., 2002). In the future, the effect of K41 on root or dentin caries should be fully investigated.

In conclusion, our work demonstrated that *L. plantarum* K41 isolated from traditional Sichuan pickles had an inhibitory effect on the biofilm formation of *S. mutans*. Our results offer a potential alternative strategy for the control of oral biofilm/dental plaque and dental caries.

DATA AVAILABILITY STATEMENT

All datasets generated for this study are included in the article/**Supplementary Material**.

ETHICS STATEMENT

This study was carried out in accordance with the recommendations of the Swiss Animal Protection Ordinance. It was reviewed and approved by the Ethics Committee of the College of Life Sciences, Sichuan University (No. 20191217001; Sichuan University, Chengdu, China).

AUTHOR CONTRIBUTIONS

QS, YQL, GZ, and ML designed the studies. GZ and ML performed the experiments and wrote the manuscript. YT, RL, YL, and VV assisted the growth inhibition and biofilm formation experiments. RL, YL, and BL assisted the establishment of caries models. GZ, ML, YT, VV, AK, and BL analyzed the data. AK, QS, and YQL revised the manuscript. The manuscript has been reviewed and approved by all authors before submission.

FUNDING

This work was supported by grants from the National Natural Science Foundation of China (31870065), the National Key Research and Development Projects (SQ2019YFE010495), and the Key Research and Development Program of Sichuan (2018HH0030 and 2017FZ0018).

SUPPLEMENTARY MATERIAL

The Supplementary Material for this article can be found online at: https://www.frontiersin.org/articles/10.3389/fmicb.2020.00774/full#supplementary-material

FIGURE S1 | The growth inhibition assay plate.

FIGURE S2 | Quantitative analysis in the double-labeled biofilm observed by confocal microscopy. **(A)** Quantification of bacteria and EPS biomass. **(B)** The ratio of EPS to bacteria at different heights in biofilms. Values are expressed as mean ± SD.

FIGURE S3 | Effects of different treatments on rat weight gain. Values are expressed as mean ± S.D.

FIGURE S4 | Standard curve for EPS quantitative determination by anthrone-sulfuric method.

TABLE S1 | The concentration of antibiotics tested.

TABLE S2 | The MIC distributions and breakpoints of *L. plantarum* against antibiotics tested.

REFERENCES

Aida, K. L., Kreling, P. F., Caiaffa, K. S., Calixto, G., Chorilli, M., Spolidorio, D. M., et al. (2018). Antimicrobial peptide-loaded liquid crystalline precursor bioadhesive system for the prevention of dental caries. *Int. J. Nanomed.* 13, 3081–3091. doi: 10.2147/IJN.S155245

Andre, C. B., Rosalen, P. L., Galvao, L. C. C., Fronza, B. M., Ambrosano, G. M. B., Ferracane, J. L., et al. (2017). Modulation of *Streptococcus mutans* virulence by dental adhesives containing anti-caries agents. *Dent. Mater.* 33, 1084–1092. doi: 10.1016/j.dental.2017.07.006

Bal, F. A., Ozkocak, I., Cadirci, B. H., Karaarslan, E. S., Cakdinleyen, M., and Agaccioglu, M. (2019). Effects of photodynamic therapy with indocyanine green on *Streptococcus mutans* biofilm. *Photodiagnosis Photodyn. Ther.* 29, 226–234. doi: 10.1016/j.pdpdt.2019.04.005

Balthazar, C. F., Pimentel, T. C., Ferrão, L. L., Almada, C. N., Santillo, A., Albenzio, M., et al. (2017). Sheep milk: physicochemical characteristics and relevance for functional food development. *Compr. Rev. Food Sci. F* 16, 247–262. doi: 10.1111/1541-4337.12250

Beiraghi, S., Rosen, S., and Beck, F. (1990). The effect of stannous and sodium fluoride on coronal caries, root caries and bone loss in rice rats. *Arch. Oral Biol.* 35, 79–80. doi: 10.1016/0003-9969(90)90120-Y

Bosch, M., Nart, J., Audivert, S., Bonachera, M. A., Alemany, A. S., Fuentes, M. C., et al. (2012). Isolation and characterization of probiotic strains for improving oral health. *Arch. Oral Biol.* 57, 539–549. doi: 10.1016/j.archoralbio.2011.10.006

Bowen, W. H., and Koo, H. (2011). Biology of *Streptococcus mutans*-derived glucosyltransferases: role in extracellular matrix formation of cariogenic biofilms. *Caries Res.* 45, 69–86. doi: 10.1159/000324598

Campus, G., Cocco, F., Carta, G., Cagetti, M. G., Simark-Mattson, C., Strohmenger, L., et al. (2014). Effect of a daily dose of *Lactobacillus brevis* CD2 lozenges in high caries risk schoolchildren. *Clin. Oral Invest.* 18, 555–561. doi: 10.1007/s00784-013-0980-9

Caufield, P. W., Li, Y., and Dasanayake, A. (2005). Dental caries: an infectious and transmissible disease. *Compend. Contin. Educ. Dent.* 26(5 Suppl. 1), 10–16. doi: 10.1016/S0031-3955(05)70255-8

Cheng, X., Zheng, X., Zhou, X., Zeng, J., Ren, Z., Xu, X., et al. (2016). Regulation of oxidative response and extracellular polysaccharide synthesis by a diadenylate cyclase in *Streptococcus mutans*. *Environ. Microbiol.* 18, 904–922. doi: 10.1111/1462-2920.13123

Chun, C. C., Chen, K. C., Pin Der, D., Peng, S. W., and Shu, C. W. (2013). Antibacterial properties of *Lactobacillus plantarum* isolated from fermented mustards against *Streptococcus mutans*. *Afr. J. Microbiol. Res.* 7, 4787–4793. doi: 10.5897/ajmr12.1885

Clinical and Laboratory Standards Institute [CLSI], (2015). *Methods for Antimicrobialdilution and Disc Susceptibility Testing of Infrequently Isolated or Fastidious Bacteria; Approved Guideline*, 3rd Edn. Wayne, PA: CLSI.

Del, R. B., Sgorbati, B., Miglioli, M., and Palenzona, D. (2000). Adhesion, autoaggregation and hydrophobicity of 13 strains of *Bifidobacterium longum*. *Lett. Appl. Microbiol.* 31, 438–442. doi: 10.1046/j.1365-2672.2000.00845.x

Du, M. Q., Li, Z., Jiang, H., Wang, X., Feng, X. P., Hu, Y., et al. (2018). Dental caries status and its associated factors among 3- to 5-year-old children in China: a national survey. *Chin. J. Dent. Res.* 21, 167–179. doi: 10.3290/j.cjdr.a41076

European Food Safety Authority [EFSA], (2012). Guidance on the assessment ofbacterial susceptibility to antimicrobials of human, and veterinary importance. *EFSA J.* 10:2740. doi: 10.2903/j.efsa.2012.2740

Fernandes, T., Bhavsar, C., Sawarkar, S., and D'souza, A. (2018). Current and novel approaches for control of dental biofilm. *Int. J. Pharm.* 536, 199–210. doi: 10.1016/j.ijpharm.2017.11.019

Fitzgerald, R. J., Jordan, H. V., and Archard, H. O. (1966). Dental caries in gnotobiotic rats infected with a variety of *Lactobacillus acidophilus*. *Arch. Oral Biol.* 11, 473–476. doi: 10.1016/0003-9969(66)90153-1

Gruner, D., Paris, S., and Schwendicke, F. (2016). Probiotics for managing caries and periodontitis: systematic review and meta-analysis. *J. Dent.* 48, 16–25. doi: 10.1016/j.jdent.2016.03.002

Gunsolley, J. C. (2010). Clinical efficacy of antimicrobial mouthrinses. *J. Dent.* 38, S6–S10. doi: 10.1016/S0300-5712(10)70004-X

Guo, X., Zhang, J., and Yang, Z. (2016). Screening of lactic acid bacteria for Inhibiting oral *Streptococcus mutans* and preliminary study of antibacterial mechanism. *Food Sci.* 37, 117–122. doi: 10.7506/spkx1002-6630-201619020

Hagerman, E. M., Chao, S. J., and Wu, B. M. (2010). Surface modification and initial adhesion events for intestinal epithelial cells. *J. Biomed. Mater. Res. A* 76A, 272–278. doi: 10.1002/jbm.a.30562

Han, S., Fan, Y., Zhou, Z., Tu, H., Li, D., Lv, X., et al. (2017). Promotion of enamel caries remineralization by an amelogenin-derived peptide in a rat model. *Arch. Oral Biol.* 73, 66–71. doi: 10.1016/j.archoralbio.2016.09.009

Haps, S., Slot, D. E., Berchier, C. E., and Weijden, G. V. (2008). The effect of cetylpyridinium chloride-containing mouth rinses as adjuncts to toothbrushing on plaque and parameters of gingival inflammation: a systematic review. *Int. J. Dent. Hyg.* 6, 290–303. doi: 10.1111/j.1601-5037.2008.00344.x

Hasslöf, P., West, C. E., Videhult, F. K., Brandelius, C., and Stecksen-Blicks, C. (2013). Early intervention with probiotic *Lactobacillus paracasei* F19 has no long-term effect on caries experience. *Caries Res.* 47, 559–565. doi: 10.1159/000350524

He, J., Wang, S., Wu, T., Cao, Y., Xu, X., and Zhou, X. (2013). Effects of ginkgoneolic acid on the growth, acidogenicity, adherence, and biofilm of *Streptococcus mutans in vitro*. *Folia Microbiol.* 58, 147–153. doi: 10.1007/s12223-012-0191-9

International Organization of Standardization/International Dairy Federation (ISO10932/Idf 223), (2010). *Milk, and milk products. Determination of the (Minimalinhibitory)Concentration (MIC) of Antibiotics Applicable To Bifidobacteria and Nonenterococcal Lactic Acid Bacteria (LAB)*. Geneva: ISO and IDF.

Isabelle, L., and Teughels, W. (2015). Probiotics in the dental practice: a review. *Quintessence Int.* 46, 225–264. doi: 10.3290/j.qi.a33182

Ito, K., Ito, S., Shimamura, T., Weyand, S., Kawarasaki, Y., Misaka, T., et al. (2011). Crystal structure of glucansucrase from the dental caries pathogen *Streptococcus mutans*. *J. Mol. Biol.* 408, 177–186. doi: 10.1016/j.jmb.2011.02.028

Jang, H. J., Kang, M. S., Yi, S. H., Hong, J. Y., and Hong, S. P. (2016). Comparative study on the characteristics of *Weissella cibaria* CMU and probiotic strains for oral care. *Molecules* 21:1752. doi: 10.3390/molecules21121752

Jeong, D., Kim, D. H., Song, K. Y., and Seo, K. H. (2018). Antimicrobial and anti-biofilm activities of *Lactobacillus kefiranofaciens* DD2 against oral pathogens. *J. Oral Microbiol.* 10:1472985. doi: 10.1080/20002297.2018.1472985

Kassebaum, N. J., Bernabé, E., Dahiya, M., Bhandari, B., Murray, C. J. L., and Marcenes, W. (2015). Global burden of untreated caries. *J. Dent. Res.* 94, 650–658. doi: 10.1177/0022034515573272

Kaye, E. K. (2017). Daily intake of probiotic *Lactobacilli* may reduce caries risk in young children. *J. Evid. Based Dent. Res.* 17, 284–286. doi: 10.1016/j.jebdp.2017.07.005

Keyes, P. H. (1958). Dental caries in the molar teeth of rats. II. A method for diagnosing and scoring several types of lesions simultaneously. *J. Dent. Res.* 37, 1088. doi: 10.1177/00220345580370060901

Kidd, E. A. M., and Fejerskov, O. (2016). What constitutes dental caries? Histopathology of carious enamel and dentin related to the action of cariogenic biofilms. *J. Dent. Res.* 83, 35–38. doi: 10.1177/154405910408301s07

Kim, D., Hwang, G., Liu, Y., Wang, Y., Singh, A. P., Vorsa, N., et al. (2015). Cranberry flavonoids modulate cariogenic properties of mixed-species biofilm through exopolysaccharides-matrix disruption. *PLos One* 10:e0145844. doi: 10.1371/journal.pone.0145844

Koo, H., Duarte, S., Murata, R. M., Scott-Anne, K., Gregoire, S., Watson, G. E., et al. (2010). Influence of cranberry proanthocyanidins on formation of biofilms by *Streptococcus mutans* on saliva-coated apatitic surface and on dental caries development *in vivo*. *Caries Res.* 44, 116–126.

Koo, H., Falsetta, M. L., and Klein, M. I. (2013). The exopolysaccharide matrix: a virulence determinant of cariogenic biofilm. *J. Dent. Res.* 92, 1065–1073. doi: 10.1177/0022034513504218

Kulshrestha, S., Khan, S., Hasan, S., Khan, M. E., Misba, L., and Khan, A. U. (2016). Calcium fluoride nanoparticles induced suppression of *Streptococcus mutans* biofilm: an *in vitro* and *in vivo* approach. *Appl. Microbiol. Biotechnol.* 100, 1901–1914. doi: 10.1007/s00253-015-7154-4

Lang, C., Boettner, M., Holz, C., Veen, M., Ryser, M., Reindl, A., et al. (2010). Specific *Lactobacillus*/*mutans Streptococcus* co-aggregation. *J. Dent. Res.* 89, 175–179. doi: 10.1177/0022034509356246

Li, C., Song, J., Kwok, L. Y., Wang, J., Dong, Y., Yu, H., et al. (2017). Influence of *Lactobacillus plantarum* on yogurt fermentation properties and subsequent changes during postfermentation storage. *J. Dairy Sci.* 100, 2512–2525. doi: 10.3168/jds.2016-11864

Li, P., Gu, Q., and Zhou, Q. (2016). Complete genome sequence of *Lactobacillus plantarum* LZ206, a potential probiotic strain with antimicrobial activity against food-borne pathogenic microorganisms. *J. Biotechnol.* 238, 52–55. doi: 10.1016/j.jbiotec.2016.09.012

Lin, T.-H., and Pan, T.-M. (2014). Inhibitory effect of *Lactobacillus paracasei* subsp. paracasei NTU 101 on rat dental caries. *J. Funct. Foods* 10, 223–231. doi: 10.1016/j.jff.2014.06.015

Ma, Q., Fu, Y., Sun, H., Huang, Y., Li, L., Yu, Q., et al. (2017). Antimicrobial resistance of *Lactobacillus* spp. from fermented foods and human gut. *LWT Food Sci. Technol.* 86, 201–208. doi: 10.1016/j.lwt.2017.07.059

Martin, F. E., Nadkarni, M. A., Jacques, N. A., and Hunter, N. (2002). Quantitative microbiological study of human carious dentine by culture and real-time PCR: association of anaerobes with histopathological changes in chronic pulpitis. *J. Clin. Microbiol.* 40, 1698–1704. doi: 10.1128/JCM.40.5.1698-1704.2002

Matsumoto, N., Salam, M. A., Watanabe, H., Amagasa, T., and Senpuku, H. (2010). Role of gene E2f1 in susceptibility to bacterial adherence of oral *streptococci* to tooth surfaces in mice. *Mol. Oral Microbiol.* 19, 270–276. doi: 10.1111/j.1399-302X.2004.00151.x

Murata, R. M., Brancodealmeida, L. S., Franco, E. M., Yatsuda, R., Santos, M. H. D., Alencar, S. M. D., et al. (2010). Inhibition of *Streptococcus mutans* biofilm accumulation and development of dental caries in vivo by 7-epiclusianone and fluoride. *Biofouling* 26, 865–872. doi: 10.1080/08927014.2010.527435

Nadelman, P., Frazao, J. V., Vieira, T. I., Balthazar, C. F., Andrade, M. M., Alexandria, A. K., et al. (2017). The performance of probiotic fermented sheep milk and ice cream sheep milk in inhibiting enamel mineral loss. *Food Res. Int.* 97, 184–190. doi: 10.1016/j.foodres.2017.03.051

Nadelman, P., Monteiro, A., Balthazar, C. F., Silva, H. L. A., Cruz, A. G., De Almeida Neves, A., et al. (2019). Probiotic fermented sheep's milk containing *Lactobacillus casei* 01: effects on enamel mineral loss and *Streptococcus* counts in a dental biofilm model. *J. Funct. Foods* 54, 241–248. doi: 10.1016/j.jff.2019.01.025

Pahumunto, N., Sophatha, B., Piwat, S., and Teanpaisan, R. (2019). Increasing salivary IgA and reducing *Streptococcus mutans* by probiotic *Lactobacillus paracasei* SD1: a double-blind, randomized, controlled study. *J. Dent. Sci.* 14, 178–184. doi: 10.1016/j.jds.2019.01.008

Rams, T. E., and Alwaqyan, A. Y. (2017). *In vitro* performance of DIAGNOdent laser fluorescence device for dental calculus detection on human tooth root surfaces. *Saudi Dent. J.* 29, 171–178. doi: 10.1016/j.sdentj.2017.08.001

Ren, Z., Cui, T., Zeng, J., Chen, L., Zhang, W., Xu, X., et al. (2016). Molecule targeting glucosyltransferase inhibits *Streptococcus mutans* biofilm formation and virulence. *Antimicrob. Agents Chemother.* 60, 126–135. doi: 10.1128/AAC.00919-15

Rodríguez, G., Ruiz, B., Faleiros, S., Vistoso, A., Marró, M. L., Sánchez, J., et al. (2016). Probiotic compared with standard milk for high-caries children: a cluster randomized trial. *J. Dent. Res.* 95, 402–407. doi: 10.1177/0022034515623935

Sanders, M. E., and Marco, M. L. (2010). Food formats for effective delivery of probiotics. *Annual Rev. Food Sci. Technol.* 1, 65–85. doi: 10.1146/annurev.food.080708.100743

Schwendicke, F., Korte, F., Dörfer, C. E., Kneist, S., Fawzy, E.-S. K., and Paris, S. (2017). Inhibition of *Streptococcus mutans* growth and biofilm formation by probiotics *in vitro*. *Caries Res.* 51, 87–95.

Soderling, E. M., Marttinen, A. M., and Haukioja, A. L. (2011). Probiotic lactobacilli interfere with *Streptococcus mutans* biofilm formation *in vitro*. *Curr Microbiol.* 62, 618–622. doi: 10.1007/s00284-010-9752-9

Tahmourespour, A., and Kermanshahi, R. K. (2011). The effect of a probiotic strain (*Lactobacillus acidophilus*) on the plaque formation of oral *Streptococci*. *Bosn. J. Basic Med. Sci.* 11, 37–40.

Tian, W., Zhang, Q., Deng, Z. Z., Liu, S., Ming-Yuan, L. I., Che, Z. M., et al. (2013). Analysis of bacterial diversity in Chinese traditional fermented Sichuan pickles using 16S rRNA genes. *Food Sci.* 34, 215–218. doi: 10.7506/spkx1002-6630-201317046

Van Leeuwen, M. P., Slot, D. E., and Van, W. G. A. (2011). Essential oils compared to chlorhexidine with respect to plaque and parameters of gingival inflammation: a systematic review. *J. Periodontol.* 82, 174–194. doi: 10.1902/jop.2010.100266

Vermeiren, L., Devlieghere, F., and Debevere, J. (2004). Evaluation of meat born lactic acid bacteria as protective cultures for the biopreservation of cooked meat products. *Int. J. Food Microbiol.* 96, 149–164. doi: 10.1016/j.ijfoodmicro.2004.03.016

Vijayendra, S. V. N., Palanivel, G., Mahadevamma, S., and Tharanathan, R. N. (2009). Physico-chemical characterization of a new heteropolysaccharide produced by a native isolate of heterofermentative *Lactobacillus* sp, CFR-2182. *Arch. Microbiol.* 191, 303–310. doi: 10.1007/s00203-008-0453-8

Vries, M. C. D., Vaughan, E. E., Kleerebezem, M., and Vos, W. M. D. (2006). *Lactobacillus plantarum*- survival, functional and potential probiotic properties in the human intestinal tract. *Int. Dairy J.* 16, 1018–1028. doi: 10.1016/j.idairyj.2005.09.003

Wu, C. C., Lin, C. T., Wu, C. Y., Peng, W. S., Lee, M. J., and Tsai, Y. C. (2015). Inhibitory effect of *Lactobacillus salivarius* on *Streptococcus mutans* biofilm formation. *Mol Oral Microbiol.* 30, 16–26. doi: 10.1111/omi.12063

Xiao, J., Klein, M. I., Falsetta, M. L., Lu, B., Delahunty, C. M., Yates, J. R., et al. (2012). The exopolysaccharide matrix modulates the interaction between

3D architecture and virulence of a mixed-species oral biofilm. *PLoS Pathog.* 8:e1002623. doi: 10.1371/journal.ppat.1002623

Xu, X., Zhou, X. D., and Wu, C. D. (2012). Tea catechin epigallocatechin gallate inhibits *Streptococcus mutans* biofilm formation by suppressing gtf genes. *Arch Oral Biol.* 57, 678–683. doi: 10.1016/j.archoralbio.2011.10.021

Yue, J., Yang, H., Liu, S., Song, F., Guo, J., and Huang, C. (2018). Influence of naringenin on the biofilm formation of *Streptococcus mutans*. *J. Dent.* 76, 24–31. doi: 10.1016/j.jdent.2018.04.013

Zhang, Q., Nguyen, T., McMichael, M., Velu, S. E., Zou, J., Zhou, X., et al. (2015). New small – molecule inhibitors of dihydrofolate reductase inhibit *Streptococcus mutans*. *Int. J. Antimicrob. Agents* 46, 174–182. doi: 10.1016/j.ijantimicag.2015.03.015

Zhang, X. Q., Zhang, X. P., Xiao-Lin, A. O., Liu, X. Q., and Biao, P. U. (2013). PCR-DGGE analysis of microbial diversity of homemade pickles in sichuan region. *Food Sci.* 34, 129–134.

Zhu, X., Zhao, Y., Sun, Y., and Gu, Q. (2014). Purification and characterisation of plantaricin ZJ008, a novel bacteriocin against Staphylococcus spp. from *Lactobacillus plantarum* ZJ008. *Food Chem.* 165, 216–223. doi: 10.1016/j.foodchem.2014.05.034

Conflict of Interest: The authors declare that the research was conducted in the absence of any commercial or financial relationships that could be construed as a potential conflict of interest.

frontiers in Microbiology

ORIGINAL RESEARCH
published: 16 June 2020
doi: 10.3389/fmicb.2020.00999

Mitigation of the Toxic Effects of Periodontal Pathogens by Candidate Probiotics in Oral Keratinocytes, and in an Invertebrate Model

Raja Moman[1], Catherine A. O'Neill[2], Ruth G. Ledder[3], Tanaporn Cheesapcharoen[3] and Andrew J. McBain[3]*

[1] Department of Microbiology and Immunology, Faculty of Pharmacy, University of Tripoli, Tripoli, Libya, [2] Division of Musculoskeletal and Dermatological Sciences, School of Biological Sciences, The University of Manchester, Manchester, United Kingdom, [3] Division of Pharmacy and Optometry, School of Health Sciences, Faculty of Biology, Medicine and Health, The University of Manchester, Manchester, United Kingdom

The larvae of the wax moth *Galleria mellonella* and human oral keratinocytes were used to investigate the protective activity of the candidate oral probiotics *Lactobacillus rhamnosus* GG (LHR), *Lactobacillus reuteri* (LR), and *Streptococcus salivarius* K-12 (SS) against the periodontal pathogens *Fusobacterium nucleatum* (FN), *Porphyromonas gingivalis* (PG), and *Aggregatibacter actinomycetemcomitans* (AA). Probiotics were delivered to the larvae (i) concomitantly with the pathogen in the same larval pro-leg; (ii) concomitantly with the pathogen in different pro-legs, and (iii) before inoculation with the pathogen in different pro-legs. Probiotics were delivered as viable cells, cell lysates or cell supernatants to the oral keratinocytes concomitantly with the pathogen. The periodontal pathogens killed at least 50% of larvae within 24 h although PG and FN were significantly more virulent than AA in the order *FN* > *PG* > *AA* and were also significantly lethal to mammalian cells. The candidate probiotics, however, were not lethal to the larvae or human oral keratinocytes at doses up to 10^7 cells/larvae. Wax worm survival rates increased up to 60% for some probiotic/pathogen combinations compared with control larvae inoculated with pathogens only. SS was the most effective probiotic against FN challenge and LHR the least, in simultaneous administration and pre-treatment, SS and LR were generally the most protective against all pathogens (up to 60% survival). For *P. gingivalis*, LR > LHR > SS, and for *A. actinomycetemcomitans* SS > LHR and LR. Administering the candidate probiotics to human oral keratinocytes significantly decreased the toxic effects of the periodontal pathogens. In summary, the periodontal pathogens were variably lethal to *G. mellonella* and human oral keratinocytes and the candidate probiotics had measurable protective effects, which were greatest when administrated simultaneously with the periodontal pathogens, suggesting protective effects based on bacterial interaction, and providing a basis for mechanistic studies.

Keywords: periodontal pathogens, *Galleria mellonella*, probiotics, infection model, keratinocytes

OPEN ACCESS

Edited by:
Giovanna Batoni, University of Pisa, Italy

Reviewed by:
María Carmen Sánchez, Complutense University of Madrid, Spain
Ashu Sharma, University at Buffalo, United States

****Correspondence:***
Ruth G. Ledder
ruth.ledder@manchester.ac.uk

Specialty section:
This article was submitted to Infectious Diseases, a section of the journal Frontiers in Microbiology

Received: *21 February 2020*
Accepted: *24 April 2020*
Published: *16 June 2020*

Citation:
Moman R, O'Neill CA, Ledder RG, Cheesapcharoen T and McBain AJ (2020) Mitigation of the Toxic Effects of Periodontal Pathogens by Candidate Probiotics in Oral Keratinocytes, and in an Invertebrate Model. Front. Microbiol. 11:999. doi: 10.3389/fmicb.2020.00999

INTRODUCTION

Periodontitis is a complex infectious disease associated with inflammation and the loss of periodontal attachment and bone support. It has several etiological and contributing factors such as the accumulation of biofilm and calculus (Wolf et al., 2005; Slots, 2017) and the presence of certain bacteria that have been identified as periodontal pathogens. There are several concepts of periodontal pathogenesis including the specific plaque hypothesis, which emphasizes the importance of specific bacteria (Nisha et al., 2017); the concept of keystone pathogens (Hajishengallis and Lamont, 2012) where a given bacterium exerts effects that are disproportionate to its abundance, and the polymicrobial synergy and dysbiosis model (Lamont and Hajishengallis, 2015; Nisha et al., 2017) all of which are significantly related to oral bacteria. Gram-negative anaerobic bacteria, in particular, have been implicated in the etiology of periodontitis. *Aggregatibacter actinomycetemcomitans, Fusobacterium nucleatum,* and *Porphyromonas gingivalis,* as well as other bacterial species including *Tannerella forsythia* and *Treponema denticola* (Socransky et al., 1998) are considered to be the important contributors to periodontitis in humans (Slots et al., 1986; Dzink et al., 1988; Duncan et al., 1993; Sandros et al., 1994).

A. actinomycetemcomitans is reported to damage host tissue via the production of a leukotoxin (Johansson, 2011), and a cytolethal distending toxin (DiRienzo, 2014). *F. nucleatum* directly influences host responses and can also increase the infectivity of other pathogens via the induction of expression of the antimicrobial peptide β-defensin and pro-inflammatory cytokines in the oral epithelium (Krisanaprakornkit et al., 2000; Bhattacharyya et al., 2016; Ahn et al., 2017). *P. gingivalis* expresses two types of gingipains (Imamura, 2003), which are reportedly implicated in the progression of periodontal disease and have been strongly associated with the induction of inflammation and destruction of the host periodontium (Miyachi et al., 2007). *Porphyromonas gingivalis* has been linked to the perturbation of periodontal microbial homeostasis. Hence, this bacterium has been proposed as a keystone periodontal pathogen (Hajishengallis and Lamont, 2012).

The potential of putatively beneficial bacteria (probiotics) to prevent or treat periodontitis and other oral diseases has been investigated (Vivekananda et al., 2010; Ince et al., 2015; Bohora and Kokate, 2017; Brignardello-Petersen, 2017; Kobayashi et al., 2017). Previous investigations have demonstrated the ability of certain species of *Lactobacillus* to inhibit the growth of *P. gingivalis* and *A. actinomycetemcomitans* (Sookkhee et al., 2001; Kõll-Klais et al., 2005). Krasse et al. (2006) reported decreased gum bleeding and reduced gingivitis following the administration of a *Lactobacillus reuteri*-based candidate probiotic suggesting mechanisms including the production of bacteriocins such as reuterin, competition with oral pathogens, and anti-inflammatory activity (Krasse et al., 2006). Another study proposed that *Lactobacillus rhamnosus* GG could suppress bone loss in a mouse model of induced periodontitis (Gatej et al., 2018). The administration of *S. salivarius* K12 has been associated with reduced alveolar bone loss and resorption in a murine periodontitis model (Zhu et al., 2019).

The use of alternative animal models for studying pathogenic microorganisms has increased in recent years (Swanson and Hammer, 2000; Casadevall, 2005; Chamilos et al., 2011) for several reasons, including throughput, cost, and ethics (Ball et al., 1995). In addition to the fact that microbial virulence mechanisms may be common between different hosts (Rahme et al., 1995), larvae are simple to work with, inherently replicable, and have a short life cycle in comparison to higher animals (Tsai et al., 2016). The presence of an innate immune system in invertebrates (Boman and Hultmark, 1987; Tsai et al., 2016) is an additional advantage over the use of alternatives such as cell culture.

Galleria mellonella, the caterpillar (larva) of the greater wax moth *(Lepidoptera: pyralidae*) is widely used as a non-mammalian animal model system to study host-pathogen interactions using a variety of microorganisms including bacteria (Morton et al., 1983; Miyata et al., 2003; Fedhila et al., 2006; Aperis et al., 2007; Seed and Dennis, 2008) and fungi (Mylonakis et al., 2005). Use of the *G. mellonella* model to study the protective effects of candidate probiotics has received some research attention where for example, it has been applied in the evaluation of candidate probiotics to impair *Pseudomonas aeruginosa* biofilm formation (Berrios et al., 2018), to reduce virulence in *Candida albicans* (Vilela et al., 2015; de Oliveira et al., 2017; Rossoni et al., 2017, 2018), and to protect against gastrointestinal pathogens such as *Listeria monocytogenes* and *Escherichia coli* (Scalfaro et al., 2017). Significant correlations between observed virulence in *G. mellonella* and mammalian models have been previously reported (Jander et al., 2000; Mylonakis et al., 2005), and *G. mellonella* host immune defense mechanisms have been proposed to broadly resemble those of humans (Nathan, 2014; Kohler, 2015). Host responses of the larvae can be assessed through both the cellular response mediated by phagocytic cells and the humoral immune response pathway mediated by antimicrobial peptides (AMPs) (Kavanagh and Reeves, 2004; Scalfaro et al., 2017).

The current study aimed to study the interactions between candidate probiotics *(L. rhamnosus* GG, *L. reuteri,* and *S. salivarius* K12) and periodontopathogens *(A. actinomycetemcomitans, F. nucleatum,* and *P. gingivalis)* in oral keratinocytes and a lower animal infection model (*G. mellonella*).

MATERIALS AND METHODS

Bacterial Strains and Culture Preparations

Candidate probiotics comprised *Lactobacillus rhamnosus* Goldin and Gorbach (GG) (ATCC 53103), *Lactobacillus reuteri* ATCC 55730, and *Streptococcus salivarius* K-12. The periodontal pathogens were *Fusobacterium nucleatum* ATCC 10953, *Porphyromonas gingivalis* ATCC 33277, and *Aggregatibacter actinomycetemcomitans* ATCC 33384. *Aggregatibacter actinomycetemcomitans* was grown in Tryptic Soya Agar and broth supplemented with 0.6% yeast extract

(TSA and TSB) and incubated in a 5% CO_2 atmosphere. All other bacteria were grown using Wilkins-Chalgren broth or agar (Oxoid, Basingstoke, United Kingdom) at 37°C and incubated in an anaerobic cabinet (atmosphere, 10:10:80, H_2, CO_2, N_2). All bacteria were incubated at 37°C. For both *in vitro* and *in vivo* experiments, 10 ml volumes of each bacterium were prepared by growing cells overnight either anaerobically or in a 5% CO_2 environment. A 100-fold dilution of overnight culture was made in sterile broth, which was incubated until the desired growth phase was reached according to constructed growth curves. Cells were harvested by centrifugation at 3220 × *g* for 15 min and the pelleted cells were washed and re-suspended in sterile phosphate buffer saline (PBS) (0.01 M PBS; NaCl 8 g/L, KCL 0.2 g/L, Na_2HPO_4 1.42 g/L, and KH_2PO_4 0.24 g/L, pH 7.4). These steps were repeated twice, and the cell suspension adjusted to a final optical density at 600 nm of 0.1. Each larva received aliquots of 5 μl of this bacterial suspension injected directly to the hemocoel. For experiments using lysates and cell-free extracts, 10 ml of 10^8 Colony Forming Units (CFU)/ml of the appropriate strain was centrifuged. The supernatant was reserved to use as a cell-free extract. The pellet was washed, concentrated in 1 ml of Wilkins Chalgren broth, and lysed using a bead beater (FastPrep FP120; Thermo Electron Corporation). Samples were filter sterilized to remove any whole bacteria remaining.

TABLE 1 | Inhibition of periodontal pathogens by suspensions of candidate probiotics.

Periodontal pathogen	Candidate probiotic		
	L. rhamnosus	***L. reuteri***	***S. salivarius* K-12**
P. gingivalis	19 ± 1	15 ± 2	20 ± 2
F. nucleatum	11 ± 2	15 ± 1	20 ± 0
A. actinomycetemcomitans	33 ± 2	24 ± 0	41 ± 2

Determined using agar well-diffusion assays. Values are zones of inhibition (mm) and represent mean ± SEM from three separate experiments.

Galleria Infection Model

G. mellonella were obtained from Live Foods Direct, Sheffield, United Kingdom. The larvae were in the last instar stage (shedding of the exoskeleton), and were selected based on their weight (275–300 mg), the presence of a fresh cream color, and no gray markings. All larvae were used within 3 days from shipment.

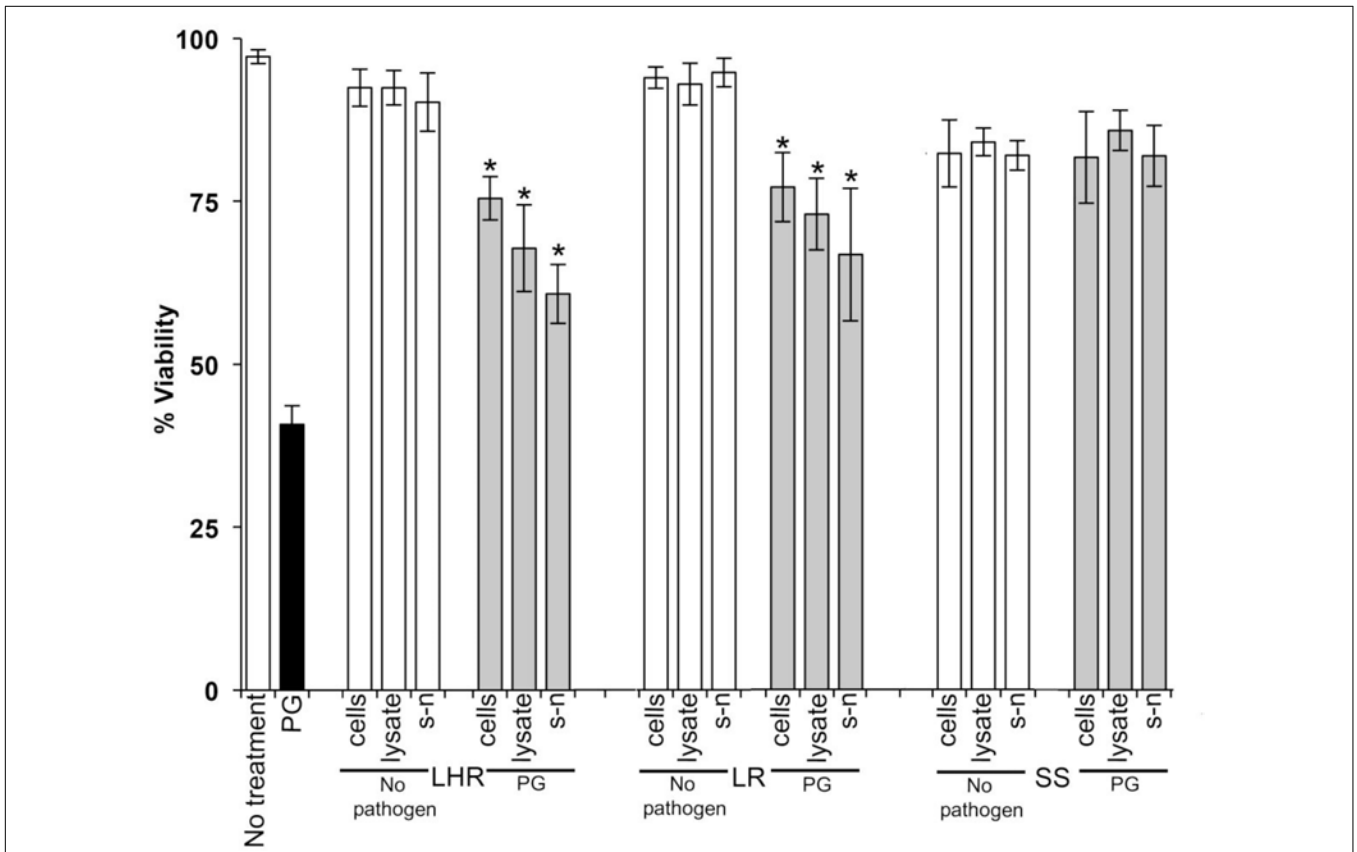

FIGURE 1 | The protective effects of candidate probiotics for human oral keratinocytes (HOKs) against *P. gingivalis.* All probiotic cells, cell lysates, and culture supernatants protected HOKs against *P. gingivalis*. HOKs were inoculated with either live *L. rhamnosus* GG (LHR), *L. reuteri* (LR), or *S. salivarius* K-12 (SS) cells, lysates and supernatants (s-n) (white bars) or simultaneously in combination with *P. gingivalis* (PG) (gray bars). All experiments were performed for a minimum of three biological replicates, with three technical replicates each time. All data are shown as mean values plus/minus standard deviations. Results expressed as the mean ± SEM, $^*p < 0.05$.

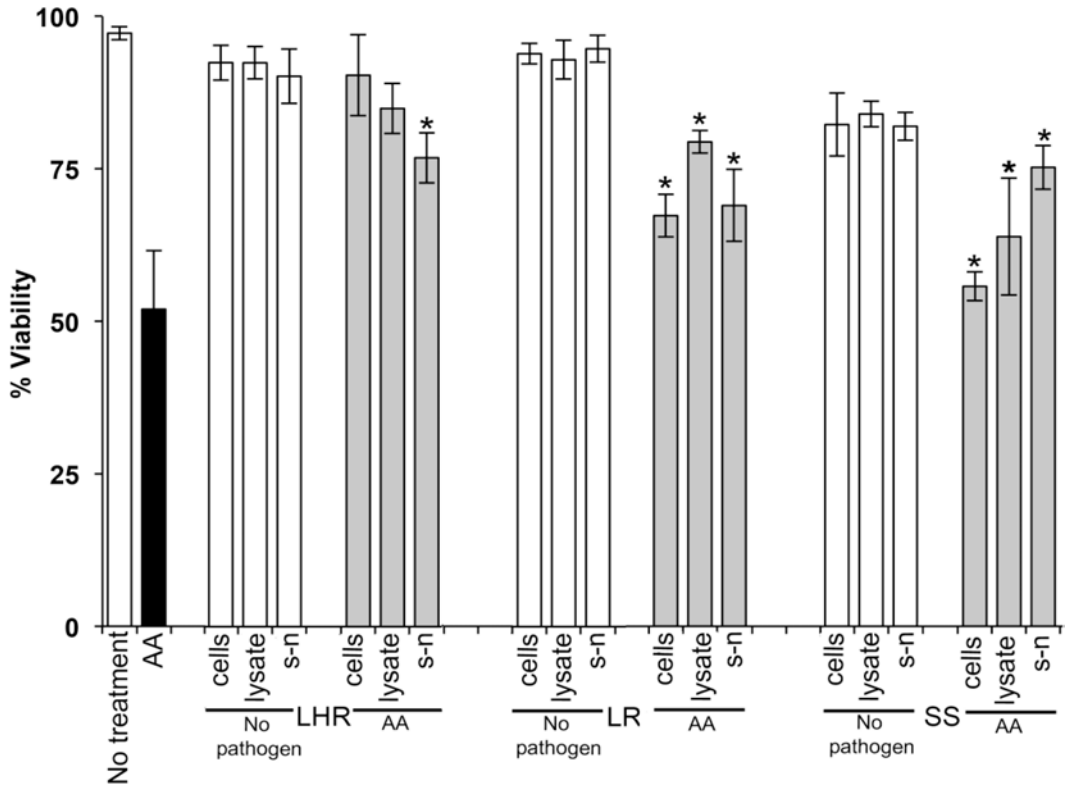

FIGURE 2 | The protective effects of candidate probiotics for human oral keratinocytes against *A. actinomycetemcomitans.* All probiotic cells, cell lysates, and culture supernatants protect HOKs against *A. actinomycetemcomitans*. HOKs were inoculated with either live *L. rhamnosus* GG (LHR), *L. reuteri* (LR), or *S. salivarius* K-12 (SS) cells, lysates and supernatants (s-n) (white bars) or simultaneously in combination with *A. actinomycetemcomitans* (AA) (gray bars). All experiments were performed for a minimum of three biological replicates, with three technical replicates each time. All data are shown as mean values plus/minus standard deviations. Results expressed as the mean ± SEM, $^*p < 0.05$.

Well-Diffusion Test

The test organisms were grown to the stationary phase (10^8 CFU/ml). Cultures of pathogenic bacteria were diluted 1:100 in Wilkins Chalgren agar. After careful mixing, 20 ml agar plates were poured and left to set. Once set, cup cuts were aseptically made within the agar (8 mm wells) and filled with 100 μl of the probiotic cell culture (∼1.5×10^8 CFU/ml) of each tested probiotic organism. The plates were incubated at 37°C anaerobically for 48 h and the diameter of the zone of inhibition produced measured using calipers.

Human Oral Keratinocyte Cell Culture

Human oral keratinocytes (HOKs, Sciencell Research Laboratories, United States) were used to assess the effect of probiotics on their viability. HOKs were maintained in oral keratinocyte medium (OKM, Sciencell Research Laboratories, United States) supplemented with oral keratinocyte growth supplement (OKGS) and 100 U/ml of both penicillin and streptomycin (OKM, Sciencell Research Laboratories, United States). The medium was substituted twice weekly and cells were incubated in a humid atmosphere with 5% CO_2 at 37°C. Cells were cultured in T-25 or T-75 vented culture flasks and 24 well plates (Corning, Sigma, United States). The cells were plated, at a density of 10×10^4 cells per cm^2, in 1 ml of the appropriate medium either in 12 or 24 well plates according to the experiment and used after 24 h incubation at 37°C at ∼90–100% confluence. Cells were exposed to 10^8 CFU/ml of each probiotic cell suspension for 24 h. Viability was determined using the trypan blue exclusion assay (Prince et al., 2012). Uninfected cells were included as a control. Probiotic lysates and cell-free extracts (100 μl) were added simultaneously with the periodontopathogen to the human oral keratinocytes.

Galleria mellonella Pathogenicity and Protection Assays

A modified version of the assay described by Ramarao et al. (2012) was performed. Larvae of *G. mellonella* were incubated for 30 min at room temperature before injection. Overnight cultures of each microorganism were centrifuged (3220 × *g*, 15 min) and suspended in PBS. This was repeated twice. Cultures were adjusted to an $OD_{600\ nm}$ of 0.1. For intrahemocoelic injection, bacterial suspensions were prepared with final concentrations in the range of 10^4 CFU/ml to 10^8 CFU/ml. Volumes of 5 μl of each strain, cell-free extract or lysate were delivered directly to the hemocoel through an injection in the rear left pro-leg using a 26-gauge needle Hamilton microsyringe

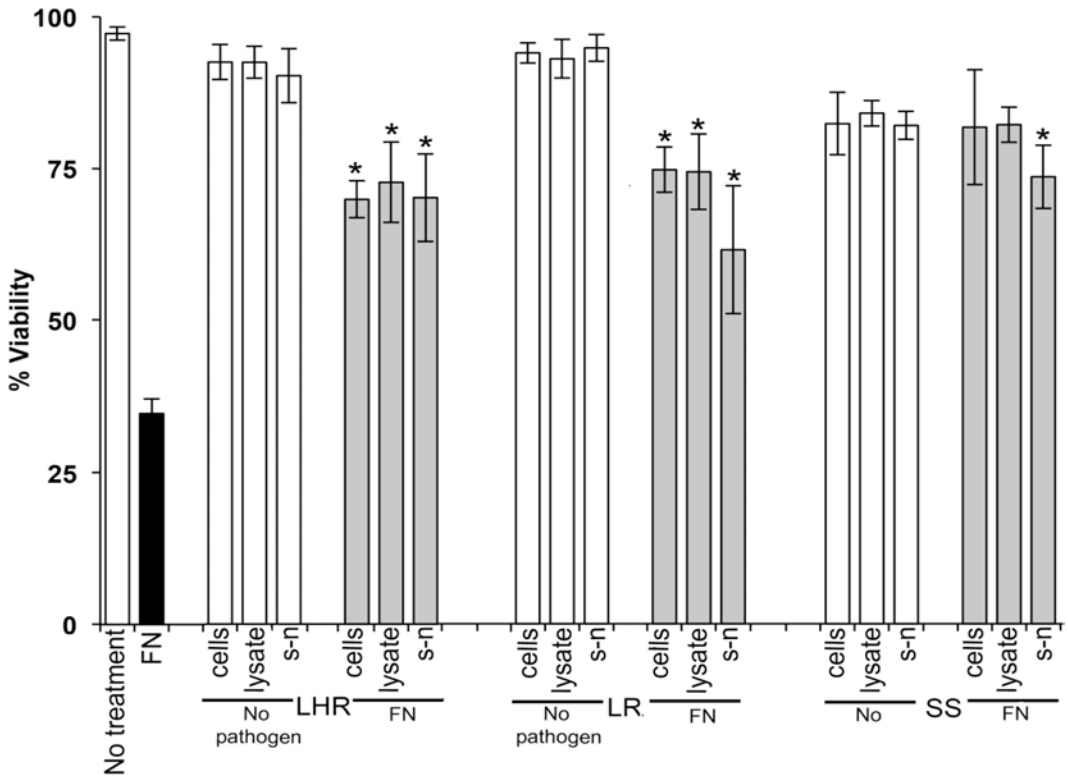

FIGURE 3 | The protective effects of candidate probiotics for human oral keratinocytes against *F. nucleatum*. All probiotic cells, cell lysates, and culture supernatants protect HOKs against *F. nucleatum*. HOKs were inoculated with either live *L. rhamnosus* GG (LHR), *L. reuteri* (LR), or *S. salivarius* K−12 (SS) lysates and supernatants (s-n) (white bars) or simultaneously in combination with *F. nucleatum* (FN) (gray bars). All experiments were performed for a minimum of three biological replicates, with three technical replicates each time. All data are shown as mean values plus/minus standard deviations. Results expressed as the mean ± SEM, $^{*}p < 0.05$.

(Sigma, United Kingdom). Sterile PBS (5 μl) was injected into the "trauma" control group and additionally, a "no treatment" control group was added. The right pro-leg was used as the injection site. Different sites were used for pathogenic and probiotic strains to reduce the risk of injection site infection. Infected larvae were incubated in a petri dish in groups of 10 at 37°C in the dark for the duration of the experiment (5–7 days).

Determination of Larval Mortality

Larval mortality was determined daily over a week. Larvae that had turned black and that were not moving in response to a gentle shaking of the dish or touching with a pipette tip were considered dead. Dead larvae were removed from the petri dish and the death was recorded. The experimental endpoint was designated by either the death of all the larvae in the tested groups or the conversion of larvae into pupae. Pupae were identified via a color change to white (Jorjao et al., 2018). Five Petri dishes containing 10 larvae each were assigned to each experiment and control groups (50 larvae total for each sample). Dead *G. mellonella* were placed into sterile Universal bottles and homogenized in 10 ml of sterile PBS. This suspension was then serially diluted, and spot plated onto Wilkins Chalgren agar to calculate bacterial load per individual larva. The experiments were terminated once two of the control individuals had died or pupated.

Statistical Analyses

Galleria mellonella data were plotted as survival curves using the Kaplan–Meier estimator in Microsoft Excel 2010. The survival values were considered significantly different if the *p*-value was < 0.05. For cell culture work paired student's *T*-tests done using Microsoft Excel 2010. Results were considered significant if $p \leq 0.05$.

RESULTS

In vitro Antibacterial Activity of Selected Probiotics

In vitro testing of antibacterial activity using an agar well-diffusion assay indicated that all three tested pathogens were inhibited by the three investigated probiotics to varying degrees. *A. actinomycetemcomitans* showed the greatest sensitivity to all probiotics with significantly larger zones of inhibition produced than for other pathogens. *Streptococcus salivarius* K-12 was the most effective against *A. actinomycetemcomitans* (**Table 1**). For both *F. nucleatum* and *P. gingivalis* the effect of all probiotics

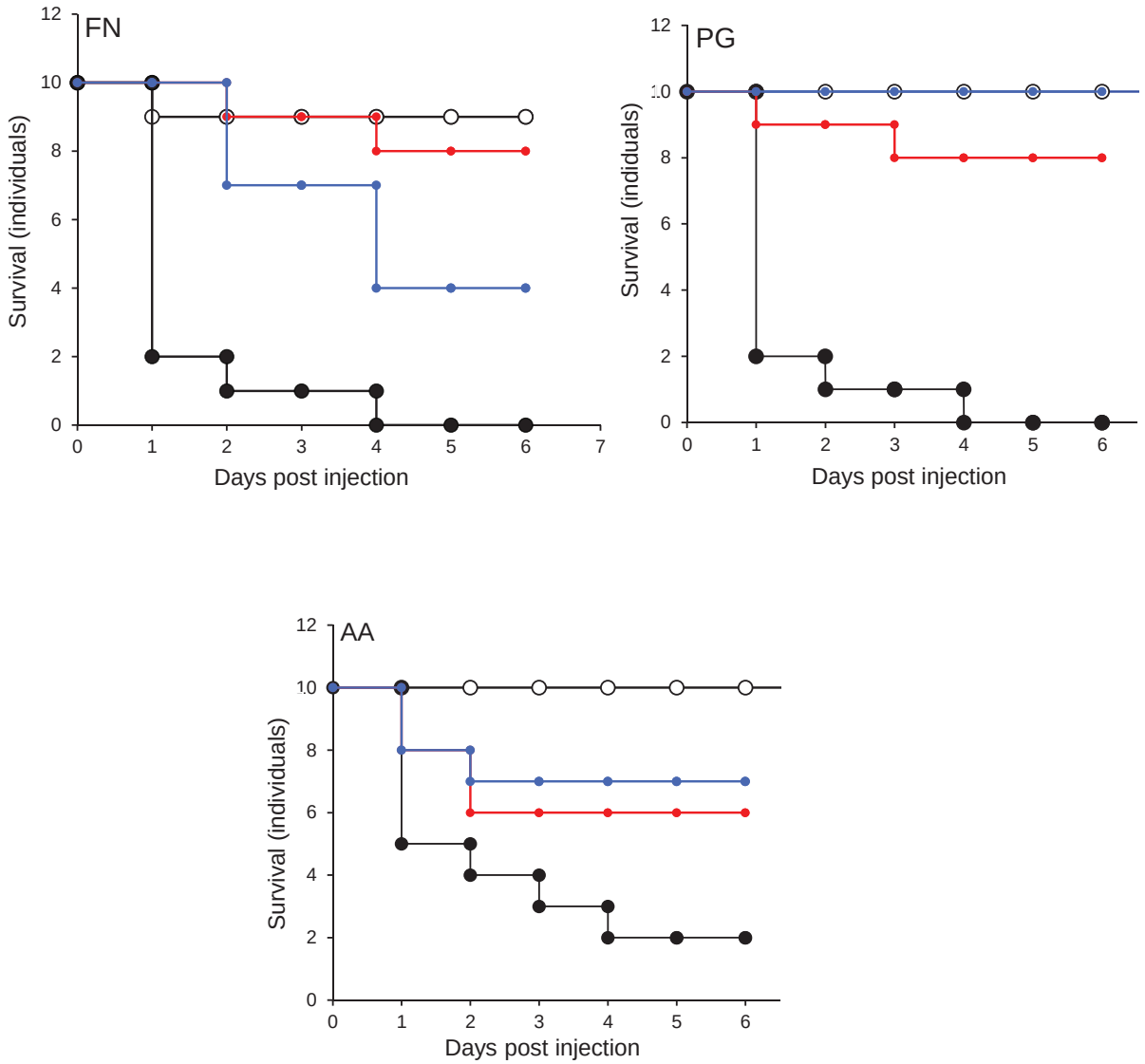

FIGURE 4 | The lethal effect of periodontal pathogens in an invertebrate model. Kaplan-Meier plots of survival of *G. mellonella* larvae after challenge with periodontal pathogens. *F. nucleatum* (FN), *Porphyromonas gingivalis* (PG), or *A. actinomycetemcomitans* (AA). Viable bacterial suspension (black symbols), cell-free culture supernatant (blue symbols), bacterial lysate (red symbols), and PBS (white symbols). All experiments were done twice on 2 consecutive weeks, with different batches of larvae and with three replica plates where each plate contains 10 larvae. All three periodontal pathogens caused at least 50% larvae morality at the endpoint of the experiment. The mortality effects of *F. nucleatum* and *P. gingivalis* were significantly greater than *A. actinomycetemcomitans* ($p < 0.05$) in the order *F. nucleatum* > *P. gingivalis* > *A. actinomycetemcomitans*. Bacterial lysates and cell-free culture supernatants contributed to the reduction of larvae viability, but the lethal effects were lower than for viable bacteria.

was comparable with *P. gingivalis* exhibiting slightly more sensitivity (**Table 1**).

The Susceptibility of Human Oral Keratinocytes and *G. mellonella* to Periodontal Pathogens

Data in **Figures 1–3** show when control HOKs were incubated for 24 h, ∼97% ± 0.2 of the cells remained viable; whereas the percentage of cells that remained viable following 24 h inoculation with the periodontopathogens was significantly ($p > 0.01$) lower. *P. gingivalis* decreased the viability of treated cell monolayers to 40% (**Figure 1**), *A. actinomycetemcomitans* decreased the viability of cell monolayers to 51% (**Figure 2**), and *F. nucleatum* decreased the viability of treated cell monolayers to 34% (**Figure 3**).

In the *G. mellonella* model (**Figure 4**), no mortality was observed in either control (non-treated control or PBS control). All three pathogens caused the death of at least 50% of larvae by the experimental endpoint. However, *P. gingivalis* and *F. nucleatum* caused significantly higher mortality ($p < 0.05$) than *A. actinomycetemcomitans* in the

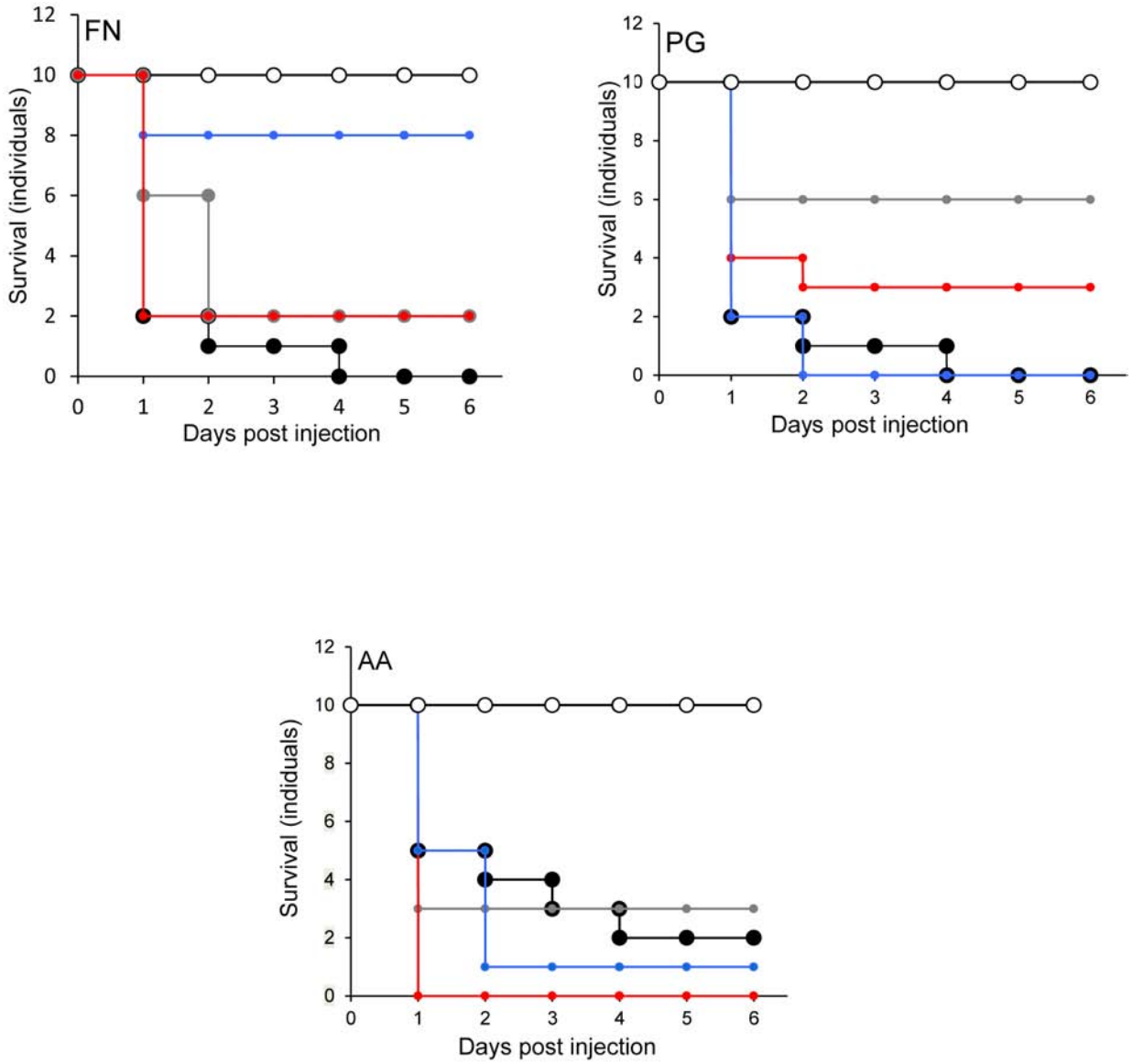

FIGURE 5 | Protection of larvae conferred by candidate probiotics following simultaneous administration of periodontal pathogens into the same larval proleg. Pathogen only (black symbols) and PBS (white symbols). Pathogen administered simultaneously with *L. rhamnosus* (gray symbols), *L. reuteri* (red symbols), *S. salivarius* (blue symbols). All experiments were done twice on 2 consecutive weeks, with different batches of larvae and with three replica plates where each plate contains 10 larvae. *S. salivarius* K-12 had a protective effect ($p \leq 0.01$) when administered simultaneously with *F. nucleatum* but not for *A. actinomycetemcomitans* or *P. gingivalis*. *L. reuteri* conferred protection against *P. gingivalis,* limited protection against *F. nucleatum,* and was not protective against *A. actimomycetemcomitans*. *L. rhamnosus* GG had some protective effect on larvae when was injected with *F. nucleatum* and *P. gingivalis* but reduced the larval viability when injected combined with *A. actinomycetemcomitans.*

order *F. nucleatum* > *P. gingivalis* > *A. actinomycetemcomitans* (**Figure 4**). Bacterial lysates and broth culture filtrates of pathogens reduced the viability of larvae, but the mortality rate was less than with live bacteria. Lysates were more lethal than cell-free extracts. These data show that HOKs and *G. mellonella* are susceptible to infection with selected periodontal pathogens. By contrast, none of the candidate probiotics (*L. rhamnosus* GG, *L. reuteri,* and *S. salivarius* K-12) induced significant mortality in HOKs or *G. mellonella* (**Figures 1–4**).

Species-Dependent Protective Effects of Candidate Probiotics in *G. mellonella* and Human Oral Cell Lines Challenged With Periodontal Pathogens

When *S. salivarius* K-12 was injected with either *F. nucleatum* or *A. actinomycetemcomitans* there was a higher larval viability 24 h post-injection ($p \leq 0.01$) than when *G. mellonella* was injected with the pathogens alone (**Figure 5**). However,

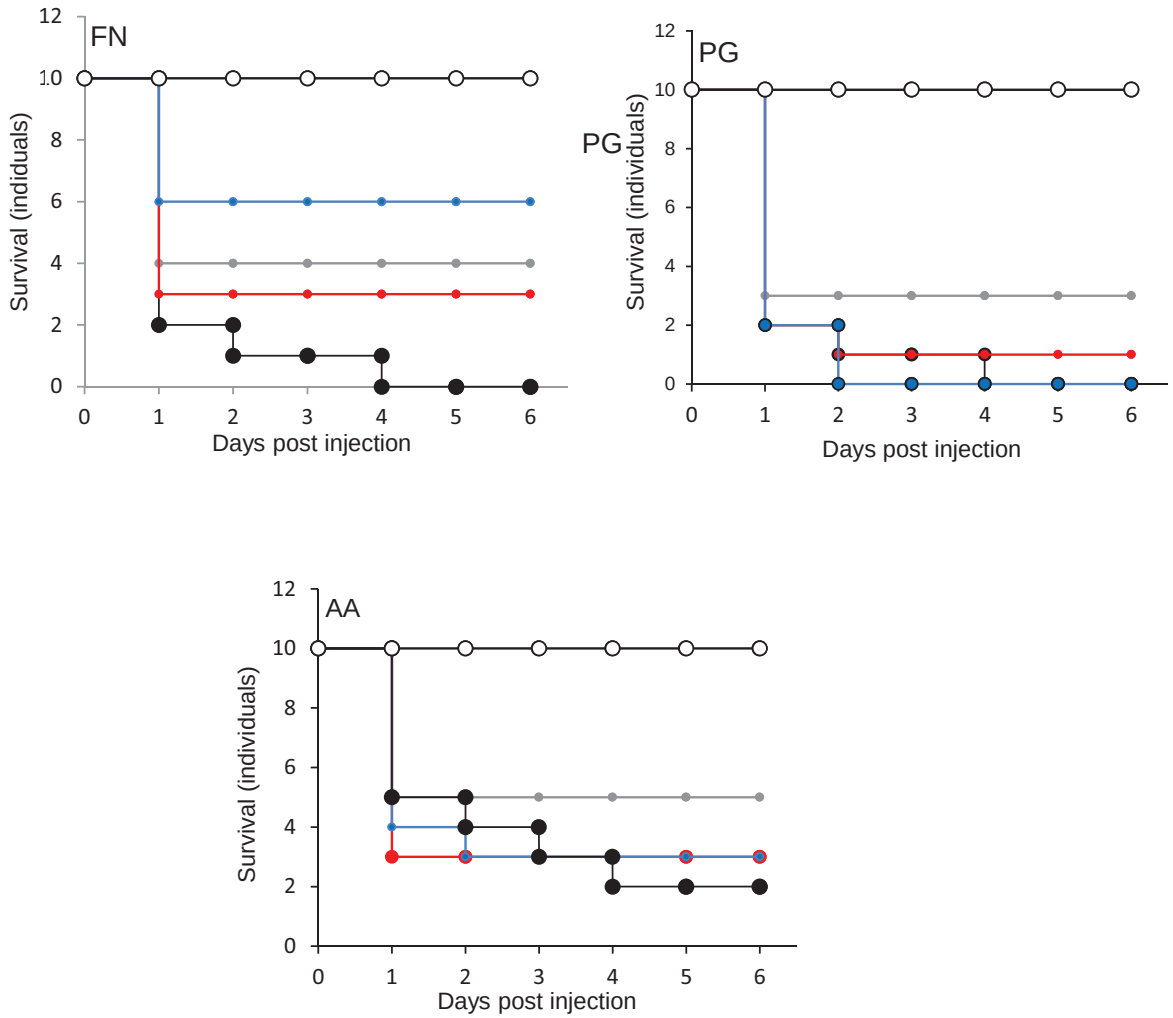

FIGURE 6 | Protection of larvae conferred by candidate probiotics following simultaneous administration of periodontal pathogens into the different larval prolegs. Pathogen only (black symbols) and PBS (white symbols). Pathogen administered simultaneously with *L. rhamnosus* (gray symbols), *L. reuteri* (red symbols), or *S. salivarius* (blue symbols). All experiments were done twice on 2 consecutive weeks, with different batches of larvae and with three replica plates where each plate contains 10 larvae. The greatest protection against *F. nucleatum* was conferred by *S. salivarius* K-12. For *P. gingivalis* and *A. actinomycetemcomitans*. *L. rhamnosus* GG was the most protective bacterium.

S. salivarius K-12 did not protect larvae from the effects of *P. gingivalis* (**Figure 5**). *L. reuteri* afforded some protection against *P. gingivalis* but had a limited effect against *F. nucleatum* and *A. actinomycetemcomitans*. *L. rhamnosus* GG had some protective effect on *G. mellonella* viability when injected in a mixture with *F. nucleatum* and *P. gingivalis* but increased the mortality of larvae when injected in a mixture with *A. actinomycetemcomitans* (**Figure 5**). Probiotic protection in *G. mellonella* according to bacterial species was in the following order: for *F. nucleatum* SS > LR > LHR, for *P. gingivalis* LR > LHR > SS, and for *A. actinomycetemcomitans,* SS > LHR = LR. Administering probiotic strains, their supernatants and lysates simultaneously with *F. nucleatum* (**Figure 3**) or *P. gingivalis* (**Figure 1**) to human oral keratinocytes significantly ($p < 0.05$) increased the viability compared to when infected with the pathogen alone. Protection against *A. actinomycetemcomitans* inoculation in HOKs (**Figure 2**) was variable and was only statistically significant ($p < 0.05$) when lysates or supernatants were administered ($p < 0.05$).

Effect of Injecting of Pathogen and Probiotic Simultaneously in Different Pro-legs on *G. mellonella* Mortality

The effects of injecting pathogens and probiotics into separate prolegs were evaluated. This was to exclude any effects due to an inhibitory interaction between microorganisms. The viability of larvae injected with *F. nucleatum* was increased when injected simultaneously with all probiotics. The most effective was *S. salivarius* K-12 (**Figure 6**). For *P. gingivalis, L. rhamnosus* GG reduced the lethal effect of *G. mellonella* (**Figure 6**), while with the other two

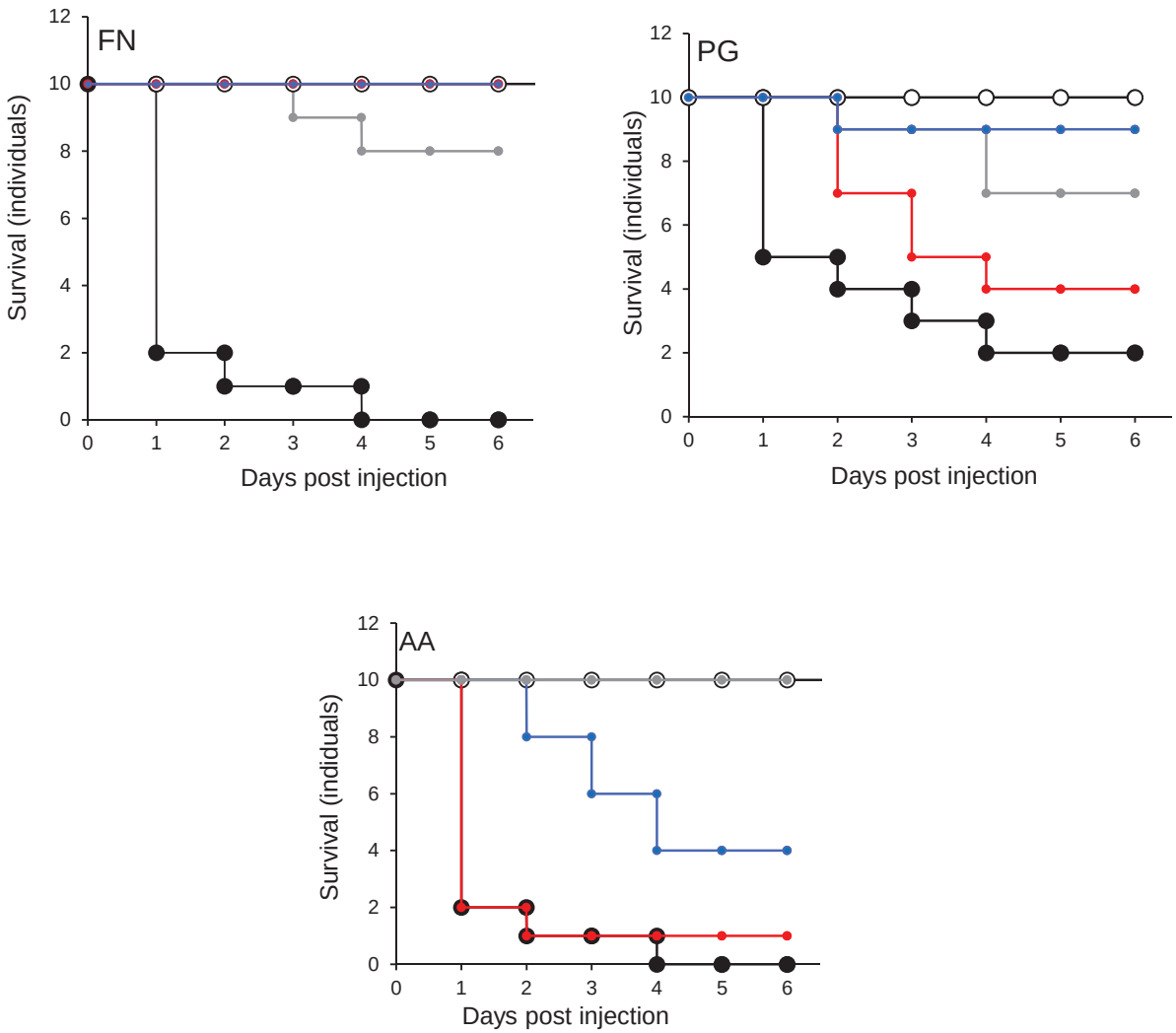

FIGURE 7 | Protection of larvae conferred by prior inoculation with candidate probiotics and administration of periodontal pathogens 24 h later, into the different larval prolegs. Pathogen only (black symbols) and PBS (white symbols). *L. rhamnosus* (gray symbols), *L. reuteri* (red symbols), or *S. salivarius* (blue symbols). All experiments were done twice on 2 consecutive weeks, with different batches of larvae and with three replica plates where each plate contains 10 larvae. Prior-injection of larvae with *L. rhamnosus* GG or *S. salivarius* K-12 was highly protective against *F. nucleatum*. *L. reuteri* had the most effective protection against the effects of *P. gingivalis,* while *S. salivarius* afforded the greatest protective effect against *A. actinomycetamcomitans*.

probiotics the viability was lower than the larvae injected with *P. gingivalis* alone. *L. reuteri* decreased conferred protection against *A. actinomycetemcomitans,* as did *L. rhamnosus* GG and *S. salivarius* K-12 to a lesser extent (**Figure 6**). Probiotic protection according to bacterial species occurred in the following order: SS > LR > LHR for *F. nucleatum*, LR > LHR > SS for *P. gingivalis,* and LR > LHR = SS for *A. actinomycetemcomitans.*

Effect of Probiotic Pre-treatment on Survival of *G. mellonella* Inoculated With Periodontal Pathogens

None of the larvae were killed when *F. nucleatum* was injected into larvae that were pre-injected with *L. rhamnosus* GG or *S. salivarius* K-12 (**Figure 7**). Furthermore, there was a highly significant decrease ($p < 0.001$) in the mortality of larvae pre-treated with *L. reuteri* (**Figure 7**). The effects of injecting *P. gingivalis* on larvae that were pre-treated for 24 h with probiotics was total protection for larvae pre-treated with *L. reuteri* whereas the least protection was conferred by *L. rhamnosus* GG (**Figure 7**). For *A. actinomycetemcomitans* the best protection was conferred by *S. salivarius* K-12 followed by *L. reuteri* and *L. rhamnosus* GG was the least effective (**Figure 7**) in terms of the increase of viability of larvae compared to larvae treated by pathogen only ($p < 0.01$). Probiotic protection according to bacterial species was in the following order: LHR > SS > LR for *F. nucleatum*, LR > SS > LHR for *P. gingivalis,* and SS > LR > LHR for *A. actinomycetemcomitans.*

DISCUSSION

We have utilized a waxworm larval pathogenicity model, and human oral keratinocytes to study interactions between candidate probiotics and periodontal pathogens. *A. actinomycetemcomitans, F. nucleatum,* and *P. gingivalis* were variably lethal to the larvae and were significantly lethal in oral keratinocytes. The candidate probiotics were not significantly pathogenic in all infection models investigated. Inoculation of larvae with the candidate probiotica before pathogen challenge gave measurable but partial protection against the periodontopathogens. Protection in mammalian culture was conferred by bacterial cells, their lysates, and cell-free extracts. There are two main mechanisms by which this protection could be conferred. The first involves direct inhibition of the periodontal pathogens by the candidate probiotics. In this respect, we observed an antagonistic effect of the probiotics against the periodontopathogens in *in vitro* tests, where *A. actinomycetemcomitans* was inhibited to the greatest extent. Previous studies have demonstrated the susceptibility of this bacterium to probiosis both *in vitro* (Jaffar et al., 2016, 2018) and *in vivo* (Morales et al., 2018). However, protection of the waxworm could also be conferred by host-dependent mechanisms. The lethality of the pathogens in the *G. mellonella* model followed the order *F. nucleatum* > *P. gingivalis* > *A. actinomycetemcomitans. F. nucleatum,* and *P. gingivalis* demonstrated significantly greater pathogenicity than *A. actinomycetemcomitans.* This finding is broadly in agreement with the Socranksy complexes (Socransky et al., 1998) where *P. gingivalis* and *F. nucleatum* form part of the red and orange complexes respectively, which have been strongly associated with periodontal disease. The toxic effects of spent culture fluid and lysates were also investigated. Both were shown to affect the viability of the larvae but to a lesser extent than with inoculation with live bacteria. This could involve extra-cellular virulence factors in addition to those that require a viable cell to be present. For example, the production of sialidase in *P. gingivalis* (Frey et al., 2019), the induction of inflammation by *F. nucleatum* (Han, 2015), and the production of toxins in *A. actinomycetemcomitans* (Belibasakis et al., 2019).

All of the candidate probiotic strains tested conferred a degree of protection to infection. However, the extent of this protection was dependent on the species of probiotic and the pathogen under test. This is in agreement with other studies demonstrating strain and species-dependent effects of probiotics when targeted toward periodontal pathogens (Teughels et al., 2013; Montero et al., 2017). The direct protection observed could be due to competition for adhesion, acid production, production of bacteriocins, and biosurfactants (Spurbeck and Arvidson, 2010; Kohler et al., 2012; Orsi et al., 2014; Sabia et al., 2014).

The effects of simultaneously administering the probiotic strain and the pathogen to *G. mellonella* but in a different pro-legs were investigated to differentiate between direct competitive effects (as seen in **Table 1**) and immunomodulation. Data in **Figure 6** suggest that there was a protective effect comparable to that observed when the probiotics were administered to the same site. This supports the hypothesis that the probiotics protect the larvae from infection *via* a mechanism distinct from direct competition, such as immunomodulation (Toshimitsu et al., 2017). Data in **Figure 7** show the effects of administering the probiotics 24 h before pathogen inoculation. Competitive inhibition of pathogens by probiotic strains has previously been indicated as important in terms of observing a significant and relevant probiotic effect (Zhu et al., 2010; Munoz-Quezada et al., 2013). **Figure 7** shows that for *F. nucleatum* injected 24 h after *Lactobacillus rhamnosus* administration, *F. nucleatum* injected after *S. salivarius* K12 and *P. gingivalis* injected after *L. reuteri* administration larval mortality was comparable to that observed in the PBS control group. This could be due to immunomodulation in *G. mellonella* that subsequently inhibited infection with the periodontopathogens. This observation is in agreement with a previous study that demonstrated that the experimental co-infection of *G. mellonella* with *L. acidophilus* and *C. albicans* reduced the number of yeast cells in the larval hemolymph and increased the survival of larvae (Ribeiro et al., 2017).

The *G. mellonella* larvae represent a cost-effective simple *in vivo* model as a preliminary investigative tool for screening the potential protective probiotic effects against periodontal and potentially other pathogens. Selected probiotic candidates showed varied probiotic activity against *F. nucleatum*, *P. gingivalis* and *A. actinomycetemcomitans* in both the larval model an in human oral keratinocytes, warranting further investigation of the mechanisms of interaction and applicability to human health.

DATA AVAILABILITY STATEMENT

The datasets generated for this study are available on request to the corresponding author.

AUTHOR CONTRIBUTIONS

RM performed the laboratory-based analyses, contributed to data analysis, and co-wrote the manuscript. TC co-wrote and contributed to data analysis. CO'N, RL, and AM designed the study, supervised the project, performed the data analysis, and co-wrote the manuscript.

FUNDING

This work was supported by a scholarship from the Faculty of Pharmacy, The University of Tripoli through the Ministry of Higher Education of Libya to RM.

REFERENCES

Ahn, S. H., Chun, S., Park, C., Lee, J. H., Lee, S. W., and Lee, T. H. (2017). Transcriptome profiling analysis of senescent gingival fibroblasts in response to *Fusobacterium nucleatum* infection. *PLoS One* 12:e0188755. doi: 10.1371/journal.pone.0188755

Aperis, G., Fuchs, B. B., Anderson, C. A., Warner, J. E., Calderwood, S. B., and Mylonakis, E. (2007). *Galleria mellonella* as a model host to study infection by the *Francisella tularensis* live vaccine strain. *Microb. Infect.* 9, 729–734. doi: 10.1016/j.micinf.2007.02.016

Ball, M., Goldberg, A., Fentem, J., Broadhead, C., Burch, R., and Festing, M. (1995). The three rs: the way forward, the report and recommendation of ECVAM (The european center for the validation of alternative methods). *Altern. Lab. Anim.* 23, 836–866.

Belibasakis, G. N., Maula, T., Bao, K., Lindholm, M., Bostanci, N., Oscarsson, J., et al. (2019). Virulence and pathogenicity properties of *Aggregatibacter actinomycetemcomitans*. *Pathogens* 8, 222. doi: 10.3390/pathogens8040222

Berrios, P., Fuentes, J. A., Salas, D., Carreno, A., Aldea, P., Fernandez, F., et al. (2018). Inhibitory effect of biofilm-forming *Lactobacillus kunkeei* strains against virulent *Pseudomonas aeruginosa* in vitro and in honeycomb moth *(Galleria mellonella)* infection model. *Benef. Microb.* 9, 257–268. doi: 10.3920/BM2017.0048

Bhattacharyya, S., Ghosh, S. K., Shokeen, B., Eapan, B., Lux, R., Kiselar, J., et al. (2016). FAD-I, a *Fusobacterium nucleatum* cell wall-associated diacylated lipoprotein that mediates human beta defensin 2 induction through toll-like receptor-1/2 (TLR-1/2) and TLR-2/6. *Infect. Immun.* 84, 1446–1456. doi: 10.1128/IAI.01311-15

Bohora, A., and Kokate, S. (2017). Evaluation of the role of probiotics in endodontic treatment: a preliminary study. *J. Int. Soc. Prev. Commun. Dent.* 7, 46–51. doi: 10.4103/2231-0762.200710

Boman, H. G., and Hultmark, D. (1987). Cell-free immunity in insects. *Annu. Rev. Microbiol.* 41, 103–126.

Brignardello-Petersen, R. (2017). Probiotics as adjuvant to scaling and root planning seem to improve periodontal parameters after 3 months of treatment. *J. Am. Dent. Assoc.* 148:e10. doi: 10.1016/j.adaj.2016.12.008

Casadevall, A. (2005). Host as the variable: model hosts approach the immunological asymptote. *Infect. Immun.* 73, 3829–3832. doi: 10.1128/IAI.73.7.3829-3832.2005

Chamilos, G., Samonis, G., and Kontoyiannis, P. (2011). Drosophila melanogaster as a model host for the study of microbial pathogenicity and the discovery of novel antimicrobial compounds. *Curr. Pharm. Design* 17, 1246–1253. doi: 10.2174/138161211795703744

de Oliveira, F. E., Rossoni, R. D., De Barros, P. P., Begnini, B. E., Junqueira, J. C., Jorge, A. O. C., et al. (2017). Immunomodulatory effects and anti-Candida activity of lactobacilli in macrophages and in invertebrate model of *Galleria mellonella*. *Microb. Pathog.* 110, 603–611. doi: 10.1016/j.micpath.2017.08.006

DiRienzo, J. M. (2014). Breaking the gingival epithelial barrier: role of the *Aggregatibacter actinomycetemcomitans* cytolethal distending toxin in oral infectious disease. *Cells* 3, 476–499. doi: 10.3390/cells3020476

Duncan, M., Nakao, S., Skobe, Z., and Xie, H. (1993). Interactions of *Porphyromonas gingivalis* with epithelial cells. *Infect. Immun.* 61, 2260–2265.

Dzink, J., Socransky, S., and Haffajee, A. (1988). The predominant cultivable microbiota of active and inactive lesions of destructive periodontal diseases. *J. Clin. Periodontol.* 15, 316–323. doi: 10.1111/j.1600-051x.1988.tb01590.x

Fedhila, S., Daou, N., Lereclus, D., and Nielsen-Leroux, C. (2006). Identification of Bacillus cereus internalin and other candidate virulence genes specifically induced during oral infection in insects. *Mol. Microbiol.* 62, 339–355. doi: 10.1111/j.1365-2958.2006.05362.x

Frey, A. M., Satur, M. J., Phansopa, C., Honma, K., Urbanowicz, P. A., Spencer, D. I. R., et al. (2019). Characterization of *Porphyromonas gingivalis* sialidase and disruption of its role in host-pathogen interactions. *Microbiology* 165, 1181–1197. doi: 10.1099/mic.0.000851

Gatej, S. M., Marino, V., Bright, R., Fitzsimmons, T. R., Gully, N., Zilm, P., et al. (2018). Probiotic *Lactobacillus rhamnosus* GG prevents alveolar bone loss in a mouse model of experimental periodontitis. *J. Clin. Periodontol.* 45, 204–212. doi: 10.1111/jcpe.12838

Hajishengallis, G., and Lamont, R. J. (2012). Beyond the red complex and into more complexity: the polymicrobial synergy and dysbiosis (PSD) model of periodontal disease etiology. *Mol. Oral Microbiol.* 27, 409–419. doi: 10.1111/j.2041-1014.2012.00663.x

Han, Y. W. (2015). *Fusobacterium nucleatum:* a commensal-turned pathogen. *Curr. Opin. Microbiol.* 23, 141–147. doi: 10.1016/j.mib.2014.11.013

Imamura, T. (2003). The role of gingipains in the pathogenesis of periodontal disease. *J. Periodontol.* 74, 111–118. doi: 10.1902/jop.2003.74.1.111

Ince, G., Gursoy, H., Ipci, S. D., Cakar, G., Emekli-Alturfan, E., and Yilmaz, S. (2015). Clinical and biochemical evaluation of lozenges containing *Lactobacillus reuteri* as an adjunct to non-surgical periodontal therapy in chronic periodontitis. *J. Periodontol.* 86, 746–754. doi: 10.1902/jop.2015.140612

Jaffar, N., Ishikawa, Y., Mizuno, K., Okinaga, T., and Maeda, T. (2016). Mature biofilm degradation by potential probiotics: *Aggregatibacter actinomycetemcomitans* versus *Lactobacillus* spp. *PLoS One* 11:e0159466. doi: 10.1371/journal.pone.0159466

Jaffar, N., Okinaga, T., Nishihara, T., and Maeda, T. (2018). Enhanced phagocytosis of *Aggregatibacter actinomycetemcomitans* cells by macrophages activated by a probiotic Lactobacillus strain. *J. Dairy Sci.* 101, 5789–5798. doi: 10.3168/jds.2017-14355

Jander, G., Rahme, L. G., and Ausubel, F. M. (2000). Positive correlation between virulence of *Pseudomonas aeruginosa* mutants in mice and insects. *J. Bacteriol.* 182, 3843–3845. doi: 10.1128/jb.182.13.3843-3845.2000

Johansson, A. (2011). *Aggregatibacter actinomycetemcomitans* leukotoxin: a powerful tool with capacity to cause imbalance in the host inflammatory response. *Toxins* 3, 242–259. doi: 10.3390/toxins3030242

Jorjao, A. L., Oliveira, L. D., Scorzoni, L., Figueiredo-Godoi, L. M. A., Cristina, A. P. M., Jorge, A. O. C., et al. (2018). From moths to caterpillars: ideal conditions for *Galleria mellonella* rearing for *in vivo* microbiological studies. *Virulence* 9, 383–389. doi: 10.1080/21505594.2017.1397871

Kavanagh, K., and Reeves, E. P. (2004). Exploiting the potential of insects for in vivo pathogenicity testing of microbial pathogens. *FEMS Microbiol. Rev.* 28, 101–112. doi: 10.1016/j.femsre.2003.09.002

Kobayashi, R., Kobayashi, T., Sakai, F., Hosoya, T., Yamamoto, M., and Kurita-Ochiai, T. (2017). Oral administration of *Lactobacillus gasseri* SBT2055 is effective in preventing *Porphyromonas gingivalis*-accelerated periodontal disease. *Sci. Rep.* 7:545. doi: 10.1038/s41598-017-00623-9

Kohler, G. (2015). Probiotics research in *Galleria mellonella*. *Virulence* 6, 3–5.

Kohler, G. A., Assefa, S., and Reid, G. (2012). Probiotic interference of *Lactobacillus rhamnosus* GR-1 and *Lactobacillus reuteri* RC-14 with the opportunistic fungal pathogen *Candida albicans*. *Infect. Dis. Obstet. Gynecol.* 2012:636474. doi: 10.1155/2012/636474

Kõll-Klais, P., Mändar, R., Leibur, E., Marcotte, H., Hammarstrom, L., and Mikelsaar, M. (2005). Oral *Lactobacilli* in chronic periodontitis and periodontal health: species composition and antimicrobial activity. *Oral Microbiol. Immunol.* 20, 354–361. doi: 10.1111/j.1399-302X.2005.00239.x

Krasse, P., Carlsson, B., Dahl, C., Paulsson, A., Nilsson, A., and Sinkiewicz, G. (2006). Decreased gum bleeding and reduced gingivitis by the probiotic *Lactobacillus reuteri*. *Swedish Dent. J.* 30, 55–60.

Krisanaprakornkit, S., Kimball, J. R., Weinberg, A., Darveau, R. P., Bainbridge, B. W., and Dale, B. A. (2000). Inducible expression of human beta-defensin 2 by *Fusobacterium nucleatum* in oral epithelial cells: multiple signaling pathways and role of commensal bacteria in innate immunity and the epithelial barrier. *Infect. Immun.* 68, 2907–2915. doi: 10.1128/iai.68.5.2907-2915.2000

Lamont, R. J., and Hajishengallis, G. (2015). Polymicrobial synergy and dysbiosis in inflammatory disease. *Trends Mol. Med.* 21, 172–183. doi: 10.1016/j.molmed.2014.11.004

Miyachi, K., Ishihara, K., Kimizuka, R., and Okuda, K. (2007). Arg-gingipain A DNA vaccine prevents alveolar bone loss in mice. *J. Dent. Res.* 86, 446–450. doi: 10.1177/154405910708600511

Miyata, S., Casey, M., Frank, D. W., Ausubel, F. M., and Drenkard, E. (2003). Use of the *Galleria mellonella* caterpillar as a model host to study the role of the type

III secretion system in *Pseudomonas aeruginosa* pathogenesis. *Infect. Immun.* 71, 2404–2413. doi: 10.1128/iai.71.5.2404-2413.2003

Montero, E., Iniesta, M., Rodrigo, M., Marin, M. J., Figuero, E., Herrera, D., et al. (2017). Clinical and microbiological effects of the adjunctive use of probiotics in the treatment of gingivitis: a randomized controlled clinical trial. *J. Clin. Periodontol.* 44, 708–716. doi: 10.1111/jcpe.12752

Morales, A., Gandolfo, A., Bravo, J., Carvajal, P., Silva, N., Godoy, C., et al. (2018). Microbiological and clinical effects of probiotics and antibiotics on nonsurgical treatment of chronic periodontitis: a randomized placebo- controlled trial with 9-month follow-up. *J. Appl. Oral Sci.* 26:e20170075. doi: 10.1590/1678-7757-2017-0075

Morton, D., Barnett, R., and Chadwick, J. (1983). Structural alterations to *Proteus mirabilis as* a result of exposure to haemolymph from the larvae of *Galleria mellonella*. *Microbios* 39, 177–185.

Munoz-Quezada, S., Bermudez-Brito, M., Chenoll, E., Genoves, S., Gomez-Llorente, C., Plaza-Diaz, J., et al. (2013). Competitive inhibition of three novel bacteria isolated from faeces of breast milk-fed infants against selected enteropathogens. *Br. J. Nutr.* 109(Suppl. 2), S63–S69. doi: 10.1017/S0007114512005600

Mylonakis, E., Moreno, R., El Khoury, J. B., Idnurm, A., Heitman, J., Calderwood, S. B., et al. (2005). *Galleria mellonella* as a model system to study *Cryptococcus neoformans* pathogenesis. *Infect. Immun.* 73, 3842–3850. doi: 10.1128/IAI.73.7.3842-3850.2005

Nathan, S. (2014). New to *Galleria mellonella*: modeling an ExPEC infection. *Virulence* 5, 371–374. doi: 10.4161/viru.28338

Nisha, S., Samyuktha, G. S., Shashikumar, P., and Chandra, S. (2017). Periodontal disease–Historical and contemporary hypothesis: a review. *SRM J. Res. Dent. Sci.* 8:121.

Orsi, C. F., Sabia, C., Ardizzoni, A., Colombari, B., Neglia, R. G., Peppoloni, S., et al. (2014). Inhibitory effects of different lactobacilli on *Candida albicans* hyphal formation and biofilm development. *J. Biol. Regul. Homeost. Agents* 28, 743–752.

Prince, T., Mcbain, A. J., and O'neill, C. A. (2012). *Lactobacillus reuteri* protects epidermal keratinocytes from *Staphylococcus aureus*-induced cell death by competitive exclusion. *Appl. Environ. Microbiol.* 78, 5119–5126. doi: 10.1128/AEM.00595-12

Rahme, L. G., Stevens, E. J., Wolfort, S. F., and Shao, J. (1995). Common virulence factors for bacterial pathogenicity in plants and animals. *Science* 268:1899. doi: 10.1126/science.7604262

Ramarao, N., Nielsen-Leroux, C., and Lereclus, D. (2012). The insect *Galleria mellonella* as a powerful infection model to investigate bacterial pathogenesis. *JoVE* 70:e4392. doi: 10.3791/4392

Ribeiro, F., Barros, P., Rossoni, R. D., Junqueira, J. C., and Jorge, A. O. C. (2017). Lactobacillus rhamnosus inhibits *Candida albicans* virulence factors *in vitro* and modulates immune system in Galleria mellonella. *J. Appl. Microbiol.* 122, 201–211. doi: 10.1111/jam.13324

Rossoni, R. D., Dos Santos Velloso, M., Figueiredo, L. M. A., Martins, C. P., Jorge, A. O. C., and Junqueira, J. C. (2018). Clinical strains of *Lactobacillus* reduce the filamentation of *Candida albicans* and protect *Galleria mellonella* against experimental candidiasis. *Folia Microbiol.* 63, 307–314. doi: 10.1007/s12223-017-0569-9

Rossoni, R. D., Fuchs, B. B., De Barros, P. P., Velloso, M. D., Jorge, A. O., Junqueira, J. C., et al. (2017). *Lactobacillus paracasei* modulates the immune system of *Galleria mellonella* and protects against Candida albicans infection. *PLoS One* 12:e0173332. doi: 10.1371/journal.pone.0173332

Sabia, C., Anacarso, I., Bergonzini, A., Gargiulo, R., Sarti, M., Condo, C., et al. (2014). Detection and partial characterization of a bacteriocin-like substance produced by *Lactobacillus fermentum* CS57 isolated from human vaginal secretions. *Anaerobe* 26, 41–45. doi: 10.1016/j.anaerobe.2014.01.004

Sandros, J., Papapanou, P., Nannmark, U., and Dahlen, G. (1994). *Porphyromonas gingivalis* invades human pocket epithelium in vitro. *J. Period. Res.* 29, 62–69. doi: 10.1111/j.1600-0765.1994.tb01092.x

Scalfaro, C., Iacobino, A., Nardis, C., and Franciosa, G. (2017). *Galleria mellonella* as an in vivo model for assessing the protective activity of probiotics against gastrointestinal bacterial pathogens. *FEMS Microbiol. Lett.* 364:fnx064. doi: 10.1093/femsle/fnx064

Seed, K. D., and Dennis, J. J. (2008). Development of Galleria mellonella as an alternative infection model for the *Burkholderia cepacia* complex. *Infect. Immun.* 76, 1267–1275. doi: 10.1128/IAI.01249-07

Slots, J. (2017). Periodontitis: facts, fallacies and the future. *Periodontology* 2000, 7–23. doi: 10.1111/prd.12221

Slots, J., Bragd, L., Wikström, M., and Dahlén, G. (1986). The occurrence of *Actinobacillus actinomycetemcomitans*, *Bacteroides gingivalis* and *Bacteroides intermedius* in destructive periodontal disease in adults. *J. Clin. Periodontol.* 13, 570–577. doi: 10.1111/j.1600-051x.1986.tb00849.x

Socransky, S. S., Haffajee, A. D., Cugini, M. A., and Smith, C. (1998). Microbial complexes in subgingival plaque. *J. Clin. Periodontol.* 25, 134–144.

Sookkhee, S., Chulasiri, M., and Prachyabrued, W. (2001). Lactic acid bacteria from healthy oral cavity of Thai volunteers: inhibition of oral pathogens. *J. Appl. Microbiol.* 90, 172–179. doi: 10.1046/j.1365-2672.2001.01229.x

Spurbeck, R. R., and Arvidson, C. G. (2010). Lactobacillus jensenii surface-associated proteins inhibit *Neisseria gonorrhoeae* adherence to epithelial cells. *Infect. Immun.* 78, 3103–3111. doi: 10.1128/IAI.01200-09

Swanson, M., and Hammer, B. (2000). *Legionella pneumophila* pathogenesis: a fateful journey from amoebae to macrophages. *Annu. Rev. Microbiol.* 54, 567–613. doi: 10.1146/annurev.micro.54.1.567

Teughels, W., Durukan, A., Ozcelik, O., Pauwels, M., Quirynen, M., and Haytac, M. C. (2013). Clinical and microbiological effects of *Lactobacillus reuteri* probiotics in the treatment of chronic periodontitis: a randomized placebo-controlled study. *J. Clin. Periodontol.* 40, 1025–1035. doi: 10.1111/jcpe.12155

Toshimitsu, T., Ozaki, S., Mochizuki, J., Furuichi, K., and Asami, Y. (2017). Effects of *Lactobacillus plantarum* strain OLL2712 culture conditions on the anti-inflammatory activities for murine immune cells and obese and type 2 diabetic mice. *Appl. Environ. Microbiol.* 83, e3001–e3016. doi: 10.1128/AEM.03001-16

Tsai, C. J., Loh, J. M., and Proft, T. (2016). *Galleria mellonella* infection models for the study of bacterial diseases and for antimicrobial drug testing. *Virulence* 7, 214–229. doi: 10.1080/21505594.2015.1135289

Vilela, S. F., Barbosa, J. O., Rossoni, R. D., Santos, J. D., Prata, M. C., Anbinder, A. L., et al. (2015). Lactobacillus acidophilus ATCC 4356 inhibits biofilm formation by *C. albicans* and attenuates the experimental candidiasis in *Galleria mellonella*. *Virulence* 6, 29–39. doi: 10.4161/21505594.2014.981486

Vivekananda, M. R., Vandana, K. L., and Bhat, K. G. (2010). Effect of the probiotic *Lactobacillus reuteri* (Prodentis) in the management of periodontal disease: a preliminary randomized clinical trial. *J. Oral Microbiol.* 2:2. doi: 10.3402/jom.v2i0.5344

Wolf, H. F., Rateitschak-Plüss, E. M., Hassell, T. M., and Rateitschak, K. H. (2005). *Color Atlas of Periodontology*. New York, NY: Thieme.

Zhu, L., Li, H., Yang, X., Xue, L., Li, X., and Du, J. (2019). Effects of *Streptococcus salivarius* K12 on experimental periodontitis and oral microbiota in mice. *J. Biosci. Med.* 7, 95–111.

Zhu, Y., Xiao, L., Shen, D., and Hao, Y. (2010). Competition between yogurt probiotics and periodontal pathogens in vitro. *Acta Odontol. Scand.* 68, 261–268. doi: 10.3109/00016357.2010.492235

Conflict of Interest: The authors declare that the research was conducted in the absence of any commercial or financial relationships that could be construed as a potential conflict of interest.

Advantages of publishing in Frontiers

OPEN ACCESS
Articles are free to read for greatest visibility and readership

FAST PUBLICATION
Around 90 days from submission to decision

HIGH QUALITY PEER-REVIEW
Rigorous, collaborative, and constructive peer-review

TRANSPARENT PEER-REVIEW
Editors and reviewers acknowledged by name on published articles

Frontiers
Avenue du Tribunal-Fédéral 34
1005 Lausanne | Switzerland

Visit us: www.frontiersin.org
Contact us: info@frontiersin.org | +41 21 510 17 00

REPRODUCIBILITY OF RESEARCH
Support open data and methods to enhance research reproducibility

DIGITAL PUBLISHING
Articles designed for optimal readership across devices

FOLLOW US
@frontiersin

IMPACT METRICS
Advanced article metrics track visibility across digital media

EXTENSIVE PROMOTION
Marketing and promotion of impactful research

LOOP RESEARCH NETWORK
Our network increases your article's readership